EMERGING INFECTIOUS DISEASES®

CDC
Centers for Disease Control and Prevention

Antimicrobial Resistance

January 2019

Anna Dumitriu (1969). *Make Do and Mend* (detail), 2017. Ampicillin antibiotic susceptibility discs and fabric, 12 in x 12 in/30.48 cm x 30.48 cm.
First exhibited at LifeSpace Dundee, 2017. Made in collaboration with Nicola Fawcett (University of Oxford) and Sarah Goldberg (Technion). Digital image courtesy of Anna Dumitriu.

EMERGING INFECTIOUS DISEASES

EDITOR-IN-CHIEF
D. Peter Drotman

Emerging Infectious Diseases is published monthly by the Centers for Disease Control and Prevention, 1600 Clifton Rd NE, Mailstop H16-2, Atlanta, GA 30329-4027, USA. Telephone 404-639-1960, fax 404-639-1954, email eideditor@cdc.gov.

EMERGING INFECTIOUS DISEASES®

January 2019

On the Cover

Anna Dumitriu (1969). *Make Do and Mend* (detail), **2017**. Ampicillin antibiotic susceptibility discs and fabric, 12 in x 12 in/30.48 cm x 30.48 cm. First exhibited at LifeSpace Dundee, 2017. Made in collaboration with Nicola Fawcett (University of Oxford) and Sarah Goldberg (Technion). Digital image courtesy of Anna Dumitriu.

About the Cover p. 198

Perspective

Synopses

Medscape EDUCATION ACTIVITY

Research

EMERGING INFECTIOUS DISEASES®
January 2019

Medscape EDUCATION ACTIVITY

Dispatches

The installation *Make Do and Mend* by Anna Dumitriu explores CRISPR gene editing and antibiotic resistance. It features an altered antique women's suit with CC41 mark, antique toy sewing machine, silk impregnated with CRISPR edited bacteria, altered vintage leaflets, ampicillin antibiotic susceptibility discs, fabric, wood and glass frames. First exhibited at LifeSpace Dundee, 2017. Made in collaboration with Sarah Goldberg and Roee Amit (Technion) with elements in collaboration with Nicola Fawcett (University of Oxford). Digital image courtesy of Anna Dumitriu.

EMERGING INFECTIOUS DISEASES®
January 2019

Research Letters

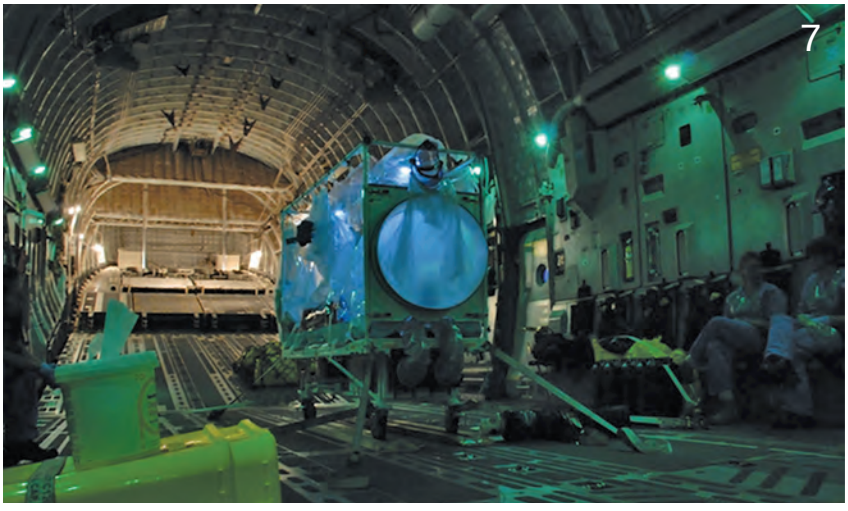

Books and Media

In Memoriam

About the Cover

Etymologia

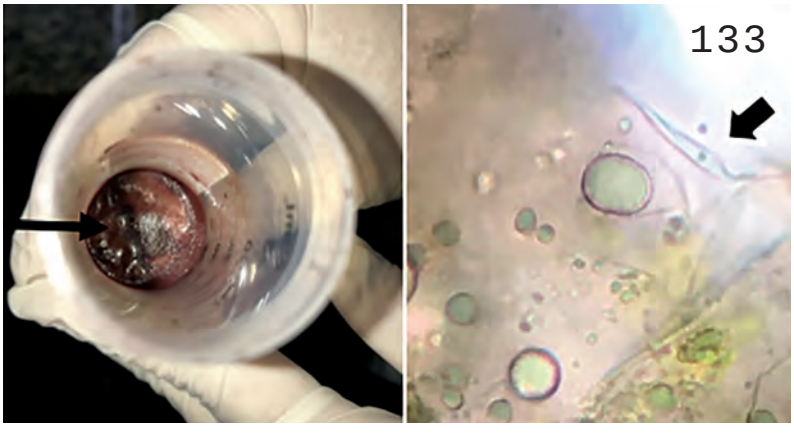

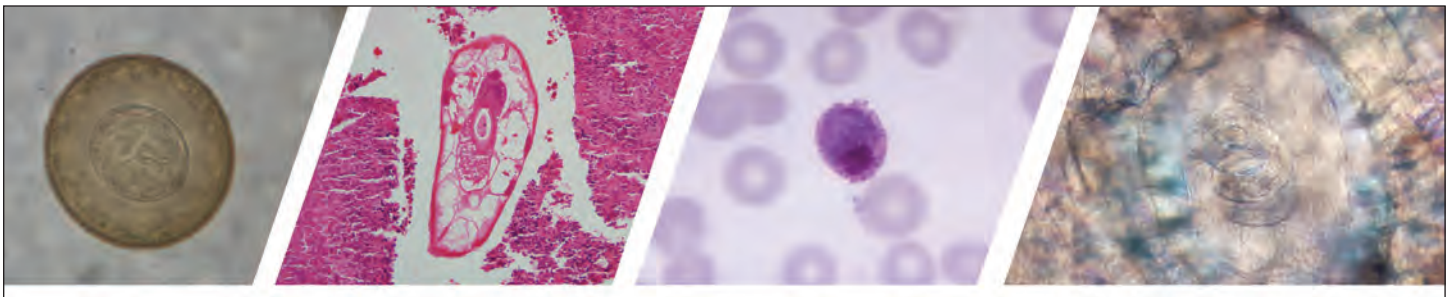

DPDx

Diagnostic Assistance and Training in Laboratory Identification of Parasites

A free service of CDC available to laboratorians, pathologists, and other health professionals in the United States and abroad

- Diagnosis from photographs of worms, histological sections, fecal, blood, and other specimen types
- Expert diagnostic review
- Formal diagnostic laboratory report
- Submission of samples via secure file share

Visit the DPDx website for information on laboratory diagnosis, geographic distribution, clinical features, parasite life cycles, and training via Monthly Case Studies of parasitic diseases.

www.cdc.gov/dpdx
dpdx@cdc.gov

U.S. Department of Health and Human Services
Centers for Disease Control and Prevention

CS272346-DE

Complexity of the Basic Reproduction Number (R_0)

Paul L. Delamater, Erica J. Street, Timothy F. Leslie, Y. Tony Yang, Kathryn H. Jacobsen

The basic reproduction number (R_0), also called the basic reproduction ratio or rate or the basic reproductive rate, is an epidemiologic metric used to describe the contagiousness or transmissibility of infectious agents. R_0 is affected by numerous biological, sociobehavioral, and environmental factors that govern pathogen transmission and, therefore, is usually estimated with various types of complex mathematical models, which make R_0 easily misrepresented, misinterpreted, and misapplied. R_0 is not a biological constant for a pathogen, a rate over time, or a measure of disease severity, and R_0 cannot be modified through vaccination campaigns. R_0 is rarely measured directly, and modeled R_0 values are dependent on model structures and assumptions. Some R_0 values reported in the scientific literature are likely obsolete. R_0 must be estimated, reported, and applied with great caution because this basic metric is far from simple.

The basic reproduction number (R_0), pronounced "R naught," is intended to be an indicator of the contagiousness or transmissibility of infectious and parasitic agents. R_0 is often encountered in the epidemiology and public health literature and can also be found in the popular press (*1–6*). R_0 has been described as being one of the fundamental and most often used metrics for the study of infectious disease dynamics (*7–12*). An R_0 for an infectious disease event is generally reported as a single numeric value or low–high range, and the interpretation is typically presented as straightforward; an outbreak is expected to continue if R_0 has a value >1 and to end if R_0 is <1 (*13*). The potential size of an outbreak or epidemic often is based on the magnitude of the R_0 value for that event (*10*), and R_0 can be used to estimate the proportion of the population that must be vaccinated to eliminate an infection from that population (*14,15*). R_0 values have been published for measles, polio, influenza, Ebola virus disease, HIV disease, a diversity of vectorborne infectious diseases, and many other communicable diseases (*14,16–18*).

Affiliations: University of North Carolina at Chapel Hill, Chapel Hill, North Carolina, USA (P.L. Delamater); George Mason University, Fairfax, Virginia, USA (E.J. Street, T.F. Leslie, K.H. Jacobsen); George Washington University, Washington, DC, USA (Y.T. Yang)

DOI: https://doi.org/10.3201/eid2501.171901

The concept of R_0 was first introduced in the field of demography (*9*), where this metric was used to count offspring. When R_0 was adopted for use by epidemiologists, the objects being counted were infective cases (*19*). Numerous definitions for R_0 have been proposed. Although the basic conceptual framework is similar for each, the operational definitions are not always identical. Dietz states that R_0 is "the number of secondary cases one case would produce in a completely susceptible population" (*19*). Fine supplements this definition with the description "average number of secondary cases" (*17*). Diekmann and colleagues use the description "expected number of secondary cases" and provide additional specificity to the terminology regarding a single case (*13*).

In the hands of experts, R_0 can be a valuable concept. However, the process of defining, calculating, interpreting, and applying R_0 is far from straightforward. The simplicity of an R_0 value and its corresponding interpretation in relation to infectious disease dynamics masks the complicated nature of this metric. Although R_0 is a biological reality, this value is usually estimated with complex mathematical models developed using various sets of assumptions. The interpretation of R_0 estimates derived from different models requires an understanding of the models' structures, inputs, and interactions. Because many researchers using R_0 have not been trained in sophisticated mathematical techniques, R_0 is easily subject to misrepresentation, misinterpretation, and misapplication. Notable examples include incorrectly defining R_0 (*1*) and misinterpreting the effects of vaccination on R_0 (*3*). Further, many past lessons regarding this metric appear to have been lost or overlooked over time. Therefore, a review of the concept of R_0 is needed, given the increased attention this metric receives in the academic literature (*20*). In this article, we address misconceptions about R_0 that have proliferated as this metric has become more frequently used outside of the realm of mathematical biology and theoretic epidemiology, and we recommend that R_0 be applied and discussed with caution.

Variations in R_0

For any given infectious agent, the scientific literature might present numerous different R_0 values. Estimations of the R_0 value are often calculated as a function of 3 primary parameters—the duration of contagiousness after a person becomes infected, the likelihood of infection per contact between a susceptible person and an infectious person or

vector, and the contact rate—along with additional parameters that can be added to describe more complex cycles of transmission (*19*). Further, the epidemiologic triad (agent, host, and environmental factors) sometimes provides inspiration for adding parameters related to the availability of public health resources, the policy environment, various aspects of the built environment, and other factors that influence transmission dynamics and, thus, are relevant for the estimation of R_0 values (*21*). Yet, even if the infectiousness of a pathogen (that is, the likelihood of infection occurring after an effective contact event has occurred) and the duration of contagiousness are biological constants, R_0 will fluctuate if the rate of human–human or human–vector interactions varies over time or space. Limited evidence supports the applicability of R_0 outside the region where the value was calculated (*20*). Any factor having the potential to influence the contact rate, including population density (e.g., rural vs. urban), social organization (e.g., integrated vs. segregated), and seasonality (e.g., wet vs. rainy season for vectorborne infections), will ultimately affect R_0. Because R_0 is a function of the effective contact rate, the value of R_0 is a function of human social behavior and organization, as well as the innate biological characteristics of particular pathogens. More than 20 different R_0 values (range 5.4–18) were reported for measles in a variety of study areas and periods (*22*), and a review in 2017 identified feasible measles R_0 values of 3.7–203.3 (*23*). This wide range highlights the potential variability in the value of R_0 for an infectious disease event on the basis of local sociobehavioral and environmental circumstances.

Various Names for R_0

Inconsistency in the name and definition of R_0 has potentially been a cause for misunderstanding the meaning of R_0. R_0 was originally called the basic case reproduction rate when George MacDonald introduced the concept into the epidemiology literature in the 1950s (*17*,*19*,*24*,*25*). Although MacDonald used Z_0 to represent the metric, the current symbolic representation (R_0) appears to have remained largely consistent since that time. However, multiple variations of the name for the concept expressed by R_0 have been used in the scientific literature, including the use of basic and case as the first word in the term, reproduction and reproductive for the second word, and number, ratio, and rate for the final part of the term (*13*). Although the frequent use of the term basic reproduction rate is in line with MacDonald's original terminology (*9*), some users interpret the use of the word rate as suggesting a quantity having a unit with a per-time dimension (*7*). If R_0 were a rate involving time, the metric would provide information about how quickly an epidemic will spread through a population. But R_0 does not indicate whether new cases will occur within 24 hours after the initial case or months later, just as R_0 does not indicate whether the disease produced by the infection is severe. Instead, R_0 is most accurately described in terms of cases per case (*7*,*13*). Calling R_0 a rate rather than a number or ratio might create some undue confusion about what the value represents.

R_0 and Vaccination Campaigns

Vaccination campaigns reduce the proportion of a population at risk for infection and have proven to be highly effective in mitigating future outbreaks (*26*). This conclusion is sometimes used to suggest that an aim of vaccination campaigns is to remove susceptible members of the population to reduce the R_0 for the event to <1. Although the removal of susceptible members from the population will affect infection transmission by reducing the number of effective contacts between infectious and susceptible persons, this activity will technically not reduce the R_0 value because the definition of R_0 includes the assumption of a completely susceptible population. When examining the effect of vaccination, the more appropriate metric to use is the effective reproduction number (R), which is similar to R_0 but does not assume complete susceptibility of the population and, therefore, can be estimated with populations having immune members (*16*,*20*,*27*). Efforts aimed at reducing the number of susceptible persons within a population through vaccination would result in a reduction of the R value, rather than R_0 value. In this scenario, vaccination could potentially end an epidemic, if R can be reduced to a value <1 (*16*,*27*,*28*). The effective reproduction number can also be specified at a particular time t, presented as $R(t)$ or R_t, which can be used to trace changes in R as the number of susceptible members in a population is reduced (*29*,*30*). When the goal is to measure the effectiveness of vaccination campaigns or other public health interventions, R_0 is not necessarily the best metric (*10*,*20*).

Measuring and Estimating R_0

Counting the number of cases of infection during an epidemic can be extremely difficult, even when public health officials use active surveillance and contact tracing to attempt to locate all infected persons. Although measuring the true R_0 value is possible during an outbreak of a newly emerging infectious pathogen that is spreading through a wholly susceptible population, rarely are there sufficient data collection systems in place to capture the early stages of an outbreak when R_0 might be measured most accurately. As a result, R_0 is nearly always estimated retrospectively from seroepidemiologic data or by using theoretical mathematical models (*31*). Data-driven approaches include the use of the number of susceptible persons at endemic equilibrium, average age at infection, final size equation, and intrinsic growth rate (*10*). When mathematical models are used, R_0 values are often estimated by using ordinary differential equations (*8–10*,*19*,*31*), but high-quality data

are rarely available for all components of the model. The estimated values of R_0 generated by mathematical models are dependent on numerous decisions made by the modeler (*8*,*32*,*33*). The population structure of the model, such as the susceptible-infectious-recovered model or susceptible-exposed-infectious-recovered model, which includes compartments for persons who are exposed but not yet infectious, as well as assumptions about demographic dynamics (e.g., births, deaths, and migration over time), are critical model parameters. Population mixing and contact patterns must also be considered; for example, for homogeneous mixing, all population members are equally likely to come into contact with one another, and for heterogeneous mixing, variation in contact patterns are present among age subgroups or geographic regions. Other decisions include whether to use a deterministic (yielding the same outcomes each time the model is run) or stochastic (generating a distribution of likely outcomes on the basis of variations in the inputs) approach and which distributions (e.g., Gaussian or uniform distributions) to use to describe the probable values of parameters, such as effective contact rates and duration of contagiousness. Furthermore, many of the parameters included in the models used to estimate R_0 are merely educated guesses; the true values are often unknown or difficult or impossible to measure directly (*31*,*34*,*35*). This limitation is compounded as models become more complex and, thus, require more input parameters (*20*,*35*), such as when using models to estimate the value of R_0 for infectious pathogens with more complex transmission pathways, which can include vectorborne infectious agents or those with environmental or wildlife reservoirs. In summary, although only 1 true R_0 value exists for an infectious disease event occurring in a particular place at a particular time, models that have minor differences in structure and assumptions might produce different estimates of that value, even when using the same epidemiologic data as inputs (*20*,*31*,*32*,*36*,*37*).

Obsolete R_0 Values

New estimates of R_0 have been produced for infectious disease events that occurred in recent history, such as the West Africa Ebola outbreak (*34*,*38*,*39*). However, for many vaccine-preventable diseases, the scientific literature reports R_0 values calculated much further back in history. For example, the oft-reported measles R_0 values of 12–18 are based on data acquired during 1912–1928 in the United States (R_0 of 12.5) and 1944–1979 in England and Wales (R_0 of 13.7–18.0) (*14*), even though more recent estimates of the R_0 for measles highlight a much greater numeric range and variation across settings (*23*). For pertussis (R_0 of 12–17), the original data sources are 1908–1917 in the United States (R_0 of 12.2) and 1944–1979 in England and Wales (R_0 of 14.3–17.1) (*14*). The major changes that have occurred in how humans organize themselves both socially and geographically make these historic values extremely unlikely to match present day epidemiologic realities. Behavioral changes undoubtedly have altered contact rates, which are a key component of R_0 calculations. Yet, these R_0 values have been repeated so often in the literature that newer R_0 values generated by using modern data might be dismissed if they fall outside the range of previous estimates. Given that R_0 is often considered when designing and implementing vaccination strategies and other public health interventions, the use of R_0 values derived from older data is likely inappropriate (*23*). Decisions about public health practice should be made with contemporaneous R_0 values or *R* values instead.

Conclusions

Although R_0 might appear to be a simple measure that can be used to determine infectious disease transmission dynamics and the threats that new outbreaks pose to the public health, the definition, calculation, and interpretation of R_0 are anything but simple. R_0 remains a valuable epidemiologic concept, but the expanded use of R_0 in both the scientific literature and the popular press appears to have enabled some misunderstandings to propagate. R_0 is an estimate of contagiousness that is a function of human behavior and biological characteristics of pathogens. R_0 is not a measure of the severity of an infectious disease or the rapidity of a pathogen's spread through a population. R_0 values are nearly always estimated from mathematical models, and the estimated values are dependent on numerous decisions made in the modeling process. The contagiousness of different historic, emerging, and reemerging infectious agents cannot be fairly compared without recalculating R_0 with the same modeling assumptions. Some of the R_0 values commonly reported in the literature for past epidemics might not be valid for outbreaks of the same infectious disease today.

R_0 can be misrepresented, misinterpreted, and misapplied in a variety of ways that distort the metric's true meaning and value. Because of these various sources of confusion, R_0 must be applied and discussed with caution in research and practice. This epidemiologic construct will only remain valuable and relevant when used and interpreted correctly.

This research was supported through a grant from the George Mason University Provost Multidisciplinary Research Initiative.

About the Author

Dr. Delamater is an assistant professor in the Department of Geography and a faculty fellow at the Carolina Population Center at the University of North Carolina at Chapel Hill, Chapel Hill, North Carolina, USA. His research focuses on the geographic aspects of health, disease, and healthcare.

References

1. Johnson R. The 10 epidemics that almost wiped out mankind. Business Insider. 2011 Sep 19 [cited 2017 Nov 17]. http://www.businessinsider.com/epidemics-pandemics-that-almost-wiped-out-mankind-2011-9
2. Coy P. A primer on the deadly math of Ebola. Bloomberg Business-week. 2014 Sep 26 [cited 2017 Nov 17]. http://www.bloomberg.com/news/articles/2014-09-26/ebolas-deadly-math
3. Doucleff M. No, seriously, how contagious is Ebola? NPR. 2014 Oct 2 [cited 2017 Nov 17]. http://www.npr.org/sections/health-shots/2014/10/02/352983774/no-seriously-how-contagious-is-ebola
4. Freeman C. Magic formula that will determine whether Ebola is beaten. Telegraph. 2014 Nov 6 [cited 2017 Nov 17]. http://www.telegraph.co.uk/news/worldnews/ebola/11213280/Magic-formula-that-will-determine-whether-Ebola-is-beaten.html
5. McKenna M. The mathematics of Ebola trigger stark warnings: act now or regret it. WIRED. 2014 Sep 14 [cited 2017 Nov 17]. https://www.wired.com/2014/09/r0-ebola/
6. Fox M. Ebola epidemic was driven by just a few infected people, study finds. NBC News. 2017 Feb 13 [cited 2017 Nov 17]. https://www.nbcnews.com/storyline/ebola-virus-outbreak/superspreaders-drove-ebola-epidemic-study-finds-n720321
7. Heesterbeek JAP, Dietz K. The concept of R_0 in epidemic theory. Stat Neerl. 1996;50:89–110. http://dx.doi.org/10.1111/j.1467-9574.1996.tb01482.x
8. Keeling MJ, Grenfell BT. Individual-based perspectives on R_0. J Theor Biol. 2000;203:51–61. http://dx.doi.org/10.1006/jtbi.1999.1064
9. Heesterbeek JAP. A brief history of R_0 and a recipe for its calculation. Acta Biotheor. 2002;50:189–204. http://dx.doi.org/10.1023/A:1016599411804
10. Heffernan JM, Smith RJ, Wahl LM. Perspectives on the basic reproductive ratio. J R Soc Interface. 2005;2:281–93. http://dx.doi.org/10.1098/rsif.2005.0042
11. Roberts MG. The pluses and minuses of R_0. J R Soc Interface. 2007;4:949–61. http://dx.doi.org/10.1098/rsif.2007.1031
12. Pellis L, Ball F, Trapman P. Reproduction numbers for epidemic models with households and other social structures. I. Definition and calculation of R_0. Math Biosci. 2012;235:85–97. http://dx.doi.org/10.1016/j.mbs.2011.10.009
13. Diekmann O, Heesterbeek JAP, Metz JAJ. On the definition and the computation of the basic reproduction ratio R_0 in models for infectious diseases in heterogeneous populations. J Math Biol. 1990;28:365–82. http://dx.doi.org/10.1007/BF00178324
14. Anderson RM, May RM. Directly transmitted infections diseases: control by vaccination. Science. 1982;215:1053–60. http://dx.doi.org/10.1126/science.7063839
15. Anderson RM, May RM. Vaccination and herd immunity to infectious diseases. Nature. 1985;318:323–9. http://dx.doi.org/10.1038/318323a0
16. Anderson RM, May RM. Infectious diseases of humans: dynamics and control. Oxford: Oxford University Press; 1991.
17. Fine PEM. Herd immunity: history, theory, practice. Epidemiol Rev. 1993;15:265–302. http://dx.doi.org/10.1093/oxfordjournals.epirev.a036121
18. Chowell G, Nishiura H. Transmission dynamics and control of Ebola virus disease (EVD): a review. BMC Med. 2014;12:196. http://dx.doi.org/10.1186/s12916-014-0196-0
19. Dietz K. The estimation of the basic reproduction number for infectious diseases. Stat Methods Med Res. 1993;2:23–41. http://dx.doi.org/10.1177/096228029300200103
20. Ridenhour B, Kowalik JM, Shay DK. Unraveling R_0: considerations for public health applications. Am J Public Health. 2014;104:e32–41. http://dx.doi.org/10.2105/AJPH.2013.301704
21. Lloyd-Smith JO, Schreiber SJ, Kopp PE, Getz WM. Superspreading and the effect of individual variation on disease emergence. Nature. 2005;438:355–9. http://dx.doi.org/10.1038/nature04153
22. Anderson RM. Directly transmitted viral and bacterial infections of man. In: Anderson RM, editor. The population dynamics of infectious diseases: theory and applications. London: Chapman and Hall; 1982. p. 1–37.
23. Guerra FM, Bolotin S, Lim G, Heffernan J, Deeks SL, Li Y, et al. The basic reproduction number (R_0) of measles: a systematic review. Lancet Infect Dis. 2017;17:e420–8. http://dx.doi.org/10.1016/S1473-3099(17)30307-9
24. MacDonald G. The analysis of equilibrium in malaria. Trop Dis Bull. 1952;49:813–29.
25. MacDonald G. The epidemiology and control of malaria. London: Oxford University Press; 1957.
26. Bärnighausen T, Bloom DE, Cafiero-Fonseca ET, O'Brien JC. Valuing vaccination. Proc Natl Acad Sci U S A. 2014;111:12313–9. http://dx.doi.org/10.1073/pnas.1400475111
27. Anderson RM. The concept of herd immunity and the design of community-based immunization programmes. Vaccine. 1992;10:928–35. http://dx.doi.org/10.1016/0264-410X(92)90327-G
28. Plans Rubió P. Is the basic reproductive number (R0) for measles viruses observed in recent outbreaks lower than in the pre-vaccination era? Euro Surveill. 2012;17:22. http://dx.doi.org/10.2807/ese.17.31.20233-en
29. Nishiura H, Chowell G. The effective reproduction number as a prelude to statistical estimation of time-dependent epidemic trends. In: Chowell G, Hyman JM, Bettencourt LMA, Castillo-Chavez C, editors. Mathematical and statistical estimation approaches in epidemiology. Dordrecht (the Netherlands): Springer Netherlands; 2009. p. 103–21.
30. Mercer GN, Glass K, Becker NG. Effective reproduction numbers are commonly overestimated early in a disease outbreak. Stat Med. 2011;30:984–94.
31. Li J, Blakeley D, Smith RJ. The failure of R0. Comput Math Methods Med. 2011;2011:527610. http://dx.doi.org/10.1155/2011/527610
32. Breban R, Vardavas R, Blower S. Theory versus data: how to calculate R_0? PLoS One. 2007;2:e282. http://dx.doi.org/10.1371/journal.pone.0000282
33. Artalejo JR, Lopez-Herrero MJ. On the exact measure of disease spread in stochastic epidemic models. Bull Math Biol. 2013;75:1031–50. http://dx.doi.org/10.1007/s11538-013-9836-3
34. Khan A, Naveed M, Dur-E-Ahmad M, Imran M. Estimating the basic reproductive ratio for the Ebola outbreak in Liberia and Sierra Leone. Infect Dis Poverty. 2015;4:13. http://dx.doi.org/10.1186/s40249-015-0043-3
35. Roberts M, Heesterbeek H. Bluff your way in epidemic models. Trends Microbiol. 1993;1:343–8. http://dx.doi.org/10.1016/0966-842X(93)90075-3
36. Bani-Yaghoub M, Gautam R, Shuai Z, van den Driessche P, Ivanek R. Reproduction numbers for infections with free-living pathogens growing in the environment. J Biol Dyn. 2012;6:923–40. http://dx.doi.org/10.1080/17513758.2012.693206
37. Nishiura H. Correcting the actual reproduction number: a simple method to estimate R_0 from early epidemic growth data. Int J Environ Res Public Health. 2010;7:291–302. http://dx.doi.org/10.3390/ijerph7010291
38. Legrand J, Grais RF, Boelle PY, Valleron AJ, Flahault A. Understanding the dynamics of Ebola epidemics. Epidemiol Infect. 2007;135:610–21. http://dx.doi.org/10.1017/S0950268806007217
39. Fisman D, Khoo E, Tuite A. Early epidemic dynamics of the West African 2014 Ebola outbreak: estimates derived with a simple two-parameter model. PLoS Curr. 2014;6:ecurrents.outbreaks.89c0d3783f36958d96ebbae97348d571. https://doi.org/10.1371/currents.outbreaks.89c0d3783f36958d96ebbae97348d571

Address for correspondence: Paul L. Delamater, University of North Carolina at Chapel Hill, Campus Box 3220, Chapel Hill, NC 27599-3220, USA; email: pld@email.unc.edu

Aeromedical Transfer of Patients with Viral Hemorrhagic Fever

Edward D. Nicol, Stephen Mepham, Jonathan Naylor, Ian Mollan, Matthew Adam, Joanna d'Arcy, Philip Gillen, Emma Vincent, Belinda Mollan, David Mulvaney, Andrew Green, Michael Jacobs

For ≥40 years, the British Royal Air Force has maintained an aeromedical evacuation facility, the Deployable Air Isolator Team (DAIT), to transport patients with possible or confirmed highly infectious diseases to the United Kingdom. Since 2012, the DAIT, a joint Department of Health and Ministry of Defence asset, has successfully transferred 1 case-patient with Crimean-Congo hemorrhagic fever, 5 case-patients with Ebola virus disease, and 5 case-patients with high-risk Ebola virus exposure. Currently, no UK-published guidelines exist on how to transfer such patients. Here we describe the DAIT procedures from collection at point of illness or exposure to delivery into a dedicated specialist center. We provide illustrations of the challenges faced and, where appropriate, the enhancements made to the process over time.

In the 1970s, the British Royal Air Force (RAF) was tasked with developing a portable isolation facility that could retrieve patients with infectious diseases. The original Vickers Isolator was manufactured at RAF Lyneham in 1982 and first used in 1985 (*1*). The Trexler Air Transport Isolator (T-ATI) system has since undergone modifications and improvements. Separate T-ATIs are owned by the Ministry of Defence (MOD) and the Department of Health, and both capabilities are operated by a dedicated MOD team that includes the medical operations directorate, the RAF Aeromedical Evacuation Coordination Cell (AECC), and the Deployable Air Isolator Team (DAIT). Civilian and military colleagues have trained and deployed together since 1996. Since 2012, this team has successfully transferred 1 patient with advanced Crimean-Congo hemorrhagic fever (*2*) and 5 patients with Ebola virus disease (EVD) (*3*–*5*), 2 with recrudescence or late neurologic complications (*6*,*7*). In addition, 5 patients with Ebola exposures, including 2 high-risk and 2 intermediate-risk exposures, have been transferred (*4*,*8*–*10*) (Table 1).

In the United Kingdom, 2 high-level isolation units (HLIU) are primarily responsible for the care of patients with viral hemorrhagic fevers (VHFs): the Royal Free Hospital, London, and the Royal Victoria Infirmary, Newcastle. Both units use the Trexler patient isolator, in which patient care is provided within an isolation tent. End-to-end maximal patient containment from overseas to the receiving hospital and subsequent discharge is achieved through the T-ATI (Figure 1), which is designed to interface with the Trexler isolator. The T-ATI is transported on a suitable aircraft and from the airhead using a dedicated ambulance, the Jumbulance (Figure 2).

Aeromedical Evacuation of Patients with High-Consequence Infectious Disease

The UK T-ATI

There are 2 basic designs of Air Transport Isolator systems, closed and open, both of which offer maximum containment of highly infectious biologic agents. Open systems provide a portable isolation facility large enough for both the patient and attending medical staff wearing personal protective equipment (PPE), whereas closed systems separate the patient from attending physicians (*11*). Several commercially available closed isolation systems have been developed from chemical, biologic, radiologic, and nuclear biodefense funding streams. These are stretcher isolators (S-ATI) designed to manage patients exposed to infectious agents, as opposed to patients with symptoms of infectious diseases. Because S-ATI are small, their capability to support the transfer of sick patients is limited. The United Kingdom uses a larger closed T-ATI system for the transfer of infected patients (Figure 1), a design that provides patient comfort and medical care while maintaining containment for the duration of the transfer mission. These systems have been used on Lockheed Martin C-130 and Boeing C-17 Globemaster (Figures 3,4) aircraft, enabling rapid delivery of the T-ATI and clinical team to both standard and austere landing strips at great distance from the United Kingdom.

Author affiliations: Royal Air Force Brize Norton, Oxfordshire, UK (E.D. Nicol, J. Naylor, I. Mollan, M. Adam, J. d'Arcy, P. Gillen, E. Vincent, B. Mollan, D. Mulvaney); Royal Air Force Henlow, Bedfordshire, UK (E.D. Nicol, J. Naylor, I. Mollan, J. d'Arcy); Royal Free London NHS Foundation Trust, London, UK (S. Mepham, M. Adam, M. Jacobs); Level 2 Queen Elizabeth Hospital Birmingham, Birmingham, UK (A. Green)

DOI: https://doi.org/10.3201/eid2501.180662

Table 1. Aeromedical transfers of patients with confirmed and exposed viral hemorrhagic fever to the United Kingdom, 2012–2016*

Mission	Date	Infection	Origin	Patient signs/symptoms (stable/unstable)	Isolator type	Aircraft	Patient outcome
1	2012 Oct 4	CCHF	Afghanistan† (*1*)	Blood, diarrhea (unstable)	T-ATI	Lockheed C-130 Hercules	Died
2	2014 Aug 23	EVD	Sierra Leone (*4*)	None (stable)	T-ATI	Boeing C-17	Survived
3	2014 Dec 29	EVD	Sierra Leone† (*2*)	None (stable)	T-ATI	Lockheed C-130 Hercules	Survived
4	2015 Jan 29	Ebola exposure	Sierra Leone (*10*)	None	SI	Boeing C-17	Survived
5	2015 Jan 31	Ebola exposure	Sierra Leone (*10*)	None	SI	Boeing C-17	Survived
6	2015 Mar 13	EVD	Sierra Leone (*3*)	Diarrhea (stable)	T-ATI	Boeing C-17	Survived
		Ebola exposure	Sierra Leone (*10*)	None	SI		Survived
		Ebola exposure	Sierra Leone (*10*)	None	SI		Survived
7	2015 Mar 11	Ebola exposure	Sierra Leone (*10*)	None	SI	Boeing C-17	Survived
8	2015 Oct 9	EVD	United Kingdom (*5*)	Meningitis	T-ATI	Boeing C-17	Survived
9	2016 Mar 22	EVD	United Kingdom (*6*)	Late neurologic complications	T-ATI	Lockheed C-130 Hercules	Survived

*CCHF, Crimean-Congo hemorrhagic fever; EVD, Ebola virus disease; SI, stretcher isolator; T-ATI, Trexler Air Transport Isolator; UK, United Kingdom.
†Aeromedical transfer originated within the United Kingdom.

The sealed T-ATI system includes an ATI frame and disposable envelope. It is maintained under negative pressure by a HEPA-filtered ventilation system that uses aircraft power when emplaned and battery power when outside the aircraft, while the cabin pressure is maintained at a standard cabin altitude of 8,000 feet. Clinically, this system maintains the arterial oxygen hemoglobin saturation at ≈90% in healthy patients, even inside the negative-pressure envelope. Additional oxygenation is possible through the use of portable oxygen cylinders and tubing passed into the envelope through sealed delivery ports. Cables for monitoring equipment, such as electrocardiogram electrodes, pulse oximeters, and blood pressure sensors, also pass through the ports, as does tubing for parenteral fluids or medication.

Clinical access consists of a half-suit on either side of the T-ATI; an additional half-suit can be fitted to permit access to the head and neck of the patient for intubation, if required (Figure 5). Arm and glove ports along the side of isolator enable multiple staff to access the patient simultaneously (Figure 1). At the foot of the envelope are 2 clinical waste disposal areas. Medical equipment likely to be needed for the management of the patient during the flight, such as intubation equipment, bag-valve mask, suction units, and intravenous access equipment, must be placed within the envelope before sealing the unit.

Logistical challenges overseas make moving the ATI away from the aircraft impractical, so the patient is usually

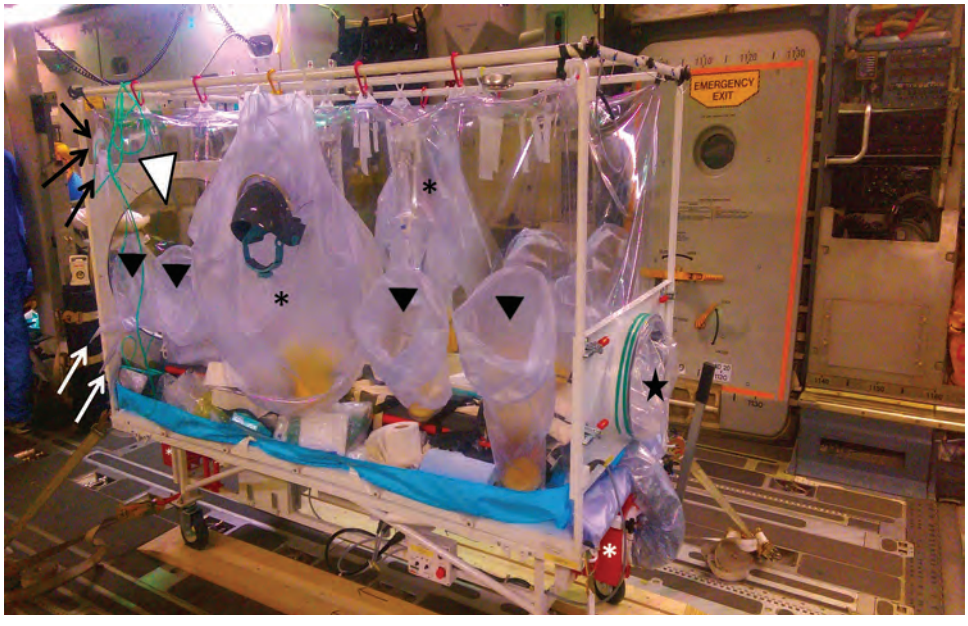

Figure 1. The Trexler Air Transport Isolator, a portable isolation facility used to transfer patients with serious infectious diseases. The sealed system is maintained under negative pressure by a HEPA-filtered ventilation system (red boxes, marked with white asterisk). Portable oxygen cylinders and tubing passed into the envelope through sealed delivery ports (black arrows) permit additional oxygenation of the patient. Additional ports allow cables for monitoring equipment and tubing for parenteral fluids or medication (white arrows). A half-suit on either side of the isolator (black asterisk) enables healthcare workers' clinical access to the patient, and an additional half-suit can be fitted to the head of the patient for intubation (white arrowhead). Additional arm and glove ports along the side (black arrowheads) allow multiple workers to access the patient simultaneously. Two larger-bore disposable waste areas are available at the foot of the envelope (black star).

Figure 2. Dedicated road transport that can accommodate the Air Transport Isolator patient transport system, such as the Jumbulance shown enables seamless end-to-end transfer from patient pickup to the destination facility.

moved to the airhead using appropriate and proportional infection prevention control (IPC) measures tailored to the location (*12*). Aeromedical personnel, who are fully trained in the use of PPE and decontamination, assist the patient into the T-ATI before boarding. Once the T-ATI is sealed, the patient's care does not require staff PPE. Upon the aircraft's return to the United Kingdom, a dedicated T-ATI Jumbulance is positioned at the receiving airbase to transport the T-ATI and to minimize the risk for external contamination.

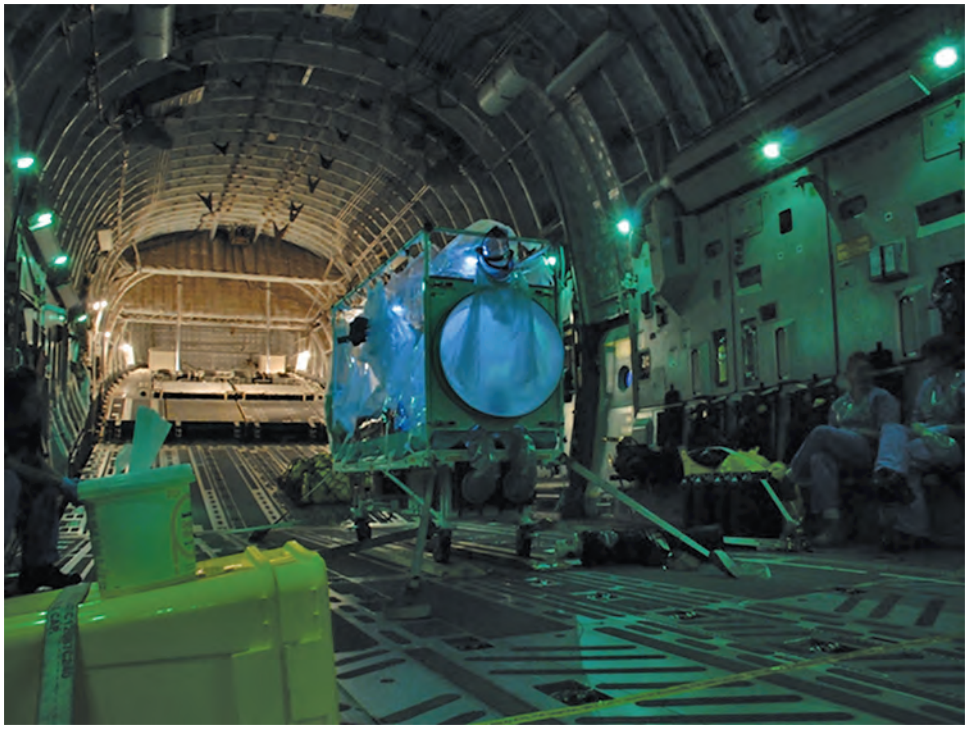

Figure 3. A single Trexler Air Transport Isolator patient transport system ready for use on a Boeing C-17 Globemaster transport aircraft.

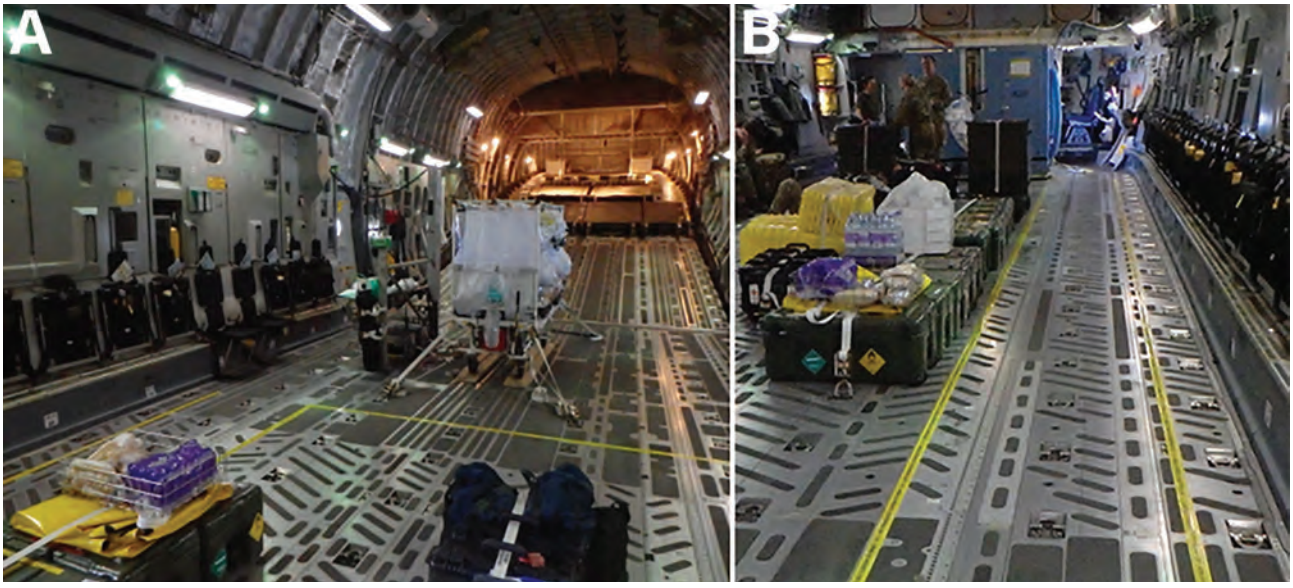

Figure 4. Demarcation of clean and dirty zones during use of the Trexler Air Transport Isolator patient transport system on a Boeing C-17 Globemaster transport aircraft. A) Yellow lines clearly demarcate clean and dirty zones as required for transporting both confirmed and exposed viral hemorrhagic fever case-patients. B) For exposed patients, the demarcation zone should extend to a corridor leading to isolated toileting and comfort facilities.

Guidance on the Air Transfer of VHF

Before 2014, UK guidance focused on the public health response to inadvertent importation of cases of VHF on domestic aircraft (*13*); some US guidance existed on the use of closed isolator procedures (*14*). In response to the 2014–2016 Ebola crisis in West Africa, the US Centers for Disease Control and Prevention (*15*), Canadian Critical Care Society (CCCS) (*16*), and European Centre for Disease Prevention and Control (*11*) have published patient transport guidelines. As the sole UK provider of air transfer of highly infectious patients, the MOD has extensive standard operating procedures for the retrieval of both civilian and military patients with EVD. In 2014, the United States, through license with Phoenix Air (*17*), developed an open system with VHF capability and now has 2 options for transporting highly contagious patients: in single-patient isolator units that are similar to the T-ATI (the Phoenix Air Airborne Biologic Containment System [*18*]) or in fully contained medical transport units (developed by MRIGlobal, with support from the US Department of State and the Paul G. Allen Ebola Program [*19*]).

Case Referral

The decision to evacuate patients with highly infectious diseases from their point of infection or diagnosis to the United Kingdom is a complex process that considers the clinical, public health, and political contexts. The clinical decision is made between the clinical lead in-country, the on-call HLIU physician at the Royal Free Hospital, and the on-call RAF medical consultant, with additional advice from the RAF public health lead as required. The flight details are planned in conjunction with AECC.

The initial call to the United Kingdom referring confirmed or suspected VHF cases or a high-risk exposure is taken by either the National Health Service England Emergency Preparedness Resilience and Response Duty Officer, the RAF, or the HLIU, Royal Free Hospital (London, UK). The transfer is coordinated by National Health Service England Emergency Preparedness Resilience and Response and approved and enabled through Cabinet Office Briefing Room meetings and Ministers of State. Once approved there is a cross-governmental process to coordinate local and national UK government, the receiving HLIU, MOD Med Ops, and RAF AECC staff.

DAIT Activation

Ultimately, the transfer of a patient is authorized only if it is deemed in the best interest of the patient, after which AECC activates the DAIT. After receiving the order to deploy, the DAIT personnel convene at RAF Brize Norton (Oxfordshire, UK) to plan and execute the mission, and communicate with receiving hospitals, specialist ambulance services, police and security services, government agencies, ministerial offices, and multiple agencies involved in flight planning and diplomatic clearances (*20*). For T-ATI transfers, the Jumbulance is prepositioned to the receiving airfield to enable a seamless, contained transfer of the patient within the T-ATI by road from the aircraft to the receiving hospital. The length of the mission, from start to the return of the aircraft, is often >24 hours.

Figure 5. Larger Trexler Air Transport Isolator patient transport systems enable care providers to access a patient via half-suits along the side of the patient; however, manual dexterity is severely impaired.

For asymptomatic exposure cases in which isolation of the source patient is not deemed necessary at the outset, a T-ATI is brought aboard to ensure immediate appropriate isolation if symptoms develop in flight. The DAIT is responsible for the planning, preparation, and conduct of the clinical aeromedical recovery, from the point of origin to the destination hospital, in a manner that protects the aircrew, aeromedical staff, and local populations while providing high-quality clinical care to the patient. For flights that require overflying other nations, the DAIT routinely seeks diplomatic clearance. In the cases we described, either there was no requirement for clearance (over-sea flight route to Sierra Leone) or the flight was within UK airspace.

The DAIT is continuously available, held at a high level of readiness, with DAIT staff on call for a month at a time on average every 3 months. At times of high operational demand, the call period may be longer or the frequency of service higher. When on call, DAIT staff convene for monthly PPE/T-ATI training and refresher training, reinforcing the team ethos required for these arduous and emotive missions and ensures skill retention.

UK DAIT Team Composition

The team composition is tailored to the requirements of the specific mission. To move a single highly contagious patient requires 12 personnel, including IPC nurses, an RAF consultant physician and anesthetist, a civilian infectious diseases consultant from the Royal Free HLIU team, medical assistants, a medical and dental support system technician to assess and monitor T-ATI integrity, and a medical support officer, who acts as a liaison with the host nation nonclinical staff, ensures involvement of legitimate personnel only, and minimizes press access. Oversight of the whole mission is provided by a team leader/flight director who remains removed from direct clinical care and allows the clinical team to focus solely on the patient's needs without distraction. Additional staff are considered for flights involving >2 patients, depending on the clinical scenario, and the United Kingdom maintains the capability to activate 2 teams concurrently if required.

Deployment of the DAIT

Before the DAIT departs the United Kingdom, and before equipment is loaded onto the airplane, final preparations ensure that all potential in-flight needs have been addressed, and that all personnel have appropriate travel and health documentation (visas, antimalarial medication, and immunization evidence). As part of the risk assessment conducted in the United Kingdom, an advance military reconnaissance team may conduct an initial assessment with the local treatment facility staff in the country of patient origin, with respect to the patient and the clinical context. If in-country retrieval by the DAIT can be avoided, the benefits for both the DAIT and patient include minimized safety and security risks in volatile regions, time spent in PPE, and fatigue on the return flight. Alternatively, the DAIT can split into 2 parts on arrival: a reconnaissance team to assess the patient, and the main party to prepare the T-ATI, decontamination area, and aircraft.

The reconnaissance team, usually consisting of the clinical lead, civilian ID consultant, an infection control nurse, and a medic, performs the initial assessment of the patient, either at the host hospital or preferably at the airhead. Ideally, the team conducts the assessment wearing full PPE consistent with UK national guidance (*18*) for confirmed cases. However, local sensibilities need to be considered and may dictate that a more practical compromise is required while minimizing risk to medical attendants and maximizing patient safety; thus, the DAIT reconnaissance team may alter PPE only if appropriate. An example is evacuating a foreign aid worker from a facility that is the only option for local patients. The team must quickly and efficiently assess the patient's clinical and mental status for entering a T-ATI, as well as assess the potential effects of the hypobaric, hypoxic aeromedical environment, the overall safety of the transfer, and the underlying conditions on the ground. Once at the airhead, the team usually conducts a final assessment immediately before transferring the patient to the ATI.

As with any aeromedical evacuation, a full risk assessment that considers the safety of the patient, team, aircrew, and aircraft must be performed before embarkation. Whereas it might appear to be futile to cancel a mission at this stage, if the risk to transfer is deemed too high (such as in advanced disease), the flight environment deemed unwise (high risk for hypoxia or long transfer with limited available intervention), or the risk for deterioration too great, the reconnaissance team and team leader must make this judgment call. Alternatively, the team may deem a case less infectious, which requires a lower level of isolation (for example, management of exposure to contacts). The team must also consider interventions, such as cannulation or catheterization, that may be easier to perform while in PPE on the ground before boarding the plane.

Meanwhile, the main team positions the T-ATI and sets up the decontamination area for the reconnaissance team. The aircraft is set up with demarcated clean and dirty zones and, for VHF exposure cases in which the T-ATI is not deemed necessary at the outset of the flight, an identified corridor (Figure 4, panels A, B) for the patient to access a dedicated area for eating and toileting. These measures separate the patient from all but immediate clinical staff and ensure safe IPC measures in the event of clinical deterioration.

For confirmed cases, the DAIT leader coordinates the safe loading of the patient into the T-ATI and its subsequent loading onto the aircraft. This process is followed by the reconnaissance team decontamination, with assistance from trained RAF regiment staff for PPE doffing (Figure 6) and clinical waste management.

Delivery of In-Flight Care

The challenges of delivering in-flight clinical care to a patient within the T-ATI are substantial; time needed to enter the half-suits, limited visibility, reduced manual dexterity, and aircraft noise and vibration make any action beyond observations and simple intervention difficult. Drugs and parenteral fluids for hydration or to replace electrolyte abnormalities are administered through closed circuits and longer lines with larger volume flushes to minimize exposure risk and permit rapid administration from outside the isolator. In extreme cases, if a patient deteriorates, the team could consider administering drugs such as vasopressors but would need to deliver them through existing venous access (either peripheral or central). If the patient's condition includes agitation, anxiety, or confusion, the team can offer anxiolytic or sedative therapy and should be prepared to manage a potentially compromised airway. To date, most patients transferred have not been critically ill, with the exception of the Crimean-Congo hemorrhagic fever transfer from Glasgow to London in October 2012. Unless it is critical to move an unstable patient, or one who is expected to significantly deteriorate, the patient may be best served with local medical care. Nonmedical requirements, such as hydration and food, must be considered before patient isolation, and the risk from human waste can be minimized by using containers with absorbent powders or gels that solidify fluids.

Figure 6. The Deployable Air Isolator Team lead, a senior infection and prevention control nurse, is responsible for overseeing the preparation of the Air Transport Isolator patient transport system on the ground (A), the transfer of the patient into the isolator, and the safe transfer of the patient onto the aircraft by the main team while the reconnaissance team performs their decontamination drills (B).

The DAIT team members do not need to remain in full PPE once the patient is inside the isolator. Rotating the nursing team every hour on the inbound flight minimizes fatigue and ensures delivery of quality care. A death in flight is managed with standard procedures, which vary depending on the jurisdiction of the flight.

Patient Delivery in the United Kingdom

The aircraft always lands as close to the receiving hospital as possible to reduce the transfer time; close coordination between the airport staff, police, and ambulance services ensures a secure arrival process. For cases of exposure only, transfer in a standard ambulance is often appropriate without the need for PPE; for confirmed VHF cases in the T-ATI, Jumbulance transfer with a police escort minimizes delay and ensures adequate security. Coordinating arrival at the specialist center (Figure 2) permits securing and clearing the transfer route to allow smooth passage to either the patient isolator (Figure 7) in the HLIU or a negative-pressure room.

After delivery of the patient to the receiving unit, the envelope, T-ATI frame, and Jumbulance require decontamination. After the HLIU staff's thorough assessment of the envelope to determine if any breaches have occurred, the T-ATI envelope and frame are fumigated with vaporized hydrogen peroxide (*21*). The envelope is then collapsed, autoclaved, and disposed as conventional clinical waste onsite. After the removal of patient's clinical waste, DAIT and HLIU personnel decontaminate the Jumbulance. Staff then shower and don fresh scrubs. The decontamination of the Jumbulance takes a few hours, and the T-ATI frame is returned within 7 days for reuse. Twice-yearly training between the RAF and HLIU includes the review of protocols and equipment.

Aeromedical evacuations are often long, with DAIT staff working for 24–36 hours. Aircrew manage aeromedical evacuations, including those using the T-ATI, as for any other flight operation, with consideration of crew hours in accordance with standard procedure. During the 2014–2016 Ebola outbreak, a typical move to Sierra Leone would involve activating the team with a "6-hour wheels up" policy from point of activation. Within these 6 hours, the DAIT would travel to RAF Brize Norton and undertake equipment checks, aircrew would conduct flight preparation, and AECC staff would undertake ongoing communications and diplomatic clearances. The flight time to Sierra Leone was 8–10 hours each way, and crews spent up to 3 hours on the ground. After the return flight, the road transfer and handover to the receiving unit typically took 4 hours, including recovery of the DAIT to RAF Brize Norton.

Discussion

The 2014–2016 Ebola outbreak in West Africa reaffirmed the requirement for aeromedical evacuation capability (a combination of both the appropriate equipment and suitable expert personnel trained in both the management of VHF and AE) for highly infectious diseases. During 2014 and 2015, the DAIT successfully transferred 5 patients with confirmed VHF and 5 with Ebola virus exposure. Each mission provided an opportunity to refine policy and

Figure 7. Isolator–isolator transfer is the safest means of transfer for patients with serious infectious diseases and requires practice in dedicated training exercises, as shown.

procedure (Table 2), with resulting improvements to policy, training, and equipment. A larger number of T-ATIs and more efficient VHF decontamination have shortened turnaround time between transports and enabled versatility through accommodation of multiple T-ATIs and exposure cases (Figure 8). Information transfer is more robust between clinical staff at all levels and among the aircrew, logistic support teams, and senior military, civil, and political stakeholders. A clear organizational structure supports rapid decision making from the highest political level down to service delivery.

We expect this resource to continue to evolve, shaped by future collaborations. The greatest challenge that emerged after the 2014–2016 Ebola epidemic is maintaining corporate knowledge and expertise; to ensure competence and confidence managing VHF requires continuous training. Regular exercises that test not only individual staff but the whole system, with particular focus

Table 2. Limitations and challenges in Deployable Air Isolator Team missions and subsequent enhancements, United Kingdom*

Limitations and challenges	Enhancements
Mission 1: Advanced CCHF in Glasgow—400-mile transfer to HLIU London (*2*)	
UK cross-governmental communication and media interest: Identifying the correct persons within the relevant UK and Scottish government departments to authorize the substantial costs involved was challenging because the Department of Health had restructured and NHS England formed with a loss of critical contact details. The coordination of the clinical transfer, with limited clinical experience of VHF and lack of standard operating procedures, and concurrent management of the extensive media interest, was time consuming and, at times, risked distraction from patient care, particularly for the lead clinician.	• Allocation of roles out with the front-line team for liaison with and arranging authorization by governmental departments. • Addition of Liaison Officer to manage extensive media interest (*3–5,8*) and minimize intrusion on patient dignity. • RAF anesthetic consultant for support of assessment, transfer and airway management such as in the event of neurologic compromise (*2,6*). • Civilian infectious diseases expert to allow an independent critical eye to assess and modify DAIT procedures and equipment. • Review of service level agreement between Department of Health and MOD for national air transfer (only international prior provision existed). • Recognition that road transfer in standard VHF PPE (*20*) posed increased risk.
Mission 2: Decontamination	
Before 2014, the T-ATI was decontaminated using formaldehyde before it was incinerated. This relatively slow and intensive process was potentially limited by lack of access to the whole T-ATI frame and by requiring physical cleaning by humans, increasing risk to staff.	• A new vaporized hydrogen peroxide protocol has enabled much faster turnaround time and safer T-ATI decontamination (*21*).
Missions 2 and 3: Environmental effects on working in PPE	
Heat and humidity while wearing chemical-resistant Tychem F PPE suits (Figure 6) posed challenges in Sierra Leone, while steamed-up goggles and sweat-filled gloves resulted in the loss of vision and dexterity. Gusting wind made decontamination and equipment containment difficult, compounding communication difficulties due to PPE and aircraft noise. Conversely, at Glasgow International Airport, Glasgow, Scotland, UK, near-freezing temperatures were experienced during the T-ATI transfer and decontamination procedures, and the hours of darkness presented visibility problems when working in PPE.	• Subsequent mission staff numbers, previously kept low to minimize VHF exposure, were revised upward for confirmed cases, and the use of lighter Tychem B/C suits offered the same protection.
Missions 4 and 5: Needle-stick exposure	
The DAIT were deployed to Sierra Leone to assess and transport HCWs who sustained a needle-stick injury while working in an Ebola treatment center (*4,8,9*). An in-country risk assessment permitted HCWs to return to the United Kingdom as standard aeromedical evacuations with DAIT as escorts, after initially being deemed too high risk to travel on a commercial airline. A T-ATI was kept on standby in case of clinical deterioration.	• In-country risk assessment modified the role of the DAIT to provide standard aeromedical evacuation with T-ATI on standby for those with high-risk exposure rather than confirmed EVD. • Civilian infectious diseases consultant enabled more rapid access to advanced EVD treatments for the injured HCWs.
Mission 6: Multiple patients on one platform, one confirmed in T-ATI and 2 exposed contacts with T-ATI on standby (Figure 5)	
Three military HCW exposed to Ebola were returned from the Ebola Treatment Centre, Kerrytown, Sierra Leone, alongside a confirmed Ebola case-patient. After an in-country risk assessment, 3 T-ATIs were flown on a single C-17 airframe (Figure 5) to Sierra Leone (*4*). Two exposed HCWs joined the RAF flight to the HLIU, Royal Free Hospital; 2 were flown back 48 h later by commercial flight to the HLIU, Royal Victoria Hospital in Newcastle.	• Team augmented to 22 personnel for 3 T-ATI. Marked out floating clean/dirty line through aircraft should all 3 T-ATI be used.

*CCHF, Crimean-Congo hemorrhagic fever; DAIT, Deployable Air Isolation Team; EVD, Ebola virus disease; HCW, healthcare worker; HLIU, high-level isolation units; MOD, Ministry of Defence; NHS, National Health Service; PPE, personal protective equipment; RAF, Royal Air Force; T-ATI, Trexler Air Transport Isolator; VHF, viral hemorrhagic fever.

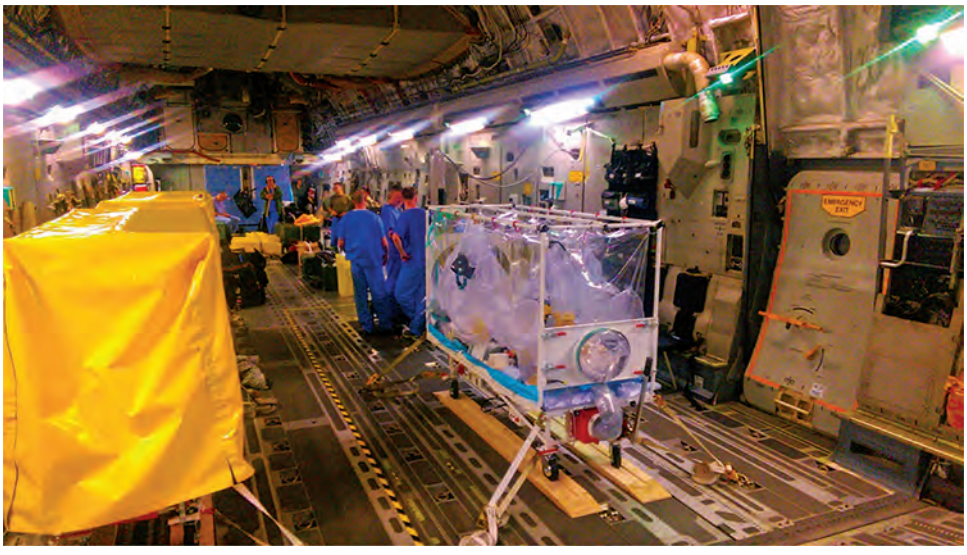

Figure 8. Multiple Air Transport Isolator patient transport systems on a single aircraft (Boeing C-17 Globemaster). A single isolator is set up for the confirmed viral hemorrhagic fever case-patient; 2 additional isolators (left, covered) are available for the 2 exposed patients should they deteriorate or become symptomatic in flight.

on interagency collaboration, are required. Most patients transferred during the Ebola outbreak had been asymptomatic or were in the early stages of disease; innovation in closed T-ATI development is required to optimize the care provided to symptomatic patients, such as improved ergonomic design to make clinical intervention as simple as possible and PPE development to facilitate easier patient management. There is an ongoing role for single-person isolation units and portable biocontainment units that can provide for multiple patients and providers in a more functional medical unit. The clinical disadvantages of the current T-ATI include its size (it is not transportable on helicopters, or without a dedicated Jumbulance) and reduced dexterity that challenges staff in delivering optimal patient care.

For the past 40 years, the UK T-ATI system has provided end-to-end biologic containment from overseas site to specialist unit. Since 2012, a total of 8 successful missions have provided learning opportunities that have greatly improved the service. The system allows for a highly specialized capability, providing both moral support to those combating the disease overseas and safe transfer of potentially isolated cases to or within the United Kingdom (*22*).

Although the United Kingdom expects to continue to use the T-ATI, more advanced systems have been developed that are smaller and more versatile and may also provide easier clinical access to the patient. The United Kingdom is not currently looking to use larger transportable medical units. If the mission changes, the T-ATI, developed in the United States, remains an alternative solution if the numbers of patients requiring transfer increase or there is a demand to provide a higher level of care to VHF patients. It is possible that a greater future threat comes from airborne infectious disease; the flexible, adaptable, responsive, and safe capability of T-ATI and DAIT allows the transport of patients with highly transmissible airborne diseases back to the United Kingdom if required.

Because many nations do not have an aeromedical evacuation facility, it is unclear whether the RAF should repatriate patients to non–United Kingdom destinations. If it should, considerations include logistics of patient delivery from airstrip to the receiving unit (either in the T-ATI or in PPE); appropriate in-hospital transfer; and safe clinical waste and T-ATI envelope disposal and decontamination.

About the Author

Dr. Nicol is a Royal Air Force general physician and the RAF Clinical Director of Deployed Hospital Care. He has conducted transfers of patients with viral hemorrhagic fever using the Trexler Air Transport Isolator system.

References

1. Fisher-Hoch SP, Craven RB, Forthall DN, Scott SM, Price ME, Price FM, et al. Safe intensive-care management of a severe case of Lassa fever with simple barrier nursing techniques. Lancet. 1985; 326:1227–9. http://dx.doi.org/10.1016/S0140-6736 (85)90752-4
2. Barr DA, Aitken C, Bell DJ, Brown CS, Cropley I, Dawood N, et al. First confirmed case of Crimean-Congo haemorrhagic fever in the UK. Lancet. 2013;382:1458. http://dx.doi.org/10.1016/S0140-6736(13)61718-3
3. BBC News. Ebola nurse Pauline Cafferkey transferred to London unit. 2014 Dec 30 [cited 2018 Nov 1]. http://www.bbc.co.uk/news/uk-scotland-30629397
4. BBC News. Ebola: British patient and five colleagues flown home. 2015 Mar 13 [cited 2018 Nov 1]. http://www.bbc.co.uk/news/uk-31845947
5. BBC News. Briton in Sierra Leone "tests positive for Ebola." 2014 Aug 23 [cited 2018 Nov 1]. http://www.bbc.co.uk/news/world-africa-28914614
6. BBC News. Ebola nurse Pauline Cafferkey back in hospital. 2015 Oct 9 [cited 2018 Nov 1]. http://www.bbc.co.uk/news/uk-34483882
7. BBC News. Ebola nurse Pauline Cafferkey "stable" after night in London hospital. 2016 Feb 24 [cited 2018 Nov 1]. http://www.bbc.co.uk/news/uk-scotland-35639748

8. BBC News. Possible Ebola cases flown to UK. 2015 Jan 16 [cited 2018 Nov 1]. http://www.bbc.co.uk/news/health-30846704
9. BBC News. Second UK health worker monitored for Ebola. 2015 Feb 2 [cited 2018 Nov 1]. http://www.bbc.co.uk/news/health-31091528
10. Jacobs M, Aarons E, Bhagani S, Buchanan R, Cropley I, Hopkins S, et al. Post-exposure prophylaxis against Ebola virus disease with experimental antiviral agents: a case-series of health-care workers. Lancet Infect Dis. 2015;15:1300–4. http://dx.doi.org/10.1016/S1473-3099(15)00228-5
11. European Centre for Disease Prevention and Control. Assessment and planning for medical evacuation by air to the EU of patients with Ebola virus disease and people exposed to Ebola virus. 2014 [cited 2018 Nov 1]. https://ecdc.europa.eu/en/publications-data/assessment-and-planning-medical-evacuation-air-eu-patients-ebola-virus-disease
12. Ewington I, Nicol E, Adam M, Cox AT, Green AD. Transferring patients with Ebola by land and air: the British military experience. J R Army Med Corps. 2016;162:217–21. http://dx.doi.org/10.1136/jramc-2016-000623
13. Gilsdorf A, Morgan D, Leitmeyer K. Guidance for contact tracing of cases of Lassa fever, Ebola or Marburg haemorrhagic fever on an airplane: results of a European expert consultation. BMC Public Health. 2012;12:1014. http://dx.doi.org/10.1186/1471-2458-12-1014
14. Christopher GW, Eitzen EM Jr. Air evacuation under high-level biosafety containment: the aeromedical isolation team. Emerg Infect Dis. 1999;5:241–6. http://dx.doi.org/10.3201/eid0502.990208
15. US Centers for Disease Control and Prevention. Guidance on air medical transport (AMT) for Patients with Ebola virus disease (EVD). 2015 [cited 2018 Nov 1]. http://www.cdc.gov/vhf/ebola/healthcare-us/emergency-services/air-medical-transport.html
16. Canadian Critical Care Society. Ebola clinical care guidelines. 2014 [cited 2018 Nov 1] http://www.canadiancriticalcare.org/resources/Pictures/Ebola%20Clinical%20Care%20Guidelines_ENG.pdf
17. Aviation Week Network. How Phoenix Air entered the "Ebola business" 2015 [cited 2018 Nov 1]. http://aviationweek.com/bca/how-phoenix-air-entered-ebola-business
18. Scientific American. SARS outbreak isolators helped "Ebola Air" fly infected patients. 2014 [cited 2018 Nov 1]. www.scientificamerican.com/article/sars-outbreak-isolators-helped-ebola-air-fly-infected-patients/
19. MRI Global. Containerized Bio-Containment Unit (CBCS). 2016 [cited 2018 Nov 1]. http://www.mriglobal.org/portfolio-item/containerized-bio-containment-unit-cbcs/
20. Department of Health and Social Care, Public Health England. (2014) Management of Hazard Group 4 viral haemorrhagic fevers and similar human infectious diseases of high consequence. November 2014 [cited 2018 Nov 6]. https://assets.publishing.service.gov.uk/government/uploads/system/uploads/attachment_data/file/534002/Management_of_VHF_A.pdf
21. Otter JA, Mepham S, Athan B, Mack D, Smith R, Jacobs M, et al. Terminal decontamination of the Royal Free London's high-level isolation unit after a case of Ebola virus disease using hydrogen peroxide vapor. Am J Infect Control. 2016; 44:233-5.
22. World Health Organization. International health regulations (2005), second edition. 2005 [cited 2018 Nov 1]. http://whqlibdoc.who.int/publications/2008/9789241580410_eng.pdf

Address for correspondence: Edward D. Nicol, Aviation Medicine Consultation Service, Bldg 108, Royal Air Force Henlow, Henlow SG16 6DN, UK; email: e.nicol@nhs.net

Clinical and Radiologic Characteristics of Human Metapneumovirus Infections in Adults, South Korea

Hyun Jung Koo, Han Na Lee, Sang-Ho Choi, Heungsup Sung, Hwa Jung Kim, Kyung-Hyun Do

Clinical features of human metapneumovirus (HMPV) infection have not been well documented for adults. We investigated clinical and radiologic features of HMPV infection in 849 adults in a tertiary hospital in South Korea. We classified patients into groups on the basis of underlying diseases: immunocompetent patients, solid tumor patients, solid organ transplantation recipients, hematopoietic stem cell transplant recipients, hematologic malignancy patients, and patients receiving long-term steroid treatment. Of 849 HMPV-infected patients, 756 had community-acquired infections, 579 had pneumonia, and 203 had infections with other pathogens. Mortality rates were highest in hematopoietic stem cell transplantation recipients (22% at 30 days). Older age, current smoking, and underlying disease were associated with HMPV pneumonia. Body mass index and an immunocompromised state were associated with 30-day mortality rates in HMPV-infected patients. Bronchial wall thickening, ground-glass opacity, and ill-defined centrilobular nodules were common computed tomography findings for HMPV pneumonia. Macronodules and consolidation were observed in <50% of patients.

Human metapneumovirus (HMPV), first described in 2001, is a common pathogen that causes acute respiratory tract infections in all age groups (*1*). Seropositivity for IgG against HMPV has been detected in up to 100% of persons 20 and >65 years of age, and reinfection is common (*2*–*4*). HMPV infection shows a seasonal pattern in the United States, Asia, and countries in Europe, and most infections occur in spring (*3*,*5*–*9*). Although HMPV infection is usually asymptomatic or causes mild and self-limiting symptoms in young healthy adults, it can cause severe pneumonia in elderly and immunocompromised persons (*10*–*13*). HMPV infection progresses from upper respiratory tract infection (URI) to lower respiratory tract disease in up to 60% of hematopoietic stem cell transplant (HCT) recipients (*14*), and mortality rates are 6%–40% (*15*,*16*). Moreover, ≈50% of patients with solid organ transplants (SOT) infected with HMPV progress to pneumonia (*13*,*17*,*18*), and HMPV infection is frequently detected in patients with exacerbated chronic obstructive pulmonary disease (*19*).

Clinical characteristics such as host immunity in patients with HMPV infection and radiologic findings of HMPV pneumonia are needed for early detection of HMPV infection and for studies of HMPV pneumonia-related outcomes (*14*,*20*,*21*). Although a recent study of 3 long-term care facilities in Japan reported clinical and radiologic characteristics of HMPV pneumonia, that study did not assess the proportion of URIs, included only immunocompetent persons, and did not determine overall outcomes of HMPV pneumonia. Therefore, we conducted a study that included a large consecutive cohort of adults infected with HMPV and assessed the proportions of HMPV-associated URI and pneumonia in patients with various underlying disease, and laboratory findings, radiologic findings, including computed tomography (CT) images, and overall outcomes.

Methods

This retrospective consecutive cohort study covered the period January 2010–February 2016. The study was approved by the institutional review board of Asan Medical Center (approval no. 2017–0016), which waived the requirement for informed consent because of the retrospective nature of this study. During the study period, all patients who came to this hospital, regardless of whether they were in the outpatient clinic, hospitalized, or in the emergency department, and who had respiratory symptoms suggestive of URI or pneumonia underwent routine collection of nasopharyngeal swab specimens, blood cultures, or both. Testing decisions were made by the clinicians. We assessed pathogens before giving any antimicrobial drugs

Author affiliations: Asan Medical Center, University of Ulsan College of Medicine, Seoul, South Korea (H.J. Koo, S-H. Choi, H. Sung, H.J. Kim, K.-H. Do); Kyung Hee University Hospital at Gangdong, Seoul H.N. Lee)

DOI: https://doi.org/10.3201/eid2501.181131

to patients with no history of treatment at another hospital. If relevant pathogens could not be identified, bronchoalveolar lavage (BAL) fluid was obtained. BAL fluid was not obtained if there was no evidence of pneumonia and symptoms were eliminated by conservative management. The decisions for laboratory testing and BAL procedures were clinician directed, and laboratory results were assessed retrospectively.

During January 2010–February 2016, a total of 15,311 patients had tests performed for respiratory virus infections. For these patients, 817 patients had multiple tests because of multiple different episodes (> a 2-month interval between tests); 591 patients had 2 tests, 149 had 3 tests, 46 had 4 tests, 15 had 5 tests, 10 had 6 tests, 3 had 7 tests, 1 had 8 tests, and 2 had 9 tests. The total number of tests was 16,489. If a patient was infected more than once with HMPV during the study period, we used only the first episode for analysis. We thoroughly reviewed electronic medical records of patients, and their clinical characteristics; immune status, such as transplant history and steroid or immunosuppressant use; presence of other pathogens; length of hospital stay; and clinical course, such as admission to an intensive care unit; and death.

Definitions

Community-acquired infection indicated respiratory infection detected in a person in a community without a history of hospitalization or living in a long-term care facility within the previous 14 days. Hospital-acquired infection was defined as respiratory infection that occurred ≥48 hours after hospital admission with new onset respiratory symptoms. We assessed respiratory virus infection in nasopharyngeal secretions and BAL fluid by using a multiplex reverse transcription PCR and a Seeplex RV 15 ACE Detection Kit (March 2010–October 2013) or an Anyplex II RV 16 Detection Kit (November 2013–August 2017) (both from Seegene Inc., http://www.seegene.com).

Patients positive for HMPV, but with no evidence of pneumonia by chest radiographs or CT images, were defined as having URI. Patients who had new pulmonary infiltrates by chest radiographs or CT images and HMPV in nasopharyngeal samples or BAL fluid were defined as having pneumonia. Patients with other pathogens in nasopharyngeal or blood samples within 2 days of diagnosis of HMPV infection were defined as co-detection positive for another pathogen (*14*). Long-term steroid use was defined as steroid treatment (≥5 mg/d of prednisolone or an equivalent drug) for >6 months because of an underlying condition or disease (Appendix Table 1, https://wwwnc.cdc.gov/EID/article/25/1/18-1131-App1.pdf), such as adrenal insufficiency, interstitial lung disease, or asthma. The mean dose of steroid was 1.80 mg/kg/d (range 0.53–2.02 mg/kg/d).

Radiologic Evaluation

For patients given a diagnosis of HMPV infection, we evaluated the presence of pneumonic infiltrates on chest radiographs to detect pneumonia. We also evaluated bilaterality and the number of involved zones (total of 6 zones; i.e., right and left upper, middle, and lower zones).

We performed CT examinations by using 16- or 64-detector CT scanners (SOMATOM Sensation 16; Siemens Medical Solutions, https://www.siemens.com/global/de/home.html; and LightSpeed VCT; General Electric Healthcare, https://www.gehealthcare.com). We reviewed all axial and coronal CT images on the picture archiving and communication system by using the mediastinal (width, 450 hounsfield units [HUs]; level, 50 HUs), lung (width, 1,500 HUs; level, –700 HUs), and bone (width, 1,000 HUs; level, 200 HUs) window settings.

We assessed CT findings for distribution of parenchymal abnormalities (number of involved lobes and bilaterality); the presence and extent of centrilobular nodules; consolidation; ground-glass opacities; and the presence of macronodules, bronchial wall thickening, bronchiectasis, lymphadenopathy, and pleural effusion. CT patterns were defined on the basis of the glossary of terms for thoracic imaging (*22*). All CT results were reviewed in consensus by 2 chest radiologists (1 with 2 years of experience and 1 with 15 years of experience) in thoracic imaging. Results were independently reviewed by a third radiologist to evaluate the reliability of the CT findings (percent extent of centrilobular nodules, consolidation, and ground-glass opacities).

Statistical Analysis

Patients were subgrouped according to underlying conditions: immunocompetent patients, patients with solid tumors, SOT recipients, HCT recipients, patients with hematologic malignancy (HM), and patients receiving long-term steroid treatment. We compared characteristics and outcomes of HMPV infection for each of these groups. We compared proportions of HMPV pneumonia in immunocompetent and immunocompromised patients by using the χ^2 test. Univariate and multivariable logistic regression analyses were performed to identify clinical factors associated with HMPV pneumonia and the 30-day mortality rate in HMPV-infected patients. Body mass index (BMI) was analyzed as a continuous variable. We assessed interobserver agreement for CT findings by determining intraclass correlation coefficients with κ statistics. We compared categorical variables by using the χ^2 test or Fisher exact test. We compared continuous variables by using the Student *t*-test or the Mann-Whitney U test. CT findings for HMPV pneumonia without another pathogen were compared in

immunocompetent and immunocompromised patients. A 2-sided p value <0.05 was defined as statistically significant. We performed all statistical analyses by using SPSS version 21.0 (SPSS Inc., https://www.ibm.com/analytics/spss-statistics-software).

Results

Patient Characteristics

For the study period, January 2010–February 2016, we identified 850 adults infected with HMPV (Figure 1). There was 1 patient in the long-term steroid use group who had 2 episodes, and the interval between the 2 episodes was 1 year. The overall percentage of patients with HMPV infection among all those tested was 5.6% (850/15,311). HMPV was detected in 5.2% (851/16,489) of all tests. Most (82.0%, 696/850) patients were given a diagnosis during March–June (Figure 2). One patient who did not undergo radiologic examination was excluded, and 579 (68.2%) of the 849 HMPV-infected patients were given a diagnosis of pneumonia. For pneumonia patients, 14 patients with negative results for chest radiographs had pneumonia on the next CT scan. The percentage of pneumonia in immunocompetent patients (72.5%, 333/459) was slightly higher than that for immunocompromised patients (63.1%, 246/390) (p = 0.003).

We determined characteristics of the HMPV-infected patients (Table 1). Of the 849 patients, 459 were immunocompetent, 174 had solid tumors, 59 had a history of SOT, 9 underwent HCT, 58 had underlying HM, and 90 had a history of long-term steroid use. We provide details of their underlying diseases (Appendix Table 1). Median age of immunocompetent HMPV-infected patients was 67 years, which was higher than that for the solid tumor, SOT, HCT, and HM patient groups. Most (89%) HMPV infections were community-acquired; the remaining infections (11%) were nosocomial. C-reactive protein concentration (6.5 mg/dL vs. 2.6 mg/dL; p<0.001), leukocyte count (7.5×10^3 cells/μL vs. 6.5×10^3 cells/μL; p = 0.001), and neutrophil count (5.5×10^3 cells/μL vs. 4.3×10^3 cells/μL; p<0.001) were significantly higher in patients with pneumonia than in those without pneumonia.

Overall, 23.9% (203/849) of patients had a pathogen other than HMPV, and 16.5% (140/849) had pneumonia and another pathogen (Appendix Table 2). Rates for other pathogens ranged from 20% to 33% in subgroups and were highest for patients with HM (32.8%, 19/58) and those receiving long-term steroid treatment (32.2%, 29/90). Bacteria were the most common co-detected pathogens (57.1%, 116/203).

Of the HMPV-infected patients, 65% were hospitalized for a median of 7 days (range 4 days–13 days) (Table 2). An

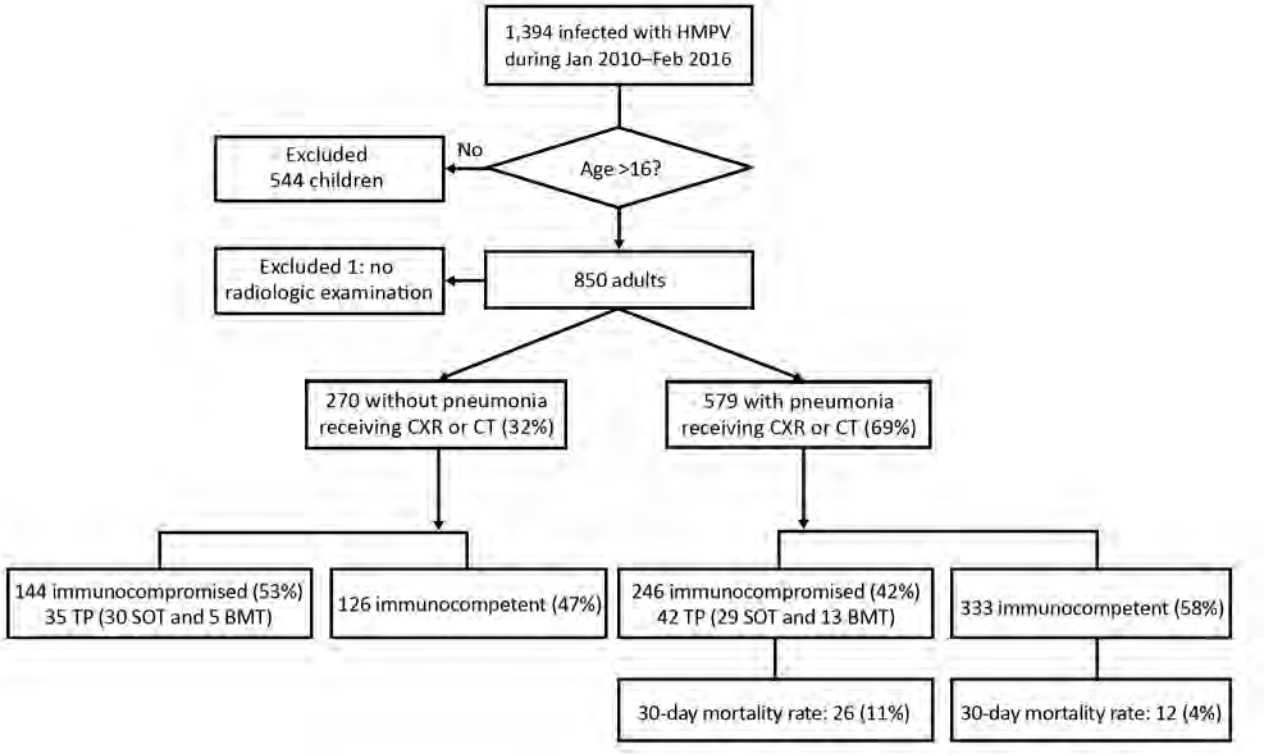

Figure 1. Flowchart for analysis of clinical and radiologic characteristics of adults with HMPV infections, South Korea. BMT, bone marrow transplant; CT, computed tomography; CXR, chest radiograph; HMPV, human metapneumovirus; SOT, solid organ transplants; TP, transplant.

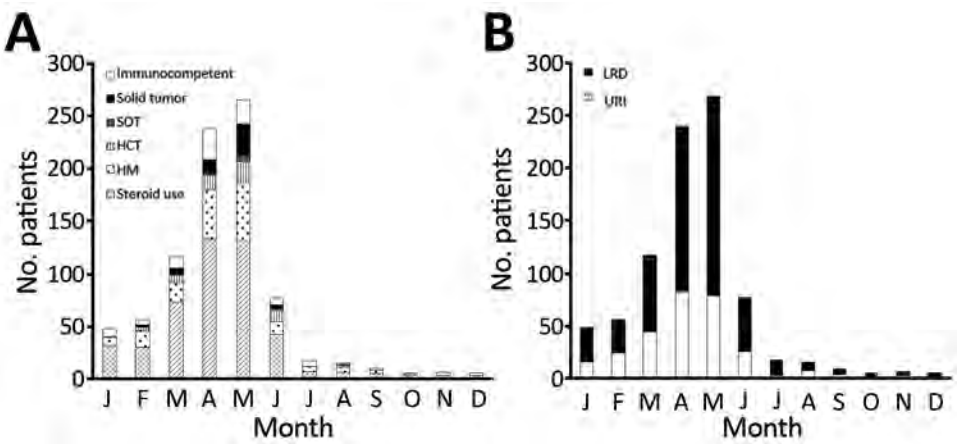

Figure 2. Monthly distribution of HMPV infection, South Korea. A) Rates of underlying diseases; B) proportions of upper respiratory tract infection and lower respiratory tract disease. HCT, hematopoietic stem cell transplantation; HM, hematologic malignancy; HMPV, human metapneumovirus; LRD, lower respiratory tract disease; SOT, solid organ transplants; URI, upper respiratory infection. A color version of this figure is available online (http://wwwnc.cdc.gov/EID/article/25/1/18-1131-F2.htm).

antiviral agent (oral ribavirin) was used in 129 patients, and intravenous immunoglobulin was used in 11 patients. For patients hospitalized for pneumonia, 68 (8%) required admission to the intensive care unit. HCT recipients had the highest all-cause 30-day (22%) and 90-day (33%) mortality rates.

Clinical Factors Related to HMPV Pneumonia

We compared clinical characteristics for patients with HMPV and URI or pneumonia by using logistic regression analysis to identify factors associated with HMPV pneumonia (Table 3). Univariate analysis showed that median age was higher in patients with pneumonia than in those with URI (66.0 vs. 59.0 years, odds ratio [OR] 1.02, 95% CI 1.01–1.03; p<0.001). Current cigarette smoking (OR 2.10, 95% CI 1.47–2.99; p<0.001) and diabetes (OR 1.47, 95% CI 1.08–2.01; p = 0.02) were also significantly associated with HMPV pneumonia. The proportion of HMPV pneumonia was higher for immunocompetent patients (73%, 333/459) than for patients with solid tumors (61%, 106/174) or SOT (49%, 29/59) (p<0.001), However, differences for patients with HCT (89%, 8/9), HM (66%, 38/58), and steroid use (70%, 63/90) were not statistically significant (p = 0.36) (Figure 3).

Multivariable logistic regression analysis showed that age (OR 1.02, 95% CI 1.01–1.03; p = 0.001) and current smoking (OR 2.07, 95% CI 1.30–3.29; p = 0.002) were independently associated with HMPV pneumonia, and that diabetes showed marginal significance (OR 1.37, 95% CI 0.96–1.95; p = 0.08). The proportion of HMPV pneumonia was significantly lower for patients with solid tumors (OR 0.57, 95% CI 0.38–0.84; p = 0.005) or SOT (OR 0.35, 95% CI 0.19–0.65; p = 0.001) than for immunocompetent patients; no major differences were observed for the HCT, HM, and steroid use groups.

Clinical Factors Related to 30-Day Mortality Rates in HMPV-Infected Patients

We found that current smoking (OR 1.92, 95% CI 1.04–3.56; p = 0.04), BMI (OR 0.89, 95% CI 0.79–0.95; p = 0.001), and underlying immunocompromised status, such as patients with solid tumor, (OR 3.00, 95% CI 1.48–6.08; p = 0.002), but not SOT, were significantly associated with 30-day mortality rates in HMPV-infected patients (Table 4). The association of 30-day mortality rate was highest for HCT patients (OR 7.91, 95% CI 1.52 – 41.1; p<0.01). Multivariable logistic regression analysis showed that BMI (OR 0.86, 95% CI 0.79–0.95; p = 0.002) and underlying immunocompromised status, such as patients with solid tumor (OR 3.43, 95% CI 1.58–7.44; p = 0.002), remained associated factors with 30-day mortality rate.

Radiologic Findings for HMPV Pneumonia

We detected HMPV pneumonia radiographically for 68% (579/849) of all patients, and 56.0% (324/579) of these patients had bilateral involvement. Median number of involved zones in patients with HMPV pneumonia was 3 (range 2–5). To evaluate CT findings for HMPV pneumonia, we analyzed 251 patients without another pathogen who had CT performed at the time of diagnosis (Table 5). Of these patients, 76% (192/251) showed bilateral involvement. Of the patients with HMPV pneumonia, 69% (174/251) had centrilobular nodules, 43% (107/251) had consolidations, and 79% (199/251) had ground-glass opacities (Figure 4). Macronodules (45%, 114/251) and bronchial wall thickening (88%, 222/251) were common findings, whereas mediastinal lymphadenopathy (27%, 68/251) and pleural effusion (22%, 56/251) were less common. Intraclass correlation coefficients of radiologists for CT findings (percent extents of centrilobular nodules, consolidation, and ground-glass opacities) ranged from 0.84 to 0.95 (p<0.001). The number of involved lobes was greater and pleural effusion was more frequent in immunocompromised patients than in immunocompetent patients (Figure 5; Appendix Table 3).

Discussion

We found that HMPV pneumonia in adults was associated with older age, current cigarette smoking, and underlying

diseases. Lower BMI and immunocompromised state, except SOT, were associated with 30-day mortality rates in HMPV-infected patients. Chest radiographs showed bilateral lung involvement in 56% of patients, and CT scans showed bilateral lung involvement in 76% of patients. Bronchial wall thickening, ground-glass opacities, and

Table 1. Clinical characteristics of patients infected with human metapneumovirus, South Korea*

Characteristic	Immunocompetent	Solid tumors†	SOT	HCT	HM	Steroid use	Total
Total	459 (54)	174 (20)	59 (7)	9 (1)	58 (7)	90 (11)	849
Age, y	67 (56–75)	62 (53–70)	56 (49–62)	54 (32–63)	60 (47–67)	67 (52–75)	64 (53–73)
Sex							
M	229 (50)	89 (51)	25 (42)	6 (67)	24 (41)	50 (56)	442 (52)
F	230 (50)	85 (49)	34 (58)	3 (33)	34 (59)	40 (44)	407 (48)
Smoking status							
Never	326 (71)	104 (60)	43 (73)	5 (56)	40 (69)	47 (52)	565 (67)
Former	99 (22)	63 (36)	16 (27)	3 (33)	14 (24)	38 (42)	233 (6)
Current	34 (7)	7 (4)	0	1 (11)	4 (7)	5 (6)	51 (27)
BP, mm Hg							
Systolic	134 (120–152)	124 (115–137)	131 (116–146)	130 (113–136)	128 (120–140)	134 (120–151)	131 (119–147)
Diastolic	80 (73–90)	80 (73–88)	82 (74–92)	88 (82–90)	82 (76–90)	82 (74–90)	80 (73–90)
Temperature, °C	36.6 (36.4–37.2)	36.6 (36.4–37.2)	36.4 (36.2–36.8)	36.7 (36.5–37.7)	36.5 (36.2–36.7)	36.6 (36.3–36.9)	36.6 (36.4–37.1)
Temperature, >37°C	70 (15)	25 (14)	4 (7)	3 (33)	5 (9)	16 (18)	123 (14.5)
Heart rate, beats/min	83 (70–99)	88 (78–103)	82 (73–91)	100 (90–110)	87 (77–100)	93 (84–106)	87 (74–100)
Respiratory rate, breaths/min	20 (18–22)	20 (18–20)	18 (18–20)	22 (20–27)	20 (18–22)	22 (20–24)	20 (18–22)
Body mass index, kg/m^2	23.2 (20.4–25.9)	23.1 (20.3–25.5)	23.2 (21.3–25.1)	20.2 (17.0–25.1)	22.4 (20.5–25.2)	22.6 (20.2–24.4)	23.1 (20.4–25.5)
Hypertension	239 (52)	71 (41)	47 (80)	3 (33)	22 (38)	51 (57)	433 (51)
Diabetes mellitus	157 (34)	42 (24)	44 (75)	4 (44)	20 (35)	29 (32)	296 (35)
Location of patients‡							
Outpatient clinic	22	1	2	0	0	2	27
Hospitalized	131	137	21	3	24	35	351
ED	306	36	36	6	34	53	471
Type of infection							
CA	415 (90)	150 (86)	51 (86)	7 (88)	47 (81)	84 (93)	756 (89)
Nosocomial	44 (10)	24 (14)	8 (14)	2 (22)	11 (19)	6 (7)	93 (11)
URI	126 (28)	68 (39)	30 (51)	1 (11)	20 (35)	27 (30)	270 (32)
LRD	333 (73)	106 (61)	29 (49)	8 (89)	38 (66)	63 (70)	579 (68)
Initial CRP level at hospital admission, mg/L	4.3 (1.5–9.9)	6.5 (2.6–13.3)	4.6 (1.0–7.7)	10.6 (5.5–19.7)	5.8 (2.8–12.0)	4.4 (1.9–4.4)	4.9 (1.8–11.0)
Leukocyte count at diagnosis, × $10^3/\mu L$	7.7 (5.5–10.5)	5.4 (2.8–8.7)	8.5 (4.8–10.6)	12.0 (6.5–13.6)	4.8 (2.3–7.4)	8.3 (5.7–11.5)	7.2 (4.9–10.3)
>10	128 (28)	33 (19)	16 (27)	5 (56)	7 (12)	34 (38)	223 (26)
≤10	331 (72)	141 (81)	43 (73)	4 (44)	51 (88)	56 (62)	626 (74)
Neutrophil count at diagnosis, × $10^3/\mu L$§	5.5 (3.4–8.3)	3.9 (1.7–6.5)	6.1 (3.3–8.5)	7.9 (5.9–9.5)	2.9 (1.3–5.1)	6.2 (3.9–9.6)	5.1 (3.0–8.1)
>5.0	252 (55)	67 (39)	35 (59)	6 (67)	14 (24)	56 (62)	430 (51)
≤5.0	205 (45)	106 (61)	24 (41)	1 (11)	42 (72)	32 (36)	410 (48)
Lymphocyte count at diagnosis, × $10^3/\mu L$§	1.3 (0.9–1.8)	0.8 (0.5–1.3)	1.0 (0.6–1.4)	2.9 (0.7–4.2)	0.8 (0.4–1.7)	1.1 (0.7–1.6)	1.1 (0.7–1.6)
>0.7	380 (83)	97 (56)	41 (70)	5 (56)	33 (57)	65 (72)	621 (73)
≤0.7	77 (17)	76 (44)	18 (31)	2 (22)	23 (40)	23 (26)	219 (26)
Platelet count, × $10^3/\mu L$	193 (145–243)	149 (101–223)	166 (116–231)	82 (35–187)	86 (36–146)	198 (143–245)	176 (124.5–233)
Blood urea nitrogen, mg/Dl	14 (10–22)	13 (9–19)	21 (14–31)	15.0 (8.5–27.0)	14.5 (10–20.3)	15 (11–23.5)	14.0 (10.0–21.0)
Creatinine, mg/dL	0.8 (0.7–1.1)	0.8 (0.6–1.0)	1.3 (1.0–1.8)	0.9 (0.7–1.4)	0.8 (0.6–1.2)	0.8 (0.6–1.1)	0.8 (0.7–1.1)
Procalcitonin, ng/mL	0.2 (0.1–1.2)	0.2 (0.1–0.7)	0.2 (0.1–1.2)	0.2 (0.1–1.1)	0.2 (0.1–0.6)	0.2 (0.1–0.9)	0.2 (0.1–0.9)

*Values are no. (%) or median (interquartile range) unless otherwise indicated. BP, blood pressure; CA, community acquired; CRP, C-reactive protein; ED, emergency department; HCT, hematologic stem cell transplantation; HM, hematologic malignancy; HMPV, human metapneumovirus; LRD, lower respiratory tract disease; SOT, solid organ transplants; URI, upper respiratory tract infection.
†Patients with solid tumors were given chemotherapy within 6 mo.
‡Locations at which patients were tested for HMPV.
§Detailed laboratory results, including neutrophil and lymphocyte counts, were unavailable for 9 patients who visited outpatient clinics

Table 2. Co-detection of other pathogens and clinical course of patients infected with human metapneumovirus, South Korea*

Characteristic	Immunocompetent	Solid tumors	SOT	HCT	HM	Steroid use	Total
Total	459 (54)	174 (20)	59 (7)	9 (1)	58 (7)	90 (11)	849
URI	126 (28)	68 (39)	30 (51)	1 (11)	20 (35)	27 (30)	270 (32)
LRD	333 (73)	106 (61)	29 (49)	8 (89)	38 (66)	63 (70)	579 (68)
Ribavirin use	44 (10)	22 (13)	10 (17)	5 (56)	23 (40)	22 (24)	126 (15)
IVIG use	3 (1)	0	1 (2)	0	1 (2)	3 (3)	8 (1)
Both ribavirin and IVIG use	2 (0.4)	0	0	0	0	1 (1)	3 (0.4)
Co-detection of other pathogen, n = 126							
URI	17 (13)	18 (26)	10 (33)	1 (100)	10 (50)	7 (26)	63 (23)
LRD	72 (21)	23 (22)	13 (45)	1 (13)	9 (24)	22 (35)	140 (24)
Bacteria	48	20	16	1	11	20	116
Virus	32	14	7	0	6	5	64
Fungi	3	5	0	1	0	0	9
Bacteria and virus	6	1	0	0	2	3	12
Bacteria and fungi	0	1	0	0	0	0	1
Virus and fungi	0	0	0	0	0	1	1
Hospital admission	279 (65)	98 (56)	32 (54)	6 (67)	35 (60)	64 (71)	552 (65)
Length of hospital stay, days	6.0 (4.0–13.0)	7.0 (4.0–12.0)	6.0 (4.0–14.0)	7.0 (5.3–55.3)	10.5 (5.8–32.5)	7.0 (4.0–16.0)	7.0 (4.0–13.0)
ICU admission	42 (9)	4 (2)	5 (10)	1 (11)	5 (10)	11 (12)	68 (8)
All-cause mortality rate at 30 d	16 (3)	17 (10)	0 (0)	2 (22)	5 (9)	7 (8)	47 (6)
All-cause mortality rate at 90 d	18 (4)	22 (13)	1 (2)	3 (33)	7 (12)	8 (9)	59 (7)
Overall mortality rate	42 (9)	34 (20)	3 (5)	4 (44)	21 (36)	22 (24)	126 (15)

*Values are no. (%) or median (interquartile range) unless otherwise indicated. HCT, hematologic stem cell transplantation; HM, hematologic malignancy; ICU, intensive care unit; IVIG, intravenous immunoglobulin; LRD, lower respiratory tract disease; SOT, solid organ transplants; URI, upper respiratory tract infection.

ill-defined centrilobular nodules were common CT findings in patients with HMPV pneumonia.

Recent studies have demonstrated that low BMI was a major risk factor for hospitalization of patients with pneumonia (*23*,*24*). A U-shaped relationship between BMI and pneumonia has been shown in a recent meta-analysis, in which an underweight condition (BMI <18.5) and morbid obesity (BMI ≥40) are both associated with the risk for community-acquired pneumonia (*25*). Conversely, being overweight and obese (BMI 25.0–39.9) were major factors in reducing the risk for death from pneumonia (*26*). In our study, the risk for HMPV pneumonia associated with BMI was not evident because only 14 patients were underweight, and there was no patient with a BMI ≥32. However, lower BMI increased the mortality rate for HMPV pneumonia. This finding coincides with the obesity survival paradox, which shows a decreased pneumonia mortality rate for overweight and obese patients (*26*).

Although most young healthy adults with HMPV infection are asymptomatic or have mild symptoms, HMPV pneumonia can cause severe symptoms in elderly (*7*) and immunocompromised (*14*,*17*,*27*,*28*) patients. Mortality

Table 3. Clinical characteristics of patients associated with pneumonia for patients with human metapneumovirus, South Korea*

			Univariate analysis		Multivariable analysis	
Characteristic	URI, n = 270	LRD, n = 579	OR (95% CI)	p value	OR (95% CI)	p value
Age	59.0 (49.3–69.8)	66.0 (56.0–74.0)	1.02 (1.01–1.03)	<0.001	1.02 (1.01–1.03)	0.001
Male sex	121 (45)	321 (55)	1.57 (1.17–2.09)	0.002	0.95 (0.65–1.40)	0.81
Smoking				<0.001		0.01
Never	209 (77)	356 (61)	1		1	
Former	12 (4)	39 (7)	1.91 (0.98–3.73)	0.59	1.66 (0.80–3.43)	0.17
Current	51 (19)	182 (31)	2.10 (1.47–2.99)	<0.001	2.07 1.30–3.29)	0.002
Body mass index, kg/m^2	23.4 (21.0–25.7)	22.7 (20.1–25.4)	0.97 (0.94–1.00)	0.09	0.97 (0.93–1.00)	0.07
Diabetes mellitus	79 (29)	217 (37)	1.47 (1.08–2.01)	0.02	1.37 (0.96–1.95)	0.08
Community-acquired pneumonia	238 (88)	516 (89)	0.83 (0.53–1.30)	0.41	1.10 (0.68–1.79)	0.69
Other pathogen	63 (23)	140 (24)	0.92 (0.66–1.30)	0.64	1.05 (0.73–1.52)	0.80
Underlying condition				0.002		0.003
Immunocompetent	126 (47)	333 (58)	1		1	
Solid tumor	68 (25)	106 (18)	0.59 (0.41–0.85)	0.005	0.57 (0.38–0.84)	0.005
SOT	30 (11)	29 (5)	0.37 (0.21–0.63)	<0.001	0.35 (0.19–0.65)	0.001
HCT	1 (0.4)	8 (1)	3.03 (0.38–24.45)	0.30	3.75 (0.44–31.85)	0.23
HM	20 (7)	38 (7)	0.72 (0.40–1.28)	0.26	0.79 (0.43–1.45)	0.45
Steroid use	27 (10)	63 (11)	0.88 (0.54–1.45)	0.62	0.72 (0.43–1.22)	0.22

*Values are no. (%) or median (interquartile range). HT, hematologic stem cell transplantation; HM, hematologic malignancy; LRD, lower respiratory tract disease; OR, odds ratio; SOT, solid organ transplants; URI, upper respiratory tract infection.

Table 4. Clinical characteristics associated with 30-day mortality rate for patients with human metapneumovirus, South Korea*

Characteristic	Recovered, n = 802	30-day mortality rate, n = 47	Univariate analysis		Multivariable analysis	
			OR (95% CI)	p value	OR (95% CI)	p value
Age	63.5 (53.0–73.0)	67.0 (55.0–77.0)	(0.99–1.04)	0.15	1.02 (1.00–1.05)	0.11
Male sex	416 (52)	26 (55)	0.87 (0.48–1.57)	0.65		
Smoking				0.04		0.54
Never	540 (67)	25 (53)	1		1	
Former	48 (6)	3 (6)	1.35 (0.39–4.63)	0.63	0.67 (0.15–3.04)	0.61
Current	214 (27)	19 (40)	1.92 (1.04–3.56)	0.04	1.35 (0.69–2.64)	0.39
Body mass index, kg/m^2	23.1 (20.5–25.6)	20.5 (18.2–24.1)	0.89 (0.79–0.95)	0.001	0.86 (0.79–0.95)	0.002
Diabetes mellitus	277 (35)	19 (40)	1.29 (0.71–2.35)	0.41	1.48 (0.77–0.95)	0.24
Community-acquired pneumonia	715 (89)	40 (85)	0.70 (0.30–1.60)	0.39	0.83 (0.32–2.11)	0.69
Other pathogen	193 (24)	10 (21)	0.86 (0.42–1.76)	0.68	0.75 (0.35–1.60)	0.45
Underlying condition				0.02		0.02
Immunocompetent	443 (55)	16 (34)	1			
Solid tumor	157 (20)	17 (36)	3.00 (1.48–6.08)	0.002	3.43 (1.58–7.44)	0.002
SOT	59 (7)	0	0.00 (0.00–0.00)	1.00	0.00 (0.00–0.00)	1.00
HCT	7 (0.9)	2 (4)	7.91 (1.52–41.1)	0.01	9.19 (1.47–57.37)	0.02
HM	53 (7)	5 (11)	2.61 (0.92–7.42)	0.07	3.44 (1.14–10.34)	0.03
Steroid use	83 (10)	7 (15)	2.34 (0.93–5.85)	0.07	2.40 (0.91–6.34)	0.08

*Values are no. (%) or median (interquartile range). HCT, hematologic stem cell transplantation; HM, hematologic malignancy; OR, odds ratio; SOT, solid organ transplants.

rates for HMPV pneumonia have been reported to be higher (up to 40%) in HCT recipients (*15*). A recent meta-analysis showed that the overall HMPV mortality rate for HCT recipients was 6% and that the HMPV-associated mortality rate was 5.9 times higher in patients with pneumonia (27%) than in patients with URI (*16*). In our study, although the number of HCT patients was small (n = 9), the mortality rate was highest for HCT recipients, and the all-cause 30-day mortality rate was 22%. Conversely, the proportion of SOT patients with pneumonia was lower than that for immunocompetent patients, and mortality rates were lower for SOT patients than for all other groups.

The proportion of patients with HMPV pneumonia among those with HMPV infection was smaller for the solid tumor and SOT groups than for immunocompetent patients, whereas the mortality rate was highest for HCT recipients, followed by those with HM. This finding might be explained by the fact that immunocompetent patients visited the tertiary hospital only when respiratory symptoms were not eliminated by management in a primary clinic, whereas patients about to receive organ transplants or HCT visited the tertiary hospital if they had less severe symptoms, and had more periodical follow-up visits. Therefore, the proportion of pneumonia in the immunocompetent group was high in this study.

In our study, use of ribavirin was more common in ICU admitted patients, and mortality rates were also higher in patients who received ribavirin. However, this study was not designed to analyze the efficacy of ribavirin, and ribavirin might been have used more often for treatment in severely ill patients. Thus, the effect of ribavirin use was not determined in this study.

We found that, radiologically, most patients with HMPV pneumonia had bilateral involvement; the main findings on CT images included ill-defined centrilobular

Table 5. CT findings for 251 patients with HMPV pneumonia without another pathogen, South Korea*

Characteristic	Immunocompetent	Solid tumors	SOT	HCT	HM	Steroid use	Total
Patients with HMPV pneumonia without another pathogen	259	81	36	7	29	41	453
Patients who underwent CT scans	138	43	26	3	23	18	251
Bilateral	100 (72.5)	34 (79.1)	21 (80.8)	3 (100)	20 (87.0)	14 (77.8)	192 (76)
No. involved lobes	3 (2–6)	5 (3–6)	4 (2–5)	6 (6–6)	5 (3–6)	4 (3–5)	4 (2–6)
Macronodule	67 (49)	19 (44)	11 (31)	1 (33)	12 (52)	4 (22)	114 (45)
Patients with centrilobular nodules	101 (73)	28 (65)	17 (47)	2 (67)	13 (57)	13 (72)	174 (69)
Extent of centrilobular nodules	10 (5–30)	10 (0–20)	10 (0–20)	20 (10–20)	10 (0–20)	10 (0–23)	10 (5–20)
Patients with consolidation	57 (41)	20 (47)	13 (50)	0	8 (35)	9 (50)	107 (43)
Extent of consolidation	0 (0–10)	0 (0–15)	3 (0–10)	0 (0–0)	0 (0–10)	8 (0–20)	0 (0–10)
Patients with ground-glass opacity	109 (79)	38 (88)	21 (81)	2 (67)	15 (65)	14 (78)	199 (79)
Extent of ground-glass opacity	10 (10–20)	10 (10–30)	10 (10–23)	10 (10–10)	10 (5–20)	18 (9–33)	10 (10–20)
Bronchial wall thickening	121 (88)	35 (81)	25 (96)	3 (100)	1 (4)	17 (94)	222 (88)
Bronchiectasis	17 (12)	4 (9)	4 (15)	1 (33)	3 (13)	5 (28)	34 (14)
Cavitation	1 (0.7)	0	0	0	0	1 (6)	2 (1)
Lymphadenopathy	40 (29)	14 (33)	6 (23)	0 (0)	2 (9)	6 (33)	68 (27)
Pleural effusion	24 (17)	15 (35)	7 (27)	1 (33)	5 (22)	4 (22)	56 (22)

*Values are no. (%) or median (interquartile range) unless otherwise indicated. CT, computed tomography; HCT, hematologic stem cell transplantation; HM, hematologic malignancy; LRD, lower respiratory tract disease; SOT, solid organ transplants; URI, upper respiratory tract infection.

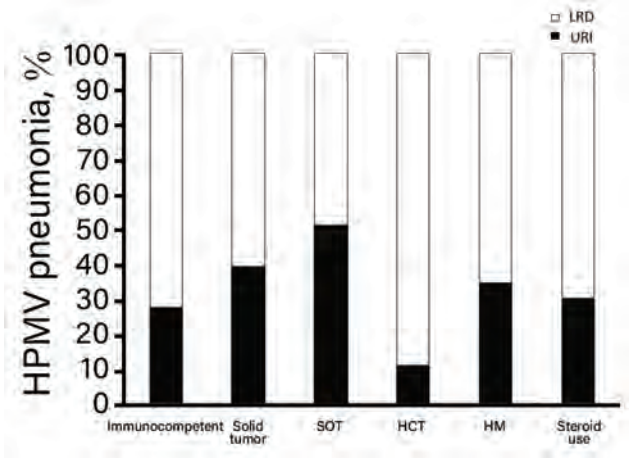

Figure 3. Proportion of HMPV-infected patients with various underlying diseases having HMPV pneumonia, South Korea. HCT, hematopoietic stem cell transplantation; HM, hematologic malignancy; HMPV, human metapneumovirus; LRD, lower respiratory tract disease; SOT, solid organ transplants; URI, upper respiratory tract infection.

nodules, ground-glass opacities, and irregular nodular consolidations. These findings suggested bronchitis and bronchiolitis and were consistent with those of previous studies (*28*–*32*). Findings of bronchial wall thickening, bronchiolitis, and centrilobular nodules were likely caused by pathogenesis of HMPV pneumonia, which affects the airways and lung epithelia and induces inflammatory cascades (*33*–*35*). Because these CT findings are also observed for bacterial pneumonia, they might be insufficient for excluding the possibility of another pathogen. CT scans of patients infected with HMPV but without another pathogen showed that the number of involved lobes and the frequency of pleural effusion were greater in the immunocompromised patients than in the immunocompetent patients.

This study had several limitations. First, patients with mild symptoms and no definite lesions by chest radiography might not undergo CT examinations. Therefore, patients with mild pneumonia that is not clearly visible on chest radiographs and who have not undergone CT scans might be classified as being in the URI group. Second, patients with low virus loads might be undetected because the Seeplex PCR has a sensitivity of 88% and the Anyplex test has a sensitivity of 96% for detecting HMPV infection (*36*). In addition, we did not routinely assess virus loads in specimens by using quantitative methods. Therefore, the effect of virus load on development of HMPV pneumonia could not be assessed, although virus load was shown not to be a major factor for HCT recipients (*14*). Third, we routinely checked patients who had respiratory infection symptoms by using nasopharyngeal swab specimens or blood cultures in our hospital. However, the decision for testing was made by clinicians, and patients with subtle respiratory symptoms might not be identified.

In conclusion, we report clinical and radiologic findings for HMPV infection in patients with various immune states. About half of these patients, even those who were immunocompetent, had HMPV pneumonia. Older age and current smoking were strongly associated with HMPV pneumonia, and the mortality rate was high in HCT recipients. CT showed that bilateral bronchial wall thickening, ground-glass opacities, and ill-defined centrilobular nodules were common.

H.J.K., H.N.L., S.H.C., and K.-H.D. designed the study; H.J.K., H.N.L., S.H.C, H.S., and K.-H.D. wrote the article; H.J.K., H.N.L., S.H.C, H.S., and K.-H.D. conducted the study; H.J.K., H.J. Kim, and H.S. developed new reagents or analytic tools; and H.J.K. and H.J. Kim analyzed data.

About the Author

Dr. Koo is a diagnostic radiologist in the Chest and Cardiovascular section, Department of Radiology and Research Institute of Radiology, Asan Medical Center, University of Ulsan College of Medicine, Seoul, South Korea. Her research interests include emerging respiratory infections.

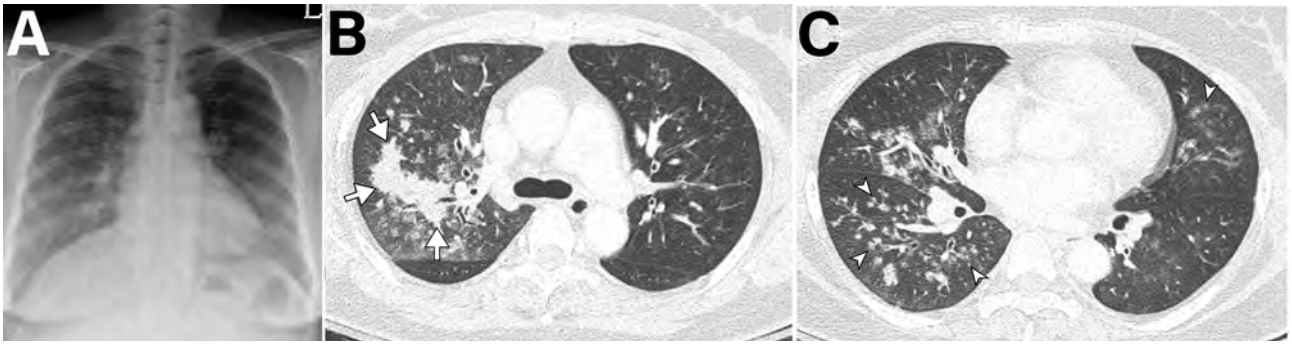

Figure 4. Imaging of 55-year-old immunocompetent woman with human metapneumovirus pneumonia, South Korea. A) Initial chest radiograph showing ill-defined patchy and nodular ground-glass opacities in the right lung and left lower lung zone. B, C) Chest computed tomography showing irregular nodular consolidation (arrows in panel B) and multiple ill-defined centrilobular nodular opacities (arrowheads in panel C) with mild bronchial wall thickening. Five days later, the lesions had resolved completely.

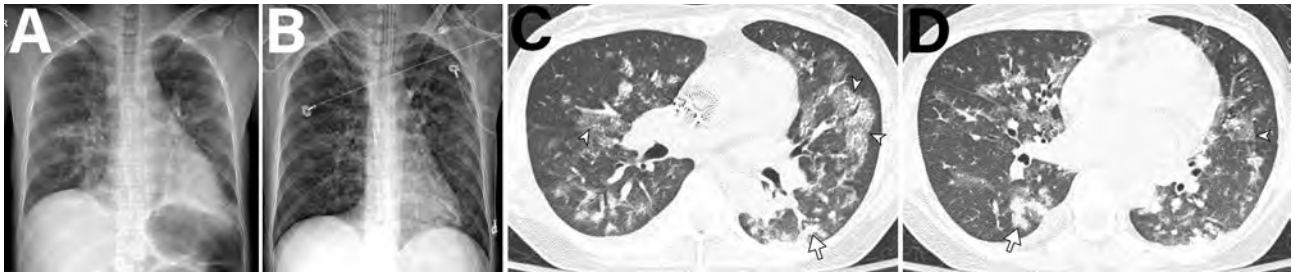

Figure 5. Imaging of 38-year-old woman in South Korea who underwent liver transplantation 2 months earlier, followed by immunosuppressant therapy, who visited the emergency department because of dyspnea, chills, and fever. A) Initial chest radiograph showing bilateral peribronchial infiltration in the central areas of both lungs and minimal pleural effusion. B) Five days later, the patient was admitted to the intensive care unit and underwent intubation because of progressive dyspnea. Radiograph showed extensive bilateral peribronchial nodular infiltrates. C, D) Computed tomography performed on the same day as in panel B showing multifocal peribronchial nodular consolidation (arrows), ground-glass opacities (arrowheads), and irregular small nodules, along with small amounts of bilateral pleural effusion. The patient was given ribavirin and prophylactic antimicrobial drugs and recovered after 10 days in the intensive care unit.

References

1. van den Hoogen BG, de Jong JC, Groen J, Kuiken T, de Groot R, Fouchier RA, et al. A newly discovered human pneumovirus isolated from young children with respiratory tract disease. Nat Med. 2001;7:719–24. http://dx.doi.org/10.1038/89098
2. Lu G, Gonzalez R, Guo L, Wu C, Wu J, Vernet G, et al. Large-scale seroprevalence analysis of human metapneumovirus and human respiratory syncytial virus infections in Beijing, China. Virol J. 2011;8:62. http://dx.doi.org/10.1186/1743-422X-8-62
3. Kahn JS. Epidemiology of human metapneumovirus. Clin Microbiol Rev. 2006;19:546–57. http://dx.doi.org/10.1128/CMR.00014-06
4. Lüsebrink J, Wiese C, Thiel A, Tillmann RL, Ditt V, Müller A, et al. High seroprevalence of neutralizing capacity against human metapneumovirus in all age groups studied in Bonn, Germany. Clin Vaccine Immunol. 2010;17:481–4. http://dx.doi.org/10.1128/CVI.00398-09
5. Boivin G, De Serres G, Hamelin ME, Côté S, Argouin M, Tremblay G, et al. An outbreak of severe respiratory tract infection due to human metapneumovirus in a long-term care facility. Clin Infect Dis. 2007;44:1152–8. http://dx.doi.org/10.1086/513204
6. El Chaer F, Shah DP, Kmeid J, Ariza-Heredia EJ, Hosing CM, Mulanovich VE, et al. Burden of human metapneumovirus infections in patients with cancer: risk factors and outcomes. Cancer. 2017;123:2329–37. http://dx.doi.org/10.1002/cncr.30599
7. Falsey AR, Erdman D, Anderson LJ, Walsh EE. Human metapneumovirus infections in young and elderly adults. J Infect Dis. 2003;187:785–90. http://dx.doi.org/10.1086/367901
8. Kim S, Sung H, Im HJ, Hong SJ, Kim MN. Molecular epidemiological investigation of a nosocomial outbreak of human metapneumovirus infection in a pediatric hemato-oncology patient population. J Clin Microbiol. 2009;47:1221–4. http://dx.doi.org/10.1128/JCM.01959-08
9. Te Wierik MJ, Nguyen DT, Beersma MF, Thijsen SF, Heemstra KA. An outbreak of severe respiratory tract infection caused by human metapneumovirus in a residential care facility for elderly in Utrecht, the Netherlands, January to March 2010. Euro Surveill. 2012;17:17.
10. Englund JA, Boeckh M, Kuypers J, Nichols WG, Hackman RC, Morrow RA, et al. Brief communication: fatal human metapneumovirus infection in stem-cell transplant recipients. Ann Intern Med. 2006;144:344–9. http://dx.doi.org/10.7326/0003-4819-144-5-200603070-00010
11. Sumino KC, Agapov E, Pierce RA, Trulock EP, Pfeifer JD, Ritter JH, et al. Detection of severe human metapneumovirus infection by real-time polymerase chain reaction and histopathological assessment. J Infect Dis. 2005;192:1052–60. http://dx.doi.org/10.1086/432728
12. Walsh EE, Peterson DR, Falsey AR. Human metapneumovirus infections in adults: another piece of the puzzle. Arch Intern Med. 2008;168:2489–96. http://dx.doi.org/10.1001/archinte.168.22.2489
13. Koo HJ, Lee HN, Choi SH, Sung H, Oh SY, Shin SY, et al. Human Metapneumovirus infection: pneumonia risk factors in patients with solid organ transplantation and computed tomography findings. Transplantation. 2018;102:699–706. http://dx.doi.org/10.1097/TP.0000000000001965
14. Seo S, Gooley TA, Kuypers JM, Stednick Z, Jerome KR, Englund JA, et al. Human metapneumovirus infections following hematopoietic cell transplantation: factors associated with disease progression. Clin Infect Dis. 2016;63:178–85. http://dx.doi.org/10.1093/cid/ciw284
15. Renaud C, Xie H, Seo S, Kuypers J, Cent A, Corey L, et al. Mortality rates of human metapneumovirus and respiratory syncytial virus lower respiratory tract infections in hematopoietic cell transplantation recipients. Biol Blood Marrow Transplant. 2013;19:1220–6. http://dx.doi.org/10.1016/j.bbmt.2013.05.005
16. Shah DP, Shah PK, Azzi JM, El Chaer F, Chemaly RF. Human metapneumovirus infections in hematopoietic cell transplant recipients and hematologic malignancy patients: a systematic review. Cancer Lett. 2016;379:100–6. http://dx.doi.org/10.1016/j.canlet.2016.05.035
17. Niggli F, Huber LC, Benden C, Schuurmans MM. Human metapneumovirus in lung transplant recipients: characteristics and outcomes. Infect Dis (Lond). 2016;48:852–6. http://dx.doi.org/10.1080/23744235.2016.1204661
18. Noel N, Rammaert B, Zuber J, Sayre N, Mamzer-Bruneel MF, Leruez-Ville M, et al. Lower respiratory tract infection in a renal transplant recipient: do not forget metapneumovirus. Case Rep Transplant. 2012;2012:353871.
19. Martinello RA, Esper F, Weibel C, Ferguson D, Landry ML, Kahn JS. Human metapneumovirus and exacerbations of chronic obstructive pulmonary disease. J Infect. 2006;53:248–54. http://dx.doi.org/10.1016/j.jinf.2005.11.010
20. Renaud C, Campbell AP. Changing epidemiology of respiratory viral infections in hematopoietic cell transplant recipients and solid organ transplant recipients. Curr Opin Infect Dis. 2011;24:333–43. http://dx.doi.org/10.1097/QCO.0b013e3283480440
21. Weigt SS, Gregson AL, Deng JC, Lynch JP III, Belperio JA. Respiratory viral infections in hematopoietic stem cell and

solid organ transplant recipients. Semin Respir Crit Care Med. 2011;32:471–93. http://dx.doi.org/10.1055/s-0031-1283286
22. Hansell DM, Bankier AA, MacMahon H, McLoud TC, Müller NL, Remy J. Fleischner Society: glossary of terms for thoracic imaging. Radiology. 2008;246:697–722. http://dx.doi.org/10.1148/radiol.2462070712
23. Blumentals WA, Nevitt A, Peng MM, Toovey S. Body mass index and the incidence of influenza-associated pneumonia in a UK primary care cohort. Influenza Other Respi Viruses. 2012;6:28–36. http://dx.doi.org/10.1111/j.1750-2659.2011.00262.x
24. Phung DT, Wang Z. Risk of pneumonia in relation to body mass index in Australian aboriginal people. Epidemiol Infect. 2013; 141:2497–502. http://dx.doi.org/10.1017/S0950268813000605
25. Phung DT, Wang Z, Rutherford S, Huang C, Chu C. Body mass index and risk of pneumonia: a systematic review and meta-analysis. Obes Rev. 2013;14:839–57. http://dx.doi.org/10.1111/obr.12055
26. Nie W, Zhang Y, Jee SH, Jung KJ, Li B, Xiu Q. Obesity survival paradox in pneumonia: a meta-analysis. BMC Med. 2014;12:61. http://dx.doi.org/10.1186/1741-7015-12-61
27. Fisher CE, Preiksaitis CM, Lease ED, Edelman J, Kirby KA, Leisenring WM, et al. Symptomatic respiratory virus infection and chronic lung allograft dysfunction. Clin Infect Dis. 2016;62:313–9. http://dx.doi.org/10.1093/cid/civ871
28. Franquet T, Rodríguez S, Martino R, Salinas T, Giménez A, Hidalgo A. Human metapneumovirus infection in hematopoietic stem cell transplant recipients: high-resolution computed tomography findings. J Comput Assist Tomogr. 2005;29:223–7. http://dx.doi.org/10.1097/01.rct.0000157087.14838.4c
29. Kamboj M, Gerbin M, Huang CK, Brennan C, Stiles J, Balashov S, et al. Clinical characterization of human metapneumovirus infection among patients with cancer. J Infect. 2008;57:464–71. http://dx.doi.org/10.1016/j.jinf.2008.10.003
30. Karimata Y, Kinjo T, Parrott G, Uehara A, Nabeya D, Haranaga S, et al. Clinical features of human metapneumovirus pneumonia in non-immunocompromised patients: an investigation of three long-term care facility outbreaks. J Infect Dis. 2018;218:868–75. http://dx.doi.org/10.1093/infdis/jiy261
31. Shahda S, Carlos WG, Kiel PJ, Khan BA, Hage CA. The human metapneumovirus: a case series and review of the literature. Transpl Infect Dis. 2011;13:324–8. http://dx.doi.org/10.1111/j.1399-3062.2010.00575.x
32. Syha R, Beck R, Hetzel J, Ketelsen D, Grosse U, Springer F, et al. Human metapneumovirus (HMPV) associated pulmonary infections in immunocompromised adults: initial CT findings, disease course and comparison to respiratory-syncytial-virus (RSV) induced pulmonary infections. Eur J Radiol. 2012;81:4173–8. http://dx.doi.org/10.1016/j.ejrad.2012.06.024
33. Kuiken T, van den Hoogen BG, van Riel DA, Laman JD, van Amerongen G, Sprong L, et al. Experimental human metapneumovirus infection of cynomolgus macaques (*Macaca fascicularis*) results in virus replication in ciliated epithelial cells and pneumocytes with associated lesions throughout the respiratory tract. Am J Pathol. 2004;164:1893–900. http://dx.doi.org/10.1016/S0002-9440(10)63750-9
34. Koo HJ, Lim S, Choe J, Choi SH, Sung H, Do KH. Radiographic and CT features of viral pneumonia. Radiographics. 2018;38: 719–39. http://dx.doi.org/10.1148/rg.2018170048
35. Chang A, Masante C, Buchholz UJ, Dutch RE. Human metapneumovirus (HMPV) binding and infection are mediated by interactions between the HMPV fusion protein and heparan sulfate. J Virol. 2012;86:3230–43. http://dx.doi.org/10.1128/JVI.06706-11
36. Kim HK, Oh SH, Yun KA, Sung H, Kim MN. Comparison of Anyplex II RV16 with the xTAG respiratory viral panel and Seeplex RV15 for detection of respiratory viruses. J Clin Microbiol. 2013;51:1137–41. http://dx.doi.org/10.1128/JCM.02958-12

Address for correspondence: Kyung-Hyun Do, Department of Radiology and Research Institute of Radiology, University of Ulsan College of Medicine, Asan Medical Center, 88, Olympic-ro 43-gil, Songpa-gu, Seoul 05505, South Korea; email: dokh@amc.seoul.kr

Enterovirus A71 Infection and Neurologic Disease, Madrid, Spain, 2016

Carmen Niño Taravilla,[1] Isabel Pérez-Sebastián,[1] Alberto García Salido, Claudia Varela Serrano, Verónica Cantarín Extremera, Anna Duat Rodríguez, Laura López Marín, Mercedes Alonso Sanz, Olga María Suárez Traba, Ana Serrano González

Medscape EDUCATION ACTIVITY

In support of improving patient care, this activity has been planned and implemented by Medscape, LLC and Emerging Infectious Diseases. Medscape, LLC is jointly accredited by the Accreditation Council for Continuing Medical Education (ACCME), the Accreditation Council for Pharmacy Education (ACPE), and the American Nurses Credentialing Center (ANCC), to provide continuing education for the healthcare team.

Medscape, LLC designates this Journal-based CME activity for a maximum of 1.00 ***AMA PRA Category 1 Credit(s)™***. Physicians should claim only the credit commensurate with the extent of their participation in the activity.

All other clinicians completing this activity will be issued a certificate of participation. To participate in this journal CME activity: (1) review the learning objectives and author disclosures; (2) study the education content; (3) take the post-test with a 75% minimum passing score and complete the evaluation at http://www.medscape.org/journal/eid; and (4) view/print certificate. For CME questions, see page 201.

Release date: December 14, 2018; Expiration date: December 14, 2019

Learning Objectives

Upon completion of this activity, participants will be able to:

- Assess the epidemiology of possible enterovirus infections among children
- Analyze the symptoms of children with possible enterovirus infection in the current study
- Evaluate possible prognostic factors among children with possible enterovirus infection
- Distinguish the most common sequela after enterovirus infection associated with neurologic symptom

CME Editor

P. Lynne Stockton Taylor, VMD, MS, ELS(D), Technical Writer/Editor, Emerging Infectious Diseases. *Disclosure: P. Lynne Stockton Taylor, VMD, MS, ELS(D), has disclosed no relevant financial relationships.*

CME Author

Charles P. Vega, MD, Clinical Professor, Health Sciences, Department of Family Medicine, University of California, Irvine School of Medicine, Irvine, California. *Disclosure: Charles P. Vega, MD, FAAFP, has disclosed the following relevant financial relationships: served as an advisor or consultant for Johnson & Johnson Pharmaceutical Research & Development, L.L.C.; Shire Pharmaceuticals; and Sunovion Pharmaceuticals Inc.; served as a speaker or a member of a speakers bureau for Shire Pharmaceuticals.*

Authors

Disclosures: ***Carmen Niño Taravilla, MD; Isabel Pérez-Sebastián, MD; Alberto García-Salido, MD, PhD; Claudia Varela Serrano, MD; Verónica Cantarín Extremera, MD,; Anna Duat Rodríguez, PhD; Laura López Marín, MD; Mercedes Alonso Sanz, MD; Olga María Suárez Traba, MD;*** *and* ***Ana Serrano-González, MD, PhD,*** *have disclosed no relevant financial relationships.*

Author affiliation: Hospital Infantil Universitario Niño Jesús, Madrid, Spain

[1]These authors contributed equally to this article.

DOI: https://doi.org/10.3201/eid2501.181089

We conducted an observational study from January 2016 through January 2017 of patients admitted to a reference pediatric hospital in Madrid, Spain, for neurologic symptoms and enterovirus infection. Among the 30 patients, the most common signs and symptoms were fever, lethargy, myoclonic jerks, and ataxia. Real-time PCR detected enterovirus in the cerebrospinal fluid of 8 patients, nasopharyngeal aspirate in 17, and anal swab samples of 5. The enterovirus was genotyped for 25 of 30 patients; enterovirus A71 was the most common serotype (21/25) and the only serotype detected in patients with brainstem encephalitis or encephalomyelitis. Treatment was intravenous immunoglobulins for 21 patients and corticosteroids for 17. Admission to the pediatric intensive care unit was required for 14 patients. All patients survived. At admission, among patients with the most severe disease, leukocytes were elevated. For children with brainstem encephalitis or encephalomyelitis, clinicians should look for enterovirus and not limit testing to cerebrospinal fluid.

Enteroviruses (family *Picornaviridae*) are RNA viruses; the >100 recognized enterovirus types are classified into 4 species, A–D. Enterovirus infections are common worldwide and occur mostly among children; infections are usually asymptomatic or mild but can produce severe neurologic disease (*1*). Enterovirus A71 (EV-A71) has emerged as an etiologic agent of aseptic meningitis, encephalitis, encephalomyelitis, acute flaccid paralysis, and other severe systemic disorders, including neurogenic pulmonary edema, and cardiopulmonary failure (*2*). The first outbreak of EV-A71–associated neurologic disease occurred in California in the 1960s (*3*). Since then, epidemics have been reported in the Asia-Pacific region (*4*–*7*). In Europe, an outbreak was first described in Bulgaria and Hungary in the 1970s (*8*,*9*). During 2016, an outbreak of enterovirus with neurologic involvement was detected in Spain. The first case described was that of acute flaccid paralysis associated with enterovirus D68 in Catalonia, followed by another 3 cases in Aragón, Galicia, and Asturias. During April–June 2016 in Catalonia, several cases of brainstem encephalitis and encephalomyelitis associated with EV-A71 infection affected >100 children (*10*–*16*). Since May 2016, increased numbers of enterovirus central nervous system (CNS) infections have been observed in Madrid.

In this article, we describe the epidemiology, clinical data, therapies, and clinical progression of children hospitalized at Hospital Infantil Universitario Niño Jesús of Madrid during 2016 because of neurologic signs and symptoms and confirmed enterovirus infection. We also describe which variables were associated with severe disease and worst prognoses.

We enrolled only patients for whom written informed consent was obtained from the next of kin, caretakers, or guardians on behalf of the children. The study was approved by the Hospital Infantil Universitario Niño Jesús of Madrid (Spain) ethics committee. The research was conducted according to The Code of Ethics of the World Medical Association (Declaration of Helsinki).

Material and Methods

Study Design

This study was an observational prospective study of children admitted to the Hospital Infantil Universitario Niño Jesús of Madrid from January 2016 to January 2017 because of neurologic symptoms with suspicion of enterovirus infection (meningitis, meningoencephalitis, encephalomyelitis, brainstem encephalitis, or acute flaccid paralysis). The hospital is a 230-bed reference medical center for patients with high-complexity pathologic conditions.

We included children with a clinical diagnosis of meningitis, encephalitis, brainstem encephalitis, encephalomyelitis with or without autonomic dysfunction, or flaccid paralysis resulting from spinal cord involvement. We excluded children with neurologic impairment but no enterovirus isolation.

Data Collection and Diagnosis

For each patient, we collected demographic, clinical, biological, microbiological, and radiographic data. Demographic data were patient sex, age in months, and hospitalization duration. Clinical data were past medical condition(s); fever duration; respiratory, gastrointestinal, and neurologic symptoms; and mucocutaneous manifestations. Biological data were leukocytosis (>15,000 leukocytes/mm^3), thrombocytosis (>400,000 thrombocytes/mm^3), and C-reactive protein and procalcitonin levels. Microbiological data were blood and cerebrospinal fluid (CSF) analysis and bacterial culture results. For each patient, we tested CSF for enterovirus by real-time PCR and for herpes simplex virus by reverse transcription PCR. If those PCRs were negative, we collected nasopharyngeal aspirates and anal swab samples for enterovirus detection by real-time PCR. Enterovirus-positive samples were genotyped at the Enterovirus Unit of the National Centre for Microbiology (Institute of Public Health "Carlos III," Madrid, Spain). Radiologic data were from imaging studies performed on all children with rhomboencephalitis, acute flaccid paralysis, or neurologic deterioration. Studies included brain and spine magnetic resonance imaging (MRI).

Management and Follow-Up

Patients with meningoencephalitis or rhomboencephalitis and substantial somnolence or incipient bulbar clinical signs received intravenous immunoglobulins (IVIG) (400 mg/kg 1×/d for 5 d). Patients with signs of bulbar or medullary involvement or with lesions suggestive of

rhomboencephalitis seen on MR images received methylprednisolone (30 mg/kg 1×/d for 3–5 d) and fluoxetine (0.3 mg/kg 1×/d for 14 d). Each patient underwent a follow-up examination at 1 and 3 months after hospital admission. To stratify the severity of illness, we used the World Health Organization (WHO) Guide to Clinical Management and Public Health Response for Hand, Foot and Mouth Disease (*15*). The 6 clinical conditions classified by WHO are aseptic meningitis, encephalitis, brainstem encephalitis (rhomboencephalitis), encephalomyelitis, autonomic nervous system dysfunction, and cardiopulmonary failure.

Statistical Analyses

We report descriptive statistics in terms of absolute frequencies and percentages. For data comparisons of categorical variables, we used Pearson χ^2 or Fisher exact tests when appropriate. We describe continuous nonnormal distributed variables as median values and interquartile ranges (IQRs) and compared them by using the Mann-Whitney U test and Kruskal-Wallis analysis. Statistical analyses were performed with SPSS version 22.0 software (https://www.ibm.com/es-es/marketplace/spss-statistics). We considered $p<0.05$ as statistically significant.

Results

Epidemiologic Data

During the study period, 42 patients were hospitalized for suspected enterovirus neurologic disease. For 12 patients, other causes for their neurologic signs were identified or enterovirus was not isolated. Of the 30 remaining patients, median age was 23 months (IQR 16–41 months), 18 were male, and 26 became ill during May–September (peak incidence [8 cases] in July) (Table; Figure 1).

Clinical Manifestations

Of the 30 patients included in the study, fever (axillary temperature ≥38°C [100.4°F]) was observed for 22, vomiting for 21, fatigue for 20, headache for 11, catarrhal symptoms for 6, and diarrhea for 2. Mucocutaneous manifestations were observed for 6 patients; the main manifestation was petechial rash on the extremities. The most common neurologic sign among the 30 patients was lethargy or drowsiness for 24, followed by myoclonic jerks for 4, tremor for 7, and ataxia for 17. One patient had tetraparesis and another had paresis isolated to the right arm. Cardiorespiratory failure (cardiogenic shock and neurogenic pulmonary edema) developed in 3 patients; 1 experienced cardiac arrest, which was reversed with advanced cardiopulmonary resuscitation maneuvers. For those who experienced them, fever and neurologic signs started a median of 3 days (IQR 1.25–5 days) before hospitalization.

Supplementary Testing

Blood analysis revealed leukocytosis in 10 patients and thrombocytosis in 9. No patient had significant alterations in plasma C-reactive protein levels, and only 1 showed elevated procalcitonin levels (3.6 ng/mL [reference value 0.5 ng/mL]).

All patients underwent lumbar puncture. CSF analyses showed a median leukocyte count of 112 leukocytes/mm^3 (IQR 28–211 leukocytes/mm^3) and an average mononuclear cell percentage of 56% (IQR 19.5%–90.0%). For only 3 patients CSF contained <10 leukocytes/mm^3 (reference count). In the CSF, the median level of protein was 32.5 mg/dL (IQR 26–46 mg/dL) and of glucose 62.5 mg/dL (IQR 55–67 mg/dL). In no patient was the glucose level <50 mg/dL.

Real-time PCR detected enterovirus in CSF of 8 of the 30 patients, all of whom had aseptic meningitis. Patients for whom CSF analysis was negative underwent nasopharyngeal aspirate or anal swab sample testing for enterovirus by the same real-time PCR. An enterovirus was isolated from nasopharyngeal aspirate of 17 of the 30 patients and from anal swab samples of 5. The enterovirus from 25 of 30 patients was genotyped; most frequently identified was EV-A71 (21 patients), followed by echovirus (2 patients), enterovirus B (1 patient), and rhinovirus (1 patient). EV-A71 was the only serotype detected in patients with brainstem encephalitis or encephalomyelitis and was isolated from respiratory and fecal samples. Patients from whom other enteroviruses (echovirus, enterovirus B, or rhinovirus) were isolated received a diagnosis of meningitis or encephalitis. No cultures of CSF or blood were positive for bacteria. In no patient was herpes simplex virus detected in CSF.

MRI was performed for 26 of the 30 patients; results were within normal limits for 5. Among the 26 patients, the radiologic abnormalities identified were leptomeningeal enhancement in 5, alteration of the signal of the white matter in the rhomboencephalic region (bulb, protuberance, cerebellum, or fourth ventricle) in 16, and cervical myelopathy in 3 (Figures 2, 3).

Treatment

Of the 30 patients, 21 received IVIG; 17 received corticosteroids, and 11 of those 17 received corticosteroids and fluoxetine. No patient with aseptic meningitis or encephalitis received treatment.

Outcomes and Variables Associated with More Severe Disease

Median hospital stay was 10 days (IQR 6–14.5 days). Fourteen patients were admitted to the pediatric intensive care unit (PICU) because of decreased consciousness level (9 patients), paresis (1 patient), or automatic nervous system

Table. Enterovirus serotype, localization of isolation, WHO clinical classification, and outcomes for 30 patients with enterovirus infection and neurologic disease, Madrid, 2016*

Patient no.	Patient age/sex	WHO clinical classification	Enterovirus source	Enterovirus serotype	Patient outcome
1	2 mo/M	Aseptic meningitis	CSF	Genotyped negative	Recovered
2	16 d/F	Aseptic meningitis	CSF	ND	Recovered
3	3 mo/F	Encephalitis	Nasopharyngeal aspirate	A71	Recovered
4	10 mo/F	Encephalitis	Nasopharyngeal aspirate	A71	Recovered
5	12 mo/M	Brainstem encephalitis	Nasopharyngeal aspirate	A71	Unknown
6	17 mo/F	Brainstem encephalitis	Nasopharyngeal aspirate	Genotyped negative	Unknown
7	21 mo/F	Brainstem encephalitis	Nasopharyngeal aspirate	A71	Cerebellar dysfunction
8	22 mo/F	Encephalitis	Nasopharyngeal aspirate	Rhinovirus	Recovered
9	19 mo/M	Encephalitis	Nasopharyngeal aspirate	A71	Unknown
10	18 mo/M	Encephalitis	Anal swab sample	A71	Cerebellar dysfunction
11	2 y/M	Brainstem encephalitis	Nasopharyngeal aspirate	A71	Recovered
12	2 y/M	Cardiopulmonary failure	Nasopharyngeal aspirate	A71	Acquired brain damage
13	23 mo/F	Cardiopulmonary failure	Anal swab sample	A71	Cerebellar dysfunction
14	2 y/M	Encephalitis	Nasopharyngeal aspirate	B	Recovered
15	3 y/M	Brainstem encephalitis	Nasopharyngeal aspirate	A71	Recovered
16	3 y/F	Brainstem encephalitis	Anal swab sample	A71	Recovered
17	3 y/F	Cardiopulmonary failure	Nasopharyngeal aspirate	A71	Paresis of the right upper limb
18	4 y/F	Brainstem encephalitis	Nasopharyngeal aspirate	A71	Cerebellar dysfunction
19	4 y/M	Aseptic meningitis	CSF	ND	Recovered
20	4 y/M	Brainstem encephalitis	Nasopharyngeal aspirate	A71	Cerebellar dysfunction
21	4 y/M	Aseptic meningitis	CSF	Echovirus	Recovered
22	6 y/M	Aseptic meningitis	CSF	ND	Recovered
23	6 y/F	Aseptic meningitis	CSF	Echovirus	Recovered
24	7 y/M	Brainstem encephalitis	Nasopharyngeal aspirate	A71	Cerebellar dysfunction
25	1 mo/M	Encephalitis	CSF	A71	Recovered
26	4 y/M	Encephalitis	Nasopharyngeal aspirate	A71	Recovered
27	5 y/M	ANS dysfunction	Nasopharyngeal aspirate	A71	Cerebellar dysfunction
28	2 y/F	Encephalitis	Nasopharyngeal aspirate	A71	Recovered
29	2 y/M	Brainstem encephalitis	Anal swab sample	A71	Recovered
30	20 mo/M	Brainstem encephalitis	Anal swab sample	A71	Peripheral facial paralysis

*ANS, autonomic nervous system; CSF, cerebrospinal fluid; ND, not done; WHO, World Health Organization.

dysregulation (4 patients, among whom 3 exhibited cardiorespiratory failure and required mechanical ventilation and treatment with an inotrope such as milrinone). The median PICU stay was 9.5 days (IQR 1.5–47 days). None of these patients died.

At the time of hospital discharge, 20 children experienced no sequelae, 7 had cerebellar dysfunction that consisted of slightly wide foot placement while walking or slight instability while sitting, 1 had paresis of the right upper limb, and 1 had peripheral facial paralysis. Another patient had acquired brain damage. Follow-up examination at 3 months after hospital admission detected only slight cerebellar alteration in 2 patients and a mild motor deficit with difficulty extending the right upper limb in 1 patient.

Of the patients with autonomic nervous system dysregulation and cardiorespiratory failure, 1 had acquired brain damage requiring a tracheostomy and a nasogastric tube for feeding. At the time of the most recent follow-up examination (June 30, 2018), the patient no longer required mechanical ventilation or the nasogastric tube for feeding.

In terms of clinical and analytical criteria, only the number of leukocytes in the blood at the time of admission was significantly higher in patients with the most severe disease (according to WHO classification) ($p = 0.00$). Of the 30 patients, all 3 with cardiopulmonary failure exhibited bulbar inflammatory lesions on MR images, but this finding was also found in 13 patients without autonomic nervous system dysfunction.

Discussion

The outbreak we report occurred in spring and summer, the typical prevalence pattern of enterovirus in Spain (*17*). The first outbreak of CNS disease associated with EV-A71 in Spain occurred in March 2016, when the

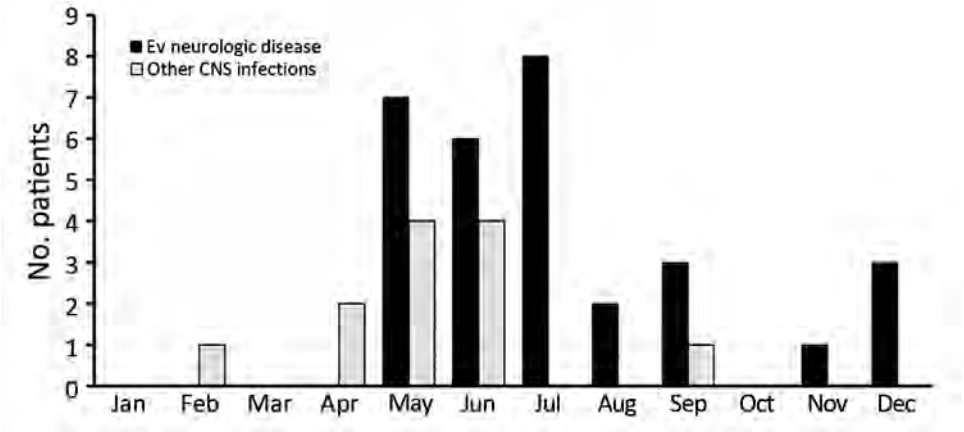

Figure 1. Monthly distribution of patients admitted to Hospital Infantil Universitario Niño Jesús, Madrid, Spain, for CNS infections in 2016. CNS, central nervous system; EV, enterovirus.

number of children with neurologic syndromes caused by enterovirus infection in Catalonia increased (*13*,*15*). In the rest of Spain, some sporadic cases occurred, but no reports were published. In our case series of concurrent neurologic disease and enterovirus infection, the main cause was EV-A71. In the Catalonia outbreak and in the cases reported here, infection with enterovirus D68, a serotype that may cause an acute flaccid polio-like paralysis in children with previous respiratory infections, was ruled out. Since 2012, the incidence of fever and hand, foot, and mouth disease (HFMD) caused by EV-A71 was increasing in Spain, but until 2016 this virus had not produced severe neurologic disease (*16*).

The clinical characteristics of the patients in our study were similar to those of patients described in other case series: young children (<5 years of age) with fever and respiratory or gastrointestinal symptoms, followed 3–5 days later by neurologic signs. The rate of mucocutaneous manifestations in patients in our study was low. The neurologic signs were drowsiness, ataxia, and positive meningeal signs, concordant with signs described in the literature (*12*,*13*,*18*,*19*). Myoclonic jerks were rare among patients in our study compared with patients in other case series (*20*,*21*).

Detection of EV-A71 from sterile sites is specific but usually insensitive. Virus is detected in 0%–5% of CSF samples from patients with neurologic disease. Real-time PCR for enterovirus in CSF was negative for 83.3% of patients in our study, and most diagnoses were made from nasopharyngeal aspirates or anal swab samples, as described elsewhere (*1*,*2*,*10*–*15*,*18*,*19*,*22*). This finding may be because the neurologic involvement is caused by an immune-mediated response (*22*,*23*) or because of earlier enterovirus elimination from CSF (*19*). Consequently, diagnostic assessments should include specimens from multiple sites. Disease was less severe for patients with positive PCR results for enterovirus in CSF.

Of the radiologic studies, the most specific was the MRI, which showed tegmental-protuberancial involvement (characteristic high-signal intensities on T2-weighted images). A restricted diffusion pattern was observed in images of patients with severe disease (the 3 patients with

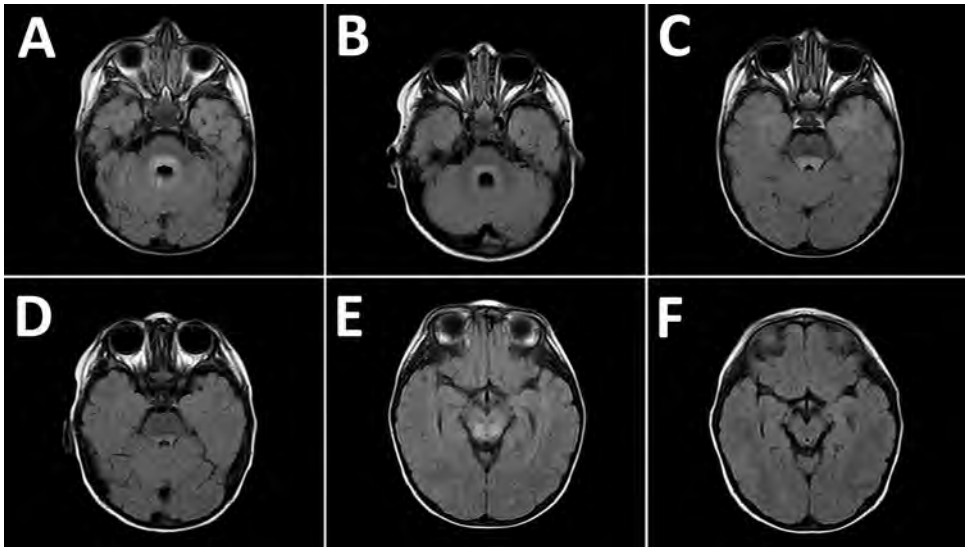

Figure 2. Magnetic resonance images of the brain of a 2-year-old boy with enterovirus meningoencephalitis. A–C) Brain at time of diagnosis. FLAIR sequences show hyperintense lesions around ventricle IV (A), posterior region of the pons (B), and posterior region of the mesencephalon (C). D–F) Control images of cerebrum 6 months after diagnosis. FLAIR sequences show slight hyperintensity of signal around ventricle IV, lower than in the initial study (D), and complete resolution of lesions in the posterior region of the pons (E) and mesencephalon (F).

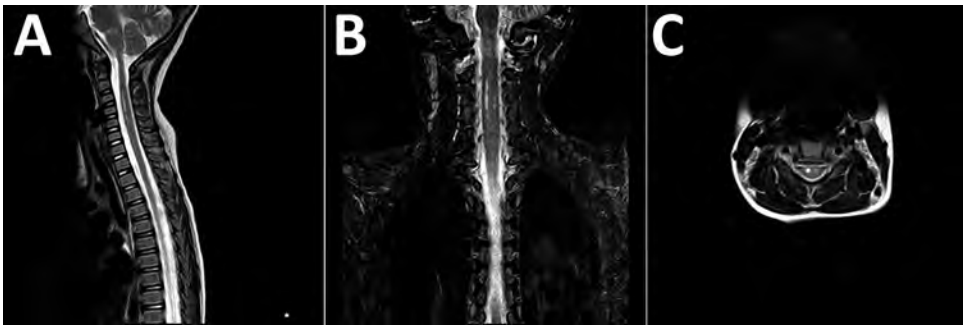

Figure 3. Magnetic resonance images of brain of a 3-year-old girl with enterovirus encephalomyelitis (paresis of the right upper limb). A) Image of the cervical spine: sagittal T2 sequence; B) short tau inversion recovery (STIR) coronal sequence; C) T2 axial sequence. Hyperintense filiform lesions in the anterolateral regions of the spinal cord (C3–C5), predominantly right, are suggestive of myelitis.

cardiopulmonary failure). In this study, lesions detected on MR images coincided with those described in the literature (*12*,*19*,*24*,*25*); we found a high number of patients who had nonsevere symptoms and MR images indicating bulbar involvement.

There is no proven effective therapy for EV-A71 infections. Antiviral drugs, corticosteroids, and IGIV have been used. The treatment given to patients in this series was chosen because it had been effective in other patients with enterovirus infection and CNS disease (*1*,*2*,*11*–*15*,*18*–*22*,*26*–*30*) and because it is a common treatment for viral and inflammatory myelitis (*31*). During the first outbreaks in Asia, IGIV was already in use, and a retrospective comparison suggests that this treatment was beneficial (*32*,*33*). However, the use of corticosteroids has been questioned after publication of a comparative study (*34*). In our experience, all patients with severe disease received corticosteroids, even though WHO does not recommend them for patients with HFMD of any severity.

Fluoxetine inhibits replication of enterovirus B and D but not of enterovirus A or C or of rhinovirus (*35*–*37*). At the time of admission, some of our patients received fluoxetine because we did not know the type of enterovirus; after the serotype was known to be A71, use of fluoxetine was not indicated.

Several antiviral drugs are available. Pleconaril is an antiviral drug that inhibits the entry of enteroviruses into cells, but it is not active against enterovirus serotypes A71 or D68 (*28*). Other antiviral drugs, such as pocapavir and vapendavir, have not been shown to be effective (*38*).

Concern about enterovirus outbreaks and the lack of effective treatment is growing. Many EV-A71 vaccines have been studied (*39*–*45*). In China, 2 inactivated EV-A71 vaccines have been approved for the prevention of severe HFMD (*46*). Efficacy, immunogenicity, and safety were reported, concluding that vaccine efficacy was 94.84% (CI 83.53%–98.38%) and, in the second year, 100% (CI 84.15%–100%) against HFMD related to EV-A71 (*47*). No serious adverse events related to the vaccine have been described (*47*). As a result of these data, the potential severity of disease, and the lack of etiologic treatment, this vaccination could be the most useful preventive strategy.

The severity of the neurologic involvement and the lethality of the different outbreaks described for enterovirus vary (*1*,*2*,*10*–*15*,*18*–*22*). In our case series, prognoses were favorable, and no patients died. However, 1 in 2 patients was admitted to the PICU. Three patients with autonomic nervous system dysfunction and cardiopulmonary failure required mechanical ventilation and inotropes. One required tracheostomy and feeding by nasogastric tube, and another experienced paresis of the right upper limb. We found statistically significant leukocytosis only in the most severely affected children, as has been described (*1*,*2*,*19*).

Our study has several limitations because it is an observational single-center study. The treatment used was empirically prescribed, thus limiting conclusions about effectiveness. The rate of sequelae was low, but long-term follow-up was not conducted. A multicenter study would be desirable.

In conclusion, the serotype most frequently isolated from the patients in our series was EV-A71. PCRs from respiratory and gastrointestinal tract samples had higher diagnostic value than PCRs of CSF. Treatment with IVIGs and corticosteroids was administered according to disease severity. Higher leukocyte counts were associated with more severe disease. There were no deaths and only 2 patients experienced significant sequelae, but almost half of the patients required admission to the PICU. For children with brainstem encephalitis or encephalomyelitis, infection with EV-A71 should be suspected. Diagnostic testing should include nasopharyngeal and anal swab samples as well as CNS fluid.

About the Author

Dr. Niño Taravilla is a pediatrician who works in the PICU at the Hospital Infantil Universitario Niño Jesús, Madrid, Spain. Her research interest is CNS infections.

References

1. Lugo D, Krogstad P. Enteroviruses in the early 21st century: new manifestations and challenges. Curr Opin Pediatr. 2016;28:107–13. http://dx.doi.org/10.1097/MOP.0000000000000303
2. Ooi MH, Wong SC, Lewthwaite P, Cardosa MJ, Solomon T. Clinical features, diagnosis, and management of enterovirus 71.

Lancet Neurol. 2010;9:1097–105. http://dx.doi.org/10.1016/S1474-4422(10)70209-X
3. Schmidt NJ, Lennette EH, Ho HH. An apparently new enterovirus isolated from patients with disease of the central nervous system. J Infect Dis. 1974;129:304–9. http://dx.doi.org/10.1093/infdis/129.3.304
4. Ho M, Chen ER, Hsu KH, Twu SJ, Chen KT, Tsai SF, et al.; Taiwan Enterovirus Epidemic Working Group. An epidemic of enterovirus 71 infection in Taiwan. N Engl J Med. 1999;341:929–35. http://dx.doi.org/10.1056/NEJM199909233411301
5. Komatsu H, Shimizu Y, Takeuchi Y, Ishiko H, Takada H. Outbreak of severe neurologic involvement associated with enterovirus 71 infection. Pediatr Neurol. 1999;20:17–23. http://dx.doi.org/10.1016/S0887-8994(98)00087-3
6. Ooi MH, Wong SC, Podin Y, Akin W, del Sel S, Mohan A, et al. Human enterovirus 71 disease in Sarawak, Malaysia: a prospective clinical, virological, and molecular epidemiological study. Clin Infect Dis. 2007;44:646–56. http://dx.doi.org/10.1086/511073
7. Chan KP, Goh KT, Chong CY, Teo ES, Lau G, Ling AE. Epidemic hand, foot and mouth disease caused by human enterovirus 71, Singapore. Emerg Infect Dis. 2003;9:78–85. http://dx.doi.org/10.3201/eid1301.020112
8. Chumakov M, Voroshilova M, Shindarov L, Lavrova I, Gracheva L, Koroleva G, et al. Enterovirus 71 isolated from cases of epidemic poliomyelitis-like disease in Bulgaria. Arch Virol. 1979;60:329–40. http://dx.doi.org/10.1007/BF01317504
9. Nagy G, Takátsy S, Kukán E, Mihály I, Dömök I. Virological diagnosis of enterovirus type 71 infections: experiences gained during an epidemic of acute CNS diseases in Hungary in 1978. Arch Virol. 1982;71:217–27. http://dx.doi.org/10.1007/BF01314873
10. Launes C, Casas-Alba D, Fortuny C, Valero-Rello A, Cabrerizo M, Muñoz-Almagro C. Utility of FilmArray meningitis/encephalitis panel during an outbreak of enterovirus brainstem encephalitis in Catalonia in 2016. J Clin Microbiol. 2016;55:336–8. http://dx.doi.org/10.1128/JCM.01931-16
11. European Centre for Disease Prevention and Control. Rapid risk assessment: enterovirus detections associated with severe neurological symptoms in children and adults in European countries, 8 August 2016 [cited 2017 Aug 5]. https://ecdc.europa.eu/en/publications-data/rapid-risk-assessment-enterovirus-detections-associated-severe-neurological
12. Felipe-Rucián A, Macaya-Ruiz A. Outbreak of acute neurological disease associated to enterovirus in Catalonia: neuropaediatric aspects [in Spanish]. Rev Neurol. 2016;63:3–4.
13. Casas-Alba D, de Sevilla MF, Valero-Rello A, Fortuny C, García-García JJ, Ortez C, et al. Outbreak of brainstem encephalitis associated with enterovirus-A71 in Catalonia, Spain (2016): a clinical observational study in a children's reference centre in Catalonia. Clin Microbiol Infect. 2017;23:874–81. https://dx.doi.org/10.1016/j.cmi.2017.03.016
14. Otero-Romero S, Campins-Marti M. Outbreak of acute neurological disease associated to enterovirus in Catalonia: epidemiological aspects [in Spanish]. Rev Neurol. 2016;63:1–2.
15. Cardosa J, Farrar J, Yeng C. A guide to clinical management and public health response for hand, foot and mouth disease (HFMD) [cited 2017 Aug 5]. http://www.wpro.who.int/publications/docs/GuidancefortheclinicalmanagementofHFMD.pdf
16. Cabrerizo M, Tarragó D, Muñoz-Almagro C, Del Amo E, Domínguez-Gil M, Eiros JM, et al. Molecular epidemiology of enterovirus 71, coxsackievirus A16 and A6 associated with hand, foot and mouth disease in Spain. Clin Microbiol Infect. 2014;20:O150–6. http://dx.doi.org/10.1111/1469-0691.12361
17. Rodà D, Pérez-Martínez E, Cabrerizo M, Trallero G, Martínez-Planas A, Luaces C, et al. Clinical characteristics and molecular epidemiology of enterovirus infection in infants <3 months in a referral paediatric hospital of Barcelona. Eur J Pediatr. 2015;174:1549–53. http://dx.doi.org/10.1007/s00431-015-2571-z
18. Rudolph H, Schroten H, Tenenbaum T. Enterovirus infection of the central nervous system in children: an update. Pediatr Infect Dis J. 2016;35:567–9. http://dx.doi.org/10.1097/INF.0000000000001090
19. Teoh HL, Mohammad SS, Britton PN, Kandula T, Lorentzos MS, Booy R, et al. Clinical characteristics and functional motor outcomes of enterovirus 71 neurological disease in children. JAMA Neurol. 2016;73:300–7. http://dx.doi.org/10.1001/jamaneurol.2015.4388
20. Hu Y, Jiang L, Peng HL. Clinical analysis of 134 children with nervous system damage caused by enterovirus 71 infection. Pediatr Infect Dis J. 2015;34:718–23. http://dx.doi.org/10.1097/INF.0000000000000711
21. Zhang Q, MacDonald NE, Smith JC, Cai K, Yu H, Li H, et al. Severe enterovirus type 71 nervous system infections in children in the Shanghai region of China: clinical manifestations and implications for prevention and care. Pediatr Infect Dis J. 2014;33:482–7. http://dx.doi.org/10.1097/INF.0000000000000194
22. Huang PN, Shih SR. Update on enterovirus 71 infection. Curr Opin Virol. 2014;5:98–104. http://dx.doi.or g/10.1016/j.coviro.2014.03.007
23. Lin JY, Shih SR. Cell and tissue tropism of enterovirus 71 and other enteroviruses infections. J Biomed Sci. 2014;21:18. http://dx.doi.org/10.1186/1423-0127-21-18
24. Shen WC, Chiu HH, Chow KC, Tsai CH. MR imaging findings of enteroviral encephalomyelitis: an outbreak in Taiwan. AJNR Am J Neuroradiol. 1999;20:1889–95.
25. Chen CY, Chang YC, Huang CC, Lui CC, Lee KW, Huang SC. Acute flaccid paralysis in infants and young children with enterovirus 71 infection: MR imaging findings and clinical correlates. AJNR Am J Neuroradiol. 2001;22:200–5.
26. Pérez-Vélez CM, Anderson MS, Robinson CC, McFarland EJ, Nix WA, Pallansch MA, et al. Outbreak of neurologic enterovirus type 71 disease: a diagnostic challenge. Clin Infect Dis. 2007;45:950–7. http://dx.doi.org/10.1086/521895
27. Prager P, Nolan M, Andrews IP, Williams GD. Neurogenic pulmonary edema in enterovirus 71 encephalitis is not uniformly fatal but causes severe morbidity in survivors. Pediatr Crit Care Med. 2003;4:377–81. http://dx.doi.org/10.1097/01.PCC.0000074274.58997.FE
28. Wang SM, Lei HY, Liu C. Cytokine immunopathogenesis of enterovirus 71 brain stem encephalitis. Clin Dev Immunol. 2012;2012:876241.https://dx.doi.org/10.1155/2012/876241
29. Wang SM, Lei HY, Huang MC, Su LY, Lin HC, Yu CK, et al. Modulation of cytokine production by intravenous immunoglobulin in patients with enterovirus 71-associated brainstem encephalitis. J Clin Virol. 2006;37:47–52. http://dx.doi.org/10.1016/j.jcv.2006.05.009
30. Tan CW, Lai JK, Sam IC, Chan YF. Recent developments in antiviral agents against enterovirus 71 infection. J Biomed Sci. 2014;21:14. http://dx.doi.org/10.1186/1423-0127-21-14
31. Defresne P, Meyer L, Tardieu M, Scalais E, Nuttin C, De Bont B, et al. Efficacy of high dose steroid therapy in children with severe acute transverse myelitis. J Neurol Neurosurg Psychiatry. 2001;71:272–4. http://dx.doi.org/10.1136/jnnp.71.2.272
32. Ooi MH, Wong SC, Mohan A, Podin Y, Perera D, Clear D, et al. Identification and validation of clinical predictors for the risk of neurological involvement in children with hand, foot, and mouth disease in Sarawak. BMC Infect Dis. 2009;9:3. http://dx.doi.org/10.1186/1471-2334-9-3

33. Chang LY, Hsia SH, Wu CT, Huang YC, Lin KL, Fang TY, et al. Outcome of enterovirus 71 infections with or without stage-based management: 1998 to 2002. Pediatr Infect Dis J. 2004; 23:327–32. http://dx.doi.org/10.1097/00006454-200404000-00010
34. Zhang G, Wang J, Yao G, Shi B. Efficacy of high-dose methylprednisolone pulse therapy in the treatment of enterovirus 71 encephalitis. Pak J Pharm Sci. 2016;29(Suppl):1421–7.
35. Holm-Hansen CC, Midgley SE, Fischer TK. Global emergence of enterovirus D68: a systematic review. Lancet Infect Dis. 2016;16:e64–75. http://dx.doi.org/10.1016/S1473-3099(15)00543-5
36. Tyler KL. Rationale for the evaluation of fluoxetine in the treatment of enterovirus D68-associated acute flaccid myelitis. JAMA Neurol. 2015;72:493–4. http://dx.doi.org/10.1001/jamaneurol. 2014.4625
37. Ulferts R, van der Linden L, Thibaut HJ, Lanke KH, Leyssen P, Coutard B, et al. Selective serotonin reuptake inhibitor fluoxetine inhibits replication of human enteroviruses B and D by targeting viral protein 2C. Antimicrob Agents Chemother. 2013;57:1952–6. http://dx.doi.org/10.1128/AAC.02084-12
38. Chen TC, Weng KF, Chang SC, Lin JY, Huang PN, Shih SR. Development of antiviral agents for enteroviruses. J Antimicrob Chemother. 2008;62:1169–73. http://dx.doi.org/10.1093/jac/dkn424
39. Zhu FC, Meng FY, Li JX, Li XL, Mao QY, Tao H, et al. Efficacy, safety, and immunology of an inactivated alum-adjuvant enterovirus 71 vaccine in children in China: a multicentre, randomised, double-blind, placebo-controlled, phase 3 trial. Lancet. 2013;381:2024–32. http://dx.doi.org/10.1016/S0140-6736(13)61049-1
40. Zhu F, Xu W, Xia J, Liang Z, Liu Y, Zhang X, et al. Efficacy, safety, and immunogenicity of an enterovirus 71 vaccine in China. N Engl J Med. 2014;370:818–28. http://dx.doi.org/10.1056/NEJMoa1304923
41. Li R, Liu L, Mo Z, Wang X, Xia J, Liang Z, et al. An inactivated enterovirus 71 vaccine in healthy children. N Engl J Med. 2014;370:829–37. http://dx.doi.org/10.1056/NEJMoa1303224
42. Chung YC, Ho MS, Wu JC, Chen WJ, Huang JH, Chou ST, et al. Immunization with virus-like particles of enterovirus 71 elicits potent immune responses and protects mice against lethal challenge. Vaccine. 2008;26:1855–62. http://dx.doi.org/10.1016/j.vaccine.2008.01.058
43. Tung WS, Bakar SA, Sekawi Z, Rosli R. DNA vaccine constructs against enterovirus 71 elicit immune response in mice. Genet Vaccines Ther. 2007;5:6. http://dx.doi.org/10.1186/1479-0556-5-6
44. Foo DG, Alonso S, Phoon MC, Ramachandran NP, Chow VT, Poh CL. Identification of neutralizing linear epitopes from the VP1 capsid protein of enterovirus 71 using synthetic peptides. Virus Res. 2007;125:61–8. http://dx.doi.org/10.1016/j.virusres.2006.12.005
45. Xu J, Qian Y, Wang S, Serrano JM, Li W, Huang Z, et al. EV71: an emerging infectious disease vaccine target in the Far East? Vaccine. 2010;28:3516–21. http://dx.doi.org/10.1016/j.vaccine.2010.03.003
46. Reed Z, Cardosa MJ. Status of research and development of vaccines for enterovirus 71. Vaccine. 2016;34:2967–70. http://dx.doi.org/10.1016/j.vaccine.2016.02.077
47. Wei M, Meng F, Wang S, Li J, Zhang Y, Mao Q, et al. 2-Year efficacy, immunogenicity, and safety of Vigoo enterovirus 71 vaccine in healthy Chinese children: a randomized open-label study. J Infect Dis. 2017;215:56–63. http://dx.doi.org/10.1093/infdis/jiw502

Address for correspondence: Carmen Niño Taravilla, Hospital Infantil Universitario Niño Jesús, Pediatric Intensive Care, Avenida Menéndez Pelayo 65, 28009 Madrid, Spain; email: carmen.nino@hotmail.com

Epidemiology of Imported Infectious Diseases, China, 2005–2016

Yali Wang,[1] Xuan Wang,[1] Xiaobo Liu,[1] Ruiqi Ren, Lei Zhou, Chao Li, Wenxiao Tu, Daxin Ni, Qun Li, Zijian Feng, Yanping Zhang

Imported infectious diseases are becoming a serious public health threat in China. However, limited information concerning the epidemiologic characteristics of imported infectious diseases is available. In this study, we collected data related to imported infectious diseases in mainland China from the National Information Reporting System of Infectious Diseases and analyzed demographic, temporal, and spatial distributions. The number of types of imported infectious diseases reported increased from 2 in 2005 to 11 in 2016. A total of 31,740 cases of infectious disease were imported to mainland China during 2005–2016; most of them were found in Yunnan Province. The cases were imported mainly from Africa and Asia. As a key and effective measure, pretravel education should be strengthened for all migrant workers and tourists in China, and border screening, cross-border international cooperation, and early warning should be further improved.

The advance of globalization, frequent personnel exchanges, and close international trade cooperation make it possible for infectious diseases from all over the world to be imported into China. The number of persons entering and leaving China has been steadily increasing, from 302 million person-times in 2005 to 570 million person-times in 2016, and the number of visitor arrivals in Yunnan Province has increased from 1.5 million (1.0 million foreigners) in 2005 to 6.0 million (4.5 million foreigners) in 2016 (*1*). According to the China Statistical Yearbook (http://www.stats.gov.cn/english/Statisticaldata/AnnualData), the number of inbound tourists from Africa has grown from 238,000 in 2005 to 589,000 in 2016, whereas the number of inbound tourists from Asia has grown from 12.5 million in 2005 to 18.0 million in 2016. The number of migrant workers leaving China rose in the same period, from 272,900 to 494,200. Some infectious diseases have been reemerging, such as epidemic hemorrhagic fever and malaria, which previously had basically been controlled, and wild poliovirus, which had been eliminated in China in 2000. After >10 years without a case of wild poliovirus infection in China, an outbreak of wild poliovirus infection occurred in 2011 in Xinjiang Uyghur Autonomous Region (*2*). A few emerging infectious diseases, such as Middle East respiratory syndrome (MERS), yellow fever, and Zika virus disease, have also been imported into China.

Since 2010, annual numbers of autochthonous malaria cases in China have fallen to unprecedentedly low levels; only hundreds of cases now occur in limited areas (*3*–*5*), whereas the number of imported cases has risen substantially (*6*). Malaria is a mosquitoborne infectious disease that caused a heavy health and economic burden in the past. *Anopheles sinensis*, *An. lesteri*, *An. minimus*, and *An. dirus* mosquitoes are considered to be 4 major malaria vectors in China. As a main vector of transmitting malaria, *An. sinensis* mosquitoes are present in all provinces and regions except Qinghai and Xinjiang; *An. lesteri* mosquitoes are found in areas south of 34°N latitude, *An. minimus* mosquitoes in mountainous and hilly areas south of 33°N latitude, and *An. dirus* mosquitoes mainly in the tropical jungles of Hainan. In China, *Aedes albopictus* and *Ae. aegypti* mosquitoes are 2 major vectors that can transmit flaviviruses and alphaviruses, which cause diseases such as dengue fever, chikungunya, and yellow fever. According to a recent investigation by the Chinese Center for Disease Control and Prevention (CDC), *Ae. aegypti* mosquitoes are found in 10 cities or counties in Yunnan Province, 7 cities or counties in Hainan Province, 1 city in Guangdong Province, and areas south of the Tropic of Cancer in Taiwan. *Ae. albopictus* mosquitoes are widely present in 25 provinces in China, in the southeastern parts of a line between Shenyang in Liaoning Province and Motuo County in Tibet (*7*,*8*).

This study describes the epidemiologic characteristics of imported infectious disease cases during 2005–2016 in mainland China. It also provides scientific information for prevention and control in the future.

Author affiliations: Chinese Center for Disease Control and Prevention, Beijing, China (Y. Wang, R. Ren, L. Zhou, C. Li, W. Tu, D. Ni, Q. Li, Z. Feng, Y. Zhang); National Institute for Communicable Disease Control and Prevention, Chinese Center for Disease Control and Prevention, Beijing (X. Liu); 302 Military Hospital of China, Beijing (X. Wang)

DOI: https://doi.org/10.3201/eid2501.180178

[1]These authors contributed equally to this article.

Materials and Methods

Surveillance System

In China, since the establishment in the 1950s of the Notifiable Disease Reporting System (NDRS), which was the main communicable disease surveillance system, many disease-specific surveillance systems have been developed as complements to NDRS. In 2004, the National Information Reporting System of Infectious Diseases, an internet-based real-time information reporting technique, was integrated into NDRS to improve case-based reporting. The workflow includes data collection, data management, data use, and report dissemination. Once a case of notifiable infectious disease or emerging infectious disease is identified, it is mandatory for doctors in all hospitals and clinics to report to the network within the statutory period. CDCs at various levels (e.g., provincial) are in charge of data checking, utilization, and timely information feedback by uploading the reports on the websites. All the hospitals and CDCs at different levels can download these reports and know the national status in a timely manner, which makes the epidemic information transparent. The completeness and timeliness of case reporting have improved dramatically since 2004 (*9*). Therefore, this study takes 2005 as the first year of analysis, considering data quality and stability.

Once an emerging infectious disease is found that is not yet included in statutory reporting but is of considerable interest, the National Health Commission of the People's Republic of China usually organizes relevant experts in clinical, epidemiologic, etiologic, and other areas to assess its risk of becoming epidemic, spreading range, influence extent, and social burden to determine whether the disease should be added to the list of notifiable infectious diseases. The results are submitted to the National People's Congress for deliberation and adoption. At the same time, the emerging infectious disease is required to be reported under "other categories of infectious diseases" in the National Information Reporting System of Infectious Diseases.

Data Collection

Using data from the National Information Reporting System of Infectious Diseases (which does not include Hong Kong, Macao, and Taiwan), we performed a retrospective analysis of imported infectious diseases in mainland China during January 1, 2005–December 31, 2016. We selected data according to reporting date, reporting area, and final confirmation. The cases reported in the National Information Reporting System of Infectious Diseases, including laboratory-confirmed cases and clinically diagnosed cases, were diagnosed by clinicians according to the unified national diagnostic criteria (*10*).

Population and Case Definition

We divided the population into citizens of China and foreign citizens according to their native countries, so the imported cases included not only citizens of China returning from migrant work or other travel abroad but also foreign visitors, expatriates, and migrant workers in China. The major occupational categories of patients were migrant workers, doctors, teachers, students, and retirees.

Local CDC staff ascertained a potential imported case according to the field investigation results after diagnosis. A case in a patient who had visited or lived in an endemic or epidemic area outside China within the longest incubation period before the date of onset was classified as an imported case. Conversely, a case would be classified as a domestic case if there was no evidence of an infection acquired abroad.

Statistical Analysis

We entered and managed the data using Microsoft Excel 2010 (https://office.microsoft.com/excel). We used SPSS 18.0 (https://www.ibm.com/analytics/spss-statistics-software) to describe characteristics of imported infectious diseases regarding geographic and temporal distribution, gender, age, region, or country of origin. We created distribution maps of imported cases using ArcGIS 10.3 (http://www.arcgis.com).

Results

During 2005–2016, a total of 31,740 cases of infectious diseases were imported into China. These included 27,497 cases of malaria, 3,351 cases of dengue fever, 773 cases of influenza A(H1N1), 24 cases of Zika virus disease, 18 cases of chikungunya fever, 11 cases of yellow fever, 2 cases of acute flaccid paralysis caused by poliomyelitis, 1 case of MERS, and 65 cases of other infectious diseases (Table 1). The study revealed that Yunnan Province witnessed the largest number of imported cases of infectious diseases during the study period.

Epidemiologic Profile of Imported Cases in Mainland China, 2005–2016

Demographic Characteristics of Imported Cases

Most persons with imported cases were male. The median age of patients with imported cases of malaria was 39 years; of patients with dengue fever, 32 years; and of influenza A(H1N1), 20 years (Table 2; Figure 1). Among these imported cases, 2,470 were reported in foreigners and 29,270 in travelers from China; 18,932 cases were reported in migrant workers from China and 12,808 in persons with other occupations. Migrant workers from China accounted for 65.2% of imported malaria cases and 28.1% of imported dengue fever cases.

Table 1. Imported infectious diseases in mainland China, 2005–2016*

Disease	Indigenous cases	Imported cases	Total cases	Imported cases, %	Main reporting provinces/cities	Main location(s) of acquisition
Malaria						
Plasmodium vivax	149,675	10,506	160,181	6.6	Yunnan	Asia (Myanmar)
P. falciparum	8,080	14,896	22,976	64.8	Yunnan, Guangxi	Asia (Myanmar), Africa (Ghana)
Undetermined species	29,929	2,095	32,024	6.5	NA	NA
Subtotal	187,684	27,497	215,181	8.1	NA	NA
Dengue fever	58,602	3,351	61,953	5.4	Yunnan	Asia (Myanmar)
Influenza A(H1N1)	75,924	773	76,697	1.0	Beijing, Guangdong	Asia, USA
Chikungunya	244	18	262	6.9	Guangdong, Zhejiang	Angola, Philippines
Lyme disease	162	2	164	1.2	Beijing	Germany
EHF	44,682	7	44,689	0.0	NA	NA
Scrub typhus	68,841	7	68,848	0.0	Hubei	Thailand
VL	1,317	14	1,331	1.1	Hubei, Sichuan	Afghanistan, Spain
JE	5,656	17	5,673	0.3	NA	NA
AFP	27,056	2	27,058	0.0	NA	NA
Loiasis	0	11	11	100.0	Beijing, Shandong, Hubei	Cameroon, Congo, Gabon
EHEC	4	3	7	42.9	Jiangsu	Thailand
CCHF	0	1	1	100.0	Beijing	Congo
Schistosomiasis	0	1	1	100.0	Beijing	Nigeria
MERS	0	1	1	100.0	Guangdong	South Korea
Yellow fever	0	11	11	100.0	Fujian	Africa (Angola)
Zika virus	0	24	24	100.0	Guangdong	South America (Venezuela)
Total	470,172	31,740	501,911	6.3		

*AFP, acute flaccid paralysis; CCHF, Crimean-Congo hemorrhagic fever; EHEC, *Escherichia coli* O157:H7; EHF, epidemic hemorrhagic fever; JE, Japanese encephalitis; MERS, Middle East respiratory syndrome; NA, not applicable; VL, visceral leishmaniasis

Trends in Imported Cases in Mainland China, 2005–2016

In 2005, only 2 types of imported infectious diseases were reported in mainland China: malaria and dengue fever. Chikungunya was imported into China in 2008 and influenza A(H1N1) in 2009; Lyme disease has been imported since 2012. Since 2013, the number of types of imported infectious diseases reported has increased each year. A total of 6 types of diseases, including scrub typhus, visceral leishmaniasis (VL), Japanese encephalitis (JE), epidemic hemorrhagic fever, loiasis, and Crimean-Congo hemorrhagic fever, started to be imported in 2013. Imported cases of *Escherichia coli* O157:H7 infection, schistosomiasis, and MERS

Table 2. Demographic characteristics of persons with imported cases of infectious disease in mainland China, 2005–2016*

	Sex, no. (%)			Native country, no. (%)		Occupation, no. (%)		
Disease	M	F	Mean age, y (range)	China	Other	Migrant worker	Other	Total
Malaria	25,819 (93.9)	1,678 (6.1)	39 (1–83)	26,048 (94.7)	1,449 (5.3)	17,929 (65.2)	9,568 (34.8)	27,497
Dengue fever	2,138 (63.8)	1,213 (36.2)	32 (1–86)	2,403 (71.7)	948 (28.3)	943 (28.1)	2,408 (71.9)	3,351
Influenza A(H1N1)	758 (98.1)	15 (1.9)	20 (0.7–75)	731 (94.6)	42 (5.4)	15 (1.9)	758 (98.1)	773
Chikungunya	15 (83.3)	3 (16.7)	25 (20–47)	15 (83.3)	3 (16.7)	4 (22.2)	14 (77.8)	18
Lyme disease	1	1	NA	1	1	0	2	2
Scrub typhus	3 (42.9)	4 (57.1)	23 (3–42)	2 (28.6)	5 (71.4)	0	7	7
VL	13 (92.9)	1 (7.1)	34 (25–49)	14 (100.0)	0 (0.0)	13 (92.9)	1 (7.1)	14
JE	12 (70.6)	5 (29.4)	8 (1–54)	5 (29.4)	12 (70.6)	0	17	17
EHF	7 (100.0)	0	48 (25–71)	6 (85.7)	1 (14.3)	5 (71.4)	2 (28.6)	7
AFP	0	2	NA	2	0	0	2	2
Loiasis	10 (90.9)	1 (9.1)	37 (22–60)	11 (100.0)	0 (0.0)	8 (72.7)	3 (27.3)	11
EHEC	3	0	63 (43–74)	3	0	0	3	3
CCHF	1	0	35	1	0	0	1	1
Schistosomiasis	1	0	28	1	0	0	1	1
MERS	1	0	43	0	1	0	1	1
Yellow fever	8 (72.7)	3 (27.3)	42 (18–53)	11 (100.0)	0 (0.0)	8 (72.7)	3 (27.3)	11
Zika virus	15 (62.5)	9 (37.5)	30 (5–55)	16 (66.7)	8 (33.3)	7 (29.2)	17 (70.8)	24
Total	28,805 (90.8)	2,935 (9.2)	NA	29,270 (92.2)	2,470 (7.8)	18,932 (59.6)	12,808 (40.4)	31,740

*AFP, acute flaccid paralysis; CCHF, Crimean-Congo hemorrhagic fever; EHEC, *Escherichia coli* O157:H7; EHF, epidemic hemorrhagic fever; JE, Japanese encephalitis; MERS, Middle East respiratory syndrome; NA, not applicable; VL, visceral leishmaniasis

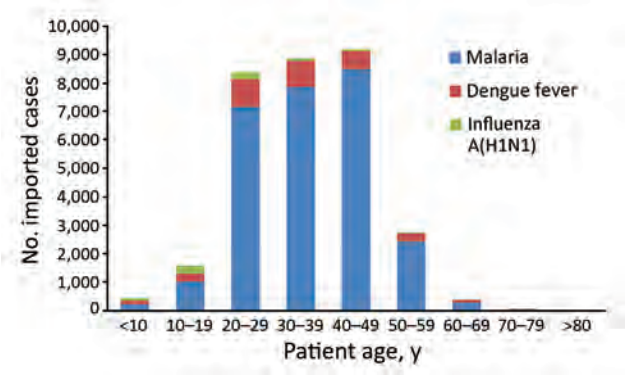

Figure 1. Distribution by age group of imported malaria, dengue fever, and influenza A(H1N1) cases in mainland China, 2005–2016.

were reported in 2015. In 2016, 24 cases of Zika and 11 cases of yellow fever were imported. The types of reported imported infectious diseases increased dramatically after 2013 and reached 11 types in 2016, compared with only 2 types in 2005.

We found that imported cases of malaria showed an upward trend from 2005 to 2016. The imported cases of dengue fever increased year by year; increased sharply in 2013 and 2015, with a peak in 2015 (1,094 cases); and declined slightly in 2016 (Figure 2).

Seasonal Distribution of Imported Cases

Many of the main imported diseases in mainland China exhibited seasonality. Most yellow fever cases were imported in March. There was usually a higher incidence of imported malaria during April–August, reaching a peak in May and June. All the JE cases were imported during June–September, whereas incidence of imported dengue fever usually peaked in October (Figure 3). In particular, the cases of Zika were imported mainly through international airports around major festival events, such as the Spring Festival (celebrating the lunar new year), May Day, the Mid-Autumn Festival, and the National Day (October 1) (*11*).

Spatial Distribution of Imported Diseases

Provinces with Imported Diseases

All 31 provinces across the country reported imported malaria (Figure 4); 36.1% (9,931 cases) were reported in Yunnan Province. The number of imported malaria cases in Yunnan Province was generally decreasing, however, whereas it had been slowly increasing in Sichuan, Henan, Jiangsu, and Zhejiang Provinces and other southeastern provinces year by year. In 2013, imported malaria increased sharply in Guangxi Province, which had the largest number of imported malaria cases in China for that year (1,261/4,067; 31.0%), accounting for 52.7% (1,261/2,394) of the total imported malaria cases in this province during 2005–2016 (data not shown).

Twenty-seven provinces across the country, all except Shanxi, Qinghai, Ningxia, and Tibet, reported dengue fever during 2005–2016. Among all imported dengue fever cases, 42.9% (1,439/3,351) were reported in Yunnan Province (data not shown). Influenza A(H1N1) was imported mainly into Beijing, Guangdong, and other major port cities (data not shown).

Origin Region/Country of Imported Diseases

According to our analysis, Africa and Asia were the main regions of origin of imported cases; 15,021 (47.3%) patients came from Africa and 12,581 (39.6%) from Asia (Figure 5). Asia was the main origin of imported dengue fever (3,097 cases, 92.4%), chikungunya, VL, JE, and other diseases. Africa was the main region of origin for imported malaria (14,854 cases, 54.0%), and others, especially *Plasmodium falciparum*, yellow fever, loiasis, and other diseases (Table 3).

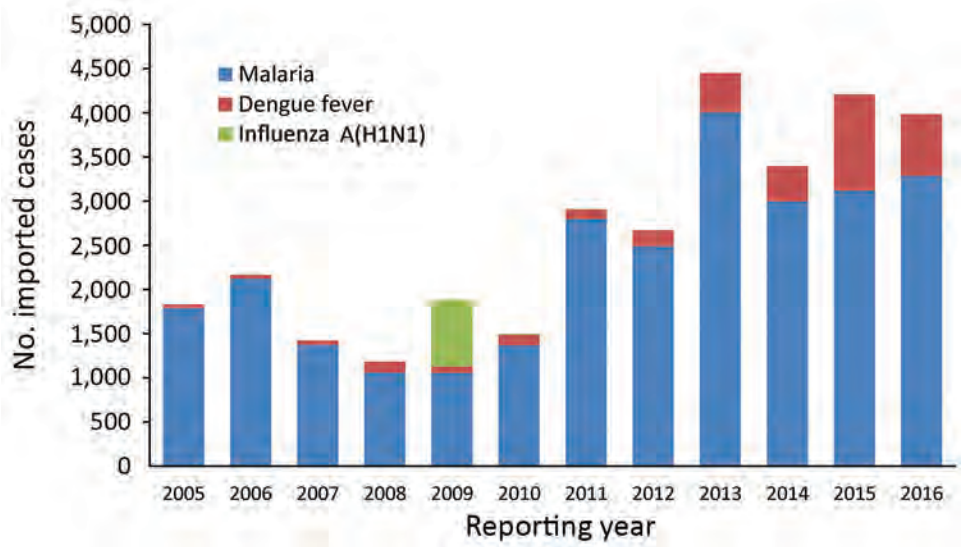

Figure 2. Annual number of imported malaria, dengue fever, and influenza A(H1N1) cases in mainland China, 2005–2016.

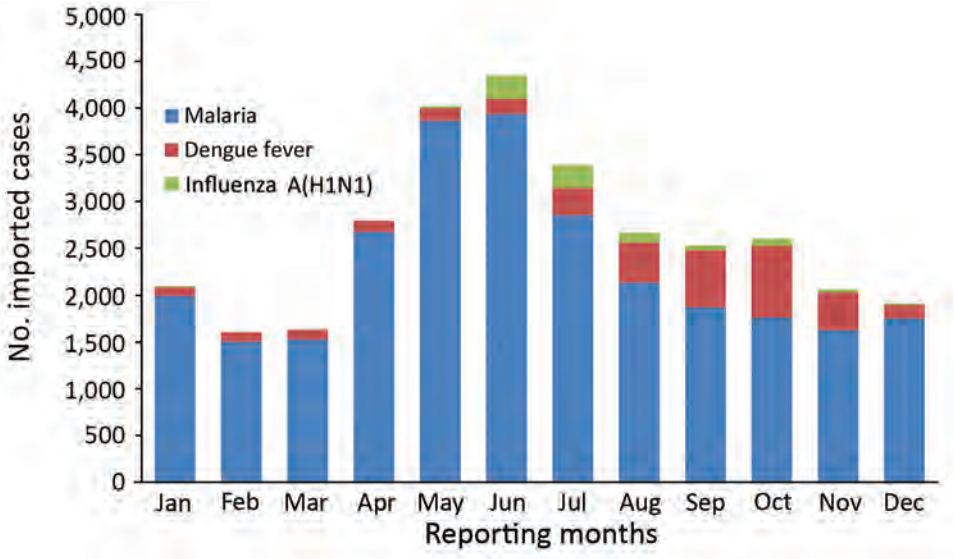

Figure 3. Monthly distribution of imported malaria, dengue fever, and influenza A(H1N1) cases in mainland China, 2005–2016.

Myanmar was the main country of origin for 5 imported diseases. These diseases were malaria (7,888 cases, 28.7%), dengue fever (1,384 cases, 41.3%), scrub typhus (6 cases, 85.7%), JE (13 cases, 76.5%), and acute flaccid paralysis (2 cases, 100.0%) (additional data not shown).

Malaria was imported mainly from Africa (14,854 cases, 54.0%) and Asia (9,160 cases, 33.3%). *P. vivax* came mainly from Asia, especially Myanmar (peaked in 2011), and was introduced into Yunnan Province during 2005–2016. There was an exception, however: Ghana exported more cases of *P. vivax* malaria to China in 2013. After that introduction, the number of imported cases of *P. vivax* malaria from Ethiopia, Angola, Equatorial Guinea, and other countries in Africa began to increase slightly. *P. falciparum* malaria also came mainly from Asia, especially from Myanmar, which exported it into Yunnan Province until 2013. In 2013, the largest number of cases of *P. falciparum* malaria came from Ghana; thereafter, most cases were imported from Angola, Nigeria, Equatorial Guinea, Ghana, and other countries in Africa, mainly into Guangxi, Jiangsu, and other southeastern provinces in China (data not shown).

Imported dengue fever cases were mainly from Asia, especially from Myanmar; most of them were brought into

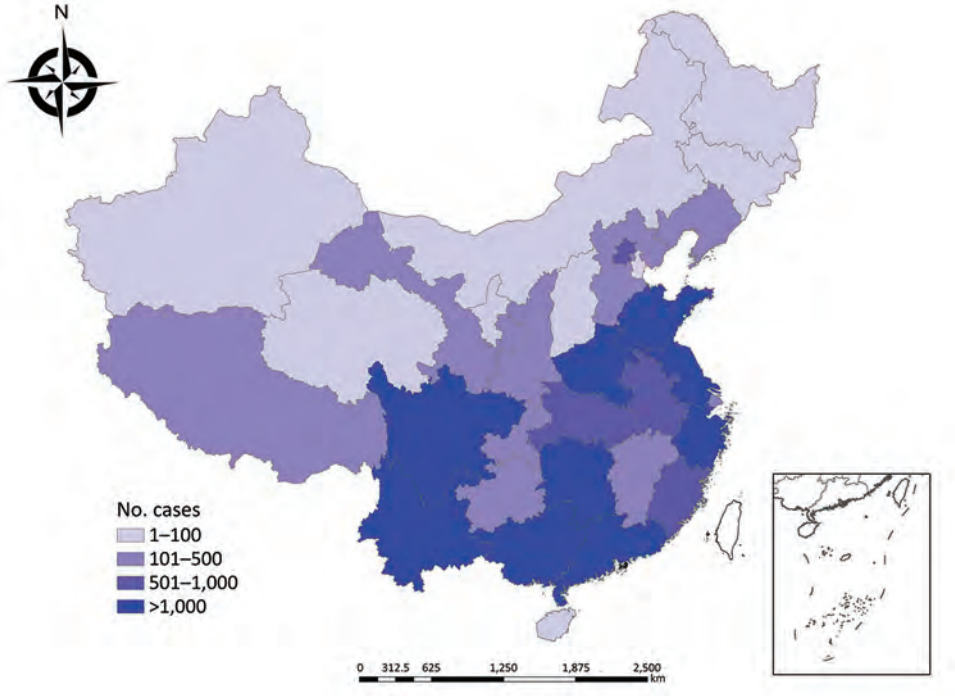

Figure 4. Number of cases of imported infectious diseases in mainland China, by province, 2005–2016.

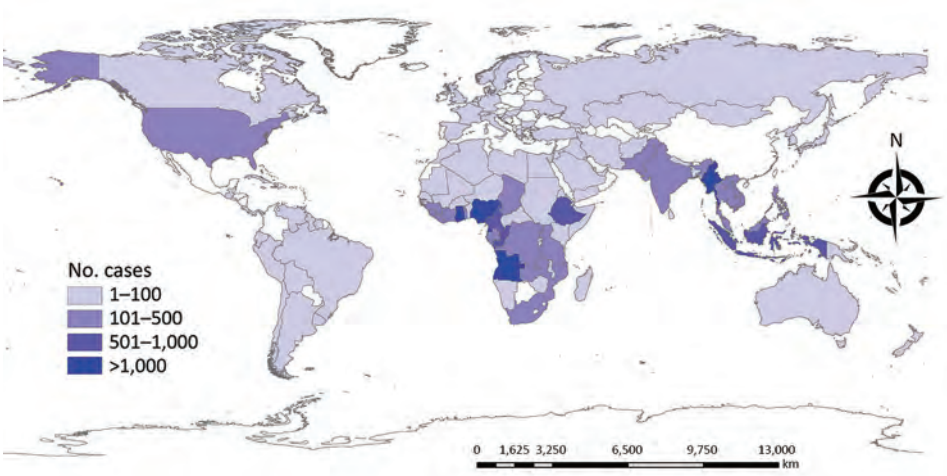

Figure 5. Number of cases of infectious diseases exported to mainland China, by country of origin, 2005–2016.

Yunnan and Guangdong Provinces. Influenza A(H1N1) was imported mainly from the United States (141 cases, 18.2%) and Australia (111 cases, 14.4%). The 1 case of MERS was imported from South Korea in 2015. All 11 imported cases of yellow fever came from Angola. Of the 24 imported Zika cases, 70.8% (17 cases) were from Venezuela.

Discussion

Many infectious diseases, such as *P. vivax* malaria, dengue fever, influenza A(H1N1), epidemic hemorrhagic fever, JE, chikungunya, Lyme disease, scrub typhus, and VL, are found frequently in the indigenous population of China, but some are found more often as imported diseases, such as *P. falciparum* malaria, yellow fever, Zika virus, and MERS. Imported *P. falciparum* malaria is a major obstacle to achieving malaria elimination in China (*12–14*). This study showed that malaria was the most frequent imported infectious disease during 2005–2016, and Yunnan was the province with the greatest number of cases of imported malaria, which was consistent with other relevant studies in China (*15–17*). The reason for the large number of imported cases is that Yunnan Province has long international borders with Myanmar, Laos, Vietnam, and other countries of the Greater Mekong Subregion that show a high incidence of malaria (*16*). The persons who cross these borders to enter or leave China increase opportunities for infectious diseases to be imported from adjacent countries (*3,14,18,19*), especially from Myanmar (*12,13,20*).

P. falciparum malaria was imported mainly from Ghana and *P. vivax* malaria mainly from Asia, which was consistent with Zhou's findings (*5*). The number of cases of *P. falciparum* malaria imported into Guangxi Province increased significantly in 2013; this increase can be attributed mainly to cases imported from Ghana in 2013, which was related to people working in Ghana and other Africa countries during a gold rush in that year (*21,22*).

Africa and Asia were the main origins of imported malaria and other mosquitoborne diseases, findings consistent with those of Tian et al. (*23*). First, as a result of the rapid development of international economic exchange, trade, and travel, the number of migrant workers from China in Africa and Asia has increased annually in recent years. Second, climate and sanitary conditions in Africa and Southeast Asia are suitable for mosquitoes. Migrant workers from China in these areas are engaged mostly in outdoor field work, and their working and living environments are not mosquito preventive. Therefore, they have greater risk for infection (*24,25*). In addition, their health education level and self-protection awareness are low. All these factors have resulted in an increased number of malaria and other mosquitoborne diseases (*26*). Therefore, the main challenges of eliminating *P. falciparum* malaria are curtailing border malaria and imported cases from Myanmar and countries in Africa (*6,14*). Cooperation between China and neighboring countries has played an important role in improving malaria control at cross-border areas and should be further strengthened.

This study revealed that imported cases of infectious diseases such as malaria, dengue fever, and chikungunya were more common in male youths, which is consistent with the findings of Jiao et al. (*24*). Industries that use labor from China generally include construction, manufacturing, and transportation; therefore, the proportion of young men was high among migrant workers from China, to meet the needs of these industries.

Because of the distributions of mosquitoes and other vectors in China, diseases such as dengue fever, *P. vivax* malaria, JE, epidemic hemorrhagic fever, and chikungunya are acquired primarily locally. However, the numbers and the types of imported infectious diseases reported have increased in recent years. We indicate 4 main reasons for this increase. First, globalization is a major factor. With growing economic globalization, ongoing development of

Table 3. Imported infectious diseases in mainland China, by region of origin, 2005–2016*

Disease	Africa	Asia	Oceania	Europe	North America	South America	Central America	Not ascertainable	Total
Malaria	14,854	9,160	68	5	2	18	0	3,390	27,497
Dengue	129	3,097	44	6	7	25	0	43	3,351
Influenza A(H1N1)	7	268	122	62	187	7	0	120	773
Chikungunya	2	12	0	0	0	1	0	3	18
Lyme disease	0	0	0	1	1	0	0	0	2
Scrub typhus	0	7	0	0	0	0	0	0	7
VL	1	12	0	1	0	0	0	0	14
JE	0	17	0	0	0	0	0	0	17
AFP	0	2	0	0	0	0	0	0	2
EHEC	0	3	0	0	0	0	0	0	3
EHF	5	2	0	0	0	0	0	0	7
Loiasis	11	0	0	0	0	0	0	0	11
Schistosomiasis	1	0	0	0	0	0	0	0	1
CCHF	1	0	0	0	0	0	0	0	1
MERS	0	1	0	0	0	0	0	0	1
Yellow fever	10	0	0	0	0	0	0	0	10
Zika virus	0	0	3	0	0	19	2	0	24
Total	15,021	12,581	237	75	197	70	2	3,556	31,740
%	47.3	39.6	0.8	0.2	0.6	0.2	0	11.2	100

*AFP, acute flaccid paralysis; CCHF, Crimean-Congo hemorrhagic fever; EHEC, *Escherichia coli* O157:H7; EHF, epidemic hemorrhagic fever; JE, Japanese encephalitis; MERS, Middle East respiratory syndrome; VL, visceral leishmaniasis.

international trade, and convenient and fast transportation in recent years, factors such as microbial mutation, global warming, floods, droughts, and natural migration of animals as disease vectors have increased the risk of disease introduction into China (*27–29*). Second, these increases are related to the increases in the number of migrant workers from China, as well as increases in the number of tourists. This study showed that migrant workers from China accounted for a large proportion of imported malaria. Migrant workers and tourists are more at risk than local residents because of lack of preexisting immunity that dramatically increases the chances that they could become infected with these diseases and bring them in from abroad (*19*). Third, the level of surveillance, diagnosis, and detection of emerging or reemerging infectious diseases improved in China during the study years, which potentially contributed to the increase in the number and the types of cases with a confirmed diagnosis. Finally, some of the increases were caused by newly discovered or emerging infections, such as MERS, which was discovered in 2012 and confirmed in 2013; the 1 case imported into China was a result of the large outbreak in South Korea in 2015.

This study has analyzed the epidemiologic characteristics of all imported infectious diseases in mainland China over a recent 10-year period to provide scientific guidance for control and prevention of imported diseases in China. The study also has limitations. First, there is currently no special reporting system for imported infectious diseases in China. The imported cases that were analyzed in this study were reported through the National Information Reporting System of Infectious Diseases and identified by local CDC staff through epidemiologic investigation; therefore, not all imported cases may have been identified. A second limitation is that the data of this study were obtained from the monitoring system and there are few denominator data to use for calculating the rates of imported infectious diseases, so conclusions are limited and risks cannot be calculated. Finally, the factors concerning imported infectious diseases are complex, whereas our data are limited. Some demographic characteristics; trip information, such as purpose and duration of travel; and climate, environmental, and other relevant information could not be obtained. In subsequent research, we will focus on the collection of more information and continue to conduct our in-depth study of imported infectious diseases.

To control and prevent imported infectious diseases, we recommend several measures. First, pretravel education targeting infectious diseases that are endemic or prevalent in the destination countries is key for the prevention of imported diseases, especially imported malaria. Such education includes pretravel special training sessions; distribution of pamphlets or leaflets; and posttravel tips via notices, banners, or scrolling electronic screens at international entry and exit ports. Also important are dispensing of free preventive medications for malaria prophylaxis, self-treatment of severe travelers' diarrhea, and vaccination against vaccine-preventable diseases such as JE and yellow fever during international travel and residence (*30*).

Second, border screening should be strengthened and improved. The effectiveness of border screening is controversial (*31*), but in recent years, China's screening practices have proven to be a crucial measure for discovering imported infectious diseases in travelers who are ill at the time they cross a border. Screening has played a major role in prevention as the first line of defense against importation of foreign infectious diseases. For example, among 25

cases of Zika virus disease imported into mainland China in 2016, border screening recognized 9 (*11*), and of 11 cases of imported yellow fever reported in 2016, border screening recognized 6 (*32*). Border screening should be strengthened and improved to prevent those epidemic diseases and others from entering China (*32*–*34*).

Third, as a second line of defense against imported diseases, fever clinics and primary clinicians need to play an active role in identifying patients with imported infectious diseases. At present, many problems exist in fever clinics set up in medical institutions, such as failure to meet requirements, unqualified procedures, or nonstandardized management, and some locations may even be out of service. Clearer management standards are needed to provide a better chance for infectious disease screening. Training of medical staff, especially primary clinicians, should be reinforced to improve the ability to identify, diagnose, and treat emerging or reemerging infectious diseases and to ensure that imported cases can be diagnosed and control measures can be implemented as early as possible to prevent these diseases from further spreading in China.

Fourth, multisectoral and regional cooperation mechanisms, especially international cooperation mechanisms in the border areas, should be further enhanced (*35*). We suggest that the relevant departments should intensify cooperation by using well-defined responsibilities and should improve communication regarding all aspects of public information sharing, training, monitoring, and control. It is critical that, in the border areas, neighboring countries develop the management of persons entering and leaving, improve the control of mosquitoes, and jointly respond to infectious diseases.

Fifth, it is necessary to improve the early warning and response capacity for emerging infectious diseases. We recommend establishing a special system of surveillance, risk assessment, and early warning. Spatiotemporal models linking disease data and different environmental factors are also urgently needed (*36*).

In summary, our study found that the numbers of emerging infectious diseases imported into China have increased year by year. Therefore, we must pay closer attention to prevention and control of imported cases, while preventing and controlling indigenous cases. These factors are crucial for preventing and controlling infectious diseases, such as *P. falciparum* malaria, that have a large number of imported cases and seriously hinder the process of China eliminating malaria and other diseases.

This study was funded by the World Bank Avian/Human Influenza Trust Fund Grant Project of Capacity Building for Emerging Infectious Diseases Control and Prevention in China (grant no. TF012401) and the National Natural Science Foundation of China (grant no. 81703280).

About the Author

Dr. Yali Wang is an epidemiologist working at the Public Health Emergency Center, Chinese Center for Disease Control and Prevention, Beijing, China. Her research interests are prevention and control of emerging infectious diseases.

References

1. Ministry of Public Security of the People's Republic of China. National Immigration Administration annual report [cited 2018 Sep 26]. http://www.mps.gov.cn/n2254996/n2254999/index.html
2. Wang HB, Yu WZ, Wang XQ, Wushouer F, Wang JP, Wang DY, et al. An outbreak following importation of wild poliovirus in Xinjiang Uyghur Autonomous Region, China, 2011. BMC Infect Dis. 2015;15:34. http://dx.doi.org/10.1186/s12879-015-0761-y
3. Feng J, Xiao H, Xia Z, Zhang L, Xiao N. Analysis of malaria epidemiological characteristics in the People's Republic of China, 2004–2013. Am J Trop Med Hyg. 2015;93:293–9. http://dx.doi.org/10.4269/ajtmh.14-0733
4. Zhang Q, Lai SJ, Zheng CJ, Zhang HL, Zhou S, Hu WB, et al. The epidemiology of *Plasmodium vivax* and *Plasmodium falciparum* malaria in China, 2004–2012: from intensified control to elimination. Malar J. 2014;13:419. http://dx.doi.org/10.1186/1475-2875-13-419
5 Zhou S, Li Z, Cotter C, Zheng C, Zhang Q, Li H, et al. Trends of imported malaria in China 2010–2014: analysis of surveillance data. Malar J. 2016;15:39. http://dx.doi.org/10.1186/s12936-016-1093-0
6. Hu T, Liu YB, Zhang SS, Xia ZG, Zhou SS, Yan J, et al. Shrinking the malaria map in China: measuring the progress of the National Malaria Elimination Programme. Infect Dis Poverty. 2016;5:52. http://dx.doi.org/10.1186/s40249-016-0146-5
7. Liu XB, Wu HX, Lu L. Dialogue on Liu Qiyong: sustainable *Aedes* management is the trump card to the prevention of Zika [in Chinese]. Chinese Sci Bull. 2016;61:2323–5.</jrn>
8. Li CM, Dong XS, Yang MD. Geographical distribution and seasonal variations of *Aedes aegypti* in Yunnan province [in Chinese]. Chin J Vector Biol Control. 2018;29:388–90.
9. Xiong W, Lv J, Li L. A survey of core and support activities of communicable disease surveillance systems at operating-level CDCs in China [in Chinese]. BMC Public Health. 2010;10:704. http://dx.doi.org/10.1186/1471-2458-10-704
10. National Health Commission of the People's Republic of China. Hygienic standard for diagnosis of infectious diseases [cited 2018 Sep 26]. http://www.nhfpc.gov.cn/zhuz/s9491/wsbz.shtml
11. Wang YL, Zhang XY, Ren RQ, Li C, Xiang NJ, Tu WX, et al. Epidemiological and clinical characteristics of 25 imported Zika cases in mainland China [in Chinese]. Chin J Vector Biol Control. 2017;28:535–7.
12. Li Z, Zhang Q, Zheng C, Zhou S, Sun J, Zhang Z, et al. Epidemiologic features of overseas imported malaria in the People's Republic of China. Malar J. 2016;15:141. http://dx.doi.org/ 10.1186/s12936-016-1188-7
13 Wang RB, Zhang J, Zhang QF. Malaria baseline survey in four special regions of northern Myanmar near China: a cross-sectional study. Malar J. 2014;13:302. http://dx.doi.org/10.1186/1475-2875-13-302
14. Zhang Q, Sun J, Zhang Z, Geng Q, Lai S, Hu W, et al. Risk assessment of malaria in land border regions of China in the context of malaria elimination. Malar J. 2016;15:546. http://dx.doi.org/10.1186/s12936-016-1590-1
15. He ZY, Wang XM, Li X, Dou LF, Li XY, Wang QY. Analysis of status and control measures for the imported malaria in Beijing from 2005 to 2011 [in Chinese]. J Trop Dis Parasitol. 2012;10:225–7.

16. Clements AC, Barnett AG, Cheng ZW, Snow RW, Zhou HN. Space-time variation of malaria incidence in Yunnan province, China. Malar J. 2009;8:180. http://dx.doi.org/10.1186/1475-2875-8-180
17. Zhang SX, Wang Y, Yan L, Wang SW, Wang XF. The epidemiological characteristics of dengue fever in China from 2005–2012 [in Chinese]. Guide of China Medicine. 2013;11:401–2.
18. Wang RB, Dong JQ, Xia ZG, Cai T, Zhang QF, Zhang Y, et al. Lessons on malaria control in the ethnic minority regions in Northern Myanmar along the China border, 2007–2014. Infect Dis Poverty. 2016;5:95. http://dx.doi.org/10.1186/s40249-016-0191-0
19. Chen TM, Zhang SS, Feng J, Xia ZG, Luo CH, Zeng XC, et al. Mobile population dynamics and malaria vulnerability: a modelling study in the China–Myanmar border region of Yunnan Province, China. Infect Dis Poverty. 2018;7:36. http://dx.doi.org/10.1186/s40249-018-0423-6
20. Xu JW, Li Y, Yang HL, Zhang J, Zhang ZX, Yang YM, et al. Malaria control along China–Myanmar border during 2007–2013: an integrated impact evaluation. Infect Dis Poverty. 2016;5:75. http://dx.doi.org/10.1186/s40249-016-0171-4
21 Li Z, Yang Y, Xiao N, Zhou S, Lin K, Wang D, et al. Malaria imported from Ghana by returning gold miners, China, 2013. Emerg Infect Dis. 2015;21:864–7. http://dx.doi.org/10.3201/eid2105.141712
22. Lai S, Wardrop NA, Huang Z, Bosco C, Sun J, Bird T, et al. *Plasmodium falciparum* malaria importation from Africa to China and its mortality: an analysis of driving factors. Sci Rep. 2016;6:39524. http://dx.doi.org/10.1038/srep39524
23. Tian LL, Liu Y, Dou XF, Ren HL, Li X, Lu YN, et al. Epidemiologic features of the imported cases of main mosquito-borne diseases in Beijing during 2006–2016 [in Chinese]. Acta Parasitol Med Entomol Sin. 2016;23:137–9.
24. Jiao YM, Yang G, Xie M, Fang Q, Tao ZY, Wang XM, et al. Epidemic characterstics of malaria in China from 2008 to 2012 [in Chinese]. Acta Parasitol Med Entomol Sin. 2013;20:80–3.
25. Lu G, Zhou S, Horstick O, Wang X, Liu Y, Müller O. Malaria outbreaks in China (1990–2013): a systematic review. Malar J. 2014;13:269. http://dx.doi.org/10.1186/1475-2875-13-269
26. Yang ZJ. An intervention study of common imported mosquito-borne disease among laborers who go to Africa and Southeast Asia [in Chinese]. Port Health Control. 2012;17:39–41.
27. Sang S, Yin W, Bi P, Zhang H, Wang C, Liu X, et al. Predicting local dengue transmission in Guangzhou, China, through the influence of imported cases, mosquito density and climate variability. PLoS One. 2014;9:e102755. http://dx.doi.org/10.1371/journal.pone.0102755
28. Wu T, Perrings C, Kinzig A, Collins JP, Minteer BA, Daszak P. Economic growth, urbanization, globalization, and the risks of emerging infectious diseases in China: a review. Ambio. 2017;46:18–29. http://dx.doi.org/10.1007/s13280-016-0809-2
29. Liu Q, Cao L, Zhu XQ. Major emerging and re-emerging zoonoses in China: a matter of global health and socioeconomic development for 1.3 billion. Int J Infect Dis. 2014;25:65–72. http://dx.doi.org/10.1016/j.ijid.2014.04.003
30. Riddle MS, Connor BA, Beeching NJ, DuPont HL, Hamer DH, Kozarsky P, et al. Reply to JTM-17-106 Comment: 'Guidelines for the prevention and treatment of travelers' diarrhoea: a graded expert panel report' by Riddle et al. J Travel Med. 2017;24(Suppl_1):S57–74. http://dx.doi.org/10.1093/jtm/tax060
31. Priest PC, Jennings LC, Duncan AR, Brunton CR, Baker MG. Effectiveness of border screening for detecting influenza in arriving airline travelers. Am J Public Health. 2015;105(Suppl 4):S607–13, S600–6. http://dx.doi.org/10.2105/AJPH.2012.300761r
32. Wang KL. ShangGuan WX, Dai XL, Tian R,Zhang N,Huang JH. Application of the four defenses policy against imported infectious diseases in the prevention and control of yellow fever at Beijing port [in Chinese]. Chinese Frontier Health Quarantine. 2016;39:158–61.
33. Cui L, Yan G, Sattabongkot J, Cao Y, Chen B, Chen X, et al. Malaria in the greater Mekong subregion: heterogeneity and complexity. Acta Trop. 2012;121:227–39. http://dx.doi.org/10.1016/j.actatropica.2011.02.016
34. Xu JW, Li JJ, Guo HP, Pu SW, Li SM, Wang RH, et al. Malaria from hyperendemicity to elimination in Hekou County on China–Vietnam border: an ecological study. Malar J. 2017;16:66. http://dx.doi.org/10.1186/s12936-017-1709-z
35. Wangdi K, Gatton ML, Kelly GC, Clements AC. Cross-border malaria: a major obstacle for malaria elimination. Adv Parasitol. 2015;89:79–107. http://dx.doi.org/10.1016/bs.apar.2015.04.002
36. Lai S, Li Z, Wardrop NA, Sun J, Head MG, Huang Z, et al. Malaria in China, 2011–2015: an observational study. Bull World Health Organ. 2017;95:564–73. http://dx.doi.org/10.2471/BLT.17.191668

Address for correspondence: Yanping Zhang, Chinese Center for Disease Control and Prevention, Public Health Emergency Center, No. 155 Changbai Rd, Changping District, Beijing 102206, China; email: zhangyp@chinacdc.cn

Risk Factors for *Elizabethkingia* Acquisition and Clinical Characteristics of Patients, South Korea

Min Hyuk Choi, Myungsook Kim, Su Jin Jeong, Jun Yong Choi,[1] In-Yong Lee, Tai-Soon Yong, Dongeun Yong, Seok Hoon Jeong, Kyungwon Lee[1]

Elizabethkingia infections are difficult to treat because of intrinsic antimicrobial resistance, and their incidence has recently increased. We conducted a propensity score–matched case–control study during January 2016–June 2017 in South Korea and retrospectively studied data from patients who were culture positive for *Elizabethkingia* species during January 2009–June 2017. Furthermore, we conducted epidemiologic studies of the hospital environment and mosquitoes. The incidence of *Elizabethkingia* increased significantly, by 432.1%, for 2016–2017 over incidence for 2009–2015. Mechanical ventilation was associated with the acquisition of *Elizabethkingia* species. Because *Elizabethkingia* infection has a high case-fatality rate and is difficult to eliminate, intensive prevention of contamination is needed.

The genus *Elizabethkingia* comprises glucose-nonfermenting, gram-negative rods that are widely distributed in natural environments, including in soil and freshwater, and in hospital environments (*1*). *E. meningoseptica* (originally named *Chryseobacterium meningoseptica*) has been associated with opportunistic infections, such as sepsis in immunocompromised patients and meningitis in neonates (*2*). Two new species of *Elizabethkingia* have been proposed: *E. miricola*, which was first isolated from water from the Russian space station MIR in 2003 (*3*,*4*); and *E. anophelis*, which was first isolated from the midgut of the *Anopheles gambiae* mosquito in 2011 (*5*). Because *E. anophelis* was the most frequently isolated *Elizabethkingia* species in recent clinical studies, as confirmed by 16s rRNA gene sequencing (*6*,*7*), but is commonly misidentified as *E. meningoseptica*, many previously reported cases of *E. meningoseptica* could actually have been caused by *E. anophelis* (*8*,*9*).

Infection caused by *Elizabethkingia* species is difficult to treat and results in a high case-fatality rate, probably because of intrinsic antimicrobial resistance (*10*). *E. meningoseptica* has been documented to carry class A extended-spectrum β-lactamases and 2 chromosomal metallo-β-lactamases (*11*,*12*).

Some outbreaks of *Elizabethkingia* species have been reported to have resulted from a contaminated water source (*13*–*15*). Furthermore, recent increases in the annual incidence of *Elizabethkingia* species. have been reported in many countries (*14*,*16*–*19*). However, knowledge about host risk factors associated with the acquisition of *Elizabethkingia* species is lacking, and no evidence exists that mosquitoes or other sources act as vectors in transmitting it to humans. Thus, we investigated the annual incidence and clinical characteristics of *Elizabethkingia* acquisition in a tertiary teaching hospital in Seoul, South Korea. We aimed to determine whether the incidence of *Elizabethkingia* species had increased in this hospital and to analyze the risk factors associated with *Elizabethkingia* acquisition. To identify the source of *Elizabethkingia*, we obtained and analyzed epidemiologic studies from the hospital environment and mosquitoes.

Methods

Study Participants

We retrospectively collected data from all nonduplicate persons who had positive culture results for *Elizabethkingia* species from Severance Hospital, a >2,000-bed tertiary teaching hospital in South Korea, during January 1, 2009–June 30, 2017. The hospital had 10 intensive care units (ICUs) for adults and 2 for children. During this period, the annual number of inpatient-days was >670,000.

Author affiliations: National Health Insurance Service Ilsan Hospital, Goyang, South Korea (M.H. Choi); Yonsei University College of Medicine, Seoul, South Korea (M.H. Choi, M. Kim, S.J. Jeong, J.Y. Choi, I.-Y. Lee, T.-S. Yong, D. Yong, S.H. Jeong, K. Lee)

DOI: https://doi.org/10.3201/eid2501.171985

[1]These authors contributed equally to this article.

Because we had identified strains in our previous study (*7*), we updated our in-house library of matrix-assisted laser desorption/ionization time-of-flight mass spectrometry (MS) (Bruker Daltonic GmbH, https://www.bruker.com). *Elizabethkingia* species were identified by 2 matrix-assisted laser desorption/ionization time-of-flight MS systems; the Bruker MS used the updated in-house library and the Vitek MS (bioMèrieux, https://www.biomerieux.com) used the latest version of IVD (in vitro diagnostic database) V3.2. Strains with discrepant results were confirmed by 16S rRNA gene sequencing using universal primers.

We collected the following clinical data using electronic medical records: age-adjusted Charlson comorbidity index (*20*), sex, sites of specimen collection, date of specimen collection, date of patient death, pulse rate, oxygen saturation, body temperature, chest radiograph results, and any antimicrobial agents administered during hospitalization. We also obtained available laboratory findings from the same day as specimen collection and within 7 days from the same day as specimen collection, including C-reactive protein level, erythrocyte sedimentation rate, and leukocyte count. The Institutional Review Board at Severance Hospital, affiliated with Yonsei University Health System (2017–2101–001), approved this study.

Epidemiologic Study of Environmental Sources and Mosquitoes

We obtained extensive surveillance cultures of 281 common environmental sources by swab culture of equipment and surfaces within patient rooms, restrooms, nursing stations, electronics, furniture, patient care devices, patient transport carts, sinks, and water taps. Additionally, during July–September 2017, we collected adult mosquitoes in 1 urban site (Seodaemun-gu, Seoul, where Severance Hospital is located) and 3 rural areas (Hwaseong-si, Gyeonggi-do; Paju-si, Gyeonggi-do; and Chungju-si, Chungbuk, where annual zoonotic disease monitoring had taken place for their dense population of animal farms) (Figure 1). Mosquitoes were collected using Insect Light Traps Model SR-2000 (Sin Young Inc., Seoul, South Korea) and identified under a stereomicroscope after cold anesthesia, as in the previous study (*21*).

All swab samples and midguts of mosquitoes were inoculated on sheep blood agar and MacConkey agar and incubated overnight. DNA was extracted from mosquitoes using a simple boiling method, and PCR was performed using *Elizabethkingia* species–specific primers (forward, GAACACGTGTGCAACCTGCC; reverse, TCCAGCCACTTCAACCTTAC) and the following cycle parameters: 95°C for 5 min, followed by 35 cycles of 95°C for 30 s, 58°C for 2 min, and 72°C for 1 min; followed by a final extension step at 72°C for 7 min (*22*).

Pulsed-Field Gel Electrophoresis

We conducted pulsed-field gel electrophoresis (PFGE) analysis of XbaI-digested isolated chromosomal DNA from a total of 12 strains isolated from the environment (7 *E. anophelis*, 3 *E. miricola*, 2 *E. meningoseptica*) and 54 stored strains isolated from inpatients since 2017. PFGE patterns were analyzed using the CHEF DR II system (Bio-Rad, http://www.bio-rad.com) as previously described (*9*).

Definition

We defined true pathogen cases according to the definitions of Moore et al. and the Centers for Disease Control and Prevention. In brief, we defined these cases as patients with the monomicrobial acquisition of *Elizabethkingia* species and 1 of the following parameters within 2 days before and after acquisition without any other recognized cause: body temperature <36°C or >38°C, pulse rate >90 beats/min

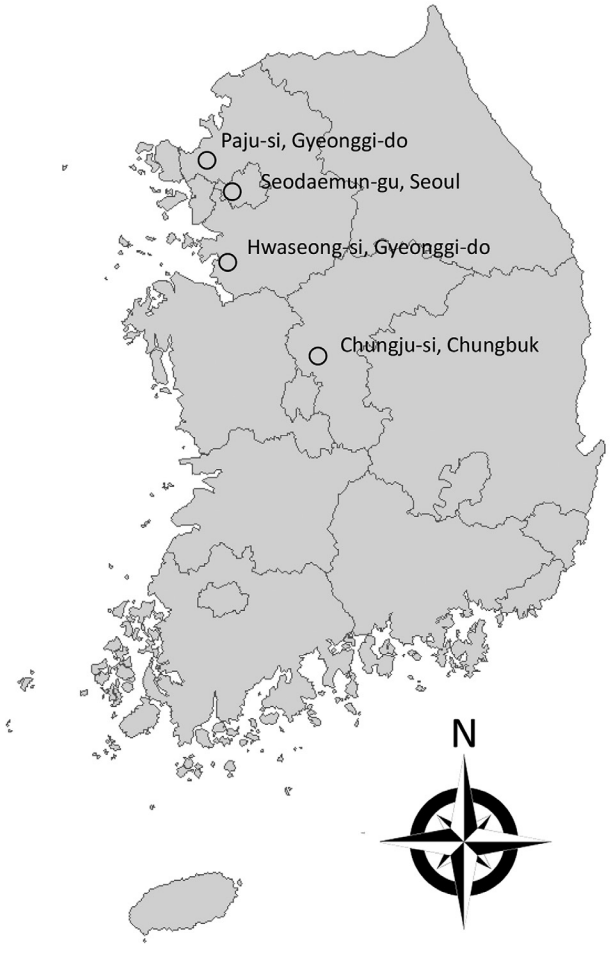

Figure 1. Rural areas of South Korea (Hwaseong-si, Gyeonggi-do; Paju-si, Gyeonggi-do; and Chungju-si, Chungbuk) where adult mosquitoes were collected during July–September 2017 and the urban location of the tertiary teaching hospital (Seodaemun-gu, Seoul) where the study of *Elizabethkingia* infection in patients was conducted during January 2009–June 2017.

(reference range 60–100 beats/min), leukocyte count <4 or >12 × 10^9 cells/L (reference range 4.0–10.9 × 10^9 cells/L), C-reactive protein >100 mg/L (reference range 0–8 mg/L), or chest radiography showing new pulmonary infiltrations (*13*,*23*). According to previous studies, outbreaks are determined by whether they exceed 2 SD of the previous disease incidence (*24*,*25*).

Propensity Score–Matched Analysis

After 2016, the incidence of isolated *Elizabethkingia* species increased significantly. To analyze the increased incidence, we conducted surveillance culture study and compared clinical characteristics of patients who acquired *Elizabethkingia* species before and after 2016. In both the surveillance culture study and the statistical analysis, only 3 study wards showed positive results for the acquisition of *Elizabethkingia*: an ICU (ICU 1, 18 beds) used for cardiovascular disease, an isolation ward (ward A, 50 beds) used for patients with vancomycin-resistant *Enterococcus*, and a general ward (ward B, 50 beds) used for pulmonary disease patients. A total of 6,583 patients have been hospitalized in these wards since 2016.

To adjust confounding factors for the acquisition of *Elizabethkingia* species, we conducted a propensity score (PS)–matched case–control study. We defined case-patients as patients with *Elizabethkingia* species isolated from any clinical specimens during January 2016–June 2017 in ICU 1, ward A, or ward B and control patients as patients without *Elizabethkingia* species in these 3 study wards. We selected 3 variables—hospital ward ($p<0.001$), period of admission ($p = 0.041$), and length of stay in the 3 study wards ($p<0.001$)—for adjustment by univariate analysis (*26*,*27*). We estimated a PS for the predicted probability of acquisition of *Elizabethkingia* species in each patient using the logistic regression model. Then we performed a PS-matched analysis by attempting to match case-patients and control patients (1:3 match) using the nearest-neighbor-matching method. A match occurred when the difference in the logits of the PS was <0.2 times the SD of the scores.

Statistical Analysis

We assessed all variables using the Shapiro-Wilk test to evaluate Gaussian distributions. Descriptive statistics are presented as a median and interquartile range (IQR) for continuous variables or numbers and percentage for categorical variables. Comparisons between groups were analyzed using the Mann-Whitney U test for continuous variables and the Fisher exact test for categorical variables.

Using conditional logistic regression, we conducted univariate and multivariate regressions between case-patients and control patients of the 3 study wards. Dependent variables included in the multivariate analysis were selected based on statistical significance provided by univariate analysis. Incidence rate ratios and 95% CIs were calculated by comparing the mean incidences between 2009–2015 and 2016–2017 by Poisson regression.

All reported p values are 2-tailed, and p values <0.05 indicate statistical significance. We conducted statistical analyses using R statistical software (R Studio, Inc., https://www.r-project.org).

Results

The annual incidence of *Elizabethkingia* acquisition in Severance Hospital increased in 2011 (Table 1; Figure 2). According to the defined threshold, years with incidence >2 SD were 2011, 2012, 2013, 2014, and 2016. In particular, incidence increased most significantly to 109.82 cases/1 million inpatient-days in 2016 ($p<0.001$). An additional 50 cases were reported during January–June 2017, which corresponded to 127.79 cases/1 million inpatient-days. The acquisition incidence of *Elizabethkingia* species increased significantly, by 432.1%, during 2016–2017 over the acquisition incidence during 2009–2015 (relative risk [RR] 4.17, 95% CI 3.28–5.29; $p<0.001$), mainly because of the

Table 1. Annual incidence and characteristics of *Elizabethkingia* acquisitions at a tertiary teaching hospital, Seoul, South Korea

Characteristic	2009	2010	2011	2012	2013	2014	2015	2016	2017 Jan–Jun
No. cases	2	2	10	23	29	39	30	84	50
Incidence									
Per 1 million inpatient-days	2.93	2.98	14.60	33.14	42.43	55.74	40.66	109.82	127.79
Per 1,000 inpatients	0.02	0.02	0.10	0.23	0.30	0.39	0.28	0.75	0.88
Sample type, no., may be multiple									
Respiratory	2	0	2	14	25	27	26	76	48
Blood culture	0	2	2	2	2	3	1	4	3
Urine culture	0	0	5	2	2	3	1	1	0
Other*	0	0	1	5	1	7	2	6	1
Species, no.									
E. anophelis	1	2	2	7	16	17	15	45	34
E miricola	0	0	5	1	4	5	11	25	12
E. meningoseptica	1	0	3	3	5	4	1	4	2
Unconfirmed†	0	0	0	12	4	13	3	10	2

*Includes 12 from body fluids, 4 wound swabs, 3 catheter tips, 2 oral swabs, 1 eye swab, and 1 ear swab.
†Includes strains that were not stored for identification.

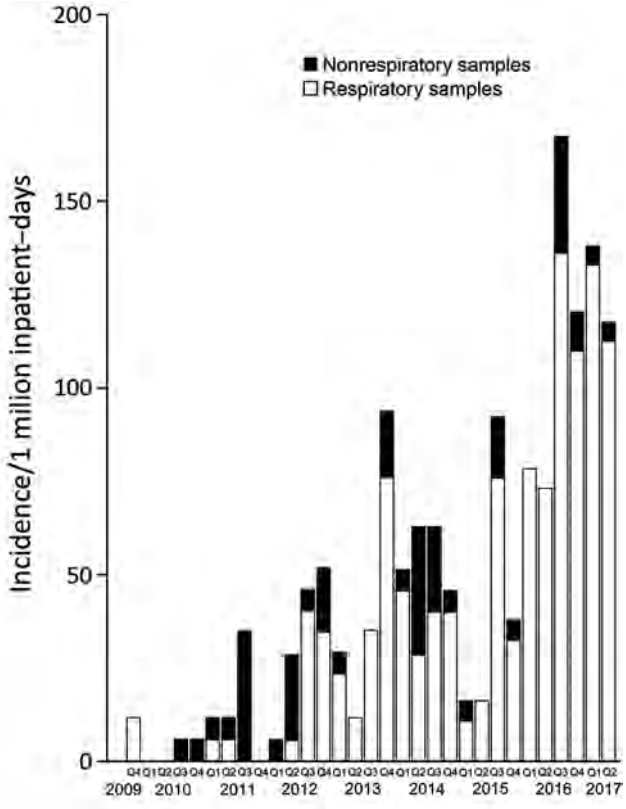

Figure 2. Trends in the quarterly incidence of *Elizabethkingia* infection or colonization in a tertiary teaching hospital, Seoul, South Korea, January 2009–June 2017. Q1, January–March; Q2, April–June; Q3, July–September; Q4, October–December.

increase in strains isolated from respiratory specimens (incidence rate ratio 3.22, 95% CI 2.46–4.20; p<0.001).

We identified 269 patients who acquired *Elizabethkingia* species during January 2009–June 2017, of whom 134 (49.8%) were reported during 2016–June 2017 (Table 2, https://wwwnc.cdc.gov/EID/article/25/1/17-1985-T2.htm). Patients who acquired *Elizabethkingia* during 2016–June 2017 were more frequently classified as having contracted a nosocomial infection than were patients who acquired *Elizabethkingia* during 2009–2015. The number of cases in the 3 study wards increased significantly but not in the other wards. In addition, more patients with chronic pulmonary disease or diabetes mellitus were seen during 2016–2017. More patients had a history of mechanical ventilation, a longer length of hospital stay, and a history of steroid use during 2009–2015 than during 2016–2017.

Surveillance Studies

We isolated 12 *Elizabethkingia* strains; all were derived from the 3 study wards. Seven *E. anophelis* isolates (4 from water taps in ICU 1, 2 from washbasins in ICU 1, and 1 from the suction regulator in ward A), 3 *E. miricola* isolates (3 from washbasins in ward A), and 2 *E. meningoseptica* isolates (1 from the mechanical ventilator after removal from a patient and 1 from the suction regulator in ward B) were identified by surveillance cultures.

We conducted PFGE typing on 54 clinical isolates (40 *E. anophelis*, 10 *E. miricola*, and 4 *E. meningoseptica*) from inpatients and 7 *E. anophelis*, 3 *E. miricola*, and 2 *E. meningoseptica* isolates from environmental samples. PFGE patterns showed that *E. anophelis* isolates belonged to 8 different PFGE groups, *E. miricola* to 4 groups, and *E. meningoseptica* to 2 groups (Figure 3). Five patients with *E. anophelis* (1 patient from ward B and 4 patients from other locations) had a history of admission to ICU 1 (Figure 3, panel A). Of patients from other locations, 1 had a history of admission to ward A and 2 had histories of admission to ward B. One patient in ICU 1 had moved from ward A, where the major cluster of environmental samples was isolated (Figure 3, panel B). Similarly, 1 patient in ICU 1 was transferred from ward B (Figure 3, panel C). This patient's history of ward transfers suggests that transmission of the bacteria from patient to patient might be a cause of spreading. However, we cannot rule out the existence of other environmental sources.

We conducted PCR on 30 *Anopheles sinensis*, 8 *Culex tritaeniorhynchus*, and 3 *Aedes vexans* mosquitoes and on surveillance cultures collected from the midgut of mosquitoes. All yielded negative results.

Epidemiologic Results Before and After PS Matching

Of the 6,583 patients potentially exposed on the 3 study wards, 74 were colonized or infected with *Elizabethkingia* species (Table 3). Case-patients and control-patients differed significantly in the proportion of hospitalized wards. The case-patient group, had higher admission rates to ward A and ward B, whereas control-patients had a higher rate of admission to ICU 1. Furthermore, case-patients had a significantly longer stay in the 3 study wards than did control-patients. In the 3 study wards, case-patients spent a median of 55 days (IQR 20–131 days), significantly longer than that of control patients (3 days [IQR 2–8 days]; p<0.001).

We conducted PS matching to adjust baseline demographics and clinical variables between the case-patient and control-patient groups. PS matching resulted in 52 matched pairs at a 1:3 ratio. After matching, we included 52 of 74 case-patients in the analysis. Confounding variables were well balanced in the 2 groups, including hospitalization ward and the period of admission and length of stay in the 3 study wards. Furthermore, the 2 comorbidities after PS matching did not differ significantly because there was an adjustment to the proportions of admission to ward A, which had high rates of patients with hematologic malignancy, and ward B, which had high rates of patients with chronic pulmonary disease. However, use of

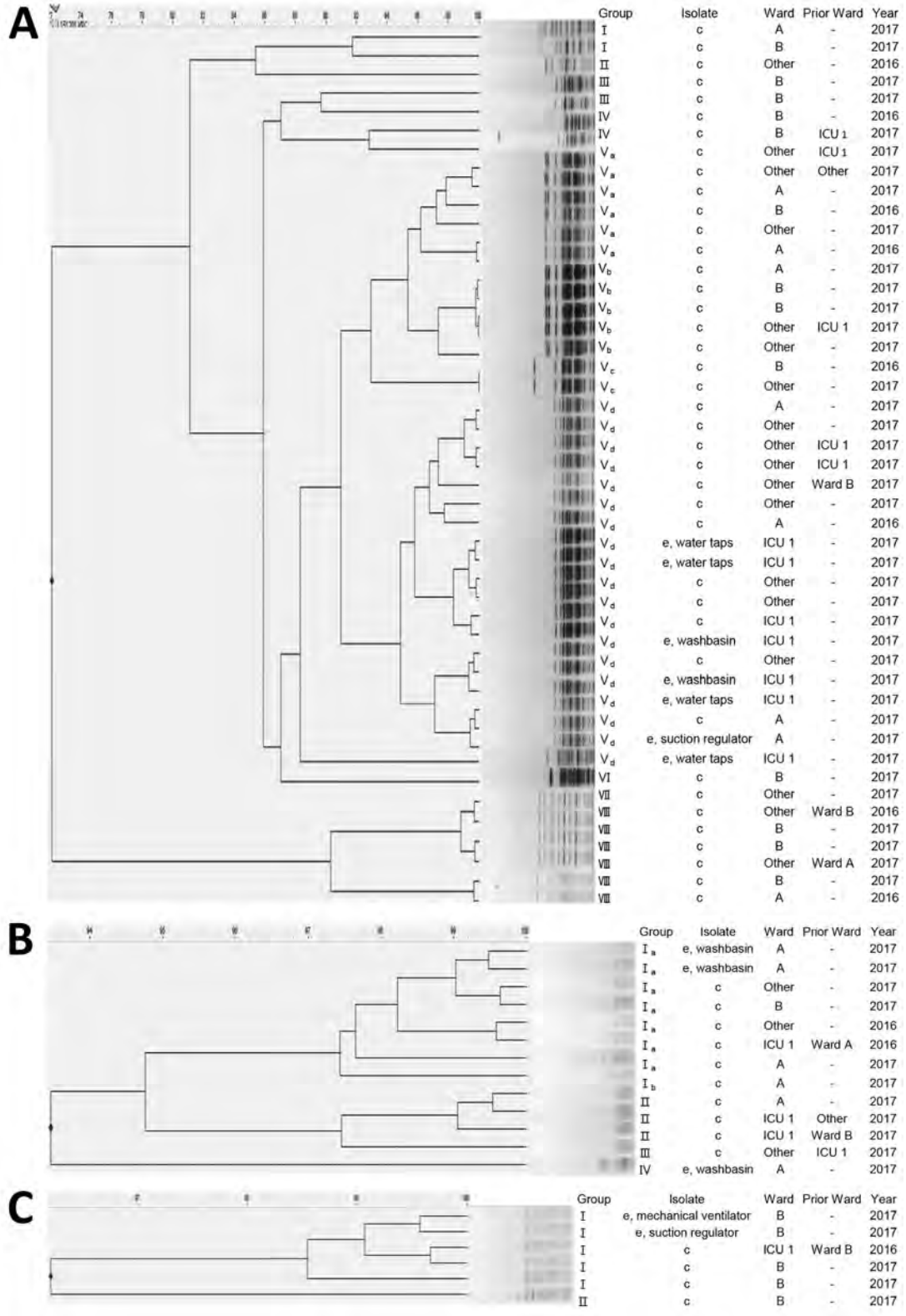

Figure 3. Pulsed-field gel electrophoresis dendrograms for 54 clinical isolates and 12 environmental isolates of *Elizabethkingia* species, Seoul, South Korea, 2017. *E. anophelis* (40 clinical isolates and 7 environmental isolates) showed 8 pulsotypes (A), *E. miricola* (10 clinical isolates and 3 environmental isolates) 4 pulsotypes (B), and *E. meningoseptica* (4 clinical isolates and 2 environmental isolates) 2 pulsotypes (C). c, clinical; e, environmental; ICU, intensive care unit. Scale bar indicates percent relatedness.

Table 3. Variables possibly associated with acquisition of *Elizabethkingia* species, before and after propensity score matching, in a tertiary teaching hospital, Seoul, South Korea

	Before matching			After matching		
Variable	Case-patients, n = 74	Control-patients, n = 6,509	p value	Case-patients, n = 52	Control-patients, n = 156	p value
Ward, no. (%)			<0.01			0.54
Ward A	24 (32.4)	587 (9.0)		21 (40.4)	76 (48.7)	
Ward B	36 (48.6)	2,607 (40.1)		25 (48.1)	62 (39.7)	
Intensive care unit 1	14 (18.9)	3,315 (50.9)		6 (11.5)	18 (11.5)	
Period of admission, no. (%)			0.26			0.79
2016 Jan–Mar	14 (18.9)	1,073 (16.5)		6 (11.5)	32 (20.5)	
2016 Apr–Jun	14 (18.9)	1,172 (18.0)		10 (19.2)	27 (17.3)	
2016 Jul–Sep	11 (14.9)	1,078 (16.6)		11 (21.2)	30 (19.2)	
2016 Oct–Dec	16 (21.6)	1,141 (17.5)		6 (11.5)	13 (8.3)	
2017 Jan–Mar	15 (20.3)	1,058 (16.3)		10 (19.2)	27 (17.3)	
2017 Apr–Jun	4 (5.4)	987 (15.2)		9 (17.3)	27 (17.3)	
Median stay in 3 wards, d (range)	55 (20–131)	3 (2–8)	<0.01	32 (6–59)	20 (5–49)	0.27
Median age, y (range)	66.5 (59.0–76.0)	67.0 (57.0–75.0)	0.72	63.5 (57.5–73.0)	66.5 (54.0–77.0)	0.79
Sex, no. (%)			0.44			0.63
M	44 (59.5)	4,197 (64.5)		28 (53.8)	76 (48.7)	
F	30 (40.5)	2,312 (35.5)		24 (46.2)	80 (51.3)	
Median Charlson comorbidity index (range)	6 (4.0–7.0)	5 (4.0–7.0)	0.14	6 (4.0–6.5)	6 (3.0–7.0)	0.99
Comorbidities, no. (%)*						
Solid-organ tumor	18 (24.3)	1,766 (27.1)	0.68	11 (21.2)	53 (34.0)	0.12
Diabetes mellitus	11 (14.9)	894 (13.7)	0.91	7 (13.5)	21 (13.5)	0.99
Chronic pulmonary disease	9 (12.2)	207 (3.2)	<0.01	5 (9.6)	9 (5.8)	0.52
Chronic kidney disease	11 (14.9)	618 (9.5)	0.17	8 (15.4)	16 (10.3)	0.45
Hematologic malignancy	6 (8.1)	164 (2.5)	0.01	4 (7.7)	9 (5.8)	0.87
Dementia	3 (4.1)	147 (2.3)	0.52	2 (3.8)	8 (5.1)	0.99
Connective tissue disease	3 (4.1)	253 (3.9)	0.99	3 (5.8)	9 (5.8)	0.99
Mild liver disease	2 (2.7)	82 (1.3)	0.56	1 (1.9)	3 (1.9)	0.99
Steroid use	23 (31.1)	562 (8.6)	<0.01	14 (26.9)	34 (21.8)	0.57
Mechanical ventilation	72 (97.3)	1,258 (19.3)	<0.01	50 (96.2)	62 (39.7)	<0.01
Antimicrobial exposure, no. (%)						
Penicillin†	5 (6.8)	393 (6.0)	0.99	2 (3.8)	15 (9.6)	0.31
1st-generation cephalosporin	2 (2.7)	445 (6.8)	0.24	1 (1.9)	11 (7.1)	0.30
2nd-generation cephalosporin	2 (2.7)	184 (2.8)	0.99	2 (3.8)	2 (1.3)	0.56
3rd-generation cephalosporin	26 (35.1)	1,089 (16.7)	<0.01	15 (28.8)	40 (25.6)	0.79
4th-generation cephalosporin	0	1	0.99	0	0	NA
Aminoglycoside	13 (17.6)	118 (1.8)	<0.01	10 (19.2)	12 (7.7)	0.04
Glycopeptide	40 (54.1)	481 (7.4)	<0.01	27 (51.9)	40 (25.6)	<0.01
Linezolid	6 (8.1)	40 (0.6)	<0.01	5 (9.6)	5 (3.2)	0.13
Carbapenem	42 (56.8)	416 (6.4)	<0.01	27 (51.9)	42 (26.9)	<0.01
Tetracycline	12 (16.2)	58 (0.9)	<0.01	5 (9.6)	7 (4.5)	0.30
Trimethoprim–sulfamethoxazole	17 (23.0)	245 (3.8)	<0.01	11 (21.2)	15 (9.6)	0.05
Lincosamide	7 (9.5)	40 (0.6)	<0.01	2 (3.8)	2 (1.3)	0.56
Macrolide	1 (1.4)	286 (4.4)	0.32	1 (1.9)	4 (2.6)	0.99
Fluoroquinolone	43 (58.1)	871 (13.4)	<0.01	30 (57.7)	45 (28.8)	<0.01
Other	5 (6.8)	100 (1.5)	<0.01	4 (7.7)	5 (3.2)	0.33

*May be multiple.
†Includes aminopenicillin, β-lactam/β-lactamase inhibitor.

mechanical ventilation still differed significantly after PS matching (p<0.001).

We used univariate and multivariate analyses with conditional logistic regression to identify independent risk factors (Table 4). Only use of mechanical ventilation (adjusted odds ratio [OR] 50.44 [95% CI 6.74–377.48]; p<0.001) was associated with the acquisition of *Elizabethkingia* species.

Only 30 patients were classified as true pathogen cases (Table 5). In the hospital mortality group, the median total hospitalization stay was longer than that of the nonhospital mortality group (77.5 vs. 38.5 days; p = 0.04). More case-patients were treated with carbapenem or trimethoprim/sulfamethoxazole than were those in the nonhospital mortality group (5 vs. 2 case-patients; p = 0.05).

Discussion

The incidence of infection with *Elizabethkingia* species has increased in recent years in many countries (*14*,*16*–*19*). Furthermore, a large-scale outbreak was reported in community settings in the United States (*28*).

In previous studies, the reported annual incidence of *E. meningoseptica* ranged from 0.007 to 0.399 cases per 1,000 admissions (*19*,*29*). We reported the antimicrobial resistance

Table 4. Results of univariate and multivariate analysis using conditional logistic regression of risk factors for the acquisition of *Elizabethkingia* species at a tertiary teaching hospital after propensity score matching, Seoul, South Korea*

	Univariate analysis		Multivariate analysis†	
Variable	OR (95% CI)	p value	OR (95% CI)	p value
Ward				
Ward A	Reference			
Ward B	0.87 (0.41–1.79)	0.70		
Intensive care unit 1	0.69 (0.18–2.22)	0.56		
Period of admission				
2016 Jan–Mar	Reference			
2016 Apr–Jun	8.03 (0.79–81.98)	0.08		
2016 Jul–Sep	8.87 (0.74–105.84)	0.08		
2016 Oct–Dec	10.62 (0.64–176.77)	0.10		
2017 Jan–Mar	8.87 (0.97–81.16)	0.05		
2017 Apr–Jun	8.34 (0.71–98.76)	0.09		
Median stay in 3 wards, d	1.01 (0.99–1.02)	0.25		
Age, y	1.00 (0.98–1.02)	0.87		
Male sex	1.06 (0.55–2.02)	0.87		
Charlson comorbidity index	0.97 (0.85–1.12)	0.69		
Comorbidities‡				
Solid organ tumor	0.48 (0.21–1.08)	0.08		
Diabetes mellitus	0.89 (0.34–2.31)	0.81		
Chronic pulmonary disease	1.85 (0.55–6.28)	0.32		
Chronic kidney disease	1.52 (0.60–3.85)	0.38		
Hematologic malignancy	1.00 (0.25–4.00)	0.99		
Dementia	0.57 (0.12–2.77)	0.49		
Connective tissue disease	0.80 (0.21–3.05)	0.75		
Mild liver disease	1.00 (0.10–9.61)	0.99		
Steroid use	1.55 (0.62–3.89)	0.35		
Mechanical ventilation	64.54 (8.76–475.30)	<0.01	50.44 (6.74–377.48)	<0.01
Antimicrobial exposure				
Penicillin§	0.32 (0.07–1.54)	0.16		
1st-generation cephalosporin	0.29 (0.03–2.88)	0.29		
2nd-generation cephalosporin	3.00 (0.42–21.30)	0.27		
3rd-generation cephalosporin	0.97 (0.46–2.01)	0.93		
4th-generation cephalosporin	NA			
Aminoglycoside	3.18 (1.21–8.31)	0.02	2.30 (0.62–8.47)	0.21
Glycopeptide	3.96 (1.82–8.63)	<0.01	1.72 (0.50–5.86)	0.39
Linezolid	8.84 (0.97–80.69)	0.05		
Carbapenem	4.16 (1.99–8.72)	<0.01	1.63 (0.55–4.85)	0.38
Tetracycline	1.65 (0.42–6.43)	0.47		
Trimethoprim/sulfamethoxazole	2.11 (0.90–4.91)	0.09		
Lincosamide	6.00 (0.54–66.17)	0.14		
Macrolide	0.75 (0.08–6.71)	0.80		
Fluoroquinolone	3.42 (1.70–6.87)	<0.01	2.01 (0.71–5.69)	0.19
Other	2.09 (0.48–9.03)	0.33		

*OR, odds ratio; NA, not available.
†Only variables with p<0.05 in the univariate model were included in the multivariate model.
‡May be multiple.
§Includes aminopenicillin, β-lactam/β-lactamase inhibitor.

mechanisms and susceptibility rates of *Elizabethkingia* species isolated from Severance Hospital in 2010 (*11*) and 2016 (*7*). Recently, the incidence of isolation in this hospital increased significantly, from 0.02 to 0.88 per 1,000 admissions during 2009–2017, mainly in the 3 study wards.

We analyzed the risk factors associated with the acquisition of *Elizabethkingia* species after controlling for other confounding variables. Using multivariate analysis, we found that the probability of acquiring *Elizabethkingia* species was significantly influenced by whether a patient received mechanical ventilation, even after PS matching and adjustment for other variables. Although some previous studies have suggested that mechanical ventilators could be a risk factor for colonization or infection with *Elizabethkingia* species, they did not provide a statistical analysis and included only a small number of patients (*16*,*30*). In our study, a total of 214 (79.6%) patients from among the 269 patients seen during January 2009–June 2017 received mechanical ventilation, as did 72 (97.3%) of 74 case-patients admitted to the 3 study wards during January 2016–June 2017. We included a large number of cases and tried to control for confounding variables using PS matching, thus ensuring that mechanical ventilation is related to the acquisition of *Elizabethkingia* species.

Water or water-related equipment can serve as a waterborne pathogen reservoir in the hospital environment (*31*). Previous studies also have associated a water source with acquisition of *Elizabethkingia* because of the bacterium's

Table 5. Results of univariable and multivariable analyses of risk factors for in-hospital mortality of patients with a true pathogen of *Elizabethkingia* in a tertiary teaching hospital, Seoul, South Korea

In-hospital mortality	Total, n = 30	Survived, n = 20	Died, n = 10	p value
Median age, y (range)	68.5 (61.0–80.0)	69.5 (60.5–79.5)	66.5 (63.0–80.0)	0.86
Male sex, no. (%)	19 (63.3)	11 (55.0)	8 (80.0)	0.35
Patients from the 3 study wards, no. (%)	7 (23.3)	5 (25.0)	2 (20.0)	0.99
Nosocomial infection, no. (%)	29 (96.7)	19 (95.0)	10 (100.0)	0.99
Median Charlson comorbidity index (range)	6 (5.0–9.0)	6 (4.5–7.5)	6 (5.0–9.0)	0.93
Clinical condition				
Median hospitalization day of acquisition (range)	26.5 (13.0–58.0)	20.5 (12.0–32.0)	52.5 (26.0–81.0)	0.03
Median length of hospitalization, d (range)	47.5 (29.0–89.0)	38.5 (27.5–67.5)	77.5 (54.0–210.0)	0.04
Mechanical ventilation, no. (%)	24 (80.0)	15 (75.0)	9 (90.0)	0.63
Steroid use, no. (%)	14 (46.7)	9 (45.0)	5 (50.0)	0.99
Antimicrobial treatment, no. (%)				
Penicillin*	5 (16.7)	3 (15.0)	2 (20.0)	0.99
1st-generation cephalosporin	3 (10)	2 (10.0)	1 (10.0)	0.99
2nd-generation cephalosporin	5 (16.7)	4 (20.0)	1 (10.0)	0.86
3rd-generation cephalosporin	8 (26.7)	4 (20.0)	4 (40.0)	0.47
4th-generation cephalosporin	7 (23.3)	4 (20.0)	3 (30.0)	0.88
Aminoglycoside	1 (3.3)	1 (5.0)	0	0.99
Glycopeptide	13 (43.3)	6 (30.0)	7 (70.0)	0.09
Linezolid	4 (13.3)	2 (10.0)	2 (20.0)	0.85
Carbapenem	7 (23.3)	2 (10.0)	5 (50.0)	0.05
Tetracycline	8 (26.7)	7 (35.0)	1 (10.0)	0.30
Colistin	3 (10)	0	3 (30.0)	0.05
Trimethoprim/sulfamethoxazole	7 (23.3)	2 (10.0)	5 (50.0)	0.05
Lincosamide	5 (16.7)	1 (5.0)	4 (40.0)	0.06
Macrolide	1 (3.3)	0	1 (10.0)	0.72
Fluoroquinolone	9 (30)	4 (20.0)	5 (50.0)	0.21
Other	5 (16.7)	2 (10.0)	3 (30.0)	0.39

*Includes aminopenicillin, β-lactam/β-lactamase inhibitor.

ability to form a biofilm in moist environments. Balm et al. reported the infections of 5 patients in 1 outbreak with *E. meningoseptica* were related to a hand hygiene sink aerator (*14*). Moore et al. identified 30 patients as having acquired *E. meningoseptica* during an outbreak; at least 10 of these infections were associated with 5 environmental samples isolated from sinks (*13*). *Elizabethkingia* can spread from a humid environment to the surface of medical devices or dry materials by the hands of hospital staff or patients (*32*). In our current study, all 12 environmental isolates shared identical PFGE patterns with clinical isolates. Our finding is consistent with prior reports that *Elizabethkingia* acquisition might be related to water sources within the hospital environment. In contrast, we could not find any evidence that the local mosquitoes of South Korea act as vehicles of *Elizabethkingia* transmission.

As extended-spectrum β-lactamase–producing bacteria have increased, the use of carbapenems has inevitably increased. Previous reports have suggested that antimicrobial selective pressure may increase the prevalence of bacteria with natural resistance to carbapenems, such as *Elizabethkingia* species (*33*,*34*). Unlike in our univariate analysis, our multivariate analysis showed no association between antimicrobial exposure to carbapenem and the acquisition of *Elizabethkingia*. One possible explanation for this finding could be that host factors are a more important selection factor than the antimicrobial drug in the selection of this strain. Another explanation could be that our data lacked the statistical power to detect differences in *Elizabethkingia* acquisition by antimicrobial exposure to carbapenem.

Difficulties in eradicating and terminating outbreaks of *Elizabethkingia* caused by a strong biofilm biotype have been reported (*13*,*14*,*35*). Furthermore, the failure of 1,000-ppm sodium hypochlorite and posthandwashing alcohol gel has been documented (*34*). The acquisition risk can be reduced by regular sink flushing and improvements to the workflow that minimize contamination (*13*). Fortunately, we succeeded in eliminating *Elizabethkingia* species in ward B in September 2017. After all structures from which bacteria were isolated were dismantled, the outer surface and inner spaces were cleaned. A sheer force was applied using a sodium hypochlorite solution and a brush, then structures were reinstalled. In ward B, no new patient acquisitions of *Elizabethkingia* occurred after this effort. These findings also support the possibility that *Elizabethkingia* acquisition may be related to water source and the contaminated devices. However, a previous study documented that *Elizabethkingia* species have been re-isolated after a month, even after all contaminated devices were replaced (*14*). Continuous monitoring, including surveillance culture systems and education for medical staff, may be more important than decontamination in reducing the acquisition of and infection with *Elizabethkingia*.

Among our data on treatment outcomes for true pathogen cases, none of the antimicrobial agents used after reporting the culture results were related to reducing in-hospital

death. Alternatively, patients treated with carbapenem or trimethoprim/sulfamethoxazole had significantly higher in-hospital death rates. However, this analysis included only 30 true pathogen cases, and results could not be adjusted for other potential confounding factors.

The retrospective and single-center nature of the study limited our results. Thus, selection bias might exist in the tests performed on environmental samples and mosquito samples, and we could not identify the species of bacteria that were not stored. It is also difficult to perform additional surveillance cultures in the hospital setting because we have conducted elimination procedures to manage bacterial spread. However, we tried to analyze risk factors for *Elizabethkingia* acquisition by minimizing the selection bias using a PS-matched study and multivariate analysis.

Even after controlling for potential biases using PS matching analysis, we found mechanical ventilation to be an independent risk factor for the acquisition of *Elizabethkingia* species. Because *Elizabethkingia* infection has a high rate of death and is difficult to eliminate, intensive prevention of contamination is needed.

About the Author

Dr. Choi is a microbiologist at the Department of Laboratory Medicine and Research Institute of Bacterial Resistance, Yonsei University College of Medicine, Seoul, South Korea. His primary research interests include antimicrobial resistance.

References

1. Vandamme P, Bernardet J-F, Kersters SK, Holmes B. New perspectives in the classification of the flavobacteria: description of *Chryseobacterium* gen. nov., *Bergeyella* gen. nov., and *Empedobacter* nom. rev. Int J Syst Evol Microbiol. 1994;44:827–31.
2. Bloch KC, Nadarajah R, Jacobs R. *Chryseobacterium meningosepticum*: an emerging pathogen among immunocompromised adults. Report of 6 cases and literature review. Medicine (Baltimore). 1997;76:30–41. http://dx.doi.org/10.1097/00005792-199701000-00003
3. Li Y, Kawamura Y, Fujiwara N, Naka T, Liu H, Huang X, et al. *Chryseobacterium miricola* sp. nov., a novel species isolated from condensation water of space station Mir. Syst Appl Microbiol. 2003;26:523–8. http://dx.doi.org/10.1078/072320203770865828
4. Green O, Murray P, Gea-Banacloche JC. Sepsis caused by *Elizabethkingia miricola* successfully treated with tigecycline and levofloxacin. Diagn Microbiol Infect Dis. 2008;62:430–2. http://dx.doi.org/10.1016/j.diagmicrobio.2008.07.015
5. Kämpfer P, Matthews H, Glaeser SP, Martin K, Lodders N, Faye I. *Elizabethkingia anophelis* sp. nov., isolated from the midgut of the mosquito *Anopheles gambiae*. Int J Syst Evol Microbiol. 2011;61:2670–5. http://dx.doi.org/10.1099/ijs.0.026393-0
6. Lau SK, Chow WN, Foo CH, Curreem SO, Lo GC, Teng JL, et al. *Elizabethkingia anophelis* bacteremia is associated with clinically significant infections and high mortality. Sci Rep. 2016;6:26045. http://dx.doi.org/10.1038/srep26045
7. Han MS, Kim H, Lee Y, Kim M, Ku NS, Choi JY, et al. Relative prevalence and antimicrobial susceptibility of clinical isolates of *Elizabethkingia* species based on 16S rRNA gene sequencing. J Clin Microbiol. 2016;55:274–80. http://dx.doi.org/10.1128/JCM.01637-16
8. Teo J, Tan SY, Tay M, Ding Y, Kjelleberg S, Givskov M, et al. First case of *E. anophelis* outbreak in an intensive-care unit. Lancet. 2013;382:855–6. http://dx.doi.org/10.1016/S0140-6736(13)61858-9
9. Lau SK, Wu AK, Teng JL, Tse H, Curreem SO, Tsui SK, et al. Evidence for *Elizabethkingia anophelis* transmission from mother to infant, Hong Kong. Emerg Infect Dis. 2015;21:232–41. http://dx.doi.org/10.3201/eid2102.140623
10. Matyi SA, Hoyt PR, Hosoyama A, Yamazoe A, Fujita N, Gustafson JE. Draft genome sequences of *Elizabethkingia meningoseptica*. Genome Announc. 2013;1:e00444-13. http://dx.doi.org/10.1128/genomeA.00444-13
11. Yum JH, Lee EY, Hur SH, Jeong SH, Lee H, Yong D, et al. Genetic diversity of chromosomal metallo-β-lactamase genes in clinical isolates of *Elizabethkingia meningoseptica* from Korea. J Microbiol. 2010;48:358–64. http://dx.doi.org/10.1007/s12275-010-9308-5
12. Chen GX, Zhang R, Zhou HW. Heterogeneity of metallo-β-lactamases in clinical isolates of *Chryseobacterium meningosepticum* from Hangzhou, China. J Antimicrob Chemother. 2006;57:750–2. http://dx.doi.org/10.1093/jac/dkl019
13. Moore LS, Owens DS, Jepson A, Turton JF, Ashworth S, Donaldson H, et al. Waterborne *Elizabethkingia meningoseptica* in adult critical care. Emerg Infect Dis. 2016;22:9–17. http://dx.doi.org/10.3201/eid2201.150139
14. Balm MN, Salmon S, Jureen R, Teo C, Mahdi R, Seetoh T, et al. Bad design, bad practices, bad bugs: frustrations in controlling an outbreak of *Elizabethkingia meningoseptica* in intensive care units. J Hosp Infect. 2013;85:134–40. http://dx.doi.org/10.1016/j.jhin.2013.05.012
15. Lin PY, Chen HL, Huang CT, Su LH, Chiu CH. Biofilm production, use of intravascular indwelling catheters and inappropriate antimicrobial therapy as predictors of fatality in *Chryseobacterium meningosepticum* bacteraemia. Int J Antimicrob Agents. 2010;36:436–40. http://dx.doi.org/10.1016/j.ijantimicag.2010.06.033
16. Weaver KN, Jones RC, Albright R, Thomas Y, Zambrano CH, Costello M, et al. Acute emergence of *Elizabethkingia meningoseptica* infection among mechanically ventilated patients in a long-term acute care facility. Infect Control Hosp Epidemiol. 2010;31:54–8. http://dx.doi.org/10.1086/649223
17. Pereira GH, Garcia DO, Abboud CS, Barbosa VL, Silva PS. Nosocomial infections caused by *Elizabethkingia meningoseptica*: an emergent pathogen. Braz J Infect Dis. 2013;17:606–9. http://dx.doi.org/10.1016/j.bjid.2013.02.011
18. Ghafur A, Vidyalakshmi PR, Priyadarshini K, Easow JM, Raj R, Raja T. *Elizabethkingia meningoseptica* bacteremia in immunocompromised hosts: the first case series from India. South Asian J Cancer. 2013;2:211–5. http://dx.doi.org/10.4103/2278-330X.119912
19. Hsu MS, Liao CH, Huang YT, Liu CY, Yang CJ, Kao KL, et al. Clinical features, antimicrobial susceptibilities, and outcomes of *Elizabethkingia meningoseptica* (*Chryseobacterium meningosepticum*) bacteremia at a medical center in Taiwan, 1999–2006. Eur J Clin Microbiol Infect Dis. 2011;30:1271–8. http://dx.doi.org/10.1007/s10096-011-1223-0
20. Charlson ME, Pompei P, Ales KL, MacKenzie CR. A new method of classifying prognostic comorbidity in longitudinal studies: development and validation. J Chronic Dis. 1987;40:373–83. http://dx.doi.org/10.1016/0021-9681(87)90171-8
21. Tanaka K, Mizusawa K, Saugstad ES. A revision of the adult and larval mosquitoes of Japan (including the Ryukyu Archipelago and the Ogasawara Islands) and Korea (Diptera: Culicidae): San Francisco: US Army Medical Lab Pacific; 1979.
22. Lindh JM, Terenius O, Faye I. 16S rRNA gene-based identification of midgut bacteria from field-caught *Anopheles gambiae* sensu lato

and *A. funestus* mosquitoes reveals new species related to known insect symbionts. Appl Environ Microbiol. 2005;71:7217–23. http://dx.doi.org/10.1128/AEM.71.11.7217-7223.2005
23. Garner JS, Jarvis WR, Emori TG, Horan TC, Hughes JM. CDC definitions for nosocomial infections, 1988. Am J Infect Control. 1988;16:128–40. http://dx.doi.org/10.1016/0196-6553(88)90053-3
24. Brady OJ, Smith DL, Scott TW, Hay SI. Dengue disease outbreak definitions are implicitly variable. Epidemics. 2015;11:92–102. http://dx.doi.org/10.1016/j.epidem.2015.03.002
25. Wagner MM, Tsui FC, Espino JU, Dato VM, Sittig DF, Caruana RA, et al. The emerging science of very early detection of disease outbreaks. J Public Health Manag Pract. 2001;7:51–9. http://dx.doi.org/10.1097/00124784-200107060-00006
26. Wyss R, Girman CJ, LoCasale RJ, Brookhart AM, Stürmer T. Variable selection for propensity score models when estimating treatment effects on multiple outcomes: a simulation study. Pharmacoepidemiol Drug Saf. 2013;22:77–85. http://dx.doi.org/10.1002/pds.3356
27. Hill J. Discussion of research using propensity-score matching: comments on 'A critical appraisal of propensity-score matching in the medical literature between 1996 and 2003' by Peter Austin, Statistics in Medicine. Stat Med. 2008;27:2055–61, discussion 2066–9. http://dx.doi.org/10.1002/sim.3245
28. Perrin A, Larsonneur E, Nicholson AC, Edwards DJ, Gundlach KM, Whitney AM, et al. Evolutionary dynamics and genomic features of the *Elizabethkingia anophelis* 2015 to 2016 Wisconsin outbreak strain. Nat Commun. 2017;8:15483. http://dx.doi.org/10.1038/ncomms15483
29. Jean SS, Lee WS, Chen FL, Ou TY, Hsueh PR. *Elizabethkingia meningoseptica*: an important emerging pathogen causing healthcare-associated infections. J Hosp Infect. 2014;86:244–9. http://dx.doi.org/10.1016/j.jhin.2014.01.009
30. Lin YT, Chiu CH, Chan YJ, Lin ML, Yu KW, Wang FD, et al. Clinical and microbiological analysis of *Elizabethkingia meningoseptica* bacteremia in adult patients in Taiwan. Scand J Infect Dis. 2009;41:628–34. http://dx.doi.org/10.1080/ 00365540903089476
31. Kanamori H, Weber DJ, Rutala WA. Healthcare outbreaks associated with a water reservoir and infection prevention strategies. Clin Infect Dis. 2016;62:1423–35. http://dx.doi.org/ 10.1093/cid/ciw122
32. Ceyhan M, Yildirim I, Tekeli A, Yurdakok M, Us E, Altun B, et al. A *Chryseobacterium meningosepticum* outbreak observed in 3 clusters involving both neonatal and non-neonatal pediatric patients. Am J Infect Control. 2008;36:453–7. http://dx.doi.org/10.1016/j.ajic.2007.09.008
33. Sader HS, Jones RN. Antimicrobial susceptibility of uncommonly isolated non-enteric gram-negative bacilli. Int J Antimicrob Agents. 2005;25:95–109. http://dx.doi.org/10.1016/j.ijantimicag.2004.10.002
34. Kirby JT, Sader HS, Walsh TR, Jones RN. Antimicrobial susceptibility and epidemiology of a worldwide collection of *Chryseobacterium* spp: report from the SENTRY Antimicrobial Surveillance Program (1997–2001). J Clin Microbiol. 2004;42:445–8. http://dx.doi.org/10.1128/JCM.42.1.445-448.2004
35. Price E, Hoffman P, Weaver G, Gilks J, Jones M, O'Brien V, et al. Difficulty with decontaminating dummies (pacifiers, soothers or comforters) for infants in hospital. J Hosp Infect. 2017;97:316. http://dx.doi.org/10.1016/j.jhin.2017.07.024

Address for correspondence: Jun Yong Choi, Department of Internal Medicine and AIDS Research Institute, Severance Hospital, Yonsei University College of Medicine, 50-1 Yonsei-ro, Seodaemun-gu, Seoul 03722, South Korea; email: seran@yuhs.ac; or Kyungwon Lee, Department of Laboratory Medicine, Severance Hospital, Research Institute of Bacterial Resistance, Yonsei University College of Medicine, 50-1 Yonsei-ro, Seodaemun-gu, Seoul 03722, South Korea; email: leekcp@yuhs.ac

Effects of Antibiotic Cycling Policy on Incidence of Healthcare-Associated MRSA and *Clostridioides difficile* Infection in Secondary Healthcare Settings

Geraldine Mary Conlon-Bingham,[1] Mamoon Aldeyab, Michael Scott, Mary Patricia Kearney, David Farren, Fiona Gilmore, James McElnay

This quasi-experimental study investigated the effect of an antibiotic cycling policy based on time-series analysis of epidemiologic data, which identified antimicrobial drugs and time periods for restriction. Cyclical restrictions of amoxicillin/clavulanic acid, piperacillin/tazobactam, and clarithromycin were undertaken over a 2-year period in the intervention hospital. We used segmented regression analysis to compare the effect on the incidence of healthcare-associated *Clostridioides difficile* infection (HA-CDI), healthcare-associated methicillin-resistant *Staphylococcus aureus* (HA-MRSA), and new extended-spectrum β-lactamase (ESBL) isolates and on changes in resistance patterns of the HA-MRSA and ESBL organisms between the intervention and control hospitals. HA-CDI incidence did not change. HA-MRSA incidence increased significantly in the intervention hospital. The resistance of new ESBL isolates to amoxicillin/clavulanic acid and piperacillin/tazobactam decreased significantly in the intervention hospital; however, resistance to piperacillin/tazobactam increased after a return to the standard policy. The results question the value of antibiotic cycling to antibiotic stewardship.

Restrictive antimicrobial prescribing guidelines have successfully reduced the incidence of *Clostridioides difficile* infection (CDI; formerly *Clostridium difficile*) and methicillin-resistant *Staphylococcus aureus* (MRSA) (*1*–*6*). However, these guidelines have been suggested to create an environment of antimicrobial homogeneity that may enhance the development and spread of antimicrobial resistance (*7*,*8*). Antibiotic cycling has been proposed as an effective strategy to increase antimicrobial heterogeneity and decrease the development of antimicrobial resistance (*8*,*9*). This method of increasing antimicrobial heterogeneity has had mixed effects on antimicrobial resistance; however, investigations have been conducted mainly in intensive care units (ICUs) and in patients with specific infections (neutropenic sepsis, ventilator-associated pneumonia), and cycling periods have been arbitrarily defined, ranging from 1 week to 6 months (*10*–*22*). In a meta-analysis of studies investigating antibiotic cycling, the optimal cycling period was identified as 30 days (*23*). When the cycling period is too long, the effect becomes equivalent to continuous use of a single agent, increasing antimicrobial homogeneity.

We aimed to evaluate the effect of an antibiotic cycling policy, derived using time-series analysis of retrospective epidemiologic data, on the incidence of healthcare-associated MRSA (HA-MRSA) and healthcare-associated CDI (HA-CDI). A secondary aim was to evaluate the effect of this policy on the incidence of infections caused by extended-spectrum β-lactamase (ESBL)–producing organisms.

Methods

We conducted the main intervention involving antibiotic cycling in Antrim Area Hospital (AAH), a 447-bed district general teaching hospital in Northern Ireland. Comparative data were collected in Causeway Hospital (CH), a 213-bed district general teaching hospital in Northern Ireland. Both hospitals form part of the Northern Health and Social Care Trust (NHSCT), which serves 436,000 persons. AAH and CH contain general medical, surgical, maternity, and gynecology wards and ICU departments (AAH ICU, 8 beds; CH ICU, 6 beds). AAH also contains a pediatric ward, a neonatal ICU, and a hematology/oncology ward and provides outpatient chemotherapy and renal dialysis services. Other specialist services, such as burn and transplant units, are provided on a regional basis by a neighboring trust. The Office of Research Ethics

Author affiliations: Queen's University Belfast, Belfast, Northern Ireland, UK (G.M. Conlon-Bingham, J. McElnay); Antrim Hospital, Antrim, Northern Ireland, UK (M. Aldeyab); Ulster University, Coleraine, Northern Ireland, UK (M. Aldeyab); Northern Health and Social Care Trust, Antrim (M. Scott, M.P. Kearney, D. Farren, F. Gilmore)

DOI: https://doi.org/10.3201/eid2501.180111

[1]Current affiliation: Craigavon Area Hospital, Craigavon, Northern Ireland, UK.

Committees of Northern Ireland (reference no. 11/NI/0110) and the NHSCT Research Governance Committee (reference no. 10-0219/11) provided ethics approval for this project.

Study Design

The study comprised 3 phases. First was development of an antibiotic cycling policy using retrospective data for April 2007–March 2012; second, implementation and assessment of the effect of this policy in AAH and comparative data collected in CH, where the policy was not implemented; and third, postintervention follow-up after return to the standard antibiotic policy in AAH (Table 1; Figures 1, 2).

Data Collection

For the retrospective part of the study (Figure 1), we determined monthly incidence of the output variables (HA-MRSA, HA-CDI) and input variables (other MRSA; other CDI; antimicrobial and infection control agent use; pharmacy, medical, and nursing staffing levels [full-time equivalents (FTEs), where 1 FTE equals 1 full-time worker]; and age-adjusted Charlson comorbidity index of all patients discharged from AAH). We obtained a record of all MRSA-positive patients identified in AAH from the hospital microbiology laboratory. Cases were classified as HA-MRSA or other MRSA (Table 1). MRSA isolates

Table 1. Overview of a study on the effects of an antibiotic drug cycling policy on the incidence of HA-MRSA and HA-CDI in 2 hospitals according to the Orion Statement, Northern Ireland, UK*

Variable	Definition
Population characteristics	The NHSCT is 1 of 5 Health and Social Care Trusts in Northern Ireland, serving ≈436,000 persons. The NHSCT has 2 acute care hospitals: AAH (intervention hospital), containing 447 beds, and CH (control hospital) containing 213 beds. These hospitals provide acute medical, surgical ICU, neonatal, pediatric, and maternity services for the NHSCT. Study wards comprised all adult inpatient wards; ICU, NNU, pediatric, and palliative care wards were excluded.
Retrospective study, 2007 Apr–2012 Mar	The intervention design was as follows: An antibiotic cycling policy was devised based on results of an analysis of HA-CDI and HA-MRSA incidence in AAH during April 2007–March 2012. This analysis identified macrolides and TZP as significantly associated with HA-MRSA with lag times of 1 mo. AMC was identified as significantly associated with HA-CDI with a lag time of 2 mo. Consequently, an antibiotic cycling policy was implemented in AAH that restricted the use of TZP and macrolides in alternate months, and AMC was restricted for 2 consecutive months in every 4 months over a 2-year period.
Comparison of effect of antibiotic cycling policy between AAH and CH, 2011 Nov–2016 Sep†	Comparison of outcome measures before and after the introduction of an antibiotic cycling policy in AAH and between the intervention hospital (AAH) and control hospital (CH). Reintroduction of standard antibiotic policy in AAH during October 2015–September 2016 to determine whether any effect observed during the intervention period was reversed upon return of the standard policy. Comparison of outcome measures between intervention and postintervention periods occurred for AAH only.
General infection control measures	Chlorine dioxide 275 ppm was used for routine environmental decontamination through the study period in both hospitals. Monthly environmental cleanliness audits were conducted on all wards. Throughout the intervention period, infection control practices did not change.
Isolation and elimination policy	All patients in whom CDI was diagnosed were placed in an isolation room. Patients identified as colonized or infected with MRSA were placed in an isolation room when one was available. However, in the event of a shortage of these rooms, these patients were placed in cohort bays.
MRSA admission screening	In both hospitals all patients with a history of MRSA; admitted from a residential or nursing home; admitted from another hospital; admitted to the ICU, NNU, or renal unit; and oncology patients were screened.
Antibiotic stewardship activities	After a CDI outbreak in 2008, restrictions were put in place throughout the NHSCT regarding use of fluoroquinolones, cephalosporins, clindamycin, and carbapenems (*4*). All requests for restricted antibiotic drugs are reviewed by the antimicrobial pharmacists and consultant microbiologists. Weekly audits were conducted on adherence to empirical antibiotic guidelines on all wards.
Definitions	1. HA-CDI incidence: No. patients presenting with CDI >48 h after admission to AAH or CH or any patient presenting with CDI ≤48 h after admission to these hospitals who had an admission to the same hospital in the preceding 4 wks (*24*). 2. Other CDI incidence: No. patients presenting with CDI ≤48 h from admission with no admission to AAH or CH in the preceding 4 wks. 3. HA-MRSA incidence: No. patients who tested negative or were not screened for MRSA on admission but tested positive for MRSA >48 h after admission (*24*). Each patient was counted once per admission. 4. Other MRSA incidence: No. patients who tested positive for MRSA ≤48 h after admission. 5. New ESBL incidence: No. newly identified patients from whom an ESBL-producing organism was isolated or known patients from whom a new ESBL strain was isolated. Each patient was counted once per admission 6. Resistant patterns (MRSA and ESBL): No. isolates per month. Duplicate isolates identified within 7 d were excluded.

*Based on (*25*). AAH, Antrim Area Hospital; AMC, amoxicillin/clavulanic acid; CDI, *Clostridioides difficile* infection; CH, Causeway Hospital; ESBL, extended-spectrum β-lactamase; HA, healthcare-associated; ICU, intensive care unit; MRSA, methicillin-resistant *Staphylococcus aureus*; NHSCT, Northern Health and Social Care Trust; NNU, neonatal unit; TZP, piperacillin/tazobactam.
†Preintervention period, 2011 Nov–2013 Sep; intervention period, 2013 Oct–2015 Sep; postintervention period, 2015 Oct–2016 Sep.

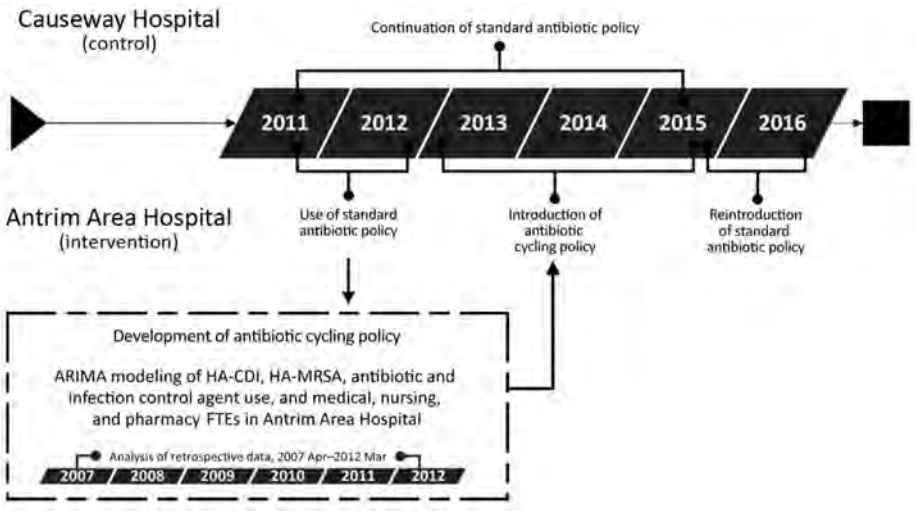

Figure 1. Investigation of the effects of an antibiotic drug cycling policy on the incidence of HA-MRSA and HA-CDI in 2 hospitals, Northern Ireland, UK. ARIMA, autoregressive integrated moving average; HA-CDI, healthcare-associated *Clostridioides difficile* infection; HA-MRSA, healthcare-associated methicillin-resistant *Staphylococcus aureus*; FTE, full-time equivalent.

from clinical samples and screening swab samples were detected according to routine microbiological procedures (*26*). Throughout the study period, targeted MRSA screening was undertaken on admission to AAH or CH for oncology patients; patients with a history of MRSA; patients admitted from a residential or nursing home; and patients admitted to the ICU, neonatal unit, or renal unit. For each patient, repeat isolates during the same admission period were excluded.

We obtained data on the number of patients in whom CDI was diagnosed from the microbiology laboratory and identified HA-CDI and other CDI cases (Table 1). During March 2007–April 2009, we identified *C. difficile* through detection of toxins A and B from the feces of patients with diarrhea using the PremierToxin A and B kit (Meridian Bioscience, Europe, http://www.meridianbioscience.eu) and an ELISA technique. In May 2009, this identification process was changed to a 3-step technique using the Techlab C.diff Quik Chek complete (Abbott, https://www.alere.com) combined glutamate dehydrogenase and toxin A and B enzyme immunoassay and the Cepheid Xpert C.difficile PCR (http://www.cepheid.com) for detection of potentially toxigenic strains (*27*).

We obtained records of monthly systemic antimicrobial drug use from the pharmacy computer system and converted to defined daily doses (DDD) (*26*,*28*). The use of antiseptic agents, such as chlorhexidine skin wash (liters), alcohol-impregnated wipes (number of wipes), and alcohol-based hand rub (liters), acted as a proxy measure for hand hygiene in the study hospitals (*29*). We determined monthly use of these agents across both hospitals during the study period from the pharmacy computer system and the National Health Service Supply Chain. We obtained the monthly number of nursing, auxiliary nursing, clinical pharmacy, and medical FTEs in AAH from the NHSCT Finance Department. We determined the monthly average age-adjusted comorbidity for AAH by calculating the Charlson age-adjusted comorbidity index of all patients discharged each month (*30*). For all of these variables, we adjusted the value to an incidence or use per 100 occupied bed days (OBD).

Using linear regression, we determined the trends in each of the explanatory variables. We constructed autoregressive integrated moving average models to model the relationship between the input and output variables in AAH for April 2007–March 2012 (Appendix, https://wwwnc.cdc.gov/EID/

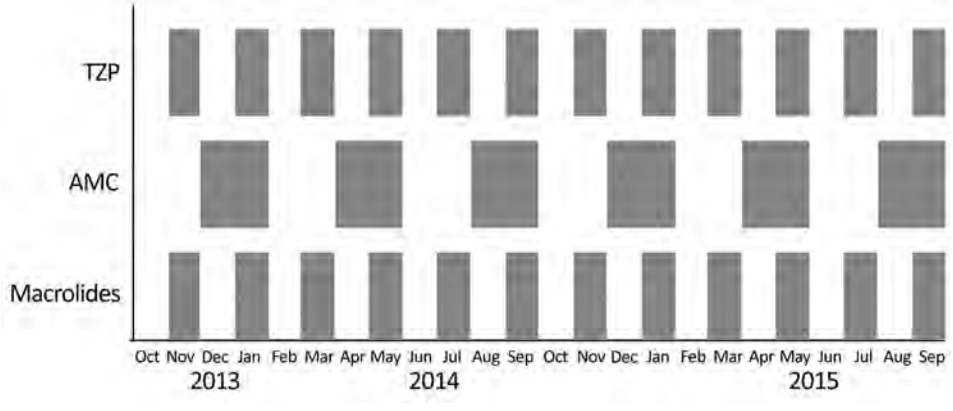

Figure 2. Antibiotic cycling schedule in Antrim Area Hospital, Northern Ireland, UK, showing the months where each antibiotic was recommended. Restrictions in the use of each antibiotic were in place during all other times. AMC, amoxicillin/clavulanic acid; TZP, piperacillin/tazobactam.

article/25/1/18-0111-App1.pdf). Based on the antimicrobial drugs that were significantly associated with HA-CDI and HA-MRSA, together with the time lag between observing a change in the antimicrobial drug use and a corresponding change in HA-MRSA or HA-CDI incidence, we developed an antibiotic cycling policy and implemented it in AAH over a 2-year period (October 13–September 15) (Figure 2).

Implementation of Cycling Policy

The antibiotic cycling policy was implemented on wards in AAH except pediatrics, neonatal unit, palliative care ward, and ICU. We excluded the palliative care ward and ICU because patients in these departments usually have received multiple previous courses of antimicrobial drugs; therefore, empirical guidelines do not apply, and antimicrobial therapy is guided by advice from the NHSCT Consultant Microbiologists. The cycling policy affected the antimicrobial recommendations for community-acquired pneumonia, hospital-acquired pneumonia, intraabdominal sepsis, and urinary tract infections. In months during which all 3 antimicrobial drugs (amoxicillin/clavulanic acid [AMC], piperacillin/tazobactam [TZP], and macrolides) were restricted, levofloxacin was recommended for the treatment of severe community-acquired pneumonia and intraabdominal sepsis. However, levofloxacin could be supplied only on receipt of an order form signed by medical staff. All patients prescribed levofloxacin were followed up for 12 weeks. During this time, the NHSCT laboratory system was used to determine the proportion of patients from whom *C. difficile* was isolated from fecal samples or MRSA from screening swab samples and clinical samples. We constructed life tables to determine the probability of remaining CDI- and MRSA-free for each week after levofloxacin treatment. After this, the cumulative probability of remaining CDI- or MRSA-free was determined and expressed as a percentage.

Before implementation of this policy, clinical staff were trained on the intervention. Monthly reminders about the policy changes were sent to staff groups, and each month a new antibiotic policy was displayed on participating wards.

During periods of restriction of a cycled antimicrobial drug, stock was removed from all bulk orders, and these drugs could be supplied only on receipt of a request form signed by a clinician, outlining the patient's details and indication for treatment. During this time, the Trustwide antibiotic stewardship activities continued as usual. These included review of requests of all restricted antimicrobial drugs by the pharmacist and consultant microbiologist and weekly audits on adherence to the Trust antibiotic policy. Where inappropriate use was identified, it was fed back to the prescriber in real time and monthly to all consultants and the medical director.

For the preintervention (November 11–September 13), intervention (October 13–September 15), and postintervention (October 15–September 2016) periods in AAH, the incidence of HA-CDI, other CDI, HA-MRSA, other MRSA, and the use of antimicrobial drugs and infection control agents were collected as described. Furthermore, HA-MRSA resistance patterns and new ESBL incidence and resistance patterns were determined. These variables were also identified in CH (November 2011–September 2015) for comparative analysis. For HA-MRSA isolates identified from clinical samples, we determined the percentage change in ciprofloxacin, erythromycin, AMC, and TZP resistance during the preintervention and intervention periods for both hospitals. Duplicate isolates identified within 7 days of the initial isolate were excluded.

We identified ESBL isolates from clinical samples using the method described by the European Committee on Antimicrobial Sensitivity Testing for the detection of ESBLs (*31*). The monthly number of new ESBL isolates and percentage change in gentamicin, ciprofloxacin, AMC, and TZP resistance during the preintervention and intervention periods was determined for both hospitals.

We assessed the effect of the antibiotic cycling policy on HA-MRSA, HA-CDI, and new ESBL incidence in AAH using segmented regression analysis (*32*). Segmented regression analysis was used to identify changes in the outcome measures in CH during the study period. We examined the effect of the antibiotic cycling policy on changes in HA-MRSA and new ESBL resistance patterns in AAH in comparison with CH using χ^2 analysis.

For AAH only, we used the aforementioned techniques to determine the effect of reverting to the standard antibiotic policy on HA-MRSA, HA-CDI, and new ESBL incidence during October 2015–September 2016. We also determined changes in resistance patterns of HA-MRSA and new ESBL isolates.

For all analyses, we considered $p<0.05$ to be statistically significant. All analyses were conducted using Eviews 8 software (QMS, http://www.eviews.com/home.html) and Microsoft Excel version 13 (https://www.microsoft.com/en-us).

Results

Retrospective Analysis

During April 2007–March 2012, a total of 275 cases of HA-CDI (average monthly incidence 0.047 cases/100 OBD [range 0–0.18 cases/100 OBD]) and 653 cases of HA-MRSA (average monthly incidence 0.11 cases/100 OBD [range 0.03–0.21 cases/100 OBD]) were reported in AAH (Appendix Table 1, Figures 1, 2). Temporal variations in HA-CDI incidence followed temporal variations in fluoroquinolone use (coefficient 0.005, $p<0.01$), with a 1-month

lag time, and AMC use (coefficient 0.0004, p = 0.02; Appendix Table 2), with a 2-month lag time. We identified significant temporal associations between HA-MRSA incidence and fluoroquinolone use (coefficient 0.004, p<0.01), with a 3-month lag time; macrolide use (coefficient 0.002, p <0.01), with a 1-month lag time; and TZP use (coefficient 0.010, p<0.01), with a 1-month lag time (Appendix Table 3). Based on these findings, an antibiotic cycling policy was implemented in AAH during October 2013–September 2015 (Figure 2).

Evaluation of Effect of Intervention

During the preintervention period, AMC use increased significantly in AAH (coefficient 0.3603, p<0.01) and CH (coefficient 0.3848, p = 0.01) (Appendix Table 4). In AAH, we observed a significant increase in TZP (coefficient 0.1119, p = 0.02), penicillins with extended-spectrum (coefficient 0.4702, p = 0.02), and first-generation cephalosporins (coefficient 0.022, p<0.01) during this period. In addition, a borderline significant increase in total antimicrobial drug use was evident. During the intervention period in both hospitals, no change in the overall use of TZP (AAH coefficient 0.1211, p = 0.25; CH coefficient 0.086, p = 0.16), AMC (AAH coefficient 0.1212, p = 0.64; CH coefficient 0.0056, p = 0.95), and macrolide (AAH coefficient –0.0126, p = 0.96; CH coefficient 0.0756, p = 0.5272) was observed. Despite this, in AAH, the monthly use of these antimicrobial drugs followed the trend that would be expected during the use of the antibiotic cycling policy (Figure 3). In AAH, during the intervention period, use of β-lactamase–sensitive penicillins (coefficient –0.1171, p<0.01) and carbapenems (coefficient –0.1124, p<0.01) decreased significantly. In CH during the intervention period, use of penicillins with extended-spectrum (coefficient 0.7081, p<0.01), tetracyclines (coefficient 0.3596, p<0.01), and total antimicrobial drugs (coefficient 1.5278, p<0.01) increased significantly. Use of carbapenems, first-generation cephalosporins, and β-lactam–sensitive penicillins also decreased significantly (Appendix Table 4).

Throughout the preintervention period, the average monthly adherence to the standard antibiotic policy was 92% in AAH and 91% in CH. HA-CDI and new ESBL incidence did not change significantly in either hospital; however, after the antibiotic cycling policy was introduced in AAH, a significant increasing trend in HA-MRSA incidence was observed, which was not evident in CH (Table 2; Figure 4). A subset analysis of the AAH HA-MRSA isolates from clinical samples also demonstrated a significant increase in the HA-MRSA trend (coefficient 0.0023, p<0.01).

During the intervention period, 792 patients received levofloxacin; 15 tested MRSA positive before receiving levofloxacin and were excluded from the MRSA cohort (Appendix Figure 3). Eleven patients tested MRSA positive during the follow-up period, and 81 patients died. The probability of remaining MRSA-free after the 12-week follow-up period was 98.5% (Appendix Figure 4). The CDI cohort comprised 792 patients, of whom 87 died during the follow-up period. Two patients tested *C. difficile* glutamate dehydrogenase–positive and *C. difficile* toxin negative, and 9 patients tested *C. difficile* toxin positive (Appendix Figure 5). The probability of remaining free of CDI during the 12-week follow-up period was 98.5% (Appendix Figure 6).

Evaluation of Postintervention Effect

During the postintervention period, the average monthly adherence to the standard antibiotic policy in AAH remained at 92% (Appendix Table 4). The overall trend in the use of each of the cycled antimicrobial drugs remained unchanged

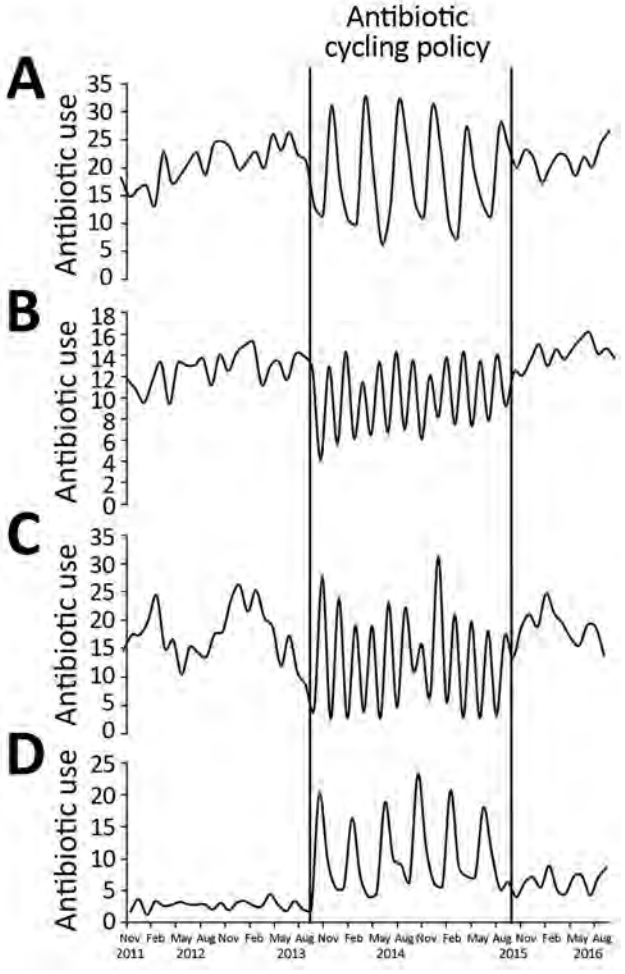

Figure 3. Trends in antibiotic use throughout preintervention (November 2011–September 2013), intervention (October 2013–September 2015), and postintervention (October 15–September 2016) periods in Antrim Area Hospital, Northern Ireland, UK. A) amoxicillin/clavulanic acid; B) piperacillin/tazobactam; C) macrolides; D) fluoroquinolones. Antibiotic use is defined daily doses/100 bed days.

Table 2. Segmented regression analysis of the incidence of HA-CDI, HA-MRSA, and infections caused by new ESBL isolates in a hospital with a cycling policy and a hospital with a standard policy, Northern Ireland, UK*

	AAH, cycling policy				CH, standard policy			
Variable	Coefficient	95% CI	SE	p value	Coefficient	95% CI	SE	p value
HA-CDI								
Constant	0.0236	0.0099 to 0.0373	0.0068	**<0.01**	–2.9873†	–3.669 to –2.3055	0.3378	**<0.01**
Trend	9.34×10^{-5}	–0.0009 to 0.0011	0.0005	0.85	–0.01905†	–0.0603 to 0.0222	0.0204	0.36
Change								
In level	–0.0084	–0.0270 to 0.0102	0.0092	0.36	–0.1335†	–0.6324 to 0.3654	0.2472	0.59
In trend	0.0004	–0.0010 to 0.0017	0.0007	0.58	0.0053†	–0.0394 to 0.0500	0.0221	0.81
HA-MRSA								
Constant	0.1100	0.0856 to 0.1343	0.0121	**<0.01**	0.0849	0.0562 to 0.1135	0.01421	**<0.01**
Trend	-2.96×10^{-3}	–0.0047 to –0.0012	0.0009	**<0.01**	–0.0008	–0.0029 to 0.0013	0.0010	0.46
Change								
In level	0.0196	–0.0134 to 0.05261	0.01634	0.24	0.0230	–0.0158 to 0.0618	0.01925	0.24
In trend	0.0041	0.0017–0.0066	0.0012	**<0.01**	–0.0005	–0.0034 to 0.0023	0.0014	0.72
New ESBL								
Constant	–3.7851†	–4.3481 to –3.2222	0.2790	**<0.01**	0.0370	0.0119 to 0.0621	0.0124	**<0.01**
Trend	–0.0018†	–0.0428 to 0.0393	0.0203	0.93	–0.0004	–0.0023 to 0.0015	0.0009	0.68
Change								
In level	0.4846†	–0.2776 to 1.2469	0.3777	0.21	–0.0093	–0.0440 to 0.0045	0.0172	0.59
In trend	0.0099†	–0.0464 to 0.0662	0.0279	0.72	0.0019	–0.0006 to 0.1564	0.0013	0.13
Outlier at 2013 Jul, CH only	NA	NA	NA	NA	0.0949	0.0333 to 0.1564	0.0305	**<0.01**

*Bold indicates statistical significance. AAH, Antrim Area Hospital; CH, Causeway Hospital; CDI, *Clostridioides difficile* infection; ESBL, extended-spectrum β-lactamase; HA, healthcare-associated; MRSA, methicillin-resistant *Staphylococcus aureus*; NA, not applicable.
†Data logarithmically transformed.

during the postintervention period (TZP trend coefficient 0.147, p = 0.12; macrolide trend coefficient –0.1699, p = 0.55; AMC trend coefficient 0.2996, p = 0.16; fluoroquinolone trend coefficient 0.148, p = 0.30). However, in AAH, use of monobactams decreased significantly (coefficient –0.2382, p<0.01 [Appendix Table 4]). Segmented regression analysis identified an immediate borderline significant decrease in HA-MRSA incidence and an immediate significant increase in new ESBL incidence (Table 3). A subset analysis of AAH HA-MRSA isolates from clinical samples demonstrated no change in the incidence of this organism after the end of antibiotic cycling; however, the level of HA-MRSA from clinical samples immediately decreased significantly (coefficient –0.029, p = 0.0261).

Effect of Antibiotic Cycling on Antimicrobial Resistance

During the preintervention, intervention, and postintervention periods in AAH and the equivalent periods in CH, HA-MRSA resistance to ciprofloxacin and erythromycin did not change (Table 4). We observed a significant decrease in resistance to AMC (–31.85% change, p<0.01) and TZP (–54.79% change, p<0.01) among new ESBL isolates in AAH during the intervention period (Table 5). In AAH after reintroduction of the standard antibiotic policy, new ESBL resistance to TZP (+11.75% change, p = 0.04), gentamicin (+23.5% change, p<0.01), and ciprofloxacin (+16.32% change, p<0.01) increased significantly.

Discussion

The use of antibiotic cycling to reduce antimicrobial resistance has been heavily debated, and many studies have produced conflicting results (*10*–*22*,*33*). We aimed to implement an antibiotic cycling policy throughout a hospital where the analysis of local epidemiologic data using autoregressive integrated moving average modeling provided the framework for the antibiotic cycling policy. The cycling of AMC, TZP, and macrolides, which the initial retrospective study predicted would decrease the incidence of HA-CDI and HA-MRSA, did not achieve this objective. HA-CDI incidence did not change during the intervention period. In addition, for patients who received levofloxacin, the probability of remaining free from CDI or MRSA in the 12 weeks after treatment was 98.5%. The incidence of new ESBL isolates during the intervention period remained unchanged, but resistance of new ESBL isolates to TZP and AMC decreased. During the postintervention period, when the standard antibiotic policy was in place, resistance of ESBL-producing organisms to TZP increased.

During the antibiotic cycling period, the incidence of HA-MRSA from clinical and surveillance samples increased significantly in AAH but reversed when the standard antibiotic policy was reintroduced. Many studies have highlighted the increased risk for MRSA infection in MRSA carriers. Recent studies reported an increased risk for invasive MRSA infection in persistent and intermittent MRSA carriage compared with placebo (*34*–*36*). The findings in our study are supported by those of a subset analysis of HA-MRSA isolates from clinical samples but must be interpreted with caution because of the small number of clinical samples included in the total HA-MRSA sample.

A recent meta-analysis hypothesized that a 1-month cycling period is the optimum time frame to reduce antimicrobial resistance (*23*). In our study, the monthly

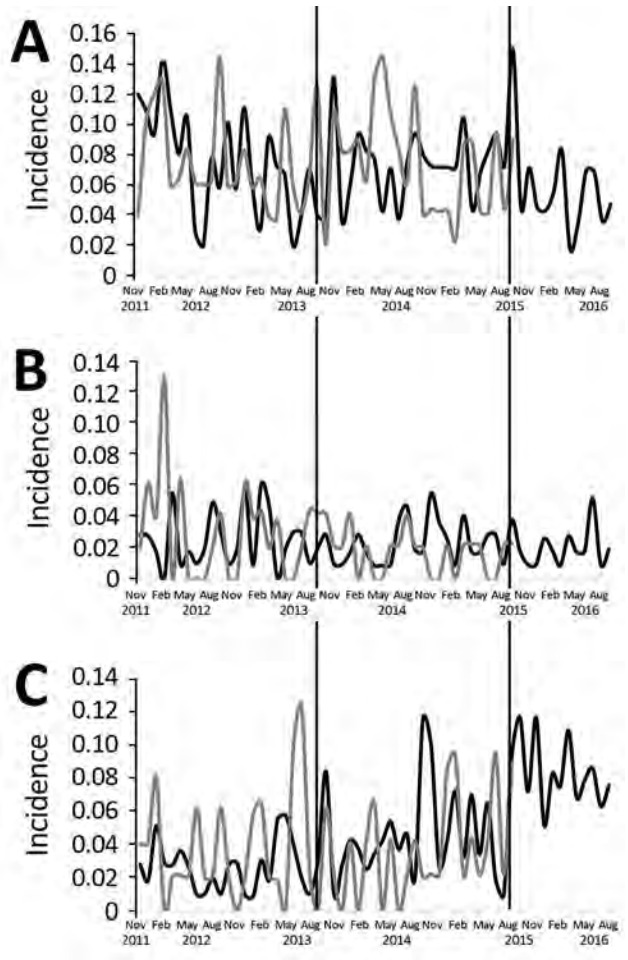

Figure 4. Incidence of healthcare-associated methicillin-resistant *Staphylococcus aureus* (A), healthcare-associated *Clostridium difficile* infection (B), and new extended-spectrum β-lactamase (C) cases throughout preintervention (November 2011–September 2013), intervention (October 2013–September 2015), and postintervention (October 15–September 2016) periods in Antrim Area Hospital and Causeway Hospital, Northern Ireland, UK. Black lines, Antrim Area Hospital; gray lines, Causeway Hospital. Incidence is number of cases per 100 occupied bed days.

cycling of clarithromycin and TZP did not decrease the incidence of HA-MRSA and HA-CDI. The reintroduction of fluoroquinolones, which are known to be associated with CDI and MRSA, may have contributed to the increase in HA-MRSA (*4*,*37*,*38*). In CH, fluoroquinolone use (5.86 DDD/100 OBD) was about half that in AAH (10.38 DDD/100 OBD), and HA-MRSA incidence did not change. Despite increased fluoroquinolone use in AAH, HA-CDI incidence did not change during the intervention and postintervention periods, when fluoroquinolone use decreased. Other studies have demonstrated decreases in CDI after reductions in AMC, fluoroquinolones, cephalosporin, clindamycin, and amoxicillin use (*39*,*40*). However, in these studies, the baseline incidence of CDI was ≈10-fold higher than in our investigation (0.2 cases/100 OBD vs. 0.02 cases/100 OBD in AAH). Furthermore, fluoroquinolones are particularly associated with *C. difficile* ribotype 027 (*4*). During an outbreak of this ribotype in AAH, average monthly fluoroquinolone use was 13 DDD/100 OBD, which was less than the highest levels (23 DDD/100 OBD) during the intervention period in our investigation (*4*). Despite these well-documented associations, we observed no such increase in HA-CDI during the cycling period. Vernaz et al. found no significant association between fluoroquinolone use and CDI in a setting where the baseline incidence was similar to that in AAH (0.027 cases/100 OBD) (*40*). That study suggested that in the nonoutbreak situation with an absence of the 027 strain and low baseline CDI incidence, when coupled with good infection control practices, antimicrobial drugs might play a less important role in transmitting this organism.

Although the antibiotic cycling policy was not designed to reduce ESBL incidence, we monitored this organism to ensure it did not increase as an inadvertent effect of the intervention, particularly the reintroduction of fluoroquinolones. New ESBL incidence did not change during the intervention period, but upon return of the standard policy, new ESBL incidence immediately increased in AAH. Because this increase did not continue throughout the postintervention period, it might have been a delayed effect of the antibiotic cycling policy. An association between ESBL incidence in AAH and both hospital fluoroquinolone use and community AMC use has previously been described; therefore, the increase in new ESBL-producing organisms in our study might have resulted from the increased use of fluoroquinolones during the intervention and postintervention periods (*41*). Primary care antimicrobial drug use also might have contributed to the increase in ESBL-producing organisms, but because we did not measure that variable, we cannot quantify the association.

Previous studies have demonstrated reversal in fluoroquinolone resistance after continuous restriction of this drug (*41*). However, our study demonstrated a reduction in TZP and AMC resistance after cycling of these agents, which was reversed for TZP upon its return to the policy, suggesting that through cycling, the balance between using TZP and reducing resistance can be achieved. Several studies have demonstrated the effectiveness of β-lactam/β-lactamase combinations in treating infections caused by ESBL-producing organisms, particularly infections with organisms for which the MICs for TZP are <16 μg/L (*42*–*45*). Harris et al. highlighted the lack of well-designed studies proving that β-lactam/β-lactamase combinations are inferior to carbapenems in treating these infections and called for more robust studies in this area (*46*). The findings of our study may provide a treatment option in less severe

Table 3. Segmented regression analysis of effect of stopping cycling on the incidence of HA-CDI, HA-MRSA, and new ESBL isolates in Antrim Area Hospital, Northern Ireland, UK*

Variable	Coefficient	95% CI	SE	p value
HA-CDI				
Constant	0.0173	0.0062 to 0.0284	0.0054	**<0.01**
Trend	4.73×10^{-4}	−0.0003 to 0.0012	0.0004	0.22
Change				
In level	−0.0159	−0.0352 to 0.0033	0.0094	0.10
In trend	0.0005	−0.0018 to 0.0028	0.0011	0.65
HA-MRSA				
Constant	0.0598	0.0388 to 0.0810	0.0102	**<0.01**
Trend	0.0012	−0.0002 to 0.0027	0.0007	0.10
Change				
In level	−0.0350	−0.0711 to −0.001	0.0179	**0.0**6
In trend	−0.0016	−0.002 to 0.0027	0.0022	0.45
New ESBL				
Constant	0.0438	0.0200 to 0.0672	0.0115	**<0.01**
Trend	0.0005	−0.0011 to 0.0021	0.0008	0.56
Change				
In level	0.0419	0.0017 to 0.0820	0.0199	**0.04**
In trend	−0.0026	−0.0074 to 0.0023	0.0024	0.30

*In this hospital, a cycling policy was in place during October 2013–September 2015, and a standard policy was in place during October 2015–September 2016. Bold indicates statistical significance. ESBL, extended-spectrum β-lactamase; HA-CDI, healthcare-associated *Clostridioides difficile* infection; HA-MRSA, healthcare-associated methicillin-resistant *Staphylococcus aureus*.

infections caused by ESBL-producing organisms, enabling carbapenems to be spared.

The successful implementation of the antibiotic cycling policy relied heavily on face-to-face engagement with all hospital staff during its development. We sought feedback from each department about potential issues with the proposed restrictions. A main difficulty was managing the restriction at ward level, ensuring restricted stock could not be unnecessarily prescribed. AAH benefited from the presence of a clinical pharmacist and pharmacy technician on all inpatient wards. These pharmacists were vital in ensuring that all ward staff were aware of the restrictions in a given month. Pharmacy technicians removed restricted antimicrobial drugs from the ward stock lists so the ward could not order a restricted drug without a preorder form outlining the patient's details and the reason for the prescription. This resource-intense intervention might be challenging to deliver in other settings, particularly where clinical pharmacy resources are limited.

Because this study was ecological in design, it suffers from the ecological fallacy, where inferences made at the population level cannot be extrapolated to the patient level. However, because of the complex dynamics of healthcare-associated infection transmission, antimicrobial drug use at the population level contributes to the individual risk for healthcare-associated infections (*47*). The use of alcohol-based hand rub and chlorhexidine skin wash was used as proxy for infection control practices because obtaining consistent data on compliance with isolation and infection control policies was not possible. During the intervention and postintervention periods, the use of other groups of antibiotics in AAH and CH changed significantly because controlling the use of all antimicrobial drugs was not possible. The decrease in monobactam use in AAH during the postintervention period resulted from ending the intervention, whereby aztreonam was replaced by the previously restricted AMC and TZP.

Table 4. Changes in resistance patterns of healthcare-associated methicillin-resistant *Staphylococcus aureus* clinical isolates, Northern Ireland, UK*

	AAH, no. resistant isolates/total tested (%)			CH, no. resistant isolates/total tested (%)		
Antibiotic comparison	Preintervention resistance	Intervention resistance	p value	Preintervention resistance	Intervention resistance	p value
Preintervention vs. intervention						
Amoxicillin/clavulanic acid	2/2 (100)	2/2 (100)	NA	2/2 (100)	0	NA
Piperacillin/tazobactam	1/1 (100)	1/1 (100)	NA	1/1 (100)	0	NA
Ciprofloxacin	66/66 (100)	77/78 (98.7)	0.99	31/31 (100)	33/34 (97.1)	0.17
Erythromycin	54/70 (77.1)	69/80 (86.3)	0.18	23/32 (71.9)	22/35 (65.9)	0.43
Intervention vs. postintervention						
Amoxicillin/clavulanic acid	2/2 (100)	2/2 (100)	NA	NR	NR	NR
Piperacillin/tazobactam	1/1 (100)	0	NA	NR	NR	NR
Ciprofloxacin	77/78 (98.7)	27/27 (100)	0.74	NR	NR	NR
Erythromycin	69/80 (86.3)	23/28 (82.1)	0.40	NR	NR	NR

*In AAH (antibiotic cycling policy) and CH (standard antibiotic policy), the preintervention period was November 2011–September 2013, and the intervention period was October 2013–September 2015. In AAH, the postintervention period was October 2015–September 2016. AAH, Antrim Area Hospital; CH, Causeway Hospital; NA, no isolates tested against amoxicillin/clavulanic acid and piperacillin/tazobactam; NR, data not recorded.

Table 5. Changes in resistance patterns of new extended-spectrum β-lactamase isolates during the preintervention period, Northern Ireland, UK*

	AAH, no. resistant isolates/total tested (%)			CH, no. resistant isolates/total tested (%)		
Antibiotic comparison	Preintervention resistance	Intervention resistance	p value	Preintervention resistance	Intervention resistance	p value
Preintervention vs. intervention						
Amoxicillin/clavulanic acid	59/65 (90.8)	76/129 (58.9)	**<0.0**1	38/41 (92.7)	33/42 (78.6)	0.07
Piperacillin/tazobactam	50/65 (76.9)	29/131 (22.1)	**<0.0**1	28/41 (68.3)	21/41 (51.2)	0.11
Ciprofloxacin	43/66 (65.2)	78/132 (59.1)	0.41	25/40 (62.5)	26/40 (65.0)	0.82
Gentamicin	20/67 (29.9)	38/135 (28.1)	0.81	15/41 (36.6)	22/42 (52.4)	0.15
Intervention vs. postintervention						
Amoxicillin/clavulanic acid	76/129 (58.9)	80/122 (65.6)	0.28	NR	NR	NR
Piperacillin/tazobactam	29/131 (22.1)	41/121 (33.9)	**0.04**	NR	NR	NR
Ciprofloxacin	78/132 (59.1)	92/122 (75.4)	**<0.01**	NR	NR	NR
Gentamicin	38/135 (28.1)	63/122 (51.6)	**<0.01**	NR	NR	NR

*In AAH (antibiotic cycling policy) and CH (standard antibiotic policy), the preintervention period was November 2011–September 2013, and the intervention period was October 2013–September 2015. In AAH, the postintervention period was October 2015–September 2016. Bold indicates statistical significance. AAH, Antrim Area Hospital; CH, Causeway Hospital; NR, data not recorded.

For analysis of changes in HA-MRSA resistance patterns, we included only clinical samples, which accounted for 30% of total MRSA isolates. Before the intervention, the trend in new ESBL resistance to AMC and TZP was decreasing as a result of a change in interpretative standards from Clinical and Laboratory Standards Institute to European Committee on Antimicrobial Susceptibility Testing breakpoints in November 2011 (*31*). Selection and information biases were limited in this study through the inclusion of all patients with HA-MRSA, HA-CDI, and a new ESBL-producing organism. All data were collected from electronic databases that were populated as part of routine microbiology procedures. This study is also limited by the relatively short intervention period of 2 years, compared with other studies with intervention periods of 5–9 years, which resulted in changes in antimicrobial resistance (*13*,*18*).

Our results suggest that antibiotic cycling is not an appropriate strategy to reduce the incidence of HA-MRSA or HA-CDI but might be effective in reducing ESBL resistance. The increased use of fluoroquinolones in a cyclical fashion was not associated with any increase in HA-CDI, suggesting that this method may help diversify antimicrobial drug use while mitigating adverse effects.

This work was supported by a grant from the Northern Ireland Health and Social Care Research and Development Office (EAT/4375/10 to G.M.C.B.).

About the Author

Dr. Conlon-Bingham is the lead antimicrobial pharmacist in the Southern Health and Social Care Trust, Craigavon. Her research interests include antibiotic surveillance and stewardship and interventions to control healthcare-acquired infections.

References

1. Specialist Advisory Committee on Antimicrobial Resistance (SACAR). Specialist Advisory Committee on Antimicrobial Resistance Antimicrobial Framework. J Antimicrob Chemother. 2007;60(Suppl1):i87–90. http://dx.doi.org/10.1093/jac/dkm185
2. Ashiru-Oredope D, Budd EL, Bhattacharya A, Din N, McNulty CA, Micallef C, et al.; English Surveillance Programme for Antimicrobial Utilisation and Resistance (ESPAUR). Implementation of antimicrobial stewardship interventions recommended by national toolkits in primary and secondary healthcare sectors in England: TARGET and Start Smart Then Focus. J Antimicrob Chemother. 2016;71:1408–14. http://dx.doi.org/10.1093/jac/dkv492
3. Ashiru-Oredope D, Hopkins S; English Surveillance Programme for Antimicrobial Utilization and Resistance Oversight Group. Antimicrobial stewardship: English Surveillance Programme for Antimicrobial Utilization and Resistance (ESPAUR). J Antimicrob Chemother. 2013;68:2421–3. http://dx.doi.org/10.1093/jac/dkt363
4. Aldeyab MA, Devine MJ, Flanagan P, Mannion M, Craig A, Scott MG, et al. Multihospital outbreak of *Clostridium difficile* ribotype 027 infection: epidemiology and analysis of control measures. Infect Control Hosp Epidemiol. 2011;32:210–9. http://dx.doi.org/10.1086/658333
5. Aldeyab MA, Scott MG, Kearney MP, Alahmadi YM, Magee FA, Conlon G, et al. Impact of an enhanced antibiotic stewardship on reducing methicillin-resistant *Staphylococcus aureus* in primary and secondary healthcare settings. Epidemiol Infect. 2014;142:494–500. http://dx.doi.org/10.1017/S0950268813001374
6. Cook PP, Gooch M. Long-term effects of an antimicrobial stewardship programme at a tertiary-care teaching hospital. Int J Antimicrob Agents. 2015;45:262–7. http://dx.doi.org/10.1016/j.ijantimicag.2014.11.006
7. Livermore DM. Of stewardship, motherhood and apple pie. Int J Antimicrob Agents. 2014;43:319–22. http://dx.doi.org/10.1016/j.ijantimicag.2014.01.011
8. Bal AM, Kumar A, Gould IM. Antibiotic heterogeneity: from concept to practice. Ann N Y Acad Sci. 2010;1213:81–91. http://dx.doi.org/10.1111/j.1749-6632.2010.05867.x
9. Masterton RG. Antibiotic heterogeneity. Int J Antimicrob Agents. 2010;36(Suppl 3):S15–8. http://dx.doi.org/10.1016/S0924-8579(10)70005-4
10. Martínez JA, Nicolás JM, Marco F, Horcajada JP, Garcia-Segarra G, Trilla A, et al. Comparison of antimicrobial cycling and mixing strategies in two medical intensive care units. Crit Care Med. 2006; 34:329–36. http://dx.doi.org/10.1097/01.CCM.0000195010.63855.45
11. Gruson D, Hilbert G, Vargas F, Valentino R, Bebear C, Allery A, et al. Rotation and restricted use of antibiotics in a medical intensive care unit. Impact on the incidence of ventilator-associated pneumonia caused by antibiotic-resistant gram-negative bacteria. Am J Respir Crit Care Med. 2000;162:837–43. http://dx.doi.org/10.1164/ajrccm.162.3.9905050
12. Gruson D, Hilbert G, Vargas F, Valentino R, Bui N, Pereyre S, et al. Strategy of antibiotic rotation: long-term effect on incidence

and susceptibilities of gram-negative bacilli responsible for ventilator-associated pneumonia. Crit Care Med. 2003; 31:1908–14. http://dx.doi.org/10.1097/01.CCM.0000069729.06687.DE
13. Sarraf-Yazdi S, Sharpe M, Bennett KM, Dotson TL, Anderson DJ, Vaslef SN. A 9-year retrospective review of antibiotic cycling in a surgical intensive care unit. J Surg Res. 2012;176:e73–8. http://dx.doi.org/10.1016/j.jss.2011.12.014
14. Toltzis P, Dul MJ, Hoyen C, Salvator A, Walsh M, Zetts L, et al. The effect of antibiotic rotation on colonization with antibiotic-resistant bacilli in a neonatal intensive care unit. Pediatrics. 2002;110:707–11. http://dx.doi.org/10.1542/peds.110.4.707
15. Sandiumenge A, Diaz E, Rodriguez A, Vidaur L, Canadell L, Olona M, et al. Impact of diversity of antibiotic use on the development of antimicrobial resistance. J Antimicrob Chemother. 2006;57:1197–204. http://dx.doi.org/10.1093/jac/dkl097
16. Sandiumenge A, Lisboa T, Gomez F, Hernandez P, Canadell L, Rello J. Effect of antibiotic diversity on ventilator-associated pneumonia caused by ESKAPE Organisms. Chest. 2011;140:643–51. http://dx.doi.org/10.1378/chest.11-0462
17. Takesue Y, Ohge H, Sakashita M, Sudo T, Murakami Y, Uemura K, et al. Effect of antibiotic heterogeneity on the development of infections with antibiotic-resistant gram-negative organisms in a non-intensive care unit surgical ward. World J Surg. 2006;30:1269–76. http://dx.doi.org/10.1007/s00268-005-0781-7
18. Cadena J, Taboada CA, Burgess DS, Ma JZ, Lewis JS II, Freytes CO, et al. Antibiotic cycling to decrease bacterial antibiotic resistance: a 5-year experience on a bone marrow transplant unit. Bone Marrow Transplant. 2007;40:151–5. http://dx.doi.org/10.1038/sj.bmt.1705704
19. Nijssen S, Fluit A, van de Vijver D, Top J, Willems R, Bonten MJ. Effects of reducing beta-lactam pressure on intestinal colonisation of antibiotic resistant gram-negative bacteria. J Intensive Care Med. 2010;36:512–9. http://dx.doi.org/10.1007/s00134-009-1714-y
20. Ginn AN, Wiklendt AM, Gidding HF, George N, O'Driscoll JS, Partridge SR, et al. The ecology of antibiotic use in the ICU: homogeneous prescribing of cefepime but not tazocin selects for antibiotic resistant infection. PLoS One. 2012;7:e38719. http://dx.doi.org/10.1371/journal.pone.0038719
21. Chong Y, Shimoda S, Yakushiji H, Ito Y, Miyamoto T, Kamimura T, et al. Antibiotic rotation for febrile neutropenic patients with hematological malignancies: clinical significance of antibiotic heterogeneity. PLoS One. 2013;8:e54190. http://dx.doi.org/10.1371/journal.pone.0054190
22. Puzniak LA, Mayfield J, Leet T, Kollef M, Mundy LM. Acquisition of vancomycin-resistant enterococci during scheduled antimicrobial rotation in an intensive care unit. Clin Infect Dis. 2001;33:151–7. http://dx.doi.org/10.1086/321807
23. Abel zur Wiesch P, Kouyos R, Abel S, Viechtbauer W, Bonhoeffer S. Cycling empirical antibiotic therapy in hospitals: meta-analysis and models. PLoS Pathog. 2014;10:e1004225. http://dx.doi.org/10.1371/journal.ppat.1004225
24. Cohen AL, Calfee D, Fridkin SK, Huang SS, Jernigan JA, Lautenbach E, et al.; Society for Healthcare Epidemiology of America and the Healthcare Infection Control Practices Advisory Committee. Recommendations for metrics for multidrug-resistant organisms in healthcare settings: SHEA/HICPAC Position paper. Infect Control Hosp Epidemiol. 2008;29:901–13. http://dx.doi.org/ 10.1086/591741
25. Stone SP, Cooper BS, Kibbler CC, Cookson BD, Roberts JA, Medley GF, et al. The ORION statement: guidelines for transparent reporting of outbreak reports and intervention studies of nosocomial infection. Lancet Infect Dis. 2007;7:282–8. http://dx.doi.org/10.1016/S1473-3099(07)70082-8
26. Aldeyab MA, Monnet DL, López-Lozano JM, Hughes CM, Scott MG, Kearney MP, et al. Modelling the impact of antibiotic use and infection control practices on the incidence of hospital-acquired methicillin-resistant *Staphylococcus aureus*: a time-series analysis. J Antimicrob Chemother. 2008;62:593–600. http://dx.doi.org/10.1093/jac/dkn198
27. Crobach MJT, Dekkers OM, Wilcox MH, Kuijper EJ. European Society of Clinical Microbiology and Infectious Diseases (ESCMID): data review and recommendations for diagnosing *Clostridium difficile*-infection (CDI). Clin Microbiol Infect. 2009;15:1053–66. http://dx.doi.org/10.1111/j.1469-0691.2009.03098.x
28. WHO Collaborating Center for Drug Statistics Methodology. Guidelines for ATC classifications and DDDs assignment [cited 2015 Apr 4]. http://www.whocc.no/atc_ddd_index/
29. Stone SP, Fuller C, Savage J, Cookson B, Hayward A, Cooper B, et al. Evaluation of the national Cleanyourhands campaign to reduce *Staphylococcus aureus* bacteraemia and *Clostridium difficile* infection in hospitals in England and Wales by improved hand hygiene: four year, prospective, ecological, interrupted time series study. BMJ. 2012;344:e3005. 10.1136/bmj.e3005 http://dx.doi.org/10.1136/bmj.e3005
30. Charlson ME, Pompei P, Ales KL, MacKenzie CR. A new method of classifying prognostic comorbidity in longitudinal studies: development and validation. J Chronic Dis. 1987;40:373–83. http://dx.doi.org/10.1016/0021-9681(87)90171-8
31. European Committee on Antimicrobial Susceptibility Testing (EUCAST). EUCAST guidelines for the detection of resistance mechanisms and specific resistances of clinical and/or epidemiological importance. Sweden. 2013 [cited 2016 Aug 19]. http://www.eucast.org/fileadmin/src/media/PDFs/EUCAST_files/Resistance_mechanisms/EUCAST_detection_of_resistance_mechanisms_v1.0_20131211.pdf
32. Cochrane Effective Practice and Organisation of Care Group. Interrupted time series (ITS) analyses-SPSS time series analysis.2013 [cited 2016 Aug 18]. https://epoc.cochrane.org/sites/epoc.cochrane.org/files/uploads/21%20Interrupted%20time%20series%20analyses%202013%2008%2012_1.pdf
33. Tsukayama DTL, van Loon HJ, Cartwright C, Chmielewski B, Fluit AC, van der Werken C, et al.; RADAR trial. The evolution of Pseudomonas aeruginosa during antibiotic rotation in a medical intensive care unit: the RADAR-trial. Int J Antimicrob Agents. 2004;24:339–45. http://dx.doi.org/10.1016/j.ijantimicag.2004.04.011
34. Gupta K, Martinello RA, Young M, Strymish J, Cho K, Lawler E. MRSA nasal carriage patterns and the subsequent risk of conversion between patterns, infection, and death. PLoS One. 2013;8:e53674. http://dx.doi.org/10.1371/journal.pone.0053674
35. Safdar N, Bradley EA. The risk of infection after nasal colonization with *Staphylococcus aureus*. Am J Med. 2008;121:310–5. http://dx.doi.org/10.1016/j.amjmed.2007.07.034
36. Vigil DI, Harden WD, Hines AE, Hosokawa PW, Henderson WG, Bessesen MT. Risk of MRSA infection in patients with intermittent versus persistent MRSA nares colonization. Infect Control Hosp Epidemiol. 2015;36:1292–7. http://dx.doi.org/10.1017/ice.2015.190
37. Couderc C, Jolivet S, Thiebaut ACM, Ligier C, Remy L, Alvarez AS, et al. on behalf of the Antibiotic Use and Staphylococcus aureus Resistance to Antibiotics (ASAR) Study Group. Fluoroquinolone use is a risk factor for methicillin resistant *Stapylococcus aureus* acquisition in long-term care facilities: a nested case–control study. Clin Infect Dis. 2014;39:206–15. http://dx.doi.org/10.1093/cid/ciu236
38. Bertrand X, Lopez-Lozano JM, Slekovec C, Thouverez M, Hocquet D, Talon D. Temporal effects of infection control practices and the use of antibiotics on the incidence of MRSA. J Hosp Infect. 2012;82:164–9. http://dx.doi.org/10.1016/j.jhin.2012.07.013
39. Talpaert MJ, Gopal Rao G, Cooper BS, Wade P. Impact of guidelines and enhanced antibiotic stewardship on reducing broad-spectrum antibiotic usage and its effect on incidence of *Clostridium difficile* infection. J Antimicrob Chemother. 2011;66:2168–74. http://dx.doi.org/10.1093/jac/dkr253
40. Vernaz N, Sax H, Pittet D, Bonnabry P, Schrenzel J, Harbarth S. Temporal effects of antibiotic use and hand rub consumption on

the incidence of MRSA and *Clostridium difficile.* J Antimicrob Chemother. 2008;62:601–7. http://dx.doi.org/10.1093/jac/dkn199
41. Aldeyab MA, Harbarth S, Vernaz N, Kearney MP, Scott MG, Darwish Elhajji FW, et al. The impact of antibiotic use on the incidence and resistance pattern of extended-spectrum beta-lactamase-producing bacteria in primary and secondary healthcare settings. Br J Clin Pharmacol. 2012;74:171–9. http://dx.doi.org/10.1111/j.1365-2125.2011.04161.x
42. Lagacé-Wiens PRS, Nichol KA, Nicolle LE, DeCorby M, McCracken M, Mulvey MR, et al. Treatment of lower urinary tract infection caused by multidrug-resistant extended-spectrum-β-lactamase-producing *Escherichia coli* with amoxicillin/clavulanate: case report and characterization of the isolate. J Antimicrob Chemother. 2006;57:1262–3. http://dx.doi.org/10.1093/jac/dkl102
43. Rodríguez-Baño J, Alcalá JC, Cisneros JM, Grill F, Oliver A, Horcajada JP, et al. Community infections caused by extended-spectrum beta-lactamase–producing *Escherichia coli.* Arch Intern Med. 2008;168:1897–902. http://dx.doi.org/10.1001/archinte.168.17.1897
44. Vardakas KZ, Tansarli GS, Rafailidis PI, Falagas ME. Carbapenems versus alternative antibiotics for the treatment of bacteraemia due to *Enterobacteriaceae* producing extended-spectrum β-lactamases: a systematic review and meta-analysis. J Antimicrob Chemother. 2012;67:2793–803. http://dx.doi.org/10.1093/jac/dks301
45. Rodriguez Bano J, Navarro MD, Retamar P, Picon E, Pascual A. The extended spectrum beta lactamases group. β-lactam/β-lactam inhibitor combinations for the treatment of bacteraemia due to extended spectrum β-lactamase producing *Escherichia coli*: a post hoc analysis of prospective cohorts. Clin Infect Dis. 2012;54:167–74. http://dx.doi.org/10.1093/cid/cir790
46. Harris PNA, Tambyah PA, Paterson DL. β-lactam and β-lactamase inhibitor combinations in the treatment of extended-spectrum β-lactamase producing *Enterobacteriaceae*: time for a reappraisal in the era of few antibiotic options? Lancet Infect Dis. 2015;15:475–85. http://dx.doi.org/10.1016/S1473-3099(14)70950-8
47. Muller A, Mauny F, Talon D, Donnan PT, Harbarth S, Bertrand X. Effect of individual- and group-level antibiotic exposure on MRSA isolation: a multilevel analysis. J Antimicrob Chemother. 2006;58:878–81. http://dx.doi.org/10.1093/jac/dkl343

Address for correspondence: Geraldine Mary Conlon-Bingham, Pharmacy Department, Craigavon Area Hospital, 68 Lurgan Rd, Portadown, Craigavon, Northern Ireland BT63 5QQ, UK; email: geraldine.conlonbingham@southerntrust.hscni.net

etymologia

Penicillin [pen"ĭ-sil'in]

Ronnie Henry

In 1928, while studying *Staphylococcus* bacteria at Saint Mary's Hospital in London, Alexander Fleming noticed that one of his petri dishes was contaminated with mold, which was causing the bacteria near it to lyse. Because the mold was identified as belonging to the genus *Penicillium* (Latin for "brush," referring to the chains of conidia that resemble a paintbrush or broom), Fleming named the antibacterial substance penicillin.

Among the earliest known clinical uses of penicillin was by Cecil George Paine, a pathologist at the Sheffield Royal Infirmary, who successfully used it in 1930 to treat gonococcal conjunctivitis in neonates. Thereafter, the therapeutic potential of penicillin went largely unexplored until 1940, when a team of researchers headed by Howard Florey and Ernst Chain showed that it produced dramatic improvements in mice with streptococcal infections. Penicillin was instrumental in treating infections in Allied soldiers in World War II; however, shortly thereafter, resistance became a substantial clinical problem.

Two conidiophores of *Penicillium frequentans* fungi, also known as *P. glabrum*. The conidiophore is the stalked structure whose distal end produces asexual spores (conidia) by budding. Original magnification x1,200. Photo: CDC/Lucille Georg/1971.

Sources

1. Petri WA Jr. Penicillins, cephalosporins, and other β-lactam antibiotics. In: Brunton LL, Chabner BA, Knollmann BC, editors. Goodman and Gilman's the pharmacological basis of therapeutics. 12th ed. New York: McGraw Hill; 2011. p. 1477–503.
2. Wainwright M, Swan HT. C.G. Paine and the earliest surviving clinical records of penicillin therapy. Med Hist. 1986;30:42–56. http://dx.doi.org/10.1017/S0025727300045026

Address for correspondence: Ronnie Henry, Centers for Disease Control and Prevention, 1600 Clifton Rd NE, Mailstop E28, Atlanta, GA 30329-4027, USA; email: boq3@cdc.gov

DOI: https://doi.org/10.3201/eid2501.ET2501

Association of Increased Receptor-Binding Avidity of Influenza A(H9N2) Viruses with Escape from Antibody-Based Immunity and Enhanced Zoonotic Potential

Joshua E. Sealy, Tahir Yaqub, Thomas P. Peacock,[1] Pengxiang Chang, Burcu Ermetal, Anabel Clements, Jean-Remy Sadeyen, Arslan Mehboob,[2] Holly Shelton, Juliet E. Bryant, Rod S. Daniels, John W. McCauley, Munir Iqbal

We characterized 55 influenza A(H9N2) viruses isolated in Pakistan during 2014–2016 and found that the hemagglutinin gene is of the G1 lineage and that internal genes have differentiated into a variety of novel genotypes. Some isolates had up to 4-fold reduction in hemagglutination inhibition titers compared with older viruses. Viruses with hemagglutinin A180T/V substitutions conveyed this antigenic diversity and also caused up to 3,500-fold greater binding to avian-like and ≥20-fold greater binding to human-like sialic acid receptor analogs. This enhanced binding avidity led to reduced virus replication in primary and continuous cell culture. We confirmed that altered receptor-binding avidity of H9N2 viruses, including enhanced binding to human-like receptors, results in antigenic variation in avian influenza viruses. Consequently, current vaccine formulations might not induce adequate protective immunity in poultry, and emergence of isolates with marked avidity for human-like receptors increases the zoonotic risk.

Since their first detection in China in 1992, avian influenza A(H9N2) viruses of the G1 and BJ94 lineages have become enzootic to poultry in Asia and parts of Africa (*1–3*). These viruses frequently cause outbreaks in these regions and sporadic outbreaks in Europe and North America (*4–9*). H9N2 viruses cause moderate illness and death rates in domestic poultry, leading to major economic burden to small-scale and large-scale poultry industries, and increased risk for zoonotic infection (*6*,*10*,*11*).

Author affiliations: The Pirbright Institute, Pirbright, UK (J.E. Sealy, T.P. Peacock, P. Chang, A. Clements, J.-R. Sadeyen, H. Shelton, M. Iqbal); University of Veterinary and Animal Sciences, Lahore, Pakistan (T. Yaqub, A. Mehboob); The Francis Crick Institute, London (B. Ermetal, R.S. Daniels, J.W. McCauley); Fondation Mérieux, Lyon, France (J.E. Bryant)

DOI: https://doi.org/10.3201/eid2501.180616

Severe illness in humans infected with this virus is rare, but seroepidemiologic data suggest that infection might be most common in those working at the human–animal interface (*12–14*). It is evident that there is a major genetic host barrier between currently circulating H9N2 viruses and humans, despite detection of molecular markers of mammalian tropism in avian isolates (*15*,*16*). Adaptation to humans requires permissive mutations throughout the genome of avian influenza viruses that affect multiple factors, such as receptor binding, pH stability, virus polymerase activity, innate immune responses, and viral egress (*17–21*).

Hemagglutinin (HA) and neuraminidase (NA) play critical roles in overcoming this genetic host barrier, as shown by recent zoonotic infections with H7N9, H10N8, and H5Nx viruses, all containing H9N2 internal genes, compared with the remarkable dearth of reported human infections with H9N2 viruses, despite their higher incidence in poultry (*15*,*22*,*23*). Efficient virus replication is dependent, in part, on the concerted activities of HA and NA binding and eluting cells and is a balance maintained by matching HA substitutions that alter receptor-binding avidity with changes to NA stalk length and sialidase activity (*24–26*).

HA is a membrane-bound homotrimer that becomes functionally active through proteolytic cleavage of precursor HA0 into HA1 and HA2 polypeptides. The HA1 globular head domain facilitates host-cell binding, which initiates infection, and the HA2 fusion peptide, primed during cleavage activation, facilitates pH-dependent fusion between virus and host-cell membranes (*27*). Human-to-

[1]Current affiliation: Imperial College London, London, UK.

[2]Current affiliation: Chinese Academy of Agricultural Sciences, Beijing, China.

human transmissible influenza viruses typically display preferential binding to glycans containing terminal α2,6-linked sialic acids (SAs), which are prevalent in the upper respiratory tract of humans (*19*,*28*,*29*); avian-origin viruses typically bind preferentially to glycans having terminal α2,3-linked SAs, which are found throughout the avian gastrointestinal and respiratory tracts (*30*). The 3′-sialyllactosamine and 6′-sialyllactosamine receptor analogs are commonly used in influenza receptor-binding assays representing α2,3-linked (3SLN) and α2,6-linked (6SLN) SAs (*31*). The switch in binding preference of H9N2 viruses from avian-like α2,3-linked to human-like α2,6-linked SAs has been attributed to amino acid substitutions in the receptor-binding site (RBS) of HA1, with residue 216 [226] (mature H9 numbering used throughout; H3 numbering within brackets) frequently shown to play a critical role (*32*–*34*).

Increasing evidence suggests that the combination and nature of amino acids at additional positions (e.g., 180 [190] and 217 [227]) needs to be determined for assessing receptor binding and zoonotic potential of H9 subtype viruses (*17*). H9N2 viruses commonly have alanine at HA1 position 180 (A180), which correlates with a preference for binding of 3SLN, viruses with glutamic acid (E180) generally show greater binding avidity for 6SLN; and viruses with valine (V180) have been shown to show appreciable binding to 6SLN, together with greater replicative fitness in mammals than viruses with A180 (*17*,*35*,*36*).

The HAs of H9N2 viruses in Pakistan typically contain the RBS residues A180, L216, and I217. A/chicken/Pakistan/UDL-01/2008 (UDL-01/08) and A/chicken/Pakistan/UDL-02/2008 were shown to preferentially bind a variant of the 3SLN receptor analog, which is sulfated at the 6′ position of the penultimate sugar Neu5Ac α2,3 β1–4(6-HSO3)GlcNAc (3SLN(6Su)). Although these viruses contain the classical humanizing residue L216, they show negligible binding to 6SLN in quantitative receptor-binding assays (*16*,*17*).

Methods

For this study, we conducted influenza surveillance for poultry farms in Pakistan during 2014–2016. Since the late 1990s, H9N2 virus has become enzootic in Pakistan (*37*). In addition, periodic outbreaks of infection with highly pathogenic avian influenza A(H5N1) and A(H7N3) viruses during 1995–2006 have occurred, resulting in intersubtype reassortment events and new viruses, some of which have subsequently spread to become predominant virus strains in the region (*9*,*16*,*38*). We aimed to characterize the genetics and antigenicity of circulating H9N2 viruses in Pakistan and link the molecular basis of differences seen in circulating viruses with zoonotic potential. Specifically, we sought to show that emergence of substitutions at HA1 position 180 are driving increases in virus receptor-binding avidity, including for human-like receptor analogs, and concurrently enabling virus to escape antibody-based immunity (Appendix, https://wwwnc.cdc.gov/EID/article/25/1/18-0616-App1.pdf).

Results

Virus Isolation and Phylogenetic Analysis

We collected 1,374 oropharyngeal and cloacal swab specimens from poultry during surveillance of farms for avian influenza viruses in Pakistan during 2014–2016. Of these specimens, 78 (5.7%) were confirmed by hemagglutinin inhibition (HI) assay to be positive for H9, and sequencing data for 55 virus isolates were generated. Next-generation sequencing of isolates yielded 43 complete genomes and 12 partial genomes. No other avian influenza virus subtypes were detected in this study.

Similar to previous results for H9N2 viruses from Pakistan, phylogenetic analysis showed that all HA and NA genes from specimens collected during 2014–2016 continued to belong to the G1 lineage, and all HA genes clustered within the Middle East B clade. Viruses isolated during this study show continued evolution, as shown by phylogenies that demonstrated drift of subclades away from previous isolates (Appendix Figures 1–3). BLASTn (https://blast.ncbi.nlm.nih.gov/Blast.cgi) comparisons for each gene segment of the 2014–2016 viruses against National Center for Biotechnology Information (https://www.ncbi.nlm.nih.gov) and GISAID (https://www.gisaid.org) databases showed the closest related viruses to be previous isolates from Pakistan, which had >95% nucleotide homology, suggesting continuous in situ evolution.

Comparison of maximum pairwise nucleotide differences between viruses isolated during 2014–2016 showed variable genetic diversity within each gene segment. Segment 8 (nonstructural) showed the greatest diversity (7% nucleotide difference), and segment 5 (nucleoprotein) showed the least diversity (2% nucleotide difference). In many instances, this diversity could be attributed to a small subset of sequenced viruses: when these segments were removed from the pairwise comparison, virus diversity was reduced. Diversity of gene segments of these outlier viruses that was affected (Appendix Figures 1–3) decreased for gene segments affected from 7% to 2.6% for nonstructural, from 6.1% to 1.1% for polymerase basic 2, and from 6.4% to 2% for HA. Diversity of gene segments remained constant even after removal of those outlier viruses from the pairwise comparison: polymerase basic 1, 4.5%; polymerase acidic, 4.5%; nucleoprotein, 2%; NA, 4.8%; and matrix, 5.5%.

It has previously been shown that H9N2 viruses in Pakistan are reassortants between G1 lineage H9N2 and either H7N3 or clade 2.2 H5N1 subtype viruses (*16*). All

internal genes of viruses isolated in this study clustered with the H7N3 virus isolate A/chicken/Pakistan/NARC-100/2004, indicating that this genotype had become predominant in Pakistan. We found no evidence of further intersubtype reassortment.

Using viruses for which we had full-genome sequences and a >2% nt difference cutoff for each segment, we found that viruses isolated during 2014–2016 could be divided into 7 distinct genotypes (Appendix Figures 1–3). Genotypes PK1 and PK2 showed variable intrasubtype reassortment between H9N2 viruses circulating in Pakistan, as shown by phylogenetic incongruence for some genes. Similar patterns of reassortment have been found in Vietnam and China (*15*,*39*). PK3 showed less intrasubtype reassortment than PK1 and PK2.

Molecular Characteristics of H9N2 Viruses Isolated during 2014–2016

Influenza virus HA requires activation by host proteases at a conserved cleavage site between the HA1 and HA2 subunits. This site is a key determinant of pathogenicity in avian species and describes the switch between low pathogenicity and highly pathogenic avian influenza viruses. Low pathogenicity avian influenza viruses contain monobasic cleavage sites, and highly pathogenic avian influenza viruses contain polybasic cleavage sites (*40*). All H9 HA cleavage sites we sequenced were either KSNR/GLF (10/55) or KSSR/GLF (45/55); viruses containing KSNR/GLF grouped in the PK3 genotype. Previously, HA of H9N2 viruses from Pakistan could be separated into 2 groups containing either KSSR/GLF or RSSR/GLF cleavage sites (*16*), indicating that the KSSR motif has persisted and undergone some evolution to KSNR. These motifs are dibasic and unlikely to be susceptible to activation by endogenous furin-like proteases, leading to classification of these viruses as low pathogenicity avian influenza viruses. However, such dibasic motifs have been described as being susceptible to an extended group of proteases present in a wider range of tissues, potentially enabling these viruses to show increased tissue tropism and pathogenicity (*41*).

All viruses we sequenced in this study contained HA L216, which has been associated with mammalian tropism of H9N2 viruses (*32*). However, recent evidence suggests that L216 alone is a poor marker for human-like receptor-binding preference in H9N2 viruses without considering surrounding amino acids, notably at positions 180 and 217 (*17*). All viruses sequenced contained I217; 52 viruses contained A180 and 3 contained T180.

Antigenic Characterization of H9N2 Viruses from Pakistan

To assess antigenic diversity of the 2014–2016 H9N2 virus subtype population (referred to as contemporary viruses), we compared amino acid sequences of HA to identify substitutions in the surface of HA1 (Figure 1). We cloned HA of a 2016 isolate (SKP-827/16) and used it as a backbone to introduce amino acid substitutions by site-directed mutagenesis, which represented the surface diversity of HA1 of the viruses isolated during 2014–2016. Viruses rescued by reverse genetics (RG) differed by only 1 or 2 aa substitutions that reflected diversity seen between individual sequenced isolates. We then assessed HI titers of viruses isolated during 2014–2016 by using chicken postinfection polyclonal antiserum raised against the closely related Pakistan 2008 isolate UDL-01/08. Most viruses were inhibited at titers equivalent to that with the homologous UDL-01/08 virus, but we observed 4-fold reductions in

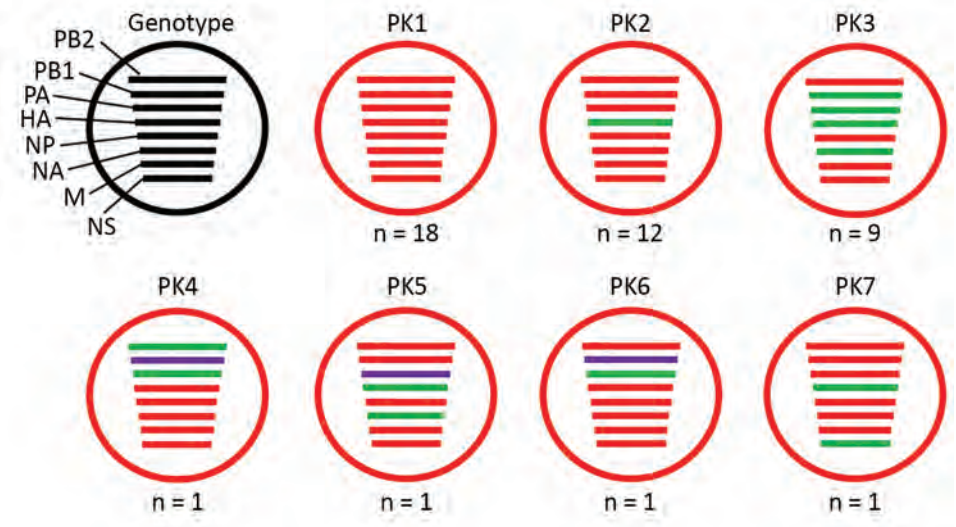

Figure 1. Genotypes of influenza A(H9N2) viruses from Pakistan. Full-genome sequences of 43 contemporary H9N2 avian influenza viruses from Pakistan were used to generate 7 unique genotypes, designated PK1–PK7. Each circle represents a genotype, and n values indicate the total number of viruses assigned to the given genotype. Each line within a circle represents a virus gene segment, and different segment colors between the same gene correspond to a >2% nucleotide difference. Black indicates wild-type virus genes; red, green, and purple indicate mutated genes. HA, hemagglutinin; M, matrix; NA, neuraminidase; NP, nucleoprotein; NS, nonstructural; PA, polymerase acidic; PB, polymerase basic.

HI titers for viruses containing the HA A180T substitution (Table 1). We observed the same effect when the HA A180T substitution was introduced into wild-type UDL-01/08. Wild-type SKP-827/16 naturally has HA T180, and a 4-fold increase in microneutralization (MNT) titer with antiserum raised against UDL-01/08 was seen when the T180A substitution was introduced, again indicating that this residue alone was responsible for most antigenic diversity in the sequenced viruses. Conversely, for the UDL-01/08 virus, the A180T substitution caused a 3-fold reduction in MNT titer compared with the titer that had the homologous virus (Table 2).

V180 has also been identified as a potential modulator of receptor binding (*35*) because the HA A180T substitution caused a major reduction in HI titer with antiserum raised against UDL-01/08. Thus, we assessed whether the A180V substitution had the same effect. Introduction of the HA V180 substitution into UDL-01/08 and SKP-827/16 RG viruses caused 4-fold greater reductions in HI titer by antiserum raised against UDL-01/08 than for parental RG viruses (Table 1). In a similar fashion, we found a 3-fold greater reduction in MNT titer for virus SKP-827/16 containing the T180V substitution and a >6-fold greater reduction in MNT titer for virus UDL-01/08 containing the A180V substitution than for titers with respective parental RG viruses (Table 2). Our results showed that A180V and A180T substitutions were sufficient to produce virus neutralization escape variants, as assessed by HI and MNT assays, when using postinfection polyclonal antiserum raised against UDL-01/08, which contains HA A180 and which recognizes epitopes in 2 discrete antigenic sites (*42*).

Table 1. Change in HI titers of influenza A(H9N2) viruses from Pakistan during 2014–2016 viruses compared to UDL-01/08 virus*

HA backbone and substitution	Fold change in HI titer (titer)†
SKP-827/16	
I116L	– (2,048)
P118S	– (2,048)
S134L	– (2,048)
N135D	– (2,048)
N148S	– (2,048)
A156V	1‡ (4,096)
R162Q + D262N	– (2,048)
G163E	– (2,048)
K164N	1‡ (4,096)
180T	4 (128)
A180T + K164N	4 (128)
A180V	4 (128)
N198D	(2,048)
D262N	(2,048)
S265I	1‡ (4,096)
UDL-01/08	
A180T	4 (128)
A180V	4 (128)

*Postinfection polyclonal antiserum raised in a single chicken inoculated with UDL-01/08 was used in all HI assays. Amino acid substitutions were introduced into a contemporary virus HA backbone (SKP-827/16 with A180) or the UDL-01/08 HA backbone and rescued by reverse genetics. HI titers between contemporary viruses and UDL-01/08 virus were compared. HA, hemagglutinin; HI, hemagglutination inhibition; –, no change.
†The homologous HI titer for UDL-01/08 antiserum was 2,048.
‡Indicates fold decrease compared with UDL-01/08.

Determination of Receptor-Binding Avidity by Residue 180

The HA RBS is located on the head domain of HA1 and is responsible for recognition of sialylated host cell receptors (*27*). To assess the receptor-binding avidity of the 2014–2016 virus population, we identified amino acid substitutions located within the RBS (Figure 2). The only amino acid variation within the RBS of the 2014–2016 viruses was residue A/T180; thus, we generated 3 RG viruses with the HA genes of wild-type SKP-827/16, which naturally contains T180, and viruses A/chicken/LH-55/2014 (LH-55/14) and A/chicken/SKP-989/2015 (SKP-989/15), which contain A180. All 3 viruses have L216 and I217. We used biolayer interferometry (*31*) to characterize the receptor-binding profiles of these viruses and compared them with those of UDL-01/08. LH-55/14 and SKP-989/15, with A180, had UDL-01/08-like receptor-binding profiles, and SKP-827/16, with T180, showed increased receptor-binding avidity for all tested receptor analogs, including an increase in human-receptor binding (Figure 3).

We then used biolayer interferometry on our previously generated UDL-01/08 and SKP-827/16 RG viruses containing A/T/V180 substitutions to define the effect of residue 180. Within the UDL-01/08 backbone, which naturally has A180, A180T caused an ≈50-fold increased binding avidity for 3SLN(6Su) and a >10-fold increased binding to 6SLN. A180V caused an ≈1,000-fold increased binding of 3SLN(6Su) and a >20-fold increased binding of 6SLN (Figure 4, panels A, B). Within the SKP-827/16 backbone, which naturally has T180, T180A caused an ≈30-fold decrease in binding to 3SLN(6Su) and a complete loss of quantifiable binding to 6SLN and 3SLN; T180V caused an ≈130-fold increase in binding to 3SLN(6Su), an ≈4-fold increase in binding to 6SLN, and detectable

Table 2. Changes in MNT titers influenza A(H9N2) viruses with HA A/T/V180 substitutions*

HA backbone and substitution	Fold change in MNT titer (titer)†
SKP-827/16	
T180A	4‡ (1,024)
T180V	3§ (4)
UDL-01/08	
A180T	3§ (32)
A180V	>6§ (2)

*MNT assays were conducted by using antiserum raised against UDL-01/08 as before and RG viruses at 100 50% tissue culture infectious doses. Wild-type virus UDL-01/08 was compared to UDL-01/08 HA backbone variants with A180T and A180V substitutions, and wild-type virus SKP-827/16 was compared with SKP-827/16 HA backbone variants with T180A and T180V substitutions. HA, hemagglutinin; MNT, microneutralization.
†The homologous MNT titer for UDL-01/08 antiserum was 256.
‡Value indicates fold increase,
§Values indicate fold decrease.

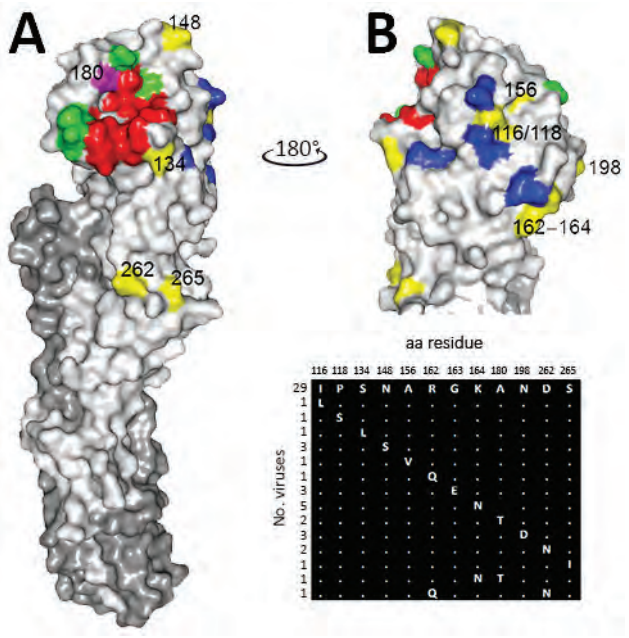

Figure 2. A) H9 HA monomer showing position of each amino acid substitution on the surface of HA1 of contemporary avian influenza A(H9N2) viruses isolated from Pakistan. HA1 is shown in light gray, HA2 in dark gray, receptor binding site in red, previously identified antigenic sites in green and blue (*42,43*), and substituted residues identified in this study in yellow. Residue 180 is shown in magenta. B) aa alignment of the HA coding region was used to identify substituted residues within the 2014–2016 population of Pakistan viruses. Shown is the crystal structure of swine H9 hemagglutinin PDB ID:1JSD (*44*), which was drawn by using PyMol software (https://pymol.org/2). Matrix diagram shows diversity of HA1 surface substitutions and the total number of viruses with a given substitution. Mature H9 numbering is used throughout. aa, amino acid; HA, hemagglutinin.

binding to 3SLN (Figure 4, panels C, D). These results indicated that A180T/V increases the receptor-binding avidity toward all sialylated receptor analogs tested and suggest that the receptor-binding phenotype of wild-type UDL-01/08 could become SKP-827/16-like through substituting A180, and vice versa.

Requirement of Enhanced Sialidase Activity by Viruses with Enhanced Binding Avidity for Elution from Erythrocytes

For new virions to be released from the surface of infected cells, the NA glycoprotein must have sufficient sialidase activity to outcompete the receptor-binding ability of its cognate HA; this equilibrium is known as HA–NA balance. We investigated A/T180A/T/V variants for their ability to elute from erythrocytes of different species. We used an adapted erythrocyte elution assay whereby different concentrations of bacterial receptor-destroying enzyme (RDE) were added to virus-hemagglutinated erythrocytes and elution monitored for 24 h at 37°C. This assay showed that viruses containing A180 eluted most rapidly, at earlier time points and lower concentrations of RDE than T/V180 viruses, indicating lower receptor avidity (Figure 5). Elution of V180 variants from chicken erythrocytes did not occur even at the highest tested RDE concentration after 24 h of incubation (Figure 5, panel B). Elution from guinea pig erythrocytes was minimal for T180 and V180 variants for which detectable elution only occurred after 24 h at the highest RDE concentrations (Figure 5, panel C). After 24 h incubation, elution from canine erythrocytes was complete for 5 of the test viruses for at least the top 4 RDE concentrations, but the SKP-827/16 T180 variant did not elute even at the highest concentration of RDE (Figure 5, panel A). In agreement with results of receptor-binding assays, we found that viruses with T/V180 have higher avidity toward sialylated receptors that naturally occur on erythrocytes and therefore require more time or better matched sialidase activity to elute efficiently. A control containing virus-hemagglutinated erythrocytes with no RDE treatment was included to show that, by 24 h, viruses containing A180 eluted from guinea pig and chicken erythrocytes but not from canine erythrocytes.

Effects of Receptor-Binding Avidity on Replication In Vitro

To evaluate further the effect on virus replication of the A/T/V180 viruses and variants, we assessed the propagation for each of our viruses by using mammalian and avian cell cultures: MDCKs, MDCK-SIAT1, and primary chicken kidney cells. These cell types express a mixture of α2,3- and α2,6-linked SA, making them suitable for assessing the correlation between growth kinetics and receptor binding (*45*). Viruses with HA T180 or V180 that showed greater receptor-binding avidities replicated to lower titers than did viruses with HA A180 for all cell types (Figure 6). However, at later time points in MDCK-SIAT1 cells, UDL-01/08 A180V replicated to comparable titers with UDL-01/08 A180. These differences in replication efficiency were reflected in MDCK plaque morphology: HA T180 or V180 produced smaller plaque sizes than viruses with HA A180 (Figure 7). This morphology could be seen for the UDL-01/08 and the SKP-827/16 HA backbones in a manner consistent with other avidity increasing amino acid substitutions in H9 virus subtype HAs (*46*).

Discussion

To effectively control enzootic avian influenza virus infections, it is vital to perform poultry surveillance and virus characterization to inform vaccine composition and use and warn of potential pathogenic or zoonotic threats. The data generated in our study showed that only H9N2 avian influenza viruses were detected among poultry in Pakistan and, although genetically diverse, these viruses were distinct from H9N2 viruses in neighboring countries,

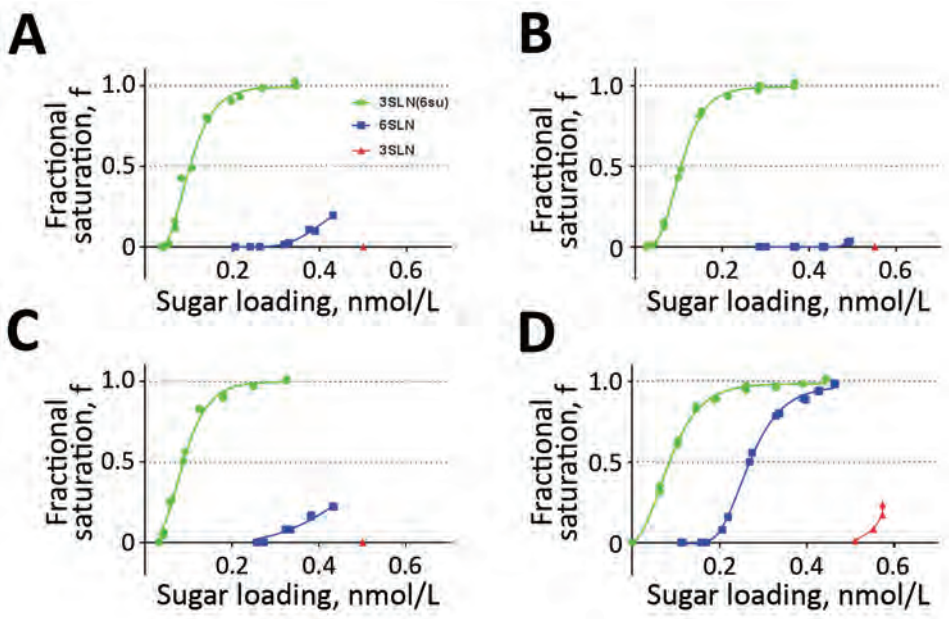

Figure 3. Receptor-binding profiles of wild-type influenza A(H9N2) viruses from Pakistan. Wild-type UDL-01/08 virus and 3 contemporary wild-type viruses were generated by using reverse genetics, and receptor-binding to 3 receptor analogs was assayed by using biolayer interferometry. Sugars tested were 3SLN(6Su) (green), 6SLN (blue), and 3SLN (red). A) H9N2 A/chicken/Pakistan/UDL-01/2008; B) H9N2 A/chicken/LH-55/2014; C) H9N2 A/chicken/SKP-989/2015; D) H9N2 A/chicken/SKP-827/2016.

implying in situ evolution rather than continuous cross-border spread. Furthermore, H9N2 avian influenza viruses from Pakistan retain internal gene cassettes that are partially derived from an H7N3 virus from Pakistan. Of particular concern is the detection of genotype PK3, which includes viruses that naturally have T180 in HA1, a dibasic motif at the HA cleavage site and truncated polymerase basic 1–F2 (Appendix). We have shown that the A180T substitution causes these viruses to be antigenically distinct from other contemporary H9N2 viruses in Pakistan, possibly leading to escape from vaccine-induced immunity. Moreover, T180 facilitates virus binding to human-like receptors, thus highlighting enhanced zoonotic potential.

Protective immunity generated by infection or conventional inactivated influenza vaccines is mediated though neutralizing antibodies against the major influenza antigen HA. However, viruses are able to evade neutralization by these antibodies through a process known as antigenic drift in human influenza viruses, whereby certain amino acid substitutions in HA are selected that directly prevent antibody binding (*27*,*42*,*47*). Although the mechanism of antigenic drift in avian influenza virus is poorly understood, there is evidence of comparable drivers of antigenic drift, whereby amino acid substitutions around the HA RBS decrease HI antibody titers (*48*). An alternative antibody escape mechanism proposed to be

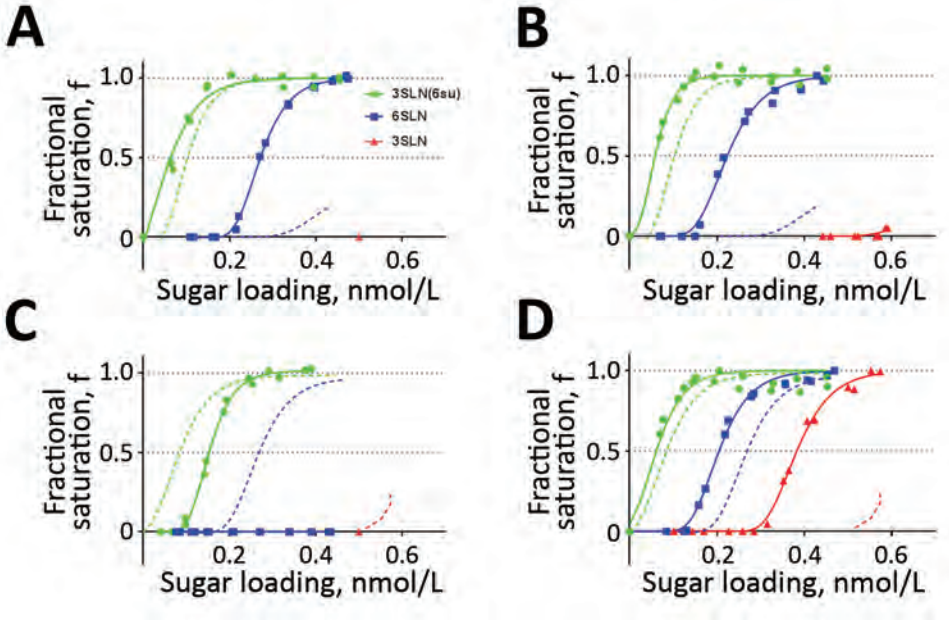

Figure 4. Receptor-binding profiles of influenza A(H9N2) virus isolates from Pakistan with HA residue 180 substitutions. A, B) UDL-01/08 viruses containing A180T/V substitutions: A) H9N2 A/chicken/Pakistan/UDL-10/2008 A180T; B) H9N2 A/chicken/Pakistan/UDL-10/2008 A180V. C, D) SKP-827/16 viruses containing T180A/V substitutions: C) H9N2 A/chicken/Pakistan/SKP-227/2016 T180A; D) H9N2 A/chicken/Pakistan/SKP-227/2016 T180V. Dashed lines indicate binding profiles of wild-type viruses UDL-01/08 with A180 and SKP-827/16 with T180, and solid lines indicate binding profiles of variant viruses. HA, hemagglutinin.

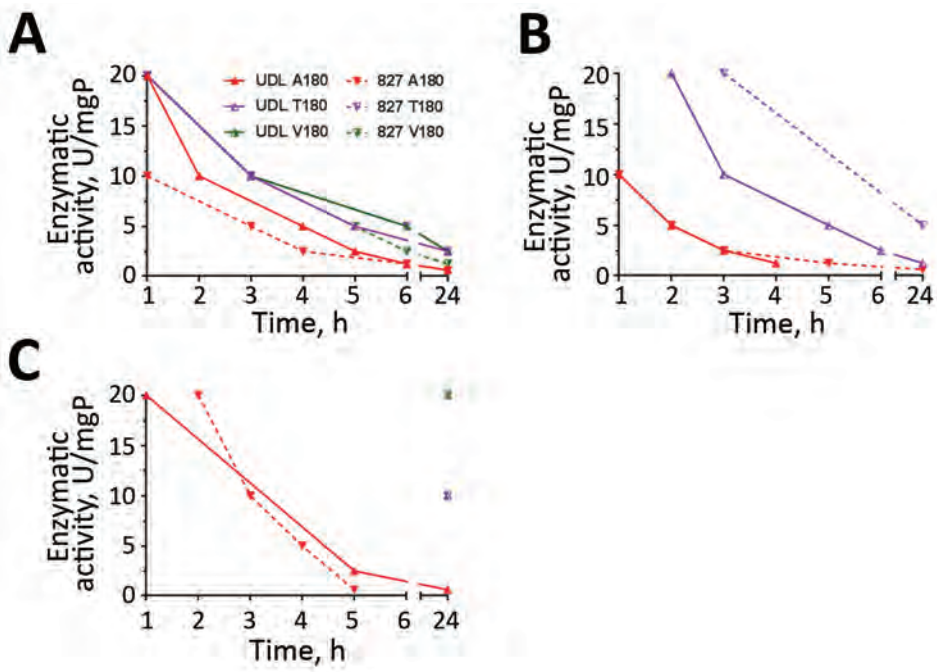

Figure 5. Elution of influenza A(H9N2) viruses (UDL-01/08 and SKP-827/16 A/T/V180) from Pakistan from erythrocytes. Virus elution was recorded at 1, 2, 3, 4, 5, 6, and 24 hours posttreatment with bacterial receptor-destroying enzyme. Points plotted indicate hour at which full loss of hemagglutination was achieved for each concentration of receptor-destroying enzyme. A) Canine erythrocyte elution with UDL and 827 A/T/V180; B) chicken erythrocyte elution with UDL and 827 A/T/V180; C) guinea pig erythrocyte elution with UDL and 827 A/T/V180. mgP, milligram of protein.

used by influenza viruses is to increase receptor-binding avidity, enabling HA–SA interactions to outcompete inhibition by neutralizing antibodies (*49*,*50*). In this study, we describe avian influenza A(H9N2) viruses that exhibit characteristics of adsorptive mutants in the field, and recently circulating viruses isolated from the field with HA amino acid substitutions that enhance binding avidity toward several different receptor analogs and have reduced HI and MNT titers compared with older viruses, thereby linking receptor-binding avidity to antigenicity. We also showed that HA A180T/V substitutions provide H9N2 viruses with enhanced binding to a human-like 6SLN receptor analog, although these viruses preferentially bind the avian-like 3SLN(6Su) receptor analog. This enhanced binding to 6SLN could enhance zoonotic potential of avian influenza viruses and further highlights the role of HA residue 180 as a marker for mammalian adaptation.

The ability to escape neutralization through enhanced receptor-binding avidity might come at a fitness cost. Virus replication of high-avidity viruses and mutants was attenuated in tested cell lines. An explanation for this finding might be an imbalance in the receptor-binding/cleaving synergy between virus HA and NA; additional HA or NA mutations might be required to rescue the attenuation observed in HA T180 and V180 viruses. Previous studies have investigated the role of residue V180 in mammalian adaptation of H9N2 avian influenza viruses (*20*,*35*,*36*). Teng et al. showed that viruses containing V180 had enhanced replication in mouse lungs and preferential receptor-binding toward α2,6-linked SA compared with α2,3-linked SA, highlighting their inherent ability to bind human-like receptors, which could be possibly attributed to possession of HA L216 (*35*). However, the 3SLN(6Su) receptor analog was not tested by Teng et al., and it is likely that their viruses would have binding preference for this avian-like receptor (*17*). Each of the viruses examined contained a 3-aa deletion in the stalk region of the NA glycoprotein, similar to that previously shown in H9N2 viruses with enhanced NA activity (*25*). All experiments conducted in our study used full-length wild-type UDL-01/08 NA (no stalk deletion), which is naturally paired with UDL-01/08 HA containing A180 and might not be well matched with viruses containing HA T/V180.

Yang et al. (*36*) showed that passage of an avian influenza A(H9N2) virus in differentiated swine airway epithelial cells led to an HA A180V substitution that facilitated α2,6-linked SA binding compare with that of parental virus, which preferentially bound α2,3-linked SA. However, these viruses did not show enhanced replication in porcine cell culture and did not have stalk deletions within the NA glycoprotein (*36*). Chan et al. showed attenuated growth in human lung organ culture of a human H9N2 virus containing HA V180 than in isolates containing D/E180 (*20*). These viruses also did not have any NA stalk deletions. Thus, we postulate that the ability of an H9N2 avian influenza virus containing HA T/V180 to cause efficient infection is at least partially dependent on a stalk deletion within its cognate NA glycoprotein, thus making HA residue 180 a good molecular marker for mammalian adaptation when considered alongside an appropriate NA. We aligned NA glycoproteins from viruses generated in this study and from aforementioned studies, but found that no additional modifications could be correlated with A/T/V180.

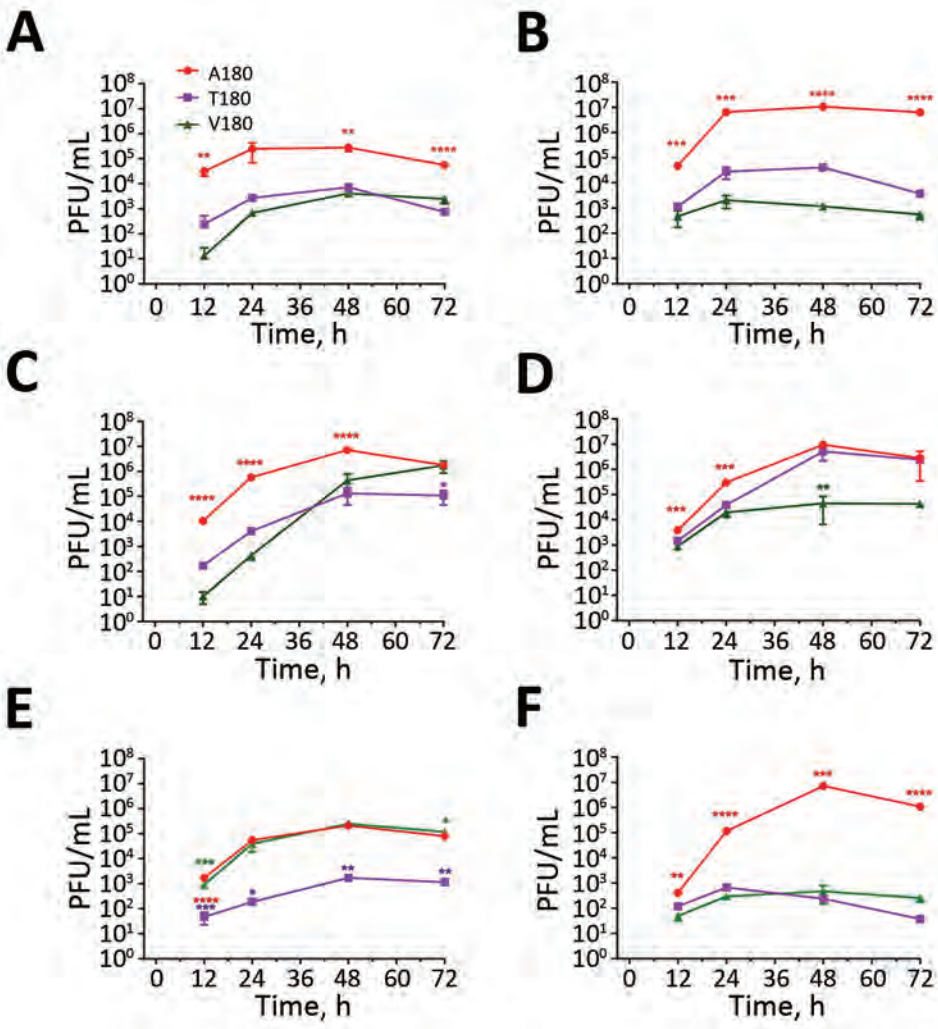

Figure 6. Replication kinetics of influenza A(H9N2) viruses from Pakistan in CKC, MDCK, and MDCK-SIAT1 cells. A, C, E) Replication in CKC, MDCK, and MDCK-SIAT1 cells of UDL-01/08 viruses containing A/T/V180 substitutions; B, D, F) replication in CKC, MDCK, and MDCK-SIAT1 cells of SKP-827/16 viruses containing A/T/V180 substitutions. Virus supernatants were titrated by plaque assay in MDCK cells by using culture supernatants harvested at 12, 24, 48, and 72 hours postinoculation. One-way analysis of variance with multiple comparisons was used to compare virus titers from each time point. A) CKC growth curve: A/chicken/UDL-01/2008 A/T/V/180; B) CKC growth curve: A/chicken/Pakistan/SKP-827/2016 A/T/V/180; C) MDCK growth curve: A/chicken/UDL-01/2008 A/T/V/180; D) MDCK growth curve: A/chicken/Pakistan/SKP-827/2016 A/T/V/180; E) SIAT1 growth curve: A/chicken/Pakistan/UDL-01/2008 A/T/V/180; F) SIAT1 growth curve: A/chicken/Pakistan/SKP-827/2016 A/T/V/180. *p<0.05; **p<0.01; ***p<0.001; ****p<0.0001).

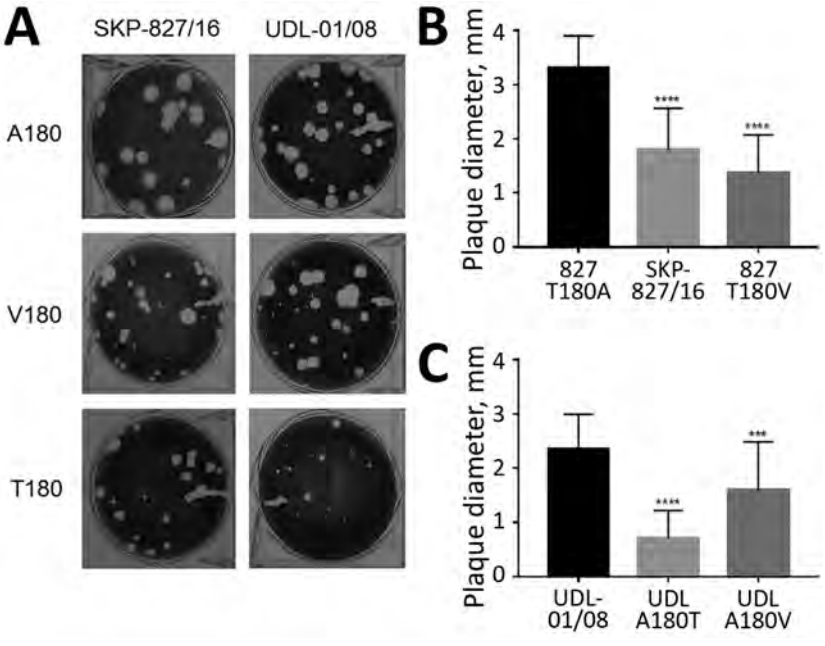

Figure 7. Plaque phenotype of influenza A(H9N2) viruses in UDL-01/08 and SKP-827/16 A/T/V180 variants in MDCK cells. A) Plaque morphology of wild-type UDL-01/08 (containing A180) and SKP-827/16 (containing T180) viruses and variants containing A/T/V180 substitutions. B, C) 30 plaques were selected for each virus, and ImageJ software (https://imagej.nih.gov/ij) was used to measure plaque diameter. Comparisons were conducted between viruses of the same hemagglutinin backbone with different substitutions (A/T/V180). Error bars indicate SEM. ***p<0.001; ****p<0.0001.

In conclusion, we have assessed the pathogenic and zoonotic risks posed by enzootic influenza A(H9N2) viruses in Pakistan by characterizing field isolates. Because of circulation of viruses with potential to escape vaccine-induced immunity, regular updating of vaccines to match circulating strains and protect poultry is needed in Pakistan. Furthermore, isolation of viruses from the G1 lineage with enhanced human receptor-binding avidity warrants continued surveillance for poultry and persons working with or near poultry.

Acknowledgments

We thank the veterinary staff and students at the University of Veterinary and Animal Sciences in Lahore, Pakistan, for their sample collection from poultry farms in Pakistan and Steve Martin for allowing us to use his Octet analysis software.

This study was supported by Biotechnology and Biological Sciences Research Council (BBSRC) Zoonoses and Emerging Livestock Systems (ZELS) Zoonoses and Emerging Livestock Systems (ZELS) award no. BB/L018853/1, BBSRC ZELS-AS award no. BB/N503563/1, BBSRC award no. BBS/E/I/0000198, BBSRC ISPG award no. BBS/E/I/00007034, BBS/E/I/00007035, BBS/E/I/00007038, and BBS/E/I/00007039; Cancer Research UK (FC001030); the Medical Research Council (FC001030); and the Wellcome Trust (FC001030).

About the Author

Dr. Sealy is a doctoral student at The Pirbright Institute, Pirbright, UK. His research interests include evolution of influenza viruses and the effects that molecular changes have on virus fitness and the propensity to persist and spread.

References

1. Dalby AR, Iqbal M. A global phylogenetic analysis in order to determine the host species and geography dependent features present in the evolution of avian H9N2 influenza hemagglutinin. PeerJ. 2014;2:e655. http://dx.doi.org/10.7717/peerj.655
2. Chen B, Zhang Z, Chen W. The study of avian influenza: I. The isolation and preliminary serological identification of avian influenza virus in chicken [in Chinese]. Chinese Journal of Veterinary Medicine 1994;20:3–5.
3. Zecchin B, Minoungou G, Fusaro A, Moctar S, Ouedraogo-Kaboré A, Schivo A, et al. Influenza A (H9N2) virus, Burkina Faso. Emerg Infect Dis. 2017;23:2118–9. http://dx.doi.org/10.3201/eid2312.171294
4. Aamir UB, Wernery U, Ilyushina N, Webster RG. Characterization of avian H9N2 influenza viruses from United Arab Emirates 2000 to 2003. Virology. 2007;361:45–55. http://dx.doi.org/10.1016/j.virol.2006.10.037
5. Alexander DJ. Report on avian influenza in the Eastern Hemisphere during 1997–2002. Avian Dis. 2003;47(Suppl):792–7. http://dx.doi.org/10.1637/0005-2086-47.s3.792
6. Kim JA, Cho SH, Kim HS, Seo SH. H9N2 influenza viruses isolated from poultry in Korean live bird markets continuously evolve and cause the severe clinical signs in layers. Vet Microbiol. 2006;118:169–76. http://dx.doi.org/10.1016/j.vetmic.2006.07.007
7. Lindh E, Ek-Kommonen C, Väänänen V-M, Vaheri A, Vapalahti O, Huovilainen A. Molecular epidemiology of H9N2 influenza viruses in northern Europe. Vet Microbiol. 2014;172:548–54. http://dx.doi.org/10.1016/j.vetmic.2014.06.020
8. Monne I, Hussein HA, Fusaro A, Valastro V, Hamoud MM, Khalefa RA, et al. H9N2 influenza A virus circulates in H5N1 endemically infected poultry population in Egypt. Influenza Other Respi Viruses. 2013;7:240–3. http://dx.doi.org/10.1111/j.1750-2659.2012.00399.x
9. Naeem K, Siddique N, Ayaz M, Jalalee MA. Avian influenza in Pakistan: outbreaks of low- and high-pathogenicity avian influenza in Pakistan during 2003–2006. Avian Dis. 2007;51(Suppl):189–93. http://dx.doi.org/10.1637/7617-042506R.1
10. Butt KM, Smith GJ, Chen H, Zhang LJ, Leung YH, Xu KM, et al. Human infection with an avian H9N2 influenza A virus in Hong Kong in 2003. J Clin Microbiol. 2005;43:5760–7. http://dx.doi.org/10.1128/JCM.43.11.5760-5767.2005
11. Huang Y, Li X, Zhang H, Chen B, Jiang Y, Yang L, et al. Human infection with an avian influenza A (H9N2) virus in the middle region of China. J Med Virol. 2015;87:1641–8. http://dx.doi.org/10.1002/jmv.24231
12. Khan SU, Anderson BD, Heil GL, Liang S, Gray GC. A systematic review and meta-analysis of the seroprevalence of influenza A (H9N2) infection among humans. J Infect Dis. 2015;212:562–9. http://dx.doi.org/10.1093/infdis/jiv109
13. Pawar SD, Tandale BV, Raut CG, Parkhi SS, Barde TD, Gurav YK, et al. Avian influenza H9N2 seroprevalence among poultry workers in Pune, India, 2010. PLoS One. 2012;7:e36374. http://dx.doi.org/10.1371/journal.pone.0036374
14. Hoa LN, Tuan NA, My PH, Huong TT, Chi NT, Hau Thu TT, et al.; The Vizions Consortium. Assessing evidence for avian-to-human transmission of influenza A/H9N2 virus in rural farming communities in northern Vietnam. J Gen Virol. 2017;98:2011–6. http://dx.doi.org/10.1099/jgv.0.000877
15. Thuy DM, Peacock TP, Bich VT, Fabrizio T, Hoang DN, Tho ND, et al. Prevalence and diversity of H9N2 avian influenza in chickens of northern Vietnam, 2014. Infect Genet Evol. 2016;44(suppl C):530–40. http://dx.doi.org/10.1016/j.meegid.2016.06.038
16. Iqbal M, Yaqub T, Reddy K, McCauley JW. Novel genotypes of H9N2 influenza A viruses isolated from poultry in Pakistan containing NS genes similar to highly pathogenic H7N3 and H5N1 viruses. PLoS One. 2009;4:e5788. http://dx.doi.org/10.1371/journal.pone.0005788
17. Peacock TP, Benton DJ, Sadeyen J-R, Chang P, Sealy JE, Bryant JE, et al. Variability in H9N2 haemagglutinin receptor-binding preference and the pH of fusion. Emerg Microbes Infect. 2017;6:e11. http://dx.doi.org/10.1038/emi.2016.139
18. Taubenberger JK, Reid AH, Lourens RM, Wang R, Jin G, Fanning TG. Characterization of the 1918 influenza virus polymerase genes. Nature. 2005;437:889–93. http://dx.doi.org/10.1038/nature04230
19. Rogers GN, Paulson JC, Daniels RS, Skehel JJ, Wilson IA, Wiley DC. Single amino acid substitutions in influenza haemagglutinin change receptor binding specificity. Nature. 1983;304:76–8. http://dx.doi.org/10.1038/304076a0
20. Chan RW, Chan LL, Mok CK, Lai J, Tao KP, Obadan A, et al. Replication of H9 influenza viruses in the human ex vivo respiratory tract, and the influence of neuraminidase on virus release. Sci Rep. 2017;7:6208. http://dx.doi.org/10.1038/s41598-017-05853-5
21. Seo SH, Hoffmann E, Webster RG. Lethal H5N1 influenza viruses escape host anti-viral cytokine responses. Nat Med. 2002;8:950–4. http://dx.doi.org/10.1038/nm757
22. Cui L, Liu D, Shi W, Pan J, Qi X, Li X, et al. Dynamic reassortments and genetic heterogeneity of the human-infecting influenza A (H7N9) virus. Nat Commun. 2014;5:3142. http://dx.doi.org/10.1038/ncomms4142

23. Cameron KR, Gregory V, Banks J, Brown IH, Alexander DJ, Hay AJ, et al. H9N2 subtype influenza A viruses in poultry in Pakistan are closely related to the H9N2 viruses responsible for human infection in Hong Kong. Virology. 2000;278:36–41. http://dx.doi.org/10.1006/viro.2000.0585
24. Mitnaul LJ, Matrosovich MN, Castrucci MR, Tuzikov AB, Bovin NV, Kobasa D, et al. Balanced hemagglutinin and neuraminidase activities are critical for efficient replication of influenza A virus. J Virol. 2000;74:6015–20. http://dx.doi.org/10.1128/JVI.74.13.6015-6020.2000
25. Sun Y, Tan Y, Wei K, Sun H, Shi Y, Pu J, et al. Amino acid 316 of hemagglutinin and the neuraminidase stalk length influence virulence of H9N2 influenza virus in chickens and mice. J Virol. 2013;87:2963–8. http://dx.doi.org/10.1128/JVI.02688-12
26. Baigent SJ, McCauley JW. Influenza type A in humans, mammals and birds: determinants of virus virulence, host-range and interspecies transmission. BioEssays. 2003;25:657–71. http://dx.doi.org/10.1002/bies.10303
27. Skehel JJ, Wiley DC. Receptor binding and membrane fusion in virus entry: the influenza hemagglutinin. Annu Rev Biochem. 2000;69:531–69. http://dx.doi.org/10.1146/annurev.biochem.69.1.531
28. Shinya K, Ebina M, Yamada S, Ono M, Kasai N, Kawaoka Y. Avian flu: influenza virus receptors in the human airway. Nature. 2006;440:435–6. http://dx.doi.org/10.1038/440435a
29. Connor RJ, Kawaoka Y, Webster RG, Paulson JC. Receptor specificity in human, avian, and equine H2 and H3 influenza virus isolates. Virology. 1994;205:17–23. http://dx.doi.org/10.1006/viro.1994.1615
30. França M, Stallknecht DE, Howerth EW. Expression and distribution of sialic acid influenza virus receptors in wild birds. Avian Pathol. 2013;42:60–71. http://dx.doi.org/10.1080/03079457.2012.759176
31. Lin YP, Xiong X, Wharton SA, Martin SR, Coombs PJ, Vachieri SG, et al. Evolution of the receptor binding properties of the influenza A(H3N2) hemagglutinin. Proc Natl Acad Sci U S A. 2012;109:21474–9. http://dx.doi.org/10.1073/pnas.1218841110
32. Wan H, Perez DR. Amino acid 226 in the hemagglutinin of H9N2 influenza viruses determines cell tropism and replication in human airway epithelial cells. J Virol. 2007;81:5181–91. http://dx.doi.org/10.1128/JVI.02827-06
33. Sang X, Wang A, Ding J, Kong H, Gao X, Li L, et al. Adaptation of H9N2 AIV in guinea pigs enables efficient transmission by direct contact and inefficient transmission by respiratory droplets. Sci Rep. 2015;5:15928. http://dx.doi.org/10.1038/srep15928
34. Gambaryan AS, Tuzikov AB, Pazynina GV, Desheva JA, Bovin NV, Matrosovich MN, et al. 6-sulfo sialyl Lewis X is the common receptor determinant recognized by H5, H6, H7 and H9 influenza viruses of terrestrial poultry. Virol J. 2008;5:85. http://dx.doi.org/ 10.1186/1743-422X-5-85
35. Teng Q, Xu D, Shen W, Liu Q, Rong G, Li X, et al. A single mutation at position 190 in hemagglutinin enhances binding affinity for human type sialic acid receptor and replication of H9N2 avian influenza virus in mice. J Virol. 2016;90:9806–25. http://dx.doi.org/10.1128/JVI.01141-16
36. Yang W, Punyadarsaniya D, Lambertz RL, Lee DC, Liang CH, Höper D, et al. Mutations during the adaptation of H9N2 avian influenza virus to the respiratory epithelium of pigs enhance sialic acid binding activity and virulence in mice. J Virol. 2017;91:e02125–16. http://dx.doi.org/10.1128/JVI.02125-16
37. Naeem K, Ullah A, Manvell RJ, Alexander DJ. Avian influenza A subtype H9N2 in poultry in Pakistan. Vet Rec. 1999;145:560. http://dx.doi.org/10.1136/vr.145.19.560
38. Shanmuganatham K, Feeroz MM, Jones-Engel L, Walker D, Alam S, Hasan M, et al. Genesis of avian influenza H9N2 in Bangladesh. Emerg Microbes Infect. 2014;3:e88. http://dx.doi.org/10.1038/emi.2014.84
39. Pu J, Wang S, Yin Y, Zhang G, Carter RA, Wang J, et al. Evolution of the H9N2 influenza genotype that facilitated the genesis of the novel H7N9 virus. Proc Natl Acad Sci U S A. 2015;112:548–53. http://dx.doi.org/10.1073/pnas.1422456112
40. Chen J, Lee KH, Steinhauer DA, Stevens DJ, Skehel JJ, Wiley DC. Structure of the hemagglutinin precursor cleavage site, a determinant of influenza pathogenicity and the origin of the labile conformation. Cell. 1998;95:409–17. http://dx.doi.org/10.1016/S0092-8674(00)81771-7
41. Baron J, Tarnow C, Mayoli-Nüssle D, Schilling E, Meyer D, Hammami M, et al. Matriptase, HAT, and TMPRSS2 activate the hemagglutinin of H9N2 influenza A viruses. J Virol. 2013;87:1811–20. http://dx.doi.org/10.1128/JVI.02320-12
42. Peacock T, Reddy K, James J, Adamiak B, Barclay W, Shelton H, et al. Antigenic mapping of an H9N2 avian influenza virus reveals two discrete antigenic sites and a novel mechanism of immune escape. Sci Rep. 2016;6:18745. http://dx.doi.org/10.1038/srep18745
43. Matrosovich M, Matrosovich T, Carr J, Roberts NA, Klenk H-D. Overexpression of the α-2,6-sialyltransferase in MDCK cells increases influenza virus sensitivity to neuraminidase inhibitors. J Virol. 2003;77:8418–25. http://dx.doi.org/10.1128/JVI.77.15.8418-8425.2003
44. Wiley DC, Skehel JJ. The structure and function of the hemagglutinin membrane glycoprotein of influenza virus. Annu Rev Biochem. 1987;56:365–94. http://dx.doi.org/10.1146/annurev.bi.56.070187.002053
45. Ha Y, Stevens DJ, Skehel JJ, Wiley DC. X-ray structures of H5 avian and H9 swine influenza virus hemagglutinins bound to avian and human receptor analogs. Proc Natl Acad Sci U S A. 2001;98:11181–6. http://dx.doi.org/10.1073/pnas.201401198
46. Peacock TP, Benton DJ, James J, Sadeyen J-R, Chang P, Sealy JE, et al. Immune escape variants of H9N2 influenza viruses containing deletions at the haemagglutinin receptor binding site retain fitness in vivo and display enhanced zoonotic characteristics. J Virol. 2017;91:e002187–17. http://dx.doi.org/10.1128/JVI.00218-17
47. Both GW, Sleigh MJ, Cox NJ, Kendal AP. Antigenic drift in influenza virus H3 hemagglutinin from 1968 to 1980: multiple evolutionary pathways and sequential amino acid changes at key antigenic sites. J Virol. 1983;48:52–60.
48. Cattoli G, Milani A, Temperton N, Zecchin B, Buratin A, Molesti E, et al. Antigenic drift in H5N1 avian influenza virus in poultry is driven by mutations in major antigenic sites of the hemagglutinin molecule analogous to those for human influenza virus. J Virol. 2011;85:8718–24. http://dx.doi.org/10.1128/JVI.02403-10
49. Hensley SE, Das SR, Bailey AL, Schmidt LM, Hickman HD, Jayaraman A, et al. Hemagglutinin receptor binding avidity drives influenza A virus antigenic drift. Science. 2009;326:734–6. http://dx.doi.org/10.1126/science.1178258
50. Li Y, Bostick DL, Sullivan CB, Myers JL, Griesemer SB, Stgeorge K, et al. Single hemagglutinin mutations that alter both antigenicity and receptor binding avidity influence influenza virus antigenic clustering. J Virol. 2013;87:9904–10. http://dx.doi.org/10.1128/JVI.01023-13

Address for correspondence: Munir Iqbal, Department of Avian Influenza, The Pirbright Institute, Ash Rd, Pirbright GU24 0NF, UK; email: munir.iqbal@pirbright.ac.uk or dr.muniriqbal@gmail.com

Variable Protease-Sensitive Prionopathy Transmission to Bank Voles

Romolo Nonno,[1] Silvio Notari,[1] Michele Angelo Di Bari, Ignazio Cali, Laura Pirisinu, Claudia d'Agostino, Laura Cracco, Diane Kofskey, Ilaria Vanni, Jody Lavrich, Piero Parchi, Umberto Agrimi, Pierluigi Gambetti

Variably protease-sensitive prionopathy (VPSPr), a recently described human sporadic prion disease, features a protease-resistant, disease-related prion protein (resPrP^D) displaying 5 fragments reminiscent of Gerstmann-Sträussler-Scheinker disease. Experimental VPSPr transmission to human PrP–expressing transgenic mice, although replication of the VPSPr resPrP^D profile succeeded, has been incomplete because of second passage failure. We bioassayed VPSPr in bank voles, which are susceptible to human prion strains. Transmission was complete; first-passage attack rates were 5%–35%, and second-passage rates reached 100% and survival times were 50% shorter. We observed 3 distinct phenotypes and resPrP^D profiles; 2 imitated sporadic Creutzfeldt-Jakob disease resPrP^D, and 1 resembled Gerstmann-Sträussler-Scheinker disease resPrPD. The first 2 phenotypes may be related to the presence of minor PrP^D components in VPSPr. Full VPSPr transmission confirms permissiveness of bank voles to human prions and suggests that bank vole PrP may efficiently reveal an underrepresented native strain but does not replicate the complex VPSPr PrP^D profile.

Sporadic prion diseases are classified according to phenotype as well as the pairing of the prion protein (PrP) genotype at the methionine (M)/valine (V) polymorphic codon 129 and the conformational characteristics of the abnormal or disease-associated PrP (PrP^D). These characteristics include electrophoretic mobility and the ratio of the PrP^D fragments that are resistant to proteinase K (PK) digestion (Appendix Table 1, https://wwwnc.cdc.gov/EID/article/25/1/18-0807-App1.pdf) (*1*). According to these criteria, the 3 major types of sporadic prion disease are sporadic Creutzfeldt-Jakob disease (sCJD), sporadic fatal insomnia, and variably protease-sensitive prionopathy (VPSPr) (*2*–*5*).

VPSPr was first reported in 2008 and further defined in 2010 (*6*–*8*) as a sporadic prion disease distinct from sCJD. Since then, 37 cases have been reported, consistent with a prevalence rate of 1%–2% for all sporadic prion diseases (*8*). Similar to sCJD, VPSPr targets all 3 PrP genotypes. However, the prevalence of the 3 genotypes at codon 129 (MM, MV, and VV) greatly differs, indeed is almost inverted, in the 2 diseases: homozygosity VV is the most common (65%) genotype in VPSPr and the least common (16%) in sCJD (*2*,*9*). Furthermore, at variance with sCJD, in which the 129 genotype is a determinant of disease phenotype and PrP^D characteristics, the 129 genotype influence on phenotype, although present, is subtle (*3*,*7*,*8*). These differences point to a distinct role of the 129 genotype as a risk factor and imply that the etiologic-pathogenetic mechanisms of the 2 diseases differ.

Although the histopathology of VPSPr is distinct (e.g., spongiform degeneration, frequent presence of PrP microplaques, and a recognizable PrP^D immunostaining pattern), the hallmarks of VPSPr are the characteristics of its PrP^D. In contrast to virtually all other sporadic human prion diseases, in which PK-resistant PrP^D (resPrP^D) electrophoretically separates into 3 major bands, VPSPr resPrP^D characteristically separates into 5 bands. Furthermore, although the 3 bands of resPrP^D are all cleaved by PK exclusively at the N terminus and separate according to the presence of 2, 1, or 0 sugar moieties, VPSPr resPrP^D bands include only the monoglycosylated and unglycosylated forms, which are cleaved either only at the N terminus or at both the N- and C-termini. Thus, the C-terminus–truncated resPrP^D lacks the GPI (glycosylphosphatidylinositol) anchor. Additional variances concerning immunoreactivity characteristics, ratios of PK-resistant and PK-sensitive PrP^D species, and conformational properties including aggregate size, have also been observed (*6*–*8*). These distinctive properties point to VPSPr PrP^D as a prion strain different from those of other

Author affiliations: Istituto Superiore di Sanità, Rome, Italy (R. Nonno, M.A. Di Bari, L. Pirisinu, C. d'Agostino, I. Vanni, U. Agrimi); Case Western Reserve University, Cleveland, Ohio, USA (S. Notari, I. Cali, L. Cracco, D. Kofskey, J. Lavrich, P. Gambetti); University of Bologna, Bologna, Italy (P. Parchi); Istituto delle Scienze Neurologiche di Bologna (P. Parchi)

DOI: https://doi.org/10.3201/eid2501.180807

[1]These authors contributed equally to this article.

sporadic prion diseases. However, the VPSPr prion shares the multiplicity of the resPrP^{D} electrophoretic bands with prions from a subset of inherited prion diseases referred to as Gerstmann-Sträussler-Scheinker disease (GSS), prompting the suggestion that VPSPr is the sporadic form of GSS (*7*,*10*). Furthermore, the presence of small amounts of sCJD-like 3-band resPrP^{D} has also been signaled in VPSPr (*6*,*11*,*12*).

Disease transmission to receptive hosts is a valuable way to further define the characteristics of strains associated with prion diseases. VPSPr has been experimentally transmitted to 3 lines of transgenic mice expressing normal PrP or cellular human PrP (PrP^{C}), harboring residue M, V, or MV at residue 129 (*13*,*14*). Data in all experiments were essentially similar. Inoculated mice remained asymptomatic, but half showed focal PrP^{D} plaques with minimal spongiform degeneration, and PrP^{D} mimicking the electrophoretic profile of the native PrP^{D} on immunoblot was demonstrated in about one third of the inoculated mice. No transmission was observed at second passage.

The bank vole, a small rodent resembling the mouse with which it shares the entire sequence of normal PrP or PrP^{C} except for 8 aa, but whose sequence differs from human PrPC by 15 aa, has recently emerged as a particularly permissive host. Bank voles and transgenic mice expressing bank vole PrP^{C} have been successfully infected after challenge with human and animal prion diseases that are hard to transmit even to recipients expressing homologous PrP^{C} (*15*–*18*).

We studied transmission of VPSPr from patients with MM, MV, and VV codon 129 genotypes to bank voles harboring either the PrP genotype 109M (bv109M) or 109I (bv109I). Although the attack rate was generally low at first passage, it consistently raised to 100% at second passage, when survival times also decreased on average by >50%. We identified 3 PrP^{D} isoforms with the characteristics of distinct strains in the affected bank voles.

Materials and Methods

The inocula used in the first passage were brain homogenates from 7 persons with a definitive diagnosis of VPSPr: 2 with genotypes 129MM, 3 with 129MV, and 2 with 129VV. Homogenate was inoculated into the cerebrum of 205 bank voles according to previously described procedures (*16*). The bank vole brains were processed for histopathology, immunohistochemistry, lesion profiles, and paraffin-embedded tissue (PET) blots according to previously reported procedures (*15*). Western blot was performed according to Notari et al. (*19*). The insoluble fraction was prepared according to previously described procedures (*20*). Preparation of monoclonal antibodies is described in the Appendix. Statistical significance was determined by 1-way analysis of variance, followed by the Tukey multiple comparison test.

Results

Transmission Characteristics

At first passage, attack rates of VPSPr were 35% (29/82) in bv109I and 5% (3/59) in bv109M (Table 1; Appendix Table 2). The 2 bank vole genotypes diverged as to disease transmission in 2 ways. First, all VPSPr 129 genotypes were transmitted to bv109I, but bv109M were not susceptible to VPSPr-VV. Second, bv109I propagated 3 distinct histopathologic phenotypes and matching PrP^{D} types (hereafter identified as T1, T2, and T3), but bv109M replicated the T1 phenotype exclusively. A more detailed analysis in bv109I,

Table 1. VPSPr transmission to bank voles*

	Bv109I							Bv109M					
	1st passage			2nd passage				1st passage			2nd passage		
Inoculum	PrP^{D} type	Attack rate	Survival time, dpi ± SD	PrP^{D} type	Attack rate	Survival time, dpi ± SD	Survival reduction, %	PrP^{D} type	Attack rate	DPI	PrP^{D} type	Attack rate	Survival time, dpi ± SD
VPSPr-MM, n = 2	T1	1/20†	901	NA	NA	NA	NA	T1	1/15	356	T1	11/11	148 ± 12
	T2	1/20	839	NA	NA	NA	NA						
	T3	5/20	413 ± 102	T3	9/9	247 ± 35‡	40						
VPSPr-MV, n = 3	T1	13/44†	458 ± 137	T1	10/10	195 ± 9§	57	T1	2/30	290, 588	T1	11/11	142 ± 11
	T2	6/44	872 ± 110¶	T2	14/14	338 ± 100#	61						
	T3	1/44	554	NA	NA	NA	NA						
VPSPr-VV, n = 2	T3	2/18	596, 535	T3	9/9	255 ± 24**	55	NA	0/14	NA	NA	NA	NA

*bv, bank voles; dpi, days postinoculation; NA, not available; neg, negative; PRP^{D}, disease-associated prion protein; VPSPr, variably protease-sensitive prionopathy.
†Total no. bank voles inoculated with either VPSPr-MM or VPSPr-MV; statistics of survival times at 1st vs. 2nd passages.
‡p<0.05.
§p<0.0001.
¶Incubation periods of T2 vs. T1 p<0.0001.
#p<0.0001.
**p<0.001.

Table 2. Itemized VPSPr transmission features in bv109I at first passage, by phenotype*

Genotype	T1 Prevalence, %	T1 Survival time, dpi ± SD	T2 Prevalence, %	T2 Survival time, dpi ± SD	T3 Prevalence, %	T3 Survival time, dpi ± SD	Attack rate for all phenotypes, %
MM	5	901	5	839	25	413 ± 102†	35
MV	29.5	458 ± 137†	13.6	872 ± 110†	2.3	554	45.5
VV	0	NA	0	NA	11.1	596, 535	11.1
All affected genotypes	11.5‡	490 ± 177†	6.2‡	867 ± 101†	12.8‡	469 ± 110†	30.5‡

*bv, bank voles; dpi, days postinoculation; VPSPr, variably protease-sensitive prionopathy.
†Weighted average ± SD.
‡Unweighted average.

although limited by the low number of animals in each subset, suggested a lower attack rate for VPSPr-VV, the most common form of human VPSPr, compared with the MM and MV genotypes and a prevalence for T3 that was 11% higher than that for T1 and 106% higher than that for T2 (Table 2). Overall survival times were 575 days postinoculation (dpi) for bv109I and 411 dpi for bv109M. However, when we considered only the bank voles associated with the T1 phenotype, because bv109M were exclusively associated with T1, the dpi difference became smaller: 490 dpi for bv109I and 411 dpi for bv109M (Tables 1, 2). As for survival times related to T1–T3 phenotypes and VPSPr genotypes, the survival times for T2 were nearly twice those for T1 and T3 (Table 2).

Second passage in bv109I was invariably characterized by a 100% attack rate, a 40%–61% decrease in survival times, and conservation of the original phenotype (Table 1). A similar trend was observed for bv109M.

Histopathology and Immunohistochemistry

Phenotype T1 featured finely vacuolated spongiform degeneration often involving the entire thickness of the neocortex, including the molecular layer but occasionally also showing a laminar distribution (Figure 1, https://wwwnc.cdc.gov/eid/article/25/1/18-0807-f1). On second passage, the spongiform degeneration appeared to be more widespread, also affecting the hippocampus and subcortical structures such as basal nuclei, thalamus, and superior colliculi but not the cerebellum. PrP immunohistochemistry demonstrated punctate deposits often co-distributed with spongiform degeneration (Figure 1, column T1, row ii). At second passage, T1 features did not differ significantly between bv109M and bv109I. Furthermore, T1 also resembled the histopathologic phenotype shown by bv109M and bv109I after inoculation with sCJDMM1 or sCJDMV1, respectively (Figures 2, 3; Appendix Figure 1)

In phenotype T2, spongiform degeneration affected predominantly subcortical structures over neocortical regions, especially the hypothalamus with the apparent exclusion of the mammillary bodies (Figure 1, column T2, row iii). PrP immunohistochemistry showed granular deposits occasionally resembling miniature plaquelike formations rather than the punctate deposits of the T1 phenotype (Figure 1, column T2, row iv).

Phenotype T3 was characterized by the paucity of spongiform degeneration in the cerebral neocortex and subcortical gray matter structures; spongiform degeneration was often prominent in the regions of the hemispheric white matter lying above the hippocampus and in the corpus callosum, where parenchyma was occasionally disorganized with glial reaction. PrP immunostaining was mostly limited to those regions where it often aggregated in confluent plaque-like deposits but not well-formed plaques (Figure 1, column T3, row v, and column Tc, row vi). No remarkable differences were detected between first and second passages. Overall, the T3 histopathologic phenotype resembled that shown by bv109I after inoculation with brain homogenates from some GSS subtypes (*16*).

It is noteworthy that the T1–T3 phenotypes were never observed to coexist in 1 animal, although distinct phenotypes were often observed in bank voles receiving the same inoculum. Although all 3 phenotypes occurred after inoculation with VPSPr-MM or -MV, the sole phenotype associated with VPSPr-VV inoculation was T3 (Table 1).

Lesion Profiles and PET Blots

Profiles of spongiform degeneration as a function of lesion severity and brain anatomic location confirmed the distinctive characteristics of the T1–T3 phenotypes (Figure 2, panel A; Appendix Figure 1). The T1 spongiform degeneration profile in bv109I did not differ significantly from that of bv109M; both mirrored the profiles of bv109I inoculated with sCJDMV1 and bv109M inoculated with sCJDMM1 brain homogenate (Figure 2, panel B; Appendix Figure 1).

The PET blot patterns of brain PrP^D distribution were also quite distinct in the 3 phenotypes and, overall, reproduced the spongiform degeneration distribution (Figures 2, 3). In T1, PrP^D was well represented in selected regions including cerebral neocortex and hippocampus, basal nuclei, thalamus, superior colliculi, geniculate nuclei, and substantia nigra but not in the cerebellum and lower brain stem. No significant variations were detected between PrP^D distributions at first and second passages (data not shown). PrP^D distributions were also similar in bv109I and bv109M inoculated with classic sCJDMV1 and sCJDMM1 prions, respectively (Figure 3, panel B). In the T2 phenotype, PrP^D appeared to be present in moderate and uniform amounts in several

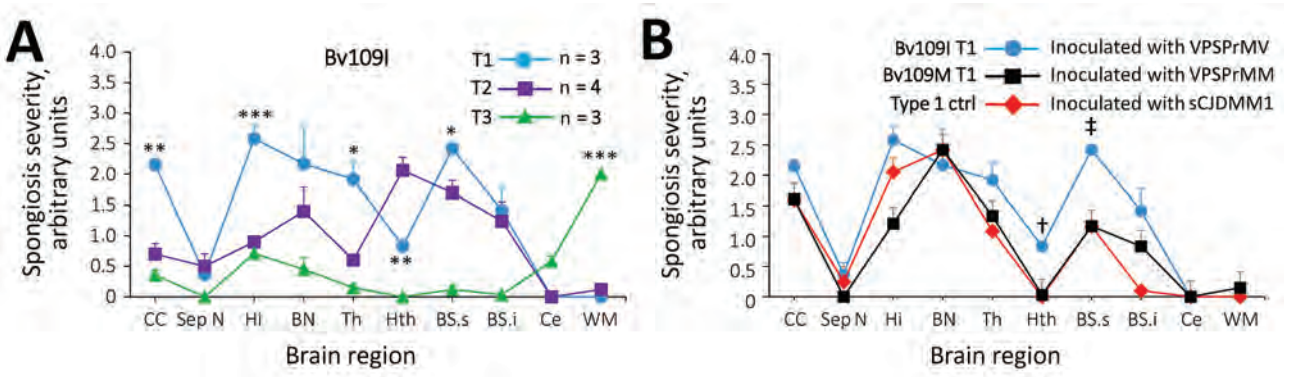

Figure 2. Profiles of topographic distribution and severity of spongiform degeneration in the brains of bank voles harboring T1–T3 phenotypes after inoculation with brain homogenate from variably protease sensitive prionopathy (VPSPr) and control bank voles inoculated with sCJD. A) Spongiform degeneration characterized both T1 and T2 phenotypes but displayed significantly divergent distributions in 5 of the 10 anatomic locations examined; spongiform degeneration affected primarily the cerebral cortex in T1 and the hypothalamus and brain stem in T2; no difference in vacuolar mean diameter was observed between T1 and T2. Spongiform degeneration scores associated with the T3 phenotype were minimal or absent in most locations except for the white matter, especially in the corpus callosum, which was virtually unaffected in T1 and T2. *p<0.5; **p<0.006; ***p<0.0001 of T1 versus T2 and T3 WM versus T1 and T2; inocula: T1 and T2 VPSPr-129MV, T3 VPSPr-129MM; vacuoles measured (n = ≈2,000) in T1 and T2 combined. B) Comparative study of T1 profiles generated in bv109M and bv109I revealed an overall more severe spongiform degeneration in bv109I but no significant difference in distribution (†, p<0.001, ‡, p<0.003; N = 3 Bv109I and Bv109M). The T1 spongiform degeneration profile generated by bv109M after inoculation with VPSPr-129MM reproduced the profile generated with sCJDMM1 extracts used as control for human type 1 (bv109M N = 3 for each profile). Similar results were obtained when comparing the T1 profile of bv109I inoculated with VPSPr-129MV and profiles of bv109I inoculated with sCJDMV1 (data not shown). BN, basal nuclei; BSs and BSi, brainstem superior and inferior; bv, bank vole; CC, cerebral cortex; Ce, cerebellum; ctrl, control; Hi, hippocampus; Hth, hypothalamus; sCJD, sporadic Creutzfeldt-Jakob disease; Sept.N, septal nuclei; Th, thalamus; WM, white matter.

anatomic regions such as neocortex and hippocampus, thalamus, and superior colliculi (Figure 3). The T3 phenotype was characterized by the striking presence of PrP^D in hippocampus and white matter structures (Figure 3).

PrP^D Characterization

Immunoblot analysis confirmed the presence of 3 distinct $resPrP^D$ electrophoretic profiles that matched the 3 histopathologic phenotypes. When probed with antibodies 9A2 and 12B2, $resPrP^D$ associated with the T1 phenotype populated 3 bands of ≈32, 26, and 21 kDa, representing the 3 $resPrP^D$ glycoforms, and by a fragment of 7 kDa (Figure 4). An additional C-terminal fragment of ≈13 kDa, possibly homologous to the human C-terminal fragment 12/13 (*20*), was detected by the C-terminal antibody SAF84 (Figure 4). Glycoform ratios showed a comparable representation of the diglycosylated and monoglycosylated forms of $resPrP^D$ (Figure 5; Appendix Figure 2). The electrophoretic profile and glycoform ratios of $resPrP^D$ T1 conformer were indistinguishable from those of $resPrP^D$ observed in bank voles inoculated with sCJDMM1 or sCJDMV1 prions, used as controls for human $resPrP^D$ type 1 in bank voles (Figures 4, 5; Appendix Figure 2; data not shown).

The $resPrP^D$ profile associated with the T2 phenotype showed 3 bands of ≈30, 24, and 19 kDa (i.e., all that had an ≈2-kDa faster electrophoretic mobility than the corresponding bands of $resPrP^D$ T1) (Figure 4). The 7-kDa fragment was not detected in T2 (Figure 4). In contrast to T1, the T2 glycoform ratio was characterized by the unambiguous predominance of the monoglycosylated component (Figure 5). In summary, bank vole $resPrP^D$ T2 differed from the T1 conformer by overall 2-kDa faster mobility, the absence of the 7-kDa fragment, and marked predominance of the monoglycoform. The striking feature of the $resPrP^D$ associated with the T3 phenotype was the predominant presence of the 7-kDa fragment detected by 9A2 and 12B2 but not by SAF84, demonstrating its internal origin and the absence of glycosylation sites (Figure 4).

Additional divergent features emerged when amounts of $totPrP^D$ (i.e., PK-sensitive plus $resPrP^D$ fractions) were assessed as percentages of total PrP, comprising PrP^C and $totPrP^D$ (Figure 6). A significantly larger component of $totPrP^D$ was $resPrP^D$ in T1 than in T2 (81% vs. 33%); $totPrP^D$ fractions were similar (93% for T1, 91% for T2). T3 differed significantly: $totPrP^D$ accounted for 8% and $resPrP^D$ accounted for 0.2% of total PrP (Figure 6; Appendix Figure 3).

Discussion

The permissiveness of bank vole PrP^C is well known (*15*,*16*,*18*,*21*–*27*); it is exemplified by the observation that, despite the mere 8-aa PrP^C divergence between bank voles and mice, a variety of human and animal prion diseases not transmissible to mice are infectious to bank voles and

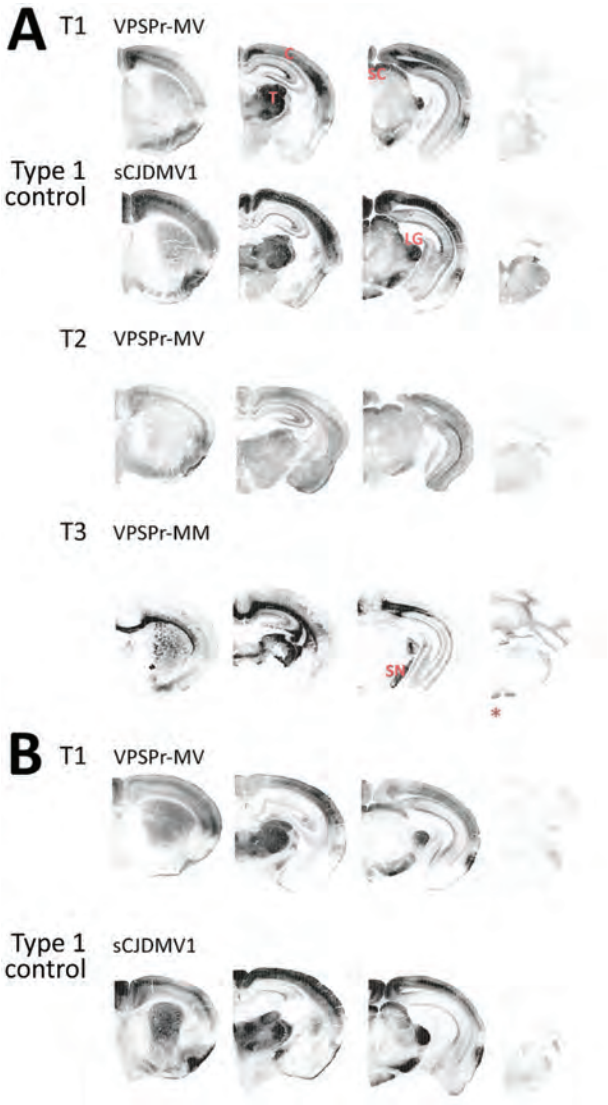

Figure 3. Representative paraffin-embedded tissue (PET) blots of protease-resistant, disease-related prion protein (resPrP^{D}) distribution in phenotypes T1–T3 and controls. A) For T1, PrP^{D} predominated in cerebral cortex (C), thalamus (T), superior colliculus (SC), lateral geniculate nucleus (LG), and substantia nigra (SN). A similar PrP^{D} distribution was observed with transmission of sCJDMV1 used as type control. T2 showed a more uniform distribution in cerebral cortex and subcortical nuclei of an apparently lesser amount of PrP^{D}; T3 appeared to preferentially affect the hemispheric white matter and other subcortical regions such as the alveus, the corpus callosum, the anterior commissure, and fascicles surrounding thalamus as well as other white matter formations such as fimbria, brachium of superior colliculus, medial lemniscus, and cerebral peduncles. Small amounts of PrP^{D} were also observed in cerebellar and medullary white matter (asterisk [*]). B) PrP^{D} T1 distribution resembled that of bank voles (bv) 109I after transmission of the same VPSPr-MV brain homogenate (compare with T1 in A). A similar distribution was also observed after inoculation with sCJDMV1. Left to right: coronal sections of telencephalon midlevel caudate nucleus; diencephalon midlevel thalamus; midbrain; and hindbrain-level medulla and cerebellum. sCJD, sporadic Creutzfeldt-Jakob disease; VPSPr, variably protease-sensitive prionopathy.

transgenic mice expressing bank vole PrP (*15,16,18,22,24*). Conversely, the 15-aa difference from the human PrP^{C} primary sequence does not impede the efficient transmission of a wealth of sporadic and inherited human prion diseases (*15,16*). This striking permissiveness has been attributed to the presence of several asparagine and glutamine residues in and around the β2–α2 loop that would result in a PrP^{C} conformation compatible with the conformations of a large number of PrP^{D} strains (*21*). Furthermore, the polymorphism at bank vole codon 109 adds further complexity to the interaction with exogenous strains (*18,28*).

We undertook systematic transmission of VPSPr brain homogenates to bv109M and bv109I after failure to consistently transmit VPSPr to humanized transgenic mice. Overall, transmission was favored by the 109I genotype, which propagated all 3 VPSPr 129 genotypes while bv109M failed to transmit VPSPr-VV. However, at first passage in bv109I, the mean attack rate (35%) was fairly low and the mean survival time (575 dpi) quite extended (Table 1). These conditions changed at second passage, when the attack rate became 100% in all transmission experiments and survival times decreased on average by 53% (Table 1). These findings point to the existence of a substantial barrier at first passage, which, judging from the 100% attack rate, is probably largely diminished or vanished at second passage. In view of the aforementioned easy transmissibility of other human prion diseases, the barrier appears to be conformational rather than caused by species-related variations in amino acid sequence of PrP^{C} (*15,16*); the barrier might be associated with the misfolding of VPSPr PrP^{D}, which may be peculiar because after PK digestion it results in an array of highly heterogeneous fragments and apparently the failure to convert one of the glycoforms (*6,7*). Similarly, the clear effect of the genotype at codon 129 on the attack rate (which was 3–4 times lower for bank voles inoculated with VPSPr-VV prions compared with VPSPr-MM and -MV), along with the lack of transmission of VPSPr-VV to bv109M but not to bv109I, points to conformational differences between PrP^{D} species associated with the 129 genotypes in VPSPr (*16*). This notion is further supported by previous data showing higher PK sensitivity (*7*) and conformational stability of PrP^{D} (*29*) in VPSPr-VV compared with VPSPr-MM and -MV.

The comparative study of VPSPr bioassay in bank voles and humanized transgenic mice revealed substantial differences. VPSPr-challenged mice invariably remained asymptomatic, and all histologically positive mice failed to transmit at second passage. Furthermore, the VPSPr-MV subtype was never transmitted to mice 129M or 129V, and the general attack rate (assessed histopathologically) was low (54%); resPrP^{D} was demonstrated in only 34% of the challenged mice despite the 2–8 times normal levels of PrP expression for most mice (*13*). However, in contrast to bank voles, positive mice generated a resPrP^{D} conformer

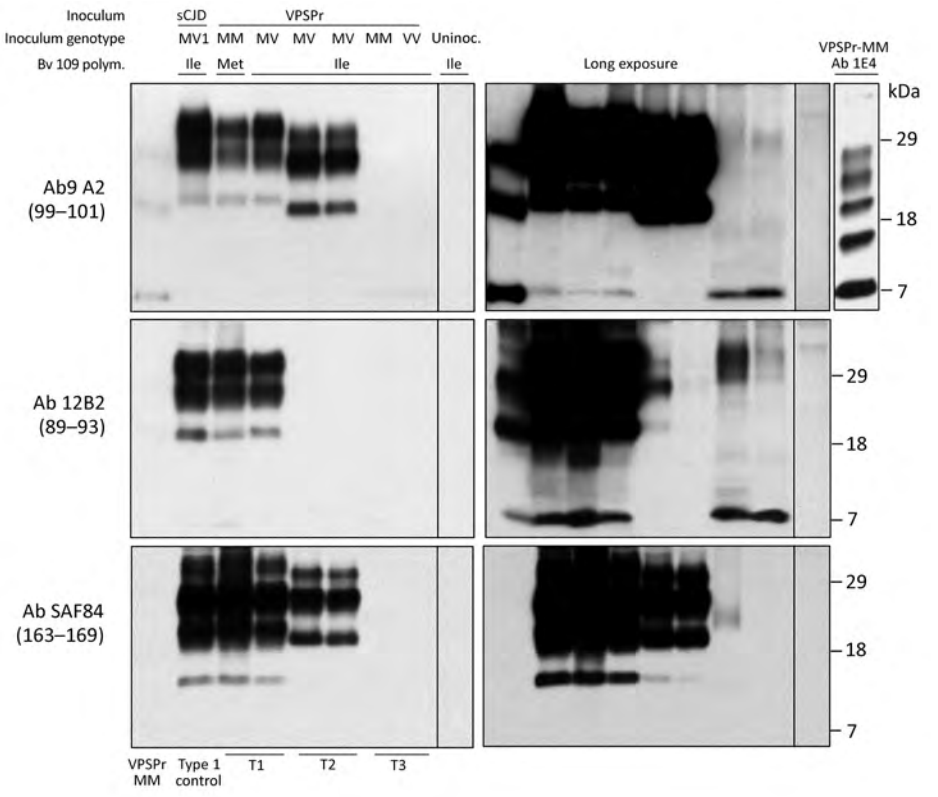

Figure 4. Immunoblot characteristics of protease-resistant, disease-related prion protein ($resPrP^D$) distribution in phenotypes T1–T3 and controls. Regular and long exposures revealed the overall similarity of the 3-band profiles in T1 and T2, but $resPrP^D$ profile, including glycoform representation, differed in the 2 phenotypes with all 3 monoclonal antibodies (Ab) used. T1 included a 7-kDa band, not detected in T2, similar to mobility and Ab immunoreactivity of the T3 7-kDa fragment. The T1 profile matched the profile generated in isogenic bank voles inoculated with sCJDMV1 used as human $resPrP^D$ type 1 control (ctrl) (lane 2). The T3 profile, visible only after long film exposures, featured a 7-kDa band, but slower migrating bands with variable immunoreactivity were also visible. None of the T1–T3 profiles matched the original VPSPr profile (first lane) although the ≈7-kDa and both 23-kDa and 19-kDa bands were shared with T1 and T2, respectively (compare first with T1 and T2 lanes). The complexity of the native $resPrP^D$ profile from VPSPr homogenate is demonstrated by probing with 1E4, a monoclonal Ab to human PrP highly reactive to VPSPr $resPrP^D$ (top right panel) (*6*). Monoclonal Ab 12B2 (middle panels) with high affinity for human $resPrP^D$ type 1 confirmed the type 1 characteristics of the $resPrP^D$ associated with the T1 phenotype. The small amount of $resPrP^D$ type 1 in 1 T2 bank vole probably represents incomplete proteinase K (PK) digestion (lane 5, right panel) (*19*). Monoclonal Ab SAF84 to the PrP C-terminus, unreactive to human PrP, further underlined the divergence in $resPrP^D$ primary structure in T1 and T2 compared with T3. Aside from revealing an additional 13-kDa fragment, strongly detected in T1 and T2 and weakly in T3, SAF84 did not detect the 7-kDa fragment, supporting its internal origin (i.e., cleaved at both N- and C-termini). Uninoculated bank voles were negative for $resPrP^D$. All samples were PK treated. sCJD, sporadic Creutzfeldt-Jakob disease; uninoc., not inoculated; polym., polymorphism; VPSPr, variably protease-sensitive prionopathy.

very similar to that of VPSPr for electrophoretic profile, glycosylation pattern, and antibody immunoreactivity, although it exhibited higher protease resistance.

Data from a previous study of transmission to humanized transgenic mice and bv109M of an sCJDMV variant with an atypical glycoform profile ($CJD\text{-}MV^{AG}$) partially resembled ours (*17*). Challenged transgenic mice remained asymptomatic and negative at neuropathologic examination, but 22% of them reproduced the original $resPrP^D$ electrophoretic profile and glycotype of the inoculum. In contrast to humanized transgenic mice, bank voles had full-blown disease develop featuring 3, although partially merging, histopathologic phenotypes along with 3 distinct $resPrP^D$ conformers, none of which mimicked the profile and glycotype of the inoculum (*17*). Remarkably, the glycoform variation of $sCJDMV^{AG}$ resembles that of VPSPr because both $resPrP^D$ species lack the diglycosylated isoform, implicating this variation as one of the possible causes of bank vole failure to accurately replicate exogenous PrP^D (*17*).

Three subtypes of GSS (which VPSPr resembles in terms of the ladder-like electrophoretic profile and the sensitivity to PK of $resPrP^D$) have also recently been transmitted to bank voles and 1 GSS subtype to humanized transgenic mice (*16*,*30*). Despite the well-known difficulty of transmitting GSS to rodents, bank voles challenged with 2 major GSS subtypes associated with PrP mutations A117V and F198S (GSS^{A117V}, GSS^{F198S}) showed no evidence of species or mutation barrier. Transmission was comparatively more difficult with the third GSS^{P102L} subtype, in which $resPrP^D$ displays 2 sets of fragments: either the 8-kDa fragment associated with the 30–21 kDa glycoform triplet (*31*,*32*) or the 8-kDa fragment alone. After inoculation, the 2-fragment set was never replicated, and the ≈8-kDa fragment alone occasionally was inaccurately reproduced as a 7-kDa fragment (*16*,*28*). To date, only GSS^{A117V} has been transmitted to 2 lines of transgenic mice expressing human PrP^D harboring the A117V transition (*30*). Although transmission features diverged in the 2 lines, both seemed

to reproduce the 7-kDa fragment that is the only strongly resPrP^{D} fragment in this disease.

Combined, these experiments indicate that PrP^{C} characteristics, and possibly other host factors (*25*), enable bank voles to be more permissive hosts (despite the species barrier) than transgenic mice expressing conspecific PrP^{C}, confirming the empirical aspect of the species barrier. However, bank vole PrP^{C} can hardly reproduce faithfully complex features of human atypical prion isolates, a task that may require PrP^{C} from the same species.

A remarkable finding of this study is the occurrence of 3 well-defined histopathologic phenotypes (T1–T3), which displayed discrete PrP^{D} brain distribution and were linked to PrP^{D} conformers easily distinguishable by electrophoretic profile and glycosylation characteristics. The 3 phenotypes also differed by mean survival times at first and second passages. Remarkably, the T1–T3 phenotypes were often generated by the same inoculum but never co-occurred in the same bank vole. Combined, these features define the T1–T3 PrP^{D} conformers as distinct strains, raising the issue of their origin. Both histopathologic and resPrP^{D} electrophoretic characteristics of the T1 phenotype are essentially indistinguishable from those of bank voles inoculated with sCJDMV1. Data on transmission of sCJDMM2, available only for bv109M, show that the electrophoretic profile of the newly formed resPrP^{D} matches the T2 resPrP^{D} of this study (*15*). Although the T1 and T2 representations of totPrP^{D} and resPrP^{D} are not known in bank voles inoculated with sCJDMM1 and sCJDMM2 prions, the values we observed after VPSPr inoculation are comparable to those reported for the original sCJD, in which totPrP^{D} and resPrP^{D} reportedly accounted for 53.5% and 48.2% of total PrP in sCJDMM1 (*6*; L. Cracco et al., unpub. data). Therefore, transmission to bank voles suggests that VPSPr PrP^{D} T1 and T2 are related to human PrP^{D} types 1 and 2, respectively. In contrast, phenotype T3 is the most divergent, especially for spongiform degeneration and PrP^{D} deposition, mostly limited to white matter regions, and electrophoretic profile, where resPrP^{D} recovered as a band of 7 kDa, was the major component shared with the complex pattern of VPSPr resPrP^{D}. The T3 histopathologic phenotypes including the PrP immunostaining pattern matched also the bank vole phenotype of GSS^{A117V} and GSS^{P102L} associated with the 8-kDa fragment only (*16*). The exceedingly low representation of the totPrP^{D} and resPrP^{D} components of total PrP in T3 is reminiscent of the corresponding data reported in VPSPr-VV, in which totPrP^{D} accounted for 3.4% and resPrP^{D} for 0.83% of total PrP (*6*). The marked underrepresentation of totPrP^{D} and resPrP^{D} in T3 is especially puzzling considering that attack rate and survival time are not very different from those of T2 and T1, respectively. The apparent relative high efficiency of T3 might be explained by the high representation of oligomers (*33*). Alternatively, the T3 underrepresentation of totPrP^{D} relative to total PrP might reflect the lack of PrP^{C} down-regulation by T3 compared with T1 and T2, which would result in the relative increase of the total PrP pool (*33*,*34*).

A mechanism put forward for the lack of fidelity in cross-species transmission of the prion strain (*25*,*35*–*37*) is

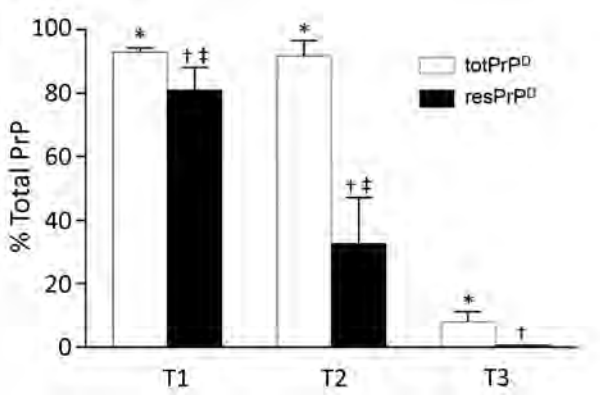

Figure 6. Relative quantities of totPrPD and resPrPD in T1–T3 phenotypes. totPrPD accounted for 93.1% and resPrPD for 81.3% of total PrP recovered from bank voles harboring the T1 phenotype. Corresponding percentages for T2 were 91.0% and 33.0%, and T3 totPrPD and resPrPD accounted only for 8.0% and 0.2% of total PrP and differed significantly from both T1 and T2 in each of the 2 components. ResPrPD also differed significantly between T1 and T2 (each bar represents the mean ± SD of n = 3 T1, n = 3 T2, and n = 5 T3; all data are from bank voles 109I; antibody 9A2). bv, bank vole; resPrPD protease-resistant, disease-related prion protein; totPrPD, comprising protease-sensitive PrPD and resPrPD. *p<0.0001; †p<0.0001 vs. T1 and p<0.05 vs. T2; ‡p<0.01.

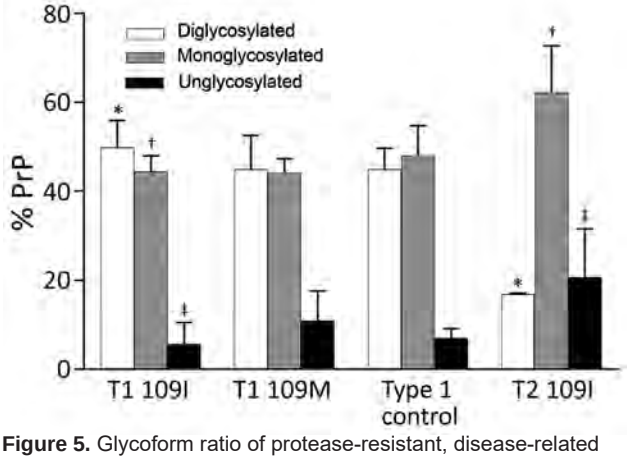

Figure 5. Glycoform ratio of protease-resistant, disease-related prion protein (resPrP^{D}) in phenotypes T1 and T2. The ratio of resPrP^{D} associated with T1 (T1 109I) was 48% for diglycosylated, 44% for monoglycosylated, and 8% for unglycosylated conformers and significantly differed in each glycoform from the 17%, 63%, and 20% corresponding ratio of T2 (T2 109I). *p<0.0001; †p<0.005; ‡p<0.05. Glycoform ratios of T1 109I and T1 109M as well as that of type 1 control (from bank voles 109I inoculated with sporadic Creutzfeldt-Jakob disease MV1 and used as human type 1 controls) did not significantly differ from each other. Each bar represents mean ± SD of n = 4 for T1 109M, n = 6 for T1 109I, n = 6 for T2, and n = 2 for type 1 control.

based on evidence that the dominant strain is selected from an array of strains that persist as substrains. In cross-species transmissions, substrains may be selected over the dominant strain (*38–40*). In the context of VPSPr, this mechanism is particularly intriguing, given that small quantities of PrP^D conformers with electrophoretic mobilities similar to those of human PrP^D type 1 were originally observed in a few cases by Gambetti et al (*6*); more recently, the presence of PrP^D type 2 in VPSPr, mostly in subcortical nuclei and in cerebellum, has been reported (*11*,*12*). These 2 components would be propagated faithfully in T1 and T2, and T3, which consistently shares only the 7-kDa fragment with the VPSPr resPrP^D, might represent the isolation of this GSS-like component of VPSPr resPrPD or the unsuccessful attempt to fully reproduce the dominant strain associated with this disease. We and others have occasionally observed an underrepresented 7-kDa fragment in sCJDMM1 (*41*; S. Notari, P. Gambetti, P. Parchi, unpub. data). Thus, it is tempting to speculate that the 7-kDa fragment observed in bank voles inoculated with sCJDMM1 and sCJDMV1 prions is related to the presence and possibly the infectivity of such fragment in the sCJDMM(MV)1 subtype.

In conclusion, on the basis of the first full transmission of VPSPr, our study confirms the permissiveness of bank voles to human prion diseases and suggests that bank voles are competent to reveal minor strain variants in prion diseases, such as resPrP^D types 1 and 2 reported in VPSPr and, possibly, the ≈7-kDa fragment observed in sCJDMM1 and sCJDMV1. However, our study also underscores the limited competence of bank vole PrP^C to faithfully reproduce the multiband profile of VPSPr resPrP^D that probably reflects the complex conformation of the prion seed in this disease.

Acknowledgments

We thank Janis Blevins, Katie Eppich, Yvonne Cohen, and the other personnel of the National Prion Disease Pathology Surveillance Center as well as Geraldina Riccardi, Stefano Marcon, Paolo Frassanito, and Marcello Rossi for their skillful assistance provided during the course of this study.

This work was supported by the National Institutes of Health (P01AI106705, 5R01NS083687) and the Charles S. Britton Fund (to P.G.).

About the Author

Dr. Nonno is a research scientist in the Emerging Zoonosis Unit at the Istituto Superiore di Sanità in Rome, Italy; his primary research interests include prion strain characterization and the zoonotic potential of animal prion diseases. Dr. Notari is an instructor in the Department of Pathology at Case Western Reserve University, Cleveland, Ohio, USA; his research focuses mainly on prion diseases, particularly prion molecular characteristics and infectivity.

References

1. Gambetti P. Creationism and evolutionism in prions. Am J Pathol. 2013;182:623–7. http://dx.doi.org/10.1016/j.ajpath.2012.12.016
2. Gambetti P, Cali I, Notari S, Kong Q, Zou WQ, Surewicz WK. Molecular biology and pathology of prion strains in sporadic human prion diseases. Acta Neuropathol. 2011;121:79–90. http://dx.doi.org/10.1007/s00401-010-0761-3
3. Puoti G, Bizzi A, Forloni G, Safar JG, Tagliavini F, Gambetti P. Sporadic human prion diseases: molecular insights and diagnosis. Lancet Neurol. 2012;11:618–28. http://dx.doi.org/10.1016/S1474-4422(12)70063-7
4. Parchi P, Strammiello R, Giese A, Kretzschmar H. Phenotypic variability of sporadic human prion disease and its molecular basis: past, present, and future. Acta Neuropathol. 2011;121:91–112. http://dx.doi.org/10.1007/s00401-010-0779-6
5. Poggiolini I, Saverioni D, Parchi P. Prion protein misfolding, strains, and neurotoxicity: an update from studies on mammalian prions. Int J Cell Biol. 2013;2013:910314. http://dx.doi.org/10.1155/2013/910314
6. Gambetti P, Dong Z, Yuan J, Xiao X, Zheng M, Alshekhlee A, et al. A novel human disease with abnormal prion protein sensitive to protease. Ann Neurol. 2008;63:697–708. http://dx.doi.org/10.1002/ana.21420
7. Zou WQ, Puoti G, Xiao X, Yuan J, Qing L, Cali I, et al. Variably protease-sensitive prionopathy: a new sporadic disease of the prion protein. Ann Neurol. 2010;68:162–72. http://dx.doi.org/10.1002/ana.22094
8. Notari S, Appleby B, Gambetti P. Variably protease sensitive prionopathy. In: Pocchiari M, Manson J. editors. Handbook of clinical neurology, vol. 153. San Diego: Elsevier; 2018. p. 175–190.
9. Collins SJ, Sanchez-Juan P, Masters CL, Klug GM, van Duijn C, Poleggi A, et al. Determinants of diagnostic investigation sensitivities across the clinical spectrum of sporadic Creutzfeldt-Jakob disease. Brain. 2006;129:2278–87. http://dx.doi.org/10.1093/brain/awl159
10. Pirisinu L, Nonno R, Esposito E, Benestad SL, Gambetti P, Agrimi U, et al. Small ruminant nor98 prions share biochemical features with human Gerstmann-Sträussler-Scheinker disease and variably protease-sensitive prionopathy. PLoS One. 2013;8:e66405. http://dx.doi.org/10.1371/journal.pone.0066405
11. Rodríguez-Martínez AB, López de Munain A, Ferrer I, Zarranz JJ, Atarés B, Villagra NT, et al. Coexistence of protease sensitive and resistant prion protein in 129VV homozygous sporadic Creutzfeldt-Jakob disease: a case report. J Med Case Reports. 2012;6:348. http://dx.doi.org/10.1186/1752-1947-6-348
12. Peden AH, Sarode DP, Mulholland CR, Barria MA, Ritchie DL, Ironside JW, et al. The prion protein protease sensitivity, stability and seeding activity in variably protease sensitive prionopathy brain tissue suggests molecular overlaps with sporadic Creutzfeldt-Jakob disease. Acta Neuropathol Commun. 2014;2:152. http://dx.doi.org/10.1186/s40478-014-0152-4
13. Notari S, Xiao X, Espinosa JC, Cohen Y, Qing L, Aguilar-Calvo P, et al. Transmission characteristics of variably protease-sensitive prionopathy. Emerg Infect Dis. 2014;20:2006–14. http://dx.doi.org/10.3201/eid2012.140548
14. Diack AB, Ritchie DL, Peden AH, Brown D, Boyle A, Morabito L, et al. Variably protease-sensitive prionopathy, a unique prion variant with inefficient transmission properties. Emerg Infect Dis. 2014;20:1969–79. http://dx.doi.org/10.3201/eid2012.140214
15. Nonno R, Angelo Di Bari M, Agrimi U, Pirisinu L. Transmissibility of Gerstmann-Sträussler-Scheinker syndrome in rodent models: new insights into the molecular underpinnings of prion infectivity. Prion. 2016;10:421–33. http://dx.doi.org/10.1080/19336896.2016.1239686
16. Pirisinu L, Di Bari MA, D'Agostino C, Marcon S, Riccardi G, Poleggi A, et al. Gerstmann-Sträussler-Scheinker disease subtypes

efficiently transmit in bank voles as genuine prion diseases. Sci Rep. 2016;6:20443. http://dx.doi.org/10.1038/srep20443
17. Galeno R, Di Bari MA, Nonno R, Cardone F, Sbriccoli M, Graziano S, et al. Prion strain characterization of a novel subtype of Creutzfeldt-Jakob disease. J Virol. 2017;91:e02390–16. http://dx.doi.org/10.1128/JVI.02390-16
18. Watts JC, Giles K, Patel S, Oehler A, DeArmond SJ, Prusiner SB. Evidence that bank vole PrP is a universal acceptor for prions. PLoS Pathog. 2014;10:e1003990. http://dx.doi.org/10.1371/journal.ppat.1003990
19. Notari S, Capellari S, Langeveld J, Giese A, Strammiello R, Gambetti P, et al. A refined method for molecular typing reveals that co-occurrence of PrP(Sc) types in Creutzfeldt-Jakob disease is not the rule. Lab Invest. 2007;11:1103–12.
20. Zou WQ, Capellari S, Parchi P, Sy MS, Gambetti P, Chen SG. Identification of novel proteinase K-resistant C-terminal fragments of PrP in Creutzfeldt-Jakob disease. J Biol Chem. 2003;278:40429–36. http://dx.doi.org/10.1074/jbc.M308550200
21. Agrimi U, Nonno R, Dell'Omo G, Di Bari MA, Conte M, Chiappini B, et al. Prion protein amino acid determinants of differential susceptibility and molecular feature of prion strains in mice and voles. PLoS Pathog. 2008;4:e1000113. http://dx.doi.org/10.1371/journal.ppat.1000113
22. Di Bari MA, Chianini F, Vaccari G, Esposito E, Conte M, Eaton SL, et al. The bank vole (*Myodes glareolus*) as a sensitive bioassay for sheep scrapie. J Gen Virol. 2008;89:2975–85. http://dx.doi.org/10.1099/vir.0.2008/005520-0
23. Cosseddu GM, Nonno R, Vaccari G, Bucalossi C, Fernandez-Borges N, Di Bari MA, et al. Ultra-efficient PrPSc amplification highlights potentialities and pitfalls of PMCA technology. PLoS Pathog. 2011;7:e1002370. http://dx.doi.org/10.1371/journal.ppat.1002370 PMID: 22114554
24. Di Bari MA, Nonno R, Castilla J, D'Agostino C, Pirisinu L, Riccardi G, et al. Chronic wasting disease in bank voles: characterisation of the shortest incubation time model for prion diseases. PLoS Pathog. 2013;9:e1003219. http://dx.doi.org/10.1371/journal.ppat.1003219
25. Espinosa JC, Nonno R, Di Bari M, Aguilar-Calvo P, Pirisinu L, Fernández-Borges N, et al. PrPC governs susceptibility to prion strains in bank vole, while other host factors modulate strain features. J Virol. 2016;90:10660–9. http://dx.doi.org/10.1128/JVI.01592-16
26. Orrú CD, Groveman BR, Raymond LD, Hughson AG, Nonno R, Zou W, et al. Bank vole prion protein as an apparently universal substrate for RT-QuIC-based detection and discrimination of prion strains. PLoS Pathog. 2015;11:e1004983. http://dx.doi.org/10.1371/journal.ppat.1004983
27. Fernández-Borges N, Eraña H, Castilla J. Behind the potential evolution towards prion resistant species. Prion. 2018;12:83–7. http://dx.doi.org/10.1080/19336896.2018.1435935
28. Nonno R, Di Bari MA, Cardone F, Vaccari G, Fazzi P, Dell'Omo G, et al. Efficient transmission and characterization of Creutzfeldt-Jakob disease strains in bank voles. PLoS Pathog. 2006;2:e12. http://dx.doi.org/10.1371/journal.ppat.0020012
29. Pirisinu L, Marcon S, Di Bari MA, D'Agostino C, Agrimi U, Nonno R. Biochemical characterization of prion strains in bank voles. Pathogens. 2013;2:446–56. http://dx.doi.org/10.3390/pathogens2030446
30. Asante EA, Linehan JM, Smidak M, Tomlinson A, Grimshaw A, Jeelani A, et al. Inherited prion disease A117V is not simply a proteinopathy but produces prions transmissible to transgenic mice expressing homologous prion protein. PLoS Pathog. 2013;9:e1003643. http://dx.doi.org/10.1371/journal.ppat.1003643
31. Parchi P, Chen SG, Brown P, Zou W, Capellari S, Budka H, et al. Different patterns of truncated prion protein fragments correlate with distinct phenotypes in P102L Gerstmann-Sträussler-Scheinker disease. Proc Natl Acad Sci U S A. 1998;95:8322–7. http://dx.doi.org/10.1073/pnas.95.14.8322
32. Piccardo P, Manson JC, King D, Ghetti B, Barron RM. Accumulation of prion protein in the brain that is not associated with transmissible disease. Proc Natl Acad Sci U S A. 2007;104:4712–7. http://dx.doi.org/10.1073/pnas.0609241104
33. Mays CE, Kim C, Haldiman T, van der Merwe J, Lau A, Yang J, et al. Prion disease tempo determined by host-dependent substrate reduction. J Clin Invest. 2014;124:847–58. http://dx.doi.org/10.1172/JCI72241
34. Mays CE, van der Merwe J, Kim C, Haldiman T, McKenzie D, Safar JG, et al. Prion infectivity plateaus and conversion to symptomatic disease originate from falling precursor levels and increased levels of oligomeric PrPSc species. J Virol. 2015;89:12418–26. http://dx.doi.org/10.1128/JVI.02142-15
35. Weissmann C. Mutation and selection of prions. PLoS Pathog. 2012;8:e1002582. http://dx.doi.org/10.1371/journal.ppat.1002582
36. Makarava N, Savtchenko R, Alexeeva I, Rohwer RG, Baskakov IV. New molecular insight into mechanism of evolution of mammalian synthetic prions. Am J Pathol. 2016;186:1006–14. http://dx.doi.org/ 10.1016/j.ajpath.2015.11.013
37. Moreno JA, Telling GC. Insights into mechanisms of transmission and pathogenesis from transgenic mouse models of prion diseases. Methods Mol Biol. 2017;1658:219–52. http://dx.doi.org/10.1007/978-1-4939-7244-9_16
38. Weissmann C, Li J, Mahal SP, Browning S. Prions on the move. EMBO Rep. 2011;12:1109–17. http://dx.doi.org/10.1038/embor.2011.192
39. Collinge J, Clarke AR. A general model of prion strains and their pathogenicity. Science. 2007;318:930–6. http://dx.doi.org/10.1126/science.1138718
40. Li J, Mahal SP, Demczyk CA, Weissmann C. Mutability of prions. EMBO Rep. 2011;12:1243–50. http://dx.doi.org/10.1038/embor.2011.191
41. Benedetti D, Fiorini M, Cracco L, Ferrari S, Capucci L, Brocchi E, et al. Molecular characterization of low molecular mass C-terminal fragments in different Creutzfeldt-Jakob disease subtypes. Presented at: Prion 2008; 2008 Oct 8–10; Madrid, Spain.

Address for correspondence: Pierluigi Gambetti, Case Western Reserve University, 2085 Adelbert Rd, Rm 419, Cleveland, OH 44160, USA; email: pxg13@case.edu; Umberto Agrimi, Istituto Superiore di Sanità, Viale Regina Elena 299, Rome 00161, Italy; email: umberto.agrimi@iss.it

Zoonotic Source Attribution of *Salmonella enterica* Serotype Typhimurium Using Genomic Surveillance Data, United States

Shaokang Zhang, Shaoting Li, Weidong Gu, Henk den Bakker, Dave Boxrud, Angie Taylor, Chandler Roe, Elizabeth Driebe, David M. Engelthaler, Marc Allard, Eric Brown, Patrick McDermott, Shaohua Zhao, Beau B. Bruce, Eija Trees, Patricia I. Fields, Xiangyu Deng

Increasingly, routine surveillance and monitoring of foodborne pathogens using whole-genome sequencing is creating opportunities to study foodborne illness epidemiology beyond routine outbreak investigations and case–control studies. Using a global phylogeny of *Salmonella enterica* serotype Typhimurium, we found that major livestock sources of the pathogen in the United States can be predicted through whole-genome sequencing data. Relatively steady rates of sequence divergence in livestock lineages enabled the inference of their recent origins. Elevated accumulation of lineage-specific pseudogenes after divergence from generalist populations and possible metabolic acclimation in a representative swine isolate indicates possible emergence of host adaptation. We developed and retrospectively applied a machine learning Random Forest classifier for genomic source prediction of *Salmonella* Typhimurium that correctly attributed 7 of 8 major zoonotic outbreaks in the United States during 1998–2013. We further identified 50 key genetic features that were sufficient for robust livestock source prediction.

Each year, 9.4 million episodes of foodborne illness occur in the United States (*1*). According to the Centers for Disease Control and Prevention, ≈95% of these infections are sporadic, nonoutbreak cases for which specific food exposures and contamination sources remain difficult to determine. The lack of source information for most foodborne infections substantially challenges understanding of the epidemiology of foodborne illnesses and development of intervention measures for their prevention and mitigation. Routine use of whole-genome sequencing (WGS) for foodborne illness surveillance and pathogen monitoring has created a large and quickly expanding wealth of genomes and associated metadata. Much of these data remain largely untapped beyond routine outbreak investigation.

Salmonella enterica is one of the most prevalent foodborne pathogens worldwide, causing >1 million human cases and an economic burden of $3.7 billion annually in the United States alone (*1*,*2*). *S. enterica* serotype Typhimurium is one of the most prevalent causes of human salmonellosis in many countries, including the United States (*3*). *Salmonella* Typhimurium strains display a broad host range and varying degrees of host adaptation (*4*). Diverse subtypes have caused emerging epidemics in recent decades. First isolated in the early 1980s in the United Kingdom, multidrug-resistant *Salmonella* Typhimurium definitive type 104 spread from cattle to other livestock in the country before its global dissemination during the 1990s (*5*). *Salmonella* Typhimurium sequence type (ST) 313 emerged ≈40–50 years ago in sub-Saharan Africa (*6*); its regional spread was linked to invasive disease symptoms and coincided with an HIV pandemic (*6*,*7*). The high prevalence, diverse reservoirs, and dynamic epidemiology of *Salmonella* Typhimurium have made it a paradigm for studying host specificity (*8*) and zoonotic colonization (*9*). Knowing the contribution of major sources of human illness caused by specific pathogens is critical for identifying, evaluating, and prioritizing public health intervention strategies (*10*). Microbiological source attribution relying on subtyping has shown some promise, such as a source attribution model from Denmark based on *Salmonella*

Author affiliations: University of Georgia Center for Food Safety, Griffin, Georgia, USA (S. Zhang, S. Li, H. den Bakker, X. Deng); Centers for Disease Control and Prevention, Atlanta, Georgia, USA (W. Gu, B.B. Bruce, E. Trees, P.I. Fields); Minnesota Department of Health, St. Paul, Minnesota, USA (D. Boxrud, A. Taylor); Translational Genomics Research Institute, Flagstaff, Arizona, USA (C. Roe, E. Driebe, D.M. Engelthaler); US Food and Drug Administration, College Park, Maryland, USA (M. Allard, E.W. Brown); US Food and Drug Administration, Laurel, Maryland, USA (P. McDermott, S. Zhao)

DOI: https://doi.org/10.3201/eid2501.180835

serotyping and phage typing (*11*). However, more recent models continued to use traditional phenotypes for *Salmonella* source attribution (*12*). The usefulness of more discriminating molecular subtyping for *Salmonella* source attribution has not been established (*12*).

We hypothesized that microbiological source attribution could be improved by an evolutionary understanding of pathogen populations and a mechanistic inquiry into their source association. We investigated zoonotic source attribution of *Salmonella* Typhimurium under an extensive phylogenomic framework by including a large collection of isolates from 3 major US laboratory surveillance and monitoring programs. We examined genotypic characteristics and metabolic profiles to assess livestock host adaptation and production environment colonization. Machine learning enabled comprehensive and high-resolution screening for key genetic indicators of source association throughout *Salmonella* Typhimurium genomes.

Materials and Methods

To study the population structure of *Salmonella* Typhimurium and its monophasic variant (I 4,[5],12:i:-), we first sequenced (n = 127) or collected (n = 1,140) 1,267 *Salmonella* Typhimurium genomes (Appendix 1 Table 1, https://wwwnc.cdc.gov/EID/article/25/1/18-0835-App1.xlsx; Appendix 2 section 1, https://wwwnc.cdc.gov/EID/article/25/1/18-0835-App1.pdf), comprising 4 sets of genomes. First, we selected human isolates from outbreak and sporadic cases in the United States during 1949–2014 (n = 127, sequenced for this study) to represent diverse pulsed-field gel electrophoresis patterns (n = 51) and multilocus variable-number tandem-repeat analysis patterns (n = 16, for isolates of known pattern) of *Salmonella* Typhimurium as surveyed by PulseNet USA during 1998–2014 (*13*). Second, we chose genomes in the GenomeTrakr database (*14*) as of September 2015 (n = 907) from food, environmental, and wild and livestock animal sources in the United States, Europe, South America, Asia, and Africa. Third, we included retail meat isolates sampled by the US National Antimicrobial Resistance Monitoring System (n = 157). Finally, we compiled other reported *Salmonella* Typhimurium genomes, including human ST313 isolates from sub-Saharan Africa (n = 76) (*6*). Publicly available genomes were confirmed to be *Salmonella* Typhimurium by SeqSero (*15*).

Overall metabolic potentials of 6 randomly selected representative isolates from 6 major population groups (Figure 1; Appendix 1 Table 2) were evaluated by Phenotype Microarrays (Biolog, https://biolog.com) (Appendix 2 section 8). Principal component analysis was conducted using Phenotype Microarrays results. Phylogenetic analysis, temporal signal screening and most recent common ancestor (MRCA) dating, and putative pseudogene identification

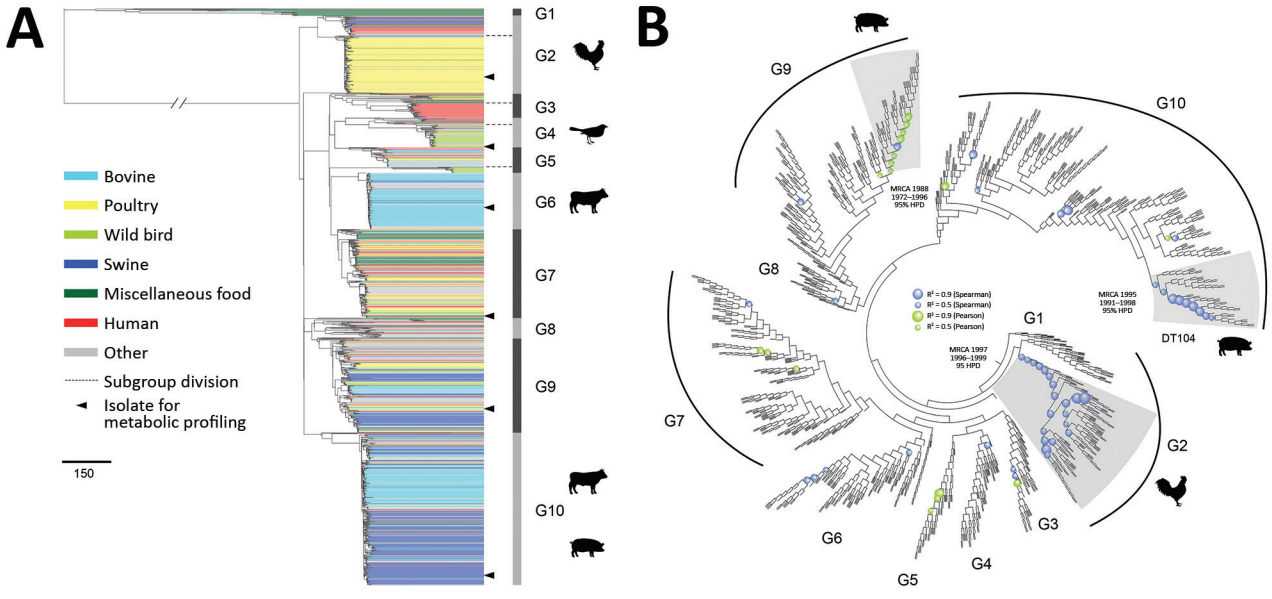

Figure 1. Phylogenetic structure of 1,267 *Salmonella enterica* serotype Typhimurium isolates. A) Maximum-likelihood phylogeny from 46 US states and 39 other countries. The tree was rooted at midpoint. Ten major population groups (G1–G10) were delineated. Each dashed line shows the division of subgroups in G2, G3, G4, and G5 (e.g., G2a and G2b). Each isolate is color coded by source. Arrowheads indicate isolates selected for metabolic profiling using Phenotype Microarrays (Biolog, https://biolog.com). Scale bar indicates number of single-nucleotide polymorphisms. B) Circular cladogram of the same maximum-likelihood phylogeny of the 1,267 isolates. Colored circles indicate internal nodes that had a squared coefficient (R^2) of the Spearman or Pearson correlation between isolation years and branch lengths >0.4. The sizes of the circle are proportional to the values of R^2 (0.0–0.9). Clades identified to exhibit temporal signals of single-nucleotide polymorphisms accumulation are shaded in gray. The inferred MRCA age of each clade is shown. HPD, highest posterior density; MRCA, most recent common ancestor.

were performed (Appendix 2 sections 2–4). A Random Forest classifier (https://www.stat.berkeley.edu/~breiman/randomforest2001.pdf) was built to predict zoonotic sources of *Salmonella* Typhimurium genomes (Appendix 2 sections 5, 6).

Results

Population Structure

We constructed a maximum-likelihood phylogeny of the 1,267 isolates based on single-nucleotide polymorphisms (SNPs) identified in the core genome alignments (Figure 1, panel A). We determined 39,562 single-nucleotide variable sites from the alignment. We excluded 154 genome segments potentially involved in recombination from the alignment and SNP identification. The recombinant regions (Appendix 1 Table 3) accounted for 269,366 nt (5.6%) of a typical *Salmonella* Typhimurium genome (4.8 Mb).

Bayesian analysis of the population structure delineated 10 population groups, designated G1–10 (Figure 1, panel A). Most population groups were monophyletic, except G5 and G8. G1 represented a highly divergent population (>9,000 SNPs) from other population groups and contained a high proportion (68.8%) of isolates from seafood, especially from Asia. Human clinical and miscellaneous food isolates (see source classification in Appendix 2 section 5) were widely distributed among population groups; clinical and food isolates were found in every group, except we found no food isolates in G6. Several groups contained major clades associated with particular sources, including G2b with poultry, G4b and G5b with wild birds, G6 with bovine, and G10 with swine and bovine sources (Figure 1, panel A; Appendix 1 Table 4). Other population groups included isolates from diverse sources. G7 accounted for all the aforementioned sources and had more human and food isolates than any other group. Representing 15.4% of the *Salmonella* Typhimurium collection, G7 had 21.6% and 40.2% of all human and food isolates. Eight major foodborne outbreaks during 1998–2012 were included. Of those, 5 were represented by isolates in G7: a 2006 picnic-associated outbreak in the United States, a 2009 multistate peanut butter–associated outbreak in the United States, a 2009 shredded lettuce–associated outbreak in the western United States and Canada, a 2010–2011 multistate alfalfa sprout–associated outbreak in the United States, and a 2012 multistate cantaloupe-associated outbreak in the United States.

To investigate the temporal history of *Salmonella* Typhimurium lineages, we searched temporal signals of SNP accumulation throughout the phylogeny by screening every internal node for strong correlation between isolation years and branch lengths (Figure 1, panel B). Although the entire phylogeny exhibited an overall weak temporal signal (R^2 <0.2), 3 clades showed moderate temporal signals (R^2 >0.4), permitting robust age inference of their MRCA. All 3 clades were associated with livestock and originated around the 1990s (Appendix 1 Table 5).

Differential Abundance of Putative Pseudogenes Among Recently Diverged Clades

We identified putative disruptive mutations (pseudogenes) in each *Salmonella* Typhimurium genome. Pseudogenes were most abundant in the sub-Saharan ST313 clade (G3b) and clades associated with wild birds (G4b and G5b) and seafood (G1). In multiple cases, we found significant differences ($p<0.01$) in pseudogene abundance between 2 recently diverged clades from a common ancestor; 1 comprised isolates from diverse sources and the other was associated predominantly with a particular source, such as wild birds (G4b), livestock (G2b, G6, and G10), and human ST313 cases in Africa (G3b) (Figure 2, panel A). We consistently observed elevated pseudogene accumulation in the source-associated and putatively host-adapted clades (Appendix 2 section 7). Most of these pseudogenes were clade-specific (Figure 2, panel B), suggesting they emerged and accumulated independently in different clades.

Differential Metabolic Potentials Among Representative Isolates

We characterized metabolic profiles of 6 representative human and animal isolates from 6 US population groups (G2b, G4b, G6, G7, G9, and G10) using Biolog Phenotype Microarrays comprising substrates of carbon, nitrogen, sulfur, and phosphorus sources. We found evidence for differential metabolic activity between any 2 isolates for 189 of the 384 substrates tested (Appendix 1 Table 2). Principal component analysis on metabolic activities suggested that a wild bird isolate (STM223) from G4b and swine isolate from G10 (STM712) deviated from each other and the rest of the isolates because of deficiency in using multiple substrates (Figure 2, panel C). Compared with a human isolate from G9 (STM988), the wild bird isolate showed reduced metabolic activity for 182 substrates and the swine isolate for 132 substrates. Some of these deficiencies correlated with the putative pseudogenes and nonsynonymous SNPs (Appendix 2 section 8).

Source Prediction Using WGS

To evaluate *Salmonella* Typhimurium source prediction using WGS, we updated the *Salmonella* Typhimurium genome collection (initially 1,267 genomes) by 1) adding 939 genomes that became available in GenomeTrakr during September 2015–January 2017; 2) sequencing another 11 isolates from 5 outbreaks with confirmed livestock origin in the United States during 2007–2013, which, together with 6 livestock isolates from 3 outbreaks in the original dataset,

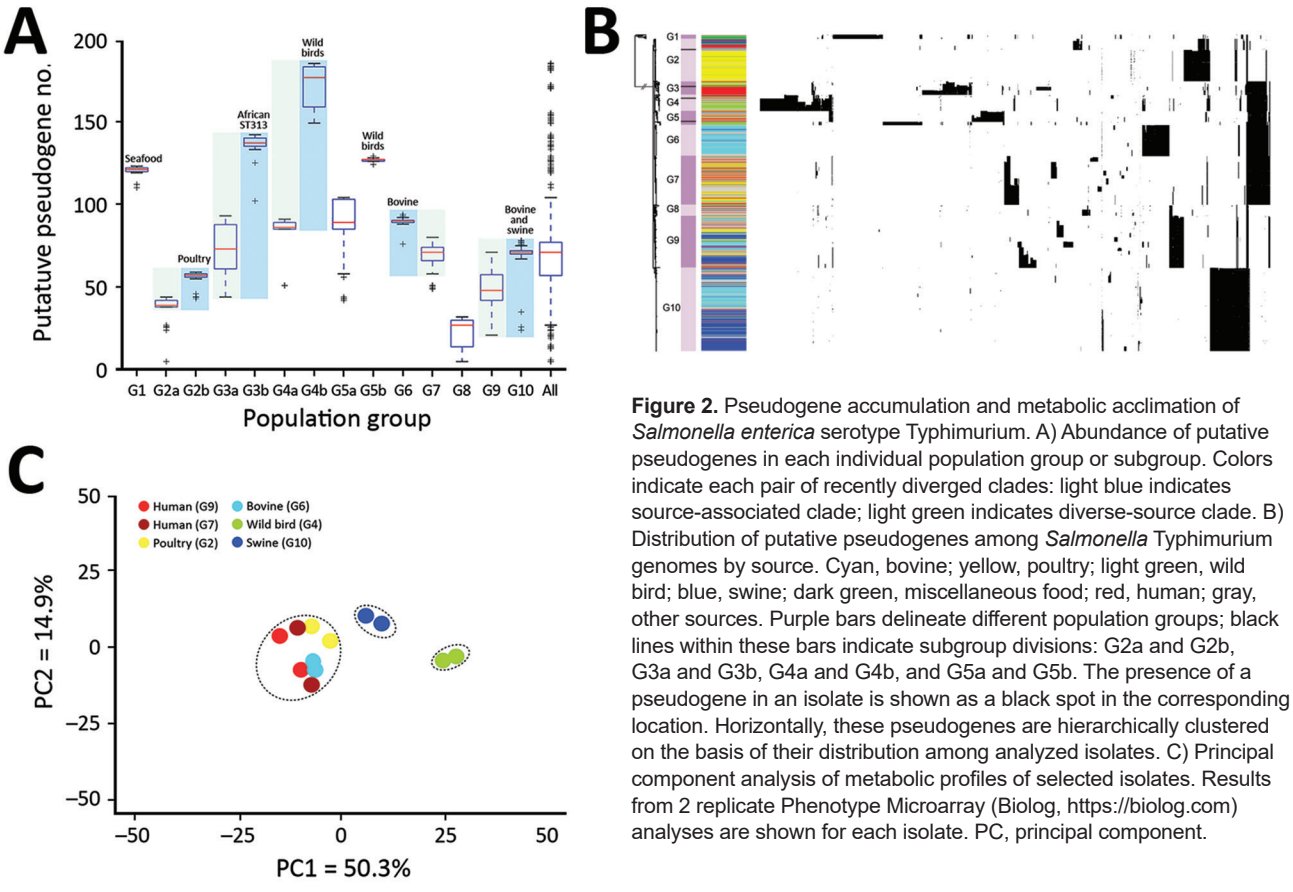

Figure 2. Pseudogene accumulation and metabolic acclimation of *Salmonella enterica* serotype Typhimurium. A) Abundance of putative pseudogenes in each individual population group or subgroup. Colors indicate each pair of recently diverged clades: light blue indicates source-associated clade; light green indicates diverse-source clade. B) Distribution of putative pseudogenes among *Salmonella* Typhimurium genomes by source. Cyan, bovine; yellow, poultry; light green, wild bird; blue, swine; dark green, miscellaneous food; red, human; gray, other sources. Purple bars delineate different population groups; black lines within these bars indicate subgroup divisions: G2a and G2b, G3a and G3b, G4a and G4b, and G5a and G5b. The presence of a pseudogene in an isolate is shown as a black spot in the corresponding location. Horizontally, these pseudogenes are hierarchically clustered on the basis of their distribution among analyzed isolates. C) Principal component analysis of metabolic profiles of selected isolates. Results from 2 replicate Phenotype Microarray (Biolog, https://biolog.com) analyses are shown for each isolate. PC, principal component.

led to 8 zoonotic outbreaks for retrospective source attribution; and 3) excluding 744 redundant genomes to minimize biases resulting from repeated sampling of closely related strains. The genome updates resulted in a modified collection of 1,473 isolates for source prediction, all belonging to the previously defined 10 populations groups.

We observed phylogenetic clustering of isolates from the same zoonotic source (Figure 1, panel A). In general, 70.3% of isolates from bovine, poultry, swine, or wild bird (BPSW) sources shared the MRCA with an isolate from the same source, suggesting the possibility of source prediction by phylogenetic placement. By assigning a query outbreak isolate to the source of the livestock isolate that shared the MRCA with the query, we correctly predicted zoonotic sources for 6 of the 8 zoonotic outbreaks. Most of the reference isolates for source prediction were epidemiologically unrelated to the query isolates (i.e., separated by years [Table 1]). By contrast, only 36.9% of human isolates and 45.5% of food isolates (excluding G1) were from the same source as their nearest phylogenetic neighbor.

In addition to overall phylogeny, we evaluated how the assortment of certain genetic features into particular *Salmonella* Typhimurium genomes could help predict zoonotic sources of *Salmonella* Typhimurium. Using a machine learning approach, we built a Random Forest (RF) classifier to interrogate a comprehensive collection of 3,137 genetic features among *Salmonella* Typhimurium genomes: core genome SNPs (n = 1,882), high-quality insertion/deletions (indels; n = 150), and source discriminatory accessory genes (n = 1,105). Trained by genomes of known BPSW origins, the classifier produced an out-of-bag accuracy rate (https://www.stat.berkeley.edu/~breiman/OOBestimation.pdf) of 82.9%. Seven of the 8 zoonotic outbreaks were attributed to the correct source by the RF method (Table 1).

Among BPSW, the classifier performed best in predicting poultry and swine sources, followed by bovine and wild bird sources (Figure 3, panel A). This result was consistent with relative sampling intensities of these sources. Rarefaction analysis suggested that phylogenetic diversity was better sampled for poultry and swine than bovine and wild bird sources; wild bird *Salmonella* Typhimurium populations were least sampled (Appendix 2 section 9). For each isolate analyzed, the RF classifier generated a predicted probability for each source class. Because the classifier was not trained by isolates from non-BPSW sources, source prediction ambiguities

Table 1. Retrospective source attribution of zoonotic outbreaks of *Salmonella enterica* serotype Typhimurium, United States*

	Outbreak		Phylogenetic reference†			Population	Phylogeny	RF
Isolate	Year	Confirmed vehicle	Isolate	Year	Source	group	prediction	prediction
STM2207	2013	Ground beef	STM296	2006	Bovine	G9	+	+
STM2208	2013	Ground beef	STM296	2006	Bovine	G9	+	+
STM2209	2007	Pot pie turkey	STM093	2005	Poultry	G7	+	+
STM2210	2007	Pot pie turkey	STM093	2005	Poultry	G7	+	+
STM2211	2007	Pot pie turkey	STM093	2005	Poultry	G7	+	+
STM2212	2007	Pot pie turkey	STM093	2005	Poultry	G7	+	+
STM2213	2013	Live poultry	STM2114	2016	Bovine	G7	–	+
STM2214	2013	Live poultry	STM2114	2016	Bovine	G7	–	+
STM2215	2011	Ground beef	STM1563	2011	Bovine	G6	+	+
STM2216	2011	Ground beef	STM1563	2011	Bovine	G6	+	+
STM2217	2015	Pork	STM2116	2016	Swine	G2a	+	+
STM1016	2010	Cattle contact	STM328	2008	Bovine	G9	+	+
STM1075	2010	Cattle contact	STM978	2010	Bovine	G2a	+	+
STM995	2010	Cattle contact	STM978	2010	Bovine	G2a	+	–
STM996	2010	Cattle contact	STM978	2010	Bovine	G2a	+	–
STM1065	1998	Raw milk	STM034	2004	Bovine	G9	+	+
STM988	2009	Chicken	STM1975	2015	Bovine	G9	–	+

*RF, Random Forest; +, correct prediction; –, incorrect prediction.
†The livestock genome that had the most recent common ancestor with an outbreak query genome.

were anticipated when it was used to predict non-BPSW isolates. Such ambiguities might present themselves as increased uncertainty in source prediction. We used the Simpson diversity indices (SDI) to measure the uncertainty of predicted probabilities between BPSW and non-BPSW isolates. The SDI of the non-BPSW group was significantly higher ($p<0.01$) than that of the BPSW group (Figure 3, panel B). We further showed that SDI of predicted probabilities made an effective binary classifier to distinguish BPSW from non-BPSW isolates in the current dataset through a receiver operating characteristic analysis, which yielded a sensitivity of 0.80 and a specificity of 0.63 adopting an arbitrary SDI cutoff of 0.45 (Figure 3, panel C).

Using this cutoff, we categorized source predictions into precise and imprecise groups (Figure 3, panel D). Precise predictions (SDI <0.45) were generated for 829 of 1,041 BPSW isolates, of which 759 (91.6%) were correct. A total of 147 non-BPSW isolates were precisely attributed to a BPSW source; among these, 51 were human isolates, which accounted for 31.9% of human isolates in the *Salmonella* Typhimurium collection.

Zoonotic source predictions by phylogenetic placement and RF analysis were generally consistent (Appendix 1 Table 6). Among the 829 isolates with precise predictions by the RF classifier, 705 (85.0%) isolates were correctly predicted by both methods. Detailed comparison of the 2 methods can be found in Appendix 2 section 10.

Genetic Indicators of Source Association

Using RF, we ranked all 3,137 genetic features by their importance for source prediction, which was measured by the mean decrease of prediction accuracy through randomly permuting feature values (Appendix 1 Table 7). To identify a subset of key features for source prediction, we incrementally incorporated features into the classifier based on their importance ranking and monitored the change of out-of-bag error rate. After an initial sharp drop, the error rate plateaued when ≈50 top-ranking features were included (Figure 4, panel A). Ten core genome mutations were among the top 50 features, 3 nonsynonymous SNPs and 7 indels (Figure 4, panel B). The 2 most important features for source prediction were nonsynonymous SNPs and related to cell surface components (Table 2). One of these was in the *fliC* gene, which is responsible for *Salmonella* flagellum formation and serotype determination. Forty of the other top 50 features were accessory genes found on plasmid- or phage-associated sequences (Figure 4, panel B). Several of these genes were involved in *Salmonella* interaction with host and environment, such as virulence genes *spvB* (*23*), *spvD* (*22*), and *pipB2* (*20*); virulence and putative host range factor *sspH2* (*19*); and multiple resistance genes to silver and copper (Table 2). Both elements are used as dietary supplements or antimicrobial drugs in livestock production (*24*,*25*). Another highly ranked accessory gene, *proQ*, was recently discovered to mediate global posttranscriptional regulation of gene expression (*21*). Twenty-four of the top 50 feature-related genes had been functionally tested for mediating intestinal colonization of livestock animals; 14 showed positive evidence for such a role (*9*). Although not ranked among the top 50 features, antimicrobial resistance genes exhibited enrichment and source-associated distribution patterns among livestock clades (Appendix 2 section 12).

Discussion

Based on our determination of the large-scale phylogeny of *Salmonella* Typhimurium, including dense sampling of US livestock isolates, we speculate emerging host adaptation associated with livestock production. Evidence to

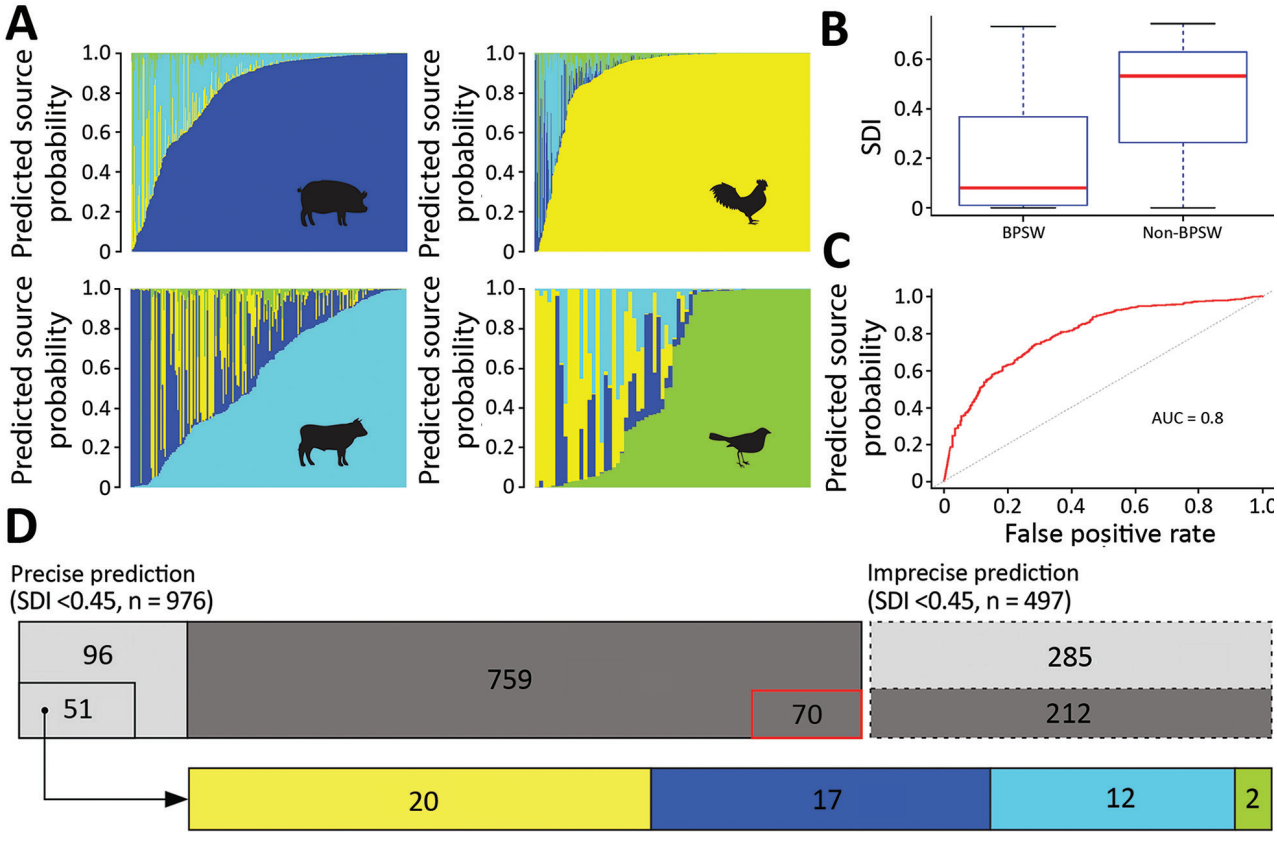

Figure 3. Source prediction by Random Forest classifier. A) Predicted source probabilities for zoonotic *Salmonella enterica* serotype Typhimurium isolates. Each vertical line in a panel is color coded by predicted source probabilities to proportion: cyan, bovine; yellow, poultry; blue, swine; light green, wild bird. B) Comparison of SDIs of predicted probabilities between BPSW and non-BPSW isolates. For each isolate, SDI was calculated among predicted probabilities of the 4 sources. Red horizontal lines indicate median SDI values; blue box tops and bottoms indicate interquartile ranges; whiskers indicate maximum and minimum SDI values. C) Receiver operating characteristics (ROC) curve of differentiating BPSW and non-BPSW isolates using SDI of predicted source probabilities. The AUC was 0.8, suggesting good binary classification. Red line indicates ROC curve; dotted line indicates diagonal line across the ROC space. D) Summary of source prediction results of 1,473 *Salmonella* Typhimurium isolates. Rectangles with solid and dashed lines represent precise (SDI <0.45) and imprecise (SDI >0.45) predictions, respectively. Dark gray rectangles, BPSW isolates; light gray rectangles, non-BPSW isolates. The number in each enclosed area is the number of isolates in the category. The sizes of enclosed and gray areas are in proportion to the numbers of isolates they represent. Red lines highlight the 70 precisely but incorrectly predicted BPSW isolates are shown with red shading. The 51 precisely predicted human isolates were attributed to zoonotic sources: cyan, bovine; yellow, poultry; blue, swine; light green, wild bird. The sizes of source colored rectangles are proportional to the numbers of isolates in the predicted source classes. AUC, area under the ROC curve; BPSW, bovine, poultry, swine, or wild bird; SDI, Simpson diversity index.

support this hypothesis includes increasing pseudogene accumulation as livestock clades diverged and metabolic deviation of a representative swine isolate. Both phenomena have been reported as possible signs of *Salmonella* host adaptation (*26*–*29*). These adaptation signals were detectable but moderate compared with the wild bird and ST313 clades, indicating emerging adaptation. Major clades of livestock isolates (G2b, G6, and G10) occupied terminal branches of the phylogeny and shared recent common ancestors with diverse-source clades, suggesting their recent emergence through clonal expansion. An exhaustive screening for temporal signals throughout the phylogeny enabled MRCA dating of 2 livestock clades in G2b and G10 around the 1990s, supporting their recent origin. The G10 clade contained the swine isolate displaying putative metabolic acclimation, as well as definitive type 104 isolates (Figure 1, panel B), whose global circulation started around the 1990s (*5*), consistent with our MRCA dating.

Major livestock clades all included animal isolates across the United States and spanned >10 years. Phylogenetic clustering of isolates spanning a wide geotemporal range also has been noticed in poultry-related *Salmonella* Enteritidis in the United States (*30*). The dissemination of

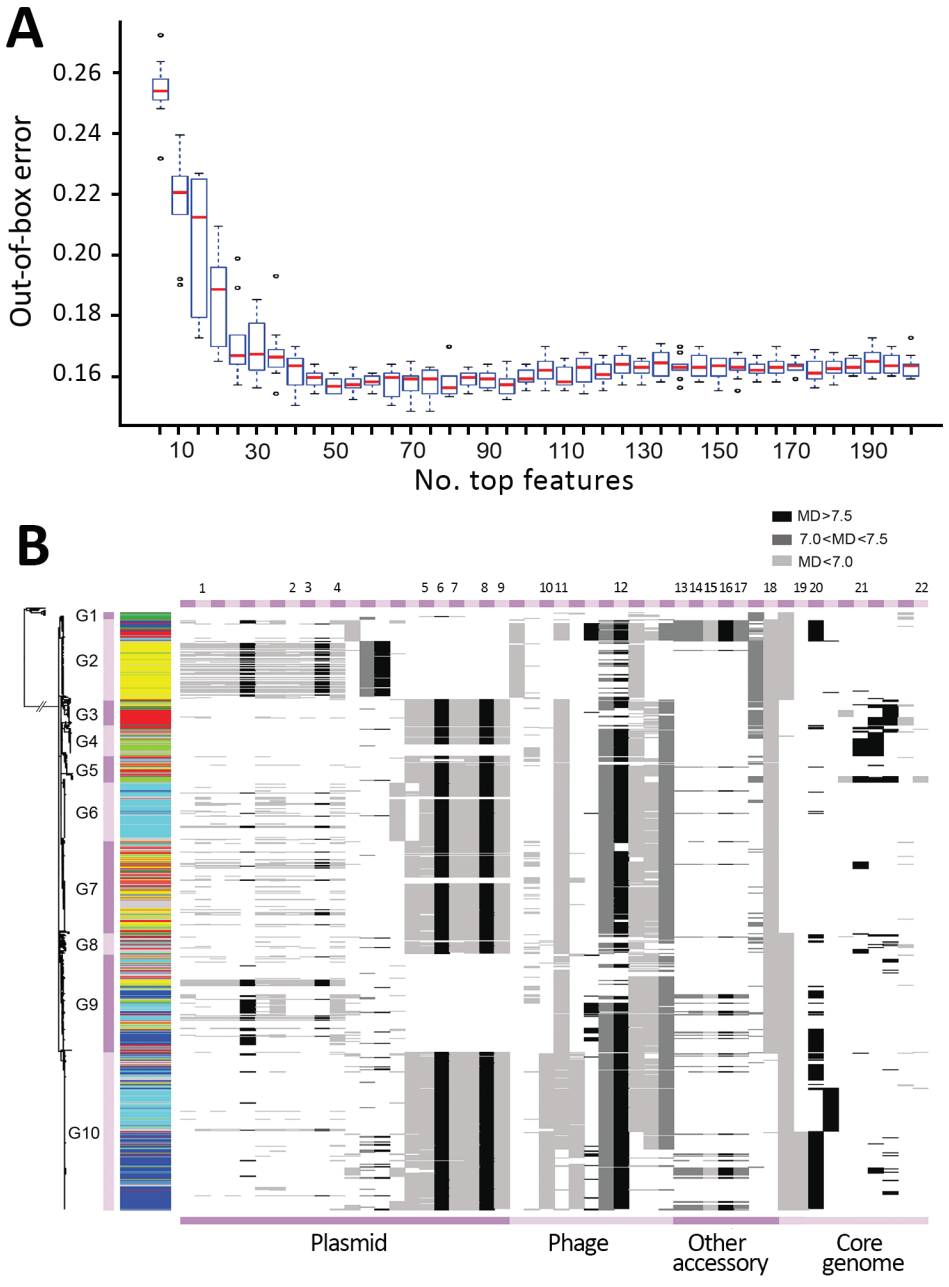

Figure 4. Key genetic features for zoonotic source prediction of *Salmonella enterica* serotype Typhimurium using Random Forest classifier. A) Change of out-of-bag prediction error rate as incremental inclusion of top ranking genetic features for source prediction. Red lines indicate median values; blue boxes indicate interquartile ranges. Upper and lower whiskers indicate maximum and minimum values. Circles indicate outliers. B) Distribution of top 50 source predicting features among *Salmonella* Typhimurium isolates on the basis of their location. Cyan, bovine; yellow, poultry; light green, wild bird; blue, swine; dark green, miscellaneous food; red, human; gray, other sources. Numbers at top reference genes: 1. *proQ*; 2. *exc*; 3. *yafA*; 4.*yceA*; 5. *Trap*; 6. *traA*; 7. *traJ*; 8. *spvB*; 9. *spvD*; 10. *pipB2*; 11. *sspH2*; 12. 1930; 13. *cusA*; 14. *siiP*; 15. *cusC*; 16. *cusF*; 17. *cusB*; 18. 0286A; 19.0835; 20. *fiiC*; 21. 1874; 22. *yhfL*. The presence of a feature in an isolate is shown as a horizontal line in the corresponding location, with its grayscale representing the level of the MD of prediction accuracy through randomly permuting values of the feature. The higher the MD, the more important the feature is for source prediction. MD, mean decrease.

closely related *Salmonella* strains from specific sources in the poultry sector could explain these observations.

Host prediction of *Salmonella* and *Escherichia coli* genomes through a machine-learning approach has been recently reported (*31*,*32*). A machine-learning classifier is inherently constrained by the representativeness of its training classes. However, for application in a realistic source attribution scenario, a classifier would be applied prospectively to isolates from sources a priori unknown to the classifier. Unlike those used in previous studies, our RF classifier was tested by isolates from various nontraining sources and capable of flagging them as imprecise predictions. This distinction might be useful for analyzing foodborne pathogens of a wide source range.

A previous support vector machine classifier had >90% accuracy in predicting the human host of *Salmonella* Typhimurium isolates using WGS data (*32*). Although human is not a source category in foodborne pathogen source attribution studies, which aim to attribute known human isolates to food and other sources, we performed a similar host specificity prediction using our RF classifier and *Salmonella* Typhimurium dataset. Only 36.9% of human isolates in our study were predicted to originate

Table 2. Selected key genetic features for zoonotic source prediction of *Salmonella enterica* serotype Typhimurium using a Random Forest classifier

Feature rank*	Affected gene	Feature type	Gene function (reference)
1	*fliC*	Single-nucleotide polymorphism	Motility, serotype diversity, intestinal colonization (*16*)
5	*traA*	Accessory gene	Pilin precursor. intestinal colonization (*16*)
6	*spvB*	Accessory gene	Virulence (*17*), intestinal colonization (*16*)
9	1930†	Accessory gene	Intestinal colonization (*16*)
11	1874†	Indel	Intestinal colonization (*16*)
13–15, 28	*cusCFBA*	Accessory gene	Putative copper efflux system (*18*)
16	*silP*	Accessory gene	Silver efflux pump (*17*)
21	*yafA*	Accessory gene	Intestinal colonization (*16*)
24	*sspH2*	Accessory gene	Virulence and potential host range factor (*19*)
27	0286A†	Accessory gene	Intestinal colonization (*16*)
31	*pipB2*	Accessory gene	Virulence (*20*)
32	*proQ*	Accessory gene	Global posttranscription regulation (*21*), intestinal colonization (*16*)
34	*spvD*	Accessory gene	Virulence (*22*)
37	*Trap*	Accessory gene	Intestinal colonization (*16*)
39	*yhfL*	Indel	Intestinal colonization (*16*)
41	0835†	Accessory gene	Intestinal colonization (*16*)
43	*traJ*	Accessory gene	Intestinal colonization (*16*)
45	*yceA*	Accessory gene	Intestinal colonization (*16*)
46	*exc*	Accessory gene	Intestinal colonization (*16*)

*Features are ranked by the mean decrease of prediction accuracy through randomly permuting values of the feature. The larger the mean decrease, the higher the rank. Only features that are located in genes that have reported involvement in intestinal colonization, virulence, and other functions related to livestock environment adaptation are listed. The full list of analyzed features, including the top 50 for zoonotic source prediction, is provided in Appendix 1 Table 6 (https://wwwnc.cdc.gov/EID/article/25/1/18-0835-App1.xlsx). Indel, insertion/deletion.
†Locus identification of the reference genome SL1344.

from a human host (Appendix 2 section 11). We found that the higher accuracy of human host prediction by the support vector machine classifier (*32*) was due mainly to an exceedingly clonal structure of its training human isolates, of which 85% shared the MRCA with another human isolate, compared with only 36.9% in our training set (Appendix 2 section 13). The percentage for the training set was consistent with our sampling of diverse human isolates in the United States based on surveillance data, including molecular subtypes. To avoid inflating source prediction accuracy by overrepresenting closely related genomes in the training set, we reduced training data redundancy by excluding 744 genomes from all training classes based on their pairwise phylogenetic distance and strain metadata (Appendix 2 section 6). Our classifier could not distinguish US human isolates from isolates of other sources by genomewide analysis of genetic features, arguing against distinct human host signals in *Salmonella* Typhimurium genomes or suggesting that the human isolates represent a mixture of strains immediately derived from multiple other sources. Higher occurrence of certain *Salmonella* Typhimurium subtypes in human cases, therefore, more likely results from their prevalent circulation in foods and the environment, as observed in G7, than from elevated infectivity or virulence.

The known zoonotic hosts and reservoirs of *Salmonella* Typhimurium appeared to be highly attributable. When the classifier was precise about a BPSW origin, 91.6% of isolates were correctly predicted. A narrow coverage of livestock isolate diversity in the United States could skew prediction accuracy. This scenario was countered by the inclusion of isolates from major US *Salmonella* Typhimurium outbreaks of livestock origins over 15 years, most of which our classifier correctly predicted. Furthermore, livestock populations of *Salmonella* Typhimurium appeared to be more clonal than human isolates (Figure 1, panel A), possibly in association with industrialized livestock production.

Our classifier performed genomewide, high-resolution interrogations of genetic features, including not only accessory genes as previously reported (*31*,*32*) but also core genome mutations, such as SNPs and indels. This approach led to the discovery of a point mutation in *fliC* that outperformed all the other features in source prediction. *fliC* encodes the filament portion of the bacterial flagella, flagellin. Flagellin shows substantial antigenic diversity across *Salmonella* that has been exploited for *Salmonella* serotyping. It remains unclear whether the 2 different FliC proteins we discovered have different biologic properties that might correlate to zoonotic source. Our demonstration that a few key genetic features were sufficient for robust source prediction paves the way for developing efficient source attribution models scalable to large and expanding volumes of WGS data, which in turn is likely to improve the training and performance of the RF classifier.

Our classifier and pilot source attribution study based on the current training set is limited to predicting major livestock sources of *Salmonella* Typhimurium. Fewer than one third (31.9%) of human isolates were precisely attributed to a BPSW source, indicating additional sources of human salmonellosis underrepresented

by the current training set. Continuing accumulation of *Salmonella* Typhimurium genomes from environmental sources might be expected to lead to the identification of additional source classes to enable source attribution of more human clinical isolates using the machine-learning approach and could potentially help generate source hypotheses for outbreak investigation. Regular update of the training set is required for incremental improvement of the classifier, particularly for tracking new and emerging strains.

Another limitation is related to the ability of certain *Salmonella* Typhimurium isolates to circulate among multiple sources, which challenges precise source prediction. For example, source prediction of BPSW isolates in the diverse-source G7 lineage was lower at 64.2% than the out-of-bag prediction accuracy at 82.9% of all BPSW isolates. Nevertheless, G7 isolates from the 2009 turkey pot pie–associated outbreak and the 2013 live poultry–associated outbreak were attributed to poultry. These successful attributions were most likely due to the inclusion of other G7 poultry isolates in the training set that informed the classifier. Growing availability of training genomes in generalist lineages may reveal fine-scale clustering of *Salmonella* Typhimurium isolates by source to help source prediction.

Finally, transmission of *Salmonella* from a zoonotic source to a nonanimal food vehicle is possible. For example, domesticated and wild animals can cause *Salmonella* contamination of irrigation water, which may subsequently contaminate fresh produce (*33*). Two G7 outbreaks with precise source predictions were linked to fresh produce, the 2010–2011 multistate alfalfa sprout–associated outbreak and the 2012 multistate cantaloupe-associated outbreak. In both cases, the outbreak isolates were attributed to poultry. Although the findings cannot be confirmed, our study provides a potential new tool to help identify root sources of foodborne *Salmonella* Typhimurium outbreaks.

Acknowledgments

We are grateful to Nadejda Lupolova and David Gally for sharing *Salmonella* genomes from their study.

About the Author

Dr. Zhang is a postdoctoral fellow at the Center for Food Safety, University of Georgia. His primary research interests include bioinformatics and genomic epidemiology of *Salmonella*.

References

1. Scallan E, Hoekstra RM, Angulo FJ, Tauxe RV, Widdowson MA, Roy SL, et al. Foodborne illness acquired in the United States—major pathogens. Emerg Infect Dis. 2011;17:7–15. http://dx.doi.org/10.3201/eid1701.P11101
2. Hoffmann S, Maculloch B, Batz M. Economic burden of major foodborne illnesses acquired in the United States [cited 2018 Oct 8]. https://www.ers.usda.gov/webdocs/publications/43984/52807_eib140.pdf
3. Hendriksen RS, Vieira AR, Karlsmose S, Lo Fo Wong DM, Jensen AB, Wegener HC, et al. Global monitoring of *Salmonella* serovar distribution from the World Health Organization Global Foodborne Infections Network Country Data Bank: results of quality assured laboratories from 2001 to 2007. Foodborne Pathog Dis. 2011;8:887–900. http://dx.doi.org/10.1089/fpd.2010.0787
4. Rabsch W, Andrews HL, Kingsley RA, Prager R, Tschäpe H, Adams LG, et al. *Salmonella enterica* serotype Typhimurium and its host-adapted variants. Infect Immun. 2002;70:2249–55. http://dx.doi.org/10.1128/IAI.70.5.2249-2255.2002
5. Helms M, Ethelberg S, Mølbak K; DT104 Study Group. International *Salmonella* Typhimurium DT104 infections, 1992–2001. Emerg Infect Dis. 2005;11:859–67. http://dx.doi.org/10.3201/eid1106.041017
6. Okoro CK, Kingsley RA, Connor TR, Harris SR, Parry CM, Al-Mashhadani MN, et al. Intracontinental spread of human invasive *Salmonella* Typhimurium pathovariants in sub-Saharan Africa. Nat Genet. 2012;44:1215–21. http://dx.doi.org/10.1038/ng.2423
7. Graham SM. Nontyphoidal salmonellosis in Africa. Curr Opin Infect Dis. 2010;23:409–14. http://dx.doi.org/10.1097/QCO.0b013e32833dd25d
8. Yue M, Han X, De Masi L, Zhu C, Ma X, Zhang J, et al. Allelic variation contributes to bacterial host specificity. Nat Commun. 2015;6:8754. http://dx.doi.org/10.1038/ncomms9754
9. Chaudhuri RR, Morgan E, Peters SE, Pleasance SJ, Hudson DL, Davies HM, et al. Comprehensive assignment of roles for *Salmonella* Typhimurium genes in intestinal colonization of food-producing animals. PLoS Genet. 2013;9:e1003456. http://dx.doi.org/10.1371/journal.pgen.1003456
10. Pires SM, Evers EG, van Pelt W, Ayers T, Scallan E, Angulo FJ, et al.; Med-Vet-Net Workpackage 28 Working Group. Attributing the human disease burden of foodborne infections to specific sources. Foodborne Pathog Dis. 2009;6:417–24. http://dx.doi.org/10.1089/fpd.2008.0208
11. Hald T, Vose D, Wegener HC, Koupeev T. A Bayesian approach to quantify the contribution of animal-food sources to human salmonellosis. Risk Anal. 2004;24:255–69. http://dx.doi.org/10.1111/j.0272-4332.2004.00427.x
12. Barco L, Barrucci F, Olsen JE, Ricci A. *Salmonella* source attribution based on microbial subtyping. Int J Food Microbiol. 2013;163:193–203. http://dx.doi.org/10.1016/j.ijfoodmicro.2013.03.005
13. Swaminathan B, Barrett TJ, Hunter SB, Tauxe RV; CDC PulseNet Task Force. PulseNet: the molecular subtyping network for foodborne bacterial disease surveillance, United States. Emerg Infect Dis. 2001;7:382–9. http://dx.doi.org/10.3201/eid0703.017303
14. Allard MW, Strain E, Melka D, Bunning K, Musser SM, Brown EW, et al. Practical value of food pathogen traceability through building a whole-genome sequencing network and database. J Clin Microbiol. 2016;54:1975–83. http://dx.doi.org/10.1128/JCM.00081-16
15. Zhang S, Yin Y, Jones MB, Zhang Z, Deatherage Kaiser BL, Dinsmore BA, et al. *Salmonella* serotype determination utilizing high-throughput genome sequencing data. J Clin Microbiol. 2015;53:1685–92. http://dx.doi.org/10.1128/JCM.00323-15
16. Chaudhuri RR, Morgan E, Peters SE, Pleasance SJ, Hudson DL, Davies HM, et al. Comprehensive assignment of roles for *Salmonella* typhimurium genes in intestinal colonization of food-producing animals. PLoS Genet. 2013;9:e1003456. http://dx.doi.org/10.1371/journal.pgen.1003456

17. Gupta A, Matsui K, Lo JF, Silver S. Molecular basis for resistance to silver cations in *Salmonella.* Nat Med. 1999;5:183–8. http://dx.doi.org/10.1038/5545
18. Franke S, Grass G, Rensing C, Nies DH. Molecular analysis of the copper-transporting efflux system CusCFBA of *Escherichia coli.* J Bacteriol. 2003;185:3804–12. http://dx.doi.org/10.1128/JB.185.13.3804-3812.2003
19. Tsolis RM, Townsend SM, Miao EA, Miller SI, Ficht TA, Adams LG, et al. Identification of a putative *Salmonella enterica* serotype typhimurium host range factor with homology to IpaH and YopM by signature-tagged mutagenesis. Infect Immun. 1999;67:6385–93.
20. Henry T, Couillault C, Rockenfeller P, Boucrot E, Dumont A, Schroeder N, et al. The *Salmonella* effector protein PipB2 is a linker for kinesin-1. Proc Natl Acad Sci U S A. 2006;103:13497–502. http://dx.doi.org/10.1073/pnas.0605443103
21. Smirnov A, Förstner KU, Holmqvist E, Otto A, Günster R, Becher D, et al. Grad-seq guides the discovery of ProQ as a major small RNA-binding protein. Proc Natl Acad Sci U S A. 2016;113:11591–6. http://dx.doi.org/10.1073/pnas.1609981113
22. Grabe GJ, Zhang Y, Przydacz M, Rolhion N, Yang Y, Pruneda JN, et al. The *Salmonella* effector SpvD Is a cysteine hydrolase with a serovar-specific polymorphism influencing catalytic activity, suppression of immune responses, and bacterial virulence. J Biol Chem. 2016;291:25853–63. http://dx.doi.org/10.1074/jbc.M116.752782
23. Lesnick ML, Reiner NE, Fierer J, Guiney DG. The *Salmonella* spvB virulence gene encodes an enzyme that ADP-ribosylates actin and destabilizes the cytoskeleton of eukaryotic cells. Mol Microbiol. 2001;39:1464–70. http://dx.doi.org/10.1046/j.1365-2958.2001.02360.x
24. Yazdankhah S, Rudi K, Bernhoft A. Zinc and copper in animal feed—development of resistance and co-resistance to antimicrobial agents in bacteria of animal origin. Microb Ecol Health Dis. 2014; 25:25.
25. Gupta A, Silver S. Silver as a biocide: will resistance become a problem? Nat Biotechnol. 1998;16:888. http://dx.doi.org/10.1038/nbt1098-888
26. Thomson NR, Clayton DJ, Windhorst D, Vernikos G, Davidson S, Churcher C, et al. Comparative genome analysis of *Salmonella* Enteritidis PT4 and *Salmonella* Gallinarum 287/91 provides insights into evolutionary and host adaptation pathways. Genome Res. 2008;18:1624–37. http://dx.doi.org/10.1101/gr.077404.108
27. Holt KE, Thomson NR, Wain J, Langridge GC, Hasan R, Bhutta ZA, et al. Pseudogene accumulation in the evolutionary histories of *Salmonella enterica* serovars Paratyphi A and Typhi. BMC Genomics. 2009;10:36. http://dx.doi.org/10.1186/1471-2164-10-36
28. Langridge GC, Fookes M, Connor TR, Feltwell T, Feasey N, Parsons BN, et al. Patterns of genome evolution that have accompanied host adaptation in *Salmonella.* Proc Natl Acad Sci U S A. 2015;112:863–8. http://dx.doi.org/10.1073/pnas.1416707112
29. Feasey NA, Hadfield J, Keddy KH, Dallman TJ, Jacobs J, Deng X, et al. Distinct *Salmonella* Enteritidis lineages associated with enterocolitis in high-income settings and invasive disease in low-income settings. Nat Genet. 2016;48:1211–7.http://dx.doi.org/10.1038/ng.3644
30. Deng X, Desai PT, den Bakker HC, Mikoleit M, Tolar B, Trees E, et al. Genomic epidemiology of *Salmonella enterica* serotype Enteritidis based on population structure of prevalent lineages. Emerg Infect Dis. 2014;20:1481–9. http://dx.doi.org/10.3201/eid2009.131095
31. Lupolova N, Dallman TJ, Matthews L, Bono JL, Gally DL. Support vector machine applied to predict the zoonotic potential of *E. coli* O157 cattle isolates. Proc Natl Acad Sci U S A. 2016;113:11312–7. http://dx.doi.org/10.1073/pnas.1606567113
32. Lupolova N, Dallman TJ, Holden NJ, Gally DL. Patchy promiscuity: machine learning applied to predict the host specificity of *Salmonella enterica* and *Escherichia coli.* Microb Genom. 2017;3:e000135. http://dx.doi.org/10.1099/mgen.0.000135
33. Hanning IB, Nutt JD, Ricke SC. Salmonellosis outbreaks in the United States due to fresh produce: sources and potential intervention measures. Foodborne Pathog Dis. 2009;6:635–48. http://dx.doi.org/10.1089/fpd.2008.0232

Address for correspondence: Xiangyu Deng, University of Georgia, Center for Food Safety, 1109 Experiment St, Griffin, GA 30223, USA; email: xdeng@uga.edu

Multiple Introductions of Domestic Cat Feline Leukemia Virus in Endangered Florida Panthers[1]

Elliott S. Chiu, Simona Kraberger, Mark Cunningham, Lara Cusack, Melody Roelke, Sue VandeWoude

The endangered Florida panther (*Puma concolor coryi*) had an outbreak of infection with feline leukemia virus (FeLV) in the early 2000s that resulted in the deaths of 3 animals. A vaccination campaign was instituted during 2003–2007 and no additional cases were recorded until 2010. During 2010–2016, six additional FeLV cases were documented. We characterized FeLV genomes isolated from Florida panthers from both outbreaks and compared them with full-length genomes of FeLVs isolated from contemporary Florida domestic cats. Phylogenetic analyses identified at least 2 circulating FeLV strains in panthers, which represent separate introductions from domestic cats. The original FeLV virus outbreak strain is either still circulating or another domestic cat transmission event has occurred with a closely related variant. We also report a case of a cross-species transmission event of an oncogenic FeLV recombinant (FeLV-B). Evidence of multiple FeLV strains and detection of FeLV-B indicate Florida panthers are at high risk for FeLV infection.

Feline leukemia virus (FeLV) is a common pathogenic infectious disease responsible for high mortality rates for domestic cats, particularly before development of effective vaccines in the 1980s (*1*). Subgroup FeLV-A, which is replication competent and horizontally transmissible, is responsible for most infections (*1*,*2*). Other FeLV subgroups (B, C, D, E, and T) arose after recombination or through mutation (*3*). FeLV causes immunosuppressive, neoplastic, and hematopoietic disorders that correlate with FeLV subgroups (*4*–*6*). Virulent FeLV-B, the most common novel variant, arises after recombination between FeLV-A and endogenous FeLV (EnFeLV) present in the domestic cat genome and resulted in altered cellular tropism (*1*,*7*–*10*). Horizontal transmission of FeLV-B is rare in domestic cats and is believed to require co-transmission with FeLV-A as a helper virus because of its replication-defective nature (*11*,*12*).

FeLV prevalence in domestic cats is variable (prevalence range 3%–18%) (*13*–*16*). FeLV has the capacity to infect nondomestic species including jaguars, bobcats, the critically endangered Iberian lynx, and pumas, most notably the endangered puma subspecies, the Florida panther (*Puma concolor coryi*) (*17*–*21*). In all non-*Felis* spp. FeLV cases, the source was believed to be domestic cats, which serve as the dominant primary host. The genus *Felis* is the only taxon known to harbor enFeLV (*22*). The presence of FeLV genetic sequences in the germline results in recombination between exogenous FeLV and FeLV-A during domestic cat infections and in emergence of more deleterious subgroups (i.e., FeLV-B) that are not considered to be replication-competent in the absence of co-infection with FeLV-A (*12*). It is assumed that felids belonging to genera other than *Felis* are only infected with FeLV-A because they do not harbor enFeLV genomes.

Outbreaks of infection with FeLV have caused concern in endangered felids that have population bottlenecks because the species might be more vulnerable to infection because of reduced genetic diversity. For example, 21% of Iberian lynx sampled during 2003–2007 were FeLV positive; 6 died from FeLV-related disease (*23*). During 2001–2004, an outbreak of infection with FeLV was documented in Florida panthers (*19*). Ten Florida panthers were FeLV PCR positive, and 5 of these panthers were also determined to be antigen ELISA positive. Three deaths were attributed to FeLV-related disease (*19*,*24*). Phylogenetic analysis of a region of the FeLV *env* gene during this outbreak indicated a single circulating FeLV strain, likely following introduction of the virus from a domestic cat (*24*). The Florida Fish and Wildlife Conservation Commission (FFWCC; Tallahassee, FL, USA) attempted to contain the FeLV outbreak by implementing a vaccination campaign spanning 2003–2007 (*19*).

Author affiliations: Colorado State University, Fort Collins, Colorado, USA (E.S. Chiu, S. Kraberger, S. VandeWoude); Florida Fish and Wildlife Conservation Commission, Gainesville, Florida, USA (M. Cunningham, L. Cusack); National Institutes of Health, Bethesda, Maryland, USA (M. Roelke)

DOI: https://doi.org/10.3201/eid2501.181347

[1]Preliminary results from this study were presented at the Ecology and Evolution of Infectious Diseases Conference, June 24–27, 2017, Santa Barbara, California, USA.

During August 2004–November 2010, ≈125 live-captured or necropsied panthers were tested for FeLV, and no additional cases were detected (FFWCC, unpub. data). However, since December 2010, a total of 6 Florida panthers found dead were positive for FeLV antigenemia. These cases are separated in both time and space from the 2001–2004 outbreak (Figure 1). Four likely scenarios exist to explain the epidemic curve. First, absence of FeLV (2004–2010) might have resulted from complete eradication of the first outbreak virus, followed by introduction of another strain from domestic cats (Figure 2, panel A). Second, contemporary cases might have arisen from infection that persisted but was unrecognized for 6 years (Figure 2, panel B). Third, new cases may have resulted from a combination of scenarios 1 and 2 (Figure 2, panel C). Fourth, new cases might be explained by introduction of multiple strains (Figure 2, panel D).

In this study, we examined the genetic relatedness between new FeLV isolates and cases described before 2004 with 3 aims. First, we attempted to establish whether recent

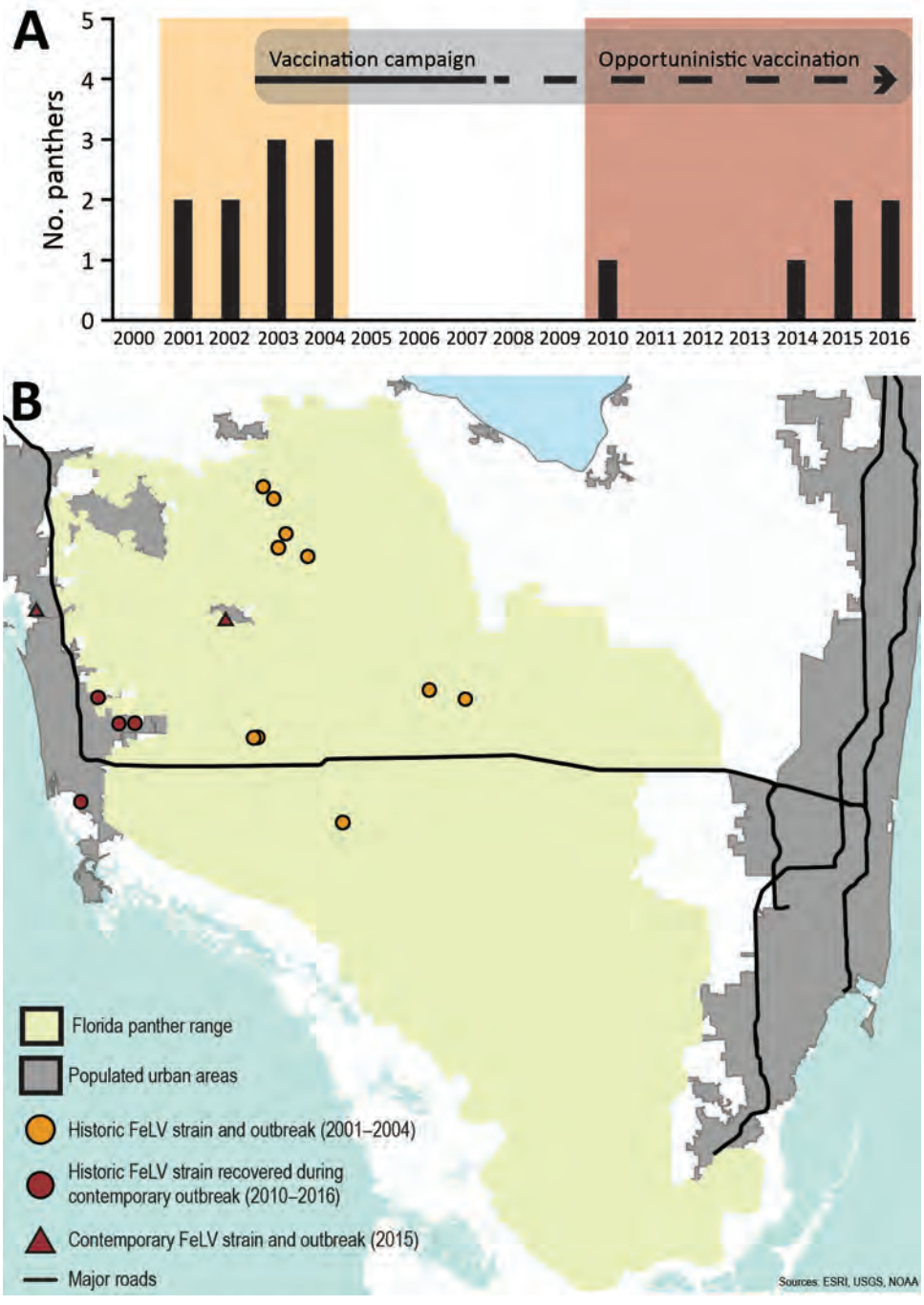

Figure 1. Temporally and spatially distinct FeLV cases in endangered Florida panthers, Florida, USA. A) Incidence of FeLV in live-caught and necropsied Florida panthers. Recaptured panthers are not represented. Different colors indicate first (yellow) and second (red) outbreak events. A vaccination campaign began in 2003 and efforts to actively vaccinate panthers continued until 2007; vaccination has continued opportunistically since the campaign. B) Distribution of historic and contemporary Florida panther FeLV cases in southern Florida. FeLV, feline leukemia virus.

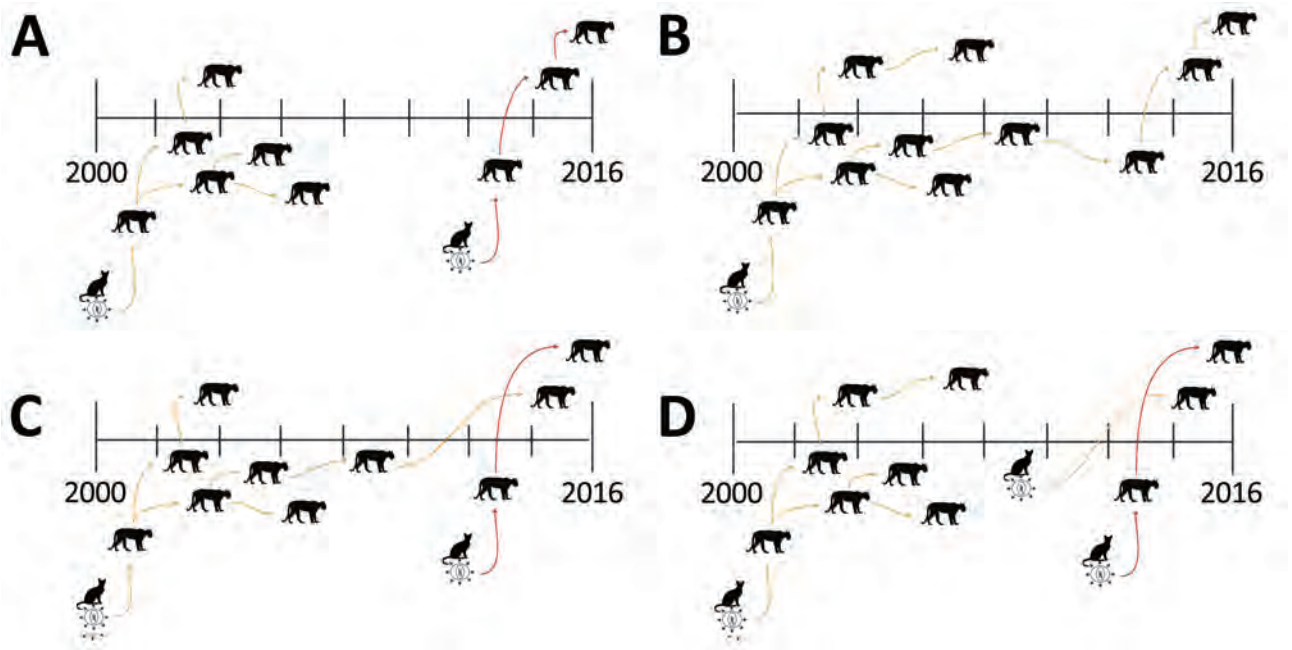

Figure 2. Hypotheses for feline leukemia virus outbreaks in Florida panthers, Florida, USA. A) Secondary infection; B) persistent transmission of 1 virus strain; C) combination of the 2 scenarios; D) multiple infections. Transmission of different virus strains is indicated by orange or red arrows.

cases represent a new outbreak or continuation of the prior infection. Second, we sought to determine the genetic relationship between Florida panther and Florida domestic cat FeLV strains. Third, we aimed to gain insights for pathogen–host interactions to better inform management practices and reduce risk for FeLV spillover from domestic cats to endangered felid populations.

Materials and Methods

Sample Collection and Processing

FFWCC routinely screens samples collected from Florida panthers for FeLV antigenemia and FIV antibodies by using commercially available test kits (SNAP Combo FeLV/FIV test; IDEXX Laboratories, https://www.idexx.com/en). Surveillance includes animals reported dead or those live captured as part of ongoing health monitoring and population management efforts. We calculated 95% CIs of prevalence for outbreak periods and the intervening quiescent period by using the Wilson score method without continuity correction (*25*).

During 2010–2016, six (2.8%) of the 214 Florida panthers (*P. concolor coryi* UCF149, UCFP 228, FP231, UCFP241, UCFP269, and UCFP275) (Table 1) reported dead to the FFWCC were positive for FeLV antigen during standard postmortem testing on heart, chest, or venous blood collected at necropsy. Lymphoid tissues from FeLV-positive and FeLV-negative controls (i.e., bone marrow, lymph node, spleen, and thymus) in addition to a fibroblast tissue culture from 1 panther (UCFP241R1) were harvested in Florida, stored at –80°C, and shipped to the Feline Retrovirus Research Laboratory at Colorado State University for additional testing.

We isolated genomic DNA from tissues by using bead-beater disruption and phenol-chloroform extraction adapted from Fan and Gulley (*26*). We extracted ≈100 mg of each tissue by using 1.4-mm ceramic spheres in a Fastprep-24 tissue homogenizer (MP Biomedicals Inc., https://www.mpbio.com). Sodium dodecyl sulfate (3 mol/L) was added to the tissue homogenates at a final concentration of 10% and incubated at 37°C overnight. Cell lysates were washed twice with phenol-chloroform. Extracted DNA was concentrated by ethanol precipitation, pelleted, dried, and resuspended in TE buffer.

In addition to tissues from the contemporary outbreak, we analyzed DNA from 3 historically infected (2002–2004; FFWCC) FeLV-infected Florida panthers (FP115, FP122, and FP132), and 4 domestic cats from Florida (x1608, x1613, x2653, and x2655) collected during 2008–2018 for FeLV genomes (Table 1). Florida panther samples were obtained as described (*19*). Domestic cat samples were remnants of archival samples from animals brought to shelters (*27*) or provided by veterinary clinics to FFWCC. An additional FeLV-positive DNA blood sample obtained from a domestic cat (x2512) was included for analysis in this study (Table 1) (*28*).

Table 1. Characteristics for Florida panthers tested for FeLV and virus genomes sequenced*

Field sample ID	Laboratory sample ID	Host species	Collection date	State	Full genome	Partial regions (LTR-gag, gag, and env)	GenBank accession nos.
FP115	x1755	*Puma concolor coryi*	2002 Nov 26	FL	No	Yes	MG020270–2
FP122	x1948	*P. concolor coryi*	2004 Jan 30	FL	Yes	Yes	MF681672
FP132	x1955	*P. concolor coryi*	2004 Mar 17	FL	No	Yes (3,688–8,396 nt)	MG020273
UCFP149	x2004	*P. concolor coryi*	2013 Dec 10	FL	Yes	Yes	MF681665
	x2004R1†				Yes	Yes	MF681666
UCFP228	x2271	*P. concolor coryi*	2014 Dec 28	FL	No	Yes	MF681676–678
UCFP231	x2270	*P. concolor coryi*	2015 Jan 20	FL	Yes	Yes	MF681667
UCFP241	x2272	*P. concolor coryi*	2015 Apr 30	FL	Yes	Yes	MF681668 and MF681671 (FeLV-B)
UCFP269	x2274	*P. concolor coryi*	2016 Feb 18	FL	No	Yes	MF681679–682, 2 *env* genotypes from 1 sample
UCFP275	x2273	*P. concolor coryi*	2016 Apr 6	FL	Yes	Yes	MF681669
517278	x1608	*Felis catus*	2011 Nov 10	FL	No	Yes	MF681673–675
517453	x1613	*F. catus*	2011 Nov 10	FL	Yes	Yes	MF681664
BDX387	x2512	*F. catus*	2015 Jul 3	MD	Yes	Yes	MF681670
	x2653	*F. catus*	2018 Jan 6	FL	Yes	Yes	MH116004
	x2655	*F. catus*	2018 Jan 31	FL	Yes	Yes	MH116005

*FeLV, feline leukemia virus; FP, Florida panther; ID, identification; UCFP, uncollared FP.
†Recaptured puma.

FeLV Genome Recovery and Analyses

We sequenced full FeLV proviral genomes (8,448 bp) from 4 domestic cats (1 from Maryland and 3 from Florida), 4 of 6 contemporary Florida panthers (2010–2016), and 1 historic Florida panther (2001–2004) (Table 1). We generated two 5-kb fragments spanning the ≈8.4-kb genome, which were overlapped 1.5 kb. PCRs contained 500 nmol/L of each primer, HiFi Kapa polymerase (Kapa Biosystems, https://www.kapabiosystems.com/region-selector), 50 200 ng of DNA template, and PCR primers (Table 2) and operated under various cycling conditions. We confirmed FeLV status in our laboratory by using FeLV-PCR and antigen ELISA tests and established protocols (*28*,*29*).

We extracted PCR products after electrophoresis from a 0.7% agarose gel, purified them by using a MEGAquick-spin Total Fragment DNA Purification Kit (iNtRON Biotechnology, http://jhscience.com/index.php?manufacturers_id=1), and cloned them into a pJET 1.2 blunt vector by using the CloneJET PCR Cloning Kit (Thermo Fisher Scientific, https://www.thermofisher.com/us/en/home.html). We transformed plasmids into XL1-Blue *E. coli* competent cells (Agilent, https://www.agilent.com). Positive clones were prepared by using DNA-Spin Plasmid Purification Kit

Table 2. Primer sequences used for PCR testing of each species and locus for FeLV*

Region	Sequence, 5′ → 3′	Species	Cycling conditions or reference
Full genome (first half)			95°C for 3 min; 30 cycles at 98°C for 20 s; 60°C for 15 s; 72°C for 2 min 40 s; 72°C for 2 min 40 s
Forward	TGAAAGACCCCCTACCCCAAAATTTAGCC	*Puma concolor coryi/Felis catus*	
Reverse	GCGGGTCCATTATCTGAACCCAATACC	*P. concolor coryi/F. catus*	
Full genome (second half)			
Forward	GAGTTCCTTGGAACTGCAGGTTACTGCC	*P. concolor coryi/F. catus*	
Reverse	TGAAAGACCCCTGAACTAGGTCTTCCTCG	*P. concolor coryi*	
Reverse 2	GCTGGCAGTGGCCTTGAAACTTCTG	*F. catus*	
FeLV-B *env*			(*28*)
Forward	CAGATCAGGAACCATTCCCAGG	*P. concolor coryi*	
Reverse	CCTCTAACTTCCTTGTATCTCATGG	*P. concolor coryi*	
LTR-*gag*			95°C for 3 min; 30 cycles at 98°C for 20 s; 60°C for 15 s; 72°C for 15 s; 72°C for 30 s
Forward	CGCAACCCTGGAAGACGTTCCA	*P. concolor coryi/F. catus*	
Reverse	TCGTCTCCGATCAACACCCTGTATTCA	*P. concolor coryi/F. catus*	
gag			
Forward	GGACCTTATGGACACCCCGACCAA	*P. concolor coryi/F. catus*	
Reverse	GGAGGGGGTAGGAACGGACGAA	*P. concolor coryi/F. catus*	
env			
Forward	CCTTTTACGTCTGCCCAGGGCAT	*P. concolor coryi/F. catus*	
Reverse	TTCCACCAAGCTTCTCCTGTGGTCT	*P. concolor coryi/F. catus*	

*The first half-genome primer set for FeLV sequencing (F/5.2R) spanning 5′-LTR/3′-pol was the same for the FeLV-positive Florida panthers and domestic cats. Reverse half-genome primers were designed to avoid amplification of domestic cat enFeLV and therefore differed for Florida panthers and domestic cats. FeLV, feline leukemia virus.

(iNtRON Biotechnology) and plasmids. Sanger sequencing used primer walking (Quintarabio, https://www.quintarabio.com). Chromatograms were verified visually to ensure that bases were scored correctly. Full genomes were assembled by using de novo assembly in Geneious version 7.0.6 (https://www.geneious.com).

Because of sample autolysis, full FeLV genomes from 4 panthers (2 contemporary, UCFP228 and UCFP269, and 2 historic, FP115 and FP132) and 1 domestic cat from Florida (x1608) were not recoverable. Partial genome sequencing was performed by using 3 fragments in the *gag* and *env* genes (Table 1). We developed forward and reverse primers to sequence a 115-bp long terminal repeat (LTR)–*gag* fragment, a 98-bp *gag* fragment, and a 121-bp *env* fragment (Table 2).

FeLV-B Screening Assay

Sequence analysis of FeLV Florida panther UCFP241 full genomes identified FeLV-B. Using FeLV-A, FeLV-B, and enFeLV sequences in GenBank (*30*), we designed a specific FeLV-B PCR and used it to screen all panther samples for FeLV-B (*28*).

Phylogenetic Analysis

We analyzed full-genome and partial *env* (1–1,294 nt) sequence datasets separately. We compared Florida panther FeLV (FeLV-Pco) and domestic cat FeLV (FeLV-Fca) sequence identity by using the SDTv1.2 nt pairwise comparison tool (*31*). A partial *env* tree was drawn to include as many GenBank FeLV sequences as possible. We aligned the 3 datasets (full genome, concatenated partial genome [3 small segments within the LTR-*gag*, *gag*, and *env* regions from FP115, UCFP228, and UCFP269], and x1608 along with those comparable regions from the FeLV full genomes available, and *env*) by using MUSCLE in MEGA version 5.3 (https://www.megasoftware.net) and manually checked open-reading frames (*32*,*33*).

To investigate phylogeny, we constructed a midpoint-rooted maximum-likelihood nucleotide tree for the full genome and concatenated partial dataset by using 1,000 bootstrap replicates. We determined best-fit substitution models by using jModelTest (*34*) in MEGA version 5.3 and phylogenetic trees constructed in PhyML implemented in SeaView4 (*35*) for the full-genome dataset TN93 + G model (*36*) and the concatenated partial sequencing nucleotide K2 + G model (*37*). A neighbor-joining tree constructed for the *env* dataset by using SeaView4 with a Jukes-Cantor substitution model was rooted with enFeLV and FeLV-B *env* genetic sequences (*38*).

Recombination was not removed from *env* sequences before constructing the tree to clearly demonstrate the phylogenetic relationship of FeLV-B in relation to enFeLV and FeLV-A. For all phylogenetic trees, branches with support <60% were collapsed. Full genomes from UCFP149, UCFP149R1, UCFP231, UCFP275, x1613, and partial sequences (LTR-*gag*, *gag*, and *env*) from FP115, FP132 (3,688 to 8,396 nt), UCFP228, UCFP269, and x1608 are available in GenBank (*30*) (Table 1). Pairwise identity of full genomes were compared for FeLV-Pco, FeLV-Fca, and FeLV-B (GenBank accession nos. JF957361 and JF957363; isolated in the United Kingdom) by using Sequence Demarcation Tool version 1.2 (*31*).

Results

FeLV Diagnosis and Case Attributes

We determined prevalence and 95% CIs for FeLV diagnosed in Florida panthers during 3 periods (Table 3). FeLV was first detected in the Florida panther in 2001 (*19*,*39*). This outbreak affected panthers residing mainly in protected areas in Florida (Figure 1), including Florida Panther National Wildlife Refuge, Big Cypress Swamp, and Okaloacoochee Slough State Forest (*24*). During 2001–2004, ≈131 animals were tested for FeLV, and 5 (3.82%) were found to be FeLV antigen positive (*19*). During 2004–2010, ≈125 animals were negative. The first FeLV case in Florida panthers after the initial outbreak was documented in a road-killed panther in December 2010. During 2014–2016, five additional FeLV-positive free-ranging Florida panthers were identified west of the historic outbreak in more populated areas (Figure 1, panel B). One of these panthers (UCFP231) might have died from infection with FeLV. Cause of death for the other 5 panthers was collision with a vehicle. Contemporary cases identified during 2010–2016 (6 of 184) primarily represented animals hit by vehicles in human populated areas (Figure 1). Prevalence (3.26%) was similar to prevalence during 2001–2004 (Table 3). Lymphadenopathy was documented in 2 of 6 animals (UCFP149, UCFP275). Animal UCFP149 had a linear stomach ulcer. The other animals were too autolyzed to identify gross abnormalities. Confirmatory FeLV PCR and antigen ELISAs reestablished positive and negative diagnoses for the contemporary outbreak.

Identification of Recombinant Subgroup FeLV-B

A clone sequenced from sample UCFP241 was identified as the recombinant subgroup FeLV-B. An *env* alignment

Table 3. Detection of 2 outbreaks of FeLV infection in Florida panthers*

Time frame	No. positive animals/no. tested	Prevalence, % (95% CI)
2001–2004	5/31	3.82 (1.64–8.62)
2004–2010	0/125	0 (0–2.98)
2010–2016	6/184	3.26 (1.50–6.93)

*Values are for historic and contemporary FeLV cases. Animals were tested by using a commercially available test that detects FeLV antigenemia. Animals tested before 2001 were uniformly negative. FeLV, feline leukemia virus.

of FeLV-Pco, FeLV-Fca, and enFeLV (Appendix Figure 1, https://wwwnc.cdc.gov/EID/article/25/1/18-1347-App1.pdf) confirmed an infection of FeLV-B resulting from a previously reported recombination event between FeLV-A and enFeLV. Multiple clones were sequenced to confirm presence of FeLV-B. All other Florida panther samples were screened for FeLV-B by PCR (*28*) but were negative.

Pairwise Comparison and Phylogenetic Analysis

FeLV-Pco showed ≈75% identity at the nucleotide level with published FeLV-Fca and ≈94%–98% identity at the nucleotide level with FeLV isolated from domestic cats in Florida (x1613, x2653, and x2655). The Florida panther FeLV-B full genome sequenced from x2272 showed ≈75% identity with sequenced FeLV-B and 95%–97% identity with FeLV-Pco subgroup A viruses (Appendix Figure 2).

Full-Genome Phylogeny

The maximum-likelihood tree of full FeLV-Pco and FeLV-Fca genomes documents 2 monophyletic lineages: a lineage composed of FeLV isolates from Florida (FeLV-Fca and FeLV-Pco) and a lineage composed of published FeLV-Fca isolates from other geographically distinct locations in the United Kingdom and the United States. FeLV-Fca isolate (x2655) from Florida groups basal to the 2 FeLV-Pco clades but within the larger Florida FeLV lineage. FeLV-Fca isolate x1613 is basal to the clade that includes all historic and related contemporary isolates. FeLV-Fca isolate x2512 was recovered as part of this study originating from Maryland and groups with FeLV-Fca isolate x2653 as part of a relatively homogeneous United States/United Kingdom clade (Figure 3, panel A).

FeLV-Pco isolates fall into ≥2 clades. Two isolates from the contemporary outbreak are monophyletic (UCFP231 and UCFP241) and are referred to as contemporary FeLV-Pco. The other FeLV-Pco clade contains 2 FeLV-Pco isolates from the contemporary outbreak (UCFP149 and UCFP275) and is most closely related to the historic FeLV-Pco isolate FP122; this group is referred to here as historic FeLV-Pco.

Partial Genotype Phylogeny

Partial genotyping FeLV-Pco sequences documented 10 single-nucleotide polymorphisms (SNPs) and a 9-nt insertion in the untranslated LTR-*gag* region, 3 SNPs in the *gag* region, and 8 SNPs in the *env* region. Phylogenetic analysis of the short concatenated sequence supported similar relationships established by full-genome nucleotide trees (Figure 3, panel B). An additional historic FeLV-Pco (FP115) is most related to other historic FeLV-Pco isolates. FeLV-Pco from a contemporary outbreak sample (UCFP228) also falls in the historic FeLV-Pco clade. Five clones sequenced from the *env* portion of FeLV-Pco UCFP269 showed 2 genotypes. Concatenated sequences from UCFP269 showed a paraphyletic relationship (Figure 3, panel B). Both isolates clustered outside the historic and contemporary FeLV-Pco strain clades (Figure 3, panel B). FeLV-Fca (x1608) groups within the major Florida FeLV clade (Figure 3, panel B).

Phylogeny of env

Phylogenetic relationships established by full-genome and concatenated partial sequence trees were supported by the *env* neighbor-joining tree (Figure 4). The *env* phylogeny clearly shows differentiation between FeLV-A/

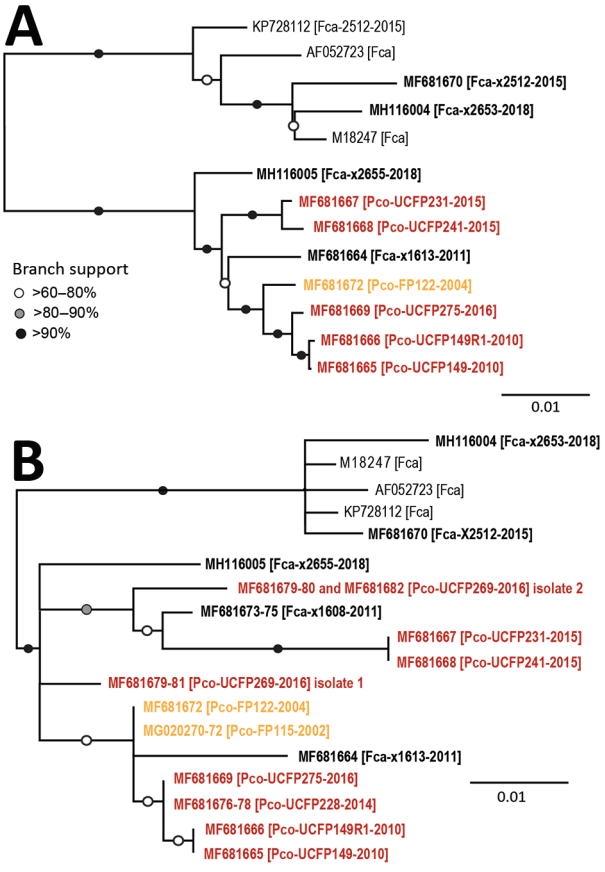

Figure 3. Maximum-likelihood phylogenetic trees showing 2 distinct FeLV-Pco clades in Florida panthers, Florida, USA. A) Full-genome phylogeny indicates Florida FeLV-A sequences are monophyletic. Historic and contemporary FeLV outbreak sequences reside in 1 clade, and a second clade consists solely of contemporary FeLV outbreak sequences. B) Genotyping sequence phylogeny generated from concatenating 3 regions of ≈100 bp (LTR-*gag*, *gag,* and *env*) compares full-genome isolates demonstrated in panel A in addition to 4 individual sequences. Black text indicates FeLV from domestic cats, orange indicates FeLV from panthers during the historic outbreak (2002–2004), and red indicates FeLV from panthers during the contemporary outbreak (2010–2016). Bold indicates isolates sequenced in this study. Scale bar indicates nucleotide substitutions per site.GenBank accession numbers are provided. FeLV, feline leukemia virus; LTR, long terminal repeat.

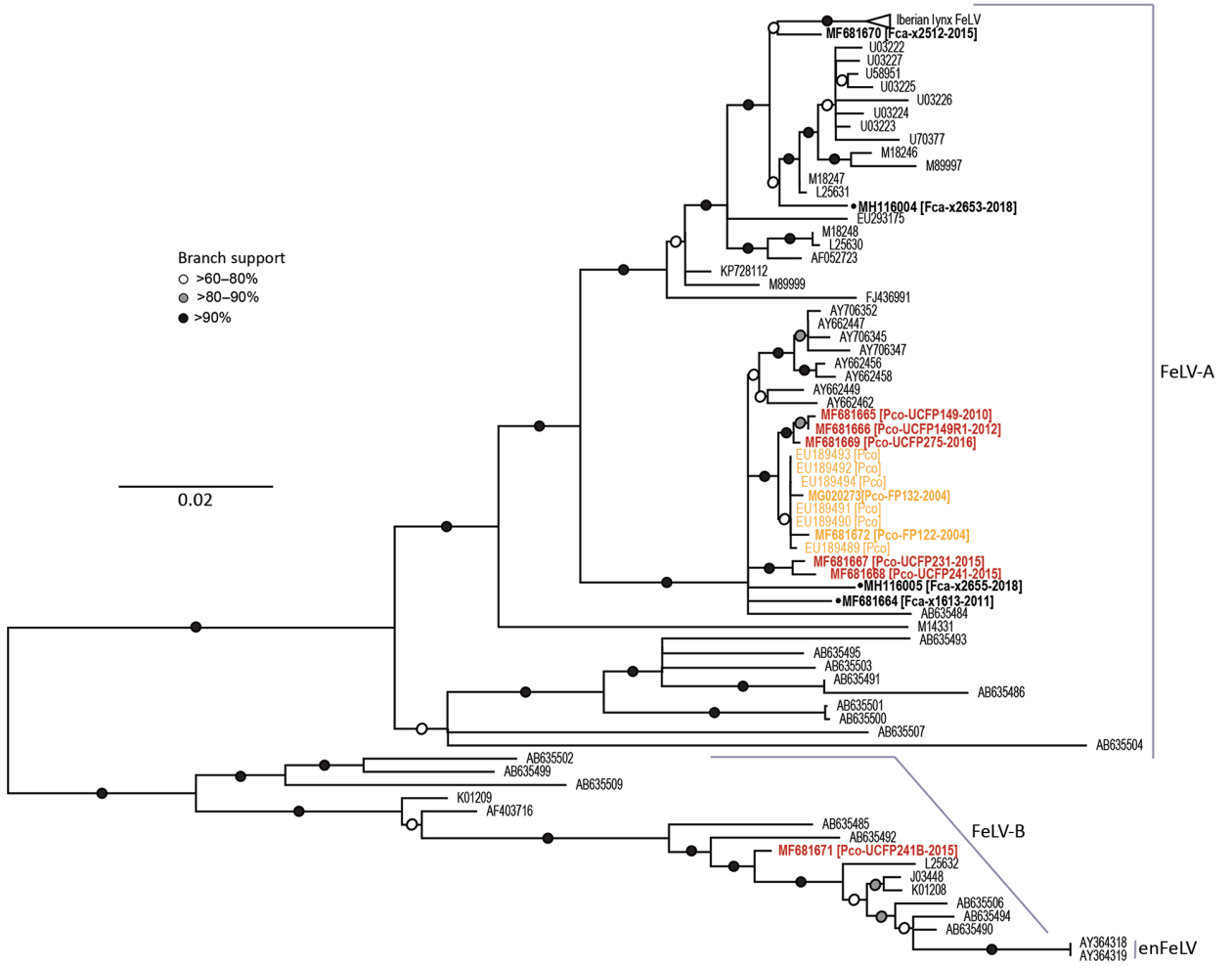

Figure 4. *Env* phylogenies support relationships established in the full-genome tree and document the Florida panther FeLV-B relationship to other known recombinant viruses in Florida panthers, Florida, USA. The *env* tree shows FeLV-A, FeLV-B, and enFeLV sequences (neighbor-joining analysis). One Florida panther sequence (MF681671) can be found in the FeLV-B cluster, identifying it as the recombinant subgroup. Black text indicates FeLV from domestic cats, orange indicates FeLV from panthers during the historic outbreak (2002–2004), and red indicates FeLV from panthers during the contemporary outbreak (2010–2016). Bold indicates isolates sequenced in this study. Scale bar indicates nucleotide substitutions per site. Black dots indicate sequences from domestic cats in Florida. GenBank accession numbers are provided. en, endogenous; FeLV, feline leukemia virus.

FeLV-B/enFeLV subgroups. FeLV-B and enFeLV subgroups clus,ter together, and FeLV-A remained a monophyletic group. All FeLV-Pco sequences detected during the historic outbreak are monophyletic (*24*). Two *env* sequences described in this study are closely related to previous sequences reported from the same animal. FP132, an isolate from a panther sample obtained in 2004, has 2 SNPs; FP122, also obtained in 2004, has 5 SNPs. FeLV-Pco sequences clustered into 2 clades, supporting previously identified relationships. One FeLV-Pco clone (UCFP241B) clusters in the FeLV-B clade.

Discussion

Two distinct FeLV outbreaks were recorded in the Florida panther population during 2001–2016 (Table 3). Phylogenetic data from both outbreaks document that FeLV-Pco resulted from initial spillover from domestic cats, presumably during a predatory event (*24*,*39*). Although FeLV prevalence in domestic cats is relatively low (≈4%) in Florida (*40*), it has been reported that domestic cats are ≈5% of the Florida panther diet (M. Cunningham et al., unpub. data). The relatively high number of domestic cats consumed, particularly in panther habitat proximal to human development, presents opportunities for FeLV spillover from cats to panthers (*40*).

Genomic analysis of contemporary FeLV-Pco identified 3 independent isolates (UCFP149, UCFP149R1, and UCFP275) that were genetically similar to historic FeLV-Pco (FP122; Figure 3, panel A). Analysis also detected FeLV in a paraphyletic clade that is similar to, but

distinct from, historic FeLV-Pco (>97% nt identity with FP122 (Appendix Figure 2). This genotype was detected in 2 panthers sampled in 2015 (UCFP231, UCFP241; Figure 3, panel A). A third FeLV strain might be present in contemporary samples and represented by partial FeLV sequences derived from 1 panther (UCFP269; Figure 3, panel B). Three Florida FeLV-Fca isolates (x1613, x2655, and x1608) clustered with Florida panther genotypes. One Florida FeLV-Fca (x2653) isolate was strongly divergent from other Florida FeLV-Fca isolates and resembled previously characterized FeLV-61E and domestic cat FeLV isolates from the United States and the United Kingdom. Movement of domestic cats by owners likely results in mixing of FeLV strains beyond geographic sites.

Full-genome and concatenated partial genome trees demonstrate that domestic cat FeLV strains are situated basal to FeLV-Pco, providing evidence of a domestic cat origin of the panther FeLV infections. Genetic distances between these Florida FeLV-Fca isolates and FeLV-Fca isolates from locations other than Florida indicate a more distant evolutionary relationship between domestic cat strains and Florida FeLV-Fca and FeLV-Pco strains (Figure 3). These findings suggest that minimal species adaptation is required for cross-species transmission between cats and panthers. Additional FeLV full-genome samples would enable a Bayesian ancestral reconstruction analysis to further resolve FeLV isolate ancestry.

Full-genome phylogenetic analysis supports the combination and hybrid panther FeLV reemergence hypotheses (Figure 2, panels C, D). Assuming that the Florida panther population was ≈300 animals during 2004–2010, sampling 125 of these animals with no FeLV detected provides a >95% CI that FeLV prevalence was ≤3%. Test results during both outbreak periods indicated an FeLV prevalence of ≈3%, which indicated that control measures initiated during the historic outbreak were successful in at least controlling, if not eliminating, additional panther FeLV infections for several years. Contemporary FeLV in Florida panthers was identified near human population centers where exposure to feral domestic cats would be more likely to occur (*41*). Although it is feasible that each contemporary case represented an individual exposure to a different domestic cat, panther-to-panther transmission cannot be excluded, particularly for cases that occurred around the same time and showed similar genotypes (i.e., UCFP231 and UCFP241 sampled in 2015; UCFP228 sampled in 2014; and UCFP275 sampled in 2016).

In addition to the common horizontally transmissible FeLV subgroup (FeLV-A), we recovered and sequenced an oncogenic FeLV subgroup (FeLV-B) from tissues from a contemporary Florida panther (UCFP241B; Figure 3, panel B; Appendix Figure 1). This subgroup is a recombinant of FeLV-A and enFeLV, an endogenous retrovirus harbored only by members of the genus *Felis*. Identification of FeLV-B infection in a Florida panther is only possible as a result of horizontal transmission of FeLV from a domestic cat because panthers lack enFeLV to support recombination (*22*). FeLV-B is common in domestic cats; recombination occurs in ≈33%–68% of cats infected with FeLV-A (*42*), presumably by independent recombination events that occur de novo after infection of domestic cats with FeLV-A.

FeLV-B horizontal transmission has been described only on 3 previous occasions (*43*). One study reported that FeLV-B was detected in a jaguar (*Panthera onca*); however, this analysis was based on a sequence amplified from a 232-bp region of the LTR (*12*,*21*). We have clearly documented a full FeLV-B genomic sequence in an endangered non-*Felis* cat species. This finding is of concern because FeLV-B is oncogenic and associated with increased illness and death in domestic cats (*6*,*44*,*45*). Because non-*Felis* cat species lack enFeLV, they might be more vulnerable to an adapted FeLV-B that is readily horizontally transmitted between animals. Thus, spillover of FeLV-B from domestic cats co-infected with this recombinant strain could represent a greater risk for vulnerable nondomestic cat populations.

Besides individual and population health effects, a potential outcome of FeLV infection in nondomestic felids is germline infection leading to endogenization. Early endogenization results in an infection in which the virus has yet to accumulate mutations rendering the endogenous retrovirus defective; therefore, at this stage, the virus might be passed horizontally to other animals (*46*). Early endogenization might result in decreased fitness, as exemplified by endogenization of koala endogenous retrovirus (*46*,*47*). Infection with this virus has also led to higher incidence of secondary infections, such as chlamydiosis and neoplasias (*48*). Therefore, FeLV infection of panthers and other non-*Felis* cat species is a greater concern for long-term population effects.

Our study demonstrated that even with efforts to control FeLV in an intensively managed population, FeLV remains a risk to Florida panthers, particularly for animals inhabiting areas near urban centers. Moss et al. reported that the proportion of diet consisting of domestic animals is increasing for Colorado pumas, which is concurrent with puma co-localization in human habitats (*49*). This trend is likely present in Florida.

This report highlights the need for continued surveillance of Florida panthers for exposure to FeLV as a major risk management strategy (*40*). Annual sampling of a proportion of the Florida panther population that is sufficient to detect an FeLV incidence of 3% with relative certainty and increased vaccination of panthers and domestic cats along sites of potential interaction are recommended measures to protect against future outbreaks.

Acknowledgments

We thank the field biologists and veterinarians at the Florida Fish and Wildlife Conservation Commission and National Park Service for their assistance with obtaining sample collections and Jenn Malmberg for helping create the map in this article.

This study was supported by the National Science Foundation–Ecology of Infectious Diseases (award no. 1413925) and the Office of the Director, National Institutes of Health (award nos. T32OD012201 and F30OD023386).

About the Author

Mr. Chiu is a doctor of veterinary medicine/PhD student at Colorado State University, Fort Collins, CO. His research interests include virology, disease ecology, and wildlife conservation medicine.

References

1. Willett BJ, Hosie MJ. Feline leukaemia virus: half a century since its discovery. Vet J. 2013;195:16–23. http://dx.doi.org/10.1016/j.tvjl.2012.07.004
2. Jarrett O, Russell PH. Differential growth and transmission in cats of feline leukaemia viruses of subgroups A and B. Int J Cancer. 1978;21:466–72. http://dx.doi.org/10.1002/ijc.2910210411
3. Chiu ES, Hoover EA, VandeWoude S. A retrospective examination of feline leukemia subgroup characterization: viral interference assays to deep sequencing. Viruses. 2018;10:E29. http://dx.doi.org/10.3390/v10010029
4. Mackey L, Jarrett W, Jarrett O, Laird H. Anemia associated with feline leukemia virus infection in cats. J Natl Cancer Inst. 1975;54:209–17. http://dx.doi.org/10.1093/jnci/54.1.209
5. Mullins JI, Hoover EA, Overbaugh J, Quackenbush SL, Donahue PR, Poss ML. FeLV-FAIDS-induced immunodeficiency syndrome in cats. Vet Immunol Immunopathol. 1989;21:25–37. http://dx.doi.org/10.1016/0165-2427(89)90127-X
6. Hartmann K. Clinical aspects of feline retroviruses: a review. Viruses. 2012;4:2684–710. http://dx.doi.org/10.3390/v4112684
7. Stewart MA, Warnock M, Wheeler A, Wilkie N, Mullins JI, Onions DE, et al. Nucleotide sequences of a feline leukemia virus subgroup A envelope gene and long terminal repeat and evidence for the recombinational origin of subgroup B viruses. J Virol. 1986;58:825–34.
8. O'Hara B, Johann SV, Klinger HP, Blair DG, Rubinson H, Dunn KJ, et al. Characterization of a human gene conferring sensitivity to infection by gibbon ape leukemia virus. Cell Growth Differ. 1990;1:119–27.
9. Takeuchi Y, Vile RG, Simpson G, O'Hara B, Collins MK, Weiss RA. Feline leukemia virus subgroup B uses the same cell surface receptor as gibbon ape leukemia virus. J Virol. 1992;66:1219–22.
10. Roy-Burman P. Endogenous env elements: partners in generation of pathogenic feline leukemia viruses. Virus Genes. 1995;11:147–61. http://dx.doi.org/10.1007/BF01728655
11. Hoover EA, Mullins JI. Feline leukemia virus infection and diseases. J Am Vet Med Assoc. 1991;199:1287–97.
12. Stewart H, Jarrett O, Hosie MJ, Willett BJ. Complete genome sequences of two feline leukemia virus subgroup B isolates with novel recombination sites. Genome Announc. 2013;1:e00036–12. http://dx.doi.org/10.1128/genomeA.00036-12
13. Yilmaz H, Ilgaz A, Harbour DA. Prevalence of FIV and FeLV infections in cats in Istanbul. J Feline Med Surg. 2000;2:69–70. http://dx.doi.org/10.1053/jfms.2000.0066
14. Muirden A. Prevalence of feline leukaemia virus and antibodies to feline immunodeficiency virus and feline coronavirus in stray cats sent to an RSPCA hospital. Vet Rec. 2002;150:621–5. http://dx.doi.org/10.1136/vr.150.20.621
15. Bandecchi P, Dell'Omodarme M, Magi M, Palamidessi A, Prati MC. Feline leukaemia virus (FeLV) and feline immunodeficiency virus infections in cats in the Pisa district of Tuscany, and attempts to control FeLV infection in a colony of domestic cats by vaccination. Vet Rec. 2006;158:555–7. http://dx.doi.org/10.1136/vr.158.16.555
16. Gleich SE, Krieger S, Hartmann K. Prevalence of feline immunodeficiency virus and feline leukaemia virus among client-owned cats and risk factors for infection in Germany. J Feline Med Surg. 2009;11:985–92. http://dx.doi.org/10.1016/j.jfms.2009.05.019
17. Sleeman JM, Keane JM, Johnson JS, Brown RJ, Woude SV. Feline leukemia virus in a captive bobcat. J Wildl Dis. 2001;37:194–200. http://dx.doi.org/10.7589/0090-3558-37.1.194
18. Luaces I, Doménech A, García-Montijano M, Collado VM, Sánchez C, Tejerizo JG, et al. Detection of feline leukemia virus in the endangered Iberian lynx (*Lynx pardinus*). J Vet Diagn Invest. 2008;20:381–5. http://dx.doi.org/10.1177/104063870802000325
19. Cunningham MW, Brown MA, Shindle DB, Terrell SP, Hayes KA, Ferree BC, et al. Epizootiology and management of feline leukemia virus in the Florida puma. J Wildl Dis. 2008;44:537–52. http://dx.doi.org/10.7589/0090-3558-44.3.537
20. Filoni C, Catão-Dias JL, Cattori V, Willi B, Meli ML, Corrêa SH, et al. Surveillance using serological and molecular methods for the detection of infectious agents in captive Brazilian neotropic and exotic felids. J Vet Diagn Invest. 2012;24:166–73. http://dx.doi.org/10.1177/1040638711407684
21. Silva CP, Onuma SS, de Aguiar DM, Dutra V, Nakazato L. Molecular detection of feline leukemia virus in free-ranging jaguars (*Panthera onca*) in the Pantanal region of Mato Grosso, Brazil. Braz J Infect Dis. 2016;20:316–7. http://dx.doi.org/10.1016/j.bjid.2016.01.005
22. Polani S, Roca AL, Rosensteel BB, Kolokotronis SO, Bar-Gal GK. Evolutionary dynamics of endogenous feline leukemia virus proliferation among species of the domestic cat lineage. Virology. 2010;405:397–407. http://dx.doi.org/10.1016/j.virol.2010.06.010
23. Meli ML, Cattori V, Martínez F, López G, Vargas A, Simón MA, et al. Feline leukemia virus and other pathogens as important threats to the survival of the critically endangered Iberian lynx (*Lynx pardinus*). PLoS One. 2009;4:e4744. http://dx.doi.org/10.1371/journal.pone.0004744
24. Brown MA, Cunningham MW, Roca AL, Troyer JL, Johnson WE, O'Brien SJ. Genetic characterization of feline leukemia virus from Florida panthers. Emerg Infect Dis. 2008;14:252–9. http://dx.doi.org/10.3201/eid1402.070981
25. Newcombe RG. Two-sided confidence intervals for the single proportion: comparison of seven methods. Stat Med. 1998;17:857–72. http://dx.doi.org/10.1002/(SICI)1097-0258(19980430)17:8<857::AID-SIM777>3.0.CO;2-E
26. Fan H, Gulley ML. DNA extraction from fresh or frozen tissues. In: Killeen AA, editor. Molecular pathology protocols. Totowa (NJ): Humana Press Inc.; 2001. p. 5–10.
27. Carver S, Bevins SN, Lappin MR, Boydston EE, Lyren LM, Alldredge M, et al. Pathogen exposure varies widely among sympatric populations of wild and domestic felids across the United States. Ecol Appl. 2016;26:367–81. http://dx.doi.org/10.1890/15-0445
28. Powers JA, Chiu ES, Kraberger SJ, Roelke-Parker M, Lowery I, Erbeck K, et al. Feline leukemia virus disease outcomes in a domestic cat breeding colony: relationship to endogenous FeLV and other chronic viral infections. J Virol. 2018;92:e00649-18. http://dx.doi.org/10.1128/JVI.00649-18

29. Chandhasin C, Coan PN, Pandrea I, Grant CK, Lobelle-Rich PA, Puetter A, et al. Unique long terminal repeat and surface glycoprotein gene sequences of feline leukemia virus as determinants of disease outcome. J Virol. 2005;79:5278–87. http://dx.doi.org/10.1128/JVI.79.9.5278-5287.2005
30. Benson DA, Cavanaugh M, Clark K, Karsch-Mizrachi I, Lipman DJ, Ostell J, et al. GenBank. Nucleic Acids Res. 2013;41 (Database issue):D36–42. http://dx.doi.org/10.1093/nar/gks1195
31. Muhire BM, Varsani A, Martin DP. SDT: a virus classification tool based on pairwise sequence alignment and identity calculation. PLoS One. 2014;9:e108277. http://dx.doi.org/10.1371/journal.pone.0108277
32. Edgar RC. MUSCLE: multiple sequence alignment with high accuracy and high throughput. Nucleic Acids Res. 2004;32:1792–7. http://dx.doi.org/10.1093/nar/gkh340
33. Tamura K, Peterson D, Peterson N, Stecher G, Nei M, Kumar S. MEGA5: molecular evolutionary genetics analysis using maximum likelihood, evolutionary distance, and maximum parsimony methods. Mol Biol Evol. 2011;28:2731–9. http://dx.doi.org/10.1093/molbev/msr121
34. Posada D. Selection of models of DNA evolution with jModelTest. Totowa (NJ): Humana Press Inc; 2009.
35. Guindon S, Dufayard J-F, Lefort V, Anisimova M, Hordijk W, Gascuel O. New algorithms and methods to estimate maximum-likelihood phylogenies: assessing the performance of PhyML 3.0. Syst Biol. 2010;59:307–21. http://dx.doi.org/10.1093/sysbio/syq010
36. Tavaré S. Some probabilistic and statistical problems in the analysis of DNA sequences. Lectures in Mathematics in the Life Sciences. 1986;17:57–86.
37. Kimura M. A simple method for estimating evolutionary rates of base substitutions through comparative studies of nucleotide sequences. J Mol Evol. 1980;16:111–20. http://dx.doi.org/10.1007/BF01731581
38. Jukes TH, Cantor CR. Evolution of protein molecules. New York: Academic Press; 1969.
39. Roelke ME, Forrester DJ, Jacobson ER, Kollias GV, Scott FW, Barr MC, et al. Seroprevalence of infectious disease agents in free-ranging Florida panthers (*Felis concolor coryi*). J Wildl Dis. 1993;29:36–49. http://dx.doi.org/10.7589/0090-3558-29.1.36
40. Lee IT, Levy JK, Gorman SP, Crawford PC, Slater MR. Prevalence of feline leukemia virus infection and serum antibodies against feline immunodeficiency virus in unowned free-roaming cats. J Am Vet Med Assoc. 2002;220:620–2. http://dx.doi.org/10.2460/javma.2002.220.620
41. Aguilar GD, Farnworth MJ. Distribution characteristics of unmanaged cat colonies over a 20 year period in Auckland, New Zealand. Applied Geography. 2013;37:160–7. http://dx.doi.org/10.1016/j.apgeog.2012.11.009
42. Jarrett O, Hardy WD Jr, Golder MC, Hay D. The frequency of occurrence of feline leukaemia virus subgroups in cats. Int J Cancer. 1978;21:334–7. http://dx.doi.org/10.1002/ijc.2910210314
43. Stewart H, Jarrett O, Hosie MJ, Willett BJ. Are endogenous feline leukemia viruses really endogenous? Vet Immunol Immunopathol. 2011;143:325–31. http://dx.doi.org/10.1016/j.vetimm.2011.06.011
44. Rojko JL, Olsen RG. The immunobiology of the feline leukemia virus. Vet Immunol Immunopathol. 1984;6:107–65. http://dx.doi.org/10.1016/0165-2427(84)90050-3
45. Tzavaras T, Stewart M, McDougall A, Fulton R, Testa N, Onions DE, et al. Molecular cloning and characterization of a defective recombinant feline leukaemia virus associated with myeloid leukaemia. J Gen Virol. 1990;71:343–54. http://dx.doi.org/ 10.1099/0022-1317-71-2-343
46. Löber U, Hobbs M, Dayaram A, Tsangaras K, Jones K, Alquezar-Planas DE, et al. Degradation and remobilization of endogenous retroviruses by recombination during the earliest stages of a germ-line invasion. Proc Natl Acad Sci U S A. 2018;115:8609–14. http://dx.doi.org/10.1073/pnas.1807598115
47. Ávila-Arcos MC, Ho SY, Ishida Y, Nikolaidis N, Tsangaras K, Hönig K, et al. One hundred twenty years of koala retrovirus evolution determined from museum skins. Mol Biol Evol. 2013;30:299–304. http://dx.doi.org/10.1093/molbev/mss223
48. Tarlinton R, Meers J, Hanger J, Young P. Real-time reverse transcriptase PCR for the endogenous koala retrovirus reveals an association between plasma viral load and neoplastic disease in koalas. J Gen Virol. 2005;86:783–7. http://dx.doi.org/10.1099/vir.0.80547-0
49. Moss WE, Alldredge MW, Logan KA, Pauli JN. Human expansion precipitates niche expansion for an opportunistic apex predator (*Puma concolor*). Sci Rep. 2016;6:39639. http://dx.doi.org/10.1038/srep39639

Address for correspondence: Sue VandeWoude, Department of Microbiology, Immunology, and Pathology, College of Veterinary Medicine and Biomedical Sciences, Colorado State University, 1619 Campus Delivery, Fort Collins, CO 80523, USA; email: sue.vandewoude@colostate.edu

Prescription of Antibacterial Drugs for HIV-Exposed, Uninfected Infants, Malawi, 2004–2010

Alexander C. Ewing, Nicole L. Davis, Dumbani Kayira, Mina C. Hosseinipour, Charles van der Horst, Denise J. Jamieson, Athena P. Kourtis, for the Breastfeeding, Antiretrovirals and Nutrition study team[1]

Medscape EDUCATION ACTIVITY

JOINTLY ACCREDITED PROVIDER™ INTERPROFESSIONAL CONTINUING EDUCATION

In support of improving patient care, this activity has been planned and implemented by Medscape, LLC and Emerging Infectious Diseases. Medscape, LLC is jointly accredited by the Accreditation Council for Continuing Medical Education (ACCME), the Accreditation Council for Pharmacy Education (ACPE), and the American Nurses Credentialing Center (ANCC), to provide continuing education for the healthcare team.

Medscape, LLC designates this Journal-based CME activity for a maximum of 1.00 ***AMA PRA Category 1 Credit(s)™***. Physicians should claim only the credit commensurate with the extent of their participation in the activity.

All other clinicians completing this activity will be issued a certificate of participation. To participate in this journal CME activity: (1) review the learning objectives and author disclosures; (2) study the education content; (3) take the post-test with a 75% minimum passing score and complete the evaluation at http://www.medscape.org/journal/eid; and (4) view/print certificate. For CME questions, see page 202.

Release date: December 12, 2018; Expiration date: December 12, 2019

Learning Objectives

Upon completion of this activity, participants will be able to:

- Assess antibiotic usage in the first year of life among 2,152 HIV-exposed, uninfected (HEU) infants who were breast-fed through 28 weeks of age, based on an analysis from the Breastfeeding, Antiretrovirals and Nutrition (BAN) Study
- Determine the factors associated with antibiotic usage in the first year of life among 2,152 HEU infants who were breast-fed through 28 weeks of age, based on an analysis from the BAN Study
- Evaluate the clinical implications of antibiotic usage in the first year of life among 2,152 HEU infants who were breast-fed through 28 weeks of age, based on an analysis from the BAN Study.

CME Editor

P. Lynne Stockton Taylor, VMD, MS, ELS(D), Technical Writer/Editor, Emerging Infectious Diseases. *Disclosure: P. Lynne Stockton Taylor, VMD, MS, ELS(D), has disclosed no relevant financial relationships.*

CME Author

Laurie Barclay, MD, freelance writer and reviewer, Medscape, LLC. *Disclosure: Laurie Barclay, MD, has disclosed the following relevant financial relationships: owns stock, stock options, or bonds from Pfizer.*

Authors

Disclosures: ***Alexander C. Ewing, MPH; Nicole L. Davis, MPH, PhD;Dumbani Kayira, MBBS, FC Paed(SA); Mina C. Hosseinipour, MD, MPH; Charles van der Horst, MD; Denise J. Jamieson, MD, MPH;*** *and* ***Athena P. Kourtis, MD, PhD,*** *have disclosed no relevant financial relationships.*

Author affiliations: Centers for Disease Control and Prevention, Atlanta, Georgia, USA (A.C. Ewing, N.L. Davis, D.J. Jamieson, A.P. Kourtis); University of North Carolina Project, Lilongwe, Malawi (D. Kayira); University of North Carolina, Chapel Hill, North Carolina, USA (M.C. Hosseinipour, C. van der Horst)

DOI: https://doi.org/10.3201/eid2501.180782

Antimicrobial drug resistance is a serious health hazard driven by overuse. Administration of antimicrobial drugs to HIV-exposed, uninfected infants, a population that is growing and at high risk for infection, is poorly studied. We therefore analyzed factors associated with antibacterial drug

[1]Team members are listed at the end of this article.

administration to HIV-exposed, uninfected infants during their first year of life. Our study population was 2,152 HIV-exposed, uninfected infants enrolled in the Breastfeeding, Antiretrovirals and Nutrition Study in Lilongwe, Malawi, during 2004–2010. All infants were breastfed through 28 weeks of age. Antibacterial drugs were prescribed frequently (to 80% of infants), and most (67%) of the 5,329 prescriptions were for respiratory indications. Most commonly prescribed were penicillins (43%) and sulfonamides (23%). Factors associated with lower hazard for antibacterial drug prescription included receipt of cotrimoxazole preventive therapy, receipt of antiretroviral drugs, and increased age. Thus, cotrimoxazole preventive therapy may lead to fewer prescriptions for antibacterial drugs for these infants.

The global rise of resistance to antibacterial drugs has resulted in longer illnesses, more deaths, and increased treatment costs (*1*–*4*). Although access to antibacterial drugs is more widespread in industrialized countries (*5*), low- and middle-income countries also experience the effects of antibacterial drug resistance and contribute to its spread (*6*). Because infants are more susceptible than adults to infectious diseases, antibacterial drug administration to infants is correspondingly higher (*7*,*8*). In sub-Saharan Africa, a growing population at especially high risk for infectious diseases is HIV-exposed, uninfected infants, many of whom breastfeed (*9*,*10*).

We studied the healthcare needs and the magnitude of antibacterial use in such populations in an underresourced setting. We used longitudinal data about antibacterial drug prescribing for HIV-exposed, uninfected infants in a large randomized controlled trial of use of maternal and infant antiretroviral therapy (ART) to prevent mother-to-child transmission of HIV during breastfeeding, conducted in Malawi during 2004–2010. Our main objectives were to describe prescriptions for antibacterial drugs for HIV-uninfected infants, in terms of frequency of prescriptions, types of drug prescribed, and clinical indications for use; and to identify factors associated with increased hazard for prescription of antibacterial drugs for this population.

Methods

Study Enrollment, Design, and Procedures

Infants were enrolled in the Breastfeeding, Antiretrovirals and Nutrition (BAN) randomized clinical trial in Lilongwe, Malawi, during March 2004–January 2010 (*11*,*12*). The study enrolled 2,369 HIV-infected pregnant women ≥14 years of age with CD4+ counts of ≥250 cells/μL (≥200 cells/μL before July 24, 2006) and their infants. Enrollment was limited to infants who weighed ≥2,000 g at birth and who had no condition precluding study interventions.

At the time of labor, all mothers received 1 dose (200 mg) of oral nevirapine followed by oral zidovudine (300 mg 2×/d) and lamivudine (150 mg 2×/d) for 7 days; their newborns received 1 dose of oral nevirapine (2 mg/kg bodyweight) and twice daily oral zidovudine (2 mg/kg bodyweight) and lamivudine (4 mg/kg) for 7 days. Using a factorial design, we randomly assigned eligible mother–infant pairs to receive or not receive a nutritional supplement while breastfeeding and to 1 of 3 ARV interventions to be initiated at birth and continued for 28 weeks or until breastfeeding cessation, if earlier. The ARV interventions were 1) daily nevirapine for the infant, 2) triple-drug ARV regimen for the mother, or 3) control (no treatment for mother or infant). According to a standardized protocol derived from the World Health Organization (WHO) Breastfeeding Counseling Training Manual (*13*), all mothers were individually counseled to breastfeed exclusively for the first 24 postpartum weeks and then wean rapidly during weeks 24–28. Because of overwhelming evidence of the intervention's effectiveness, we stopped enrolling participants in the control group after we had 668 mother–infant pairs in this group; those already enrolled were offered the choice to switch to either of the interventions.

During the BAN study, WHO and the Malawi Ministry of Health released updated guidelines for prophylaxis for HIV-infected mothers and HIV-exposed infants. To adhere to these guidelines, daily cotrimoxazole preventive therapy (CPT) was implemented for mothers (480 mg 2×/d) and infants (240 mg 1×/d) enrolled in the study as of June 13, 2006, and for all those enrolled afterward. Infants began CPT at their first study visit after 6 weeks of age and continued through 36 weeks of age or until weaning was complete and HIV infection was ruled out.

At 2, 6, 12, 18, 24, 28, 36, and 48 weeks, we collected data on anthropometrics, vital signs, illnesses and hospitalizations since the last visit, current symptoms, and physical examination findings. Participants were advised to return to the clinic (to which they had unlimited access) between visits for treatment if the woman or child was ill. Medical care was provided according to the standard of care at the study clinics, and participants were given insecticide-treated bed nets.

Guidelines for medication prescribing in Malawi are set by the Malawi Standard Treatment Guidelines, 4th Edition (*14*), and are based on the WHO Integrated Management of Childhood Illness Guidelines (http://whqlibdoc.who.int/publications/2005/9241546441.pdf). We collected data about prescriptions from the study concomitant medications log, which was abstracted from pharmacy records. If an infant had been examined by an outside healthcare provider, the mother was asked to report medications received. For hospitalized participating mothers and their infants, we obtained medical records when possible and

included in our analysis any antibacterial drugs administered. At study visits, patients were asked if they had taken any medication not prescribed by study physicians, and any such medications were recorded. As outcomes, we considered only prescriptions for antibacterial agents (Table 1); other prescriptions, including antimalarial and antiparasitic medications, were excluded. Prescription of CPT was not considered an outcome.

HIV status of infants at 2, 12, 28, and 48 weeks of age was determined by using a Roche Amplicor 1.5 DNA PCR (https://diagnostics.roche.com). Positive results were confirmed by testing an additional blood specimen. The window of infection was narrowed by testing dried blood spot specimens collected at 4, 6, 8, 18, 24, 32, and 36 weeks. We included in our analysis the 2,152 infants who were HIV negative at 2 weeks of age; we removed from the study and referred for care those who were not.

Ethics Approval

The BAN study was approved by the Malawi National Health Science Research Committee and the institutional review boards at the University of North Carolina at Chapel Hill and the US Centers for Disease Control and Prevention (CDC). All women provided written, informed consent for specimen storage and laboratory studies.

Statistical Analyses

For descriptive analyses, we calculated frequencies and medians for all exposures and covariables. Total antibacterial drug prescriptions are presented as frequencies and as medians per infant and per infant-month of follow-up. We describe frequencies of prescriptions of antibacterials by drug class, indications, indication categories, respiratory indication subcategories, and routes of administration. We compare the categorical proportions of exposures, covariables, and total antibacterial drug prescriptions by using χ^2 tests and assessed continuous variables by using the Kruskal–Wallis test. A Cox proportional hazards model with recurrent events modeled as a counting process was used to assess the hazards of antibacterial prescription by time-dependent CPT status; ARV group; malaria season (October–April); nutritional study group; maternal demographics; maternal CD4+ T-cell count at delivery; log maternal HIV viral load during pregnancy; and infant sex, birthweight, and categorical age (<1, 1–3, 3–6, or 6–12 mo). To assess the proportional hazards assumption and determine whether the effects of independent variables on the hazard of antibacterial prescription varied with infant age, we included interaction terms in Cox models. Infant follow-up ended at death, mother's death, or loss to follow-up. For the 71 infants who became HIV infected after 2 weeks of age, follow-up ended at the time of their last HIV-negative test result. The first week of life and the 5 days after prescription of an antibacterial drug do not contribute to total follow-up time, and antibacterial drug prescriptions administered during these periods were excluded. Sensitivity analyses excluded the 71 infants who became HIV infected after 2 weeks of follow-up and excluded prescriptions for topical antibacterials.

In analyses considering time-varying CPT exposure, infants were considered exposed from the first post-CPT implementation (June 13, 2006) study visit at or later than 6 weeks of age. Study group is modeled as an intent-to-treat variable. All analyses were performed by using SAS 9.4 (https://www.sas.com).

Table 1. Antibacterial drugs used in the Breastfeeding, Antiretrovirals and Nutrition study, Malawi, 2004–2010

Class	Drug
Aminoglycoside	Gentamicin
Cephalosporins	Ceftriaxone
	Cefuroxime
	Loracarbef
Nitroimidazole	Metronidazole
Penicillins	Amoxicillin
	Ampicillin
	Augmentin
	Benzathine penicillin
	Benzylpenicillin
	Cloxacillin
	Flucloxacillin
β-lactams/β-lactamase inhibitor combination	Amoxicillin/clavulanate
Phenicols	Chloramphenicol
Quinolones	Ciprofloxacin
	Nalidixic acid
Sulfonamides	Cotrimoxazole
	Sulfadiazine
Tetracyclines/macrolides	Doxycycline
	Erythromycin
	Tetracycline

Results

At delivery, the mothers of the 2,152 infants included in this analysis had a median CD4+ T-cell count of 440 cells/μL and a median HIV viral load of ≈16,000 copies/mL (Table 2). Median age of the mothers was 26 years (interquartile range [IQR] 22–29 years), and most had been educated through the primary (53%) or secondary (34%) levels. Among infants, median birthweight was 3,000 g (IQR 2,700–3,300), and 51% were male. There were fewer infants in the control (28%) than the maternal ARV (35.6%) or infant nevirapine (36.7%) groups because of early discontinuation of the control group. Half of the mothers from all 3 groups received a nutritional supplement.

Overall, 80.3% of infants received ≥1 prescription for an antibacterial drug during the follow-up period. Of the 5,107 antibacterial drug prescriptions for infants during the study, 3,437 (67.3%) were for respiratory indications, 590 (11.6%) for gastrointestinal indications, and 314 (6.1%)

Table 2. Baseline characteristics of HIV-exposed, uninfected infants in the Breastfeeding, Antiretrovirals and Nutrition study, Malawi, 2004–2010*

Characteristic	Total	Before CPT	After CPT	p value†
No. infants	2,152	692 (32.16)	1,460 (67.84)	
Maternal education				1.0
None	245 (11.4)	81 (11.7)	164 (11.3)	
Primary	1,153 (53.7)	369 (53.3)	784 (53.8)	
Secondary	730 (34.0)	236 (34.1)	494 (33.9)	
Tertiary	21 (1.0)	6 (0.9)	15 (1.0)	
Maternal CD4, cells/μL‡	440 (330–582)	437 (328–596.5)	441 (330–578)	0.8
Maternal HIV viral load during pregnancy, copies/mL‡	16,045 (4,462–48,857)	17,231 (5,194.5–51,274)	15,281 (4,339–48,192)	0.2
Maternal age at delivery, y‡	26 (22, 29)	25 (22–29)	26 (23–29)	0.047
Male infant	1,088 (50.6)	358 (51.7)	730 (50.0)	0.5
Infant birthweight, g‡	3,000 (2,700–3,300)	3,000 (2,700–3,300)	3,000 (2,700–3,300)	0.7
Treatment group				0.002
Control	597 (27.7)	227 (32.8)	370 (25.3)	
Maternal ARV	766 (35.6)	229 (33.1)	537 (36.8)	
Infant nevirapine	789 (36.7)	236 (34.1)	553 (37.9)	
Nutrition group	1,076 (50.0)	345 (49.9)	731 (50.1)	0.9

*Data from 6 wks after birth overall and according to baseline visit timing relative to cotrimoxazole prophylaxis guideline implementation in June 2006. Values are no. (%) unless otherwise indicated. ARV, antiretroviral therapy; CPT, cotrimoxazole preventive therapy.
†p values for continuous variables based on Kruskal-Wallis test; p values for categorical variables based on the Pearson χ^2 test.
‡Median (interquartile range).

for skin-related indications (Figure 1, panel A). Among antibacterial drug prescriptions for respiratory indications, 66.7% were for acute respiratory infections or upper respiratory tract infections, 6.8% were for pneumonia, and 26.5% were for other conditions (Table 3). The distribution of respiratory indications among antibacterial drug prescriptions did not vary according to timing relative to CPT implementation. Most antibacterial drug prescriptions were for penicillins (2,132, 41.8%), sulfonamides (1,194, 23.4%), and tetracyclines or macrolides (863, 16.9%) (Figure 1, panel B). Each of the remaining categories (phenicols, nitroimidazoles, cephalosporins, β-lactams/β-lactamase inhibitor combinations, aminoglycosides, and quinolones) accounted for <10% of prescriptions. In the BAN study, prescriptions for amoxicillin accounted for 1,932 (37.8%) of all antibacterial drug prescriptions for HIV-exposed, uninfected infants, followed by cotrimoxazole (23.4%), tetracycline (8.7%), erythromycin (8.2%), and chloramphenicol (6.0%). Tetracycline was prescribed as an ophthalmic solution to treat conjunctivitis. No other individual antibacterial drug accounted for >5% of all prescriptions (data not shown). Most antibacterial drugs were administered orally (85.0%); the rest, topically (8.0%) or intramuscularly (5.4%) (data not shown).

More infants were enrolled after (1,460) than before (692) CPT implementation in Malawi in June 2006 (Table 2). Median maternal age at delivery was slightly higher after CPT implementation (26 years) than before (25 years). Because of the discontinuation of the control group, infants born after CPT implementation were less likely to be in the control group ($p<0.001$ by χ^2 test). No other maternal or infant characteristics differed according to CPT implementation or ARV treatment group (Table 2).

Because more participants were enrolled after CPT implementation, the post-CPT implementation group contributed more person-time (412,697 vs. 187,865 person-days). The median length of follow-up for infants was 336 days (IQR 255–340 days); median follow-up length did not vary according to timing of birth relative to CPT implementation date ($p = 0.09$ by Kruskal–Wallis test) (Table 4). The median number of antibacterial drug prescriptions per infant was 2 (IQR 1–3) and was higher before (median 3, IQR 1–5) than after (median 2, IQR 1–3) CPT implementation. The same was true for median total antibacterial drug prescriptions per infant-month before (0.3, IQR 0.2–0.5) and after (0.2, IQR 0.1–0.3) CPT implementation (Table 4). Several infants were born before CPT implementation, but only 1 was born after and received ≥10 antibacterial drug prescriptions over the follow-up period (Figure 2).

Several factors were significantly associated with antibacterial drug prescription according to the Cox proportional hazards model. The largest reduction in hazards of prescription was for time-varying CPT exposure (hazard ratio [HR] 0.57, 95% CI 0.52–0.61) (Table 5). Assignment to each of the ARV prophylaxis groups was also associated with reduced hazard of antibacterial drug prescription (maternal ARV HR 0.85, 95% CI 0.78–0.93; infant nevirapine HR 0.90, 95% CI 0.82–0.98). Although maternal CD4+ counts at delivery were not associated with antibacterial drug prescriptions, log maternal HIV viral load at delivery was; for each 1 unit increase of log maternal viral load, hazard of infant antibacterial drug prescriptions increased by 2% (HR 1.02, 95% CI 1.003–1.04).

Removing the 71 infants who had become HIV infected by the 2-week visit reduced the median maternal viral load for CPT-exposed and CPT-unexposed infants but did

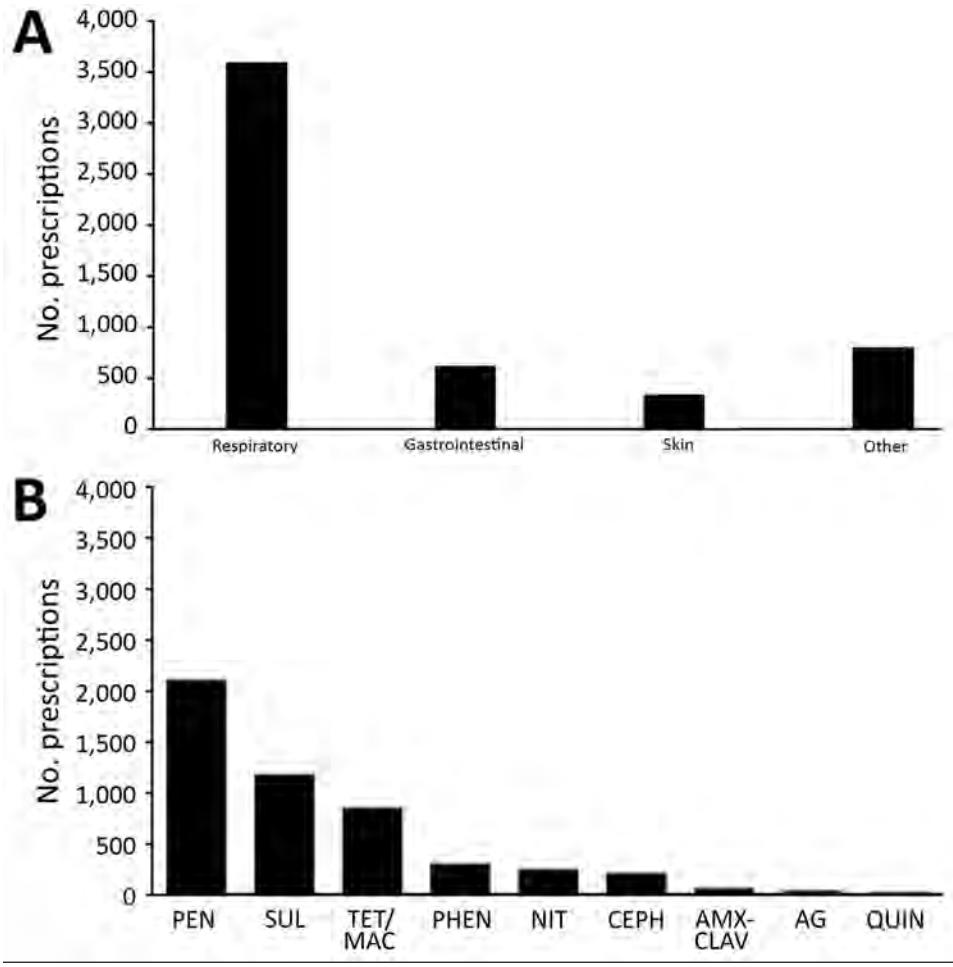

Figure 1. Numbers of prescriptions for antibacterial drugs, by clinical indication (A) and drug category (B), for HIV-exposed, uninfected infants in the Breastfeeding, Antiretrovirals and Nutrition study, Malawi, 2004–2010. AG, aminoglycosides; AMX-CLAV, amoxicillin-clavulanate; CEPH, cephalosporins; QUIN, quinolones; NIT, nitroimidazole; PEN, penicillins; PHEN, phenicols; SUL, sulfonamides; TET/MAC, tetracycline/ macrolides.

not otherwise notably affect results. Exclusion of topical antibacterial drug prescriptions did not alter any associations in the proportional hazards model (results not shown).

No maternal demographic characteristics were associated with hazard of antibacterial drug prescription, but infant characteristics were associated. Male sex (HR 1.09, 95% CI 1.02–1.17) and higher birthweight (HR 1.17, 95% CI 1.06–1.28) were each associated with increased hazard of antibacterial drug prescriptions; increasing age was associated with reduced hazard of prescriptions. Compared with the period from birth to 1 month of age, each subsequent period was associated with further reduced hazard of antibacterial drug prescription (at 1–3 months of age, HR 0.80, 95% CI 0.67, 0.95; at 3–6 months, HR 0.63, 95% CI 0.53, 0.76; at 6–12 months, HR 0.48, 95% CI 0.40, 0.58) (Table 5).

Discussion

In this study, HIV-exposed uninfected infants in Lilongwe, Malawi, received a median of 2 antibacterial drug prescriptions during the 48 weeks of study follow-up; 80% received ≥1 prescription during their first year of life. The main indicator driving these prescriptions was respiratory infections, followed by gastrointestinal infections. The most commonly prescribed drugs were in the penicillin class, specifically amoxicillin. Prescriptions became less common as study infants aged, and prophylactic CPT was associated with a 43% decrease in antibacterial drug prescriptions to treat infections; ARV administration to either the mother or the infant was associated with smaller decreases (10%–15%).

Studies of recent antibacterial drug prescribing in western Europe and Australia show rates of 0.65–0.97 prescriptions/person-year for infants in the first year of life (*15*–*19*), approximately one third to one half the rate of prescriptions for infants in the BAN study. This finding is perhaps not surprising, considering the higher rates of illness and death caused by infectious diseases among infants in Malawi compared with rates in higher income countries (*20*) and the even higher illness rates for infants born to HIV-infected mothers (*9*). Previous research has identified irrational prescribing of antibacterial drugs in health facilities in Malawi (*21*), potentially contributing to the higher observed rates of antibacterial drug use. To our knowledge, studies using person-level data to determine antibacterial

Table 3. Respiratory indications for antibacterial drugs prescribed for HIV-exposed, uninfected infants in the Breastfeeding, Antiretrovirals and Nutrition study, Malawi, 2004–2010*

Condition	No. (%)
Pneumonia	234 (6.81)
Acute respiratory infection or upper respiratory tract infection	2,291 (66.7)
Other*	912 (26.5)

*Otitis media, conjunctivitis, meningitis, sinusitis.

drug prescription for infants in low- and middle-income countries are lacking. Antibacterial drugs were prescribed for a larger proportion (80%) of infants in the BAN study than in a study in Nigeria (*22*), although that study was based on parent recall, which may have introduced error.

CPT for participants in the BAN study was implemented in June 2006. Several analyses, using data from the BAN study and from other studies, have shown CPT to be associated with reduced subclinical malaria (*23*), lower rates of illness and death caused by infectious diseases (*24–26*), and reduced incidence of severe anemia (*27*). The antibacterial properties of cotrimoxazole are probably the cause of the observed association between CPT and reduced overall antibacterial prescriptions. The malaria-preventing activity of cotrimoxazole may also contribute to better overall infant health and decreased illness rates from infectious diseases, as indicated in another analysis of BAN data (*24*). The prescriptions in this trial were driven mostly by respiratory infections. Reductions in antibacterial drug prescriptions associated with gastrointestinal symptoms and other indications were also observed; this finding is in agreement with previous results from the BAN study showing associations between CPT and reduced respiratory and diarrheal illness (*24*) and with evidence that CPT prevents a variety of infections and resulting illness and death (*28–30*). Another study, however, found that CPT for severely malnourished infants in Kenya did not reduce respiratory or diarrheal infections, although it did reduce malaria incidence (*31*).

Significant reductions in antibacterial drug prescriptions, although of smaller magnitude, were associated with use of ART by mothers during breastfeeding and with prophylactic administration of nevirapine to infants during 28 weeks of breastfeeding. Factors contributing to such increases may include overall improvements in maternal health, resulting in better ability to care for their infants, and perhaps improved immunologic or nutritional quality of breastmilk (*32*,*33*). The reasons for the effect of nevirapine on the infant are less clear but may be associated with the mother's perception of her infant's health and need to access care. Since the conclusion of the BAN study, Malawi has adopted the Option B+ strategy (http://www.who.int/hiv/pub/guidelines/arv2013/en) aiming to provide all HIV-infected persons with ART for life. Guidelines for HIV-infected pregnant women (https://aidsfree.usaid.gov/sites/default/files/malawi_art_2016.pdf) have been updated to recommend that mothers continue breastfeeding for 12–24 months and continue CPT, both of which may lead to decreased infectious disease incidence for the infants and resultant decreased prescription of antibacterial drugs.

Among antibacterial drugs given for respiratory indications, approximately two thirds were for acute respiratory infections or upper respiratory tract infections, for which Malawi Ministry of Health guidelines (http://www.pascar.org/uploads/files/Malawi_STG_Hypertension.pdf) do not support antibacterial treatment. This pattern agrees with research on prescribing practices from Malawi and other developing countries (*21*,*34*,*35*) but also the United States (*36*,*37*). After implementation of CPT, the prescriptions described and appropriate prescription of

Table 4. Antibacterial prescriptions and person-time of follow-up for HIV-exposed, uninfected infants in the Breastfeeding, Antiretrovirals and Nutrition study, Malawi, 2004–2010*

	Overall			Before CPT			After CPT			p values†	
Variable	Total no.	Per person	Per infant-month	Total no.	Per person	Per infant-month	Total no.	Per person	Per infant-month	Per person	Per person-month
No.	2,152			692			1,460				
Median follow-up time, d	600,562	336 (255–340)		187,865	337 (226–343)		412,697	336 (294–339)		0.09	
Prescriptions, total	5,107	2 (1–3)	0.2 (0.1–0.3)	2,269	3 (1–5)	0.3 (0.2–0.5)	28,38	2 (1–3)	0.2 (0.1–0.3)	<0.0001	<0.0001
For respiratory infections	3,437	1 (0–2)	0.1 (0–0.2)	1481	2 (1–3)	0.2 (0.1–0.3)	1956	1 (0–2)	0.1 (0.0–0.2)	<0.0001	<0.0001
For other infections	1,670	0 (0–1)	0 (0–0.1)	788	1 (0–2)	0.1 (0–0.2)	882	0 (0–1)	0.0 (0.0–0.1)	<0.0001	<0.0001

*Overall and according to baseline visit timing relative to CPT guideline implementation (June 2006). Values are range (IQR) except as indicated. CPT, cotrimoxazole prophylaxis; IQR, interquartile range.
†p values based on Kruskal-Wallis test for continuous variables.

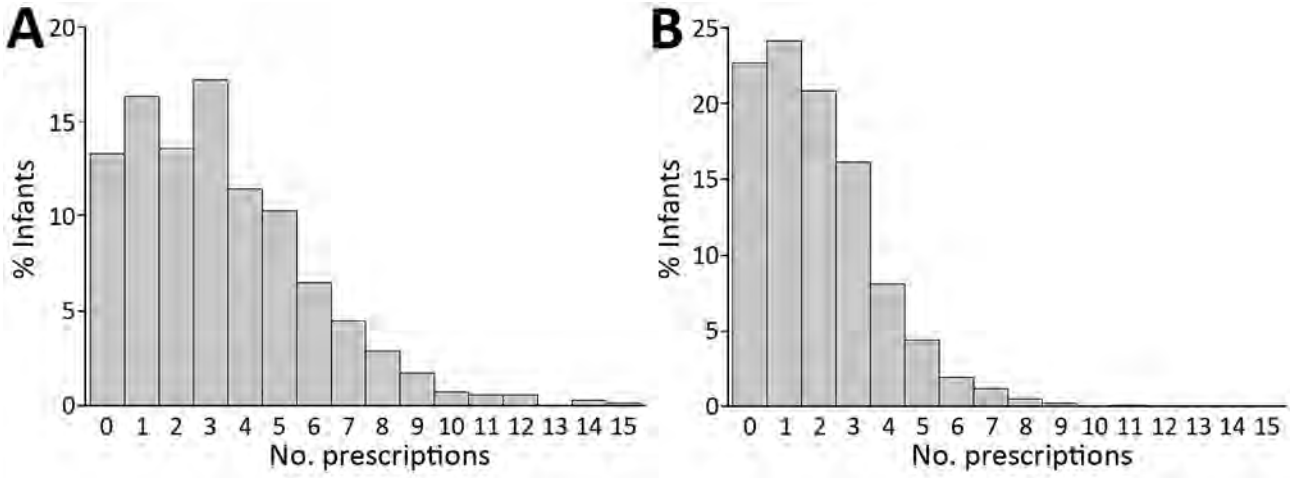

Figure 2. Distribution of HIV-exposed, uninfected infants according to total number of prescriptions for antibacterial drugs during follow-up in the Breastfeeding, Antiretrovirals and Nutrition study, Malawi, 2004–2010. Infants enrolled A) before and B) after implementation of cotrimoxazole preventive therapy.

antibacterial drugs declined, which could possibly be attributed to reductions of malaria or better overall maternal and infant health. In addition, recent research indicates that pharmacies in Malawi often do not adhere to rules requiring a prescription for antibacterial drugs (*38*), although there are no data on administration of over-the-counter antibacterial drugs for infants. The BAN study attempted to record these medications, but the self-reported nature of these data could have led to underestimation.

Maternal HIV viral load is an indicator of HIV disease status and an indirect marker of immune status; higher viral loads indicate more advanced HIV disease, a more compromised immune system, and increased susceptibility to infection (*39*). Mothers with a higher viral load at delivery may have had poorer overall health and increased susceptibility to infection, potentially explaining the increase in antibacterial drug prescriptions for infants of mothers with higher viral loads. The BAN study excluded women with CD4+ counts <250 cells/μL (<200 cells/μL early in the study). This restriction may explain why no association was found between CD4+ counts and antibacterial drug prescriptions.

Our findings also showed an association of increased antibacterial drug prescriptions for infants who were male, had higher birthweight, and were younger. Research suggests that male infants are more susceptible to most types of respiratory infections and that these infections tend to be more severe (*40*). Younger infants also have greater susceptibility to, and severity of, infectious diseases (*8*,*41*,*42*), which could trigger more aggressive treatment of younger infants. The reasons for the association of antibacterial drug prescriptions with higher birthweight are less clear; however, infants with the lowest birthweights (<2,000 g) were excluded from the BAN study.

The 13-valent pneumococcal conjugate vaccine was introduced in Malawi in November 2011, after the conclusion of the BAN study. Surveillance during implementation of this immunization program showed fewer cases of severe and fatal pneumonia (*43*). This vaccine can also prevent otitis media caused by pneumococcal infection (*44*). The rotavirus vaccine, introduced in October 2012, also after the conclusion of the BAN study, has reduced hospital admissions of infants for acute rotavirus gastroenteritis in Malawi (*45*). The reduction of severe pneumonia may reduce infants' need for antibacterial drugs, and the reduction of rotavirus infections may limit unnecessary antibacterial drug prescribing and generally improve infant health.

Our study has some limitations. One limitation is a lack of reliable data about the duration of treatment with antibacterial drugs and individual adherence. Although the study followed Malawi national treatment guidelines, as part of a large clinical trial that provided unlimited access to medical care, resources may have been available to the study clinics that are not available to clinics and persons at large in the target population in Malawi, limiting our ability to generalize the results. Also, we were not able to independently verify the reliability of providers' diagnoses used to guide prescription of antibacterial drugs. Although we requested relevant records when participants reported having received outside medical care, some antibacterial drug prescriptions may have been missed. However, because medical care was provided without charge, participants had an incentive to use that provided by the study clinic.

There may have been unmeasured variables affecting disease incidence or antibacterial drug prescribing patterns, confounding the associations we found. Because of its time-dependent nature, the association between CPT exposure and antibacterial drug use may be

Table 5. Cox proportional hazard ratio estimates for associations between prescriptions for antibacterial drugs and other variables in the Breastfeeding, Antiretrovirals and Nutrition study, Malawi 2004–2010

Factor	Hazard ratio (95% CI)
Cotrimoxazole preventive therapy	0.57 (0.52–0.61)
Malaria season (Oct–Apr)	0.98 (0.91–1.05)
Treatment group	
Maternal antiretrovirals	0.85 (0.78–0.93)
Infant nevirapine	0.90 (0.82–0.98)
Nutritional supplement	1.05 (0.98–1.12)
Maternal CD4+ T-cell count at delivery, cells/μL	1.15 (0.96–1.38)
Maternal HIV viral load during pregnancy, log copies/mL	1.02 (1.003–1.04)
Maternal age, y	1.01 (0.998–1.01)
Maternal education	
None	Reference
Primary	0.92 (0.83–1.03)
Secondary	0.99 (0.89–1.11)
Tertiary	0.93 (0.65–1.32)
Male sex	1.09 (1.02–1.17)
Infant birthweight, kg	1.17 (1.06–1.28)
Age category, mo	
Birth–1 mo	Reference
1–3	0.80 (0.67–0.95)
3–6	0.63 (0.53–0.76)
6–12	0.48 (0.40–0.58)

vulnerable to confounding by overall trends in population health. However, baseline characteristics before and after CPT implementation were broadly comparable. Prescriptions for antibacterial drugs when such treatment was not clearly indicated (e.g., fever, abdominal pain, upper respiratory tract infections, asthma) were included as outcomes. For these conditions, this study lacks sufficient clinical detail on which to base a definite determination of the appropriateness of antibacterial drug administration, and we thus cannot definitely conclude how much of the reduced antibacterial drug prescription associated with CPT resulted from prevention of bacterial infections versus other factors, such as reduced malaria or influence on clinicians' antibacterial drug prescribing threshold. A proportion of the reduced antibacterial drug prescriptions for respiratory indications associated with CPT may result from a reduction in malaria because of overlapping symptoms (*46*,*47*). In Malawi, because study clinicians commonly do not regularly test urine without a distinct indication of a urinary tract problem, urinary tract infections are probably underrepresented as causes for prescription of antibacterial drugs in the study population.

Our study also has several strengths. The study included a large sample of a population whose antibacterial drug use is underdescribed, it took advantage of the midtrial CPT introduction to assess CPT effects on use of antibacterial drugs, and it measured the effects of several factors on prescribing of antibacterial drugs for HIV-exposed, uninfected infants in an urban setting in Malawi. Data on independent variables, outcomes, and illness were collected systematically, and participants were followed up actively, which is generally not possible with studies that use administrative or surveillance data.

In conclusion, our findings indicate that antibacterial drugs were frequently prescribed for HIV-exposed, uninfected infants in the BAN study, primarily to treat respiratory infections. Antibacterial drugs were more likely to be prescribed for infants who were younger, whose mothers had higher HIV viral loads, and who were not exposed to ART. We found a strong association between CPT and lower hazard of antibacterial drug prescription. With the expansion of lifelong ART coverage in Malawi and other areas of high HIV prevalence and the increasing availability of effective vaccines, HIV-exposed, uninfected infants in Malawi may experience fewer infectious diseases and a resulting decrease in prescription of antibacterial drugs. Our study provides a useful reference point for measuring prescription of antibacterial drugs for infants at high risk for infectious diseases in a low-income country and for assessing the effects of programs to improve the health of those infants in Malawi.

Breastfeeding, Antiretrovirals and Nutrition Study team members: Linda Adair, Yusuf Ahmed, Mounir Ait-Khaled, Sandra Albrecht, Shrikant Bangdiwala, Ronald Bayer, Margaret Bentley, Brian Bramson, Emily Bobrow, Nicola Boyle, Sal Butera, Charles Chasela, Charity Chavula, Joseph Chimerang'ambe, Maggie Chigwenembe, Maria Chikasema, Norah Chikhungu, David Chilongozi, Grace Chiudzu, Lenesi Chome, Anne Cole, Amanda Corbett, Amy Corneli, Nicole Davis, Anna Dow, Ann Duerr, Henry Eliya, Sascha Ellington, Joseph Eron, Sherry Farr, Yvonne Owens Ferguson, Susan Fiscus, Valerie Flax, Ali Fokar, Shannon Galvin, Laura Guay, Chad Heilig, Irving Hoffman, Elizabeth Hooten, Mina Hosseinipour, Michael Hudgens, Stacy Hurst, Lisa Hyde, Denise Jamieson, George Joaki (deceased), David Jones, Elizabeth Jordan-Bell, Zebrone Kacheche, Esmie Kamanga, Gift Kamanga, Coxcilly Kampani, Portia Kamthunzi, Deborah Kamwendo, Cecilia Kanyama, Angela Kashuba, Damson Kathyola, Dumbani Kayira, Peter Kazembe, Caroline C. King, Rodney Knight, Athena P. Kourtis, Robert Krysiak, Jacob Kumwenda, Hana Lee, Edde Loeliger, Dustin Long, Misheck Luhanga, Victor Madhlopa, Maganizo Majawa, Alice Maida, Cheryl Marcus, Francis Martinson, Navdeep Thoofer, Chrissie Matiki (deceased), Douglas Mayers, Isabel Mayuni, Marita McDonough, Joyce Meme, Ceppie Merry, Khama Mita, Chimwemwe Mkomawanthu, Gertrude Mndala, Ibrahim Mndala, Agnes Moses, Albans Msika, Wezi Msungama, Beatrice Mtimuni, Jane Muita, Noel Mumba, Bonface Musis, Charles Mwansambo, Gerald Mwapasa, Jacqueline Nkhoma, Megan Parker, Richard Pendame, Ellen Piwoz, Byron Raines,

Zane Ramdas, John Rublein, Mairin Ryan, Ian Sanne, Christopher Sellers, Diane Shugars, Dorothy Sichali, Wendy Snowden, Alice Soko, Allison Spensley, Jean-Marc Steens, Gerald Tegha, Martin Tembo, Roshan Thomas, Hsiao-Chuan Tien, Beth Tohill, Charles van der Horst, Esther Waalberg, Elizabeth Widen, Jeffrey Wiener, Cathy Wilfert, Patricia Wiyo, Innocent Zgambo, and Chifundo Zimba.

Acknowledgments

We are grateful to the BAN Study Team at University of North Carolina–Chapel Hill, CDC, and the University of North Carolina Project in Lilongwe. Most especially, we thank all the women who agreed to participate in the study.

The BAN study was supported by grants from the Prevention Research Centers Special Interest Project of CDC (SIP 13-01 U48-CCU409660-09, SIP 26-04 U48-DP000059-01, and SIP 22-09 U48-DP001944-01); the National Institute of Allergy and Infectious Diseases; the University of North Carolina Center for AIDS Research (P30-AI50410); the Carolina Population Center (R24 HD050924); the National Institutes of Health Fogarty International Programs (AIDS International Training and Research Program [D43 TW001039] and the Scholars and Fellows Program [R24 TW007988]; the American Recovery and Reinvestment Act); and the Bill and Melinda Gates Foundation (grant no. OPP53107).

The ARV drugs used in the BAN study were donated by Abbott Laboratories, GlaxoSmithKline, Boehringer Ingelheim, Roche Pharmaceuticals, and Bristol-Myers Squibb. The Call to Action PMTCT program was supported by the Elizabeth Glaser Pediatric AIDS Foundation, the United Nations Children's Fund, the World Food Program, the Malawi Ministry of Health and Population, Johnson & Johnson, and the US Agency for International Development.

About the Author

Mr. Ewing is an epidemiologist working in the Division of Reproductive Health, National Center for Chronic Disease Prevention and Health Promotion, CDC. His research focuses on issues related to prevention and illness related to HIV and sexually transmitted infections.

References

1. World Health Organization. Antimicrobial resistance: global report on surveillance. Geneva: The Organization; 2014. p. 69–71.
2. Maragakis LL, Perencevich EN, Cosgrove SE. Clinical and economic burden of antimicrobial resistance. Expert Rev Anti Infect Ther. 2008;6:751–63. http://dx.doi.org/10.1586/14787210.6.5.751
3. Neidell MJ, Cohen B, Furuya Y, Hill J, Jeon CY, Glied S, et al. Costs of healthcare- and community-associated infections with antimicrobial-resistant versus antimicrobial-susceptible organisms. Clin Infect Dis. 2012;55:807–15. http://dx.doi.org/10.1093/cid/cis552
4. Woolhouse M, Waugh C, Perry MR, Nair H. Global disease burden due to antibiotic resistance—state of the evidence. J Glob Health. 2016;6:010306. http://dx.doi.org/10.7189/jogh.06.010306
5. Laxminarayan R, Matsoso P, Pant S, Brower C, Røttingen J-A, Klugman K, et al. Access to effective antimicrobials: a worldwide challenge. Lancet. 2016;387:168–75. http://dx.doi.org/10.1016/S0140-6736(15)00474-2
6. Van Boeckel TP, Gandra S, Ashok A, Caudron Q, Grenfell BT, Levin SA, et al. Global antibiotic consumption 2000 to 2010: an analysis of national pharmaceutical sales data. Lancet Infect Dis. 2014;14:742–50. http://dx.doi.org/10.1016/S1473-3099(14)70780-7
7. Fleming-Dutra KE, Hersh AL, Shapiro DJ, Bartoces M, Enns EA, File TM Jr, et al. Prevalence of inappropriate antibiotic prescriptions among US ambulatory care visits, 2010–2011. JAMA. 2016;315:1864–73. http://dx.doi.org/10.1001/jama.2016.4151
8. Lambert L, Culley FJ. Innate immunity to respiratory infection in early life. Front Immunol. 2017;8:1570. http://dx.doi.org/10.3389/fimmu.2017.01570
9. Afran L, Garcia Knight M, Nduati E, Urban BC, Heyderman RS, Rowland-Jones SL. HIV-exposed uninfected children: a growing population with a vulnerable immune system? Clin Exp Immunol. 2014;176:11–22. http://dx.doi.org/10.1111/cei.12251
10. Filteau S. The HIV-exposed, uninfected African child. Trop Med Int Health. 2009;14:276–87. http://dx.doi.org/10.1111/j.1365-3156.2009.02220.x
11. Chasela CS, Hudgens MG, Jamieson DJ, Kayira D, Hosseinipour MC, Kourtis AP, et al. Maternal or infant antiretroviral drugs to reduce HIV-1 transmission. N Engl J Med. 2010;362:2271–81.
12. van der Horst C, Chasela C, Ahmed Y, Hoffman I, Hosseinipour M, Knight R, et al.; Breastfeeding, Antiretroviral, and Nutrition study team. Modifications of a large HIV prevention clinical trial to fit changing realities: a case study of the Breastfeeding, Antiretroviral, and Nutrition (BAN) protocol in Lilongwe, Malawi. Contemp Clin Trials. 2009;30:24–33. http://dx.doi.org/10.1016/j.cct.2008.09.001
13. World Health Organization, United Nations International Children's Emergency Fund. Breastfeeding counselling: a training course [cited 2018 Nov 9] http://www.who.int/maternal_child_adolescent/documents/who_cdr_93_3/en
14. Malawi Ministry of Health. Malawi standard treatment guidelines, 4th edition. 2009 [cited 2018 Nov 9]. http://apps.who.int/medicinedocs/documents/s18801en/s18801en.pdf
15. Stam J, Van Stuijvenberg M, Grüber C, Mosca F, Arslanoglu S, Chirico G, et al. Antibiotic use in infants in the first year of life in five European countries. Acta Paediatrica. 2012;101:929–34.
16. Kinlaw AC, Stürmer T, Lund JL, Pedersen L, Kappelman MD, Daniels JL, et al. Trends in antibiotic use by birth season and birth year. Pediatrics. 2017;140:e20170441. http://dx.doi.org/10.1542/peds.2017-0441
17. Anderson H, Vuillermin P, Jachno K, Allen KJ, Tang MLK, Collier F, et al.; Barwon Infant Study Investigator Group. Prevalence and determinants of antibiotic exposure in infants: a population-derived Australian birth cohort study. J Paediatr Child Health. 2017;53:942–9. http://dx.doi.org/10.1111/jpc.13616
18. Dekker ARJ, Verheij TJM, van der Velden AW. Antibiotic management of children with infectious diseases in Dutch primary care. Fam Pract. 2017;34:169–74.
19. Schneider-Lindner V, Quach C, Hanley JA, Suissa S. Secular trends of antibacterial prescribing in UK paediatric primary care. J Antimicrob Chemother. 2011;66:424–33. http://dx.doi.org/10.1093/jac/dkq452
20. World Health Organization. Global health risks: mortality and burden of disease attributable to selected major risks. Geneva: The Organization; 2009. p. 7–12.
21. Johansson EW, Selling KE, Nsona H, Mappin B, Gething PW, Petzold M, et al. Integrated paediatric fever management and antibiotic over-treatment in Malawi health facilities: data mining

a national facility census. Malar J. 2016;15:396. http://dx.doi.org/10.1186/s12936-016-1439-7
22. Murphy R, Stewart AW, Braithwaite I, Beasley R, Hancox RJ, Mitchell EA; ISAAC Phase Three Study Group. Antibiotic treatment during infancy and increased body mass index in boys: an international cross-sectional study. Int J Obes. 2014;38:1115–9. http://dx.doi.org/10.1038/ijo.2013.218
23. Davis NL, Barnett EJ, Miller WC, Dow A, Chasela CS, Hudgens MG, et al. Impact of daily cotrimoxazole on clinical malaria and asymptomatic parasitemias in HIV-exposed, uninfected infants. Clin Infect Dis. 2015;61:368–74. http://dx.doi.org/10.1093/cid/civ309
24. Davis NL, Wiener J, Juliano JJ, Adair L, Chasela CS, Kayira D, et al.; Breastfeeding, Antiretrovirals and Nutrition (BAN) study team. Co-trimoxazole prophylaxis, asymptomatic malaria parasitemia, and infectious morbidity in human immunodeficiency virus–exposed, uninfected infants in Malawi: the BAN study. Clin Infect Dis. 2017;65:575–80. http://dx.doi.org/10.1093/cid/cix367
25. Mermin J, Lule J, Ekwaru JP, Malamba S, Downing R, Ransom R, et al. Effect of co-trimoxazole prophylaxis on morbidity, mortality, CD4-cell count, and viral load in HIV infection in rural Uganda. Lancet. 2004;364:1428–34. http://dx.doi.org/10.1016/S0140-6736(04)17225-5
26. Kourtis AP, Wiener J, Kayira D, Chasela C, Ellington SR, Hyde L, et al. Health outcomes of HIV-exposed uninfected African infants. AIDS. 2013;27:749–59. http://dx.doi.org/10.1097/QAD.0b013e32835ca29f
27. Ewing AC, King CC, Wiener JB, Chasela CS, Hudgens MG, Kamwendo D, et al. Effects of concurrent exposure to antiretrovirals and cotrimoxazole prophylaxis among HIV-exposed, uninfected infants. AIDS. 2017;31:2455–63. http://dx.doi.org/10.1097/QAD.0000000000001641
28. Grimwade K, Swingler G. Cotrimoxazole prophylaxis for opportunistic infections in adults with HIV. Cochrane Database Syst Rev. 2003;(3):CD003108.
29. Chintu C, Bhat GJ, Walker AS, Mulenga V, Sinyinza F, Lishimpi K, et al.; CHAP trial team. Co-trimoxazole as prophylaxis against opportunistic infections in HIV-infected Zambian children (CHAP): a double-blind randomised placebo-controlled trial. Lancet. 2004;364:1865–71. http://dx.doi.org/10.1016/S0140-6736(04)17442-4
30. Church JA, Fitzgerald F, Walker AS, Gibb DM, Prendergast AJ. The expanding role of co-trimoxazole in developing countries. Lancet Infect Dis. 2015;15:327–39. http://dx.doi.org/10.1016/S1473-3099(14)71011-4
31. Berkley JA, Ngari M, Thitiri J, Mwalekwa L, Timbwa M, Hamid F, et al. Daily co-trimoxazole prophylaxis to prevent mortality in children with complicated severe acute malnutrition: a multicentre, double-blind, randomised placebo-controlled trial. Lancet Glob Health. 2016;4:e464–73. http://dx.doi.org/10.1016/S2214-109X(16)30096-1
32. Flax VL, Bentley ME, Combs GF Jr, Chasela CS, Kayira D, Tegha G, et al. Plasma and breast-milk selenium in HIV-infected Malawian mothers are positively associated with infant selenium status but are not associated with maternal supplementation: results of the Breastfeeding, Antiretrovirals, and Nutrition study. Am J Clin Nutr. 2014;99:950–6. http://dx.doi.org/10.3945/ajcn.113.073833
33. Allen LH, Hampel D, Shahab-Ferdows S, York ER, Adair LS, Flax VL, et al. Antiretroviral therapy provided to HIV-infected Malawian women in a randomized trial diminishes the positive effects of lipid-based nutrient supplements on breast-milk B vitamins. Am J Clin Nutr. 2015;102:1468–74. http://dx.doi.org/10.3945/ajcn.114.105106
34. Kabaghe AN, Phiri MD, Phiri KS, van Vugt M. Challenges in implementing uncomplicated malaria treatment in children: a health facility survey in rural Malawi. Malar J. 2017;16:419. http://dx.doi.org/10.1186/s12936-017-2066-7
35. Istúriz RE, Carbon C. Antibiotic use in developing countries. Infect Control Hosp Epidemiol. 2015;21:394–7.
36. Grijalva CG, Nuorti JP, Griffin MR. Antibiotic prescription rates for acute respiratory tract infections in US ambulatory settings. JAMA. 2009;302:758–66. http://dx.doi.org/10.1001/jama.2009.1163
37. Shaw SY, Blanchard JF, Bernstein CN. Association between the use of antibiotics in the first year of life and pediatric inflammatory bowel disease. Am J Gastroenterol. 2010;105:2687–92. http://dx.doi.org/10.1038/ajg.2010.398
38. Chikowe I, Bliese SL, Lucas S, Lieberman M. Amoxicillin quality and selling practices in urban pharmacies and drug stores of Blantyre, Malawi. Am J Trop Med Hyg. 2018;99:233–8. http://dx.doi.org/10.4269/ajtmh.18-0003
39. Mellors JW, Muñoz A, Giorgi JV, Margolick JB, Tassoni CJ, Gupta P, et al. Plasma viral load and CD4+ lymphocytes as prognostic markers of HIV-1 infection. Ann Intern Med. 1997;126:946–54. http://dx.doi.org/10.7326/0003-4819-126-12-199706150-00003
40. Falagas ME, Mourtzoukou EG, Vardakas KZ. Sex differences in the incidence and severity of respiratory tract infections. Respir Med. 2007;101:1845–63. http://dx.doi.org/10.1016/j.rmed.2007.04.011
41. Tregoning JS, Schwarze J. Respiratory viral infections in infants: causes, clinical symptoms, virology, and immunology. Clin Microbiol Rev. 2010;23:74–98. http://dx.doi.org/10.1128/CMR.00032-09
42. Centers for Disease Control and Prevention. Pneumonia hospitalizations among young children before and after introduction of pneumococcal conjugate vaccine—United States, 1997–2006. MMWR Morb Mortal Wkly Rep. 2009;58:1–4.
43. McCollum ED, Nambiar B, Deula R, Zadutsa B, Bondo A, King C, et al. Impact of the 13-valent pneumococcal conjugate vaccine on clinical and hypoxemic childhood pneumonia over three years in central Malawi: an observational study. PLoS One. 2017;12:e0168209. http://dx.doi.org/10.1371/journal.pone.0168209
44. Ben-Shimol S, Givon-Lavi N, Leibovitz E, Raiz S, Greenberg D, Dagan R. Near-elimination of otitis media caused by 13-valent pneumococcal conjugate vaccine (PCV) serotypes in southern Israel shortly after sequential introduction of 7-valent/13-valent PCV. Clin Infect Dis. 2014;59:1724–32. http://dx.doi.org/10.1093/cid/ciu683
45. Bar-Zeev N, Kapanda L, Tate JE, Jere KC, Iturriza-Gomara M, Nakagomi O, et al.; VacSurv Consortium. Effectiveness of a monovalent rotavirus vaccine in infants in Malawi after programmatic roll-out: an observational and case-control study. Lancet Infect Dis. 2015;15:422–8. http://dx.doi.org/10.1016/S1473-3099(14)71060-6
46. English M, Punt J, Mwangi I, McHugh K, Marsh K. Clinical overlap between malaria and severe pneumonia in Africa children in hospital. Trans R Soc Trop Med Hyg. 1996;90:658–62. http://dx.doi.org/10.1016/S0035-9203(96)90423-X
47. Ukwaja KN, Aina OB, Talabi AA. Clinical overlap between malaria and pneumonia: can malaria rapid diagnostic test play a role? J Infect Dev Ctries. 2011;5:199–203. http://dx.doi.org/10.3855/jidc.945

Address for correspondence: Alexander C. Ewing, Centers for Disease Control and Prevention, 4770 Buford Hwy, Mailstop F74, Chamblee, GA 30341-3717, USA; email: yhy4@cdc.gov

Dengue Virus IgM Serotyping by ELISA with Recombinant Mutant Envelope Proteins

Alexandra Rockstroh, Luisa Barzon, Widuranga Kumbukgolla, Hoang Xuan Su, Erley Lizarazo, Maria Fernanda Vincenti-Gonzalez, Adriana Tami, Alice M.M. Ornelas, Renato Santana Aguiar, Daniel Cadar, Jonas Schmidt-Chanasit, Sebastian Ulbert

We developed an IgM-based ELISA that identifies the dengue virus serotype of recent infections. Dominant serotypes were detectable in 91.1% of samples from travelers and 86.5% of samples from residents of endemic regions; 97.1% corresponded to the serotype identified by PCR. This ELISA enables more accurate reporting of epidemiologic findings.

Dengue virus (DENV) is an arthropodborne flavivirus that is endemic in tropical and subtropical regions, causing hundreds of millions of infections annually (*1*). It is subdivided into 4 serotypes, DENV-1–4. After infection, patients have lifelong immunity against the homologous serotype but remain susceptible to infections with the others (*2*). Such secondary infections have been shown to be a risk factor for severe dengue with life-threatening clinical manifestations, including dengue hemorrhagic fever or dengue shock syndrome (*3*). Thus, monitoring the serotype is essential for outbreak management, epidemiologic studies, and patient care. Analyses are often performed by using direct virus detection methods, such as PCR and nonstructural protein 1 (NS1) antigen capture (*4*). Despite the high specificities of these assays, their main disadvantages include a rather small diagnostic window for detection and, for NS1 antigen capture tests, low sensitivities during secondary DENV infections (*5*). Identification of the infecting serotype by serologic methods is hampered by the cross-reactivity of antibodies elicited by the immune response against flaviviruses (*6*). Previous reports have shown that the insertion of mutations in the conserved fusion loop domain of flavivirus envelope proteins reduces this cross-reactivity in diagnostic testing (*7*–*9*). Using this method, we developed a DENV-specific ELISA capable of differentiating DENV from other clinically relevant flaviviruses, such as Zika virus, West Nile virus, and tick-borne encephalitis virus (*10*). In this study, we evaluated the potential of this technique to distinguish the 4 DENV serotypes during the acute phase of infection on the basis of IgM detection.

Author affiliations: Fraunhofer Institute for Cell Therapy and Immunology, Leipzig, Germany (A. Rockstroh, S. Ulbert); University of Padova, Padova, Italy (L. Barzon); Rajarata University of Sri Lanka, Mihinthale, Sri Lanka (W. Kumbukgolla); Vietnam Military Medical University, Hanoi, Vietnam (H.X. Su); University Medical Center Groningen, Groningen, the Netherlands (E. Lizarazo, M.F. Vincenti-Gonzalez, A. Tami); Federal University of Rio de Janeiro, Rio de Janeiro, Brazil (A.M.M. Ornelas, R.S. Aguiar); Bernhard Nocht Institute for Tropical Medicine, Hamburg, Germany (D. Cadar, J. Schmidt-Chanasit); German Centre for Infection Research, Hamburg (J. Schmidt-Chanasit)

DOI: https://doi.org/10.3201/eid2501.180605

The Study

We acquired DENV PCR–confirmed and, thereby, serotype-classified serum samples that we divided into 2 groups: those from returning travelers with residence in Italy or Germany (n = 45), collected from patients 5–60 days after symptom onset during 2013–2016; and those from persons residing in the DENV-endemic countries of Sri Lanka (n = 43), Vietnam (n = 24), Venezuela (n = 5), and Brazil (n = 2), collected from patients 2–8 days after symptom onset during 2013–2018. We also had a set of 14 DENV PCR–negative but NS1-positive (PLATEILA DENGUE NS1 AG; Bio-Rad, Hercules, CA, USA) serum samples from patients in Vietnam that were collected during the same outbreak as the other patients from Vietnam with DENV PCR–positive test results. Ethics approvals were obtained from the respective local authorities for all samples.

We first tested all serum samples with a DENV-specific ELISA that used 4 recombinant DENV envelope proteins (1 per serotype) containing 4 point mutations in and near the conserved fusion loop (called Equad proteins) (*9*). All samples were positive for DENV IgM (S. Ulbert, unpub. data). This Equad-based ELISA was previously shown to be capable of discriminating DENV from other flaviviruses (*9*,*10*). We took the Equad antigens from this ELISA and created a DENV serotyping ELISA. In brief, we titrated serum samples (1:100–1:12,800 in serial 2-fold dilutions) in duplicate on plates coated with DENV-1–4 Equad proteins (Appendix, https://wwwnc.cdc.gov/EID/article/25/1/18-0605-App1.pdf) (*10*). We defined the endpoint titer for every serotype as the last dilution presenting

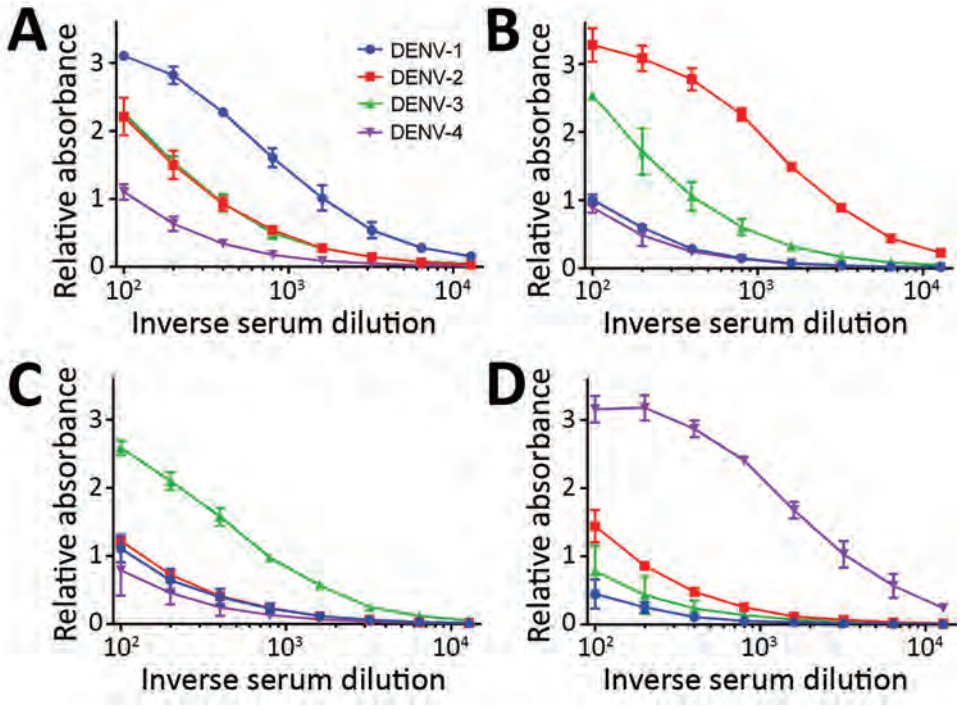

Figure 1. DENV IgM ELISA titers, by serotype, for DENV PCR–positive serum samples from travelers returning to Germany or Italy, 2013–2016. A) DENV-1; B) DENV-2; C) DENV-3; D) DENV-4. Data lines indicate average titers; error bars indicate SDs. The antigens in this ELISA were Equad proteins (i.e., envelope protein from each DENV serotype with 4 amino acid changes T76R, Q77E, W101R, and L107R). In these examples, the highest endpoint titers corresponded to the DENV serotype identified by PCR analysis. DENV, dengue virus.

a signal above the cutoff (Appendix Table), which was calculated as the mean plus 2 times the SD of 15 flavivirus-negative control serum samples (diluted 1:100) acquired from Padova University Hospital, Padova, Italy.

Results showed 1 dominant serotype (Figure 1) for 91.1% of serum samples from returning travelers and 86.5% of serum samples from residents of DENV-endemic countries (Appendix Figures 1, 2). Compared

Table 1. Dominant serotype determined by DENV serotype–specific IgM ELISA and ELISA specificity, by cohort and serotype, 2013–2018*

Cohort, DENV serotype†	No. samples	Dominant serotype, no. (%) samples	Serotype specificity‡	
			No. samples	% Samples (95% CI)
Returning travelers				
DENV-1	16	14 (87.50)	14	87.50 (61.65–98.45)
DENV-2	11	10 (90.91)	8	72.73 (39.03–93.98)
DENV-3	10	9 (90)	9	90.00 (55.50–99.75)
DENV-4	8	8 (100.00)	7	87.50 (47.35–99.68)
All serotypes	45	41 (91.11)	38	84.44 (70.54–93.51)
Residents in DENV-endemic countries				
Sri Lanka				
DENV-1	23	16 (69.57)	16	69.57 (47.08–86.79)
DENV-2	14	13 (92.86)	13	92.86 (66.13–99.82)
DENV-4	6	6 (100.00)	6	100.00 (54.07–100.00)
All serotypes	43	35 (81.40)	35	81.40 (66.60–91.61)
Vietnam				
DENV-1	20	19 (95.00)	19	95.00 (75.13–99.87)
DENV-2	4	4 (100.00)	4	100.00 (39.76–100.00)
All serotypes	24	23 (95.83)	23	95.83 (78.88–99.89)
Venezuela				
DENV-4	5	4 (80.00)	4	80.00 (23.36–99.49)
Brazil				
DENV-4	2	2 (100.00)	2	100.00 (15.81–100.00)
Total				
DENV-1	43	35 (81.40)	35	81.40 (66.60–91.61)
DENV-2	18	17 (94.44)	17	94.44 (72.71–99.86)
DENV-4	13	12 (92.31)	12	92.31 (76.55–99.81)
All serotypes	74	64 (86.49)	64	86.49 (76.55–93.32)
Total, all serotypes	119	105 (88.24)	102	85.71 (77.12–91.45)

*DENV, dengue virus.
†Determined by PCR.
‡Determined by correspondence with PCR results.

with samples from Vietnam, 15% fewer samples from Sri Lanka had a dominant serotype (Table 1). Serum samples from patients in Sri Lanka cross-reacted only between serotypes 1 and 2 (Appendix Figure 2); however, these samples were collected at a time when the dominant serotype in circulation was switching from DENV-1 to DENV-2 after a DENV-1 outbreak in early 2016 (W. Kumbukgolla, unpub. data). Therefore, this result could be explained by preexisting IgM or, alternatively, by co-infections. However, co-infections were not evident by PCR.

Overall, for 97.1% (102/105) of samples with a dominant serotype, ELISA results corresponded with PCR results; for patients residing in endemic regions, 100% (64/64) of the sample results corresponded, and for returning travelers, 92.7% (38/41) of the sample results corresponded (Table 1). When including the samples for which no dominant serotype was detectable, the overall serotype specificity of the Equad-based ELISA was 85.7% (Table 1); specificity of the ELISA for serum samples from persons in endemic countries was 86.5% and for returning travelers 84.4%. Because of the lower number of dominant serotypes detected, the cohort from Sri Lanka displayed a lower ELISA specificity (81.4%) than did the cohort from Vietnam (95.8%). The serotype results for the PCR-negative group from Vietnam were consistent with the PCR-positive group from Vietnam: ≈80% DENV-1 and ≈20% DENV-2 (Tables 1, 2).

Table 2. Dominant serotype determined by DENV serotype–specific IgM ELISA among DENV PCR–negative cohort (n = 14), Vietnam, 2013–2018*

No. (%) samples with dominant serotype	DENV serotype	No. (%) samples
13 (92.86)	1	10/14 (71.43)
	2	3/14 (21.43)

*DENV, dengue virus.

Analysis of paired serum samples suggests that the results of this Equad-based ELISA are consistent over time and with different initial antibody concentrations (Figure 2). The IgM serotype initially identified as the dominant serotype remained the dominant serotype for at least 8 days (and potentially longer) after symptom onset for both returning travelers and patients residing in DENV-endemic countries, many of whom probably had secondary DENV infections (Appendix Figure 3).

Conclusions

Early identification of the infecting DENV serotype can be a critical component of dengue diagnosis that is also essential to pathologic and epidemiologic monitoring of outbreaks. Because of its long persistence in serum, IgM is a preferred diagnostic marker, especially when viral nucleic acids and NS1 are no longer detectable. However, serologic

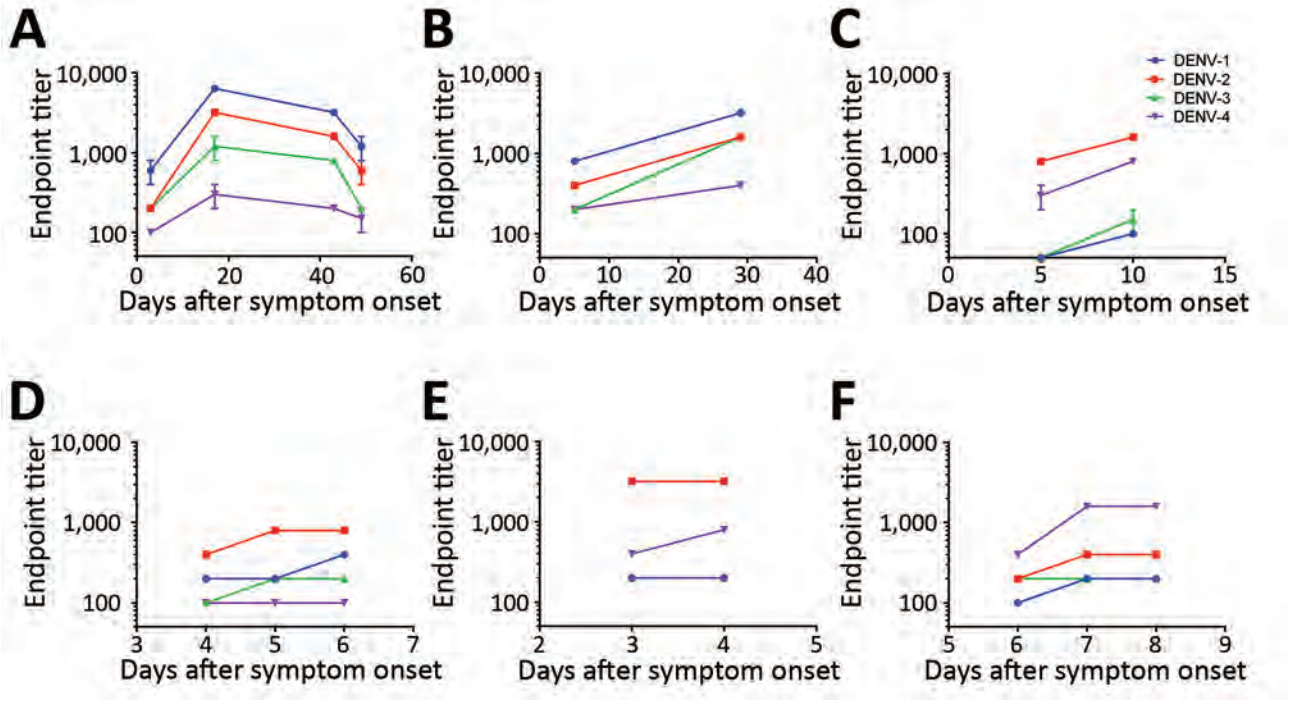

Figure 2. DENV IgM ELISA endpoint titers, by serotype, of paired patient serum samples acquired at 2–4 time points after symptom onset, 2013–2018. A–C) Serum samples from returning travelers with residence in Germany: DENV-1 positive (A, B); DENV-2 positive (C). D–F) Serum samples from residents of DENV-endemic country Sri Lanka: DENV-2 positive (D, E); DENV-4 positive (F). Data lines indicate average titers; error bars indicate SDs. The antigens in the ELISA were Equad proteins (i.e., envelope protein from each DENV serotype with 4 amino acid changes T76R, Q77E, W101R, and L107R). DENV, dengue virus.

determination of the infecting serotype is challenging. Detection of neutralizing antibodies remains the standard method for DENV identification, but interpretation is complicated by the antigenic sin phenomenon in secondary infections (*11*). The possibility of using IgM to determine the infecting serotype was attempted previously (*12–14*), but results were complicated by low specificities, especially for secondary DENV infections. In this study, we analyzed the serotype-specific IgM responses to DENV infections in returning travelers and residents in DENV-endemic regions using recombinant mutated envelope proteins with reduced cross-reactivity (*9*,*10*). The ELISA was able to specifically detect the infecting DENV serotype in 84.4% of travelers and 86.5% of residents in DENV-endemic regions. If a dominant serotype was detected, it corresponded to the PCR result in 100% of cases in DENV-endemic regions. The finding that some sample sets did not have a dominant IgM serotype remains to be explained. Factors such as a change in the DENV serotype during an outbreak (as seen in the Sri Lanka cohort) or differing patient exposure histories could be involved. The study included DENV-3–positive serum samples from returning travelers but not from persons residing in endemic regions. However, results obtained for the other serotypes indicate that specificities were similar for samples from returning travelers and inhabitants of endemic areas.

In summary, our results suggest that specific IgM serotyping can be achieved with an ELISA-based format when using as antigens DENV envelope proteins reduced in cross-reactivity. The test can be optimized further by, for example, varying the serum dilutions tested. By using IgM-based serologic tests, which have broad diagnostic windows (*15*), we can more accurately report epidemiologic outbreak findings.

Parts of this work were supported by the European Union (European Funds for Regional Development grant 100216415). S.U. and A.R. are on a patent application that includes the proteins described in this study. This does not alter their adherence to policies on sharing data and materials.

About the Author

Dr. Rockstroh is a scientist at the Department of Immunology at the Fraunhofer-Institute for Cell Therapy and Immunology in Leipzig, Germany. Her research interest focus is on the serologic diagnosis of flavivirus infections.

References

1. Bhatt S, Gething PW, Brady OJ, Messina JP, Farlow AW, Moyes CL, et al. The global distribution and burden of dengue. Nature. 2013;496:504–7. http://dx.doi.org/10.1038/nature12060
2. Gubler D, Kuno G, Markoff L. Flaviviruses. In: Knipe DM, Howley PM, editors. Fields virology, vol. 1, 5th ed. Philadelphia: Lippincott Williams & Wilkins; 2007. p. 1153–252.
3. Katzelnick LC, Gresh L, Halloran ME, Mercado JC, Kuan G, Gordon A, et al. Antibody-dependent enhancement of severe dengue disease in humans. Science. 2017;358:929–32. http://dx.doi.org/10.1126/science.aan6836
4. Bosch I, de Puig H, Hiley M, Carré-Camps M, Perdomo-Celis F, Narváez CF, et al. Rapid antigen tests for dengue virus serotypes and Zika virus in patient serum. Sci Transl Med. 2017;9:eaan1589. http://dx.doi.org/10.1126/scitranslmed.aan1589
5. Hang VT, Nguyet NM. Trung DT, Tricou V, Yoksan S, Dung NM, et al. Diagnostic accuracy of NS1 ELISA and lateral flow rapid tests for dengue sensitivity, specificity and relationship to viraemia and antibody responses. PLoS Negl Trop Dis. 2009;3:e360.
6. Koraka P, Zeller H, Niedrig M, Osterhaus ADME, Groen J. Reactivity of serum samples from patients with a flavivirus infection measured by immunofluorescence assay and ELISA. Microbes Infect. 2002;4:1209–15. http://dx.doi.org/10.1016/S1286-4579(02)01647-7
7. Crill WD, Chang G-JJ. Localization and characterization of flavivirus envelope glycoprotein cross-reactive epitopes. J Virol. 2004;78:13975–86. http://dx.doi.org/10.1128/JVI.78.24.13975-13986.2004
8. Chabierski S, Barzon L, Papa A, Niedrig M, Bramson JL, Richner JM, et al. Distinguishing West Nile virus infection using a recombinant envelope protein with mutations in the conserved fusion-loop. BMC Infect Dis. 2014;14:246. http://dx.doi.org/10.1186/1471-2334-14-246
9. Rockstroh A, Barzon L, Pacenti M, Palù G, Niedrig M, Ulbert S. Recombinant envelope-proteins with mutations in the conserved fusion loop allow specific serological diagnosis of dengue-infections. PLoS Negl Trop Dis. 2015;9:e0004218. http://dx.doi.org/10.1371/journal.pntd.0004218
10. Rockstroh A, Moges B, Barzon L, Sinigaglia A, Palù G, Kumbukgolla W, et al. Specific detection of dengue and Zika virus antibodies using envelope proteins with mutations in the conserved fusion loop. Emerg Microbes Infect. 2017;6:e99. http://dx.doi.org/10.1038/emi.2017.87
11. Midgley CM, Bajwa-Joseph M, Vasanawathana S, Limpitikul W, Wills B, Flanagan A, et al. An in-depth analysis of original antigenic sin in dengue virus infection [erratum in J Virol. 2011; 85:12100]. J Virol. 2011;85:410–21. http://dx.doi.org/10.1128/JVI.01826-10
12. Nawa M, Yamada KI, Takasaki T, Akatsuka T, Kurane I. Serotype-cross-reactive immunoglobulin M responses in dengue virus infections determined by enzyme-linked immunosorbent assay. Clin Diagn Lab Immunol. 2000;7:774–7.
13. Shu P-Y, Chen L-K, Chang S-F, Su C-L, Chien L-J, Chin C, et al. Dengue virus serotyping based on envelope and membrane and nonstructural protein NS1 serotype-specific capture immunoglobulin M enzyme-linked immunosorbent assays. J Clin Microbiol. 2004;42:2489–94. http://dx.doi.org/10.1128/JCM.42.6.2489-2494.2004
14. Zidane N, Dussart P, Bremand L, Bedouelle H. Cross-reactivities between human IgMs and the four serotypes of dengue virus as probed with artificial homodimers of domain-III from the envelope proteins. BMC Infect Dis. 2013;13:302. http://dx.doi.org/10.1186/1471-2334-13-302
15. Hunsperger EA, Yoksan S, Buchy P, Nguyen VC, Sekaran SD, Enria DA, et al. Evaluation of commercially available diagnostic tests for the detection of dengue virus NS1 antigen and anti-dengue virus IgM antibody. PLoS Negl Trop Dis. 2014;8:e3171. http://dx.doi.org/10.1371/journal.pntd.0003171

Address for correspondence: Sebastian Ulbert, Fraunhofer Institute for Cell Therapy and Immunology, Perlickstrasse 1, Leipzig 04103, Germany; email: sebastian.ulbert@izi.fraunhofer.de

Influenza H5/H7 Virus Vaccination in Poultry and Reduction of Zoonotic Infections, Guangdong Province, China, 2017–18

Jie Wu,[1] Changwen Ke,[1] Eric H.Y. Lau, Yingchao Song, Kit Ling Cheng, Lirong Zou, Min Kang, Tie Song,[2] Malik Peiris, Hui-Ling Yen[2]

We compared the detection frequency of avian influenza H7 subtypes at live poultry markets in Guangdong Province, China, before and after the introduction of a bivalent H5/H7 vaccine in poultry. The vaccine was associated with a 92% reduction in H7 positivity rates among poultry and a 98% reduction in human H7N9 cases.

Human infections with avian influenza A(H7N9) virus have been documented in China since 2013 (*1*). Among 1,220 confirmed H7N9 case-patients during 2013–2017, a total of 73% reported poultry exposure, and 57% had visited live poultry markets (LPMs) before symptom onset (*2*). Because of the lack of apparent clinical signs in poultry infected with low pathogenicity H7N9 influenza virus, it has been challenging to rapidly identify and remove infected poultry at the LPMs or farms and to justify implementation of mandatory vaccination of poultry against this virus. Interventions such as market closure during human epidemics have temporarily reduced human exposure to live poultry and decreased zoonotic infection risk (*3*). However, the effect was not sustainable because H7N9 viruses continue to circulate within the LPM supply chain, leading to recurrent waves of human infections in winter months (*4*).

During winter 2016–17, the H7N9 virus evolved into highly pathogenic avian influenza (HPAI) virus by acquiring a polybasic amino acid motif at the hemagglutinin cleavage site, rendering the virus capable of disseminating systematically and causing high mortality rates among chickens (*5*,*6*). In response to the emergence of HPAI H7N9 virus, the government of China amended the mandatory vaccination regimen for avian influenza in summer 2017. Specifically, a newly developed bivalent H5 (Re-8, based on clade 2.3.4.4 H5N1 virus A/chicken/Guizhou/4/2013) and H7 (Re-1, based on H7N9 virus A/pigeon/Shanghai/S1069/2013) vaccine replaced the previous bivalent H5 vaccine that targeted H5 clades 2.3.4.4 (Re-8) and 2.3.2.1 (Re-6, based on H5N1 virus A/duck/Guangdong/S1322/2010). The new bivalent H5/H7 vaccine was first introduced in Guangdong and Guangxi Provinces in July 2017; other provinces adopted the poultry vaccine by winter 2017–18. The vaccine coverage rate reported in November 2017 in Guangdong was 97.9% (282 million birds) among the target poultry population (*7*), which encompassed chickens, ducks, geese, quail, pigeons, and rare birds in captivity (*8*); however, the reported vaccine coverage varied in different provinces (*8*). Layers and breeders received 2 doses of the H5/H7 vaccine, whereas broilers sold within 70 days received 1 dose (*8*).

To assess the effect of poultry vaccination on H7N9 prevalence in poultry and the subsequent effect on human zoonotic infection risk, we analyzed the temporal distribution of monthly H7N9 detection rates at LPMs and of human H7N9 cases in Guangdong Province during 2013–2018. We estimated the effect of the bivalent H5/H7 vaccine using a Poisson regression model.

The Study

During January 2013–June 2018, a total of 22 collaborating laboratories collected 81,984 environmental samples from 345 retail LPMs and 24 wholesale LPMs distributed in 21 cities in Guangdong Province (*9*). Samples included poultry fecal droppings, drinking water, and various surface swab specimens from cages, chopping boards, display tables, and defeathering machines. Samples were stored in virus transport media (Zijian Biotech, Shenzhen, Lang Shan, China). Influenza A virus RNA segment 7 (M gene) was detected by quantitative real-time reverse transcription PCR (RT-PCR); positive samples underwent further testing to detect H5, H7, or H9 viral RNA using subtype-specific primers and probes (*10*). Human H7N9 infections were reported from 28 hospitals and 22 collaborating laboratories in Guangdong Province and verified by the Guangdong Provincial

Author affiliations: Guangdong Provincial Center for Disease Control and Prevention, Guangdong, China (J. Wu, C. Ke, Y. Song, L. Zou, M. Kang, T. Song); University of Hong Kong, Hong Kong, China (E.H.Y. Lau, K.L. Cheng, M. Peiris, H.-L. Yen)

DOI: https://doi.org/10.3201/eid2501.181259

[1]These authors contributed equally to this article.

[2]These senior authors contributed equally to this article.

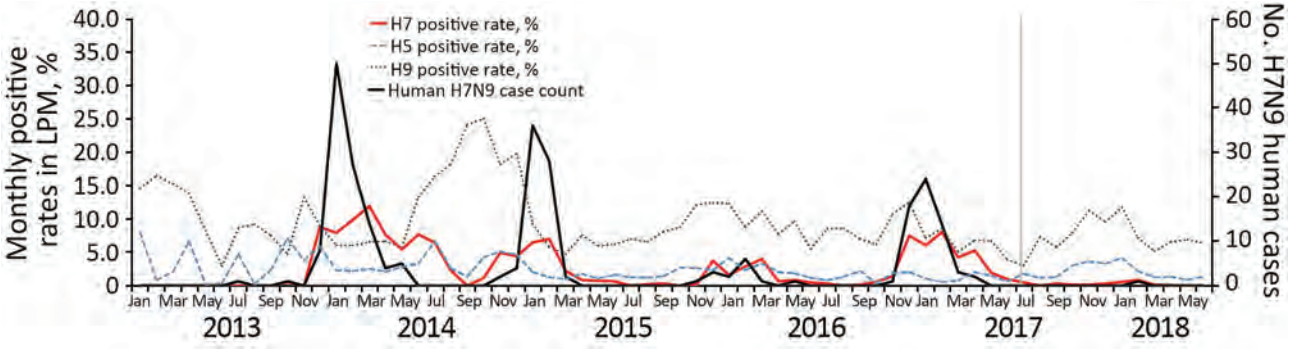

Figure 1. Monthly H5, H7, and H9 positive rates at live poultry markets (LPM) and human H7N9 cases in Guangdong Province, China, January 2013–June 2018. Vertical gray line shows the introduction (July 2017) of the bivalent H5/H7 vaccine in poultry.

Center for Disease Control and Prevention by RT-PCR, virus isolation, or both (*10*).

During the 66-month period of the study, influenza A viral RNA was detected frequently from LPMs; the median monthly positive rate was 22.0% (range 7.4%–48.3%). H9 was the most frequently detected subtype; the median monthly positive rate was 12.1% (range 4.4%–37.6%) (Figure 1). H5 subtype was detected every month at low frequency (median monthly positive rate 3.1% [range 0.3%–11.9%]), whereas H7 subtype was detected at variable frequency (median monthly positive rate 0.6% [range 0%–12.0%]).

The bivalent H5/H7 vaccine was introduced in Guangdong in July 2017. We expected to see its effect on H7 prevalence in poultry and the accompanying human infections after September 2017 because of the 45-day fattening period for broilers before they are traded to the LPMs (*11*). The median H7 positive rate detected at LPMs before (January 2013–August 2017) the introduction of the bivalent H5/H7 vaccine was 0.8% (range 0%–12%). The rate after introduction (September 2017–June 2018) was 0.1% (range 0%–0.8%; $p<0.001$ by *t*-test). The median H5 positive rates detected during the same periods were 3.1% (range 0.3%–11.9%) before introduction and 2.7% (range 1.4%–6.3%) after ($p = 0.727$ by *t*-test). These results suggest that replacing the bivalent H5 vaccine that targeted H5 clades 2.3.4.4 and 2.3.2.1 with the bivalent H5/H7 vaccine that targeted H5 clade 2.3.4.4 alone did not significantly affect the H5 positive rate at LPMs during winter 2017–18.

To further evaluate the effect of the bivalent H5/H7 poultry vaccine, we estimated the expected H7 positive rate at LPMs and the number of human H7N9 cases in Guangdong Province after September 2017 if the vaccination had not been implemented. Using baseline data collected before the vaccination period (January 2013–August 2017), we fitted separate Poisson regression models that described the risk for H7 positive detection in LPMs and of identifying human H7N9 cases in Guangdong Province, allowing for a long-term time trend, annual seasonal patterns, and lower H7N9 virus activity during winter 2015–16. This baseline model accounts for the potential effects of other intervention measures, including market rest days, which were similarly implemented in 2017–18. We plotted the predicted values during the vaccination period (Figure 2) and fitted another model for the full period (July 2013–June 2018) to test the vaccination

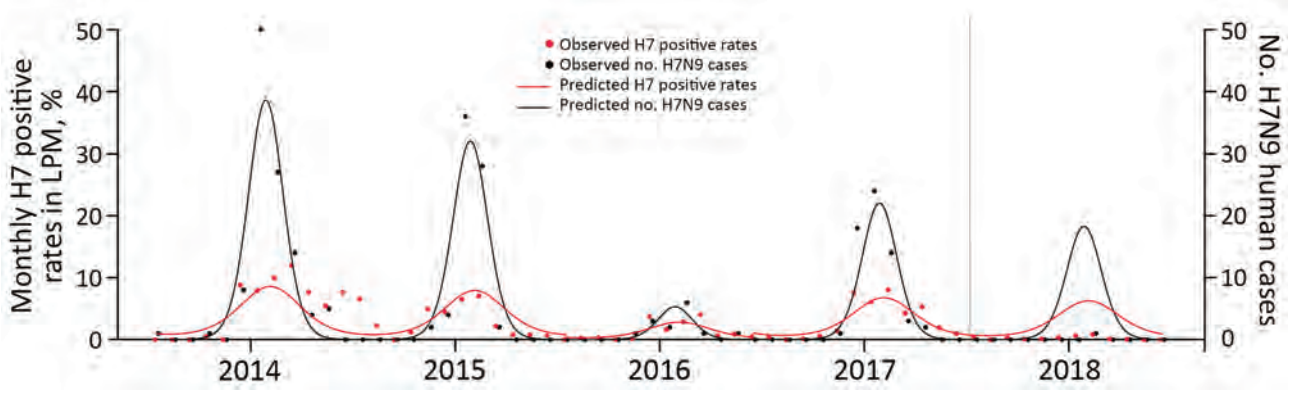

Figure 2. Observed and predicted monthly H7 positive rates at live poultry markets (LPM) and number of H7N9 human cases in Guangdong Province, China, July 2013–June 2018. Vertical gray line shows the introduction (July 2017) of the bivalent H5/H7 vaccine in poultry.

effect by including an indicator variable for the postvaccination period. We estimated relative risks (RRs) and corresponding 95% CIs by fitting the model to data. The bivalent H5/H7 vaccine was associated with a reduction of 92% (RR 0.079, 95% CI 0.057–0.106) in the H7 positive rates at LPMs and 98% (RR 0.021, 95% CI 0.001–0.096) in the number of human H7N9 cases.

Conclusions

Emergence of H7N9 highly pathogenic avian influenza virus during the fifth epidemic wave during winter 2016–17 has prompted the mandatory use of a bivalent H5/ H7 inactivated influenza vaccine in domestic poultry in China. Before then, a bivalent H5 poultry vaccine was used. Our results provided quantitative confirmation for the significant impact of the vaccine in reducing H7 detection frequency at LPMs and the corresponding reduction in human H7N9 infections in Guangdong Province, 1 year after implementation of the vaccine. The focus should be on achieving a high vaccine coverage rate in domestic poultry in which the H7N9 virus has been detected, recognizing that antigenic drift variants that escape vaccine-induced immunity may emerge. A second concern is whether H7N9, which predominantly infected chickens, may adapt to aquatic poultry, such as ducks. Such an event would prove a major challenge for the control strategy.

In conclusion, our analyses of longitudinal surveillance data support the association between the introduction of the bivalent H5/H7 vaccine for poultry and the reduction in zoonotic H7N9 disease. These results illustrate an example of combating zoonotic avian influenza virus at its source in a One Health approach.

Acknowledgments

We thank the 28 hospitals and 22 collaborating laboratories in Guangdong Province that participated in the longitudinal surveillance.

This study was supported by Contract HHSN272201400006C from the National Institute of Allergy and Infectious Diseases, National Institutes of Health, United States, and the Theme-based Research Scheme (Project No. T11-705/14N) from the Government of Hong Kong, China.

About the Author

Dr. Wu is the deputy chief technician for the Institute of Pathogenic Microbes at Guangdong Provincial Center for Disease Control and Prevention. Her research interest is monitoring human infection risk by avian influenza viruses at the human–poultry interface. Dr. Ke is the chief technician for the Institute of Pathogenic Microbes at Guangdong Provincial Center for Disease Control and Prevention. His research interest is pathogenic mechanisms of emerging pathogens.

References

1. World Health Organization. Influenza at the human-animal interface—monthly risk assessment summary. 2018 [cited 2018 Oct 9]. http://www.who.int/influenza/human_animal_interface/Influenza_Summary_IRA_HA_interface_02_03_2018.pdf
2. Wang X, Jiang H, Wu P, Uyeki TM, Feng L, Lai S, et al. Epidemiology of avian influenza A H7N9 virus in human beings across five epidemics in mainland China, 2013–17: an epidemiological study of laboratory-confirmed case series. Lancet Infect Dis. 2017;17:822–32. http://dx.doi.org/10.1016/S1473-3099(17)30323-7
3. Peiris JS, Cowling BJ, Wu JT, Feng L, Guan Y, Yu H, et al. Interventions to reduce zoonotic and pandemic risks from avian influenza in Asia. Lancet Infect Dis. 2016;16:252–8. http://dx.doi.org/10.1016/S1473-3099(15)00502-2
4. Wu J, Lau EH, Xing Q, Zou L, Zhang H, Yen HL, et al. Seasonality of avian influenza A(H7N9) activity and risk of human A(H7N9) infections from live poultry markets. J Infect. 2015;71:690–3. http://dx.doi.org/10.1016/j.jinf.2015.08.007
5. Shi J, Deng G, Kong H, Gu C, Ma S, Yin X, et al. H7N9 virulent mutants detected in chickens in China pose an increased threat to humans. Cell Res. 2017;27:1409–21. http://dx.doi.org/10.1038/cr.2017.129
6. Zhu W, Zhou J, Li Z, Yang L, Li X, Huang W, et al. Biological characterisation of the emerged highly pathogenic avian influenza (HPAI) A(H7N9) viruses in humans, in mainland China, 2016 to 2017. Euro Surveill. 2017;22:30533. http://dx.doi.org/10.2807/1560-7917.ES.2017.22.19.30533
7. Food and Agriculture Organization of the United Nations. H7N9 situation update. 2017 [cited 2018 Oct 9]. http://www.fao.org/ag/againfo/programmes/en/empres/h7n9/wave_6/Situation_update_2017_11_24.html.
8. Food and Agriculture Organization of the United Nations. Chinese-origin H7N9 avian influenza spread in poultry and human exposure. FAO Animal Health Risk Analysis—assessment No. 4. 2018 [cited 2018 Oct 9]. http://www.fao.org/3/i8705en/I8705EN.PDF
9. Kang M, He J, Song T, Rutherford S, Wu J, Lin J, et al. Environmental sampling for avian influenza A(H7N9) in live-poultry markets in Guangdong, China. PLoS One. 2015;10:e0126335. http://dx.doi.org/10.1371/journal.pone.0126335
10. Ke C, Lu J, Wu J, Guan D, Zou L, Song T, et al. Circulation of reassortant influenza A(H7N9) viruses in poultry and humans, Guangdong Province, China, 2013. Emerg Infect Dis. 2014;20:2034–40. http://dx.doi.org/10.3201/eid2012.140765
11. Bingsheng K, Yijun H. Poultry sector in China: structural changes during the past decade and future trends. In: Thieme O, Pilling D, editors. International Poultry Conference. Bangkok: Food and Agriculture Organization of the United Nations; 2007. p. 25–6.

Address for correspondence: Tie Song, Guangdong Provincial Center for Disease Control and Prevention, Guangzhou, Guangdong, China; email: 849762409@qq.com; Hui-Ling Yen, The University of Hong Kong School of Public Health, 6F, Laboratory Block, LKS Faculty of Medicine No. 21 Sassoon Rd, Hong Kong, China; email: hyen@hku.hk

Higher Viral Load of Emerging Norovirus GII.P16-GII.2 than Pandemic GII.4 and Epidemic GII.17, Hong Kong, China

Sarah K.C. Cheung, Kirsty Kwok, Lin-Yao Zhang, Kirran N. Mohammad, Grace C.Y. Lui, Nelson Lee,[1] E. Anthony S. Nelson, Raymond W.M. Lai, Ting F. Leung, Paul K.S. Chan, Martin Chi-Wai Chan

We compared viral load of emerging recombinant norovirus GII.P16-GII.2 with those for pandemic GII.Pe-GII.4 and epidemic GII.P17-GII.17 genotypes among inpatients in Hong Kong. Viral load of GII.P16-GII.2 was higher than those for other genotypes in different age groups. GII.P16-GII.2 is as replication competent as the pandemic genotype, explaining its high transmissibility and widespread circulation.

Norovirus, the leading cause of acute gastroenteritis, evolves through mutation and recombination (*1*). Noroviruses are named by dual nomenclature using the genotype of RNA-dependent RNA-polymerase (RdRp) and major capsid protein (VP1) (*2*). Recently, 2 recombinant noroviruses carrying RdRp genotype GII.P16 with 2 other VP1 genotypes emerged and spread worldwide: GII.P16-GII.4 in the United States and Europe and GII.P16-GII.2 in Europe and Asia in 2016 (*3*–*5*). GII.P16 actively recombined with ≥8 capsid genotypes (*6*–*8*) and may have pandemic potential and lead to a change in norovirus epidemiology. Phylogenetic and sequence analyses indicated that recent GII.P16-GII.2 had no remarkable change on capsid protein compared with earlier GII.2 strains, suggesting that factors other than immune escape or change in affinity for histo–blood group antigens (i.e., host susceptibility) may play a role in the recent reemergence (*6*). We compared the viral load of norovirus GII.P16-GII.2 with pandemic GII.Pe-GII.4 and epidemic GII.P17-GII.17 in a cohort of hospitalized patients in Hong Kong over a 5-year period. Our findings may explain, at least in part, the high transmissibility and widespread circulation of GII.P16-GII.2.

The Study

This study was part of an ongoing molecular surveillance study of norovirus genotype in hospitalized cases in Prince of Wales Hospital, Hong Kong, during August 2012–June 2017. Norovirus genotype distribution has been detailed in earlier reports (*9*,*10*). The fecal norovirus load was determined by a genogroup-specific quantitative real-time reverse transcription PCR (qRT-PCR) assay (*11*) (Appendix, http://wwwnc.cdc.gov/EID/article/25/1/18-0395-App1.pdf) and was expressed as cycle threshold (C_t) value that has been demonstrated in a large-scale analysis of CaliciNet data to associate with host and virologic factors (*12*). A lower C_t value represents a higher norovirus load (Appendix Figure 1). In the data analysis, we stratified cases by 3 patient age groups: <5 years, 5–65 years, and >65 years. Continuous variables between 2 and 3 groups were compared by the Mann-Whitney U test and the Kruskal-Wallis test with Dunn's multiple comparison correction, respectively, by Prism 7 for Mac (GraphPad, https://www.graphpad.com/scientific-software/prism). A 2-tailed p value <0.05 was considered statistically significant.

During the 5-year period, we collected fecal samples at admission from 1,465 hospitalized patients with laboratory-confirmed norovirus gastroenteritis. The median age of patients was 3 years (interquartile range [IQR] 1–50 years); male:female ratio was 1:1.1. Norovirus genotype was successfully determined for 1,269 (86.6%) samples. We excluded 8 (0.6%) patients co-infected with ≥1 norovirus genotype from viral load analysis. The top 3 circulating norovirus genotypes were GII.Pe-GII.4 (n = 657; 51.8%), GII.P17-GII.17 (n = 191; 15.1%), and GII.P16-GII.2 (n = 136; 10.7%).

We found that the viral load was higher for emerging GII.P16-GII.2 norovirus than for pandemic GII.Pe-GII.4 and epidemic GII.P17-GII.17 (Figure, panel A). In young children <5 years of age, the median viral load of GII.P16-GII.2 was as high as that of GII.Pe-GII.4 (median C_t [IQR]: GII.P16-GII.2, 15.2 [12.9–18.8]; GII.Pe-GII.4, 16.7 [14.8–19.0]; p = 0.200). In patients 5–65 years of age, the median viral load of GII.P16-GII.2 was 28-fold higher than that of GII.Pe-GII.4 and 42-fold higher than that of GII.P17-GII.17. In patients >65 years of age, the median viral load of GII.P16-GII.2 was 45-fold higher than that of GII.Pe-GII.4 and 274-fold higher than that of

Author affiliation: The Chinese University of Hong Kong, Hong Kong, China

DOI: https://doi.org/10.3201/eid2501.180395

[1]Current affiliation: Faculty of Medicine and Dentistry, University of Alberta, Edmonton, Alberta, Canada.

GII.P17-GII.17. The median viral load of GII.Pe-GII.4 declined with age, whereas that of GII.P16-GII.2 remained at the same high level among different age groups. GII.P17-GII.17 had the lowest viral load in most comparisons.

We did 2 additional subgroup analyses (sensitivity tests) to validate the robustness of the high viral load observation of GII.P16-GII.2. First, we compared the viral load of cases only during their first season of emergence (i.e., in an immune naive population): for GII.Pe-GII.4, August 2012–June 2013; for GII.P17-GII.17, July 2014–June 2015; and for GII.P16–GII.2, July 2016–June 2017. We observed a trend similar to that of all cases in which viral load of GII.P16-GII.2 was as high as GII.Pe-GII.4 in young children <5 years of age and higher than those of GII.Pe-GII.4 and GII.P17-GII.17 in older children, adults, and the elderly (Figure, panel B). Second, we compared co-circulating GII.P16-GII.2 and GII.Pe-GII.4 in the last season, July 2016–June 2017, to minimize sample processing variation over time. Again, we observed a trend similar to that of all cases and those during first season of emergence (Appendix Figure 2).

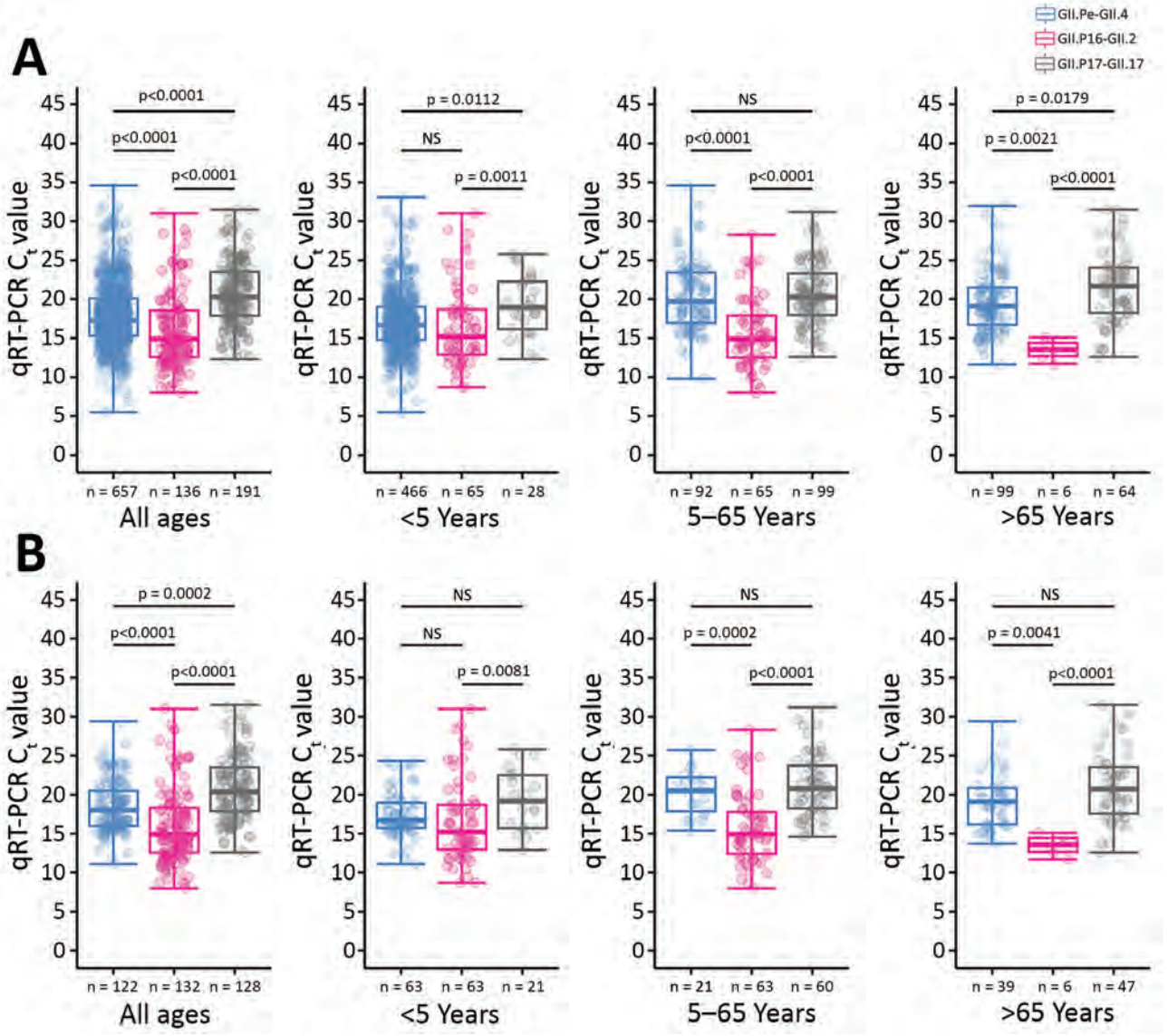

Figure. Higher fecal viral load of recombinant norovirus genotype GII.P16-GII.2 compared with pandemic GII.Pe-GII.4 and epidemic GII.P17-GII.17 among patients in Hong Kong, August 2012–June 2017. A) Results for the whole study period; B) results for the first season of emergence for each genotype: GII.Pe-GII.4, August 2012–June 2013; GII.P16-GII.2, July 2016–June 2017; and GII.P17-GII.17, July 2014–June 2015. Data shown are stratified by age group of patients. Each dot represents a patient; box tops and bottoms indicate interquartile range; horizontal lines within boxes indicate medians; error bars indicate maxima and minima. C_t values were determined by qRT-PCR and used as proxies for norovirus load. A lower C_t value indicates a higher norovirus load. p values were calculated by the Kruskal-Wallis test, with Dunn's multiple comparison corrections. C_t, cycle threshold; NS, not significant; qRT-PCR, quantitative reverse transcription PCR.

To validate the robustness of C_t values, we randomly selected 80 samples (16 samples/season) according to quality control sampling scheme ANSI/ASQ Standard Z1.4 (https://asq.org) for repeat qRT-PCR measurement and inhibition study. We found a strong association between initial and repeat measurements (Spearman r = 0.82; p<0.0001) (Appendix Figure 3). Most samples gave an ideal C_t difference of ≈1 between undiluted and 2-fold diluted templates (median C_t difference [IQR] 1.0 [0.9–1.1]), indicating minimal to mild inhibition (Appendix Figure 4). To exclude the possibility of genotype-specific quantification artifacts, we inspected the amplification efficiency of the assay by testing on 5-fold serial dilution of 3 strains for each virus genotype. The qRT-PCR efficiency in GII.Pe-GII.4 (100.8 ± 5.3%) and GII.P17-GII.17 (99.1 ± 2.6%) was equivalent to that of GII.P16-GII.2 (95.0 ± 4.3%) (p = 0.296 by 1-way ANOVA). We randomly selected 13 of 72 samples with low viral load (C_t >25.0) for primers/probe sequence mismatch analysis; mismatch was noted in only 1 case, indicating that ≥96% samples with low viral load were free of primers/probe mismatch.

Conclusions

We found that GII.P16-GII.2 shed in higher amounts than pandemic GII.Pe-GII.4 in different age groups. This new strain, which is as replication competent as pandemic GII.Pe-GII.4, may cause severe gastroenteritis and lead to poor clinical outcomes (*13*). Our findings imply that the absence of prior exposure to this newly emerged strain may result in the delayed immune response and viral clearance in most populations. Immune naivety may be attributed to equally high viral loads of GII.P16-GII.2 and GII.Pe-GII.4 in children (*1*), providing a virologic explanation for the recent upsurge in the number of outbreaks caused by GII.P16-GII.2 in nursery schools, kindergartens, and elementary schools in Japan in the winter of 2016–17 (*14*). That report found a higher reproductive number of GII.P16-GII.2 compared with the previous 4 seasons, during which other norovirus genotypes, such as GII.Pe-GII.4, predominated, a result consistent with our findings of prominent viral load of GII.P16-GII.2 in children.

Our findings agree with a previous phylogenetic analysis, which showed that the capsid of GII.P16-GII.2 was closely related to earlier GII.2 strains, when it was speculated that its recent emergence may be attributable to high replication efficiency (*6*). Furthermore, recombinants carrying GII.P16, including GII.P16-GII.4 and GII.P16-GII.2, have caused >60% of norovirus outbreaks in 2016 and 2017 in the United States (CaliciNet, https://www.cdc.gov/norovirus/reporting/calicinet/data.html). We propose that this time, rather than acquiring a new capsid variant, a new polymerase variant GII.P16 may be affecting norovirus epidemiology worldwide. This emerging and actively recombining norovirus polymerase genotype GII.P16 is highly transmissible, with pandemic risk. The mechanism behind replication difference among norovirus genotypes needs to be further studied by a virus cultivation system such as human intestinal enteroids (*15*).

Our study has limitations. First, we did not evaluate the viral load of GII.P16-GII.4 because this recombinant was sporadically (n = 21; 1.7%) observed. Second, we did not perform multivariate analysis to control for other confounding factors such as time from symptom onset to sample collection (viral load decreases over time) because of incomplete information, which may have introduced bias.

In summary, our results show that the emerging recombinant norovirus GII.P16-GII.2 is as replication competent as pandemic genotypes, which explains its high transmissibility and widespread circulation. Norovirus GII.P16-GII.2 has pandemic potential.

Acknowledgments

We thank Jenny Chan for providing proofreading and editorial assistance.

This study was supported in part by a grant from the commissioned Health and Medical Research Fund of Food and Health Bureau of the HKSAR Government (CU-15-C2, to M.C.-W.C.).

About the Author

Dr. Cheung is a postdoctoral fellow in the Department of Microbiology of the Chinese University of Hong Kong. Her research interests are norovirus epidemiology and transmission, and the use of advanced technologies such as enteroid model to study norovirus pathogenesis.

References

1. Bányai K, Estes MK, Martella V, Parashar UD. Viral gastroenteritis. Lancet. 2018;392:175–86. http://dx.doi.org/10.1016/S0140-6736(18)31128-0
2. Kroneman A, Vega E, Vennema H, Vinjé J, White PA, Hansman G, et al. Proposal for a unified norovirus nomenclature and genotyping. Arch Virol. 2013;158:2059–68. http://dx.doi.org/10.1007/s00705-013-1708-5
3. Cannon JL, Barclay L, Collins NR, Wikswo ME, Castro CJ, Magaña LC, et al. Genetic and epidemiologic trends of norovirus outbreaks in the United States from 2013 to 2016 demonstrated emergence of novel GII.4 recombinant viruses. J Clin Microbiol. 2017;55:2208–21. http://dx.doi.org/10.1128/JCM.00455-17
4. Ao Y, Wang J, Ling H, He Y, Dong X, Wang X, et al. Norovirus GII.P16/GII.2-associated gastroenteritis, China, 2016. Emerg Infect Dis. 2017;23:1172–5. http://dx.doi.org/10.3201/eid2307.170034
5. Bidalot M, Théry L, Kaplon J, De Rougemont A, Ambert-Balay K. Emergence of new recombinant noroviruses GII.p16-GII.4 and GII.p16-GII.2, France, winter 2016 to 2017. Euro Surveill. 2017;22:30508. http://dx.doi.org/10.2807/1560-7917.ES.2017.22.15.30508
6. Tohma K, Lepore CJ, Ford-Siltz LA, Parra GI. Phylogenetic analyses suggest that factors other than the capsid protein play a

role in the epidemic potential of GII.2 norovirus. mSphere. 2017; 2:e00187–17. http://dx.doi.org/10.1128/mSphereDirect.00187-17
7. van Beek J, de Graaf M, Al-Hello H, Allen DJ, Ambert-Balay K, Botteldoorn N, et al.; NoroNet. Molecular surveillance of norovirus, 2005–16: an epidemiological analysis of data collected from the NoroNet network. Lancet Infect Dis. 2018;18:545–53. http://dx.doi.org/10.1016/S1473-3099(18)30059-8
8. Wang C, Ao Y, Yu J, Xie X, Deng H, Jin M, et al. Complete genome sequence of a novel recombinant GII.P16-GII.1 norovirus associated with a gastroenteritis outbreak in Shandong Province, China, in 2017. Genome Announc. 2018;6:e01483–17. http://dx.doi.org/10.1128/genomeA.01483-17
9. Chan MC, Leung TF, Chung TW, Kwok AK, Nelson EA, Lee N, et al. Virus genotype distribution and virus burden in children and adults hospitalized for norovirus gastroenteritis, 2012–2014, Hong Kong. Sci Rep. 2015;5:11507. http://dx.doi.org/10.1038/srep11507
10. Kwok K, Niendorf S, Lee N, Hung TN, Chan LY, Jacobsen S, et al. Increased detection of emergent recombinant norovirus GII. P16-GII.2 strains in young adults, Hong Kong, China, 2016–2017. Emerg Infect Dis. 2017;23:1852–5. http://dx.doi.org/10.3201/eid2311.170561
11. Kageyama T, Kojima S, Shinohara M, Uchida K, Fukushi S, Hoshino FB, et al. Broadly reactive and highly sensitive assay for Norwalk-like viruses based on real-time quantitative reverse transcription-PCR. J Clin Microbiol. 2003;41:1548–57. http://dx.doi.org/10.1128/JCM.41.4.1548-1557.2003
12. Shioda K, Barclay L, Becker-Dreps S, Bucardo-Rivera F, Cooper PJ, Payne DC, et al. Can use of viral load improve norovirus clinical diagnosis and disease attribution? Open Forum Infect Dis. 2017;4:ofx131. http://dx.doi.org/10.1093/ofid/ofx131
13. Desai R, Hembree CD, Handel A, Matthews JE, Dickey BW, McDonald S, et al. Severe outcomes are associated with genogroup 2 genotype 4 norovirus outbreaks: a systematic literature review. Clin Infect Dis. 2012;55:189–93. http://dx.doi.org/10.1093/cid/cis372
14. Sakon N, Komano J, Tessmer HL, Omori R. High transmissibility of norovirus among infants and school children during the 2016/17 season in Osaka, Japan. Euro Surveill. 2018;23:18-00029. http://dx.doi.org/10.2807/1560-7917.ES.2018.23.6.18-00029
15. Ettayebi K, Crawford SE, Murakami K, Broughman JR, Karandikar U, Tenge VR, et al. Replication of human noroviruses in stem cell-derived human enteroids. Science. 2016;353:1387–93. http://dx.doi.org/10.1126/science.aaf5211

Address for correspondence: Martin Chi-Wai Chan, 1/F, Department of Microbiology, Lui Che Woo Clinical Sciences Building, Prince of Wales Hospital, Shatin, Hong Kong, China; email: martin.chan@cuhk.edu.hk

Autochthonous Transmission of *Coccidioides* in Animals, Washington, USA

Allison E. James, Gabrielle Pastenkos, Daniel Bradway, Timothy Baszler

We report 5 cases of coccidioidomycosis in animals that were acquired within Washington, USA, and provide further evidence for the environmental endemicity of *Coccidioides immitis* within the state. Veterinarians should consider coccidioidomycosis in animals with compatible clinical signs that reside in, or have traveled to, south central Washington.

Since 2010, a total of 13 human cases of coccidioidomycosis have been reported in Washington, USA, that were acquired within the state (*1*). Soil samples from south central Washington were also found to harbor viable *Coccidioides immitis*, and whole-genome sequencing verified that the genotype obtained from soil matched that of the clinical isolate in 1 patient (*2*,*3*). This evidence strongly supports that the organism is endemic in Washington, well north of the previously defined geographic range.

We undertook a thorough search of the Washington Animal Disease Diagnostic Laboratory (WADDL) database to identify all animal coccidioidomycosis cases in which autochthonous transmission was likely to occur. We confirm and report the 3 probable cases that were previously known to WADDL diagnosticians (*4*), as well as 2 newly identified cases. Of the 5 animal cases that have histories compatible with local transmission in Washington, 4 preceded known human cases.

Case Reports

We searched the WADDL database for diagnoses of "coccidioidomycosis," "mycosis, *Coccidioides* spp.," and"osteomyelitis, coccidioidomycosis." All records with owner addresses in Washington were further investigated for a history of travel. We identified 16 animal cases with a diagnosis of coccidioidomycosis since 1990 for which the animal's primary residence was in Washington. We then excluded any cases in animals that had an unknown or unclear travel history or those that traveled outside of Washington, Oregon, Idaho, and Montana, regardless of the amount of time between travel and onset of disease. Thereafter, 5 animals remained that were highly likely to have been exposed to the disease within Washington.

The first case, in a 6-year-old female Labrador retriever, was reported in 1997. Five months before diagnosis, the dog developed a draining abscess caudal to the stifle that recurred after antimicrobial drug and steroid treatment. Subsequent skin biopsy and histopathology examination revealed a pyogranulomatous cellulitis. Fungal culture of the lesion ultimately identified *Coccidioides*, and the diagnosis was confirmed with a fungal DNA probe-hybridization assay (Mayo Clinic, Rochester, MN, USA). The dog resided in Seattle but had a history of only intrastate travel to Yakima, Washington, before the onset of disease. Travel history was obtained from the dog's owner at the time of diagnosis and documented in the WADDL record (Figure, orange diamonds).

The next case was in a 14-year-old female quarter horse that was brought to the Washington State University Veterinary Teaching Hospital (WSU–VTH) in 1999 for a painful swelling in the region of the withers that was unresponsive to antimicrobial drugs. Ultrasound of the lesion revealed a large fluid-filled mass that released purulent fluid when drained. An aspirate of the abscess was submitted for aerobic culture and revealed *Coccidioides* spp. According to documented conversations among WADDL diagnosticians, the owner, and the referring veterinarian, this mare lived in Clarkston, Washington, and had traveled out of state to Prineville and Rufus, Oregon, and Missoula, Montana. Intrastate travel history included Wenatchee and Spokane (Figure, blue circles).

In 2000, a 6-year-old male German wirehaired pointer dog was referred to WSU–VTH for a 4-week history of lameness, diffuse swelling of the right hindlimb, and a draining abscess near the right popliteal lymph node. The lesion had been unresponsive to debridement and antimicrobial drugs. WSU clinicians submitted tissue biopsies for histopathology examination, which revealed pyogranulomatous lymphadenitis and cellulitis. Subsequent fungal culture of the lymph node identified *Coccidioides*. PCR and sequencing using previously published methods confirmed the diagnosis, although this protocol cannot discriminate *C. immitis* from *C. posadasii* (*5*). This animal resided in Prosser, Washington, and was never taken outside the Yakima Valley. Travel history was reported by the owner and documented in WADDL records (Figure, green triangle).

Author affiliation: Washington State University, Pullman, Washington, USA

DOI: https://doi.org/10.3201/eid2501.180411

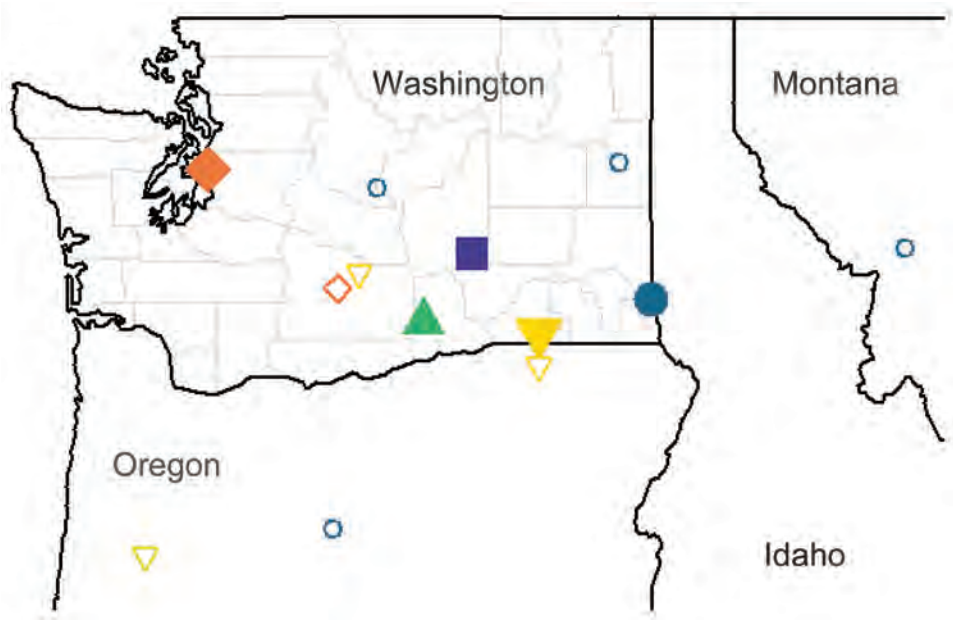

Figure. Locations of primary residence and travel of animals with apparently autochthonous coccidioidomycosis, Washington, USA. Five animals are depicted, each represented by a unique shape/color: orange diamonds, 6-year-old female Labrador retriever; blue circles, 14-year-old female quarter horse; green triangle, 6-year-old male German wirehaired pointer dog; purple square, 7-year-old female quarter horse; yellow inverted triangles, 2-year-old German shorthair pointer dog. Solid shapes depict the animal's primary residence; hollow shapes indicate all travel locations of the 3 animals with local travel history.

A 7-year-old female quarter horse that developed progressively worsening paraparesis over the course of 2 weeks was identified in 2006 after admission to WSU–VTH. A mass over the thoracic spinal vertebrae was noted. Despite aggressive treatment with antimicrobial drugs, the animal's condition rapidly deteriorated. The horse was euthanized; subsequent necropsy revealed a large, locally invasive paravertebral abscess that extended from T5 to T11. Histopathology examination revealed that the abscess was pyogranulomatous, with visible fungal spherules morphologically consistent with *Coccidioides* spp. The diagnosis was confirmed by DNA extraction from paraffin-embedded tissue blocks, followed by PCR and sequencing using methods that do not discriminate *Coccidioides* species (*5*). This horse lived in Othello, Washington, and had no out-of-state travel history according to the owner and documented in the WSU–VTH record (Figure, purple square).

The last case, a 2-year-old German shorthair pointer dog, was brought to WSU–VTH in late 2017 for persistent fever, weight loss, and severe progressive pneumonia that was refractory to multiple antimicrobial drugs. Histopathological findings from a right caudal lung lobectomy revealed severe pyogranulomatous pneumonia with rare fungal spherules. DNA was extracted from tissue samples for PCR and sequence analysis using published primers (*6*). In this case, sequencing confirmed the infection as *C. immitis* with 100% sequence identity to GenBank accession no. KF539899 and others and only 97.3% identity with *C. posadasii*. The primary residence for this dog was in College Place, Washington, although the dog frequently traveled to the Yakima area. The dog had occasionally traveled to Oregon, with multiple visits to Milton-Freewater and a visit to Eugene earlier in 2017 (Figure, yellow inverted triangles).

Conclusions

In Washington, in contrast to other areas endemic for *Coccidioides* spp., animal cases are reported infrequently. Our analysis of the WADDL database has confirmed 5 cases highly likely to have been acquired in Washington, 4 of which were verified using molecular methods. Because we excluded animals with a history of travel to geographic areas traditionally endemic for coccidioidomycosis, regardless of time before clinical signs, it is possible that other animals in the WADDL database acquired the disease locally. Although unlikely, it should also be noted that for the 2 cases with a travel history to Oregon, out-of-state transmission cannot be dismissed.

As with humans, pulmonary disease is the most common clinical finding for coccidioidomycosis in animals, whereas bone and skin lesions are relatively uncommon (*7*,*8*). Of the 5 cases that we identified, 4 initially had extrapulmonary abscesses that were refractory to antimicrobial drugs. Except in rare instances, human and animal infections are acquired from inhalation of the highly infectious environmental form of *Coccidioides*, the arthroconidia (*9*). A few human cases have been reported after exposure to live or dead animals (*10*,*11*). In these cases, the spherule/endospore form has been implicated in human disease after exposure to infected tissues or fluids.

The Washington State Department of Health has worked to increase awareness of coccidioidomycosis with human and animal health providers by hosting community workshops and disseminating informational brochures (R. Wohrle, W. Clifford, D. Kangiser, Washington State Department of Health, pers. comm., 2018 Mar 7). Even so, it is likely that animal cases in Washington are being underdiagnosed and underreported. Canine serologic surveys

would be valuable to determine the extent of exposure within the state and help to elucidate the geographic boundaries of the fungus in the region.

Acknowledgments

We thank Tom Besser and Margaret Davis for their contributions in investigating these cases and Claire Miller for providing her expertise regarding the clinical diagnosis of *Coccidioides* spp.

The Washington Animal Disease Diagnostic Laboratory provided financial support for this work.

About the Author

Dr. James is a clinical assistant professor of veterinary public health at Washington State University in Pullman, Washington, USA. Her research interests include zoonotic diseases, with her primary research focus on relapsing fever *Borrelia* spp.

References

1. Washington Department of Health. Coccidioidomycosis (Valley fever) [cited 2017 Nov 30]. https://www.doh.wa.gov/ForPublicHealthandHealthcareProviders/NotifiableConditions/Coccidioidomycosis
2. Litvintseva AP, Marsden-Haug N, Hurst S, Hill H, Gade L, Driebe EM, et al. Valley fever: finding new places for an old disease: *Coccidioides immitis* found in Washington state soil associated with recent human infection. Clin Infect Dis. 2015;60:e1–3. http://dx.doi.org/10.1093/cid/ciu681
3. Marsden-Haug N, Hill H, Litvintseva AP, Engelthaler DM, Driebe EM, Roe CC, et al.; Centers for Disease Control and Prevention (CDC). *Coccidioides immitis* identified in soil outside of its known range—Washington, 2013. MMWR Morb Mortal Wkly Rep. 2014;63:450.
4. Marsden-Haug N, Goldoft M, Ralston C, Limaye AP, Chua J, Hill H, et al. Coccidioidomycosis acquired in Washington state. Clin Infect Dis. 2013;56:847–50. http://dx.doi.org/10.1093/cid/cis1028
5. Sandhu GS, Kline BC, Stockman L, Roberts GD. Molecular probes for diagnosis of fungal infections. J Clin Microbiol. 1995 ;33:2913–9.
6. Binnicker MJ, Buckwalter SP, Eisberner JJ, Stewart RA, McCullough AE, Wohlfiel SL, et al. Detection of *Coccidioides* species in clinical specimens by real-time PCR. J Clin Microbiol. 2007;45:173–8. http://dx.doi.org/10.1128/JCM.01776-06
7. Graupmann-Kuzma A, Valentine BA, Shubitz LF, Dial SM, Watrous B, Tornquist SJ. Coccidioidomycosis in dogs and cats: a review. J Am Anim Hosp Assoc. 2008;44:226–35. http://dx.doi.org/10.5326/0440226
8. Brown J, Benedict K, Park BJ, Thompson GR III. Coccidioidomycosis: epidemiology. Clin Epidemiol. 2013;5:185–97. http://dx.doi.org/10.2147/CLEP.S34434
9. Sewell DL. Laboratory-associated infections and biosafety. Clin Microbiol Rev. 1995;8:389–405.
10. Gaidici A, Saubolle MA. Transmission of coccidioidomycosis to a human via a cat bite. J Clin Microbiol. 2009;47:505–6. http://dx.doi.org/10.1128/JCM.01860-08
11. Kohn GJ, Linné SR, Smith CM, Hoeprich PD. Acquisition of coccidioidomycosis at necropsy by inhalation of coccidioidal endospores. Diagn Microbiol Infect Dis. 1992;15:527–30. http://dx.doi.org/10.1016/0732-8893(92)90103-Z

Address for correspondence: Allison E. James, Washington State University, Paul G. Allen School for Global Animal Health, PO Box 647040, Pullman, WA 99164-7040, USA; email: allison.eavey.james@wsu.edu

Meat and Fish as Sources of Extended-Spectrum β-Lactamase–Producing *Escherichia coli*, Cambodia

Maya Nadimpalli, Yith Vuthy, Agathe de Lauzanne, Laetitia Fabre, Alexis Criscuolo, Malika Gouali, Bich-Tram Huynh, Thierry Naas, Thong Phe, Laurence Borand, Jan Jacobs, Alexandra Kerléguer, Patrice Piola, Didier Guillemot, Simon Le Hello,[1] Elisabeth Delarocque-Astagneau,[1] on behalf of the BIRDY study group[2]

We compared extended-spectrum β-lactamase–producing *Escherichia coli* isolates from meat and fish, gut-colonized women, and infected patients in Cambodia. Nearly half of isolates from women were phylogenetically related to food-origin isolates; a subset had identical multilocus sequence types, extended-spectrum β-lactamase types, and antimicrobial resistance patterns. Eating sun-dried poultry may be an exposure route.

In Europe, evidence for the spread of extended-spectrum β-lactamase (ESBL)–producing *Escherichia coli* from animals to humans via food is unclear (*1*). Few studies have been conducted in low- and middle-income countries, where colonization rates can exceed 60% (*2*). High ESBL colonization rates in low- and middle-income countries such as Cambodia are usually attributed to unrestricted consumer access to and hospital overuse of third-generation cephalosporins (*3*,*4*). However, antimicrobial drugs in classes critical for human health (e.g., β-lactams, macrolides, aminoglycosides, polymyxins) are increasingly being used in food animals (*5*). In Cambodia, weak public health protections and consumption of undercooked animal products could exacerbate the spread of ESBL-producing *E. coli* or ESBL genes from animals to humans.

We had 2 goals with this study. First, we assessed the prevalence of ESBL-producing or carbapenemase-producing *E. coli* from fish, pork, and chicken from markets in Phnom Penh, Cambodia. Second, we examined the contribution of food-origin isolates to locally disseminated ESBL *E. coli* by comparing isolates from food with isolates from healthy, colonized persons and infected patients.

The Study

During September–November 2016, we purchased 60 fish, 60 pork, and 30 chicken samples from 150 vendors at 2 markets in Steung Meanchey district, Phnom Penh (Appendix Table 2, https://wwwnc.cdc.gov/EID/article/25/1/18-0534-App1.pdf) and tested them at the Institut Pasteur du Cambodge for third-generation cephalosporin- and carbapenem-resistant *E. coli* (Appendix sections 1.1–1.3). We detected ESBL-producing *E. coli* (all CTX-M-type) among 93 (62%) of 150 food samples, including 32 (53%) of 60 fish, 45 (75%) of 60 pork, and 16 (53%) of 30 chicken samples. We identified carbapenem-resistant *E. coli* (OXA-type) from 1 pork and 1 fish sample.

We also selected ESBL-producing *E. coli* from 88 recently pregnant healthy women living in Steung Meanchey and participating in the Bacterial Infections and antibiotic Resistant Diseases among Young children in low-income countries (BIRDY) program, a surveillance program of bacterial infections among young children in low- and middle-income countries (*6*). During September 2015–December 2016, ESBL-producing *E. coli* isolates were cultured from rectal swabs or fecal samples collected at or just after delivery (Appendix Table 3).

We further included ESBL-producing *E. coli* from 15 Phnom Penh–based patients who sought care at the Sihanouk Hospital Center of Hope during November 2015–

Author affiliations: Institut Pasteur, Paris, France (M. Nadimpalli, L. Fabre, A. Criscuolo, B.-T. Huynh, D. Guillemot, S. Le Hello, E. Delarocque-Astagneau); Institut National de la Santé et de la Recherche Médicale, Université de Versailles Saint-Quentin-en-Yvelines and Université Paris-Saclay, Paris (M. Nadimpalli, B.-T. Huynh, D. Guillemot, E. Delarocque-Astagneau); Institut Pasteur du Cambodge, Phnom Penh, Cambodia (Y. Vuthy, A. de Lauzanne, M. Gouali, L. Borand, A. Kerléguer, P. Piola); Assistance Publique/Hôpitaux de Paris, Bicêtre Hospital and Université Paris-Sud, Le Kremlin-Bicêtre, France (T. Naas); Sihanouk Hospital Center of Hope, Phnom Penh (T. Phe); Institute of Tropical Medicine, Antwerp, Belgium (J. Jacobs); K.U. Leuven, Leuven, Belgium (J. Jacobs); Assistance Publique/Hôpitaux de Paris, Raymond-Poincaré Hospital, Garches, France (D. Guillemot, E. Delarocque-Astagneau)

DOI: https://doi.org/10.3201/eid2501.180534

[1]These senior authors contributed equally to this article.

[2]Additional members of the BIRDY study group are listed at the end of this article.

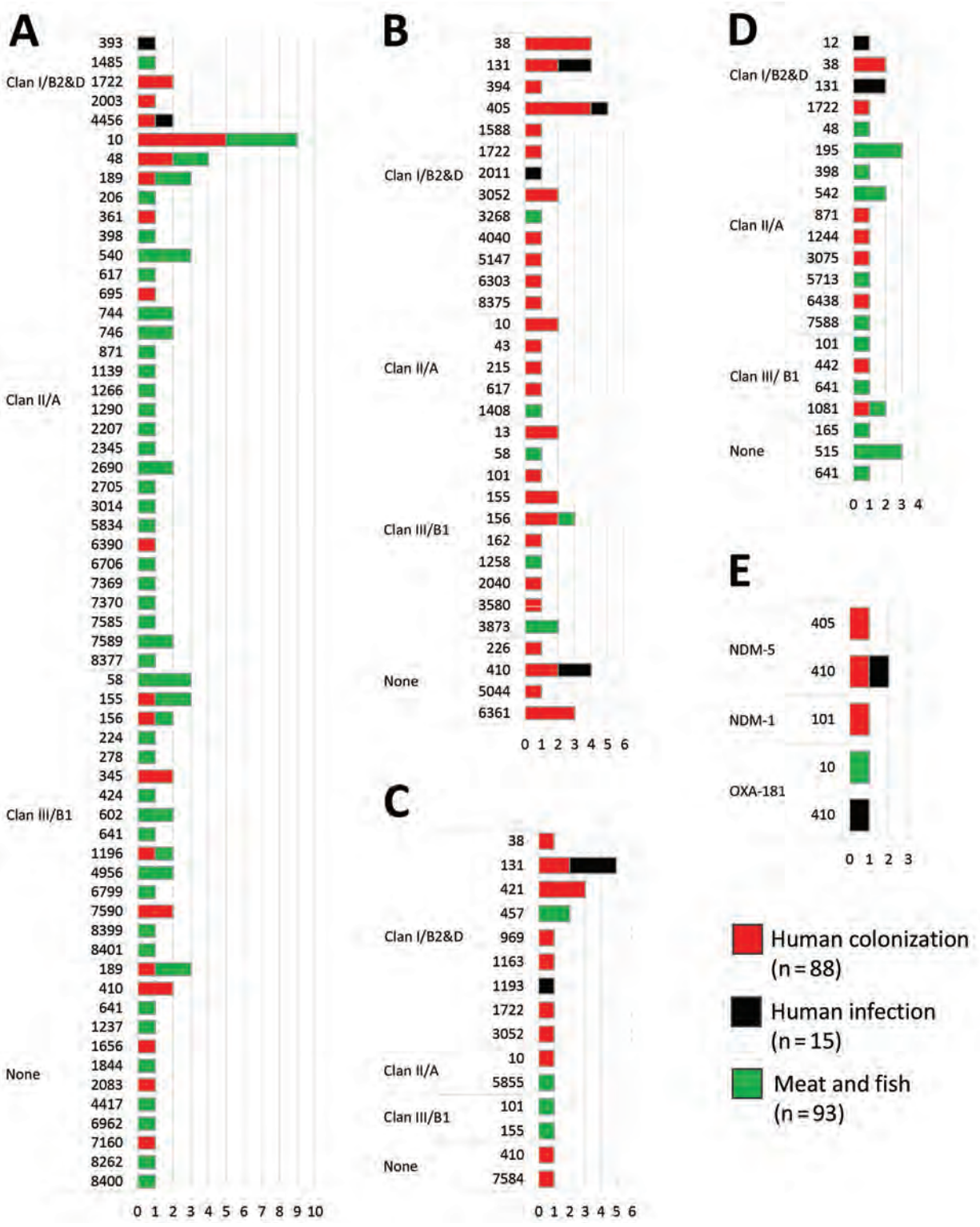

Figure 1. Distribution of 105 multilocus sequence types (MLSTs) among predominant extended-spectrum β-lactamase (ESBL) and carbapenemase gene types encoded by 196 ESBL-producing *Escherichia coli* from humans and food, Cambodia, 2015–2016. A) CTX-M-55; B) CTX-M15; C) CTX-M-27; D) CTX-M-14; E) carbapenemases. Vertical axes depict MLSTs. Horizontal axes depict the frequency of each observed MLST. CTX-M-3, CTX-M-24, and CTX-M-65 are not shown because these ESBL gene types were rare (<2%). One human colonization isolate (ST394, clan I/B2&D) encoded CTX-M-3, 1 food-origin isolate (ST10, clan II/A) encoded CTX-M-24, and 2 food-origin isolates (ST2207, clan II/A and ST7586, clan III/B1) encoded CTX-M-65.

December 2016. ESBL-producing *E. coli* were cultured from blood (12 patients), urine (2 patients), and peritoneal fluid (1 patient) (Appendix Table 4).

We performed whole-genome sequencing for 1 ESBL -producing *E. coli* isolate from each food sample and all human-origin ESBL-producing *E. coli* isolates (Appendix sections 1.4–1.6) and compiled genetic and phenotypic characteristics of these 196 isolates (Appendix Tables 6, 7). We also determined the distribution of multilocus sequence types (MLSTs) encoding predominant ESBL- or carbapenemase-gene types (Figure 1).

Phylogenetic analysis of ESBL-producing *E. coli* genomes revealed 3 distinct clans (Figure 2, panel A). Clan I/B2&D (n = 53) comprised mostly human-origin isolates, including isolates from colonized persons and most infected patients. Clans II/A (n = 69) and III/B1 (n = 47) included isolates from colonized persons and from food but not from infected patients. Each clan comprised an exclusive subset of sequence types (STs); clan I/B2&D included ST131 and clonal complex (CC) 38, clan II/A included CC10, and clan III/B1 included CC58 and CC156. Approximately half (21/39) of isolates in clans II/A and III/B1 from colonized patients belonged to STs detected in both humans and meat (Appendix Table 8).

We determined the distributions of ESBL-encoding genes and resistance patterns among isolates from colonized persons by clan (Figure 2, panels B and C). The $bla_{\text{CTX-M-55}}$ gene was more common among colonization isolates belonging to clan II/A than to clan I/B2&D ($p<0.05$). Amphenicol resistance was more common among colonization isolates belonging to clan II/A than clan I/B2&D ($p<0.05$) and was most often encoded by *floR* (Appendix Table 7).

Women colonized with amphenicol-resistant (vs. amphenicol-susceptible) ESBL-producing *E. coli* were more likely to report having ever eaten dried poultry (adjusted odds ratio 9.0, 95% CI 1.8–45.2) (Table). Women colonized with CTX-M-55–producing *E. coli* (vs. other ESBL types) were more likely to have handled live poultry (adjusted odds ratio 4.6, 95% CI 1.1–19.3), but this exposure was uncommon (11/88).

Our genomic and epidemiologic findings suggest that ESBL-producing *E. coli* that contaminates meat and fish in Phnom Penh may be disseminating to the community. ESBL-producing *E. coli* were highly prevalent among the meat and fish we sampled. More than 80% of food-origin isolates were amphenicol resistant, and two thirds produced CTX-M-55. When food-origin isolates were compared

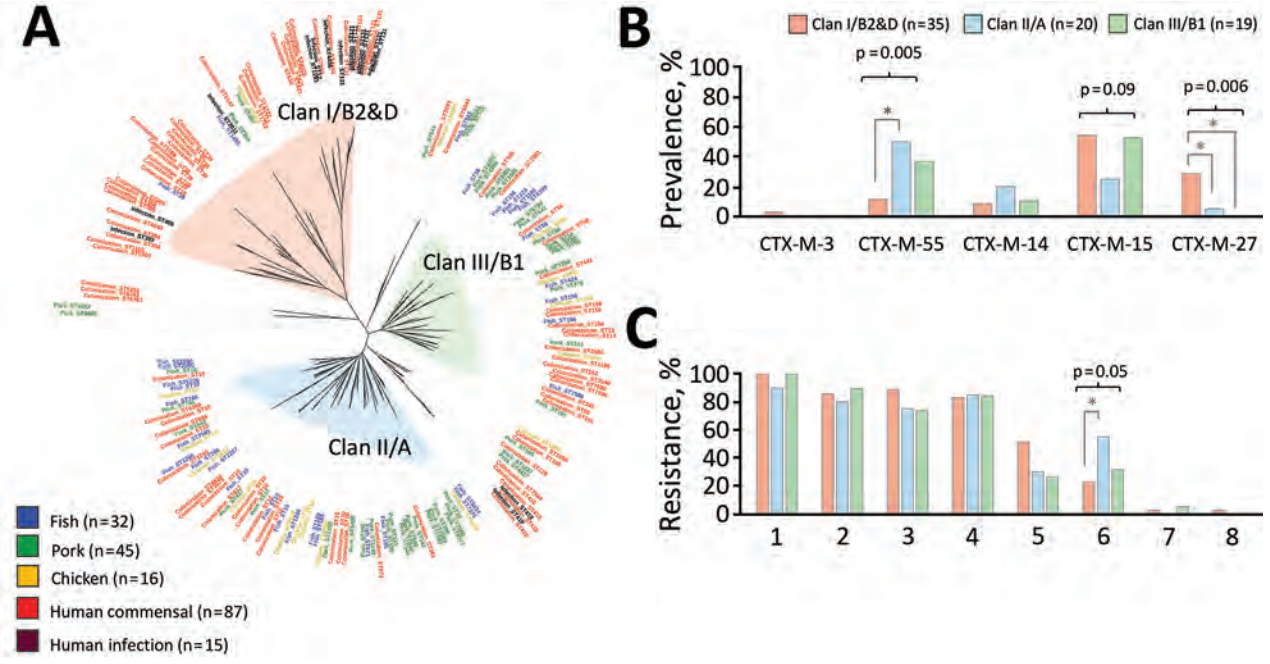

Figure 2. Genomic comparisons of extended-spectrum β-lactamase (ESBL)–producing *Escherichia coli* from humans, fish, pork, and chicken from Cambodia and differences in human colonization isolates by phylogenetic clan. All isolates were phenotypically resistant to third-generation cephalosporins (data not shown). A) Whole-genome sequence-based phylogenetic tree of 195 ESBL-producing *E. coli* genomes comprising 87 human colonization isolates, 15 human clinical isolates, and 93 isolates from fish, pork, and chicken meat and resulting phylogenetic clans I/B2&D (n = 53), II/A (n = 69), and III/B1 (n = 47). B) ESBL-encoding genes of human colonization *E. coli* isolates, by phylogenetic clan. C) Phenotypic resistance of human colonization ESBL-producing *E. coli* isolates to antimicrobial drugs of 8 classes, by phylogenetic clan. Clinical isolates are not included in panels B or C. Of 87 human colonization genomes, 13 did not group into a phylogenetic clan and thus are excluded from panels B and C. Prevalence of outcome differed significantly ($p<0.05$, indicated by *) between 2 indicated clans by post hoc Tukey test. Only statistically significant differences are depicted. 1, quinolone; 2, co-trimoxazole; 3, tetracycline; 4, aminoglycoside; 5, macrolide; 6, amphenicol; 7, carbapenem; 8, colistin.

with human-origin isolates, ≈40% of ESBL-producing *E.coli* from healthy persons grouped into the same phylogenetic clans that comprised most food-origin isolates. Approximately half of these colonization isolates had MLSTs detected among food, and a substantial portion were more likely to produce CTX-M-55 and be amphenicol resistant than colonization isolates that grouped separately. The fact that chloramphenicol has not been used in human medicine for almost 20 years in Cambodia, yet chloramphenicol analogs (e.g., florfenicol, thiamphenicol) are administered to food animals (*5*,*7*), suggests a food origin for these colonizing isolates.

Healthy women colonized with amphenicol-resistant ESBL-producing *E. coli* were more likely to eat poultry meat prepared by sun drying, a process that may not eliminate bacteria (*8*). Although we did not test dried meat samples for ESBL-producing *E. coli* contamination, our finding is consistent with those of other studies (*8*,*9*). Women reported having prepared dried poultry at home. Especially in low-resource households, sun-dried meat may become cross-contaminated by raw meat, dust, animals, and flies (*8*).

Our findings are concerning because of growing interest in using chloramphenicol as a drug of last resort for panresistant strains of bacteria (*10*). In the early 2000s, the Cambodia government stopped purchasing chloramphenicol because of concerns about side effects. Since restriction of this drug, infections in the hospital setting have reverted to a chloramphenicol-susceptible phenotype (*11*). Nevertheless, our findings suggest that amphenicol resistance genes are circulating in the

Table. Environmental exposures and colonization with chloramphenicol-resistant and CTX-M-55–encoding ESBL-producing *Escherichia coli* among healthy women, Phnom Penh, Cambodia, 2015–2016*

	CHL resistance				ESBL type			
Variable	Resistant, no. (%), n = 29	Susceptible, no. (%), n = 59	OR (95% CI)	aOR (95% CI)	CTX-M-55, no. (%), n = 26	Other, no. (%), n = 62	OR (95% CI)	aOR (95% CI)
Persons living in home								
>8	5 (17)	10 (17)	1.1 (0.3–3.7)		3 (12)	12 (19)	0.6 (0.1–2.5)	
6–8	9 (31)	19 (32)	1.1 (0.3–3.7)		10 (38)	18 (29)	1.4 (0.5–3.7)	
≤5	15 (52)	30 (51)	Referent		13 (50)	32 (52)	Referent	
Place of delivery								
Private clinic	5 (17)	17 (29)	0.4 (0.1–1.4)		4 (15)	18 (29)	0.4 (0.1–1.4)	
Hospital	11 (38)	20 (34)	0.8 (0.3–2.2)		9 (35)	22 (35)	0.7 (0.2–1.9)	
Health center	13 (45)	22 (37)	Referent		13 (50)	22 (35)	Referent	
Received antimicrobial drugs at delivery†	2 (7)	11 (19)	0.3 (0.1–1.3)	0.2 (0.0–1.1)	1 (4)	12 (19)	0.2 (0–1.3)	0.2 (0.0–1.4)
Untreated drinking water	5 (17)	7 (12)	1.5 (0.4–5.3)		4 (15)	8 (13)	1.2 (0.3–4.5)	
Toilet shared‡	11 (38)	16 (27)	1.6 (0.6–4.2)		5 (19)	22 (35)	0.4 (0.1–1.3)	
Nonflush toilet	26 (90)	47 (80)	2.2 (0.6–8.5)		24 (92)	49 (79)	3.2 (0.7–15.3)	
Pet contact	6 (21)	13 (22)	0.9 (0.3–2.7)		6 (23)	13 (21)	1.1 (0.4–3.4)	
Live poultry contact	4 (14)	7 (12)	1.2 (0.3–4.4)		6 (23)	5 (8)	3.4 (0.9–12.4)	4.6 (1.1–19.3)
Consumption habits								
Dried pork ≥1×/wk	15 (52)	32 (54)	0.9 (0.4–2.2)		11 (42)	36 (58)	0.5 (0.2–1.3)	
Dried beef	17 (59)	38 (64)	0.8 (0.3–2.1)		20 (77)	35 (56)	2.6 (0.9–7.3)	
Dried poultry	27 (93)	39 (66)	7.9 (1.7–36.4)	9.0 (1.8–45.2)	22 (85)	44 (71)	2.3 (0.7–7.5)	
Pork ≥3×/wk	22 (76)	53 (90)	0.4 (0.1–1.2)	0.2 (0.1–1.1)	23 (88)	52 (84)	1.5 (0.4–5.9)	
Insects	21 (72)	33 (56)	2.2 (0.8–5.7)		16 (62)	38 (61)	1 (0.4–2.6)	
Raw vegetables ≥1×/wk	5 (17)	8 (14)	1.3 (0.4–4.5)		3 (12)	10 (16)	0.7 (0.2–2.7)	

*Blank cells indicate variable not included in multivariate models. aOR, adjusted (for age) OR; CHL, chloramphenicol; ESBL, extended-spectrum β-lactamase; OR, odds ratio.
†Not reported for 4 women (missing data). All 4 were colonized with CHL-susceptible ESBL-producing *Escherichia coli*. One woman was colonized with CTX-M-55–type *E. coli*, whereas the other 3 were colonized with other CTX-M–encoded isolates.
‡With persons in other households.

community, potentially because amphenicol use in food animals has selected for resistant bacteria that can spread to humans (*12*). This possibility is concerning because physicians in Cambodia are often unable to assess the resistance of infectious agents before prescribing antimicrobial drugs (*4*).

Our study had several limitations. First, for logistical reasons, we sampled meat and fish during only 1 season. Contamination rates may have differed had we sampled across seasons (*13*). Second, although we included colonization samples from healthy women, all women had recently given birth in healthcare settings. However, more than half were colonized with ESBL-producing *E. coli* phylotypes A and B1, supporting community-associated, rather than healthcare-associated, acquisition. Third, we were unable to include clinical isolates from the same population that contributed colonization isolates. Thus, differences in colonization and clinical isolates could have resulted from population differences. Fourth, we did not sample food animals, which could have helped confirm that CTX-M-55–type and amphenicol-resistant ESBL-producing *E. coli* circulate among them. Last, we did not investigate additional potential pathways for ESBL-producing *E. coli* transmission to colonized women, such as contact with persons employed at farms or slaughterhouses or proximity to such operations.

Conclusions

This study, which integrated epidemiologic and genomic methods to characterize community, clinical, and environmental data, supports concerns that the dissemination of antimicrobial drug–resistant bacteria from food animals to humans may be more likely in low- and middle-income countries (*14*,*15*). This finding is concerning because meat consumption is projected to drastically increase in these countries, and animal production that relies on routine antimicrobial drug use is being promoted to meet this demand (*14*). Particularly for low- and middle-income countries such as Cambodia, implementation of multisectoral strategies to combat antimicrobial resistance from a One Health perspective must be supported, and food safety should be prioritized.

Collaborators of the BIRDY program: Bodonirina Tanjona Raheliarivao, Frédérique Randrianirina, Perlinot Herindrainy, Zafitsara Zo Andrianirina, Feno Manitra Jacob Rakotoarimanana, Benoit Garin, Jean-Marc Collard, Thida Chon, Sok Touch, Arnaud Tarantola, Sophie Goyet, Siyin Lach, Veronique Ngo, Muriel Vray, Marguerite Diatta, Joseph Faye, Abibatou Ndiaye, Vincent Richard, Abdoulaye Seck, Raymond Bercion, Amy Gassama Sow, Jean Baptiste Diouf, Pape Samba Dieye, Balla Sy, Bouya Ndao, Maud Seguy, Laurence Watier, Abdou Armya Youssouf, and Michael Padget.

Acknowledgments

We thank Kruy Sun Lay for assistance with field study design and implementation; Moul Chanta for collection of meat samples and questionnaire administration; Yem Chailly for questionnaire administration to BIRDY-enrolled women; Sem Nita and Magali Ravel for assistance with laboratory analyses; and all physicians, laboratory staff, field interviewers, and community workers involved in the project. We also thank the Plateforme de Microbiologie Mutualisée of the Pasteur International Bioresources Network from the Institut Pasteur of Paris for genomic sequencing. We are grateful to all women participating in the BIRDY program.

This work was supported by the Dennis and Mireille Gillings Foundation, the US Pasteur Foundation, MSD Avenir, the Monaco Department of International Cooperation, and the Institut Pasteur. The funders had no role in study design, data collection and analysis, decision to publish, or preparation of the manuscript.

About the Author

Dr. Nadimpalli is a postdoctoral research scientist at the Institut Pasteur. She is interested in using genomic and epidemiologic approaches to understand how exposures to animals and the environment can affect human colonization and infection with antimicrobial-resistant bacteria.

References

1. Lazarus B, Paterson DL, Mollinger JL, Rogers BA. Do human extraintestinal *Escherichia coli* infections resistant to expanded-spectrum cephalosporins originate from food-producing animals? A systematic review [cited 2017 Nov 3]. https://academic.oup.com/cid/article-lookup/doi/10.1093/cid/ciu785
2. Woerther P-L, Burdet C, Chachaty E, Andremont A. Trends in human fecal carriage of extended-spectrum β-lactamases in the community: toward the globalization of CTX-M. Clin Microbiol Rev. 2013;26:744–58. http://dx.doi.org/10.1128/CMR.00023-13
3. Laxminarayan R, Duse A, Wattal CM, Zaidi AKL, Wertheim HF, Sumpradit N, et al. Antibiotic resistance—the need for global solutions. Lancet Infect Dis. 2013;13:1057–98. http://dx.doi.org/10.1016/S1473-3099(13)70318-9
4. Om C, Daily F, Vlieghe E, McLaughlin JC, McLaws M-L. "If it's a broad spectrum, it can shoot better": inappropriate antibiotic prescribing in Cambodia. Antimicrob Resist Infect Control. 2016;5:58. http:dx.doi.org/10.1186/s13756-016-0159-7
5. Ström G, Boqvist S, Albihn A, Fernström L-L, Andersson Djurfeldt A, Sokerya S, et al. Antimicrobials in small-scale urban pig farming in a lower middle-income country–arbitrary use and high resistance levels [cited 2018 May 29]. https://aricjournal.biomedcentral.com/articles/10.1186/s13756-018-0328-y
6. Huynh B-T, Kermorvant-Duchemin E, Herindrainy P, Padget M, Rakotoarimanana FMJ, Feno H, et al. Bacterial infections in neonates, Madagascar, 2012–2014. Emerg Infect Dis. 2018;24:710–17. https://dx.doi.org/10.3201/eid2404.161977
7. Nhung NT, Cuong NV, Thwaites G, Carrique-Mas J. Antimicrobial usage and antimicrobial resistance in animal production in Southeast Asia: a review. Antibiotics (Basel). 2016;5:E37. http://dx.doi.org/10.3390/antibiotics5040037

8. Food Safety and Inspection Service. Jerky and food safety [cited 2018 Feb 6]. https://www.fsis.usda.gov/wps/portal/fsis/topics/food-safety-education/get-answers/food-safety-fact-sheets/meat-preparation/jerky-and-food-safety/CT_Index
9. Niumsup PR, Tansawai U, Na-udom A, Jantapalaboon D, Assawatheptawee K, Kiddee A, et al. Prevalence and risk factors for intestinal carriage of CTX-M-type ESBLs in Enterobacteriaceae from a Thai community. Eur J Clin Microbiol Infect Dis. 2018;37:69-75. https://dx.doi.org/10.1007/s10096-017-3102-9
10. Falagas ME, Grammatikos AP, Michalopoulos A. Potential of old-generation antibiotics to address current need for new antibiotics [cited 2017 Nov 2]. http://www.tandfonline.com/doi/full/10.1586/14787210.6.5.593
11. Fox-Lewis A, Takata J, Miliya T, Lubell Y, Soeng S, Sar P, et al. Antimicrobial resistance in invasive bacterial infections in hospitalized children, Cambodia, 2007–2016. Emerg Infect Dis. 2018; 24:841–51.
12. Trongjit S, Angkittitrakul S, Chuanchuen R. Occurrence and molecular characteristics of antimicrobial resistance of *Escherichia coli* from broilers, pigs and meat products in Thailand and Cambodia provinces. Microbiol Immunol. 2016;60:575–85. http://dx.doi.org/10.1111/1348-0421.12407
13. Cohen N, Ennaji H, Bouchrif B, Hassar M, Karib H. Comparative study of microbiological quality of raw poultry meat at various seasons and for different slaughtering processes in Casablanca (Morocco). J Appl Poult Res. 2007;16:502–8. http://dx.doi.org/ 10.3382/japr.2006-00061
14. Lam Y, Fry JP, Hu E, Kim BF, Nachman KE. Industrial food animal production in low-and middle-income countries: a landscape assessment [cited 2017 Nov 3]. https://www.jhsph.edu/research/centers-and-institutes/johns-hopkins-center-for-a-livable-future/_pdf/projects/IFAP/IFAPLowmid_income_countriesWeb1.pdf
15. Nadimpalli M, Delarocque-Astagneau E, Love DC, Price LB, Huynh BTB-T, Collard JMJ-M, et al.; Bacterial Infections and antibiotic-Resistant Diseases among Young children in low-income countries (BIRDY) study group. Combating global antibiotic resistance: emerging One Health concerns in lower- and middle-income countries. Clin Infect Dis. 2018;66:963–9. http://dx.doi.org/10.1093/cid/cix879

Address for correspondence: Maya Nadimpalli, Institut Pasteur, 25 Rue du Docteur Roux, 75724 Paris CEDEX 15, France; email: maya.nadimpalli@gmail.com

Oral Transmission of *Trypanosoma cruzi*, Brazilian Amazon

Rosa Amélia G. Santana, Maria Graças V.B. Guerra, Débora R. Sousa, Kátia Couceiro, Jessica V. Ortiz, Maurício Oliveira, Lucas S. Ferreira, Kenny R. Souza, Igor C. Tavares, Romulo F. Morais, George A.V. Silva, Gisely C. Melo, Gabriel M. Vergel, Bernardino C. Albuquerque, Ana Ruth L. Arcanjo, Wuelton M. Monteiro, João Marcos B.B. Ferreira, Marcus V.G. Lacerda, Henrique Silveira, Jorge Augusto O. Guerra

In the Brazilian Amazon, the suspected source of infection in an outbreak of acute Chagas disease involving 10 patients was *Euterpe oleracea* (açaí berry) juice. Patient blood and juice samples contained *Trypanosoma cruzi* TcIV, indicating oral transmission of the Chagas disease agent.

In Latin America, Chagas disease is prevalent in 21 countries and is one of the most worrisome public health problems on the subcontinent. The social and economic effects among poor and neglected populations are high (*1*). Increasing reports of outbreaks of acute Chagas disease have come to the attention of public health authorities, who regard the disease as emerging in the Amazon (*2*). For most reported outbreaks, epidemiologic investigation points to nonvectored transmission, implicating juices from local fruits (*3*). A major suspected source of infection is *Euterpe oleracea*, the açaí berry, consumed widely as a drink made from a blended pulp (*4*).

Author affiliations: Fundação de Medicina Tropical Dr Heitor Vieira Dourado, Manaus, Brazil (R.A.G. Santana, M.G.V.B. Guerra, D.R. Sousa, K. Couceiro, J.V. Ortiz, M. Oliveira, L.S. Ferreira, G.A.V. Silva, G.C. Melo, G.M. Vergel, W.M. Monteiro, M.V.G. Lacerda, J.A.O. Guerra); Universidade do Estado do Amazonas, Manaus (R.A.G. Santana, M.G.V.B. Guerra, D.R. Sousa, K. Couceiro, J.V. Ortiz, M. Oliveira, K.R. Souza, I.C. Tavares, R.F. Morais, G.C. Melo, W.M. Monteiro, J.M.B.B. Ferreira, J.A.O. Guerra); Fundação de Vigilância em Saúde do Amazonas, Manaus (G.M. Vergel, B.C. Albuquerque, A.R.L. Arcanjo); Instituto Leônidas & Maria Deane, Fiocruz, Manaus (M.V.G. Lacerda); Instituto de Higiene e Medicina Tropical, Universidade Nova de Lisboa, Lisbon, Portugal (H. Silveira)

DOI: https://doi.org/10.3201/eid2501.180646

The Study

On December 29, 2017, a 51-year-old woman with acute febrile syndrome visited a tertiary care center for infectious diseases (Fundação de Medicina Tropical Dr Heitor Vieira Dourado; FMT-HVD) in Manaus, the capital of Amazonas state, Brazil, where malaria is endemic. A routine thick blood smear was negative for *Plasmodium* spp. but positive for *Trypanosoma cruzi* trypomastigotes. The patient mentioned 3 sick relatives in Manaus and 6 more in Lábrea, a municipality 850 km south of Manaus, where she visited often (Table). A common exposure factor among them was ingestion of açaí berry juice, produced by local dealers in the outskirts of Lábrea and sent to Manaus for consumption. Thick blood smears from the other 9 patients, all with acute febrile syndrome, were positive for *T. cruzi*. Of these 10 patients, 8 were clinically assessed at FMT-HVD and submitted samples for direct xenodiagnosis and peripheral blood for *T. cruzi* culture and PCR. A sample of the same juice drunk by all the patients, maintained at –20°C in the family refrigerator in Lábrea, was collected by local health authorities and sent to the reference laboratory in Manaus. All patients with a diagnosis of acute Chagas disease were prescribed benznidazole for 60 days (*5*).

Blood samples were obtained by venipuncture from 8 of the 10 patients, and ≈10 mL of blood was collected into heparin-containing tubes. Next, 100 μL whole blood was distributed into 3 mL liver infusion tryptose medium containing 20% inactivated fetal calf serum and 40 mg/mL gentamycin sulfate and then incubated at 27°C. Inverted optical microscopy was used daily to search for flagellate forms. Xenodiagnosis was conducted by using 20 stage 3 nymphs of *Rhodnius robustus* and *R. prolixus* bugs. We centrifuged 5 μL blood at 4,000 rpm for 10 min and collected the buffy coat for DNA extraction by using the PureLink Kit (Invitrogen, https://www.thermofisher.com).

On December 11, a sample of the açaí juice was transported on ice to FMT-HVD, where it was immediately thawed and centrifuged in 50-mL tubes at 3,000 rpm for 5 minutes. After centrifugation, 3 layers were observed: pulp, an intermediate layer containing fat, and supernatant (Figure 1, panels A and B). From each phase, we suspended 300 μL into 1 mL liver infusion tryptose medium containing 20% inactivated fetal calf serum and 40 mg/mL gentamycin sulfate and incubated it at 27°C. We made triplicate cultures and used inverted optical microscopy to search daily for flagellate forms.

Table. Basic demographics and diagnostic methods used to confirm acute Chagas disease in 10 patients, Brazilian Amazon*

Patient	Patient age, y/sex	Date of diagnosis	Blood smear	Xenodiagnosis	Culture
1	51/F	2017 Dec 29	+	+	+
2	19/F	2017 Dec 29	+	+	+
3	22/M	2017 Dec 29	+	+	+
4	35/F	2018 Jan 5	+	+	+
5	1/F	2018 Jan 5	+	NP	+
6	21/F	2018 Dec 1	+	+	–
7	65/F	2018 Dec 1	+	+	+
8	16/F	2018 Dec 1	–	+	NP
9	11/M	2018 Dec 1	+	NP	NP
10	51/F	2018 Dec 1	+	NP	NP

*NP, not performed; +, positive for *Trypanosoma cruzi*; –, negative for *T. cruzi*.

We placed 200 μL of the açaí culture in 1.5-mL microtubes with 500 μL of phosphate-buffered saline at pH 7.2, incubated the sample in a water bath for 15 minutes at 98°C, and centrifuged it at 3,500 rpm for 3 minutes. We removed 200 μL of supernatant for genotyping.

The nontranscribed spacer of the mini-exon gene was amplified according to the multiplex protocol described elsewhere (*6*). The 150-bp product is characteristic of *T. cruzi* zymodeme Z3 of discrete typing units (DTUs) TcIII or TcIV; 100 bp is characteristic of *T. rangeli*, 200 bp of *T. cruzi* TcI, and 250 bp of *T. cruzi* TcII. Mini-exon gene analysis cannot distinguish between TcIII and TcIV.

All samples were also subjected to mitochondrial and nuclear DNA typing by analyzing polymorphisms in the cytochrome oxidase subunit II (COII) (*7*) and the glucose-phosphate isomerase (GPI) (*8*) genes, respectively. The amplified PCR products were purified by using the Wizard SV Gel and PCR Clean-up System kit (Promega, https://www.promega.com.br) and sequenced. Sequencing was performed with an ABI 3130 DNA sequencer (Applied Biosystems, https://www.thermofisher.com). We followed the BigDye Terminator v3.1 Cycle Sequencing Kit protocol (Applied Biosystems) by using 10–40 ng of purified PCR product in the sequencing reaction and the same primers used for COII and GPI gene amplification by PCR. We used sequences from standard strains: TcI (Silvio X10 cl1), TcII (Esmeraldo cl3), TcIII (M6241 cl6), TcIV (CANIII cl1), TcV (Mn cl2), and TcVI (CL Brener). Maximum-likelihood phylogenetic trees were inferred by using W-IQ-TREE (*9*).

During the outbreak, 8 patients who had drunk the açaí juice were clinically assessed at FMT-HVD. Parasite culture was successful for 6 and xenodiagnoses for 7. A total of 5 *T. cruzi* strains were isolated by blood culture and xenodiagnosis. All 8 patients were *T. cruzi* positive by PCR. Blood culture, xenodiagnoses, and PCR were not performed for 2 patients because they did not attend follow-up at FMT-HVD; their diagnoses were based only on thick blood smears.

After 24 h of incubation, we observed flagellated motile forms in the intermediate layer of fat of centrifuged açaí juice (Figure 1, panel C). *T. cruzi* from human samples and açaí juice showed an identical 150-bp band of mini-exon compatible with *T. cruzi* zymodeme Z3 (*6*), consistent with COII and GPI sequencing results. Parasites differed in position 507 (G/C) of the GPI sequence (Figure 2, panel A). COII sequences were compatible with *T. cruzi* III mitochondrial ancestral lineage (*7*). This set of samples and the reference strains TcIII, TcIV, TcV, and TcVI formed a single cluster that shared a characteristic mitochondrial genome distinct from both TcI and TcII (Figure 2, panel B). GPI sequence analysis showed that the human blood and açaí juice *T. cruzi* samples could be consistently classified as TcIV DTU (*8*) (Figure 2, panel C). Alignments of sequences from COII and GPI *T. cruzi* genes showed that the parasites in the açaí juice were the same.

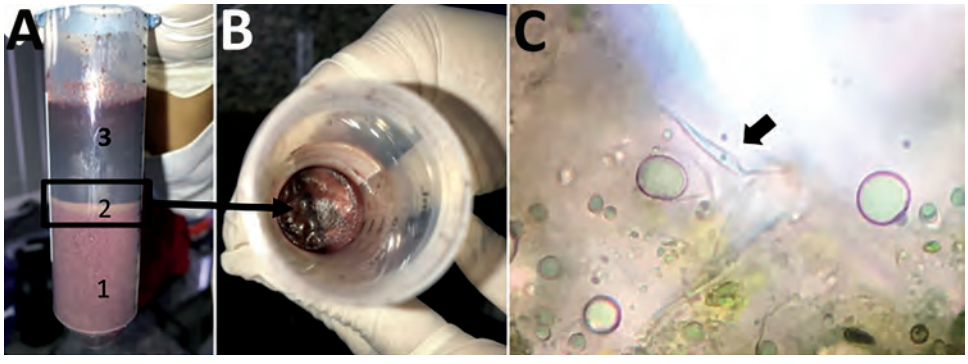

Figure 1. Açaí berry juice sample from Brazilian Amazon. A) A 50 mL-tube after centrifugation shows 3 layers: 1, pulp, 2, intermediate fat (box); and 3: supernatant. B) Top view of layer 2 (arrow). C) Fresh preparation of layer 2 showing *Trypanosoma cruzi* flagellated form (arrow).

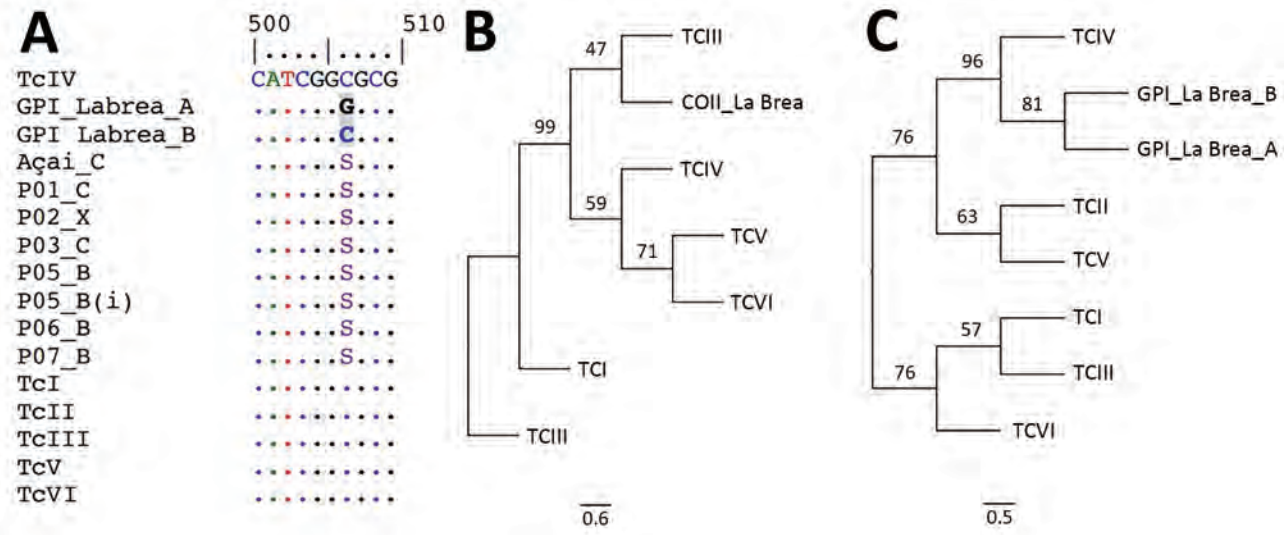

Figure 2. Comparison of *Trypanosoma cruzi* açaí juice samples and Chagas disease patient blood samples, Brazilian Amazon. A) Alignment of GPI sequences from açaí juice samples and patient blood samples. B–C) Phylogenetic position of *T. cruzi* responsible for the 2017 Chagas disease outbreak in the Brazilian Amazon, based on the cytocrome oxidase subunit II gene sequences (best-fit model: Hasegawa-Kishino-Yano) and on the GPI gene sequences (best-fit model: Kimura 2-parameter). The following standard strains obtained from GenBank (discrete typing units [strain name, access no. for COII–GPY]) were used: TcI (SilvioX10 cl4, EU302222.1–Silvio10cl1–AY540730.1), TcII (Esmeraldo cl3, AF359035.1–AY540728.1), TcIII (M6241 cl6, AF359032.1– AY484478.1), TcIV (CANIII cl1–AF359030.1), TcV (Mn cl2, DQ343718.1–AY484480.1), and TcVI (CL Brener, DQ343645.1–XM_815802.1). B, blood; C, culture; GPI, glucose-phosphate isomerase; P0, patient number; X, xenodiagnosis; (i) repetition number. Scale bars indicate number of mutations per site.

Conclusions

All patients who simultaneously exhibited febrile syndrome had consumed açaí juice from the same source in the previous weeks. They were all infected with the same *T. cruzi* DTU as that in the juice, strongly suggestive that in the Brazilian Amazon, contaminated açaí juice is a source of oral contamination with *T. cruzi*. Circumstantial association between outbreaks and contaminated açaí juice has been suggested by previous studies from South America (*10*–*12*), but our evidence of an acute Chagas disease outbreak in which oral transmission could be implicated is robust because patients and a sample of the juice consumed were analyzed in a paired manner.

The most probable hypothesis for contamination of the juice is based on the attraction of contaminated triatomines by the light used during nighttime açaí pulp extraction. Another hypothesis is that contamination occurred during collection and manipulation of açaí berries without use of proper hygiene before mashing (*1*). Triatomine infestation of Amazonian palm trees also supports the potential for oral *T. cruzi* contamination of humans (*13*).

Experimental contamination of food with *T. cruzi* shows that parasite survival varies with the type of food and presence or absence of refrigeration (*14*,*15*). In this study, we hypothesized that the long survival of the parasite is associated with freezing the sample in the presence of cryoprotectants probably present in the fatty content of the açaí juice. On the basis of our demonstration of this route of contamination, legislation should be revised to possibly require pasteurization of açaí juice (*14*).

Acknowledgments

We thank Nelson Fé, Flávio Fé, and Yolanda Noguthi for technical support in the laboratory.

This study was supported by the National Council for Scientific and Technological Development and by the Amazonas Research Foundation.

About the Author

Dr. Santana is a scientist in the Fundação de Medicina Tropical Dr. Heitor Vieira Dourado. His research interests include entomology and epidemiology of neglected infectious diseases, especially Chagas disease and malaria.

References

1. Coura JR, Junqueira AC, Fernandes O, Valente SA, Miles MA. Emerging Chagas disease in Amazonian Brazil. Trends Parasitol. 2002;18:171–6. http://dx.doi.org/10.1016/S1471-4922(01)02200-0
2. Barbosa M, Ferreira JM, Arcanjo AR, Santana RA, Magalhães LK, Magalhães LK, et al. Chagas disease in the state of Amazonas: history, epidemiological evolution, risks of endemicity and future perspectives. Rev Soc Bras Med Trop. 2015;48(Suppl 1):27–33. http://dx.doi.org/10.1590/0037-8682-0258-2013
3. Blanchet D, Brenière SF, Schijman AG, Bisio M, Simon S, Véron V, et al. First report of a family outbreak of Chagas disease

in French Guiana and posttreatment follow-up. Infect Genet Evol. 2014;28:245–50. http://dx.doi.org/10.1016/j.meegid.2014.10.004
4. Xavier SC, Roque AL, Bilac D, de Araújo VA, da Costa Neto SF, Lorosa ES, et al. Distantiae transmission of *Trypanosoma cruzi*: a new epidemiological feature of acute Chagas disease in Brazil. PLoS Negl Trop Dis. 2014;8:e2878. https://dx.doi.org/10.1371/journal.pntd.0002878
5. Rodriques Coura J, de Castro SL. A critical review on Chagas disease chemotherapy. Mem Inst Oswaldo Cruz. 2002;97:3–24. http://dx.doi.org/10.1590/S0074-02762002000100001
6. Fernandes O, Santos SS, Cupolillo E, Mendonça B, Derre R, Junqueira AC, et al. A mini-exon multiplex polymerase chain reaction to distinguish the major groups of *Trypanosoma cruzi* and *T. rangeli* in the Brazilian Amazon. Trans R Soc Trop Med Hyg. 2001;95:97–9. http://dx.doi.org/10.1016/S0035-9203(01)90350-5
7. de Freitas JM, Augusto-Pinto L, Pimenta JR, Bastos-Rodrigues L, Gonçalves VF, Teixeira SM, et al. Ancestral genomes, sex, and the population structure of *Trypanosoma cruzi.* PLoS Pathog. 2006;2:e24. http://dx.doi.org/10.1371/journal.ppat.0020024
8. Gaunt MW, Yeo M, Frame IA, Stothard JR, Carrasco HJ, Taylor MC, et al. Mechanism of genetic exchange in American trypanosomes. Nature. 2003;421:936–9. http://dx.doi.org/10.1038/nature01438
9. Trifinopoulos J, Nguyen LT, von Haeseler A, Minh BQ. W-IQ-TREE: a fast online phylogenetic tool for maximum likelihood analysis. Nucleic Acids Res. 2016;44:W232-5. http://dx.doi.org/10.1093/nar/gkw256
10. Steindel M, Kramer Pacheco L, Scholl D, Soares M, de Moraes MH, Eger I, et al. Characterization of *Trypanosoma cruzi* isolated from humans, vectors, and animal reservoirs following an outbreak of acute human Chagas disease in Santa Catarina State, Brazil. Diagn Microbiol Infect Dis. 2008;60:25–32. http://dx.doi.org/10.1016/j.diagmicrobio.2007.07.016
11. Monteiro WM, Magalhães LKC, de Sá ARN, Gomes ML, Toledo MJdO, Borges L, et al. Trypanosoma cruzi IV causing outbreaks of acute Chagas disease and infections by different haplotypes in the western Brazilian Amazonia. PLoS ONE 2012;7:e41284. https://doi.org/10.1371/journal.pone.0041284
12. Noya BA, Díaz-Bello Z, Colmenares C, Ruiz-Guevara R, Mauriello L, Muñoz-Calderón A, et al. Update on oral Chagas disease outbreaks in Venezuela: epidemiological, clinical and diagnostic approaches. Mem Inst Oswaldo Cruz. 2015;110:377–86. http://dx.doi.org/10.1590/0074-02760140285
13. Dias FB, Quartier M, Diotaiuti L, Mejía G, Harry M, Lima AC, et al. Ecology of *Rhodnius robustus* Larrousse, 1927 (Hemiptera, Reduviidae, Triatominae) in Attalea palm trees of the Tapajós River Region (Pará State, Brazilian Amazon). Parasites Vect. 2014;7:154. https://doi.org/10.1186/1756-3305-7-154
14. Añez N, Crisante G. Survival of culture forms of Trypanosoma cruzi in experimentally contaminated food [in Spanish]. Bol Malariol Salud Ambient. 2008;48:91–9.
15. Barbosa RL, Pereira KS, Dias VL, Schmidt FL, Alves DP, Guaraldo AM, et al. Virulence of *Trypanosoma cruzi* in Açai (*Euterpe oleraceae* Martius) pulp following mild heat treatment. J Food Prot. 2016;79:1807–12. http://dx.doi.org/10.4315/0362-028X.JFP-15-595

Address for correspondence: Marcus V.G. Lacerda, Fundação de Medicina Tropical Dr Heitor Vieira Dourado, Av Pedro Teixeira 25, Manaus 69040-000, AM, Brazil; email: marcuslacerda.br@gmail.com

etymologia revisited

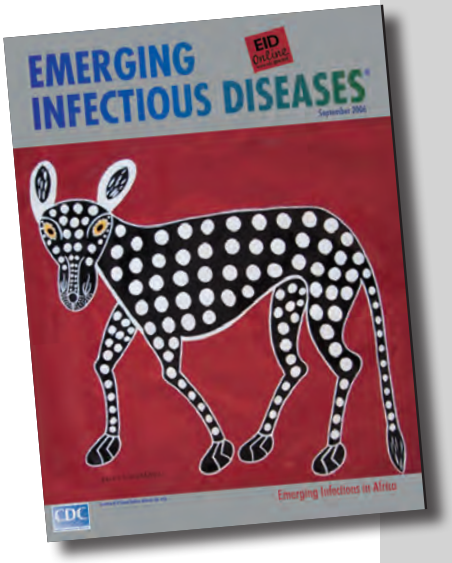

Originally published in September 2006

Trypanosoma [tri-pan′′o-so′mə]

From the Greek trypanon, "*borer*," plus sōma, "*body*," Trypanosoma is a genus of hemoflagellate protozoa, several species of which are pathogenic in humans. *Trypanosoma cruzi,* the etiologic agent of Chagas disease, is transmitted from its vector to humans in the insect's feces, not its saliva, as is the case with most other arthropodborne organisms, including *Trypanosoma brucei,* the etiologic agent of sleeping sickness.

Sources: Dorland's illustrated medical dictionary. 30th ed. Philadelphia: Saunders; 2003 and wikipedia.org

https://wwwnc.cdc.gov/eid/article/12/9/et-1209_article

Avian Influenza A(H9N2) Virus in Poultry Worker, Pakistan, 2015

Muzaffar Ali, Tahir Yaqub, Nadia Mukhtar, Muhammad Imran, Aamir Ghafoor, Muhammad Furqan Shahid, Muhammad Naeem, Munir Iqbal, Gavin J.D. Smith, Yvonne C.F. Su

Avian influenza A(H9N2) virus isolated from a poultry worker in Pakistan in 2015 was closely related to viruses detected in poultry farms. Observed mutations in the hemagglutinin related to receptor-binding affinity and antigenicity could affect cross-reactivity with prepandemic H9N2 vaccine strains.

Influenza A(H9N2) virus circulates in domestic poultry, and outbreaks have been recorded since the early 1990s in China (*1*). In Pakistan, H9N2 virus was first detected in a poultry outbreak in 1998; subsequent outbreaks have led to increased genetic diversifications of distinct viral lineages descended from H9N2 G1 lineage viruses (*2*). Serologic studies of H9 virus among persons of different occupations in Pakistan who had direct exposure to poultry (e.g., poultry workers, vaccinators, veterinarians) have shown high rates of seropositivity (30%–85%) (*3*–*5*). Although no human infection with H9N2 virus has been reported from Pakistan, sporadic clinical cases of H9N2 virus infection in humans have been reported in China (*6*), Hong Kong (*7*), and Bangladesh (*8*). We report the isolation of H9N2 virus from a poultry worker during avian influenza virus surveillance in Pakistan.

The Study

During January 2015–June 2016, avian influenza virus (AIV) surveillance was conducted in poultry farms throughout 19 districts of Punjab Province, Pakistan (*9*). In addition, after obtaining written informed consent, we collected 117 nasal swab specimens from male poultry workers 25–35 years of age. The Institutional Ethical Review Board at the Institute of Public Health (Lahore, Pakistan) reviewed and approved the study protocol.

Sterile swabs were used to take nasal swab samples from humans; the swabs were placed in sterile tubes containing 2 mL of viral transport media. To prevent cross-contamination between samples, human and chicken samples were collected in different zip-sealable plastic bags and transported on ice to the laboratory. Human and chicken samples were also processed and cultured separately on different dates. Individual human samples were inoculated in 9-day-old embryonated chicken eggs and amnio-allantoic fluid (AAF) harvested after 48 h incubation. Harvested AAF was first tested by hemagglutination assay, and positive AAF screened for H5, H7, H9, and Newcastle disease virus (NDV) using hemagglutination inhibition (HI) assay as previously described (*9*).

We detected 1 H9-positive sample collected from a poultry worker in Narowal District, Punjab, where only 1 (1.1%) of 88 chicken samples was H9N2-positive (*9*), and the flock from the same farm was H9 negative. The 36-year-old worker did not display major signs of influenza-like illness, which is typical of the mild to no symptoms shown in H9N2 virus infection (*10*). No human samples were positive for H5 or H7 virus. The virus isolate was confirmed as H9N2 by reverse transcription PCR, and the hemagglutinin (HA) and neuraminidase (NA) genes were sequenced as described (*9*). We sequenced the HA and NA genes of 8 additional viruses isolated from chickens in different districts of Punjab (Table 1).

We analyzed 2,751 H9NX and 8,059 HXN2 avian and human virus sequences (collected during 1963–2017) obtained from GenBank and the GISAID database (https://platform.gisaid.org) and reconstructed large H9-HA and N2-NA phylogenies using maximum-likelihood (ML) analysis. We then subsampled the datasets to a final dataset of 145 sequences for each H9-HA and N2-NA. Reconstruction of temporal phylogenies was performed as previously described (*11*). H9-HA (Figure; Appendix Figure 1, https://wwwnc.cdc.gov/EID/article/25/1/18-0618-App1.pdf) and N2-NA (Appendix Figure 2) phylogenies show that, within the G1 lineage, the human H9N2 isolate (A/Pakistan/486/2015) formed a strongly supported monophyletic group with chicken H9N2 viruses collected in Pakistan from 2015 to 2016. The HA and NA genes of A/Pakistan/486/2015 (H9N2) showed close genetic resemblance (99.8%–99.9% nt identity) with 2015–2016 Pakistan chicken viruses, most likely indicating direct cross-species transmission from poultry to human. These 2015–2016

Author affiliations: University of Veterinary and Animal Sciences, Lahore, Pakistan (M. Ali, T. Yaqub, M. Imran, A. Ghafoor, M.F. Shahid); Health Care Department, Government of Punjab, Lahore (N. Mukhtar); Bahauddin Zakariya University, Multan, Pakistan (M. Naeem); The Pirbright Institute, Compton Laboratory, Newbury, UK (M. Iqbal); Duke University, Durham, North Carolina, USA (G.J.D. Smith); Duke-National University Singapore Medical School, Singapore (G.J.D. Smith, Y.C.F. Su)

DOI: https://doi.org/10.3201/eid2501.180618

Table 1. H9-HA and N2-NA influenza virus sequences isolated from poultry and a human, Punjab, Pakistan, 2015–2016*

Virus isolate	Collection date	Host	District	GenBank accession no.	
				HA	NA
A/chicken/Pakistan/12CF/2015	2015 May 19	Commercial chicken	Lahore	MH930826	MH930508
A/chicken/Pakistan/540CF/2015	2015 Jun 8	Commercial chicken	Gujranwala	MH930827	MH930509
A/chicken/Pakistan/740CF/2015	2015 May 29	Commercial chicken	Layyah	MH930828	MH930510
A/chicken/Pakistan/870CF/2015	2015 Jul 11	Commercial chicken	Sharqpur	MH930829	MH930511
A/chicken/Pakistan/1108CF/2016	2016 Apr 30	Commercial chicken	Rawalpindi	MH930830	MH930512
A/chicken/Pakistan/401BYP/2015	2015 Jun 30	Backyard chicken	Narowal	MH930831	MH930513
A/chicken/Pakistan/654BYP/2015	2015 Dec 12	Backyard chicken	Rawalpindi	MH930832	MH930514
A/chicken/Pakistan/800BYP/2016	2016 Jun 26	Backyard chicken	Sharqur	MH930833	MH930515
A/Pakistan/486/2015	2015 Nov 19	Human	Narowal	MH930834	MF280171

*HA, hemagglutinin; NA, neuraminidase.

Pakistan viruses are further grouped within sublineage B2 (*2*), which also includes viruses isolated during 2008–2014 from Afghanistan, Iran, and Pakistan. The mean times to the most recent common ancestor (tMRCAs) of the HA and NA genes for the 2015–2016 Pakistan strains were both estimated as late 2010 (Table 2), and sublineage B2 mean tMRCAs were estimated as 2005–2006. Together, these results indicate the circulation of unsampled virus diversity in poultry during the past decade, hindering our ability to investigate virus transmission and evolution of H9N2 virus in Pakistan and highlighting the need for systematic surveillance.

All 2015–2016 Pakistan lineage viruses possessed a leucine (L) residue at position 226 (H3 numbering) in the HA receptor-binding site (RBS), which is associated with greater affinity for α-2,6 binding. However, HA residue 228 (H3 numbering) in the RBS was glutamine (G), known for avian-like receptor specificity. All 2015–2016 Pakistan lineage viruses possessed a low pathogenic motif (KSSR/G) in the HA cleavage site. To further characterize the recent evolution of H9N2 viruses in Pakistan, we mapped the HA and NA amino acid substitutions onto the phylogenetic trees and used Mixed Effects Model of Evolution (MEME) analysis to detect amino acids under positive selection, as previously described (*11*). Three amino acid substitutions were present at the ancestral node of the HA of the 2015–2016 Pakistan lineage, T103I, L150N, and V393I (mature H9 protein numbering), although only residue 150 (H3 numbering 160) was under positive selection. One additional substitution, T186A (H3 numbering 196), was present in the human isolate A/Pakistan/486/2015 (H9N2). Both of these mutations are situated in the antigenic region of the H9-HA globular head and correspond to H3N2 epitope B (*12*). The biologic function of mutations at the remaining residues is not known. In addition, the HA phylogeny also indicated that 2015–2016 Pakistan viruses had diverged from lineages containing the 3 H9N2 G1 lineage candidate vaccine viruses (A/Hong Kong/1073/99, A/Hong Kong/33982/2009, and A/Bangladesh/994/2011) (Appendix Figure 1). These vaccine candidates may therefore not provide efficient protection against the avian 2015–2016 Pakistan lineage, although this assumption must be confirmed by antigenic assays.

No deletion in the NA gene, associated with aquatic to terrestrial host adaptation and increased replication in ferrets (*13*), was observed in the 2015–2016 Pakistan lineage viruses. Numerous substitutions were observed in the 2015–2016 Pakistan lineage viruses (Appendix Figure 2). Of these, the Q39R, K47E, and I62T mutations are functionally key residues in the NA stalk that may be associated with host adaptation and virus virulence (*13*). The mutations at 372 and 401 residues may be responsible for hemadsorption activity of the NA (*14*). The functional importance of the remaining mutations is unknown, including V263I that was under positive selection.

Conclusions

Our detection and isolation of H9N2 virus from a poultry worker in Pakistan highlights the potential for cross-species transmission of H9 viruses in the country. The World Health Organization considers avian H9N2 viruses a consistent pandemic threat because they are widespread in poultry and cause sporadic infection in humans. H9N2 viruses have been central to the generation of other viruses of pandemic concern and have contributed the internal genes to both H5 and H7 viruses in China (*15*). Although the subtype is relatively well studied in China, investigation in other countries is generally limited in scope. Within Pakistan, H9N2 viruses in chickens have circulated endemically for at least a decade, yet systematic surveillance is lacking.

Our results show continued diversification of H9N2 viruses in Pakistan; viruses isolated during 2015–2016 formed a distinct clade to earlier viruses from Afghanistan, Iran, and Pakistan isolated during 2008–2014. Dating analysis further estimated the tMRCA of the 2015–2016 Pakistan viruses as late 2010, indicating at least 5 years of unsampled virus diversity that circulated in poultry. We also observed mutations in HA related to changes in receptor-binding affinity and antigenicity that could affect cross-reactivity with the World Health Organization–recommended prepandemic H9N2 vaccine strains. None of the 3 G1 candidate vaccine viruses are closely related to strains from Pakistan.

Phylogenetic relationships indicate H9N2 virus transmission across South Asia and the Middle East,

Figure. Evolutionary relationships of the influenza A virus H9-HA gene isolated from avian and human hosts, Pakistan, 1998–2016. The phylogeny was generated using the uncorrelated lognormal relaxed molecular clock, the SRD06 codon position model, HKY85 plus gamma substitution model, and a Gaussian Markov random field (GMRF) Bayesian skyride in BEAST version 1.8.4. Two independent runs of 100 million Markov chain Monte Carlo generations were performed. Horizontal node bars represent the 95% highest posterior density intervals. Red branches indicate new sequences generated from this study, and the new human isolate is marked by a red star. Black arrows indicate the amino acid mutations (H9 numbering) for the 2015–2016 Pakistan lineage, and asterisk indicates site under positive selection.

Table 2. Estimated tMRCA of influenza A(H9N2) virus sublineages, Pakistan*

Gene and lineage	tMRCA (date)		
	Mean	Upper 95% HPD	Lower 95% HPD
H9-HA			
Sublineage B1	2003.27 (2003 Apr 10)	2003.86 (2003 Nov 11)	2002.62 (2002 Aug 16)
Sublineage B2	2005.81 (2005 Oct 24)	2006.70 (2006 Sep 14)	2004.74 (2004 Sep 29)
2015–2016 (Pakistan)	2010.95 (2010 Dec 14)	2012.49 (2012 Jun 29)	2009.32 (2009 Apr 28)
N2-NA			
Sublineage B2	2006.84 (2006 Nov 4)	2007.89 (2007 Nov 22)	2005.74 (2005 Sep 29)
2015–2016 (Pakistan)	2010.71 (2010 Sep 18)	2012.23 (2012 Mar 26)	2009.29 (2009 Apr 17)

*HA, hemagglutinin; HPD, highest posterior density; NA, neuraminidase; tMRCA, time to the most recent common ancestor.

where the persistence and circulation of AIV are poorly understood. Increased surveillance in wild bird populations, poultry farms and markets, and occupationally exposed workers is needed in these regions to identify the emergence of antigenic variants and to maintain up-to-date H9 vaccine candidates.

Acknowledgments

We thank the Influenza Laboratory at the Department of Microbiology, University of Veterinary and Animal Sciences Lahore, Pakistan, for providing facilities, funded by Biotechnology and Biological Sciences Research Council, UK (project no. BB/L018853/1).

The study was supported by the Duke-National University Singapore Signature Research Programme funded by the Ministry of Health, Singapore, and by contract HHSN272201400006C from the National Institute of Allergy and Infectious Disease, National Institutes of Health, US Department of Health and Human Services. M.A. was supported by a fellowship from the International Research Support Initiative Program administered by the Higher Education Commission of Pakistan.

About the Author

Mr. Ali is a PhD student at the University of Veterinary and Animal Sciences, Lahore, Pakistan, and performed part of this work while an International Research Support Initiative Program fellow at Duke-National University Singapore Medical School. His research focuses on the evolution of avian influenza viruses.

References

1. Li C, Yu K, Tian G, Yu D, Liu L, Jing B, et al. Evolution of H9N2 influenza viruses from domestic poultry in Mainland China. Virology. 2005;340:70–83. http://dx.doi.org/10.1016/j.virol. 2005.06.025
2. Lee D-H, Swayne DE, Sharma P, Rehmani SF, Wajid A, Suarez DL, et al. H9N2 low pathogenic avian influenza in Pakistan (2012–2015). Vet Rec Open. 2016;3:e000171. http://dx.doi.org/10.1136/vetreco-2016-000171
3. Ahad A, Rabbani M, Yaqub T, Younus M, Mahmood A, Zubair M, et al. Serosurveillance to H9 and H7 avian influenza virus among poultry workers in Punjab Province, Pakistan. Pak Vet J. 2013;33:107–12.
4. Rasheed M, Rehmani SF, Iqbal M, Ahmad A, Akhtar F, Akhtar R, et al. Seropositivity to avian influenza virus subtype H9N2 among human population of selected districts of Punjab, Pakistan. Journal of Infection and Molecular Biology. 2013;1:32–4.
5. Ahad A, Thornton RN, Rabbani M, Yaqub T, Younus M, Muhammad K, et al. Risk factors for H7 and H9 infection in commercial poultry farm workers in provinces within Pakistan. Prev Vet Med. 2014;117:610–4. http://dx.doi.org/10.1016/j.prevetmed.2014.10.007
6. Pan Y, Cui S, Sun Y, Zhang X, Ma C, Shi W, et al. Human infection with H9N2 avian influenza in northern China. Clin Microbiol Infect. 2018;24:321–3. http://dx.doi.org/10.1016/j.cmi.2017.10.026
7. Butt KM, Smith GJ, Chen H, Zhang LJ, Leung YH, Xu KM, et al. Human infection with an avian H9N2 influenza A virus in Hong Kong in 2003. J Clin Microbiol. 2005;43:5760–7. http://dx.doi.org/10.1128/JCM.43.11.5760-5767.2005
8. Food and Agriculture Organization. EMPRES-I Global Animal Disease Information System [cited 2018 Apr 3]. http://empres-i.fao.org
9. Ali M, Yaqub T, Mukhtar N, Imran M, Ghafoor A, Shahid MF, et al. Prevalence and phylogenetics of H9N2 in backyard and commercial poultry in Pakistan. Avian Diseases. In press 2018.
10. Khan SU, Anderson BD, Heil GL, Liang S, Gray GC. A systematic review and meta-analysis of the seroprevalence of influenza A(H9N2) infection among humans. J Infect Dis. 2015;212:562–9. http://dx.doi.org/10.1093/infdis/jiv109
11. Su YC, Bahl J, Joseph U, Butt KM, Peck HA, Koay ES, et al. Phylodynamics of H1N1/2009 influenza reveals the transition from host adaptation to immune-driven selection. Nat Commun. 2015;6:7952. http://dx.doi.org/10.1038/ncomms8952
12. Wan Z, Ye J, Xu L, Shao H, Jin W, Qian K, et al. Antigenic mapping of the hemagglutinin of an H9N2 avian influenza virus reveals novel critical amino acid positions in antigenic sites. J Virol. 2014;88:3898–901. http://dx.doi.org/10.1128/JVI.03440-13
13. Diederich S, Berhane Y, Embury-Hyatt C, Hisanaga T, Handel K, Cottam-Birt C, et al. Hemagglutinin-neuraminidase balance influences the virulence phenotype of a recombinant H5N3 influenza A virus possessing a polybasic HA0 cleavage site. J Virol. 2015;89:10724–34. http://dx.doi.org/10.1128/JVI.01238-15
14. Uhlendorff J, Matrosovich T, Klenk H-D, Matrosovich M. Functional significance of the hemadsorption activity of influenza virus neuraminidase and its alteration in pandemic viruses. Arch Virol. 2009;154:945–57. http://dx.doi.org/10.1007/s00705-009-0393-x
15. Zhu H, Lam TT-Y, Smith DK, Guan Y. Emergence and development of H7N9 influenza viruses in China. Curr Opin Virol. 2016;16:106–13. http://dx.doi.org/10.1016/j.coviro.2016.01.020

Address for correspondence: Gavin J.D. Smith, Duke-National University Singapore Medical School, Programme in Emerging Infectious Diseases, 8 College Rd, Singapore 169857, Singapore; email: gavin.smith@duke-nus.edu.sg

Puumala Hantavirus Genotypes in Humans, France, 2012–2016

Jean-Marc Reynes,[1] Damien Carli, Damien Thomas,[2] Guillaume Castel

The analysis of the nucleoprotein gene of 77 Puumala hantavirus strains detected in human samples in France during 2012–2016 showed that all belonged to the Central European lineage. We observed 2 main clusters, geographically structured; one included strains with the Q64 signature and the other strains with the R64 signature.

Puumala virus (PUUV) is the main hantavirus detected in Europe. Several variants of this enveloped trisegmented RNA virus species have been reported, comprising PUUV stricto sensu, detected in humans, and the Asian Hokkaido and Muju viruses, not yet detected in humans. PUUV variant, hosted in the wild by the bank vole (*Myodes glaerolus*), is responsible for a mild hemorrhagic fever with renal syndrome called nephropathia epidemica (*1*,*2*). Within the variant PUUV, 8 lineages have been described, according to phylogenetic analysis of the small (S) RNA segment coding domain sequence (CDS) of the strains. Each lineage is constituted by well-supported and geographically structured clusters of variants, supporting the hypothesis of a hantavirus/host co-evolution (*3*,*4*). Furthermore, it has been shown that this genetic diversity may affect the molecular detection of PUUV in humans (*5*). Consequently, the genotyping of local PUUV strains is also essential for laboratory diagnostics.

PUUV is also the main hantavirus detected in France. Approximately 100 human hospitalized cases are detected annually, all of them located in the northeastern part of the country (*6*). Sequences of 7 PUUV strains have been studied so far, and all were detected in bank voles (*7*,*8*). We report the analysis of the S segment CDS for the nucleoprotein N from 77 additional strains detected in human cases in France during 2012–2016.

The Study

As part of our surveillance assignment, using serologic and molecular assays, we detected 470 laboratory-confirmed human hantavirus cases from 2012–2016 in France, including Tula virus (n = 1), Seoul virus (n = 6), and PUUV (n = 228) infections (*6*). We did not obtain strains from all samples for several reasons, including the absence of molecular testing because of lack of samples, samples being taken too long after the date of onset, and inadequate sample storage temperature before reception in our laboratory. We detected 162 PUUV strains using both real-time PCR and nested reverse transcription PCR (RT-PCR) (*9*,*10*), 33 using real-time PCR, and 33 using nested RT-PCR. The discordance of results between the 2 techniques could be explained by a viral load in the sample close to our limit of detection. We identified these 228 PUUV strains in 28 of the 34 hantavirus-endemic departments (administrative divisions) in France (*6*). We used 3 overlapping heminested RT-PCRs to obtain the S segment sequences. After sequencing by Sanger method, we obtained the entire S CDS from 77 strains coming from 17 departments (Appendix Tables 1,2, https://wwwnc.cdc.gov/EID/article/25/1/18-0270-App1.pdf). We deposited PUUV sequences in GenBank (accession nos. MG923598–MG923674). We mapped strains according to the municipality of exposure. We used ClustalW and Muscle implemented in MEGA7 (https://www.megasoftware.net) (*8*) to align the S segment CDS and to deduce aa sequences from these strains and from 115 other PUUV strains published and available in GenBank (as of December 1, 2017). We then ordered the sequences according to aa similarity. We conducted maximum-likelihood phylogenetic analysis with 1,000 bootstrap replicates by using PhyML version 3.0 (http://www.atgc-montpellier.fr/phyml) implemented in Seaview version 4.6.1 (*8*), on the basis of the S segment CDS using a representative sample in which sequences were identical at the aa level, to reduce the size of the tree. We also performed phylogenetic analysis on the generalized time-reversible model with a gamma distribution (GTR+Γ) with 4 rate categories, with the assumption that a certain fraction of sites are evolutionarily invariable according to the best-fit substitution model proposed by SMS version 1.8.2, available online on the ATGC bioinformatics platform (http://www.atgc-montpellier.fr/sms).

Author affiliations: Institut Pasteur, Lyon, France (J.-M. Reynes, D. Carli, D. Thomas); CBGP, INRA, CIRAD, IRD, Montpellier SupAgro, Université Montpellier, Montpellier, France (G. Castel)

DOI: https://doi.org/10.3201/eid2501.180270

[1]Current affiliation: Institut Pasteur, Paris, France.

[2]Current affiliation: Laboratoire P4 INSERM Jean Mérieux, Lyon, France.

The phylogenetic analysis showed that the PUUV S CDS were grouped into the 8 lineages as previously described (*3*,*4*). All of the PUUV sequences from France detected in humans belonged to the Central European lineage (Figure 1). We distinguished 2 main sublineages, the first harboring the aa signature Q64 and including strains from Belgium and Germany (*3*), and the second with strains harboring an arginine (R) amino acid at position 64. Within this cluster, strains isolated from bank voles in the Loiret department (coded 45) cluster together with branch support of 100; they share the K258 signature (*8*) with the human strain 2012.00086 isolated in the Nièvre department (coded 58), neighbor of the Loiret department (Figure 1). Of note, strains from the Q64 cluster were from the northeast part of the endemic region, whereas the strains from the R64 clusters were detected in the south of the endemic area, except for strains carrying the I276 residue; those came from the northwest part of the endemic region in the Oise department (coded 60), where the Q64 cluster was co-circulating (Figure 2).

Several real-time RT-PCRs targeting the PUUV S segment have been implemented to diagnose PUUV infection

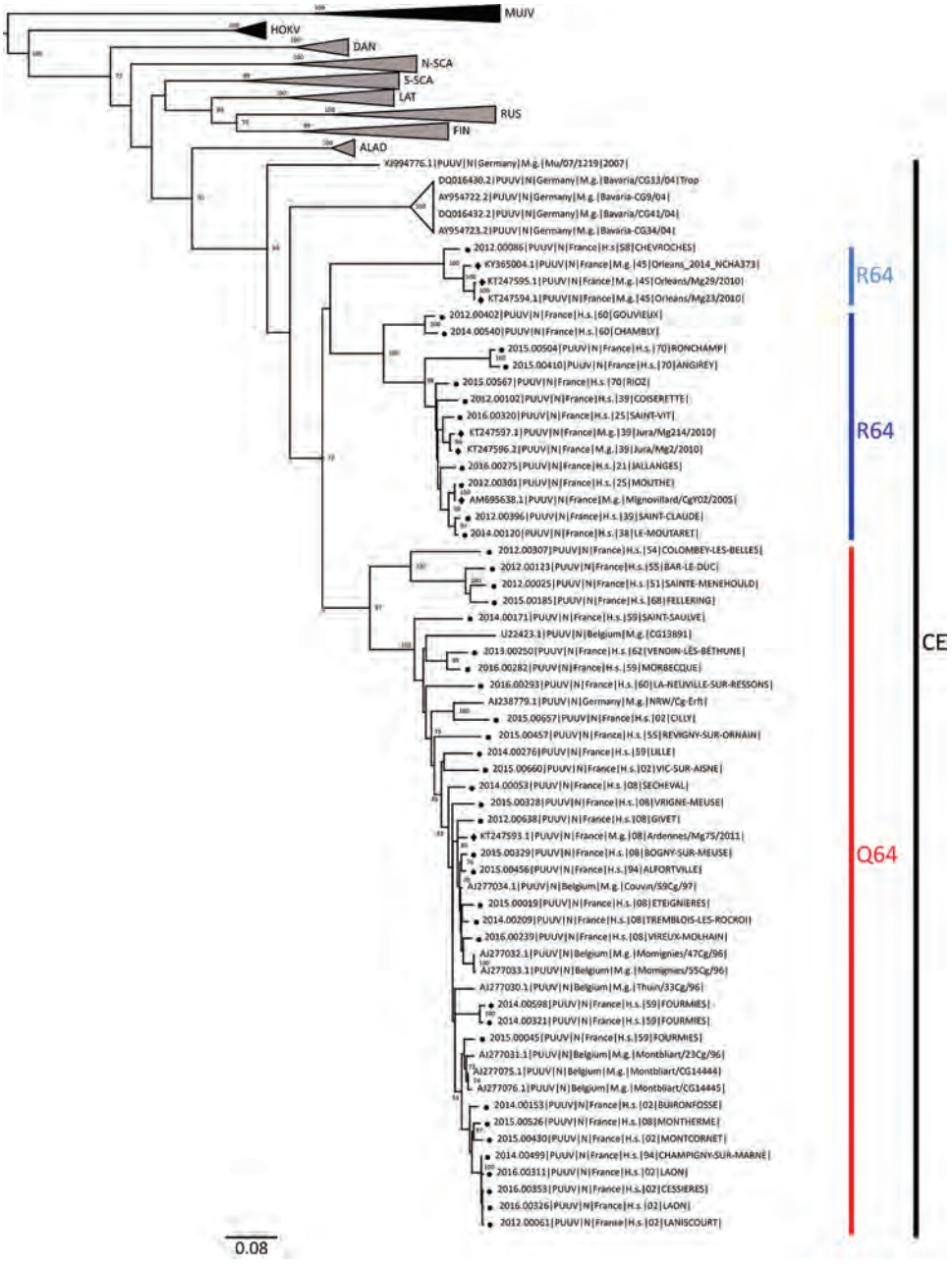

Figure 1. Phylogenetic tree constructed using the maximum-likelihood approach based on the complete small-segment RNA nucleotide coding sequences of representative Puumala virus (PUUV) strains detected in human cases in France, 2012–2016 (circles), and on those published and representative of PUUV strains detected in Europe. Diamonds indicate sequences of strains detected in rodents as reported elsewhere (*7*,*8*). Bootstrap percentages ≥70% (from 1,000 resamplings) are indicated at each node; GenBank accession numbers are indicated for reference strains. Scale bar indicates nucleotide substitutions per site. ALAD, Alpe-Adrian lineage; CE, Central European lineage; DAN, Danish lineage; FIN, Finnish lineage; LAT, Latvian lineage; N-SCA, north-Scandinavian lineage; S-SCA; south-Scandinavian lineage; RUS, Russian lineage; MUJV, Muju virus; HOKV, Hokkaido virus.

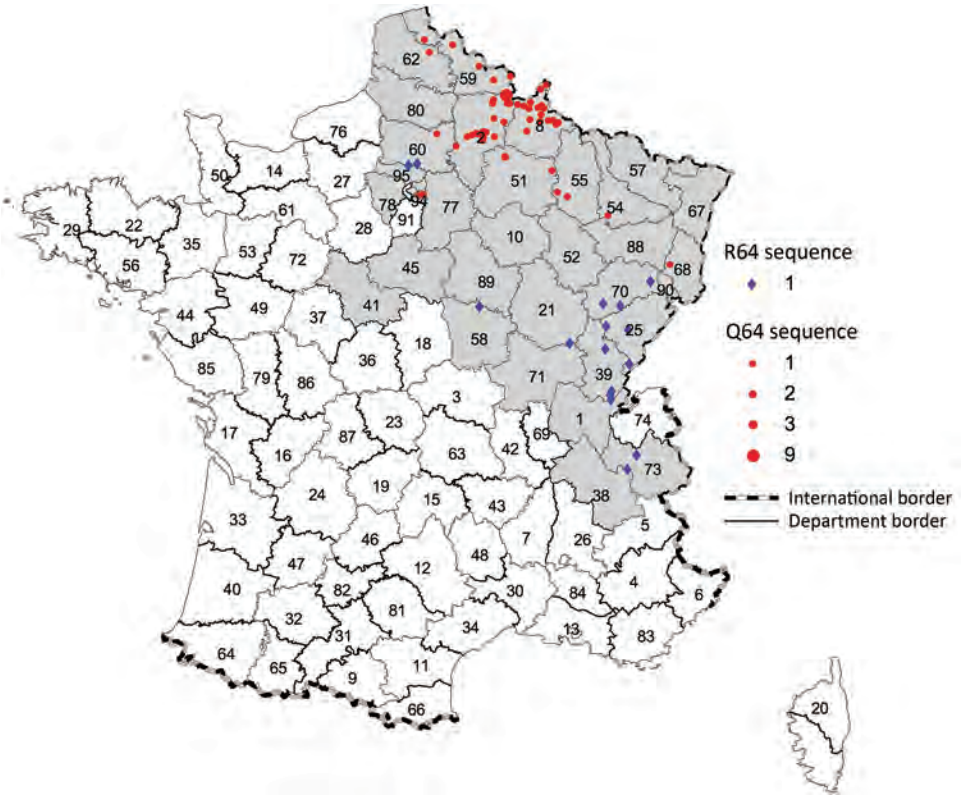

Figure 2. Location of the Puumala virus small segment RNA coding domain sequence sublineages Q64 and R64 detected in human cases, by municipality of exposure, France, 2012–2016. Gray shading indicates the hantavirus-endemic area; red circles indicate Q64 sequences, by size; blue diamonds indicate R64 sequences.

in humans (*5*,*9*,*11*–*14*). We detected some mismatches between the sequences of the France strains and those of the primers and probes (for example, at the 3′ end of the forward primer designed by Garin D et al. [*12*]), which could jeopardize the detection of some PUUV strains from France (Appendix Figure). However, we did not perform assays to evaluate this hypothesis.

Conclusions

Genomic findings from this study revealed that the 77 PUUV strains studied and detected in humans in France during 2012–2016 all belonged to the Central European lineage. Within this lineage, the strains were clustered within 2 sublineages, with marked geographical patterns: the first included strains with the Q64 signature, a hallmark of strains from Belgium, and the second carried an arginine (R) at position 64. These results confirm the clustering observed within the 7 PUUV strains from France so far studied and obtained from rodents (*7*,*8*) and highlight the geographic diversity of strains from France within this lineage.

We were unable to obtain the S segment CDS from all strains, especially from the few strains detected in the departments (e.g., 10, 52, 67, 89) located between the northeastern part and the southeastern part of the hantavirus-endemic area; these 2 parts, reported as main endemic areas in Reynes et al. (*6*), were overrepresented in our dataset. The lack of amplification could be a result of improper storage of the specimens for several days at 4°C by peripheral laboratories for serologic diagnostic testing before sending to the National Reference Center; the low viral load observed in the specimens at reception (crossing point >35); the limit of detection of our S CDS overlapping heminested RT-PCR (reduced 10-fold, compared with detection limit using our molecular diagnostic methods); or mismatch between the sequences of PUUV strains and those of our primers used for S segment CDS amplification. Therefore, other clusters may be present in France, and we cannot clearly determine the geographic overlap of the clusters we described. Furthermore, our study was limited to the S segment CDS, whereas it has been shown that intercluster reassortment of the small, medium, and large segments in PUUV strains can occur, which could be the case in the area in which the 2 sublineages co-circulate (*15*).

Future efforts will be focused on more efficient sequencing of PUUV S segment CDS and also M and L segment CDS, using next-generation sequencing and amplicon approaches for samples with low viral load. We hope to identify more sequences from more geographic areas for use in molecular diagnostic development and in implementing a comprehensive phylogeographic analysis, permitting a better molecular description of PUUV strains in France and further investigation of their evolution.

Acknowledgment

We thank the members of the laboratory network involved in first-line hantavirus diagnostics and in providing samples for expertise and surveillance.

Santé Publique France supports the Centre National de Référence des Hantavirus.

About the Author

Dr. Reynes is a veterinarian and a medical virologist at Institut Pasteur, Paris, France. He is responsible for the National Reference Center for Hantavirus in France. His research interests focus on zoonotic infectious diseases.

References

1. Vaheri A, Henttonen H, Voutilainen L, Mustonen J, Sironen T, Vapalahti O. Hantavirus infections in Europe and their impact on public health. Rev Med Virol. 2013;23:35–49. http://dx.doi.org/10.1002/rmv.1722
2. International Committee on Taxonomy of Viruses (ICTV). 2016.023a-cM Hantavirus approved proposal. 2017 March 19. [cited 2018 Feb 9]. https://talk.ictvonline.org/ICTV/proposals/2016.023a-cM.A.v2.Hantavirus_sprev.pdf
3. Sironen T, Vaheri A, Plyusnin A. Molecular evolution of Puumala hantavirus. J Virol. 2001;75:11803–10. http://dx.doi.org/10.1128/JVI.75.23.11803-11810.2001
4. Razzauti M, Plyusnina A, Niemimaa J, Henttonen H, Plyusnin A. Co-circulation of two Puumala hantavirus lineages in Latvia: a Russian lineage described previously and a novel Latvian lineage. J Med Virol. 2012;84:314–8. http://dx.doi.org/10.1002/jmv.22263
5. Evander M, Eriksson I, Pettersson L, Juto P, Ahlm C, Olsson GE, et al. Puumala hantavirus viremia diagnosed by real-time reverse transcriptase PCR using samples from patients with hemorrhagic fever and renal syndrome. J Clin Microbiol. 2007;45:2491–7. http://dx.doi.org/10.1128/JCM.01902-06
6. Reynes JM, Carli D, Renaudin B, Fizet A, Bour JB, Brodard V, et al. Surveillance of human hantavirus infections in metropolitan France 2012–2016. [in French]. Bull Epidemiol Hebd (Paris). 2017;23:492–9.
7. Plyusnina A, Deter J, Charbonnel N, Cosson JF, Plyusnin A. Puumala and Tula hantaviruses in France. Virus Res. 2007;129:58–63. http://dx.doi.org/10.1016/j.virusres.2007.04.023
8. Castel G, Couteaudier M, Sauvage F, Pons JB, Murri S, Plyusnina A, et al. Complete genome and phylogeny of Puumala hantavirus isolates circulating in France. Viruses. 2015;7:5476–88. http://dx.doi.org/10.3390/v7102884
9. Kramski M, Meisel H, Klempa B, Krüger DH, Pauli G, Nitsche A. Detection and typing of human pathogenic hantaviruses by real-time reverse transcription-PCR and pyrosequencing. Clin Chem. 2007;53:1899–905. http://dx.doi.org/10.1373/clinchem.2007.093245
10. Bowen MD, Gelbmann W, Ksiazek TG, Nichol ST, Nowotny N. Puumala virus and two genetic variants of Tula virus are present in Austrian rodents. J Med Virol. 1997;53:174–81. http://dx.doi.org/10.1002/(SICI)1096-9071(199710)53:2<174::AID-JMV11>3.0.CO;2-J
11. Aitichou M, Saleh SS, McElroy AK, Schmaljohn C, Ibrahim MS. Identification of Dobrava, Hantaan, Seoul, and Puumala viruses by one-step real-time RT-PCR. J Virol Methods. 2005;124:21–6. http://dx.doi.org/10.1016/j.jviromet.2004.10.004
12. Garin D, Peyrefitte C, Crance JM, Le Faou A, Jouan A, Bouloy M. Highly sensitive Taqman PCR detection of Puumala hantavirus. Microbes Infect. 2001;3:739–45. http://dx.doi.org/10.1016/S1286-4579(01)01424-1
13. Korva M, Saksida A, Kejžar N, Schmaljohn C, Avšič-Županc T. Viral load and immune response dynamics in patients with haemorrhagic fever with renal syndrome. Clin Microbiol Infect. 2013;19:e358–66. http://dx.doi.org/10.1111/1469-0691.12218
14. Lagerqvist N, Hagström Å, Lundahl M, Nilsson E, Juremalm M, Larsson I, et al. Molecular diagnosis of hemorrhagic fever with renal syndrome caused by Puumala virus. J Clin Microbiol. 2016;54:1335–9. http://dx.doi.org/10.1128/JCM.00113-16
15. Razzauti M, Plyusnina A, Sironen T, Henttonen H, Plyusnin A. Analysis of Puumala hantavirus in a bank vole population in northern Finland: evidence for co-circulation of two genetic lineages and frequent reassortment between strains. J Gen Virol. 2009;90:1923–31. http://dx.doi.org/10.1099/vir.0.011304-0

Address for correspondence: Jean-Marc Reynes, Centre National de Référence des Hantavirus, Unité de Recherche et d'Expertise Environnement et Risques Infectieux, Institut Pasteur, 25-28 rue du Dr Roux, 75724 Paris CEDEX 15, France; email: jean-marc.reynes@pasteur.fr

New Multidrug-Resistant *Salmonella enterica* Serovar Anatum Clone, Taiwan, 2015–2017

Chien-Shun Chiou, Yu-Ping Hong, Ying-Shu Liao, You-Wun Wang, Yueh-Hua Tu, Bo-Han Chen, Yi-Syong Chen

In 2011, a *Salmonella enterica* serovar Anatum clone emerged in Taiwan. During 2016–2017, infections increased dramatically, strongly associated with emergence and spread of multidrug-resistant strains with a plasmid carrying 11 resistance genes, including bla_{DHA-1}. Because these resistant strains infect humans and food animals, control measures are urgently needed.

Salmonella, a prevalent foodborne pathogen that causes zoonoses worldwide, comprises 2 species, *Salmonella enterica* and *S. bongori*, and ≈2,600 serovars (*1*). In Taiwan, salmonellosis has been primarily caused by the *S. enterica* serovars Enteritidis, Typhimurium, Stanley, Newport, and Albany, which together caused 70% of salmonellosis infections during 2004–2012 (*2*). During this period, *Salmonella* Anatum was not prevalent, causing only 0.4% of the infections. However, since 2015, *Salmonella* Anatum infections have increased, and most isolates are multidrug resistant (MDR). We report the epidemiologic trend of *Salmonella* Anatum infection of humans, the clonal relationships among strains recovered during 2004–2017, and the resistance mechanism of the newly emerging MDR strains.

The Study

To investigate the epidemiologic trend, we analyzed the data in the *Salmonella* fingerprint database constructed by the Taiwan Centers for Disease Control. The database comprises demographic and experimental data, including pulsed-field gel electrophoresis (PFGE) fingerprints obtained by using the PulseNet standardized PFGE protocol (*3*), serotypes obtained using PFGE pattern comparison and conventional methods (*4*), and antimicrobial drug susceptibility testing results for isolates collected from hospitals nationwide. We conducted whole-genome sequencing for 68 *Salmonella* Anatum isolates from humans and animals and 9 isolates from chicken carcasses and abbatoir environments by using the Illumina MiSeq platform (https://www.illumina.com) and identified resistance genes, incompatibility groups of plasmids, and sequence types by using the whole-genome sequencing data. To investigate clonal relationships and locations of resistance genes, we constructed a dendrogram for *Salmonella* Anatum strains with whole-genome single-nucleotide polymorphism profiles to assess genetic relatedness among strains and determined the complete genomic sequence of *Salmonella* Anatum strain R16.0676 with whole-genome sequencing data generated by using a MinION nanopore sequencer (https://nanoporetech.com/products/minion) and an Illumina MiSeq sequencer. To investigate mobility of resistance plasmids, we conducted conjugation experiments to transfer the resistance genes–carrying (R) plasmid from *Salmonella* Anatum strain R16.0676 into recipient *Escherichia coli* C600 and transferred an R plasmid from an *E. coli* transconjugant back to a rifampin-resistant mutant of *Salmonella* Anatum strain R13.0957 (Appendix, https://wwwnc.cdc.gov/EID/article/25/1/18-1103-App1.pdf).

The *Salmonella* fingerprint database of the Taiwan Centers for Disease Control contained PFGE fingerprints for 34,160 *Salmonella* isolates recovered during 2004–2017, of which antimicrobial drug sensitivity test results were available for 23,018. *Salmonella* Anatum was not a prevalent serovar among those collected during 2004–2014 (Figure 1). However, the number of *Salmonella* Anatum infections increased in 2015 and subsequently underwent another sharp increase in 2016 and 2017. In 2017, *Salmonella* Anatum accounted for 14.2% of *Salmonella* infections in Taiwan and ranked as the third most frequently identified serovar.

Whole-genome single-nucleotide polymorphism analysis of *Salmonella* Anatum recovered from humans during 2004–2017 revealed 3 distinct lineages (Figure 2). Strains of lineage (L) 1 were either pansusceptible or MDR; they mostly appeared during 2004–2009 (Appendix Table 2). L2 comprised only 2 isolates, which emerged in 2005 and were pansusceptible. L3 comprised 2 sublineages; sublineage (SL) 3_1, first detected in 2011, was mostly pansusceptible, whereas SL3_2, which first emerged in 2013, was mostly MDR. The MDR strains of SL3_2 first appeared in 2015 and were resistant or of reduced susceptibility to 10 of the 14 antimicrobial drugs tested. SMX.642 was the predominant MDR strain, but the first 2 isolates recovered

Author affiliation: Centers for Disease Control, Taichung, Taiwan

DOI: https://doi.org/10.3201/eid2501.181103

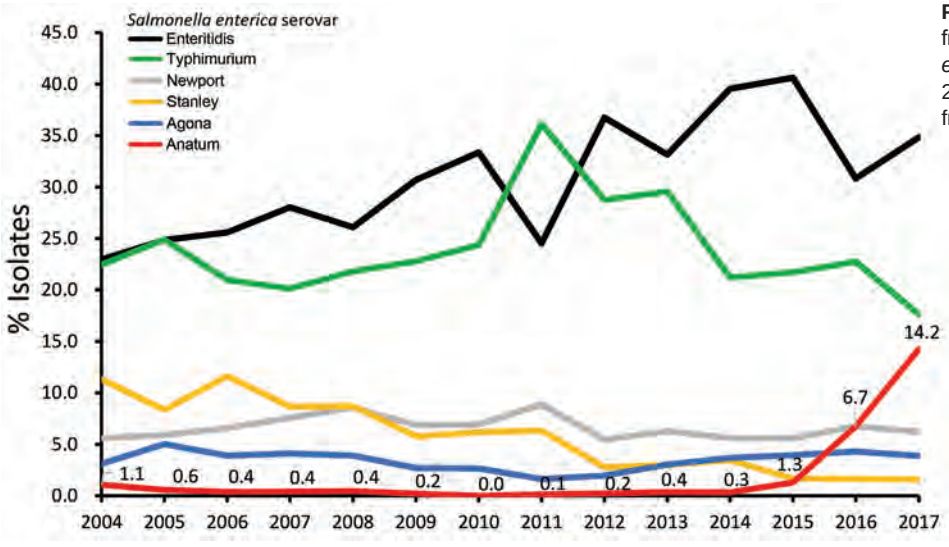

Figure 1. Distribution of the 6 most frequently identified *Salmonella enterica* serovars in Taiwan, 2004–2017. Numbers indicate increasing frequency of *Salmonella* Anatum.

in 2013 were pansusceptible. Of the 9 isolates from chicken carcasses and abattoir environments, 5 belonged to SL3_1 and 4 to SL3_2. The new clone (L3) accounted for 91.9% of the total *Salmonella* Anatum infections during 2004–2017 and 99.6% in 2017. MDR strains accounted for 90.3% of the new clone recovered during 2011–2017 and 94.1% in 2017. All *Salmonella* Anatum isolates sequenced belonged to sequence type 64.

The chromosomal sequence of strain R16.0676 was 4,674,190 bp (GenBank accession no. CP029800) and was not noted to carry any horizontally transferable resistance gene. R16.0676 harbored 2 plasmids, which were designated pR16.0676_90k (90,137 bp; IncC; accession no. CP029802) and pR16.0676_34k (34,063 bp; IncN3; accession no. CP029801). pR16.0676_90k harbored 11 resistance genes, *aadA2*, bla_{DHA-1}, *dfrA23*, *floR*, *lnu(F)*, *qnrB4*, *strA*, *strB*, *sul1*, *sul2*, and *tet(A)*, which were distributed in 2 antimicrobial resistance islands, ARI1 and ARI2 (Appendix Figure, panel A). ARI1 carried 5 resistance genes, *floR*, *strA*, *strB*, *sul2*, and *tet(A)*, and was found in many IncC plasmids in the National Center for Biotechnology Information database (*5*). ARI2 carried the other 6 resistance genes, *aadA2*, bla_{DHA-1}, *dfrA23*, *lnu(F)*, *qnrB4*, and *sul1*. The resistance genes could confer resistance to cefoxitin, cefotaxime, ceftazidime, ampicillin, chloramphenicol, streptomycin, sulfonamide, tetracycline, and trimethoprim and reduced susceptibility to ciprofloxacin as shown by antimicrobial susceptibility testing (Figure 2). pR16.0676_90k shared 79% sequence identity with a 272-kb plasmid, pECAZ155_KPC (GenBank accession no. CP019001.1), which harbored only the sequence of ARI1 but not ARI2. pR16.0676_34k did not carry any resistance gene (Appendix Figure, panel B), but it shared 98% sequence identity with a 34.8-kb plasmid, pN-Cit (GenBank accession no. JQ996149.1). All MDR SL3_2 isolates, including the 4 isolates recovered from the abattoirs, harbored an IncC plasmid and the same 11 resistance genes identified in strain R16.0676. Strain R17.0132 acquired an additional *mcr-1* gene and was resistant to colistin (Figure 2). We did not obtain any transconjugants with pR16.0676_90k, but we did obtain a transconjugant with a composite plasmid, which had the same sequences as pR16.0676_90k and pR16.0676_34k (Appendix Figure, panel C). This 125-kb composite plasmid probably resulted from insertion of pR16.0676_90k into pR16.0676_34k through an insertion sequence 26–mediated transposition process. The resulting plasmid acquired an additional copy of insertion sequence 26 and an 8-bp tandem repeat in the insertion site. More than a dozen genes are typically required for conjugation (*6*). pR16.0676_90k harbored only 3 genes, and pR16.0676_34k contained at least 12 genes related to conjugation. Fusion of the 2 plasmids caused the composite plasmid to become self-transmissible. When the composite plasmid was transferred back into a rifampin-resistant mutant of *Salmonella* Anatum strain R13.0957, we obtained transconjugants harboring only a 58-kb or 83-kb R plasmid, which were derived from the 125-kb plasmid through deletions (Appendix Figure, panel C). Accordingly, the composite plasmid was unstable in *Salmonella* Anatum.

Conclusions

We identified a new *Salmonella* Anatum clone that emerged in Taiwan in 2011. During 2011–2014, strains of the new clone were not resistant and caused few infections. The dramatic increase in *Salmonella* Anatum infections that occurred during 2016–2017 was strongly associated with the emergence of MDR strains in 2015. The most crucial concern regarding emergence of the MDR

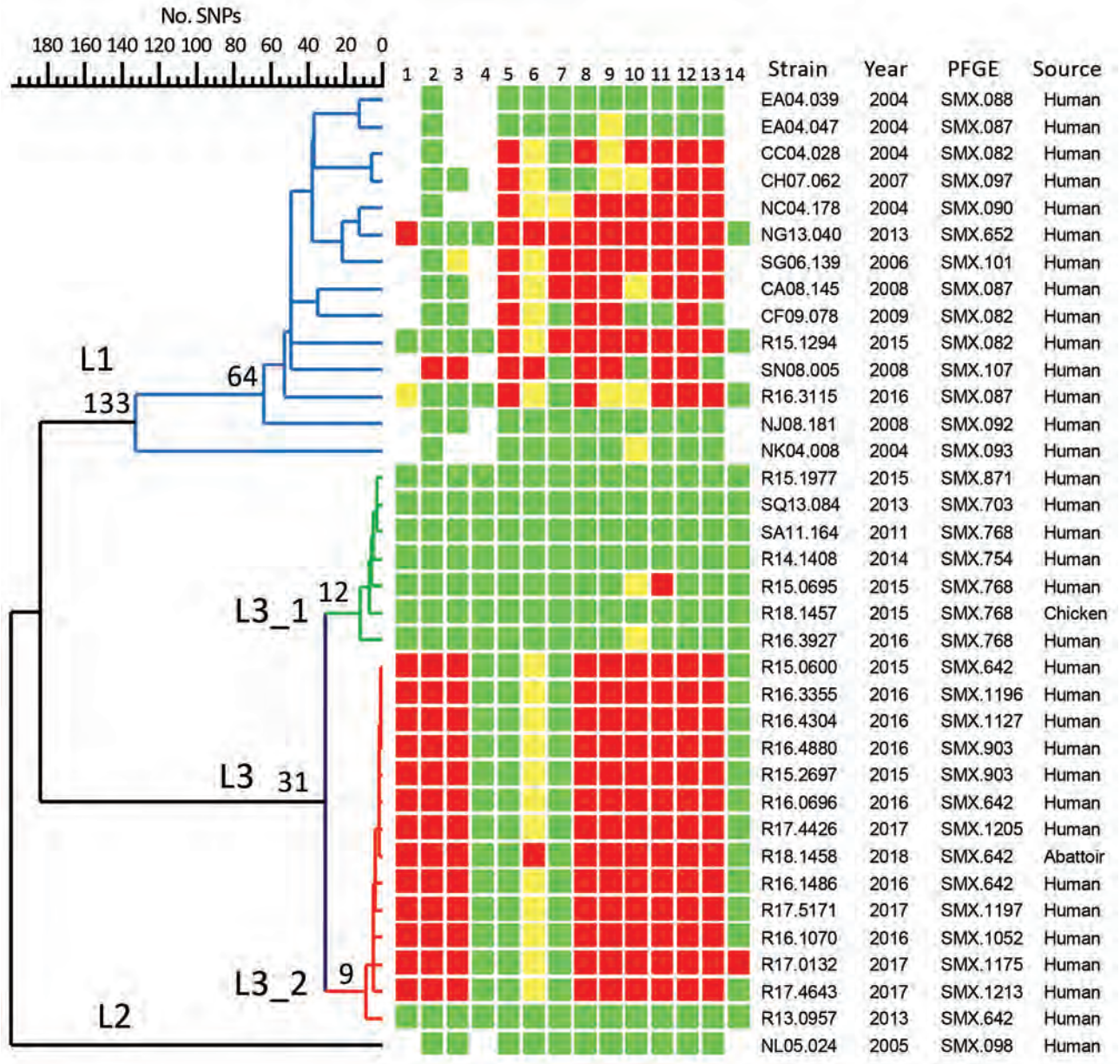

Figure 2. Dendrogram of 36 representative *Salmonella enterica* serovar Anatum strains from Taiwan, 2004–2017, constructed with whole-genome SNP profiles with 883 SNPs. The complete genomic sequence of *Salmonella* Anatum strain GT-38 (GenBank accession no. CP013226) was used as the reference for SNP calling. Red, resistant; yellow, intermediate; green, susceptible. Lanes: 1, cefoxitin; 2, cefotaxime; 3, ceftazidime; 4, ertapenem; 5, nalidixic acid; 6, ciprofloxacin; 7, gentamicin; 8, ampicillin; 9, chloramphenicol; 10, streptomycin; 11, sulfamethoxazole; 12, tetracycline; 13, sulfamethoxazole/trimethoprim; 14, colistin. L, lineage; PFGE, pulsed-field gel electrophoresis; SNP, single-nucleotide polymorphism. A color version of this figure is available online (http://wwwnc.cdc.gov/EID/article/25/1/18-1103-F2.htm).

Salmonella Anatum clone was that all MDR strains carry bla_{DHA-1}, which encodes AmpC β-lactamase and confers resistance to β-lactam drugs, including third-generation cephalosporins. This resistance cannot be overcome by using β-lactam inhibitors. Because these MDR strains can cause numerous infections in humans and are prevalent in animals used for food, urgent control measures are needed.

Acknowledgments

We thank the Bureau of Animal and Plant Health Inspection and Quarantine, Council of Agriculture and Agricultural Technology Research Institute, for providing *Salmonella* Anatum isolates recovered from chicken carcasses and abattoir environments.

This study was funded by the Ministry of Health and Welfare, Taiwan (grant no. MOHW107-CDC-C-315-124503).

About the Author

Dr. Chiou is a principal investigator at the Centers for Disease Control, Ministry of Health and Welfare, Taiwan. His research interests include genotyping, molecular epidemiology, and antimicrobial resistance of foodborne bacterial pathogens.

References

1. Guibourdenche M, Roggentin P, Mikoleit M, Fields PI, Bockemühl J, Grimont PA, et al. Supplement 2003-2007 (no. 47) to the White-Kauffmann-Le Minor scheme. Res Microbiol. 2010;161:26–9. http://dx.doi.org/10.1016/j.resmic.2009.10.002
2. Kuo HC, Lauderdale TL, Lo DY, Chen CL, Chen PC, Liang SY, et al. An association of genotypes and antimicrobial resistance patterns among *Salmonella* isolates from pigs and humans in Taiwan. PLoS One. 2014;9:e95772. http://dx.doi.org/10.1371/journal.pone.0095772
3. Ribot EM, Fair MA, Gautom R, Cameron DN, Hunter SB, Swaminathan B, et al. Standardization of pulsed-field gel electrophoresis protocols for the subtyping of *Escherichia coli* O157:H7, *Salmonella*, and *Shigella* for PulseNet. Foodborne Pathog Dis. 2006;3:59–67. http://dx.doi.org/10.1089/fpd.2006.3.59
4. Chiou CS, Torpdahl M, Liao YS, Liao CH, Tsao CS, Liang SY, et al. Usefulness of pulsed-field gel electrophoresis profiles for the determination of *Salmonella* serovars. Int J Food Microbiol. 2015;214:1–3. http://dx.doi.org/10.1016/j.ijfoodmicro.2015.07.016
5. Fernández-Alarcón C, Singer RS, Johnson TJ. Comparative genomics of multidrug resistance-encoding IncA/C plasmids from commensal and pathogenic *Escherichia coli* from multiple animal sources. PLoS One. 2011;6:e23415. http://dx.doi.org/10.1371/journal.pone.0023415
6. Cabezón E, Ripoll-Rozada J, Peña A, de la Cruz F, Arechaga I. Towards an integrated model of bacterial conjugation. FEMS Microbiol Rev. 2015;39:81–95.

Address for correspondence: Chien-Shun Chiou, Centers for Disease Control, Center for Diagnostics and Vaccine Development, 5F No. 20, Wen-Sin South Third Rd, Taichung 40855, Taiwan; email: nipmcsc@cdc.gov.tw

Seroepidemiology of Parechovirus A3 Neutralizing Antibodies, Australia, the Netherlands, and United States

Eveliina Karelehto, Lieke Brouwer, Kimberley Benschop, Jen Kok, Kerri Basile, Brendan McMullan, William Rawlinson, Julian Druce, Suellen Nicholson, Rangaraj Selvarangan, Christopher Harrison, Kamani Lankachandra, Hetty van Eijk, Gerrit Koen, Menno de Jong, Dasja Pajkrt, Katja C. Wolthers

Recent parechovirus A3 (PeV-A3) outbreaks in Australia suggest lower population immunity compared with regions that have endemic PeV-A3 circulation. A serosurvey among populations in the Netherlands, the United States, and Australia before and after the 2013 Australia outbreak showed high PeV-A3 neutralizing antibody prevalence across all regions and time periods, indicating widespread circulation.

Parechovirus A3 (PeV-A3), belonging to the Picornavirus family, can cause respiratory and gastrointestinal symptoms, as well as meningitis and sepsis-like disease in infants (*1*). PeV-A3 was isolated from a fecal specimen collected in 1999 from a child with fever, diarrhea, and transient paralysis; it has been gaining increasing interest because of reported outbreaks of severe illness in neonates (*2*–*4*). To date the largest outbreaks have been caused by a recombinant PeV-A3 strain in Australia: in New South Wales in 2013, and in Victoria in 2015 (*4*). Humoral immunity is essential in protection against PeV-A3 disease, yet seroepidemiological data on population immunity are limited (*5*,*6*). We describe the findings of a cross-sectional study on serum PeV-A3 neutralizing antibody (nAb) levels among children and adults from Victoria and New South Wales, Australia; Missouri, USA; and the Netherlands, where PeVs circulate every 2 years during summer and fall months (*3*,*7*).

Author affiliations: Academic Medical Center, Amsterdam, the Netherlands (E. Karelehto, L. Brouwer, H. van Eijk, G. Koen, M. de Jong, D. Pajkrt, K.C. Wolthers); National Institute for Public Health and the Environment, Bilthoven, the Netherlands (K. Benschop); Institute of Clinical Pathology and Medical Research, Westmead, New South Wales, Australia (J. Kok, K. Basile); Sydney Children's Hospital, Sydney, New South Wales, Australia (B. McMullan); Prince of Wales Hospital, Randwick, New South Wales, Australia (W. Rawlinson); Doherty Institute, Melbourne, Victoria, Australia (J. Druce, S. Nicholson); Children's Mercy Hospital, Kansas City, Missouri, USA (R. Selvarangan, C. Harrison); Truman Medical Center, Kansas City (K. Lankachandra)

DOI: https://doi.org/10.3201/eid2501.180352

The Study

We screened 1,288 anonymized serum samples from persons 0–91 years of age. From each geographic location, 2 independent sets of samples collected before and after the 2013 Australia PeV-A3 outbreak were used (Table 1). No ethics approval is required for anonymous use of biobank specimens in the Netherlands. Serum samples from the Netherlands in 2006–2007 came from a serum bank approved by the Medical Ethics Testing Committee of the Foundation of Therapeutic Evaluation of Medicines (ISRCTN 20164309). The institutional review board at the Children's Mercy Hospital (Kansas City, Missouri, USA) determined that anonymous use of the Missouri samples was exempt from ethics approval. The human research ethics committee at Melbourne Health approved the use of Victoria serum samples and the human research ethics committee at Western Sydney Local Health District approved the use of New South Wales serum samples (LNR/17/WMEAD/279).

We tested the serum samples with a previously described neutralization assay (*8*). We serially diluted heat-inactivated serum samples and incubated them with chloroform-treated PeV-A3 strain isolated during the 2013 outbreak in Australia (GenBank accession no. KY930881) (*4*). We subsequently added LLCMK2 cells and incubated them for 7 days. We calculated neutralizing titers based on cytopathogenic effect using the Reed and Muench method and reported them as the reciprocal titers of serum dilutions exhibiting 50% neutralization (*9*). We considered an nAb titer of ≥1:8 to be positive; we used ≥1:32 as a secondary cutoff (*5*). We compared PeV-A3 nAb seroprevalence between the timepoints within each location using χ^2 tests. We performed logistic regression to examine the association between seropositivity and location–timepoint (8 categories), gender (2 categories), and age (3 categories). We present 3 univariable models and 1 multivariable model including all 3 variables. We used the Kruskal-Wallis test with post hoc analysis and Bonferroni correction to

Table 1. Demographic information for study of parechovirus A3 neutralizing antibodies, Australia, the Netherlands, and United States*

Sample group	Institute	Sample type	No. (%) patients	Patient age, y	
				Mean	SD
Country (state) and years					
NL 2006–2007	RIVM	P	140 (11)	27.8	21.9
NL 2015–2016	AMC	R, S	140 (11)	27.8	21.5
USA (MO) 2012–2013	CMH	R	120 (9)	30.8	18.3
USA (MO) 2017	CMH, TMC	R	171 (13)	25.5	18.8
AUS (VIC) 2011–2012	VIDRL	R	138 (11)	26.5	19.9
AUS (VIC) 2015–2016	VIDRL	R	138 (11)	26.4	19.6
AUS (NSW) 2011–2012	WH, POW	R	185 (14)	26.1	23.2
AUS (NSW) 2015–2016	WH, POW	R	257 (20)	23.9	20.6
Sex†					
M			598 (46)	25.7	21.3
F			580 (45)	25.5	20.5
Age, y					
<1			148 (11)	0.4	0.3
1–2			52 (4)	1.8	0.6
3–4			41 (3)	3.8	0.6
5–9			120 (9)	7.2	1.5
10–19			220 (17)	15.8	2.7
20–29			184 (14)	24.8	2.9
30–39			172 (13)	34.2	2.8
40–49			162 (13)	44.6	2.8
50–59			89 (7)	54.8	3.2
60–69			62 (5)	64.3	2.8
>69			38 (3)	76.4	5.3
Total			1,288		

*AMC, Academic Medical Center; AUS, Australia; CMH, Children's Mercy Hospital; NL, the Netherlands; P, population-based sampling; POW, Prince of Wales Hospital; R, residual serum from hospitalized patients and community; RIVM, National Institute for Public Health and the Environment; S, AMC staff; SD, standard deviation; TMC, Truman Medical Center; VIC, Victoria; NSW, New South Wales; VIDRL, Victorian Infectious Diseases Reference Laboratory; WH, Westmead Hospital.
†Information on sex not available for US 2017 adult samples.

compare the median nAb titers. In the statistical analyses, we excluded children <1 year of age because of the presence of maternal antibodies; we merged the remaining age categories into 3 groups.

Overall PeV-A3 nAb seropositivity was similar across 3 locations: 71.1% (2006–2007) and 69.2% (2015–2016) in the Netherlands, 63.3% (2012–2013) and 66.5% (2017) in Missouri, and 58.5% (2011–2012) and 66.4% (2015–2016) in Victoria (Figure 1, panel A). In New South Wales, nAb seroprevalence was 82.9% in 2011–2012, whereas it was significantly less (68.6%) in 2015–2016 ($p = 0.005$; Figure 1, panel A).

Age was a significant determinant of PeV-A3 nAb seropositivity, which increased from 32.7% in children 1–2 years of age to 65.0% in those 5–9 years of age and peaked at 77.7% in adults 20–30 years of age (Figure 1, panel B). nAb seropositivity decreased to 42.1% in persons >30 years of age when a titer cutoff ≥1:32, the level necessary for protection against disease (*5*), was used. Furthermore, we observed that only 33.8% of infants <1 year of age had an nAb titer ≥1:32 and were thus sufficiently protected by maternal antibodies (Figure 1, panel B).

We compiled age-stratified seroprevalences for each location and timepoint (Figure 1, panels C–F). The variables location–timepoint and age were significantly associated with seroprevalence in both univariable and multivariable regression models ($p<0.002$; Table 2). We did not detect sex-dependent differences ($p = 0.309$; Table 2). In line with the age-stratified seropositivity, the geometric mean titers (GMTs) declined steadily with age (Figure 2). Overall GMT peaked at 1:53 (SD 8.5) in the 10–19-year age group and decreased thereafter. Both children 1–5 years of age ($p = 0.001$) and adults >30 years of age ($p<0.001$) had significantly lower median titers than persons 6–29 years of age.

Conclusions

In this large seroepidemiological PeV-A3 study, we compared the nAb prevalence in populations from 4 distinct geographic regions. We report high and comparable PeV-A3 nAb seropositivity across all these regions. In agreement with the reports from Japan, the overall seroprevalence was 68.9%, suggesting widespread global circulation of PeV-A3 (*10,11*). Unexpectedly, the level of PeV-A3 humoral immunity in NSW was higher before the 2013 outbreak compared with 2–3 years after the outbreak. This suggests that PeV-A3 was already endemic in Australia before or during 2011–2012. Localized smaller PeV-A3 upsurges or variations in the proportion of samples originating from hospitalized patients versus the community may explain the observed difference between the earlier and later time periods.

Age-stratified PeV-A3 nAb seropositivity and GMTs suggest that the infection generally occurs in children <10

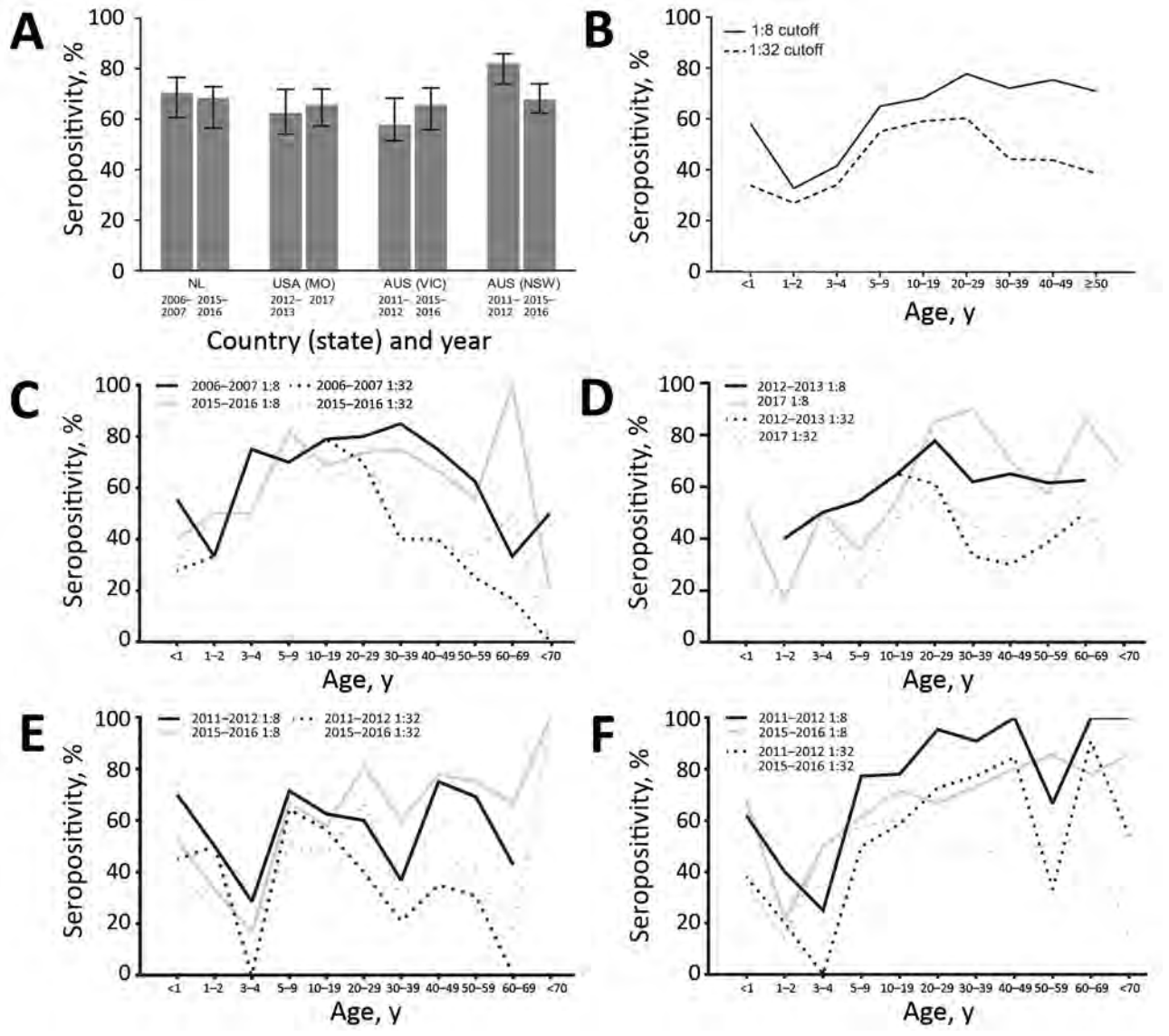

Figure 1. Parechovirus A3 (PeV-A3) neutralizing antibody (nAb) seropositivity, Australia, the Netherlands, and United States. A) Overall nAb seropositivity with associated 95% CIs. Infants <1 year of age were excluded from the analysis. Seropositivity rates between the timepoints within each location were compared by using χ^2 tests. B) Overall age-stratified PeV-A3 nAb seropositivity, including infants <1 year of age. Seropositivity was determined as a nAb titer of ≥1:8 or ≥1:32. C–F) Age-stratified PeV-A3 nAb seropositivity in C) the Netherlands; D) Missouri, USA; E) Victoria, Australia; and F) New South Wales, Australia. Complete data used in this figure can be found in the Appendix (http://wwwnc.cdc.gov/EID/article/25/1/18-0352-App1.pdf). AUS, Australia; NL, the Netherlands; NSW, New South Wales; VIC, Victoria.

years of age, although nAb titers continued to increase in adolescent children. nAb titers decreased below the proposed level of protection in adults >30 years of age. Similar observations have been reported previously (*5*,*10*,*12*). This result is in contrast to results for PeV-A1, against which high nAb seropositivity rates are maintained in adults (*11*). The large proportion of seronegative persons and gradually declining GMTs in older age categories may indicate that widespread circulation of PeV-A3 has emerged fairly recently, as previously proposed (*13*), or that the immunity elicited in childhood is waning. Because the mean age of women at first birth in developed countries is high, we hypothesize that low nAb titers in women of childbearing age, and therefore the lack of adequate maternal antibody protection, contribute to the occurrence of PeV-A3 outbreaks in infants. Moreover, the 2013 Australia outbreak strain was recently described as a novel recombinant with the capsid-encoding region of the genome originating from a PeV-A3 strain collected in Japan in 2011 and the nonstructural region from an unknown origin (*4*). Preexisting serum antibodies recognizing epitopes in the PeV-A3 capsid maintain their ability to neutralize this strain, but this factor may represent a more virulent variant of PeV-A3.

Table 2. Association between seropositivity and location–timepoint, gender, and age by univariate and multivariate logistic regression models in study of parechovirus A3 neutralizing antibodies, Australia, the Netherlands, and United States*

Parameter	Univariate model		Multivariate model	
	Odds ratio (95% CI)	p value	Odds ratio (95% CI)	p value
Location, years		**0.002**		**<0.001**
Netherlands, 2006–2007	1.124 (0.693–1.824)		1.078 (0.658–1.764)	
Netherlands, 2015–2016	1.026 (0.635–1.658)		0.963 (0.591–1.568)	
Missouri, USA, 2011–2012	0.790 (0.496–1.260)		0.725 (0.451–1.166)	
Missouri, USA, 2017	0.906 (0.585–1.403)		0.376 (0.189–0.748)	
Victoria, Australia, 2011–2012	0.644 (0.406–1.023)		0.642 (0.400–1.030)	
Victoria, Australia, 2015–2016	0.904 (0.563–1.451)		0.868 (0.536–1.406)	
New South Wales, Australia, 2011–2012	2.222 (1.354–3.647)		2.247 (1.358–3.718)	
New South Wales, Australia, 2015–2016†	1		1	
Sex‡		0.193		0.309
F	0.840 (0.646–1.092)		0.868 (0.661–1.140)	
M†	1		1	
Age, y		**<0.001**		**<0.001**
1–5†	1		1	
6–29	2.938 (1.954–4.419)		2.782 (1.821–4.251)	
≥30	3.248 (2.160–4.883)		3.081 (2.004–4.738)	

*Boldface indicates a statistically significant result. Seropositivity was determined as a neutralizing antibody titer ≥1:8. Children <1 years of age were excluded.
†Reference category.
‡Information on sex not available for US 2017 adult samples.

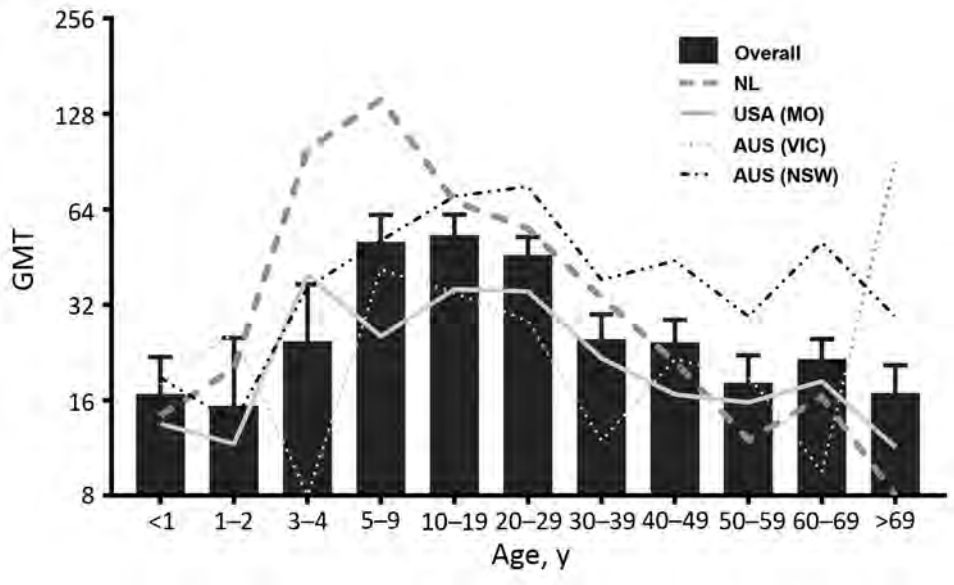

Figure 2. Age-associated GMTs of parechovirus A3 neutralizing antibodies, Australia, the Netherlands, and United States. Bars indicate overall GMTs (timepoints and locations merged); error bars indicate SDs. Lines represent GMTs in each location (timepoints merged). AUS, Australia; GMT, geometric mean titer; NL, Netherlands; VIC, Victoria; NSW, New South Wales.

This study has limitations. Cross-neutralizing antibodies resulting from exposure to other PeV genotypes may confound our findings. However, we have previously observed no evidence of PeV-A3 cross-neutralization by polyclonal and monoclonal antibodies elicited against PeV-A1 to 5 (*14*,*15*). Because we used anonymous serum samples from population-based sampling and residual serum collections, we could not relate the seroprevalence to cohort exposure history or etiologic information, and the varying sampling time periods prohibit us from making direct temporal comparisons between the locations.

Taken together, our results suggest that PeV-A3 circulation is widespread and that infection takes place in early childhood and adolescence. Nonetheless, PeV-A3 outbreaks occur regularly in young infants, and case numbers remain elevated in Australia (L. Caly, Doherty Institute, Melbourne, VIC, Australia, pers. comm. 2017 Oct 15). Why humoral immunity against PeV-A3 declines with age and what factors predispose neonates to severe PeV-A3 illness remain to be elucidated. Implementation of molecular PeV detection in routine diagnostics and continuous surveillance are warranted.

Acknowledgments

We thank Laura Teixidó for excellent technical assistance and Rebecca Holman for expert advice on statistical analyses.

This research was funded by the FP7 Marie Curie Industry Academia Partnerships and Pathways consortium Academia Industry R&D Opportunities for Picornaviruses.

About the Author

Ms. Karelehto is a PhD candidate at the Laboratory of Clinical Virology in the Department of Medical Microbiology at the Academic Medical Center in Amsterdam, the Netherlands. Her research focuses on parechovirus seroepidemiology and virus–host interactions.

References

1. Harvala H, Wolthers KC, Simmonds P. Parechoviruses in children: understanding a new infection. Curr Opin Infect Dis. 2010; 23:224–30. http://dx.doi.org/10.1097/QCO.0b013e32833890ca
2. Ito M, Yamashita T, Tsuzuki H, Takeda N, Sakae K. Isolation and identification of a novel human parechovirus. J Gen Virol. 2004;85:391–8. http://dx.doi.org/10.1099/vir.0.19456-0
3. Midgley CM, Jackson MA, Selvarangan R, Franklin P, Holzschuh EL, Lloyd J, et al. Severe parechovirus 3 infections in young infants—Kansas and Missouri, 2014. J Pediatric Infect Dis Soc. 2018;7:104–12. http://dx.doi.org/10.1093/jpids/pi
4. Nelson TM, Vuillermin P, Hodge J, Druce J, Williams DT, Jasrotia R, et al. An outbreak of severe infections among Australian infants caused by a novel recombinant strain of human parechovirus type 3. Sci Rep. 2017;7:44423. http://dx.doi.org/10.1038/srep44423
5. Aizawa Y, Watanabe K, Oishi T, Hirano H, Hasegawa I, Saitoh A. Role of maternal antibodies in infants with severe diseases related to human parechovirus type 3. Emerg Infect Dis. 2015;21:1966–72. http://dx.doi.org/10.3201/eid2111.150267
6. Westerhuis B, Kolehmainen P, Benschop K, Nurminen N, Koen G, Koskiniemi M, et al. Human parechovirus seroprevalence in Finland and the Netherlands. J Clin Virol. 2013;58:211–5. http://dx.doi.org/10.1016/j.jcv.2013.06.036
7. Janes VA, Minnaar R, Koen G, van Eijk H, Dijkman-de Haan K, Pajkrt D, et al. Presence of human non-polio enterovirus and parechovirus genotypes in an Amsterdam hospital in 2007 to 2011 compared to national and international published surveillance data: a comprehensive review. Euro Surveill. 2014;19:20964. http://dx.doi.org/10.2807/1560-7917.ES2014.19.46.20964
8. Karelehto E, van der Sanden S, Geraets JA, Domanska A, van der Linden L, Hoogendoorn D, et al. Strain-dependent neutralization reveals antigenic variation of human parechovirus 3. Sci Rep. 2017;7:12075. http://dx.doi.org/10.1038/s41598-017-12458-5
9. Reed LJ, Muench H. A simple method of estimating fifty percent endpoints. Am J Hyg. 1938;27:493–7.
10. Watanabe K, Hirokawa C, Tazawa T. Seropositivity and epidemiology of human parechovirus types 1, 3, and 6 in Japan. Epidemiol Infect. 2016; (Aug):1–10.
11. Tanaka S, Aoki Y, Matoba Y, Yahagi K, Itagaki T, Matsuzaki Y, et al. Seroepidemiology of human parechovirus types 1, 3, and 6 in Yamagata, Japan, in 2014. Microbiol Immunol. 2016;60:854–8. http://dx.doi.org/10.1111/1348-0421.12456
12. Karelehto E, Wildenbeest J, Benschop K, Koen G, Rebers S, Bouma-de Jongh S, et al. Human parechovirus 1, -3 and -4 neutralizing antibodies in Dutch mothers and infants and their role in protection against disease. Pediatr Infect Dis J. http://dx.doi.org/10.1097/INF.0000000000001986
13. Calvert J, Chieochansin T, Benschop KS, McWilliam Leitch EC, Drexler JF, Grywna K, et al. Recombination dynamics of human parechoviruses: investigation of type-specific differences in frequency and epidemiological correlates. J Gen Virol. 2010;91: 1229–38. http://dx.doi.org/10.1099/vir.0.018747-0
14. Westerhuis BM, Koen G, Wildenbeest JG, Pajkrt D, de Jong MD, Benschop KS, et al. Specific cell tropism and neutralization of human parechovirus types 1 and 3: implications for pathogenesis and therapy development. J Gen Virol. 2012;93:2363–70. http://dx.doi.org/10.1099/vir.0.043323-0
15. Westerhuis BM, Benschop KS, Koen G, Claassen YB, Wagner K, Bakker AQ, et al. Human memory B cells producing potent cross-neutralizing antibodies against human parechovirus: implications for prevalence, treatment, and diagnosis. J Virol. 2015;89:7457–64. http://dx.doi.org/10.1128/JVI.01079-15

Address for correspondence: Katja C. Wolthers, Laboratory of Clinical Virology, Rm L1-109, Department of Medical Microbiology, Academic Medical Center, University of Amsterdam, Meibergdreef 9, 1105AZ Amsterdam, the Netherlands; email: k.c.wolthers@amc.uva.nl

Identification of *Lonepinella* sp. in Koala Bite Wound Infections, Queensland, Australia

Holly Angela Sinclair, Paul Chapman, Lida Omaleki, Haakon Bergh, Conny Turni, Patrick Blackall, Lindsey Papacostas, Phillip Braslins, David Sowden, Graeme R. Nimmo

We report 3 cases of koala bite wound infection with *Lonepinella koalarum*–like bacteria requiring antimicrobial and surgical management. The pathogens could not be identified by standard tests. Phylogenetic analysis of 16S rRNA and housekeeping genes identified the genus. Clinicians should isolate bacteria and determine antimicrobial susceptibilities when managing these infections.

Lonepinella koalarum, a species present in koala (*Phascolarctos cinereus*) feces, is a gram-negative bacterium that can degrade tannin protein complexes (*1*). This bacterium is the only species of the genus *Lonepinella*, a member of the family *Pasteurellaceae*. *L. koalarum*–related strains have been identified in koala gingiva (*2*). We report 3 cases of human wound infection involving *Lonepinella*-like organisms occurring after koala bites in Queensland, Australia.

The Study

In 2014, case-patient 1, a 69-year-old female wildlife worker from the Sunshine Coast region of Queensland, Australia, sought treatment for left wrist puncture wounds and a 2-cm laceration to the dorsum of her left hand after a koala bite. The wound was cleaned, and oral amoxicillin/clavulanic acid was administered. Increased erythema and edema developed after 48 hours. Surgical debridement was required, and intravenous piperacillin/tazobactam was given for 6 days, followed by oral trimethoprim and sulfamethoxazole; full recovery was achieved. A Gram stain revealed gram-positive and -negative organisms. After 48 hours of culturing, we identified *Staphylococcus sciuri* and 2 gram-negative coccobacilli (MS14434 and MS14435).

After this case, we reviewed records and found a similar previous incident. In 2012, case-patient 2, a 62-year-old male wildlife worker from Toowoomba, Queensland, Australia, went to a general practitioner for treatment of a koala crush-bite injury to the thumb. After increased pain, swelling, fever, and malaise developed, he sought hospital care. He had an open wound (2-mm long, 5–8-mm wide, 20-mm deep) with purulent discharge. Surgical debridement was required, and intravenous ticarcillin/clavulanic acid was administered for 4 days, followed by oral amoxicillin/clavulanic acid for 7 days; clinical improvement occurred. We cultured specimens obtained during the operation and found *Fusobacterium nucleatum*, *Staphylococcus aureus*, and an unidentifiable gram-negative bacillus (MS14436).

In 2015, case-patient 3, a 66-year-old woman from Brisbane, Queensland, Australia, sought hospital treatment for a koala bite wound on her right hand. Surgical debridement and washout revealed pus within the thenar muscle compartment and metacarpophalangeal joint. Intravenous piperacillin/tazobactam was given, and the patient's condition improved. We cultured swabs of specimens acquired before and during surgery and isolated an unidentified gram-negative bacillus (MS14437).

We cultured all isolates on chocolate agar in 5% CO_2 for 48 h and recorded growth in different culture conditions (Table 1). We performed biochemical reactions, sugar utilization, and cultures using in-house methods and commercial identification products API 20NE Microbial Identification Kit (bioMérieux, https://www.biomerieux.com), RapID NH System (Remel, http://www.remel.com/Clinical/Microbiology.aspx), RapID ANA II System (Remel), and VITEK 2 GN and NH ID cards (bioMérieux). We performed matrix-assisted laser desorption/ionization time-of-flight mass spectrometry using the VITEK MS IVD database (bioMérieux) and performed antimicrobial susceptibility tests per the European Committee on Antimicrobial Susceptibility Testing (EUCAST) guidelines (http://www.eucast.org/clinical_breakpoints) for *Pasteurella multocida* (*3*). We used Etest (bioMérieux) to determine MICs.

We performed DNA amplification and sequencing of 16S rRNA (*4*), *rpoB* (*5*), *recN* (*6*), and *infB* (*7*) genes as previously published and deposited sequences in GenBank (Appendix Table 3, https://wwwnc.cdc.gov/EID/article/25/1/17-1359-App1.pdf). We used Geneious 10.0.6

Author affiliations: Pathology Queensland, Herston, Queensland, Australia (H.A. Sinclair, H. Bergh, G.R. Nimmo); Caboolture Hospital, Caboolture, Queensland, Australia (P. Chapman); Queensland Institute of Medical Research Berghofer, Herston (P. Chapman); The University of Queensland, Brisbane, Queensland, Australia (L. Omaleki, C. Turni, P. Blackall); Sunshine Coast University Hospital, Birtinya, Queensland, Australia (L. Papacostas, D. Sowden); University of New England, Armidale, New South Wales, Australia (P. Braslins); Griffith University, Gold Coast, Queensland, Australia (G.R. Nimmo)

DOI: https://doi.org/10.3201/eid2501.171359

Table 1. Phenotypic characteristics of 4 clinical isolates obtained from koala bite wound infections, Queensland, Australia, and *Lonepinella koalarum* ACM 3666

Growth characteristic or condition	MS14434	MS14435	MS14436	MS14437	ACM 3666
Growth requirement					
X factor	–	–	–	–	–
V factor	–	–	–	–	–
Biochemical reaction					
Acetoin, Voges-Proskauer test	–	+	+	–	+
Arginine arylamidase	+	–	–	+	–
β-galactosidase	–	–	–	+	–
β-glucosidase	–	+	+	+	+
β-xylosidase	+	–	–	–	+
Catalase	–	–	–	–	–
H_2S	–	–	–	–	–
Indole	–	–	–	–	–
Leucine arylamidase	+	+	+	+	+
Ornithine decarboxylase	–	–	–	–	–
Oxidase	+*	+*	+*	+*	+*
Phenylalanine arylaminidase	+	+	+	–	+
Urease	–	–	–	–	–
Courmarate	–	+	–	+	–
Maltotriose	+	+	+	+	+
N-acetyl-D-glucosamine	+	+	+	–	+
Phenylphosphonate	+	–	–	–	+
Phosphatase	+	+	+	+	+
Nitrate reduction	–	–	–	–	+
Hydrolyzed esculin	–	+	+	+	+
Sugar utilization					
Glucose	+	+	+	+	+
Sucrose	+	–	–	+	+
Lactose	–	–	–	–	–
Maltose	–	–	–	–	+
Mannose	+	+	+	+	+
Xylose	–	–	–	–	+*
Mannitol	–	–	–	–	–
Malate	+	+	+	+	+
D-cellobiose	–	–	–	+	+
Media type					
Horse blood agar	+	+	+	+	+
Chocolate agar	+	+	+	+	+
Bacitracin agar	+	+	+	+	+
Brain Heart yeast	+	+	+	+	+
MacConkey with crystal violet	–	–	–	–	–
Hemolysis on horse blood agar	–	–	–	–	–
Temperature and atmospheric conditions					
Room temperature	+	+	+	+	+
28°C Aerobic	+	+	+	+	+
35°C Aerobic	+	+	+	+	+
35°C in 5% CO_2	+	+	+	+	+
35°C Microaerophilic	+	+	+	+	+
35°C Anaerobic	+	+	+	+	+
42°C Aerobic	–	–	–	+	–

*Weak positive.

(https://www.geneious.com) to align and analyze sequences. We performed a neighbor-joining analysis of 16S rRNA sequences by using Jukes-Cantor corrections and calculated bootstrap support in MEGA version 6 (https://www.megasoftware.net). We calculated the similarity matrix using MUSCLE (https://www.ebi.ac.uk/Tools/msa/muscle) and predicted genome relatedness using a previously published formula using the *recN* gene (*8*,*9*).

The colony morphology of the 2 isolates from case-patient 1 were distinctly different from each other; MS14434 was morphologically similar to MS14437, and MS14435 was similar to MS14436. Optimal colony growth was seen on chocolate agar with 5% CO_2 and under microaerophilic conditions (Table 1). Results from commercial identification systems were mostly inconsistent (Appendix Table 1); note that *L. koalarum* is not included within the commercial databases used.

The MICs of all the antimicrobial drugs tested for MS14434 and MS14435 were low (Appendix Table 2); MICs for MS14436 and MS14437 were higher. MS14436 and MS14437 were resistant to benzylpenicillin when applying *P. multocida* breakpoints (*3*).

Table 2. Similarity matrix of 16S rRNA, *rpoB*, *infB*, and *recN* gene sequences of 4 clinical isolates obtained from koala bite wound infections, Queensland, Australia, and *Lonepinella koalarum* ACM 3666*

Gene and isolate	MS14434	MS14435	MS14436	MS14437	ACM 3666
16SrRNA					
MS14434	100				
MS14435	96.52	100			
MS14436	96.50	98.45	100		
MS14437	97.48	98.16	98.00	100	
ACM 3666	94.82	95.26	96.00	95.45	100
rpoB					
MS14434	100				
MS14435	95.77	100			
MS14436	96.54	97.69	100		
MS14437	95.96	99.42	97.88	100	
ACM 3666	95.96	95.96	95.00	96.35	100
infB					
MS14434	100				
MS14435	84.34	100			
MS14436	83.89	98.66	100		
MS14437	84.34	96.20	95.75	100	
ACM 3666	99.78	84.12	83.67	84.12	100
recN					
MS14434	100				
MS14435	83.90	100			
MS14436	84.13	99.06	100		
MS14437	83.97	99.53	99.37	100	
ACM 3666	97.17	83.97	84.21	84.05	100

*Values are percentage identity.

We compared 16S rRNA and *rpoB* gene sequences from our isolates with those available in public databases, including GenBank, but confident organism identification was not possible. The 16S rRNA phylogenetic analysis clustered all 4 isolates distantly from *L. koalarum* (ACM 3666), albeit within the same group (Figure).

For the *rpoB* gene sequence, an identity of 85%–88% for genera and 95% for species has been suggested for *Pasteurellaceae* (*2*,*10*,*11*). All isolates of this study had an identity of >95% for the *rpoB* gene of ACM 3666 (Table 2), indicating a close genetic relationship with *L. koalarum*. A minimum level of 83%–85% identity of the partial *infB* gene has been shown between members of the *Pasteurellaceae* family at the genus level (*12*). The partial *infB* gene sequence of MS14434 had a high similarity (99.78%) to the corresponding sequence in ACM 3666, and the partial *infB* genes of the other 3 isolates are at the lower limit of the 83%–85% threshold. These 3 isolates also shared <85% similarity with the *recN* gene of ACM 3666 and >99% similarity with the *recN* gene of each other. The *recN* gene of MS14434 had 97.17% similarity with that of ACM 3666. Using the *recN* similarity index (*8*), we are 95% confident that these 3 isolates are a species other than *L. koalarum* within the genus *Lonepinella*, and MS14434 is most likely *L. koalarum*.

Each case manifested with purulent skin and soft tissue infection requiring surgical washout and debridement, similar to infections linked to *Pasteurella* in dog and cat bite wounds (*13*). MICs of amoxicillin and clavulanic acid, third-generation cephalosporins, and ciprofloxacin were low for all isolates. MIC determination should be sought because 2 isolates were nonsusceptible to benzylpenicillin on the basis of *P. multocida* interpretation criteria (*3*). For

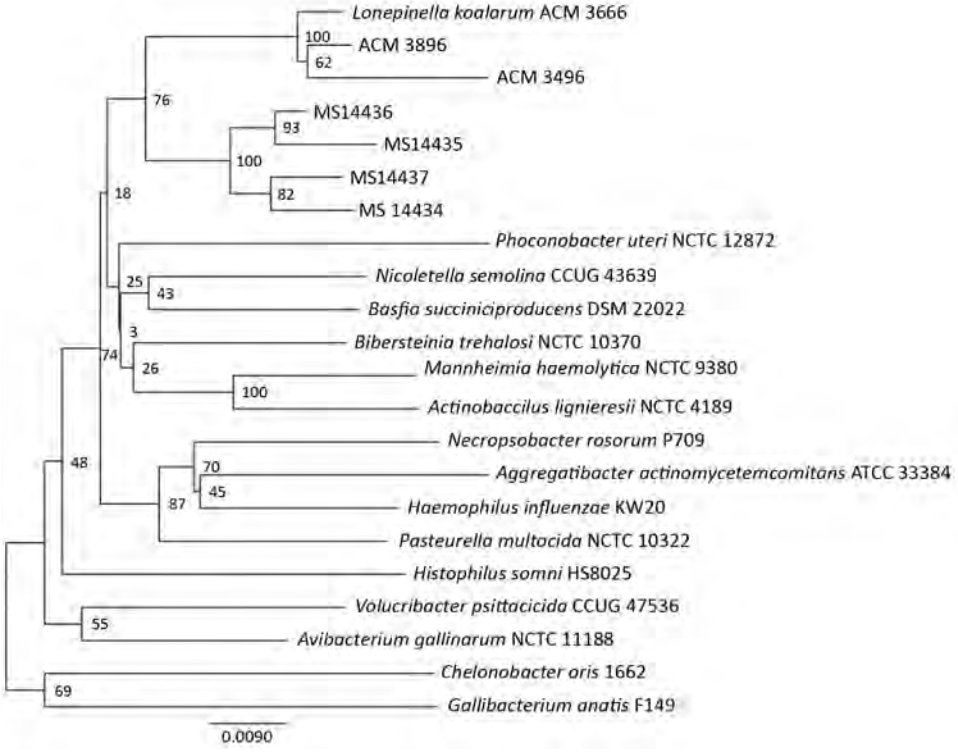

Figure. Neighbor-joining phylogenetic analysis of 16S rRNA gene sequences of 4 clinical isolates obtained from koala bite wound infections in 3 persons (MS14434–7), Queensland, Australia, 3 *Lonepinella koalarum* ACM isolates, and members of the *Pasteurellaceae* family. Scale bar represents nucleotide substitutions per site.

resolution of infection, surgical drainage might be required in addition to antimicrobial drug therapy.

In the original study of *L. koalarum* (*1*), 7 isolates were grouped into 4 biovars (a–d), and 16S rRNA sequencing demonstrated high similarity (97.6%–99.8%). A threshold of 93%–94% identity between 16S rRNA gene sequences has been described for differentiating members of *Pasteurellaceae* at the genus level (*5*) and >97% at the species level (*10*). Although all 4 isolates in our study showed >93% similarity to *L. koalarum* ACM 3666 in their 16S rRNA genes, none of them reached 97% similarity. Both *infB* and *recN* gene sequences indicated a close relationship between MS14434 and ACM 3666; however, 16S rRNA and *rpoB* gene sequences showed the same level of similarity between all 4 isolates and the reference *L. koalarum* strain. This disagreement between genes could be a result of lateral gene transfer; lateral gene transfer of housekeeping genes has been described as a reason for incongruence between 16S rRNA and housekeeping gene phylogeny (*14*).

Conclusions

Clinical and microbiological suspicion is required when assessing bacteria from koala bite wounds. Phenotypic and biochemical colony characteristics are often unreliable at assigning isolates to a genus and species within the *Pasteurellaceae* family, and identification with commercial kits is not always possible. *Pasteurellaceae* spp., including *L. koalarum,* can be identified by using matrix-assisted laser desorption/ionization time-of-flight mass spectrometry with updated spectra (*15*). Clinical laboratory identification methods involve sequencing the 16S rRNA gene and searching nucleotide databases. As seen in this investigation, this approach can be inconclusive, and phylogenetic analysis of sequences including housekeeping genes might be required.

In summary, *Lonepinella* infections acquired after koala bites can cause clinically significant human skin and soft tissue disease. In this report, we identified possibly novel *Lonepinella*-like organisms with a combination of genetic analyses.

Acknowledgments

We thank Scott A. Beatson and Leah Roberts for their scientific support.

About the Author

Dr. Sinclair is an advanced trainee in microbiology and infectious diseases with the Royal College of Pathologists Australasia and Royal Australasian College of Physicians. Her primary research interests include bacteriology, *Aeromonas* identification and infection, antimicrobial resistance, and phylogenetics.

References

1. Osawa R, Rainey F, Fujisawa T, Lang E, Busse HJ, Walsh TP, Stackebrandt E. *Lonepinella koalarum* gen. nov., sp. nov., a new tannin-protein complex degrading bacterium. Syst Appl Microbiol. 1995;18:368–73.
2. Hansen MJ, Bertelsen MF, Kelly A, Bojesen AM. Occurrence of *Pasteurellaceae* Bacteria in the Oral Cavity of Selected Marsupial Species. J Zoo Wildl Med. 2017;48:1215–8. http://dx.doi.org/10.1638/2017-0071.1
3. European Committee on Antimicrobial Susceptibility Testing. Breakpoint tables for interpretation of MICs and zone diameters. Version 5.0. 2015 Jan 1 [cited 2017 Aug 15]. http://www.eucast.org/mic_distributions_and_ecoffs/
4. Nikkari S, Lopez FA, Lepp PW, Cieslak PR, Ladd-Wilson S, Passaro D, et al. Broad-range bacterial detection and the analysis of unexplained death and critical illness. Emerg Infect Dis. 2002;8:188–94. http://dx.doi.org/10.3201/eid0802.010150
5. Korczak B, Christensen H, Emler S, Frey J, Kuhnert P. Phylogeny of the family *Pasteurellaceae* based on *rpoB* sequences. Int J Syst Evol Microbiol. 2004;54:1393–9. http://dx.doi.org/10.1099/ijs.0.03043-0
6. Mullins MA, Register KB, Brunelle BW, Aragon V, Galofré-Mila N, Bayles DO, et al. A curated public database for multilocus sequence typing (MLST) and analysis of *Haemophilus parasuis* based on an optimized typing scheme. Vet Microbiol. 2013;162:899–906. http://dx.doi.org/10.1016/j.vetmic.2012.11.019
7. Omaleki L, Barber SR, Allen JL, Browning GF. *Mannheimia* species associated with ovine mastitis. J Clin Microbiol. 2010;48:3419–22. http://dx.doi.org/10.1128/JCM.01145-10
8. Zeigler DR. Gene sequences useful for predicting relatedness of whole genomes in bacteria. Int J Syst Evol Microbiol. 2003; 53:1893–900. http://dx.doi.org/10.1099/ijs.0.02713-0
9. Kuhnert P, Korczak BM. Prediction of whole-genome DNA-DNA similarity, determination of G+C content and phylogenetic analysis within the family *Pasteurellaceae* by multilocus sequence analysis (MLSA). Microbiology. 2006;152:2537–48. http://dx.doi.org/10.1099/mic.0.28991-0
10. Christensen H, Kuhnert P, Busse HJ, Frederiksen WC, Bisgaard M. Proposed minimal standards for the description of genera, species and subspecies of the *Pasteurellaceae*. Int J Syst Evol Microbiol. 2007;57:166–78. http://dx.doi.org/10.1099/ijs.0.64838-0
11. Bisgaard M, Nørskov-Lauritsen N, de Wit SJ, Hess C, Christensen H. Multilocus sequence phylogenetic analysis of *Avibacterium.* Microbiology. 2012;158:993–1004. http://dx.doi.org/10.1099/mic.0.054429-0
12. Nicklas W, Bisgaard M, Aalbæk B, Kuhnert P, Christensen H. Reclassification of *Actinobacillus muris* as *Muribacter muris* gen. nov., comb. nov. Int J Syst Evol Microbiol. 2015;65:3344–51. http://dx.doi.org/10.1099/ijsem.0.000417
13. Dendle C, Looke D. Review article: Animal bites: an update for management with a focus on infections. Emerg Med Australas. 2008;20:458–67.
14. Christensen H, Kuhnert P, Olsen JE, Bisgaard M. Comparative phylogenies of the housekeeping genes *atpD, infB* and *rpoB* and the 16S rRNA gene within the *Pasteurellaceae.* Int J Syst Evol Microbiol. 2004;54:1601–9. http://dx.doi.org/10.1099/ijs.0.03018-0
15. Kuhnert P, Bisgaard M, Korczak BM, Schwendener S, Christensen H, Frey J. Identification of animal *Pasteurellaceae* by MALDI-TOF mass spectrometry. J Microbiol Methods. 2012;89:1–7. http://dx.doi.org/10.1016/j.mimet.2012.02.001

Address for correspondence: Holly A. Sinclair, Pathology Queensland, Department of Microbiology, Level 5, Block 7, Royal Brisbane and Women's Hospital Complex, Herston, QLD 4029, Australia; email: holly.sinclair@health.qld.gov.au or sinclair_holly@hotmail.com

Surgical Site Infections Caused by Highly Virulent Methicillin-Resistant *Staphylococcus aureus* Sequence Type 398, China

Lu Sun,[1] Yan Chen,[1] Danying Wang, Haiping Wang, Dandan Wu, Keren Shi, Ping Yan, Yunsong Yu

We identified 2 methicillin-resistant *Staphylococcus aureus* strains of sequence type 398 from surgical site infections in China. Genetic analysis and clinical data from these strains suggested that they were human-related but sporadic. Hemolysis analysis and mouse-skin infection models indicated a high virulence potential for these strains.

Methicillin-resistant *Staphylococcus aureus* (MRSA) can cause a variety of infections, such as skin and soft tissue infection (SSTI), pneumonia, and sepsis. MRSA can also cause surgical site infections (SSI), which are the most common type of healthcare-associated infections in hospitals (*1*). In addition, MRSA infection has been reported in animals, including pigs, veal calves, and poultry (*2*). Livestock-associated MRSA (LA-MRSA) was first reported in humans in the Netherlands in 2003 (*3*), and numerous countries have subsequently reported the presence of this MRSA variant. Although LA-MRSA belongs to several clone complexes, the major clone of LA-MRSA belongs to sequence type (ST) 398 (*4*).

Several infections caused by MRSA ST398 have been reported in the community, ranging from mild skin infections to serious invasive infections, both with and without livestock contact. Fatal cases of septicemia were also reported in Japan and Denmark (*5*,*6*). MRSA ST398 isolates from human postoperative surgical site infections were presented with complete genome sequencing in Canada and in a long-term MRSA surveillance study in the United Kingdom (*7*,*8*). The virulence potential of MRSA ST398 isolated from SSI has not been reported to date.

Author affiliations: Sir Run Run Shaw Hospital of Zhejiang University School of Medicine, Hangzhou, China (L. Sun, Y. Chen, D. Wang, H. Wang, D. Wu, K. Shi, Y. Yu); Fuyang Hospital of Traumatology and Orthopedics of Traditional Chinese Medicine, Hangzhou (P. Yan); Key Laboratory for Microbial Technology and Bioinformatics of Zhejiang Province, Hangzhou (Y. Yu)

DOI: https://doi.org/10.3201/eid2501.171862

We studied 2 MRSA ST398 strains from surgical site infections, focusing on their clinical characteristics, genetic features, and virulence potential. The study was approved by the local ethics committees in Sir Run Run Shaw Hospital with a waiver of informed consent (approval no. 20150115-1). Mouse experiments were performed with approval from the Institutional Animal Ethics Committee of Zhejiang University (approval no. ZJU2015-141-01).

The Study

From January 2013 through December 2014, we collected a total of 147 *Staphylococcus aureus* isolates at Fuyang Hospital of Traumatology and Orthopedics of Traditional Chinese Medicine, a tertiary hospital in Hangzhou, China, with ≈500 beds. We performed multilocus sequence type (MLST) analysis on 18 SSI MRSA isolates from patients who underwent orthopedic surgery. We detected 2 MRSA strains, FY20 and FY22, which belong to ST398.

We characterized these strains by antimicrobial drug susceptibility testing, whole-genome sequencing and comparison, hemolysis analysis, and a mouse skin infection model. We included 2 community-acquired MRSA (CA-MRSA) strains isolated from patients in 2015 at Sir Run Run Shaw Hospital for comparison; SR389 was isolated from a 32-year-old female outpatient with a left neck mass, and SR411 was isolated from a 21-year-old female outpatient with lower extremity nodules and an ulcer. We sequenced the genomes on an Illumina HiSeq2000 platform (Illumina, http://www.illumina.com). We deposited the draft genome of FY20 as GenBank accession no. NTMC00000000, for FY22 as NXFU00000000, for SR389 as PDFA00000000, and for SR411 as PDFB00000000. We imported FASTA files into SeqSphere+ software version 4.1 (Ridom GmbH, http://www.ridom.de/seqsphere) for analysis (*9*). We detected virulence and resistance genes using the Center for Genomic Epidemiology website (http://www.genomicepidemiology.org).

We collected supernatants from bacterial cultures grown at 37°C for 24 h with shaking at 180 rpm. We determined hemolytic activities by incubating samples with human red blood cells (2% vol/vol in Dulbecco's phosphate-buffered saline) for 1 h at 37°C and subsequently by

[1]These authors contributed equally to this article.

Table. Characteristics of methicillin-resistant *Staphylococcus aureus* sequence type 398 isolates from 4 patients, China*

Characteristic	Isolate			
	FY20	FY22	SR389	SR411
Patient age, y/sex	42/F	52/M	32/F	21/F
Admission diagnosis	Right tibial plateau comminuted fracture	Right tibial plateau comminuted fracture	Left neck mass	Lower extremity nodules with ulceration
Infection type	SSI	SSI	SSTI	SSTI
SCC*mec* type	V	V	V	V
spa type	t034	t034	t034	t1255
Panton–Valentine leukocidin	–	–	–	–
Resistance phenotype	PEN, OXA, CLI, ERY	PEN, OXA	PEN, OXA	PEN, OXA, CLI, ERY
Resistance genes	*mecA*, *blaZ*, *ermC*	*mecA*, *blaZ*	*mecA*, *blaZ*	*mecA*, *blaZ*, *ermC*
Virulence factors	aur, sak, scn, hlb, hlgA, hlgB, hlgC	aur, sak, scn, hlb, hlgA, hlgB, hlgC	aur, sak, scn, hlb, hlgA, hlgB, hlgC	aur, sak, scn, hlb, hlgA, hlgB, hlgC

*aur, aureolysin; CLI, clindamycin; ERY, erythromycin; hlb, β-hemolysin; hlgA, gamma-hemolysin component; OXA, oxacillin; PEN, penicillin; sak, staphylokinase; scn, staphylococcal complement inhibitor; SCC, staphylococcal cassette chromosome; SSI, surgical site infection; SSTI, skin and soft tissue infection; –, negative.

measuring the optical density at 540 nm using an ELISA reader. We performed the mouse skin infection model using BALB/c female nude mice, 4–6 weeks of age. We injected anesthetized mice subcutaneously with ≈1 × 10^7 bacterial cells in 50 μL phosphate-buffered saline in the back. We measured length and width of the abscess or lesion for 6 days with calipers, and calculated abscess size by length × width. We euthanized all mice 6 days after injection. We used South Korea CA-MRSA strain HL1 (ST72) and its mutant HL1Δ*agr* in the skin infection model and the hemolysis study for comparison (*10*). We performed statistical analysis using GraphPad Prism version 7.01 (GraphPad Software, https://www.graphpad.com).

We isolated both MRSA strains from SSIs, FY20 and FY22. FY20 was isolated from a 42-year-old female patient who had undergone steel plate–screw internal fixation after a right tibial plateau comminuted fracture in May 2014. She was discharged in June 2014 and admitted to the hospital again because of swelling and pain in her right knee 71 days after surgery. The abscess was surgically

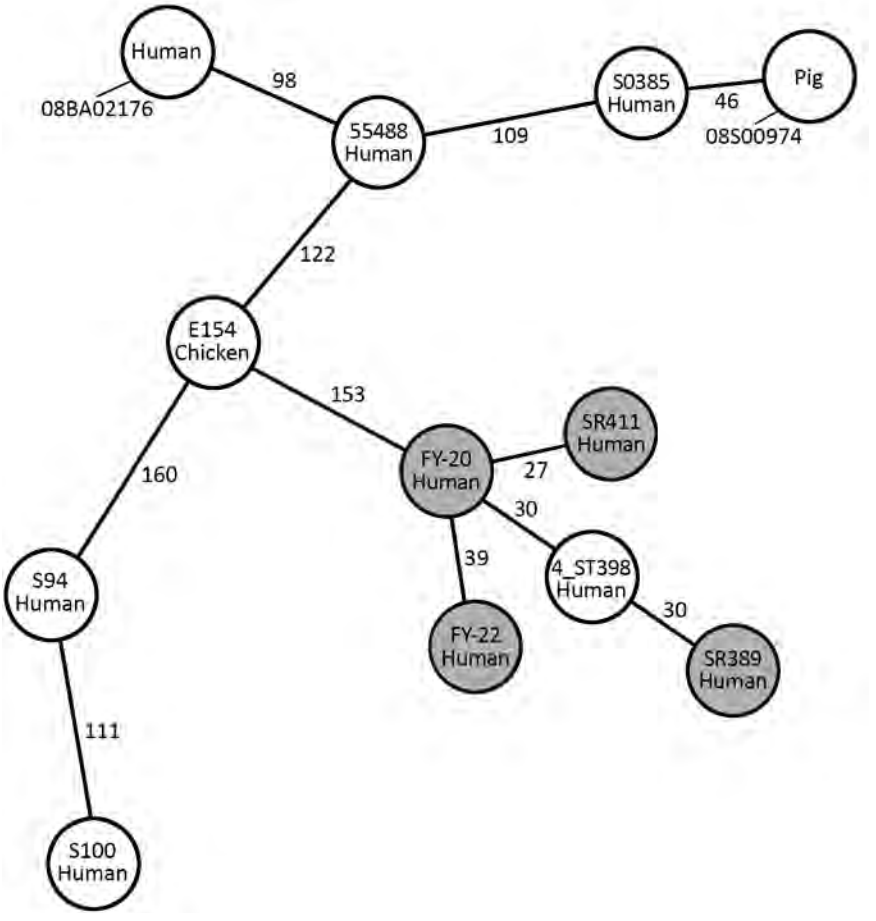

Figure 1. Minimum-spanning tree built from the core genome multilocus sequence type allelic profiles of MRSA ST398 strains from 4 patients in China (gray circles) and other ST398 strains. Each circle represents a single strain and is named with the sample and the origin. The 12 strains are based on 1,807 columns with the pairwise ignoring missing values option in Ridom SeqSphere+ software (Ridom GmbH, http://www.ridom.de/seqsphere). The numbers on the connecting lines indicate the number of allelic differences between 2 strains. *S. aureus* strain COL (GenBank accession no. NC_002951) is used as a reference. S0385 (human, MRSA, NC_017333.1), 08BA02176 (human, MRSA, CP003808.1), 55488 (human, MRSA, NZ_LAWV00000000), 4_ST398 (human, MRSA, He L et al, 2018), S94 (human, MSSA, AUPW00000000), S100 (human, MSSA, AUPV00000000), 08S00974 (animal, MRSA, NZ_CP020019.1), and E154 (animal, MRSA, CP013218.1), are used for comparison. MRSA, methicillin-resistant *Staphylococcus aureus*; ST, sequence type.

debrided, and she was treated with levofloxacin. We isolated FY22 from a 52-year-old male patient. This patient also underwent steel plate–screw internal fixation after a right tibial plateau comminuted fracture in August 2014. He was discharged in September 2014 and was admitted to the hospital again for pus and exudate from the incision site in the right knee 21 days after surgery. The wound was surgically debrided, and he was treated with cefuroxime and levofloxacin. These 2 patients were admitted to different wards and were treated by different teams during hospitalization.

Antimicrobial susceptibility testing results showed that the 4 ST398 strains in our study had a similar resistance phenotype; they displayed resistance to β-lactam antimicrobial drugs but were susceptible to most other antimicrobial drugs. FY20 and SR411 were resistant to clindamycin and erythromycin. Resistance genes detected using the Center for Genomic Epidemiology site matched the resistance phenotypes (Table). The 4 ST398 strains were negative for *tetM* and *czrC*, were positive for φSa3, and displayed susceptibility to tetracycline. We classified FY20, FY22, and SR389 into SCC*mec* V and *spa*-type t034, and SR411 into SCC*mec* V and *spa*-type t1255. We built a minimum-spanning tree based on the core genome MLST (cgMLST) allelic profiles (Figure 1). There were 27 allelic differences by cgMLST analysis between FY20 and SR411; for 5 pairs of other strains from our study (FY20 and FY22, FY20 and SR389, FY22 and SR389, FY22 and SR411, and SR389 and SR411), there were ≥30 allelic differences. From a previous study, 9–29 allelic differences can be considered possibly related, whereas >30 are considered unrelated (*11*). When we compared the strains in our study to MRSA ST398 strain 4_ST398 from a hospital in Shanghai (*12*), we found 30–40 allelic differences between each of our 4 strains and the reference strain. There were ≥150 allelic differences between the SSI strains in our study and other ST398 strains, including animal- and human-related strains, from other studies (*7,13,14*).

All 4 strains in our study contained the same virulence factors (Table). We analyzed the lysis of human erythrocytes, which is a key determinant of *S. aureus* virulence. Erythrocyte lysis by SR389, FY20, and FY22 was stronger than for CA-MRSA HL1 ($p<0.05$) (Figure 2, panel A), whereas SR411 showed a relatively weaker lytic capacity. We used a mouse skin infection model to evaluate the virulence potential of ST398 strains in vivo. In this model, abscesses caused by SSI strains (FY20 and FY22) were significantly larger than those caused by SR411 and the HL1 *agr* mutant ($p<0.05$) and were similar to those caused by SR389 and HL1 ($p>0.05$) (Figure 2, panel B). These findings demonstrated the pronounced virulence potential of SSI ST398 strains to cause invasive skin infections similar to those associated with HL1, which was a predominant CA-MRSA clone in South Korea.

Conclusions

We reported 2 ST398 MRSA strains causing SSI, which were classified into hospital-acquired MRSA according to the Centers for Disease Control and Prevention definition (*15*). The clinical data and cgMLST results indicated no clonal transmission in these 2 cases. These 2 patients denied livestock contact, and further genetic analysis showed characteristics of human-associated isolates. It is possible that the 2 patients were colonized with ST398 MRSA in the community and their infections developed later, after

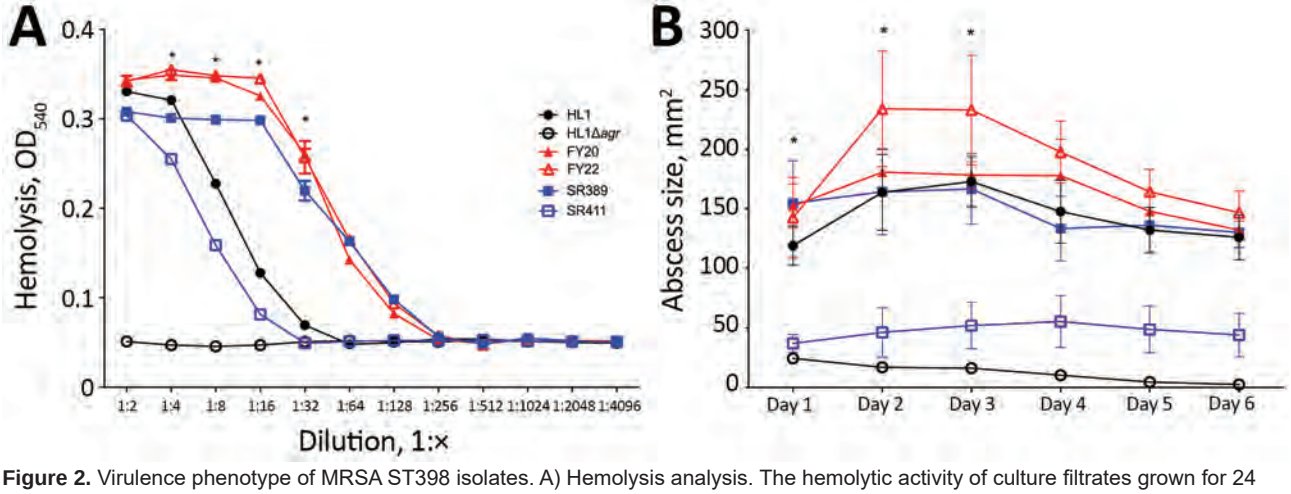

Figure 2. Virulence phenotype of MRSA ST398 isolates. A) Hemolysis analysis. The hemolytic activity of culture filtrates grown for 24 h was measured in triplicate at given dilutions. The mean and SE are shown. The statistical analysis used a 2-way analysis of variance between multiple groups. FY20 and FY22 were significantly stronger than other strains in dilution 1:4, 1:8, 1:16, and 1:32 ($p<0.05$). B) Abscess sizes in the mouse skin infection model. There were 4 mice per strain, and the mean and SE are shown. The statistical analysis used a 2-way analysis of variance to compare data for multiple groups. The abscess sizes of FY20 and FY22 were significantly larger than SR411 and the HL1 *agr* mutant ($p<0.05$) but were similar to SR389 and HL1 ($p>0.05$) at day 1, day 2, and day 3. MRSA, methicillin-resistant *Staphylococcus aureus*; OD, optical density; ST, sequence type.

surgery. A limitation of this study is that we detected only 2 ST398 HA-MRSA strains, which means that it is difficult to evaluate the spreading trend and the threat of this lineage in the healthcare setting. However, our results revealed the emergence and transmission pattern of ST398 MRSA in the surgical department of a hospital in China.

Acknowledgments

We thank Min Li for providing the sequence file of the MRSA ST398 strain.

This work was supported by grants from the National Natural Science Foundation of China (grant no. 81501788) and the Zhejiang Provincial Natural Science Foundation of China (grant no. Q16H190005). All authors report no potential conflicts.

About the Author

Miss Sun is a student at Zhejiang University School of Medicine. Her research focuses on MRSA infections and using whole-genome sequencing to investigate the changing epidemiology of CA-MRSA in China.

References

1. Baker AW, Dicks KV, Durkin MJ, Weber DJ, Lewis SS, Moehring RW, et al. Epidemiology of surgical site infection in a community hospital network. Infect Control Hosp Epidemiol. 2016;37:519–26. http://dx.doi.org/10.1017/ice.2016.13
2. Verkade E, Kluytmans J. Livestock-associated *Staphylococcus aureus* CC398: animal reservoirs and human infections. Infect Genet Evol. 2014;21:523–30. http://dx.doi.org/10.1016/j.meegid.2013.02.013
3. Voss A, Loeffen F, Bakker J, Klaassen C, Wulf M. Methicillin-resistant *Staphylococcus aureus* in pig farming. Emerg Infect Dis. 2005;11:1965–6. PubMed http://dx.doi.org/10.3201/eid1112.050428
4. Huijsdens XW, van Dijke BJ, Spalburg E, van Santen-Verheuvel MG, Heck ME, Pluister GN, et al. Community-acquired MRSA and pig-farming. Ann Clin Microbiol Antimicrob. 2006;5:26. http://dx.doi.org/10.1186/1476-0711-5-26
5. Nielsen RT, Kemp M, Holm A, Skov MN, Detlefsen M, Hasman H, et al. Fatal septicemia linked to transmission of MRSA clonal complex 398 in hospital and nursing home, Denmark. Emerg Infect Dis. 2016;22:900–2. http://dx.doi.org/10.3201/eid2205.151835
6. Koyama H, Sanui M, Saga T, Harada S, Ishii Y, Tateda K, et al. A fatal infection caused by sequence type 398 methicillin-resistant *Staphylococcus aureus* carrying the Panton-Valentine leukocidin gene: A case report in Japan. J Infect Chemother. 2015;21:541–3. http://dx.doi.org/10.1016/j.jiac.2015.03.013
7. Golding GR, Bryden L, Levett PN, McDonald RR, Wong A, Graham MR, et al. Whole-genome sequence of livestock-associated st398 methicillin-resistant *Staphylococcus aureus* isolated from humans in Canada. J Bacteriol. 2012;194:6627–8. http://dx.doi.org/10.1128/JB.01680-12
8. Bortolami A, Williams NJ, McGowan CM, Kelly PG, Archer DC, Corrò M, et al. Environmental surveillance identifies multiple introductions of MRSA CC398 in an equine veterinary hospital in the UK, 2011–2016. Sci Rep. 2017;7:5499. http://dx.doi.org/10.1038/s41598-017-05559-8
9. Leopold SR, Goering RV, Witten A, Harmsen D, Mellmann A. Bacterial whole-genome sequencing revisited: portable, scalable, and standardized analysis for typing and detection of virulence and antibiotic resistance genes. J Clin Microbiol. 2014;52:2365–70. http://dx.doi.org/10.1128/JCM.00262-14
10. Chen Y, Yeh AJ, Cheung GY, Villaruz AE, Tan VY, Joo HS, et al. Basis of virulence in a Panton-Valentine leukocidin–negative community-associated methicillin-resistant *Staphylococcus aureus* strain. J Infect Dis. 2015;211:472–80. http://dx.doi.org/10.1093/infdis/jiu462
11. Cunningham SA, Chia N, Jeraldo PR, Quest DJ, Johnson JA, Boxrud DJ, et al. Comparison of whole-genome sequencing methods for analysis of three methicillin-resistant *Staphylococcus aureus* outbreaks. J Clin Microbiol. 2017;55:1946–53. http://dx.doi.org/10.1128/JCM.00029-17
12. He L, Zheng HX, Wang Y, Le KY, Liu Q, Shang J, et al. Detection and analysis of methicillin-resistant human-adapted sequence type 398 allows insight into community-associated methicillin-resistant *Staphylococcus aureus* evolution. Genome Med. 2018;10:5. http://dx.doi.org/10.1186/s13073-018-0514-9
13. Schijffelen MJ, Boel CH, van Strijp JA, Fluit AC. Whole genome analysis of a livestock-associated methicillin-resistant *Staphylococcus aureus* ST398 isolate from a case of human endocarditis. BMC Genomics. 2010;11:376. http://dx.doi.org/10.1186/1471-2164-11-376
14. van der Mee-Marquet N, Corvaglia AR, Valentin AS, Hernandez D, Bertrand X, Girard M, et al. Analysis of prophages harbored by the human-adapted subpopulation of *Staphylococcus aureus* CC398. Infect Genet Evol. 2013;18:299–308. http://dx.doi.org/10.1016/j.meegid.2013.06.009
15. David MZ, Daum RS. Community-associated methicillin-resistant *Staphylococcus aureus*: epidemiology and clinical consequences of an emerging epidemic. Clin Microbiol Rev. 2010;23:616–87. http://dx.doi.org/10.1128/CMR.00081-09

Address for correspondence: Yunsong Yu, Zhejiang University School of Medicine, Sir Run Run Shaw Hospital—Infectious Diseases, 3# East Qingchun Rd, Hangzhou, Zhejiang 310016, China; email: yvys119@zju.edu.cn

Canine Influenza Virus A(H3N2) Clade with Antigenic Variation, China, 2016–2017

Yanli Lyu,[1] Shikai Song,[1] Liwei Zhou,[1] Guoxia Bing, Qian Wang, Haoran Sun, Mingyue Chen, Junyi Hu, Mingyang Wang, Honglei Sun, Juan Pu, Zhaofei Xia, Jinhua Liu, Yipeng Sun

During 2012–2017, we collected throat swabs from dogs in China to characterize canine influenza virus (CIV) A(H3N2) isolates. A new antigenically and genetically distinct CIV H3N2 clade possessing mutations associated with mammalian adaptation emerged in 2016 and replaced previously circulating strains. This clade probably poses a risk for zoonotic infection.

Canine influenza can be caused by a variety of influenza A viruses, including equine-origin H3N8 and avian-origin H3N2 viruses, which are both established lineages in dogs worldwide. Canine influenza virus (CIV) A(H3N8) has predominantly circulated in the United States since 2004 (*1*,*2*), and CIV A(H3N2) mainly prevails in China and South Korea (*3*,*4*). CIV H3N2 was first isolated in 2006 from Guangdong Province, China, and found to be genetically most closely related to H3N2 avian influenza viruses prevalent in aquatic birds in South Korea (*5*). Since 2006, H3N2 CIV has rapidly become prevalent in China and South Korea (*6*,*7*) and has also been isolated in Thailand and the United States (*8*,*9*).

CIV usually causes mild respiratory symptoms, and CIV-infected dogs often recover without treatment. As a consequence, animal owners and veterinarians often neglect treating CIV infections, creating an opportunity for CIVs to circulate and further adapt in dogs. Mutations leading to better growth in dogs could enhance infectiousness in other mammals (e.g., humans). Also, CIVs are antigenically novel to the human immune system and, thus, might pose a threat to public health. Therefore, we set out to characterize CIV H3N2 in dogs in China to assess the potential risk to the public.

The Study

During October 2012–July 2017, we collected 399 throat swabs from dogs with respiratory symptoms in pet hospitals and kennels in China to monitor for CIV H3N2 epidemics and virus evolution. We amplified the matrix gene by real-time reverse transcription PCR using Influenza A Virus V8 Rapid Real-Time RT-PCR Detection Kit (Beijing Anheal Laboratories Co. Ltd., http://anheal.company.weiku.com) and isolated and identified virus isolates using methods previously described (*6*). Of 399 samples, 54 (13.5%) contained CIV H3N2 isolates. Of these 54 isolates, 43 were from Beijing, 6 from Nanjing, 3 from Shanghai, and 2 from Xi'an.

To characterize the evolution of CIV H3N2, we sequenced the full genome of the 54 isolates (GenBank accession nos. MK212398–829) and performed genetic analyses using available sequences of related viruses from GenBank and the GISAID database (https://www.gisaid.org). Phylogenetic analysis of worldwide CIV H3N2 isolates indicated that each genome segment of the H3N2 isolates after 2016 formed a separate clade, distinct from other isolates from China, which grouped with isolates from South Korea and the United States (Figure 1; Appendix Figure, https://wwwnc.cdc.gov/EID/article/25/1/17-1878-App1.pdf). Each genome segment of the 41 H3N2 CIVs isolated after 2016 shared high nucleotide sequence identities (99.62% ± 0.09% to 99.88% ± 0.10%). Among these isolates, the time to most recent common ancestor computed by molecular clock analysis (*10*,*11*) was similar for each genome segment; all ancestors dated back to early to mid-2016 (Appendix Figure). Therefore, the introduction of this CIV H3N2 clade into China most likely occurred in 2016 as either a single event or multiple events involving genetically similar viruses. This clade was more closely related to earlier H3N2 CIVs than the ancestral H3N2 avian influenza viruses from South Korea (Figure 1), and viruses of this clade could have originated from H3N2 CIVs circulating in South Korea or the United States.

We then investigated the molecular characteristics of these viruses. Although all the CIV H3N2 isolates from this clade still possessed 226Q and 228G (which confer specificity to cell entry receptors in birds) in hemagglutinin, they also possessed the 4 amino acid substitutions 251R and 590S in polymerase basic 2 and 146S and 242I in hemagglutinin, which have frequently been identified in human influenza viruses. Of note, 251R and 590S in polymerase basic 2 are known determinants of adaptation to growth in mammals (Table 1) (*12*,*13*).

Author affiliations: China Agricultural University, Beijing, China (Y. Lyu, S. Song, L. Zhou, Q. Wang, Haoran Sun, M. Chen, J. Hu, M. Wang, Honglei Sun, J. Pu, Z. Xia, J. Liu, Y. Sun); China Animal Disease Control Center, Beijing (G. Bing)

DOI: https://doi.org/10.3201/eid2501.171878

[1]These authors contributed equally to this article.

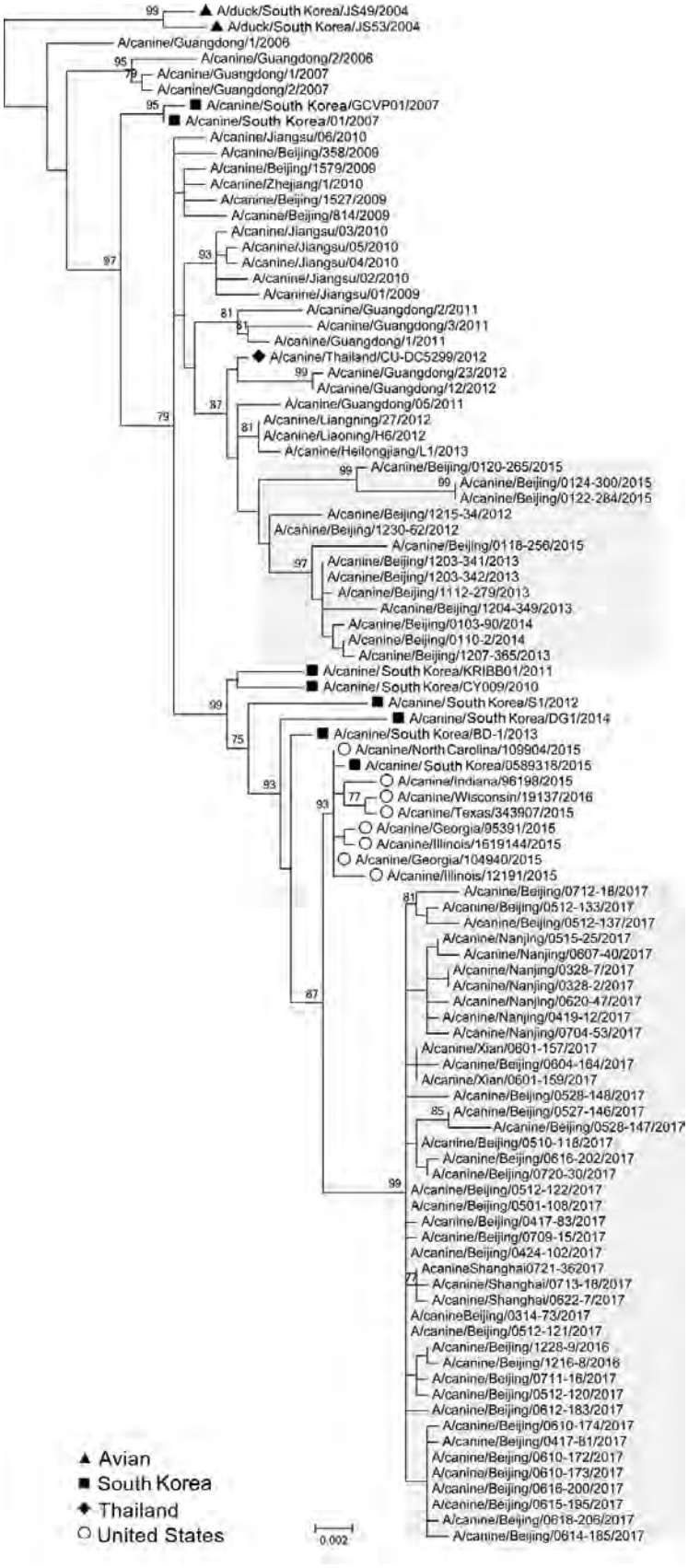

Figure 1. Maximum-likelihood phylogenetic tree of hemagglutinin genomic segment of H3N2 canine influenza viruses (CIVs). The phylogeny of 97 H3N2 CIVs available in public databases and the 8 hemagglutinin genomic segments sequenced in this study were inferred by using MEGA version 6 (https://www.megasoftware.net) under the general time-reversible plus gamma distribution model with 1,000 bootstrap replicates. Avian isolates of ancestral strain (triangles) and canine isolates from South Korea (squares), Thailand (diamonds), and the United States (circles) are indicated. Shading indicates isolates sequenced in this study. Scale bar indicates substitutions per nucleotide.

Table 1. Possible mammalian adaptation related to amino acid substitutions in CIV H3N2, China, 2016–2017*

	Virus protein, amino acid position, amino acid (frequency, %)			
	Polymerase basic 2		Hemagglutinin	
Category	251	590	146	242
CIV H3N2, 2006–2015	K (89.19), R† (8.11), G (2.70)	G (100)	G (91.89), S (8.11)	V (100)
CIV H3N2, 2016–2017	R† (100)	S† (100)	S (100)	I (100)
Influenza virus A(H3N2) in humans	R† (99.82), K (0.14), G (0.04)	S† (89.76), G (10.06), N (0.14), T (0.04), R (0.01)	S (99.57), G (0.42), F (0.01)	I (99.29), V (0.39), M (0.20), T (0.08), L (0.03), K (0.02)
Influenza A(H1N1)pdm09 virus	R† (98.99), K (0.99), I (0.02)	S† (99.43), N (0.35), G (0.22)	K (99.64), N (0.23), R (0.07), E (0.06)	F (99.99), L (0.01)

*CIV, canine influenza virus.
†Known determinant for adaptation to mammals.

Antigenic analysis with ferret antiserum against representative viruses of different clades demonstrated a diversity of reaction patterns that generally corresponded with phylogenetic relationships (Table 2). H3N2 CIVs isolated during 2016–2017 reacted well with antiserum against viruses of the same lineage and less well with antiserum against viruses of other lineages. Numeric analysis of these hemagglutinin inhibition (HI) titers with AntigenMap (http://sysbio.cvm.msstate.edu/software/AntigenMap) revealed that H3N2 CIVs isolated after 2016 had a distinguishable antigenic reaction pattern (Figure 2).

The CIV H3N2–positive dogs in this study generally had only respiratory symptoms and recovered within 10 days. However, the virus spread rapidly. Among dogs in a cohort, 1 displayed mild disease (cough, runny nose, lethargy) soon after being introduced into a kennel. Within 3 days, similar symptoms were observed in 16 more dogs within that kennel. Real-time reverse transcription PCR confirmed that all 17 dogs were CIV positive. We obtained 2 CIV H3N2 isolates (A/canine/Beijing/0512-133/2017 and A/canine/Beijing/0512-137/2017) from 2 German shepherd dogs in this kennel.

To determine the prevalence of CIV H3N2 in dogs, we randomly performed serologic surveillance for H3N2 virus among dogs visiting the Veterinary Teaching Hospital of China Agricultural University (Beijing, China) in 2017. Of 240 serum samples, 15 (6.3%) were positive for CIV H3N2 (HI titers against A/canine/Beijing/0512-137/2017 of ≥40). To evaluate whether humans can be infected by CIV H3N2, we collected serum samples from pet owners (n = 50), veterinarians (n = 5), and animal hospital staff (n = 23) who had contact with CIV-positive dogs. Serum from

Table 2. Antigenic analysis of H3N2 subtype canine influenza viruses, China, 2009–2017*

	HI titer, by antigenic group and antiserum							
Antigenic group and virus	A, 814/2009	A, 362/2009	B, 0110-2/2014	B, 0118-256/2015	B, 0120-265/2015	C, 1228-9/2016	C, 0512-13720/17	C, 0527-147/2017
A								
814/2009	1,280†	1,280	1,280	160	320	320	320	160
1527/2009	640	1,280	2,560	320	160	320	320	320
1579/2009	640	2,560	1,280	160	160	320	320	320
362/2009	640	1,280†	1,280	320	160	320	160	160
B								
1215-34/2012	160	640	1,280	160	640	1,280	640	1,280
0203-342/2013	320	640	640	640	640	640	1,280	320
1207-365/2013	320	640	1,280	640	1,280	640	1,280	640
0110-2/2014	640	2,560	1,280†	640	320	1,280	640	640
0118-256/2015	320	640	1,280	1,280†	640	640	320	320
0120-265/2015	640	640	1,280	640	1,280†	640	320	640
0124-300/2015	320	1280	1280	640	640	160	640	640
C								
1228-9/2016	80	80	80	160	1,280	1,280†	640	640
0424-102/2017	80	80	320	80	160	640	640	1,280
0512-120/2017	80	80	320	160	320	640	1,280	1,280
0512-133/2017	80	40	320	40	160	640	640	1,280
0512-137/2017	160	80	320	160	320	1,280	1,280†	640
0527-148/2017	80	80	320	80	320	640	2,560	1,280
0527-146/2017	80	40	320	80	320	640	640	640
0527-147/2017	80	320	320	160	160	2,560	1,280	1,280†
0601-159/2017	80	40	320	80	160	640	640	640
0610-173/2017	40	40	320	80	160	640	640	640
0721-36/2017	80	40	320	80	160	640	640	640

*Virus names are abbreviated as serial number and year. HI titers are the inverse of the highest dilution that inhibited hemagglutination. Cells containing moderate HI titers (160, 320) are shaded gray and high titers (≥640) black. Low HI titers (40, 80) were not shaded. HI, hemagglutinin inhibition.
†Homologous titers.

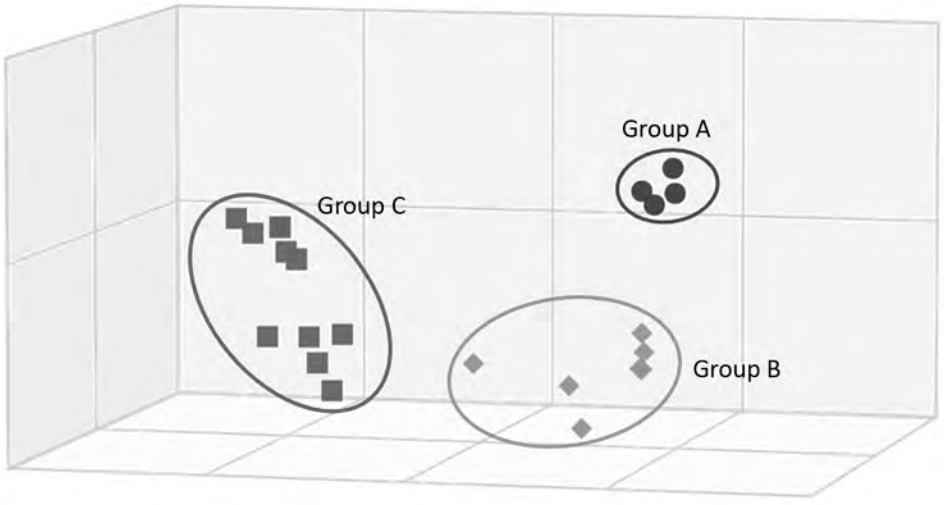

Figure 2. Antigenic cartograph representative of hemagglutinin inhibition (HI) titers of canine influenza viruses, China, 2009–2017, showing antigenic groups A–C. Map was generated by using AntigenMap 3D (http://sysbio.cvm.msstate.edu/software/AntigenMap) and HI data shown in Table 2. One unit (cell) represents a 2-fold change in HI titer.

1 pet owner tested positive for CIV H3N2 (HI titer 80), revealing that this virus is a potential threat to public health.

Conclusions

CIV H3N2 originated from avian influenza viruses in aquatic birds. We found that H3N2 viruses of a novel genetic clade and antigenicity have prevailed in dogs in some areas of China since 2016, completely replacing the previous strains; this H3N2 clade might have originated from CIVs in South Korea or the United States. However, the sparse sequence data for isolates from South Korea and the United States and the absence of CIV H3N2 sequences from these countries after 2016 prevent identification of the ancestor of this clade. Unlike the geographic clustering of isolates observed during the spread of H3N2 CIVs in the United States (*8*), the H3N2 CIVs isolated during 2016–2017 in Beijing (northern China), Shanghai and Nanjing (southeastern China), and Xi'an (western China) have high genetic identities.

In 2017, the percentage of dogs treated at the Veterinary Teaching Hospital of China Agricultural University that were seropositive for CIV H3N2 was 6.3%, higher than the percentage during 2012–2013 (3.5%) (*14*). The wide prevalence and increased seropositivity of H3N2 variants suggest the lineage that emerged in 2016 might possess greater infectivity in dogs than earlier viruses, which might have resulted in clade replacement. The possibility of stochastic events leading to the disappearance of the previous clade should not be excluded. Considering that preadaptation of influenza A(H1N1)pdm09 virus genes to mammalian hosts through prior circulation for several decades in swine might have contributed to the emergence of viruses containing these genes in humans, the potential adaptation of this CIV H3N2 clade to mammals and its public health threat should be further evaluated.

Because dog competitions and trade involving different countries are frequent and the surveillance of CIV is limited, further studies should focus on determining whether viruses of this CIV H3N2 lineage are prevalent in other countries. Global active surveillance to monitor the spread of these viruses among dogs should also be enhanced. Such efforts could prevent further CIV spread and adaptation and will be critical for identifying public health threats that could emerge at the animal–human interface.

This work was supported by the National Natural Science Foundation of China (31672573), National Natural Science Fund for Outstanding Young Scholars (31522058), Beijing New-Star Plan of Science and Technology (Z161100004916115), Beijing Municipal Science and Technology Project (Z171100001517008), and grants from the Chang Jiang Scholars Program.

About the Author

Dr. Lyu is an associate professor at the College of Veterinary Medicine, China Agricultural University, Beijing, China, and a veterinarian at the Veterinary Teaching Hospital of China Agricultural University. Her research interests include diseases that affect dogs and cats.

References

1. Crawford PC, Dubovi EJ, Castleman WL, Stephenson I, Gibbs EP, Chen L, et al. Transmission of equine influenza virus to dogs. Science. 2005;310:482–5. http://dx.doi.org/10.1126/science.1117950
2. Pecoraro HL, Bennett S, Spindel ME, Landolt GA. Evolution of the hemagglutinin gene of H3N8 canine influenza virus in dogs. Virus Genes. 2014;49:393–9. http://dx.doi.org/10.1007/s11262-014-1102-8
3. Zhu H, Hughes J, Murcia PR. Origins and evolutionary dynamics of H3N2 canine influenza virus. J Virol. 2015;89:5406–18. http://dx.doi.org/10.1128/JVI.03395-14
4. Song D, Kang B, Lee C, Jung K, Ha G, Kang D, et al. Transmission of avian influenza virus (H3N2) to dogs. Emerg Infect Dis. 2008;14:741–6. http://dx.doi.org/10.3201/eid1405.071471
5. Li S, Shi Z, Jiao P, Zhang G, Zhong Z, Tian W, et al. Avian-origin H3N2 canine influenza A viruses in Southern China.

Infect Genet Evol. 2010;10:1286–8. http://dx.doi.org/10.1016/j.meegid.2010.08.010
6. Sun Y, Sun S, Ma J, Tan Y, Du L, Shen Y, et al. Identification and characterization of avian-origin H3N2 canine influenza viruses in northern China during 2009–2010. Virology. 2013;435:301–7. http://dx.doi.org/10.1016/j.virol.2012.09.037
7. Lee E, Kim EJ, Kim BH, Song JY, Cho IS, Shin YK. Molecular analyses of H3N2 canine influenza viruses isolated from Korea during 2013–2014. Virus Genes. 2016;52:204–17. http://dx.doi.org/10.1007/s11262-015-1274-x
8. Voorhees IEH, Glaser AL, Toohey-Kurth K, Newbury S, Dalziel BD, Dubovi EJ, et al. Spread of canine influenza A(H3N2) virus, United States. Emerg Infect Dis. 2017;23:1950–7. http://dx.doi.org/10.3201/eid2312.170246
9. Bunpapong N, Nonthabenjawan N, Chaiwong S, Tangwangvivat R, Boonyapisitsopa S, Jairak W, et al. Genetic characterization of canine influenza A virus (H3N2) in Thailand. Virus Genes. 2014;48:56–63. http://dx.doi.org/10.1007/s11262-013-0978-z
10. Drummond AJ, Rambaut A. BEAST: Bayesian evolutionary analysis by sampling trees. BMC Evol Biol. 2007;7:214. http://dx.doi.org/10.1186/1471-2148-7-214
11. Smith GJ, Vijaykrishna D, Bahl J, Lycett SJ, Worobey M, Pybus OG, et al. Origins and evolutionary genomics of the 2009 swine-origin H1N1 influenza A epidemic. Nature. 2009;459:1122–5. http://dx.doi.org/10.1038/nature08182
12. Prokopyeva EA, Sobolev IA, Prokopyev MV, Shestopalov AM. Adaptation of influenza A(H1N1)pdm09 virus in experimental mouse models. Infect Genet Evol. 2016;39:265–71. http://dx.doi.org/ z10.1016/j.meegid.2016.01.022
13. Mehle A, Doudna JA. Adaptive strategies of the influenza virus polymerase for replication in humans. Proc Natl Acad Sci U S A. 2009;106:21312–6. http://dx.doi.org/10.1073/pnas.0911915106
14. Sun Y, Shen Y, Zhang X, Wang Q, Liu L, Han X, et al. A serological survey of canine H3N2, pandemic H1N1/09 and human seasonal H3N2 influenza viruses in dogs in China. Vet Microbiol. 2014;168:193–6. http://dx.doi.org/10.1016/j.vetmic.2013.10.012

Address for correspondence: Yipeng Sun, China Agricultural University, Key Laboratory of Animal Epidemiology of the Ministry of Agriculture, College of Veterinary Medicine, No. 2 Yuanmingyuan West Rd, Beijing 100193, China; email: sypcau@163.com

Isolation and Full-Genome Characterization of Nipah Viruses from Bats, Bangladesh

Danielle E. Anderson,[1] Ariful Islam,[1] Gary Crameri,[1] Shawn Todd, Ausraful Islam, Salah U. Khan, Adam Foord, Mohammed Z. Rahman, Ian H. Mendenhall, Stephen P. Luby, Emily S. Gurley, Peter Daszak, Jonathan H. Epstein,[1] Lin-Fa Wang[1]

Despite molecular and serologic evidence of Nipah virus in bats from various locations, attempts to isolate live virus have been largely unsuccessful. We report isolation and full-genome characterization of 10 Nipah virus isolates from *Pteropus medius* bats sampled in Bangladesh during 2013 and 2014.

Nipah virus (NiV) is an emerging zoonotic virus carried by bats. It is considered a global health priority by the World Health Organization and has pandemic potential because of its zoonotic nature, human-to-human transmissibility, wide geographic distribution of bat reservoir species, high case-fatality rate in humans, and lack of available vaccine or therapeutic agents (*1*). Although NiV or NiV-related infections have been demonstrated by serologic surveillance or PCR detection in several bat species across extensive areas, attempts to isolate live NiV have been unsuccessful; there have been only 3 successful reports: *Pteropus hypomelanus* bats (*2*) and *P. vapmyrus* bats (*3*) in Malaysia and *P. lylei* bats in Cambodia (*4*).

Bangladesh has reported seasonal outbreaks of infectious NiV almost annually since 2001, and India has reported 2 outbreaks in neighboring West Bengal, the last in 2007 (*5*,*6*). In May 2018, India reported an outbreak in Kerala State, which is >1,800 km southwest of West Bengal (https://www.searo.who.int/entity/emerging_diseases/links/nipah_virus_outbreaks_sear/en).

Despite sustained efforts to detect NiV in bats in this region, current infection data are largely from serologic and limited PCR detection of virus RNA from potential bat reservoirs, such as *P. medius* from Bangladesh and India (*7*–*10*). NiV genomic data from the region have come primarily from human cases (*11*,*12*). Spillover might not be limited to humans in Bangladesh; nonneutralizing antibodies against NiV in cattle, goats, and pigs (*13*) underscore the urgency of characterizing diversity of henipaviruses in *P. medius* bats and other possible animal reservoirs in the region.

We report isolation of NiVs from *P. medius* bats in Bangladesh. We performed full-genome characterization of these viruses by using enrichment-based next-generation sequencing (NGS).

The Study

During January 2011–April 2014, we collected 2,749 bat samples from various ongoing projects in the region. We collected samples nondestructively from individual bats as described (*7*) and collected environmental urine samples from underneath roosts by using polyethylene sheets. In early 2013, an outbreak of infection with NiV occurred in 13 districts of Bangladesh (Gaibandha, Jhinaidaha, Kurigram, Kushtia, Magura, Manikganj, Mymenshingh, Naogaon, Natore, Nilphamari, Pabna, Rajbari, and Rajshahi). In April 2013, we collected only urine samples during an outbreak investigation in Raipur, Manikganj. We also tested 944 underroost urine samples, 829 throat swab specimens, and 976 urine samples from 2 confirmed bat species (*P. medius* and *Rousettus leschenaultia*) for NiV. Samples were collected with permission from the Government of Bangladesh Forestry Office and under Institutional Animal Care and Use Committees (Tufts University no. G2011-12 and University of California at Davis no. 19300).

We also collected bat samples from 5 sites in Raipur that showed NiV spillover and 1 district (Sylhet) that had no reported cases (Figure 1). Samples were tested at the CSIRO Australian Animal Health Laboratory under BioSafety Level 4 containment. Individual samples were pooled into groups of 4 for initial extraction and PCR analysis. Of 688 pooled samples tested, 20 pools were positive by a nucleoprotein gene–specific 1-step reverse transcription

Author affiliations: Duke–National University of Singapore Medical School, Singapore (D.E. Anderson, I.H. Mendenhall, L.-F. Wang); EcoHealth Alliance, New York, New York, USA (Ariful Islam, P. Daszak, J.H. Epstein); CSIRO Australian Animal Health Laboratory, Geelong, Victoria, Australia (G. Crameri, S. Todd, A. Foord); icddrb, Dhaka, Bangladesh (Ausraful Islam, M.Z. Rahman, E.S. Gurley); University of Guelph, Guelph, Ontario, Canada (S.U. Khan); Stanford University, Stanford, California, USA (S.P. Luby); Johns Hopkins Bloomberg School of Public Health, Baltimore, Maryland, USA (E.S. Gurley)

DOI: https://doi.org/10.3201/eid2501.180267

[1]These authors contributed equally to this article.

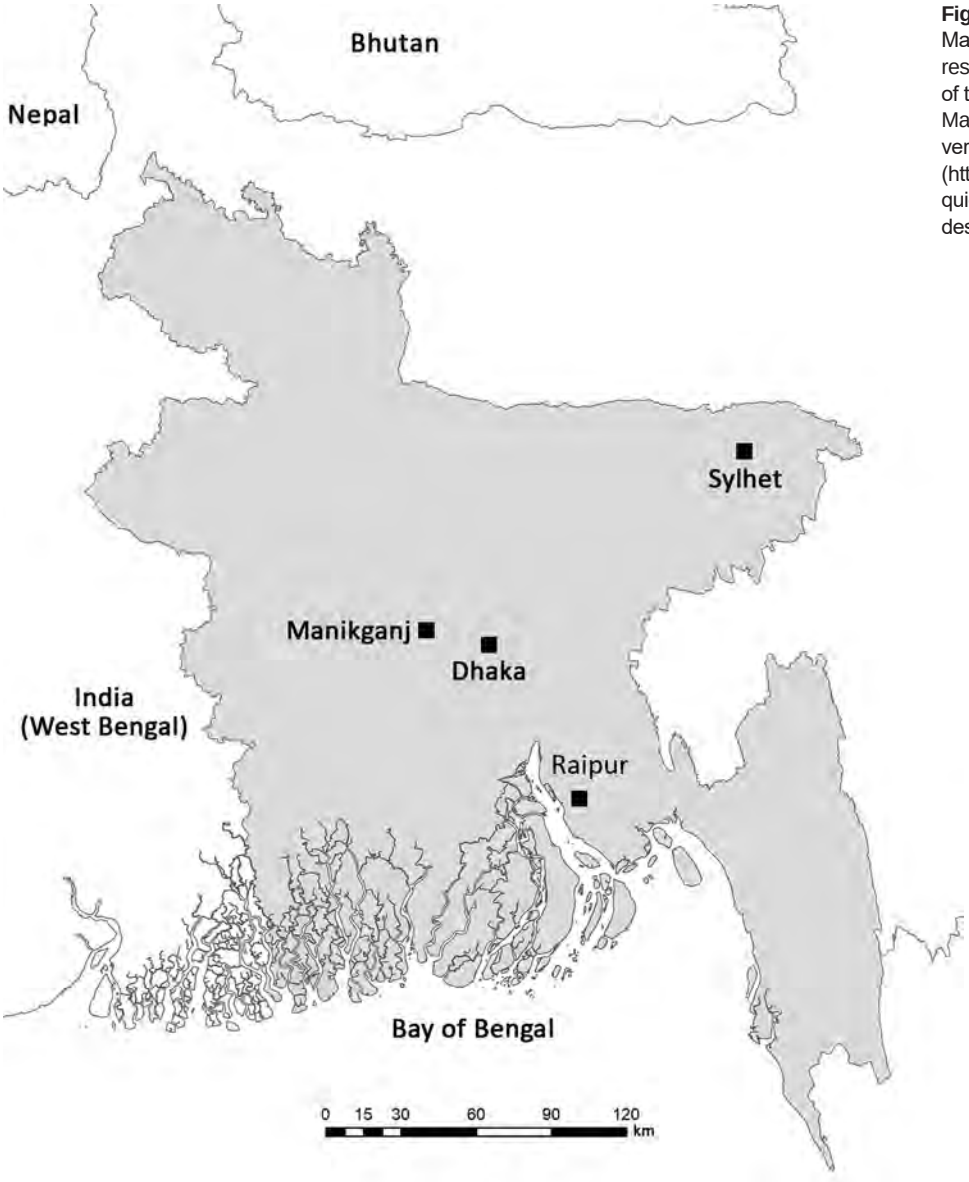

Figure 1. Sampling sites (Raipur, Manikganj, and Sylhet) for bat reservoirs of Nipah virus and location of the capital, Dhaka, in Bangladesh. Map was generated by using ArcGIS version 10.4.1 software (https://desktop.arcgis.com/en/quick-start-guides/10.4/arcgis-desktop-quick-start-guide.htm).

quantitative PCR. The 80 individual samples from positive pools were thawed for virus isolation and RNA reextracted for PCR. Of 80 samples (urine and throat swab specimens) tested by nucleoprotein gene–gene specific 1-step reverse transcription quantitative PCR, only 20 urine samples were positive. We used these 20 urine samples for virus isolation.

We performed virus isolation under BioSafety Level 4 containment. For virus isolation from PCR-positive samples, we prepared Vero cells in 96-well plates in Eagle minimum essential medium (EMEM) containing 10% fetal bovine serum and 1× antibiotic–antimycotic mixture (GIBCO, http://www.biosciences.ie/gibco). We added 50 μL of each sample to 2 wells, incubated each sample for 90 min, remove the inoculum, and added 200 μL EMEM to each well. Plates were incubated at 37°C, checked at 7 days postinfection for a cytopathic effect (CPE), and frozen at –80°C.

A total of 11 wells showed CPE, and putative virus culture from these wells was passaged a second time by inoculation of a 24-well plate containing 80% confluent Vero cells in EMEM with 80 μL of culture supernatant from each positive well. Plates were incubated at 37°C for 90 min; inoculum was removed and 1 mL EMEM added. Plates were then incubated at 37°C for 5 days. All 11 samples remained CPE positive after this second passage.

For a third passage, we harvested culture supernatant and added 300 μL to a 25-cm flask containing 80% confluent Vero cells. Flasks were incubated for 90 min at 37°C before inoculum was removed and 5 mL EMEM added. We incubated the flasks at 37°C and harvested

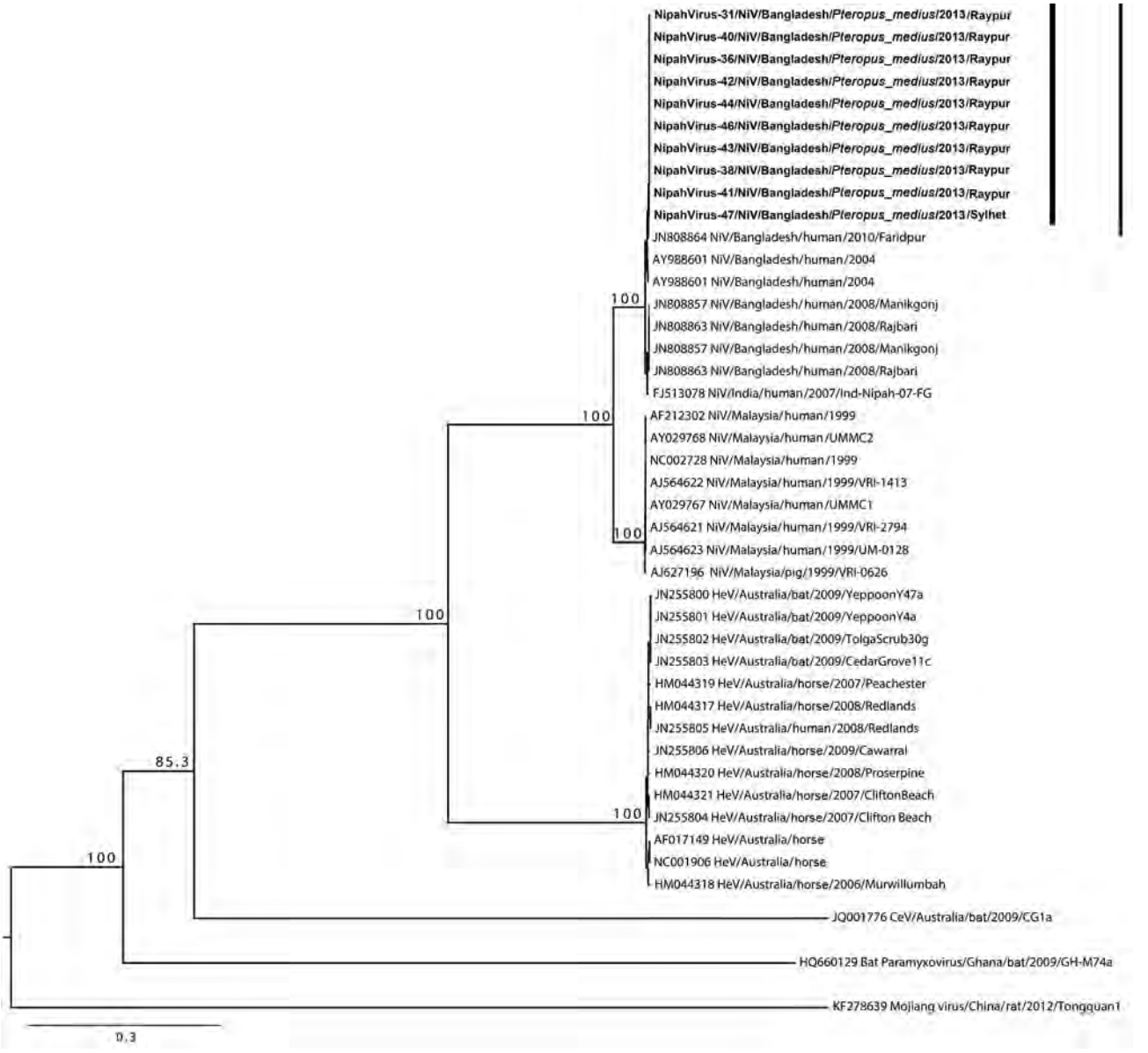

Figure 2. Phylogenetic tree of Nipah viruses from bats in Bangladesh (bold) compared with other henipaviruses, generated from full-genome sequences. Tree was constructed by using a maximum-likelihood approach, and robustness of nodes was tested with 1,000 bootstrap replicates. Sequences are labeled according to the following ordination: GenBank accession number or isolate identification number/virus type/country/host/year/strain. Numbers along branches are bootstrap values. Scale bar indicates nucleotide substitutions per site.

virus supernatants at 2–3 days postinfection. Supernatants were clarified by centrifugation at 10,000 × *g* for 5 min and frozen at –80°C.

To confirm the identity of isolated viruses, we subjected each sample to electron microscopy and PCR. All isolates had morphology consistent with NiV and were positive by NiV-specific PCR. Virus stocks were amplified in Vero cells, and supernatants were harvested and clarified by centrifugation at 10,000 × *g* for 10 min, followed by pelleting virus from supernatant by centrifugation at 200,000 × *g* for 30 min. Virus pellets were resuspended in 200 μL of Magmax Buffer (Applied Biosystems, https://www.thermofisher.com/us/en/home/brands/applied-biosystems.html) for RNA extraction according to the manufacturer's protocol.

We used a virus enrichment strategy (*14*) to obtain the full-genome sequence for NiV isolates. Total RNA was used to prepare NGS libraries (New England Biolabs, https://www.neb.com) according to the manufacturer's instructions. DNA libraries were subjected to a liquid-based

Table. Characteristics of 11 bat samples tested for Nipah virus, Bangladesh*

Sample no.	Sample ID	Date sampled	Location	Sample type*	Taqman PCR C_t	NGS	Isolate designation
1	PGB-1401B	2011 Apr 13	Raipur, Manikganj	ORU	31.9	Yes	NiV/BD/BA/2013/Raipur1401
2	PGB-1402B	2011 Apr 13	Raipur, Manikganj	ORU	30.1	Yes	NiV/BD/BA/2013/Raipur1402
3	PGB-1403B	2011 Apr 13	Raipur, Manikganj	ORU	31.0	Yes	NiV/BD/BA/2013/Raipur1403
4	PGB-1404B	2011 Apr 13	Raipur, Manikganj	ORU	31.3	Yes	NiV/BD/BA/2013/Raipur1404
5	PGB-1405B	2011 Apr 13	Raipur, Manikganj	ORU	31.0	Yes	NiV/BD/BA/2013/Raipur1405
6	PGB-1406B	2011 Apr 13	Raipur, Manikganj	ORU	31.9	Yes	NiV/BD/BA/2013/Raipur1406
7	PGB-1408B	2011 Apr 13	Raipur, Manikganj	ORU	31.3	Yes	NiV/BD/BA/2013/Raipur1408
8	PGB-1409B	2011 Apr 13	Raipur, Manikganj	ORU	31.7	Yes	NiV/BD/BA/2013/Raipur1409
9	PGB-1410B	2011 Apr 13	Raipur, Manikganj	ORU	31.0	Yes	NiV/BD/BA/2013/Raipur1410
10	PGB-1411B	2011 Apr 13	Raipur, Manikganj	ORU	30.8	No	NiV/BD/BA/2013/Raipur1411
11	PGB-191	2006 Jan 13	Sylhet	RU	39.0	Yes	NiV/BD/BA/2013/Sylhet191

*C_t, cycle threshold; ID, identification; NGS, next-generation sequencing; NIV, Nipah virus; ORU, outbreak roost urine; RU, roost urine.

target capture method to separate and enrich for specific NiV sequences. NiV-specific 120-mer biotinylated DNA baits were designed to capture the entire genome. Hybridized probes and captured NiV genetic material were immobilized on magnetic beads, and contaminating host material was washed away, which increased the number of virus-specific reads. We mapped all reads to NiV sequence JN808863 by using the Map to Reference Function in Geneious version 7.1.6 (https://www.geneious.com/previous-versions). The consensus nucleotide sequence was selected by majority rules at each site.

To ascertain 5′ and 3′ ends because of low coverage and PCR errors and chimeras, we downloaded full-genome NiV sequences from GenBank and aligned them by using MAFFT in Geneious. A 90% similarity threshold was used to generate consensus 5′ and 3′ sequences of 120 nt. Final consensus full genomes had 10× coverage. We downloaded full-genome henipaviruses from GenBank, generated alignment by using the MAFFT plugin in Geneious, and tested node robustness by using 1,000 bootstrap replicates under the general time reversible plus gamma model in PHYML (*15*).

Full-length genome sequences were obtained from 10 bat NiV isolates. We constructed a phylogenetic tree (Figure 2) that showed all bat isolates had nearly identical genome sequences; there was 99.9% conservation among all 10 genomes characterized (Table). The virus isolated in Sylhet during January 2013 was nearly identical to all other isolates obtained in 2013 in Raipur, which is ≈350 km from Sylhet, suggesting that NiV homogeneity might be supported by bat movements connecting disparate bat colonies (*10*).

Conclusions

We report isolation of NiV from *P. medius* bats, a natural virus reservoir in Bangladesh. With an improved enrichment-based NGS strategy, we generated complete genome sequences for 10 bat NiV isolates with higher efficiency than for traditional PCR-based sequencing methods. NiV has been difficult to isolate from bats and, similar to results of previous studies of Hendra virus (*10*), we observed that successful virus isolation does not correlate with cycle thresholds. The complete sequence identity match among isolates obtained during the outbreak investigation in Raipur suggests that multiple strains were not co-circulating in the bat population at the time, supporting results of a previous study in Faridpur (*10*).

None of the bat NiV isolate sequences were identical with any previously detected human NiV isolate sequences, suggesting that NiV spillover into humans is a rare event. However, the genetic diversity of bat NiV isolates needs to be fully identified.

Acknowledgments

We thank Ina Smith and Vicky Boyd for providing assistance and support during this study, Sandy Crameri for performing the electron microscopy, and Jordan Menscher for his help collecting bat roost urine samples. We also thank the Forest Department, Government of Bangladesh, for their support and for providing permission and the appropriate permits to conduct the study.

This study was supported by the National Institutes of Health Fogarty International Center (R01TW005869: P.D., J.H.E., A.I., S.P.L., and E.S.G.), the US Agency for International Development, PREDICT Project (J.H.E., A.I., A.I., and P.D.), and a National Science Foundation Research Coordination Network Award (EcoHealthNet DEB-0955897). L.-F. W. was supported by the National Research Foundation (NRF2012NRF-CRP001-056), the Ministry of Health (CDPHRG/0006/2014) and the Ministry of Defence (DIRP2015-9016102060) in Singapore. D.E.A. and I.H.M. were supported by New Investigators Grants from the National Medical Research Council of Singapore (NMRC/BNIG/2030/2015 and NMRC/BNIG/2005/2013).

About the Author

Dr. Anderson is a virologist at Duke–National University of Singapore Medical School, Singapore. Her research interests are paramyxovirus pathogenesis and pathogen discovery by using novel molecular and serologic approaches.

References

1. Sweileh WM. Global research trends of World Health Organization's top eight emerging pathogens. Global Health. 2017;13:9. http://dx.doi.org/10.1186/s12992-017-0233-9
2. Chua KB, Koh CL, Hooi PS, Wee KF, Khong JH, Chua BH, et al. Isolation of Nipah virus from Malaysian Island flying-foxes. Microbes Infect. 2002;4:145–51. http://dx.doi.org/10.1016/S1286-4579(01)01522-2
3. Rahman SA, Hassan SS, Olival KJ, Mohamed M, Chang L-Y, Hassan L, et al.; Henipavirus Ecology Research Group. Characterization of Nipah virus from naturally infected *Pteropus vampyrus* bats, Malaysia. Emerg Infect Dis. 2010;16:1990–3. http://dx.doi.org/10.3201/eid1612.091790
4. Reynes JM, Counor D, Ong S, Faure C, Seng V, Molia S, et al. Nipah virus in Lyle's flying foxes, Cambodia. Emerg Infect Dis. 2005;11:1042–7. http://dx.doi.org/10.3201/eid1107.041350
5. Chadha MS, Comer JA, Lowe L, Rota PA, Rollin PE, Bellini WJ, et al. Nipah virus–associated encephalitis outbreak, Siliguri, India. Emerg Infect Dis. 2006;12:235–40. http://dx.doi.org/10.3201/eid1202.051247
6. Hahn MB, Gurley ES, Epstein JH, Islam MS, Patz JA, Daszak P, et al. The role of landscape composition and configuration on *Pteropus gig*anteus roosting ecology and Nipah virus spillover risk in Bangladesh. Am J Trop Med Hyg. 2014;90:247–55. http://dx.doi.org/10.4269/ajtmh.13-0256
7. Epstein JH, Prakash V, Smith CS, Daszak P, McLaughlin AB, Meehan G, et al. Henipavirus infection in fruit bats (*Pteropus giganteus*), India. Emerg Infect Dis. 2008;14:1309–11. http://dx.doi.org/10.3201/eid1408.071492
8. Hsu VP, Hossain MJ, Parashar UD, Ali MM, Ksiazek TG, Kuzmin I, et al. Nipah virus encephalitis reemergence, Bangladesh. Emerg Infect Dis. 2004;10:2082–7. http://dx.doi.org/10.3201/eid1012.040701
9. Yadav PD, Raut CG, Shete AM, Mishra AC, Towner JS, Nichol ST, et al. Detection of Nipah virus RNA in fruit bat (*Pteropus giganteus*) from India. Am J Trop Med Hyg. 2012;87:576–8. http://dx.doi.org/10.4269/ajtmh.2012.11-0416
10. Epstein JH. The ecology of Nipah virus and the first identification of a bat Pegivirus in *Pteropus medius*, Bangladesh. London: Kingston University; 2017.
11. Lo MK, Lowe L, Hummel KB, Sazzad HMS, Gurley ES, Hossain MJ, et al. Characterization of Nipah virus from outbreaks in Bangladesh, 2008–2010. Emerg Infect Dis. 2012;18:248–55. http://dx.doi.org/10.3201/eid1802.111492
12. Arankalle VA, Bandyopadhyay BT, Ramdasi AY, Jadi R, Patil DR, Rahman M, et al. Genomic characterization of Nipah virus, West Bengal, India. Emerg Infect Dis. 2011;17:907–9. http://dx.doi.org/10.3201/eid1705.100968
13. Chowdhury S, Khan SU, Crameri G, Epstein JH, Broder CC, Islam A, et al. Serological evidence of henipavirus exposure in cattle, goats and pigs in Bangladesh. PLoS Negl Trop Dis. 2014;8:e3302. http://dx.doi.org/10.1371/journal.pntd. 0003302
14. Ho ZJ, Hapuarachchi HC, Barkham T, Chow A, Ng LC, Lee JM, et al.; Singapore Zika Study Group. Outbreak of Zika virus infection in Singapore: an epidemiological, entomological, virological, and clinical analysis. Lancet Infect Dis. 2017;17:813–21. http://dx.doi.org/10.1016/S1473-3099(17)30249-9
15. Guindon S, Dufayard JF, Lefort V, Anisimova M, Hordijk W, Gascuel O. New algorithms and methods to estimate maximum-likelihood phylogenies: assessing the performance of PhyML 3.0. Syst Biol. 2010;59:307–21. http://dx.doi.org/10.1093/sysbio/syq010

Addresses for correspondence: Jonathan H. Epstein, EcoHealth Alliance, 460 W 34th St, New York, NY 10001, USA,; email: epstein@ecohealthalliance.org

Burdens of Invasive Methicillin-Susceptible and Methicillin-Resistant *Staphylococcus aureus* Disease, Minnesota, USA

Mackenzie Koeck, Kathryn Como-Sabetti, Dave Boxrud, Ginette Dobbins, Anita Glennen, Melissa Anacker, Selina Jawahir, Isaac See, Ruth Lynfield

During August 1, 2014–July 31, 2015, in 2 counties in Minnesota, USA, incidence of invasive methicillin-susceptible *Staphylococcus aureus* (MSSA) (27.1 cases/100,000 persons) was twice that of invasive methicillin-resistant *S. aureus* (13.1 cases/100,000 persons). MSSA isolates were more genetically diverse and susceptible to more antimicrobial drugs than methicillin-resistant *S. aureus* isolates.

Methicillin-resistant *Staphylococcus aureus* (MRSA) infections were first reported in the 1960s in healthcare facilities (*1*). Risk factors included recent hospitalization, surgery, dialysis, having a central venous catheter or other invasive medical device, chronic wounds, residence in long-term care facilities or prisons, injection drug use, and exposure to antimicrobial drugs (*2*). In the 1990s, MRSA infections caused by genetically distinct strains were observed among healthy persons in the community (*3*).

Although *S. aureus* has long been recognized as a major human pathogen, epidemiologic studies and infection prevention precautions in recent decades have largely focused on MRSA. We compared epidemiologic, microbiologic, and molecular characteristics of invasive methicillin-susceptible *S. aureus* (MSSA) infections with those of invasive MRSA infections.

The Study

Active surveillance for invasive MSSA was added to existing invasive MRSA surveillance in Ramsey and Hennepin Counties (combined population in 2014: 1,742,806) in Minnesota, USA, during 2014. Cases were defined as *S. aureus* isolated from a normally sterile site in a catchment area resident. We collected demographic and clinical information from medical record reviews by using a standardized case report form. We epidemiologically characterized patients with invasive *S. aureus*: hospital onset (culture obtained >3 days after admission); healthcare-associated, community onset (HACO; ≥1 healthcare-associated risk factor); and community associated (CA). Healthcare-associated risk factors included in the year before culture hospital admission or residence in a long-term care facility or long-term acute-care facility for any duration, surgery, or dialysis or within 2 days before culture presence of a central vascular catheter.

Invasive MSSA and MRSA isolates were submitted to the Minnesota Department of Health for species confirmation, antimicrobial drug susceptibility testing, and molecular characterization. We confirmed species by using the tube coagulase test (Becton Dickinson, http://www.bd.com) or matrix-assisted laser desorption ionization time-of-flight mass spectrometry by using a Microflex LT/SH mass spectrometer and FlexControl 3.4 software (Bruker Daltonics, Inc., https://www.bruker.com). We subtyped isolates by using pulsed-field gel electrophoresis (PFGE) according to published protocols (*4*). PFGE patterns were analyzed by using BioNumerics software (Applied Maths, http://www.applied-maths.com); patterns without differences were considered indistinguishable. We assigned patterns a USA clonal group on the basis of an 80% similarity coefficient cutoff to a type strain. Whole-genome sequencing characterized 2 isolates that were untypable by PFGE. We determined sequence type by using short reads in Illumina Miseq as described (*5*) and retrieved sequences by uploading raw read files to the Multilocus Sequence Typing 1.8 server (*S. aureus* configuration) hosted by the Center for Genomic Epidemiology (*6*).

We performed antimicrobial drug susceptibility testing by using broth microdilution with a custom dried panel (TREK Diagnostic Systems, Inc., http://www.trekds.com/techInfoVT/default.asp) and interpreted results according to Clinical and Laboratory Standards Institute guidelines (*7*). Isolates susceptible to penicillin were examined for β-lactamase production by using nitrocefin disk test, penicillin zone-edge test, and *blaZ* β-lactamase gene confirmation by PCR. We induced β-lactamase production for

Author affiliations: Minnesota Department of Health, St. Paul, Minnesota, USA (M. Koeck, K. Como-Sabetti, D. Boxrud, G. Dobbins, A. Glennen, M. Anacker, S. Jawahir, R. Lynfield); Centers for Disease Control and Prevention, Atlanta, Georgia, USA (I. See)

DOI: https://doi.org/10.3201/eid2501.181146

nitrocefin disk testing by inoculating an isolate onto sheep blood agar with a 1-μg oxacillin disk and incubating overnight by using TREK Diagnostic Systems. Subsequent growth from the zone periphery was incubated with a nitrocefin disk (REMEL, http://www.remel.com/About.aspx) for 60 min. We also performed a penicillin zone-edge test by using standard disk diffusion, followed by assessment for fuzzy or sharp zone edges. We determined the incidence of the blaZ β-lactamase gene by using real-time PCR as described but with slight modifications (*8*).

We analyzed data by using SAS version 9.4 (SAS Institute, https://www.sas.com). Census data for 2014 were

Table 1. Epidemiologic characteristics and concurrent conditions for patients with cases of invasive MSSA and MRSA, Minnesota, USA, August 1, 2014–July 31, 2015*

Characteristic	Total, n = 701			HO, n = 65			HACO, n = 416			CA, n = 220		
	MSSA	MRSA	p value	MSSA	MRSA	p value	MSSA	MRSA	p value	MSSA	MRSA	p value
Total	473 (67)	228 (33)	NA	40 (8)	25 (11)	0.28	260 (55)	156 (68)	<0.001	173 (37)	47 (21)	<0.01
Demographic												
Median age, y	59 (0–102)	62 (0–95)	0.05	61 (0–94)	61 (17–93)	0.99	62 (0–102)	65 (5–95)	0.21	55 (0–90)	50 (0–91)	0.40
Sex												
F	175 (37)	92 (40)	0.39	15 (38)	6 (24)	0.26	108 (42)	66 (42)	0.88	52 (30)	20 (43)	0.11
M	316 (67)	153 (67)	0.94	26 (65)	13 (52)	0.30	169 (65)	109 (70)	0.31	121 (70)	31 (66)	0.60
Private residence 4 d before culture	376 (79)	146 (64)	<0.01	NA	NA	NA	211 (81)	100 (64)	<0.01	165 (95)	46 (98)	0.69
LTCF past year	53 (11)	70 (31)	<0.01	4 (10)	8 (32)	0.05	49 (19)	62 (40)	<0.01	NA	NA	NA
CVC 2 d before culture	29 (6)	19 (8)	0.28	6 (15)	5 (20)	0.74	23 (9)	14 (9)	0.97	NA	NA	NA
Length of stay, d	7 (0–121)	8 (0–58)	0.05	15 (3–121)	15 (4–48)	0.91	6 (0–43)	7 (1–39)	0.11	7 (0–53)	9 (0–58)	0.15
Inpatient death	47 (10)	26 (11)	0.55	8 (20)	2 (8)	0.29	29 (11)	23 (15)	0.28	10 (6)	1 (2)	0.46
Concurrent condition												
None	96 (20)	27 (12)	<0.01	1 (4)	5 (13)	0.39	14 (9)	35 (12)	0.17	12 (26)	56 (12)	0.37
Kidney disease	95 (20)	67 (29)	<0.01	9 (23)	9 (36)	0.24	77 (30)	54 (35)	0.29	9 (5)	4 (9)	0.48
Chronic skin breakdown	22 (5)	25 (11)	<0.01	<0.01	3 (12)	0.69	14 (5)	21 (13)	<0.01	5 (3)	1 (2)	1.00
D/PU	9 (2)	17 (7)	<0.01	0 (0)	0 (0)	NA	6 (2)	17 (11)	<0.01	3 (2)	0 (0)	1.00
CVD	58 (12)	46 (20)	<0.01	5 (13)	6 (24)	0.31	44 (17)	39 (25)	0.05	9 (5)	1 (2)	0.69
H/P	15 (3)	23 (10)	<0.01	1 (3)	2 (8)	0.55	9 (3)	20 (13)	<0.01	5 (3)	1 (2)	1.00
Other drug use†	41 (9)	25 (11)	0.33	4 (10)	2 (8)	1.00	21 (8)	11 (7)	0.70	16 (9)	12 (26)	<0.01
PVD	24 (5)	22 (10)	0.02	3 (8)	4 (16)	0.42	16 (6)	17 (11)	0.08	5 (3)	1 (2)	1.00
COPD	50 (11)	34 (15)	0.10	6 (15)	6 (24)	0.36	30 (12)	23 (15)	0.34	14 (8)	5 (11)	0.57
Current smoker	71 (15)	32 (14)	0.73	7 (18)	4 (16)	1.00	36 (14)	19 (12)	0.63	28 (16)	9 (19)	0.63
Diabetes	153 (32)	80 (35)	0.47	12 (30)	11 (44)	0.25	96 (37)	59 (38)	0.86	45 (26)	10 (21)	0.51
Injection drug use	25 (5)	12 (5)	0.99	0 (0)	0 (0)	NA	10 (4)	4 (3)	0.48	15 (9)	8 (17)	0.11
Obesity	70 (15)	43 (19)	0.17	8 (20)	7 (28)	0.46	47 (18)	29 (19)	0.90	15 (9)	7 (15)	0.27
Syndrome												
Bacteremia	328 (69)	178 (78)	0.03	30 (75)	16 (64)	0.34	181 (70)	125 (80)	0.03	117 (68)	37 (79)	0.14
Internal abscess	25 (5)	11 (5)	0.78	2 (5)	0 (0)	0.52	16 (6)	5 (3)	0.18	7 (4)	6 (13)	0.04
Pneumonia‡	39 (8)	40 (18)	<0.01	2 (5)	8 (32)	<0.01	21 (8)	22 (14)	0.06	16 (9)	10 (21)	0.02
Septic arthritis	137 (29)	35 (15)	<0.01	3 (8)	2 (8)	1.00	67 (26)	24 (15)	0.01	67 (39)	9 (19)	0.01
Skin abscess	7 (1)	4 (2)	0.76	0 (0)	1 (4)	0.39	7 (3)	0 (0)	0.05	0 (0)	3 (6)	<0.01
Bursitis	35 (7)	10 (4)	0.12	0 (0)	1 (4)	0.39	7 (3)	3 (2)	0.75	28 (16)	6 (13)	0.57
Cellulitis	73 (15)	32 (14)	0.60	6 (15)	3 (12)	1.00	38 (15)	18 (11)	0.35	29 (17)	11 (23)	0.30
Endocarditis	23 (5)	9 (4)	0.57	2 (5)	1 (4)	1.00	12 (5)	5 (3)	0.47	9 (5)	3 (6)	0.72
Osteomyelitis	51 (11)	28 (12)	0.58	1 (3)	4 (16)	0.07	38 (15)	20 (13)	0.58	12 (7)	3 (7)	0.75
Septic shock	41 (9)	19 (8)	0.86	3 (8)	4 (16)	0.42	27 (10)	11 (7)	0.24	11 (6)	4 (9)	0.53

*Values are no. (%), median (range), or no. (range). Nonsignificant ($p \geq 0.05$) differences were observed for chronic pulmonary disease, current smoker, diabetes, intravenous drug use, obesity, bursitis, cellulitis, endocarditis, osteomyelitis, and septic shock among patients with MSSA and MRSA cases and within epidemiologic classifications of MSSA and MRSA cases. CA, community associated; COPD, chronic pulmonary disease; CVC, central venous catheter; CVD, cardiovascular disease; D/PU, decubitus/pressure ulcer; HACO, healthcare-associated, community onset; HO, hospital onset; H/P, hemiplagia/paraplegia; LTCF, long-term care facility; MRSA, methicillin-resistant *Staphylococcus aureus*; MSSA, methicillin-susceptible *S. aureus;* NA, not available; PVD, peripheral vascular disease.

†Drug use other than intravenous drug use.

‡All patients with pneumonia had positive blood cultures to meet the case definition.

used to calculate incidence. We used a Wald χ^2 test and $p \leq 0.05$ to distinguish statistical significance. Infections with invasive MSSA and MRSA are reportable conditions under Minnesota State Rules, and obtaining information for surveillance purposes does not require Institutional Review Board review.

A total of 701 cases (473 invasive MSSA, 228 invasive MRSA) were reported during August 1, 2014–July 31, 2015. Incidence for invasive MSSA (27.1 cases/100,000 population) was more than twice that for invasive MRSA (13.1 cases/100,000 population) ($p<0.001$). Invasive MSSA cases were less likely to be HACO ($p<0.001$), more likely to be CA ($p<0.001$), and have no concurrent conditions ($p = 0.006$) than invasive MRSA cases. Bacteremia ($p = 0.026$) and pneumonia ($p<0.001$) were less common among invasive MSSA cases. However, septic arthritis ($p<0.001$) was more common. Injection drug use and inpatient case-fatality rate were similar for persons with invasive MSSA (6% and 10%, respectively) and invasive MRSA (5% and 11%, respectively) (Table 1).

Isolates from 40% of MSSA cases and 52% of MRSA cases were submitted. Cases with and without submitted isolates did not differ by sex, race, median age, or inpatient case-fatality rate. However, case-patients without isolates were more likely to have invasive MSSA ($p = 0.003$) or to be hospitalized in the year before culture ($p = 0.030$).

Invasive MSSA isolates were more genetically diverse than invasive MRSA isolates. We could not assign a USA clonal group for 55% of invasive MSSA isolates compared with 29% of invasive MRSA isolates. The most common clonal group among invasive MSSA isolates was USA200, which included 14% of invasive MSSA isolates; 35% of invasive MRSA isolates were clonal group USA100, and 30% were USA300 (Table 2). The 2 invasive MSSA isolates that were untypable by PFGE were characterized by whole-genome sequencing as sequence type 398; 1 was from a HACO case and 1 was from a hospital onset case.

Invasive MSSA isolates were more often susceptible than invasive MRSA isolates to all antimicrobial drug classes, except for tetracycline (Table 2). We detected penicillin susceptibility through multiple testing methods in 63 (33%) of invasive MSSA isolates. Six clonal groups were identified among penicillin-susceptible isolates.

Conclusions

The incidence of invasive MSSA was more than twice that of invasive MRSA in these counties. Invasive *S. aureus* infections were associated with a high case-fatality rate. Infection types were similar except for more frequent septic arthritis among invasive MSSA cases and bacteremia and pneumonia among invasive MRSA cases; these findings were consistent with those of other studies (*9*). Some

Table 2. Clonal groups and antimicrobial drug susceptibilities of invasive MSSA and MRSA isolates, Minnesota, USA, August 1, 2014–January 31, 2015*

Characteristic	MSSA, no. (%), n = 190	MRSA, no. (%), n = 119	p value
Clonal group			
USA100	13 (7)	42 (35)	<0.01
USA200	26 (14)	0 (0)	<0.01
USA300	5 (3)	36 (30)	<0.01
USA400	1 (1)	3 (3)	0.16
USA500	2 (1)	0 (0)	0.56
USA600	13 (7)	0 (0)	<0.01
USA700	5 (3)	3 (3)	1.00
USA900	10 (5)	0 (0)	<0.01
USA1000	6 (3)	0 (0)	0.09
USA1200	2 (1)	0 (0)	0.56
Untypeable	2 (1)	0 (0)	0.56
No USA group	105 (55)	35 (29)	<0.01
Antimicrobial drug†			
Clindamycin‡	176 (93)	61 (51)	<0.01
Ceftaroline	190 (100)	117 (98)	0.15
Doxycycline	185 (97)	118 (99)	0.41
Erythromycin	143 (75)	18 (15)	<0.01
Gentamicin	189 (99)	118 (99)	1.00
Levofloxacin	175 (92)	35 (29)	<0.01
Penicillin	63 (33)	0 (0)	<0.01
Rifampin	189 (99)	118 (99)	1.00
Tetracycline	177 (93)	118 (99)	0.01
Trimethoprim/sulfamethoxazole	188 (99)	119 (100)	0.53

*MRSA, methicillin-resistant *Staphylococcus aureus*; MSSA, methicillin-susceptible *S. aureus*.
†Proportions represent isolates susceptible to an antimicrobial drug. All isolates were susceptible to daptomycin, linezolid, telavancin, and vancomycin. A total of invasive MSSA and MRSA isolates had vancomycin MICs <0.05; 86% of invasive MSSA isolates and 81% of invasive MSSA isolates had vancomycin MICs = 1; 13% of invasive MSSA isolates and 18% of invasive MRSA isolates had vancomycin MICs = 2.
‡Isolates with inducible clindamycin resistance were classified as nonsusceptible.

studies found a higher case-fatality rate for MRSA than MSSA infections, possibly attributable to the older age and concurrent conditions among invasive MRSA case-patients (*10*). Although case-patients with invasive MSSA had fewer concurrent conditions and were less likely to have pneumonia (a syndrome associated with poor outcomes [*11*]) than case-patients with invasive MRSA, case-fatality rates were similar.

Invasive MSSA isolates were susceptible to more antimicrobial drugs and were more genetically diverse than invasive MRSA isolates, consistent with results of other reports (*12*). Penicillin susceptibility was observed in 33% of invasive MSSA isolates, which is considerably higher than for previous studies of invasive and noninvasive MSSA isolates and was seen for multiple strain types (*13*,*14*).

Infection control interventions have effectively decreased healthcare-associated invasive MRSA incidence (*15*). However, invasive *S. aureus* burden and mortality rates remain a concern. Most invasive *S. aureus* disease was HACO or CA, highlighting the need for preventing these community-onset infections through new approaches and infection prevention in settings outside acute care. Ongoing surveillance data can inform planning for future interventions, such as improved wound care, enhanced infection prevention in nursing homes and dialysis centers, and greater attention to chronic conditions and development of effective vaccines.

This study was supported in part by a cooperative agreement (U50/CCU511190) with the Centers for Disease Control and Prevention as part of the Emerging Infections Program.

About the Author

Ms. Koeck is an epidemiologist in the Emerging Infections Unit, Minnesota Department of Health, St. Paul, MN. Her primary research interest is coordinating surveillance for invasive *S. aureus*.

References

1. Jevons M. Celbenin-resistant staphylococci. BMJ. 1961;1:124–5. http://dx.doi.org/10.1136/bmj.1.5219.124-a
2. Lowy FD. *Staphylococcus aureus* infections. N Engl J Med. 1998; 339:520–32. http://dx.doi.org/10.1056/NEJM199808203390806
3. Naimi TS, LeDell KH, Como-Sabetti K, Borchardt SM, Boxrud DJ, Etienne J, et al. Comparison of community- and health care-associated methicillin-resistant *Staphylococcus aureus* infection. JAMA. 2003;290:2976–84. http://dx.doi.org/10.1001/jama.290.22.2976
4. McDougal LK, Steward CD, Killgore GE, Chaitram JM, McAllister SK, Tenover FC. Pulsed-field gel electrophoresis typing of oxacillin-resistant *Staphylococcus aureus* isolates from the United States: establishing a national database. J Clin Microbiol. 2003;41:5113–20. http://dx.doi.org/10.1128/JCM.41.11.5113-5120.2003
5. Taylor AJ, Lappi V, Wolfgang WJ, Lapierre P, Palumbo MJ, Medus C, et al. Characterization of foodborne outbreaks of *Salmonella enterica* serovar Enteritidis with whole-genome sequencing single nucleotide polymorphism–based analysis for surveillance and outbreak detection. J Clin Microbiol. 2015;53:3334–40. http://dx.doi.org/10.1128/JCM.01280-15
6. Larsen MV, Cosentino S, Rasmussen S, Friis C, Hasman H, Marvig RL, et al. Multilocus sequence typing of total-genome-sequenced bacteria. J Clin Microbiol. 2012;50:1355–61. http://dx.doi.org/10.1128/JCM.06094-11
7. Clinical and Laboratory Standards Institute. Performance standards for antimicrobial susceptibility testing. 26th ed. (M100S). Wayne (PA): The Institute; 2016.
8. Pereira LA, Harnett GB, Hodge MM, Cattell JA, Speers DJ. Real-time PCR assay for detection of *blaZ* genes in *Staphylococcus aureus* clinical isolates. J Clin Microbiol. 2014;52:1259–61. http://dx.doi.org/10.1128/JCM.03413-13
9. David MZ, Boyle-Vavra S, Zychowski DL, Daum RS. Methicillin-susceptible *Staphylococcus aureus* as a predominantly healthcare-associated pathogen: a possible reversal of roles? PLoS One. 2011;6:e18217. http://dx.doi.org/10.1371/journal.pone.0018217
10. Wang JT, Hsu LY, Lauderdale TL, Fan WC, Wang FD. Comparison of outcomes among adult patients with nosocomial bacteremia caused by methicillin-susceptible and methicillin-resistant *Staphylococcus aureus*: a retrospective cohort study. PLoS One. 2015;10:e0144710. http://dx.doi.org/10.1371/journal.pone.0144710
11. Sicot N, Khanafer N, Meyssonnier V, Dumitrescu O, Tristan A, Bes M, et al. Methicillin resistance is not a predictor of severity in community-acquired *Staphylococcus aureus* necrotizing pneumonia—results of a prospective observational study. Clin Microbiol Infect. 2013;19:E142–8. http://dx.doi.org/10.1111/1469-0691.12022
12. Hsiang MS, Shiau R, Nadle J, Chan L, Lee B, Chambers HF, et al. Epidemiologic similarities in pediatric community-associated methicillin-resistant and methicillin-sensitive *Staphylococcus aureus* in the San Francisco Bay Area. J Pediatric Infect Dis Soc. 2012;1:200–11. http://dx.doi.org/10.1093/jpids/pis061
13. Staphylococcus Laboratory, Statens Serum Institut. Annual report on *Staphylococcus aureus* bacteraemia cases in Denmark, 2012. *Staphylococcus* Laboratory, Statens Serum Institut, Copenhagen [cited 2018 Sep 28]. http://www.ssi.dk/~/media/Indhold/DK%20-%20dansk/Smitteberedskab/Referencelaboratorier/Stafylokoklaboratoriet/Rapport%202012%20%20part%20II.ashx.
14. Richter SS, Doern GV, Heilmann KP, Miner S, Tendolkar S, Riahi F, et al. Detection and prevalence of penicillin-susceptible *Staphylococcus aureus* in the United States in 2013. J Clin Microbiol. 2016;54:812–4. http://dx.doi.org/10.1128/JCM.03109-15
15. Centers for Disease Control and Prevention. Healthcare-associated infections in the United States, 2006–2016: a story of progress, January 5, 2018 [cited 2018 Apr 25]. https://www.cdc.gov/hai/surveillance/data-reports/data-summary-assessing-progress.html

Address for correspondence: Kathryn Como-Sabetti, Emerging Infections Unit, Minnesota Department of Health, 625 Robert St N, St. Paul, MN 55155, USA; email: kathy.como-sabetti@state.mn.us

Orogenital Transmission of *Neisseria meningitidis* Causing Acute Urethritis in Men Who Have Sex with Men

Arnaud Jannic, Hedi Mammeri, Lise Larcher, Vincent Descamps, William Tosini, Bao Phung, Yazdan Yazdanpanah, Fabrice Bouscarat

Author affiliations: Hôpital Bichat Claude Bernard, Paris, France (A. Jannic, H. Mammeri, L. Larcher, V. Descamps, F. Bouscarat); Université Paris Diderot, Paris (A. Jannic, H. Mammeri, V. Descamps, W. Tosini, B. Phung, Y. Yazdanpanah, F. Bouscarat); Institut National de la Santé et de la Recherche Médicale, Paris (H. Mammeri)

DOI: https://doi.org/10.3201/eid2501.171102

Neisseria meningitidis sequence type 11 is an emerging cause of urethritis. We demonstrate by using whole-genome sequencing orogenital transmission of a *N. meningitidis* sequence type 11 isolate causing urethritis in a monogamous couple of men who have sex with men. These results suggest dissemination of this clonal complex among low-risk patients.

Neisseria meningitidis is a gram-negative diplococcus that can cause severe invasive infections. It usually colonizes the oropharynx and spreads through close or prolonged contact with respiratory or throat secretions. Cases of *N. meningitidis*–associated urethritis have been reported since the 1930s, and orogenital sex has been demonstrated as a potential mode of transmission by genotyping methods (*1*).

A 22-year-old man visited a sexual health clinic for symptomatic urethritis with purulent urethral discharge and pain while urinating. Clinical examination showed no other signs or symptoms, including fever. His last sexual intercourse (including orogenital contacts) occurred 3 weeks before with his stable, unique, asymptomatic male partner. Both men reported that they had not had any other sexual partner before and since their first intercourse together <1 year before. Meningococcal vaccination statuses were unknown.

Results of nucleic acid amplification testing for *N. gonorrhoeae* and *Chlamydia trachomatis* in urine, pharyngeal, and anal samples, and serologic testing for HIV, hepatitis B and C viruses, and syphilis were negative for the patient and his partner. Urethral culture yielded growth with oxidase and Gram stain results consistent with gonococcus, but matrix-assisted laser desorption/ionization time-of-flight mass spectrometry identified *N. meningitidis* (isolate TUR1). A pharyngeal swab specimen was collected from the partner of the patient to identify a potential source of contamination. This specimen also grew *N. meningitidis* (isolate CHA1). Isolates were nongroupable by slide agglutination serogrouping.

We purified genomic DNAs by using a NucleoSpin Tissue Kit (Macherey-Nagel, http://www.mn-net.com), prepared DNA libraries by using the Nextera Library Construction Kit (Illumina, https://www.illumina.com), and sequenced these DNAs by using a MiSeq sequencer (Illumina), which yielded 62× coverage for isolate TUR1 and 66× coverage for isolate CHA1. We assembled the genomes of CHA1 and TUR1 isolates by using SPAdes version 3.10.1 (http://bioinf.spbau.ru/spades), which resulted in assemblies consisting of 395 contigs for TUR1 and 636 contigs for CHA1 and yielded draft genomes of ≈2.19 Mb. We performed genome annotation by using the MicroScope Platform (http://www.genoscope.cns.fr/agc/microscope), which yielded 2,597 coding sequences, including protein-encoding genes and RNAs.

We analyzed high-throughput sequencing data by using the PubMLST website (https://pubmlst.org) for typing the CHA1 and TUR1 isolates. These 2 isolates belonged to the clonal complex sequence type (ST) 11 and had finetype PorA 1.5,2; FetA F1-1. DNA sequence analysis of the *csw* gene of these isolates showed an open reading frame of 3,114 bp that had 99.9% nucleotide identity with that of the *N. meningitidis* W:2a:P1.7–2,4 ST11 strain (GenBank accession no. EU164779), which was consistent with genogroup W (*2*,*3*).

We used CSI Phylogeny version 1.4 (https://cge.cbs.dtu.dk/services/CSIPhylogeny) for phylogenomic analysis on the basis of single-nucleotide polymorphisms (SNPs) and called among core genomes of CHA1 and TUR1 isolates and 3 other ST11 *N. meningitidis* strains (NM3688 from Brazil [Bioproject PRJNA264543], COL-201505-31 from the United States [BioProject PRJNA324131]), and LNP27256 from France [Bioproject PRJNA215157]). Analysis showed that the CHA1 and TUR1 isolates differed by only 3 SNPs, thus demonstrating their clonal relationship. Conversely, these isolates differed by >890 SNPs from the other strains.

Nucleotide sequence accession numbers for whole-genome shotgun projects have been deposited at DNA Data Bank of Japan/European Molecular Biology Laboratory/GenBank under accession nos. MULP000000001 (Bioproject PRJNA369721) and MULO000000001 (Bioproject PRJNA369166).

The patient recovered quickly after receiving single doses of intramuscular ceftriaxone (500 mg) and azithromycin (1 g). His partner received a single dose of intramuscular ceftriaxone (500 mg) as a decontamination strategy.

Albeit rare, *N. meningitidis*–associated urethritis is emerging worldwide among men (*4*,*5*). These infections can be highly symptomatic and mimic gonococcal urethritis.

Orogenital transmission is often suspected but rarely proven (*1*). In our study, use of whole-genome sequencing strongly supported the hypothesis that the oropharyngeal carriage of *N. meningitidis* by the man who performed oral sex was the source of the urethritis. Moreover, whole-genome sequencing showed that the strains belonged to the ST11 clonal complex. Several studies reported nongonococcal urethritis caused by *N. meningitidis* ST11 in Japan and the United States (*1*,*6*,*7*). These worldwide descriptions suggest that *N. meningitidis* S11 might represent an emerging urethrotropic clade.

This case is notable because the patient had highly symptomatic urethritis without risky sexual behavior. In fact, he reported that he and his only sexual partner had not had sex with others before they met.

Since 2010, several clusters of serogroup C invasive meningococcal disease have been reported among men who have sex with men, and sexual transmission is suspected to be involved (*8*–*10*). These infections led to an extension of the meningococcal vaccine recommendations to men who have sex with men who are engaged in risky behavior in some outbreaks areas. Our case highlights that sexual transmission of *N. meningitidis* should be considered for all men.

Finally, although systematically collected information is limited, meningococcal urogenital infections are potentially increasing and raising public health concerns. These infections need to be monitored, and bacteriological culture of purulent exudate should always be considered when available. Also, because fidelity might be contested between partners when a sexually transmitted disease is being diagnosed, identification of meningococcal urethritis and its transmission might have a strong psychological effect on the couple.

About the Author

Dr. Jannic is an attending physician at the Service de Dermatologie, Hôpital Bichat Claude Bernard, Paris, France. His research interests include dermatologic infectious diseases.

References

1. Hayakawa K, Itoda I, Shimuta K, Takahashi H, Ohnishi M. Urethritis caused by novel *Neisseria meningitidis* serogroup W in men who has sex with men, Japan. Emerg Infect Dis. 2014;20:1585–7. http://dx.doi.org/10.3201/eid2009.140349
2. Harrison OB, Claus H, Jiang Y, Bennett JS, Bratcher HB, Jolley KA, et al. Description and nomenclature of *Neisseria meningitidis* capsule locus. Emerg Infect Dis. 2013;19:566–73. http://dx.doi.org/10.3201/eid1904.111799
3. Beddek AJ, Li M-S, Kroll JS, Jordan TW, Martin DR. Evidence for capsule switching between carried and disease-causing *Neisseria meningitidis* strains. Infect Immun. 2009;77:2989–94. http://dx.doi.org/10.1128/IAI.00181-09
4. McKenna JG, Fallon RJ, Moyes A, Young H. Anogenital nongonococcal neisseriae: prevalence and clinical significance. Int J STD AIDS. 1993;4:8–12. http://dx.doi.org/10.1177/095646249300400103
5. Frølund M, Lidbrink P, Wikström A, Cowan S, Ahrens P, Jensen JS. Urethritis-associated pathogens in urine from men with nongonococcal urethritis: a case–control study. Acta Derm Venereol. 2016;96:689–94. http://dx.doi.org/10.2340/00015555-2314
6. Toh E, Gangaiah D, Batteiger BE, Williams JA, Arno JN, Tai A, et al. *Neisseria meningitidis* ST11 complex isolates associated with nongonococcal urethritis, Indiana, USA, 2015–2016. Emerg Infect Dis. 2017;23:336–9. http://dx.doi.org/10.3201/eid2302.161434
7. Bazan JA, Peterson AS, Kirkcaldy RD, Briere EC, Maierhofer C, Turner AN, et al. Notes from the field: increase in *Neisseria meningitidis*–associated urethritis among men at two sentinel clinics—Columbus, Ohio, and Oakland County, Michigan, 2015. MMWR Morb Mortal Wkly Rep. 2016;65:550–2. http://dx.doi.org/10.15585/mmwr.mm6521a5
8. Taha M-K, Claus H, Lappann M, Veyrier FJ, Otto A, Becher D, et al. Evolutionary events associated with an outbreak of meningococcal disease in men who have sex with men. PLoS One. 2016;11:e0154047. http://dx.doi.org/10.1371/journal.pone.0154047
9. Aubert L, Taha M, Boo N, Le Strat Y, Deghmane AE, Sanna A, et al. Serogroup C invasive meningococcal disease among men who have sex with men and in gay-oriented social venues in the Paris region: July 2013 to December 2014. Euro Surveill. 2015;20:pii:21016. http://dx.doi.org/10.2807/1560-7917.ES2015.20.3.21016
10. Folaranmi TA, Kretz CB, Kamiya H, MacNeil JR, Whaley MJ, Blain A, et al. Increased risk for meningococcal disease among men who have sex with men in the United States, 2012–2015. Clin Infect Dis. 2017;65:756–63. http://dx.doi.org/10.1093/cid/cix438

Address for correspondence: Arnaud Jannic, Hôpital Bichat Claude Bernard, 46 Rue Henri Huchard, 75018 Paris, France; email: arnaud.jannic@aphp.fr

Trends in Azole Resistance in *Aspergillus fumigatus*, the Netherlands, 1994–2016

Jochem B. Buil, Eveline Snelders, Laura Bedin Denardi, Willem J.G. Melchers, Paul E. Verweij

Author affiliations: Radboud University Medical Center, Nijmegen, The Netherlands (J.B. Buil, W.J.G. Melchers, P.E. Verweij); Center of Expertise in Mycology Radboudumc/CWZ, Nijmegen (J.B. Buil, W.J.G. Melchers, P.E. Verweij); Wageningen University and Research, Wageningen, the Netherlands (E. Snelders); Federal University of Santa Maria, UFSM, Santa Maria, Brazil (L.B. Denardi)

DOI: https://doi.org/10.3201/eid2501.171925

We investigated azole resistance in *Aspergillus fumigatus* in a tertiary reference hospital in the Netherlands during 1994–2016. The 5-year patient-adjusted proportion of resistance increased from 0.79% for 1996–2001 to 4.25% for 2002–2006, 7.17% for 2007–2011, and 7.04% for 2012–2016. However, we observed substantial variation between years.

Azole resistance is increasingly reported in *Aspergillus fumigatus* and is now found all around the world (*1*). Most studies have investigated the presence of resistance in environmental or clinical samples over a limited time, but longitudinal resistance studies are lacking. It is important to determine if azole resistance frequency shows increasing trends over time and if the distribution of resistance mutations changes over time. We have previously reported the emergence of azole resistance from 1994–2007 for the Radboud University Medical Center (RUMC) in Nijmegen, the Netherlands (*2*). Here, we describe trends in resistance frequency and distributions of mutations over a 23-year period, from 1994 through 2016.

All clinical *A. fumigatus* isolates cultured at RUMC are screened for azole resistance. Before 2009, isolates were screened using an agar-slant supplemented with 4 mg/L itraconazole (*2*). During 2009–2011 a 4-well plate was developed containing itraconazole (4 mg/L), voriconazole (1 mg/L), posaconazole (0.5 mg/L), and a growth control. Since 2012, we have used a commercial agar-based screening system (VIPcheck, http://www.vipcheck.nl) containing 2 mg/L of voriconazole (*3*,*4*). We performed EUCAST susceptibility testing (http://www.eucast.org) and sequencing of the *cyp51A* gene and promoter on isolates that grew on azole-containing wells (*2*).

We calculated the resistance frequency of azole-resistant *A. fumigatus* isolates for each year, using the number of cultured isolates as denominator. Furthermore, we calculated the patient-adjusted proportion of resistance for each year and for each 5-year period, using the number of patients with a resistant isolate as numerator and of culture-positive patients as denominator. We determined by χ^2 test whether trends of resistance frequency were statistically significant ($p \leq 0.05$). When 2 different resistance mechanisms were recovered from a single patient, we counted the patient once for determining the resistance proportion but used both isolates to determine the resistance frequency.

Over the 23-year period, 4,268 *A. fumigatus* isolates were cultured from 2,051 patients, a resistance frequency of 4.2% (179/4,268 isolates). Azole-resistant *A. fumigatus* was found in 109/2,051 (5.3%) culture-positive patients (Figure, panel A**).** The patient-adjusted resistance proportion increased from 0% in 1997 to 9.5% in 2016 (Figure, panel B). The increase of resistance was not statistically significant when the proportion of resistance for each consecutive year was analyzed. However, the 5-year proportion of resistance increased from 0.79% for 1996–2001 to 4.25% for 2002–2006, 7.17% for 2007–2011, and 7.04% for 2012–2016 (Figure, panel A). The increases in resistance for 2002–2006 compared with 1996–2001 and for 2007–2011 compared with 2002–2006 were statistically significant ($p<0.05$) (Figure, panel B).

TR_{34}/L98H was the most prevalent resistance mutation over the 23-year period; it was present in 77/109 (70.6%) patients with drug-resistant *A. fumigatus* (Figure, panel C). TR_{46}/Y121F/T289A was found in 2 patients in 2010, 1 in 2011, and 1 in 2012 but only twice during 2013–2016. In recent years, resistant phenotypes without *Cyp51A* mutations were encountered more frequently than phenotypes with the mutation (Figure 1, panel C).

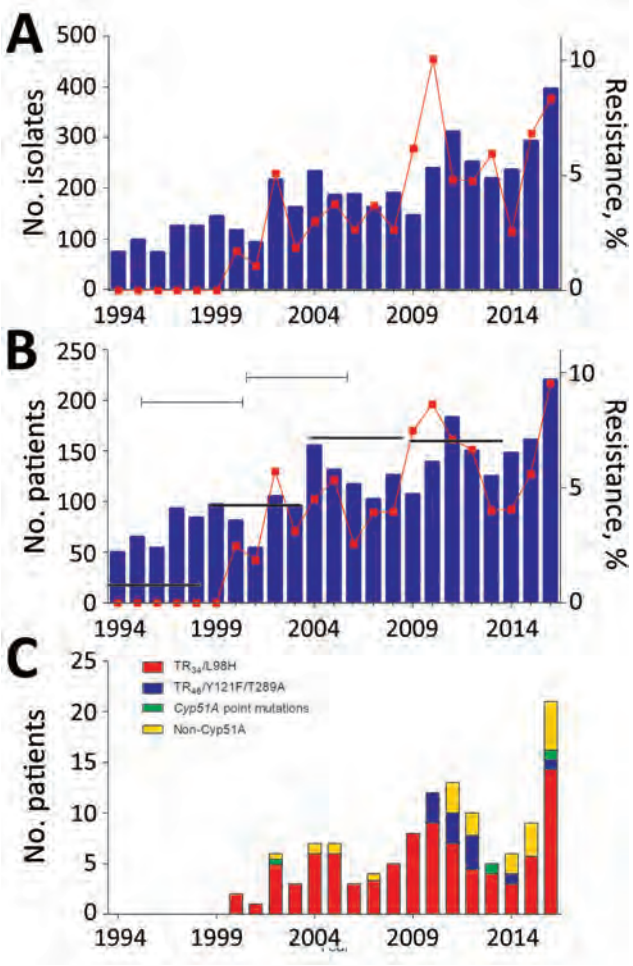

Figure. Trends in azole resistance in *Aspergillus fumigatus*, the Netherlands, 1994–2016. A) Resistance frequency by number of total cultured *A. fumigatus* isolates and percentage of azole-resistant isolates. B) Patient-adjusted proportion of resistance. Thick black horizontal bars indicate 5-year patient-adjusted proportion of resistance. $p<0.05$. C) Resistance mechanisms in azole-resistant *A. fumigatus.*

We observed an increasing trend in azole resistance prevalence in clinical *A. fumigatus* isolates until 2011, using number of patients with a positive culture as denominator. After 2011, the 5-year proportion of resistance remained stable. The advantages and disadvantages of different approaches of reporting resistance frequency remain under debate (*5*). Experts have recommended 10% resistance rate as the threshold for reconsideration of primary antifungal therapy (*6*), which indicates a need for consensus in how to determine resistance rates (*5*).

Although we found a substantial increase in azole resistance frequency over time, our study showed variation between consecutive years. Therefore, analysis of culture-positive patients over multiple years is required to determine local resistance epidemiology. Furthermore, resistance rates calculated using *Aspergillus* disease as denominator provide more information to support changes in empiric treatment decisions, but the low number of culture-positive patients in risk groups makes it difficult to obtain accurate estimates.

Various factors might have caused bias over the long period. The method of resistance detection changed from an agar-slant containing itraconazole to a system that contained 3 azoles. Voriconazole- or posaconazole-resistant isolates with low itraconazole MICs may have been initially missed, but this phenotype is very uncommon (*7*). Other factors include increased awareness of resistance, the policy to screen multiple *A. fumigatus* colonies after observation of patients with mixed azole-susceptible and azole-resistant infection (*8*), and local changes in aspergillus disease risk groups.

Resistance was dominated by environmental resistance mutations TR_{34}/L98H and TR_{46}/Y121F/T289A, although the number of patients with TR_{46}/Y121F/T289A decreased in recent years. Furthermore, in the last 5 years, ≈15% of resistant isolates harbored a wild-type *Cyp51A* gene, suggesting that other resistance mechanisms may be emerging. Because commercial PCR tests detect only resistance mechanisms with TR_{34} (*9*) or TR_{34} and TR_{46} (*10*), our observation is relevant for using these assays in culture-negative patients.

In summary, our study indicates an increasing azole resistance trend in clinical *A. fumigatus* isolates in the Netherlands. Furthermore, our results highlight difficulties encountered in establishing local epidemiology of this resistance.

This study was supported by internal funding.

Disclosures: P.E.V. has received research grants from Gilead Sciences, Astellas, Merck Sharp & Dohme (MSD), F2G, and BioRad, is a speaker for Gilead Sciences and MSD, and is on the advisory boards for Pfizer, MSD, and F2G. All other authors have nothing to declare.

About the Author

Dr. Buil is currently a resident in clinical microbiology and PhD student at Radboud University Medical Center in Nijmegen, the Netherlands. His research interests include the diagnosis of azole-resistant aspergillosis and preclinical studies of new antifungal agents.

References

1. Verweij PE, Chowdhary A, Melchers WJ, Meis JF. Azole resistance in *Aspergillus fumigatus*: can we retain the clinical use of mold-active antifungal azoles? Clin Infect Dis. 2016;62:362–8. http://dx.doi.org/10.1093/cid/civ885
2. Snelders E, van der Lee HA, Kuijpers J, Rijs AJ, Varga J, Samson RA, et al. Emergence of azole resistance in *Aspergillus fumigatus* and spread of a single resistance mechanism. PLoS Med. 2008;5:e219. http://dx.doi.org/10.1371/journal.pmed.0050219
3. Buil JB, van der Lee HAL, Rijs A, Zoll J, Hovestadt J, Melchers WJG, et al. Single centre evaluation of an agar-based screening for azole resistance in *Aspergillus fumigatus* by using VIPcheck. Antimicrob Agents Chemother. 2017;61:e01250-17. http://dx.doi.org/10.1128/AAC.01250-17
4. Arendrup MC, Verweij PE, Mouton JW, Lagrou K, Meletiadis J. Multicentre validation of 4-well azole agar plates as a screening method for detection of clinically relevant azole-resistant *Aspergillus fumigatus*. J Antimicrob Chemother. 2017;72:3325–33. http://dx.doi.org/10.1093/jac/dkx319
5. Verweij PE, Lestrade PP, Melchers WJ, Meis JF. Azole resistance surveillance in *Aspergillus fumigatus*: beneficial or biased? J Antimicrob Chemother. 2016;71:2079–82. http://dx.doi.org/10.1093/jac/dkw259
6. Verweij PE, Ananda-Rajah M, Andes D, Arendrup MC, Brüggemann RJ, Chowdhary A, et al. International expert opinion on the management of infection caused by azole-resistant *Aspergillus fumigatus*. Drug Resist Updat. 2015;21-22:30–40. http://dx.doi.org/10.1016/j.drup.2015.08.001
7. van Ingen J, van der Lee HA, Rijs TA, Zoll J, Leenstra T, Melchers WJ, et al. Azole, polyene, and echinocandin MIC distributions for wild-type, TR34/L98H and TR46/Y121F/T289A *Aspergillus fumigatus* isolates in the Netherlands. J Antimicrob Chemother. 2015;70:178–81. http://dx.doi.org/10.1093/jac/dku364
8. Kolwijck E, van der Hoeven H, de Sévaux RG, ten Oever J, Rijstenberg LL, van der Lee HA, et al. voriconazole-susceptible and voriconazole-resistant *Aspergillus fumigatus* coinfection. Am J Respir Crit Care Med. 2016;193:927–9. http://dx.doi.org/10.1164/rccm.201510-2104LE
9. Chong GM, van der Beek MT, von dem Borne PA, Boelens J, Steel E, Kampinga GA, et al. PCR-based detection of *Aspergillus fumigatus* Cyp51A mutations on bronchoalveolar lavage: a multicentre validation of the AsperGenius assay in 201 patients with haematological disease suspected for invasive aspergillosis. J Antimicrob Chemother. 2016;71:3528–35. http://dx.doi.org/10.1093/jac/dkw323
10. Dannaoui E, Gabriel F, Gaboyard M, Lagardere G, Audebert L, Quesne G, et al. Molecular diagnosis of invasive aspergillosis and detection of azole resistance by a newly commercialized PCR kit. J Clin Microbiol. 2017;55:3210–8. http://dx.doi.org/10.1128/JCM.01032-17

Address for correspondence: Jochem B. Buil, Department of Medical Microbiology, Radboud University Medical Center, PO Box 9101, 6500 HB Nijmegen, the Netherlands; email: jochem.buil@radboudumc.nl

Using the Health Belief Model to Analyze Instagram Posts about Zika for Public Health Communications

Jeanine P.D. Guidry, Kellie E. Carlyle, Jessica G. LaRose, Paul Perrin, Marcus Messner, Mark Ryan

Author affiliation: Virginia Commonwealth University, Richmond, Virginia, USA

DOI: https://doi.org/10.3201/eid2501.180824

We analyzed Instagram posts about Zika by using the Health Belief Model. We found a high presence of threat messages, yet little engagement with these posts. Public health professionals should focus on posting messages to increase self-efficacy and benefits of protective behavior, especially when a vaccine becomes available.

Many persons will not engage in health protective behaviors without first understanding that they are at risk for an adverse outcome. However, the concept of risk can be difficult for persons to grasp (*1*), especially with a health topic such as Zika, with which persons are not likely to have much experience before an outbreak. Social media provides information that can help frame the public's understanding of complex, highly contagious viruses (*2*). Instagram, especially, has potential for communicating risk information because visuals can increase attention and recall above those for text alone (*3*). In addition, women of reproductive age are particularly likely to use Instagram (*4*), making it a salient platform for Zika information. Analyzing Instagram posts about Zika lends insight into public attitudes and beliefs about Zika and the types of messages that are engaging. Understanding the target audience is a key step in the formative research process when designing effective prevention messaging.

Two studies have examined Zika-focused messages on Instagram (*5*,*6*), but neither study included health behavior theory, a major component of effective public health messaging (*7*). The Health Belief Model (HBM) provides a theoretical framework to explain the uptake of preventive behaviors by perceived susceptibility, severity, benefits, barriers, self-efficacy, and cues to action (*8*); HBM has been used successfully to develop health education messages and campaigns. To address the lack of health behavior theory in previous studies of Zika on social media, we examined the content of, and engagement with, Zika posts on Instagram through the lens of the HBM (Appendix, https://wwwnc.cdc.gov/EID/article/25/1/18-0824-App1.pdf).

We collected Instagram posts that used the hashtags #Zika and #ZikaVirus during August 1–31, 2016; hashtags, which are words/phrases preceded by the # symbol, create searchable topics on many social media platforms, including Instagram. We also used the simple random sampling in the social media mining tool Netlytic (https://netlytic.org) to select 1,000 posts for quantitative content analysis (intercoder reliability 0.71–1.00).

We found that of all HBM constructs, perceived severity (75.8%) and perceived susceptibility (59.9%) occurred most frequently, indicating that posts reflect a high level of perceived threat. However, posts mentioning fear and danger produced lower engagement (Table). One explanation for this finding might relate to how persons process a threat response. The Extended Parallel Processing Model provides 2 pathways as a threat response: danger control and fear control (*9*). Fear control takes place when a perceived threat is greater than the perceived efficacy to deal with the threat (e.g., a vaccine); as a result, responses are likely to be maladaptive. It remains to be determined whether this pattern holds once a high-efficacy response like the Zika vaccine becomes available, or whether engagement increases, as would be predicted by the danger control path of the Extended Parallel Processing Model.

Perceived barriers to Zika preventive behaviors were barely present (2.8%) as a percentage of the total sample and present in just >10% of the posts specifically mentioning

Table. Mann-Whitney U test results for dichotomous independent variables and median engagement for the Health Belief Model in analyzing Instagram posts about Zika for public health communications

Engagement variable	Variable	Median present	Median absent	U*	Z	p value
Likes	Conspiracy theories	188.00	64.00	52,426.000	3.525	<0.001
Comments	Conspiracy theories	19.00	6.00	56,533.500	5.070	<0.001
Likes	Fear	61.00	102.00	78,434.000	–4.045	<0.001
Comments	Fear	6.00	10.00	78,619.000	–4.008	<0.001
Likes	Mosquito visual	57.50	77.50	63,749.500	–2.343	0.019
Likes	Person visual	89.50	57.50	141,628.000	3.733	<0.001
Likes	Perceived benefits prevention	45.00	78.50	46,042.000	–2.277	0.023
Comments	Perceived benefits prevention	4.00	7.00	45,176.000	–2.575	0.010
Likes	Perceived severity	61.00	112.00	74.914.000	–4.356	<0.001
Comments	Perceived severity	6.00	10.00	75,207.500	–4.291	<0.001

*Test statistic for Mann-Whitney U test.

Zika preventive measures. Using mosquito repellent was mentioned most frequently, more so than other available options, such as postponing travel to areas with local Zika activity or wearing long-sleeved shirts or pants. This finding makes sense because half of all preventive measure posts originate with commercial accounts, which often are promoting mosquito repellents. In addition, using mosquito repellent is not a complex behavior, and few barriers to its use likely exist beyond mild inconvenience. However, when a Zika vaccine becomes available, the conversation about Zika preventive measures on Instagram will likely change because vaccination is not without controversy. Finally, cues to action were present in only 10.2% of the sample, and cues to self-efficacy were present in only 9.6% of the sample. Public health communications professionals should focus on increasing these forms of messaging on social media, especially when a vaccine becomes available.

Overall, the Zika-focused posts in this sample reflected a high level of perceived threat and a low level of expressed self-efficacy. At least some of the responses seem to be maladaptive in nature. To counter this trend, public health organizations should consider increasing their activity regarding Zika prevention on Instagram. For example, they could emphasize the benefits and relative ease of restricting travel to high-risk areas, using repellent, and wearing protective clothing—and that the benefits of such actions outweigh the barriers. Because the salience of Zika tends to wane after the summer, cues to action are particularly needed to remind the public of ongoing risk, especially travel-related risk. Last, once a vaccine becomes available, it will be essential to promote the safety and efficacy of the vaccine and counter misinformation about vaccination side effects more generally.

About the Author

Dr. Guidry is an assistant professor at the Richard T. Robertson School of Media and Culture at Virginia Commonweaalth University, Richmond, VA. Her research interests are information and message testing using visual social media platforms, as well as designing and evaluating health promotion campaigns using health behavior theoretical models.

References

1. Lipkus IM. Numeric, verbal, and visual formats of conveying health risks: suggested best practices and future recommendations. Med Decis Making. 2007;27:696–713. http://dx.doi.org/10.1177/0272989X07307271
2. Lee ST, Basnyat I. From press release to news: mapping the framing of the 2009 H1N1 A influenza pandemic. Health Commun. 2013;28:119–32. http://dx.doi.org/10.1080/10410236.2012.658550
3. Houts PS, Doak CC, Doak LG, Loscalzo MJ. The role of pictures in improving health communication: a review of research on attention, comprehension, recall, and adherence. Patient Educ Couns. 2006;61:173–90. http://dx.doi.org/10.1016/j.pec.2005.05.004
4. Smith A. Social media use in 2018 [cited 2018 Aug 8]. http://www.pewinternet.org/2018/03/01/social-media-use-in-2018/
5. Fung IC-H, Blankenship EB, Goff ME, Mullican LA, Chan KC, Saroha N, et al. Zika-virus-related photo sharing on Pinterest and Instagram. Disaster Med Public Health Prep. 2017;11:656–9. http://dx.doi.org/10.1017/dmp.2017.23
6. Seltzer EK, Horst-Martz E, Lu M, Merchant RM. Public sentiment and discourse about Zika virus on Instagram. Public Health. 2017;150:170–5. http://dx.doi.org/10.1016/j.puhe.2017.07.015
7. Glanz K, Rimer BK, Lewis ML. Health behavior and health education: theory, research, and practice. San Francisco: Jossey-Bass; 2008.
8. Janz NK, Becker MH. The Health Belief Model: a decade later. Health Educ Q. 1984;11:1–47. http://dx.doi.org/10.1177/109019818401100101
9. Witte K. Putting the fear back into fear appeals: The extended parallel process model. Communications Monograph. 1992;59:329–49. http://dx.doi.org/10.1080/03637759209376276

Address for correspondence: Jeanine P.D. Guidry, Robertson School of Media and Culture, Virginia Commonwealth University, 901 W Main St, Rm 2216, Richmond, VA 23284, USA; email: guidryjd@vcu.edu

Zoonotic Endocarditis in a Man, the Netherlands

Janneke Sleutjens, Dennie Meijer, Paola G. Meregalli, Leendert Bakker, Jaap A. Wagenaar, Birgitta Duim, Aldert Zomer

Author affiliations: Utrecht University, Utrecht, the Netherlands (J. Sleutjens, J.A. Wagenaar, B. Duim, A. Zomer); Academical Medical Centre, Amsterdam, the Netherlands (D. Meijer, P.G. Meregalli); Tergooi Hospital, Hilversum, the Netherlands (L. Bakker); Wageningen Bioveterinary Research, Lelystad, the Netherlands (J.A. Wagenaar)

DOI: https://doi.org/10.3201/eid2501.181029

In 2017, endocarditis caused by *Streptococcus equi* subspecies *zooepidemicus* was diagnosed in a man in the Netherlands who had daily contact with horses. Whole-genome sequencing of isolates from the man and his horses confirmed the same clone, indicating horse-to-human transmission. Systematic reporting of all zoonotic cases would help with risk assessment.

On July 23, 2017, a 62-year-old man sought care at the emergency department of Tergooi Hospital (Hilversum, the Netherlands) for general malaise and fever up to

40.6°C (105.1°F). Nine months earlier, the patient's aortic valve had been replaced with a mechanical prosthesis. The emergency department staff found no cause for his complaints. Blood test results suggested an active infection; C-reactive protein concentration was 250 mg/L (reference value <10 mg/L). Blood culture grew gram-positive cocci, which were identified by matrix-assisted laser desorption/ionization time-of-flight mass spectrometry (Microflex LT; Bruker, http://www.bruker.com) as S*treptococcus equi* subspecies *zooepidemicus.* The MIC for penicillin was 0.016 and for gentamicin was 16 mg/L.

Cardiac ultrasonography revealed a small, mobile structure adhering to the aortic valve prosthesis, at the side of the left ventricle outflow tract, which was possibly bacterial vegetation. An abscess was present in the aortic root at the side of the left coronary artery. The diagnosis was bacterial endocarditis of the prosthetic valve caused by *S. equi* subsp. *zooepidemicus.*

The patient received high doses of penicillin (2 million IU/4 h for 6 wk) and gentamicin (3 mg/kg/24 h for 2 wk) intravenously, according to national guidelines (https://www.swab.nl/richtlijnen). Results of subsequent blood cultures taken on days 4 and 8 after admission were negative, and the patient was discharged after 6 weeks of treatment.

Several case reports have described the potential for *S. equi* subsp. *zooepidemicus* to cause severe infection in humans. Contact with horses is a possible source of infection (*1*–*5*). The patient we describe had frequent contact with 7 horses stabled in his yard. Two weeks before his hospital admission, horse A showed signs of an upper airway infection: copious bilateral purulent nasal discharge, coughing, and fever up to 39.1°C (102.4°F; reference range 37.5°C–38.3°C [99.5°F–100.9°F]). Seventeen days later, horse B showed similar signs. After a nasal swab sample from horse B tested by the Animal Health Service (Deventer, the Netherlands) had a negative PCR result for *S. equi* subsp. *equi*, we collected nasal swab samples from all 7 horses and cultured them for streptococci on blood agar (Oxoid, http://www.oxoid.com) at 37°C for 48 h. Culture results were positive for *S. equi* subsp. *zooepidemicus* for 4 of the 7 horses. Horses A and B recovered uneventfully without antimicrobial drug treatment.

To investigate the relatedness of isolates, we fully sequenced 2 isolates from horse A, 4 isolates from horse B, 2 isolates from horse C, 1 isolate from horse D, and 1 isolate from the human patient. We identified sequence type (ST) 212 in 1 isolate from horse A, all 4 isolates from horse B, the 2 isolates from horse C, and the isolate from the patient (Appendix Table, https://wwwnc.cdc.gov/EID/article/25/1/18-1029-App1.pdf). All genomes were aligned with a selection of publicly available *S. equi* subsp. *zooepidemicus* isolates. We constructed a core-genome alignment of 1.55 Mb, representing 76% of the genome of the reference isolate MGCS10565. Comparison of the *S. equi* subsp. *zooepidemicus* core genomes showed that the human and animal ST212 isolates had 100% identical core genomes (Appendix Figure), strongly suggesting that the same clone was present in the human patient and the animals. Construction of core-genome alignments of the ST212 isolates resulted in a 1.94-Mb core genome, 97% of the genome of the ST212 isolates; only 3% of the genome was located in the accessory genome. We extracted single-nucleotide polymorphisms (SNPs) that differed between these isolates and used them to generate a minimal-spanning tree (Figure). The number of SNPs between the human and horse isolates did not differ significantly from the number of SNPs differing between horse isolates, thereby demonstrating animal-to-human transmission of *S. equi* subsp. *zooepidemicus*.

In healthy horses, *S. equi* subsp. *zooepidemicus* is a commensal organism of the upper respiratory and lower genital tracts and can cause secondary infections (*6*). However, in 2010, a large outbreak in Iceland showed that *S. equi* subsp. *zooepidemicus* might be a primary pathogen that spreads clinically among horses without any other predisposing factors (*7*). Infections with *S. equi* subsp. *zooepidemicus* in humans, especially confirmed cases originating from contact with horses, are rare. Only a few reports confirm a horse as the source of infection by whole-genome sequencing (*7*,*8*). Systematic reporting of suspected or confirmed transmission of pathogens between horses and humans is lacking. Such reporting would support the estimation of the burden of equine-origin zoonotic infections in humans, which is needed as the equine industry continues to grow. Collaboration among disciplines to develop such a reporting system is fundamental for enabling reliable assessment of the potential risk for humans to become ill after contact with horses and the usefulness of implementing precautionary measures for patients with specific conditions.

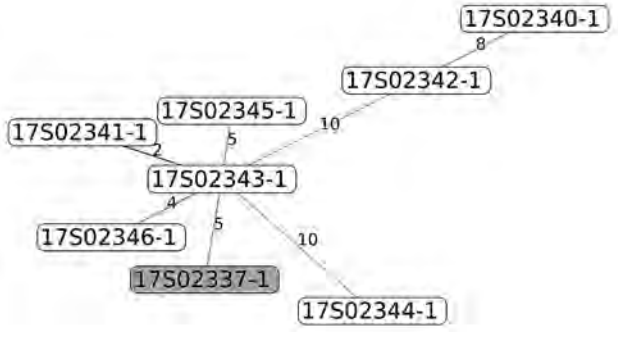

Figure. Minimal-spanning tree of 34 single-nucleotide polymorphisms. Gray indicates the human isolate. Single-nucleotide polymorphisms counts are given.

Acknowledgment

We thank Carolien Flemming for excellent support with diagnostic microbiology.

About the Author

Dr. Sleutjens is an equine ambulatory veterinarian. Her research interest is the effects of head and neck position on the welfare of the equine athlete.

References

1. Eyre DW, Kenkre JS, Bowler ICJW, McBride SJ. *Streptococcus equi* subspecies *zooepidemicus* meningitis—a case report and review of the literature. Eur J Clin Microbiol Infect Dis. 2010;29:1459–63. http://dx.doi.org/10.1007/s10096-010-1037-5
2. Minces LR, Brown PJ, Veldkamp PJ. Human meningitis from *Streptococcus equi* subsp. *zooepidemicus* acquired as zoonoses. Epidemiol Infect. 2011;139:406–10. http://dx.doi.org/10.1017/S0950268810001184
3. Altreuther M, Lange C, Myhre HO, Hannula R. Aortic graft infection and mycotic aneurysm with *Streptococcus equi zooepidemicus*: two cases with favorable outcome of antibiotic treatment. Vascular. 2013;21:6–9. http://dx.doi.org/10.1258/vasc.2011.cr0299
4. van Samkar A, Brouwer MC, van der Ende A, van de Beek D. *Streptococcus equi* meningitis. Clin Microbiol Infect. 2016;22:e3–4. http://dx.doi.org/10.1016/j.cmi.2015.09.003
5. Kittang BR, Pettersen VK, Oppegaard O, Skutlaberg DH, Dale H, Wiker HG, et al. Zoonotic necrotizing myositis caused by *Streptococcus equi* subsp. *zooepidemicus* in a farmer. BMC Infect Dis. 2017;17:147. http://dx.doi.org/10.1186/s12879-017-2262-7
6. Fulde M, Valentin-Weigand P. Epidemiology and pathogenicity of zoonotic streptococci. In: Chhatwal G, editor. Current Topics in Microbiology and Immunology. New York: Springer;2012. p. 49–81.
7. Björnsdóttir S, Harris SR, Svansson V, Gunnarsson E, Sigurðardóttir ÓG, Gammeljord K, et al. Genomic dissection of an Icelandic epidemic of respiratory disease in horses and associated zoonotic cases. MBiol. 2017;8:e00826–17.
8. Pelkonen S, Lindahl SB, Suomala P, Karhukorpi J, Vuorinen S, Koivula I, et al. Transmission of *Streptococcus equi* subspecies *zooepidemicus* infection from horses to humans. Emerg Infect Dis. 2013;19:1041–8. http://dx.doi.org/10.3201/eid1907.121365

Address for correspondence: Janneke Sleutjens, Utrecht University, Department of Equine Sciences, Faculty of Veterinary Medicine, Yalelaan 112, 3584 CM Utrecht, the Netherlands; email: j.sleutjens@uu.nl

Trachoma in 3 Amerindian Communities, Venezuelan Amazon, 2018

Oscar Noya-Alarcón, Maríapía Bevilacqua, Alfonso J. Rodríguez-Morales

Author affiliations: Universidad Central de Venezuela, Caracas, Venezuela (O. Noya-Alarcón); Asociación Venezolana para la Conservación de Áreas Naturales, Caracas (M. Bevilacqua); Universidad Tecnológica de Pereira, Pereira, Colombia (A.J. Rodríguez-Morales); Universidad Privada Franz Tamayo, Cochabamba, Bolivia (A.J. Rodríguez-Morales)

DOI: https://doi.org/10.3201/eid2501.181362

Trachoma is among the most common infectious causes of blindness. During January–May 2018, a total of 4 trachoma cases were diagnosed among Amerindians of the Yanomami ethnic group in 3 communities of southern Venezuela. This country has social and environmental conditions conducive to the endemicity of this neglected tropical disease.

Trachoma, caused by the bacterium *Chlamydia trachomatis*, is the most common infectious cause of blindness. It is endemic to many of the poorest and most remote areas of Africa, Asia, Australia, the Middle East, and Latin America (*1*). Trachoma causes visual impairment in ≈2.2 million persons worldwide, of whom 1.2 million are completely blind (*2*). As of April 2018, ≈158 million persons living in districts to which trachoma is endemic are at risk (*3*). In South America, trachoma is considered endemic to Brazil (*4*) and Colombia (*5*) but not to Venezuela. We describe 4 patients in whom trachoma was diagnosed during January–May 2018 in 3 communities in the Amazon region of southern Venezuela. All were Amerindians of the Yanomami ethnic group living near rivers in extensive, well-conserved international forest frontiers.

During January–May 2018, in the integrated healthcare system in the Venezuela states of Amazonas and Bolivar, 4 trachoma cases were detected. Two cases occurred in the Yanomami community of Kuyuwiniña, Alto Caura River basin, Bolivar, and 1 case occurred in each of 2 communities of the upper Orinoco River basin of Amazonas (Oroshi and Rashakami) (Appendix Figure 1, https://wwwnc.cdc.gov/EID/article/25/1/18-1362-App1.pdf).

Case-patient 1 was a 38-year-old woman from Oroshi with a 5-month history of trachomatous trichiasis (TT), pain, madarosis, blepharitis, and conjunctivitis in both eyes. Case-patient 2 was a 35-year-old woman from Kuyuwiniña with a 6-month history of TT, pain, madarosis, blepharitis, and conjunctivitis in both eyes; corneal opacity in the right eye; and full blindness in the left eye (Appendix Figure 2). Case-patient 3 was a 45-year-old man from Kuyuwiniña with a 5-year

history of TT, madarosis, blepharitis, conjunctivitis, and corneal opacity in both eyes. Case-patient 4 was a 22-year-old man from Rashakami with a 1-year history of TT, madarosis, blepharitis, and keratitis in both eyes; full blindness in the left eye; and decreased vision in the right eye.

All 4 patients used natural depilatory wax to improve their trachoma. No additional information on use of traditional eye medicine or epilation was obtained. These communities have no access to potable water except rivers and live crowded in open aboriginal community households (Appendix Figure 1, panel B). These patients were treated with azithromycin (1 g single dose orally) and showed clinical improvement (less inflammation) 3 months later (*6*) without surgery.

Trachoma is a neglected tropical disease (NTD) that disproportionately affects the poorest communities (*7*). Worldwide, many indigenous peoples are at risk (*4*,*5*,*7*). The geographic origin of these cases is unknown. In remote areas of the southern Venezuelan Amazon, the population moves within the Caura River basin and in the upper Orinoco basin and to and from Brazil in the headwaters of the Auaris River and other subbasins of the Branco River in Yanomami territory. The potential introduction of infected illegal gold miners also should be considered as a source of trachoma. The remoteness of these communities often means they have limited access to healthcare, making assessment of trachoma and other diseases challenging. Thus, findings of this NTD and others is not surprising.

Trachoma was originally reported in Venezuela in 1894; at least 17 cases were sporadically reported during 1903–1956. In 1982, six case-patients (2 female, 4 male) 30 months–22 years of age were described (*8*).

A resolution of the World Health Assembly in 1998 established political commitment for global elimination of trachoma as a public health problem. Much progress is being made toward that goal, but momentum may be insufficient to meet the 2020 target (*1*), particularly given emerging evidence of previously unknown endemic foci in places such as Venezuela and the Democratic Republic of the Congo. Population-based studies are needed to define the prevalence of trachoma in these communities of Venezuela, which border Brazil, a country in which this NTD is endemic in indigenous populations, with reported prevalences of up to 35.2% for the trachomatous follicular inflammation in children 1–9 years of age (*4*).

Water is necessary for face washing, and trachoma often occurs in communities or households without an adequate water supply. Several studies have identified a positive association between the distance to the water source and the prevalence of active trachoma (*1*). Because of improvement of socioeconomic and sanitary status (*9*), advent of new generations of antimicrobial drugs, and training of ophthalmologists and eye-care facilities, the prevalence of trachoma is decreasing (*2*). In the context of the onchocerciasis elimination program in the area, ophthalmologists and other specially trained physicians periodically attended these populations to assess visual health, including onchocercosis. In countries such as Brazil (*4*) and Colombia (*5*), trachoma appears to be a serious public health problem in indigenous settlements and should be prioritized in programs aimed at eliminating trachoma (*1*,*2*,*7*). The cases we report suggest that national and international health authorities should consider developing surveillance and undertaking research for trachoma in these areas of Venezuela (*6*,*10*).

About the Author

Dr. Noya-Alarcón is a research physician at the Servicio Autónomo Centro Amazónico de Investigación y Control de Enfermedades Tropicales, Puerto Ayacucho, Amazonas, Venezuela, and Instituto de Medicina Tropical, Facultad de Medicina, Universidad Central de Venezuela, Caracas, Venezuela. His primary research interests include tropical diseases, such as trachoma, onchocercosis, echinococcosis, as well as microbioma in native peoples.

References

1. Taylor HR, Burton MJ, Haddad D, West S, Wright H. Trachoma. Lancet. 2014;384:2142–52. http://dx.doi.org/10.1016/S0140-6736(13)62182-0
2. Mohammadpour M, Abrishami M, Masoumi A, Hashemi H. Trachoma: past, present and future. J Curr Ophthalmol. 2016;28:165–9.
3. WHO Alliance for the Global Elimination of Trachoma by 2020: progress report on elimination of trachoma, 2017. Wkly Epidemiol Rec. 2017;92:359–68.
4. Freitas HS, Medina NH, Lopes MF, Soares OE, Teodoro MT, Ramalho KR, et al. Trachoma in indigenous settlements in Brazil, 2000–2008. Ophthalmic Epidemiol. 2016;23:354–9. http://dx.doi.org/10.3109/09286586.2015.1131305
5. Miller H, Gallego G, Rodriguez G. Clinical evidence of trachoma in Colombian Amerindians of the Vaupes Province [in Spanish]. Biomedica. 2010;30:432–9.
6. Chidambaram JD, Bird M, Schiedler V, Fry AM, Porco T, Bhatta RC, et al. Trachoma decline and widespread use of antimicrobial drugs. Emerg Infect Dis. 2004;10:1895–9. http://dx.doi.org/10.3201/eid1011.040476
7. Trujillo JT, Jesudason T, Sankar G. Reaching remote Amazonian communities to eliminate trachoma. Community Eye Health. 2017;30:65.
8. Selle F, Gan J, Gonzalez F, Gonzalez Sirit R. Tracoma en Venezuela—nuevos casos. Revista Oftalmologica Venezolana. 1985;43:341–7.
9. Garn JV, Boisson S, Willis R, Bakhtiari A, Al-Khatib T, Amer K, et al. Sanitation and water supply coverage thresholds associated with active trachoma: modeling cross-sectional data from 13 countries. PLoS Negl Trop Dis. 2018;12:e0006110. http://dx.doi.org/10.1371/journal.pntd.0006110
10. Gaynor BD, Miao Y, Cevallos V, Jha H, Chaudary JS, Bhatta R, et al. Eliminating trachoma in areas with limited disease. Emerg Infect Dis. 2003;9:596–8. http://dx.doi.org/10.3201/eid0905.020577

Address for correspondence: Alfonso J. Rodríguez-Morales, Public Health and Infection Research Group and Incubator, Office 14-315, Scientific Research Direction, Fl 3, Bldg 14, Department of Community Medicine, School of Medicine, Faculty of Health Sciences, Universidad Tecnológica de Pereira, Sector La Julita, Pereira 660003, Risaralda, Coffe-Triangle Region, Colombia; email: arodriguezm@utp.edu.co

Phylogeographic Analysis of African Swine Fever Virus, Western Europe, 2018

Mutien Garigliany, Daniel Desmecht, Marylène Tignon, Dominique Cassart, Christophe Lesenfant, Julien Paternostre, Rosario Volpe, Ann Brigitte Cay, Thierry van den Berg, Annick Linden

Author affiliations: University of Liège, Sart Tilman, Belgium (M. Garigliany, D. Desmecht, D. Cassart, C. Lesenfant, J. Paternostre, R. Volpe, A. Linden); Sciensano Animal Health, Brussels, Belgium (M. Tignon, A.B. Cay, T. van den Berg)

DOI: https://doi.org/10.3201/eid2501.181535

In September 2018, African swine fever in wild boars was detected in Belgium. We used African swine fever–infected spleen samples to perform a phylogenetic analysis of the virus. The causative strain belongs to genotype II, and its closest relatives are viruses previously isolated in Ukraine, Belarus, Estonia, and European Russia.

African swine fever (ASF) is a devastating disease of domestic pigs and wild boars caused by a DNA arbovirus, African swine fever virus (ASFV), belonging to the family *Asfarviridae*. ASF is endemic in sub-Saharan African countries and has become more prevalent in the Caucasus region since its spread from eastern Africa to Georgia in 2007. The epizootic then spread to the surrounding countries, including the Russian Federation, and further to Belarus and Ukraine. In 2014, ASFV reached the European Union member states of Estonia, Latvia, Lithuania, and Poland; in 2016, Moldova; and, in 2017, the Czech Republic and Romania (*1*).

On September 13, 2018, authorities in Belgium reported that ASF had been confirmed in 2 wild boars near the village of Étalle (49.6833° N, 5.6° E), in the province of Luxembourg, which is located 12 km from the border with France and 17 km from the country of Luxembourg. ASFV appears to have jumped a considerable distance from previously affected countries: ≈500 km from the border with the Czech Republic, 800 km from Hungary, and 1,200 km from the border with Romania. Since then, ≈75% of the wild boars found dead near the primordial spot have been found to be ASFV positive; a total of 96 positive results had been recorded as of October 16, 2018.

To investigate the virus, we performed initial genetic characterization using standard genotyping procedure on virus DNA directly extracted from homogenized spleen or kidney tissues of each animal. First, we obtained a segment of the *B646L* gene by PCR as described by Gallardo et al. (*2*) and Ge et al. (*3*). The DNA sequence retrieved was identical in both animals (GenBank accession no. MH998358). We performed sequence alignments using ClustalW implemented in Geneious version 8.1.8 (https://www.geneious.com). We performed phylogenetic analysis using MEGA7 (http://www.megasoftware.net) and the Kimura 2-parameter substitution model, using the neighbor-joining method, as determined by a model selection analysis (Figure, panel A). The strain of ASFV found in Belgium clearly belonged to genotype II, which includes viruses that are circulating in both Eurasia and southern Africa.

To further define the most likely origin of this strain, we performed PCR targeting a ≈350-bp fragment in the variable intergenic region between the *I73R* and *I329L* genes, according to Gallardo et al. (*2*). Again, we retrieved identical DNA sequences from both animals (GenBank accession no. MH998359). Sequence alignments revealed that the isolate ASFV/Etalle/wb/2018 from Belgium contains a 10-nt (TATATAGGAA) insertion at position 106. It is therefore a so-called intergenic region (IGR) II variant, according to the nomenclature of Gallardo et al. (*2*). ASFV/Etalle/wb/2018 displays 100% identity with the sequences obtained from strains isolated in Ukraine in 2012, Belarus in 2013, Estonia in 2014, European Russia in 2015 and 2016, and China in 2018 (*3*,*4*), suggesting that the strain in Belgium most likely originates from one of these countries (Figure, panel B). Conversely, this insertion is absent in strains isolated in Armenia in 2007, in Georgia in 2007, in Poland in 2015, and in Siberia, Russia, in 2017 (*4*). Genotyping the p72 and IGR loci is compatible with the current state of the art for ASFV molecular epidemiology but still presents intrinsic limitations. A further genome-wide genotyping approach is expected to consolidate and bring more precision to the filiation revealed here.

Acknowledgments

The authors thank Laetitia Delaval and Mathieu Franssen for technical assistance.

The field part of this study is supported by a regional grant of the Public Service of Wallonia.

About the Author

Dr. Garigliany is a professor of pathology on the Veterinary Faculty of the University of Liège, Belgium. His research activities focus on the biology of viruses and related host–pathogen interactions.

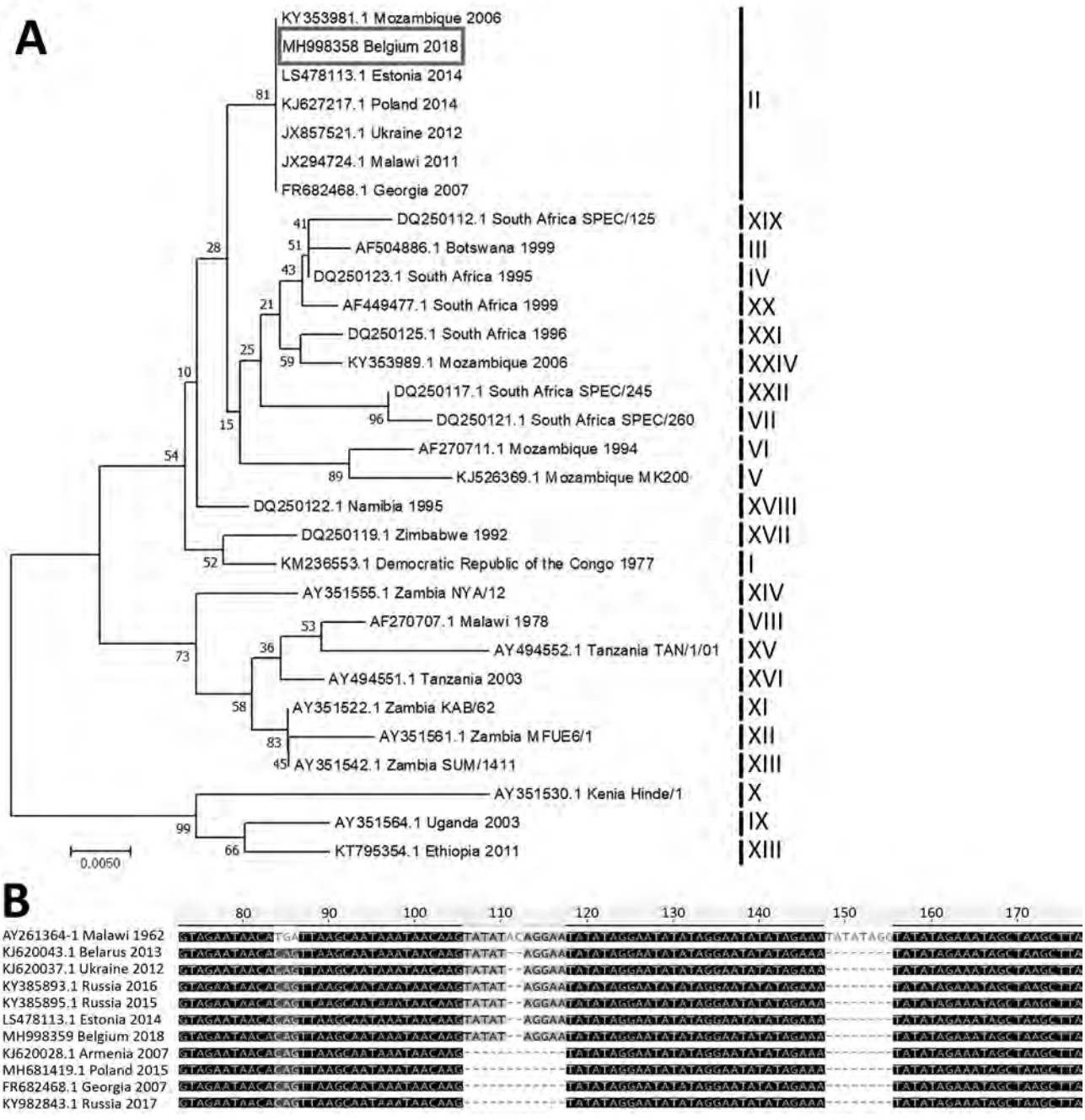

Figure. A) Evolutionary relationships of representative strains of African swine fever virus based on the neighbor-joining phylogeny of the partial p72 gene sequences. The phylogenetic analysis was performed using MEGA7 (http://www.megasoftware.net) and the Kimura 2-parameter substitution model, as determined by a model selection analysis. Bootstrap values (≥70%, based on 500 replicates) for each node are given. GenBank accession numbers, country, and year of collection are indicated for each strain; for strains for which the year of collection is not known, the strain name is indicated. Corresponding genotypes are labeled I–XXIV. Box indicates the African swine fever sequence from Belgium generated during this study. Scale bar indicates nucleotide substitutions per site. B) Nucleotide sequence alignment of the partial intergenic region between the *I73R* and *I329L* genes from representative African swine fever virus strains. GenBank accession numbers, country, and year of collection are indicated.

References

1. Chenais E, Ståhl K, Guberti V, Depner K. Identification of wild boar–habitat epidemiologic cycle in African swine fever epizootic. Emerg Infect Dis. 2018;24:810–2. http://dx.doi.org/10.3201/eid2404.172127
2. Gallardo C, Fernández-Pinero J, Pelayo V, Gazaev I, Markowska-Daniel I, Pridotkas G, et al. Genetic variation among African swine fever genotype II viruses, eastern and central Europe. Emerg Infect Dis. 2014;20:1544–7. http://dx.doi.org/10.3201/eid2009.140554
3. Ge S, Li J, Fan X, Liu F, Li L, Wang Q, et al. Molecular characterization of African swine fever virus, China, 2018. Emerg Infect Dis. 2018;24:2131–3. http://dx.doi.org/10.3201/eid2411.181274
4. Kolbasov D, Titov I, Tsybanov S, Gogin A, Malogolovkin A. African swine fever virus, Siberia, Russia, 2017. Emerg Infect Dis. 2018;24:796–8. http://dx.doi.org/10.3201/eid2404.171238

Address for correspondence: Daniel Desmecht, University of Liège, Pathology, Faculty of Veterinary Medicine, Sart Tilman B43, Liège 4000, Belgium; email: daniel.desmecht@ulg.ac.be

Inaccurate Multilocus Sequence Typing of *Acinetobacter baumannii*

Santiago Castillo-Ramírez, Lucía Graña-Miraglia

Author affiliation: Programa de Genómica Evolutiva, Centro de Ciencias Génomicas, Universidad Nacional Autónoma de México, Cuernavaca, Mexico

DOI: https://doi.org/10.3201/eid2412.180374

Multilocus sequence typing has been useful for genotyping pathogens in surveillance and epidemiologic studies. However, it cannot reflect the true relationships of isolates for species with very dynamic genomes. Using a robust genome phylogeny, we demonstrated the limitations of this method for typing *Acinetobacter baumannii*.

An adequate genotyping system is of paramount importance for infectious disease epidemiology. Two decades ago, the multilocus sequence typing (MLST) scheme was proposed as a genotyping method (*1*), and today, because of its reproducibility and portability, MLST schemes are available for many human pathogens (*2*). MLST has been instrumental in increasing understanding of the epidemiology and population structure of many bacteria. *Acinetobacter baumannii*, a major source of nosocomial infections, is no exception, and 2 MLST schemes (Oxford and Pasteur) have been established for this species (*3*,*4*). Each scheme uses just 7 loci and, therefore, only samples a small fraction of the chromosome, which could be a serious issue for genotyping species with highly variable genomes. Some studies have shown that *A. baumannii* has both high gene content variation (*5*) and substantial levels of recombination (*6*).

We revisited one of the most comprehensive genome datasets of *A. baumannii* (*5*) to construct a robust phylogeny to show that sequence type (ST) assignation in both MLST schemes does not reflect true relationships among isolates of this species. This dataset of >80 genomes covers 36 different STs according to the Oxford scheme (STox) and 19 different STs according to the Pasteur scheme (STp) (Appendix Table 1, https://wwwnc.cdc.gov/EID/article/25/1/18-0374-App1.pdf). We constructed a concatenated alignment of 574 orthologous genes and conducted statistical model selection as in a previous study (*5*) and, on that alignment, constructed a maximum-likelihood phylogeny by PhyML (*7*).

The 2 schemes showed different levels of resolution. Although in many instances a single STp had just 1 equivalent STox, 2 STs exist in the Pasteur scheme that encompass many Oxford STs (Appendix Figure, red branches). For instance, under the Pasteur scheme, STp2 represents >15 STs in the Oxford scheme and STp1 encompasses 5 STox. Thus, the Pasteur scheme seems to have considerably less resolution than the Oxford scheme to distinguish isolates. The Pasteur scheme's lack of resolution was not insignificant, however. STp2 comprises 43 isolates (approximately half of our dataset) showing considerable levels of genetic variation according to our phylogeny, but according to this MLST scheme, they constitute just 1 genotype.

Many of the STs in either scheme formed coherent (monophyletic) groups in our phylogeny. However, we recorded some clear exceptions in which isolates from some STs did not form monophyletic groups, that is, isolates with the same ST did not cluster. The most striking case is STox208 (orange tips in the phylogeny), where there are 2 well-defined groups with several isolates each and an extra isolate not close to either of those well-defined groups. We also noted that the 2 STox455 isolates did not cluster and are located far apart on the tree (green tips). Additionally, 1 of the STox369 isolates did not fall within the ST369 group (blue tips). These 3 examples show that the Oxford MLST does not accurately reflect the relationships among the isolates. Also notable is that, although for the Oxford scheme 36 STs are represented in this dataset, only 16 of them have ≥2 isolates and therefore only in these STs could we detect problems with the clustering within any given ST. Thus, 3 of these 16 STs did not cluster the isolates properly inasmuch as these STs were polyphyletic. In summary, for the Oxford scheme we demonstrated that some STs form polyphyletic groups

because 4 of the 7 loci have signals of recombination (Appendix Table 2), whereas for the Pasteur scheme, we noted a serious lack of resolution for some STs because the loci used only by this scheme have the lowest levels of genetic diversity (Appendix Table 2). Two previous studies noted problems with the MLST schemes for this species (*8*,*9*); nonetheless, neither was as extensive as our study, nor did they benchmark both schemes against a genome-based phylogeny.

In conclusion, we showed that the correct relationships among isolates cannot be recovered using either of the MLST schemes for *A. baumannii*. In addition, we highlighted the importance of using more powerful genotyping strategies when analyzing bacteria with highly dynamic genomes; in this regard, the ever-decreasing cost of genome sequencing will make this technology the perfect tool for genotyping bacterial species.

Acknowledgments

S.C.-R. thanks Timothy Read for his valuable comments on the manuscript.

This work was supported by "Programa de Apoyo a Proyectos de Investigación e Innovación Tecnológica PAPIIT" (grant no. IA201317) and CONACyT Ciencia Básica 2016 (grant no. 284276) to S.C.-R. L.G.-M. received a CONACYT doctoral fellowship (no. 585414).

About the Authors

Dr. Castillo-Ramírez is an associate professor in the Centro de Ciencias Genómicas, Universidad Nacional Autónoma de México. His primary research interests include evolutionary genomics and phylogeography of bacterial pathogens.

Ms. Graña-Miraglia is a doctoral student at the Programa de Doctorado en Ciencias Biomédicas, Universidad Nacional Autónoma de México. Her primary research interest is the comparative genomics of bacteria.

References

1. Maiden MC, Bygraves JA, Feil E, Morelli G, Russell JE, Urwin R, et al. Multilocus sequence typing: a portable approach to the identification of clones within populations of pathogenic microorganisms. Proc Natl Acad Sci U S A. 1998;95:3140–5. http://dx.doi.org/10.1073/pnas.95.6.3140
2. Jolley KA, Maiden MC. BIGSdb: scalable analysis of bacterial genome variation at the population level. BMC Bioinformatics. 2010;11:595. http://dx.doi.org/10.1186/1471-2105-11-595
3. Bartual SG, Seifert H, Hippler C, Luzon MA, Wisplinghoff H, Rodríguez-Valera F. Development of a multilocus sequence typing scheme for characterization of clinical isolates of *Acinetobacter baumannii*. J Clin Microbiol. 2005;43:4382–90. http://dx.doi.org/10.1128/JCM.43.9.4382-4390.2005
4. Diancourt L, Passet V, Nemec A, Dijkshoorn L, Brisse S. The population structure of *Acinetobacter baumannii*: expanding multiresistant clones from an ancestral susceptible genetic pool. PLoS One. 2010;5:e10034. http://dx.doi.org/10.1371/journal.pone.0010034
5. Graña-Miraglia L, Lozano LF, Velázquez C, Volkow-Fernández P, Pérez-Oseguera Á, Cevallos MA, et al. Rapid gene turnover as a significant source of genetic variation in a recently seeded population of a healthcare-associated pathogen. Front Microbiol. 2017;8:1817. http://dx.doi.org/10.3389/fmicb.2017.01817
6. Snitkin ES, Zelazny AM, Montero CI, Stock F, Mijares L, Murray PR, et al.; NISC Comparative Sequence Program. Genome-wide recombination drives diversification of epidemic strains of *Acinetobacter baumannii*. Proc Natl Acad Sci U S A. 2011;108:13758–63. http://dx.doi.org/10.1073/pnas.1104404108
7. Guindon S, Dufayard JF, Lefort V, Anisimova M, Hordijk W, Gascuel O. New algorithms and methods to estimate maximum-likelihood phylogenies: assessing the performance of PhyML 3.0. Syst Biol. 2010;59:307–21. http://dx.doi.org/10.1093/sysbio/syq010
8. Hamidian M, Nigro SJ, Hall RM. Problems with the Oxford multilocus sequence typing scheme for *Acinetobacter baumannii*: do sequence type 92 (ST92) and ST109 exist? J Clin Microbiol. 2017;55:2287–9. http://dx.doi.org/10.1128/JCM.00533-17
9. Tomaschek F, Higgins PG, Stefanik D, Wisplinghoff H, Seifert H. Head-to-head comparison of two multi-locus sequence typing (MLST) schemes for characterization of *Acinetobacter baumannii* outbreak and sporadic isolates. PLoS One. 2016; 11:e0153014. http://dx.doi.org/10.1371/journal.pone.0153014

Address for correspondence: Santiago Castillo-Ramírez, Centro de Ciencias Genomicas, Av Universidad S/N, Cuernavaca 62210, Mexico; email: iago@ccg.unam.mx

Severe Disseminated Infection with Emerging Lineage of Methicillin-Sensitive *Staphylococcus aureus*

Paul Jewell, Luke Dixon, Aran Singanayagam, Rohma Ghani, Ernie Wong, Meg Coleman, Bruno Pichon, Angela Kearns, Georgina Russell, James Hatcher

Author affiliations: Imperial College Healthcare NHS Trust, London, United Kingdom (P. Jewell, L. Dixon, A. Singanayagam, R. Ghani, E. Wong, M. Coleman, G. Russell, J. Hatcher); Public Health England, London (B. Pichon, A. Kearns)

DOI: https://doi.org/10.3201/eid2501.180684

We report a case of severe disseminated infection in an immunocompetent man caused by an emerging lineage of methicillin-sensitive *Staphylococcus aureus* clonal complex 398. Genes encoding classic virulence factors were

absent. The patient made a slow recovery after multiple surgical interventions and a protracted course of intravenous flucloxacillin.

Since being identified in 2002, methicillin-resistant *Staphylococcus aureus* (MRSA) clonal complex 398 (CC398) lineage, associated with livestock, has been a global public health concern (*1*). We know less about human infections with methicillin-sensitive *Staphylococcus aureus* (MSSA) CC398. Evidence suggests MRSA CC398 and MSSA CC398 are of distinct lineages (*2*); recently, MSSA CC398 has emerged as an invasive pathogen in humans without prior contact with animals (*3*). Here, we describe a case of severe disseminated MSSA CC398 infection in an immunocompetent man with no exposure to livestock.

Shortly after arriving in the United Kingdom, a 60-year-old man from Colombia sought medical care after experiencing malaise, sore throat, and joint and muscular pain for 7 days. At hospital admission, he had signs consistent with sepsis and evidence of spreading soft tissue infection. Results of admission blood tests included leukocytes 49.9 × 10^9/L (neutrophils 48.4), platelets 113 ×10^9/L, C-reactive protein 437 mg/dL, creatine kinase 1,277 IU/L, lactate 4.5 mmol/L, and albumin 19 g/L. Laboratorians isolated MSSA from blood cultures taken at admission. Antimicrobial susceptibility testing using disc diffusion methodology (EUCAST version 8.0, http://eucast.org) showed susceptibility to cefoxitin, rifampin, ciprofloxacin, trimethoprim, and tetracycline, but resistance to penicillin, erythromycin, and clindamycin. Oxacillin MIC testing confirmed flucloxacillin sensitivity (MIC 0.38 mg/L).

Computed tomography and magnetic resonance imaging (MRI) images taken at admission indicated pyomyositis of the left subscapularis, inferior scalene, and intercostal muscles; a large retropharyngeal (Figure, panels A, B) and right psoas collection of pus, bibasal lung consolidation; and an epidural collection of pus extending from the lower thoracic to the lumbar spine and into the paraspinal soft tissues (Figure, panels C, D). HIV testing; hepatitis A, B, and C testing; myeloma screening; and a transthoracic echocardiogram all returned negative results. A transesophageal echocardiogram was not performed.

The patient was treated with intravenous flucloxacillin (2 g every 4 h) and rifampin (300 mg 2×/d) throughout his hospital admission. Initial surgical interventions consisted of incision and drainage of the retropharyngeal, right deltoid, and left subscapular collections. A second MRI, taken on day 13 of admission, showed discitis and osteomyelitis of the C3 and C4 vertebrae, return of the retropharyngeal collection, and enlargement of the psoas and epidural collections, with evidence of compression of the distal cord. No neurosurgical intervention was undertaken because the patient showed no focal neurologic signs.

Despite images showing initial enlargement of collections, the patient experienced a slow clinical and biochemical recovery. MSSA was recovered from blood cultures until day 10, but tests were negative thereafter. A second computed tomography image, taken on day 30, showed a reduction in the size of the epidural and psoas collections. The patient returned to Colombia on medical grounds on day 46 to continue intravenous antibiotic therapy.

Whole-genome sequencing showed the MSSA to be multilocus sequence type (ST) 4371 (a single-locus variant of ST398). Sequencing also found no genes encoding superantigens (9 enterotoxins and *tst*), exfoliatins, or Panton-Valentine leukocidin. Presence of the immune evasion cluster genes and the canonical single-nucleotide polymorphisms described by Stegger et al. (*4*) confirmed the isolate

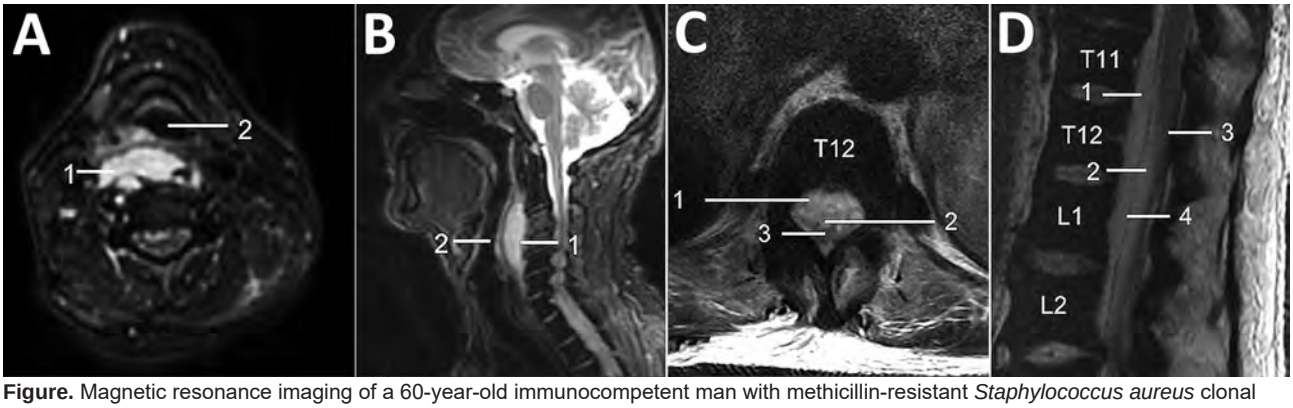

Figure. Magnetic resonance imaging of a 60-year-old immunocompetent man with methicillin-resistant *Staphylococcus aureus* clonal complex 398 infection. A, B) Axial (A) and sagittal (B) T2-weighted fat suppressed sequences of the cervical spine demonstrate a retropharyngeal abscess (1) that moderately anteriorly displaces and mildly effaces the hypopharynx (2). C, D) Axial (C) and sagittal (D) T2-weighted MRI sequences of the thoracolumbar spine (T11–L2 vertebra levels labeled) demonstrate a large ventral, combined epidural (1) and subdural (2) spinal collection that displaces the conus medullaris (3) dorsally. Note the dura mater (4) on the sagittal sequence, which delineates the theca and separates the epidural and subdural spaces.

belonged to the human clade of CC398. Resistance genes *blaZ* and *erm(T)* were identified, correlating with the observed phenotype.

This case of severe, widely disseminated infection in an immunocompetent man caused by a strain of MSSA without classic virulence factors is consistent with a growing body of evidence in support of MSSA CC398 as an emerging human pathogen. In cohorts of patients in France, CC398 MSSA has increased from being found in no cases in 1999 to 4.6% of cases in 2010 and 13.8% of cases in 2014 (*3*). Reports further indicate that nasal colonization with MSSA CC398 has increased in Europe (*5*).

A study in New York, New York, USA, found MSSA CC398 infection to be associated with a largely Dominican neighborhood, in particular; Hispanic ethnicity was a clinical predictor (*6*). Another case of invasive MSSA CC398 in a patient from Colombia has also been described (*7*).

Existing literature demonstrates evidence for MSSA CC398 as both a community- and hospital-associated pathogen (*3*). As in this case, MSSA CC398 has been shown to cause bloodstream infections (*8*), bone and joint infections (*5*,*9*) and skin and soft tissue infections (*3*,*9*). MSSA CC398 has also been associated with causing severe infection. Bouiller et al. found that 30-day all-cause mortality was higher for patients with CC398 MSSA bloodstream infection than for a control group with non-CC398 MSSA infection (*3*). Other cases of MSSA CC398 in the literature report similar resistance profiles and lack of virulence factors as we describe (*10*).

This case report aligns with existing evidence for MSSA CC398 as an emerging human pathogen. However, it is unusual in its degree of severity, with multiple extensive foci of infection, despite this strain lacking classic virulence factors. This lineage is of increasing global public health concern, and potential unidentified virulence factors and uncharacterized transmission patterns remain to be determined.

Acknowledgment

We kindly thank the patient for providing permission to publish this case.

About the Author

Dr. Jewell is a junior doctor in respiratory medicine at St Mary's Hospital, Imperial College Healthcare NHS Trust, London, with a primary research interest in infectious diseases.

References

1. Verkade E, Bergmans AMC, Budding AE, van Belkum A, Savelkoul P, Buiting AG, et al. Recent emergence of *Staphylococcus aureus* clonal complex 398 in human blood cultures. PLoS One. 2012;7:e41855. http://dx.doi.org/10.1371/journal.pone.0041855
2. Smith TC, Wardyn SE. Human infections with *Staphylococcus aureus* CC398. Curr Environ Health Rep. 2015;2:41–51. http://dx.doi.org/10.1007/s40572-014-0034-8
3. Bouiller K, Gbaguidi-Haore H, Hocquet D, Cholley P, Bertrand X, Chirouze C. Clonal complex 398 methicillin-susceptible *Staphylococcus aureus* bloodstream infections are associated with high mortality. Clin Microbiol Infect. 2016;22:451–5. http://dx.doi.org/10.1016/j.cmi.2016.01.018
4. Stegger M, Liu CM, Larsen J, Soldanova K, Aziz M, Contente-Cuomo T, et al. Rapid differentiation between livestock-associated and livestock-independent *Staphylococcus aureus* CC398 clades. PLoS One. 2013;8:e79645. http://dx.doi.org/10.1371/journal.pone.0079645
5. Valour F, Tasse J, Trouillet-Assant S, Rasigade JP, Lamy B, Chanard E, et al.; Lyon Bone and Joint Infection study group. Methicillin-susceptible *Staphylococcus aureus* clonal complex 398: high prevalence and geographical heterogeneity in bone and joint infection and nasal carriage. Clin Microbiol Infect. 2014;20:O772–5. http://dx.doi.org/10.1111/1469-0691.12567
6. Uhlemann A-C, Porcella SF, Trivedi S, Sullivan SB, Hafer C, Kennedy AD, et al. Identification of a highly transmissible animal-independent *Staphylococcus aureus* ST398 clone with distinct genomic and cell adhesion properties. MBio. 2012;3:1–9. http://dx.doi.org/10.1128/mBio.00027-12
7. Jiménez JN, Velez LA, Mediavilla JR, Ocampo AM, Vanegas JM, Rodriguez EA, et al. Livestock-associated methicillin-susceptible *Staphylococcus aureus* ST398 infection in woman, Colombia. Emerg Infect Dis. 2011;17:1970–1. http://dx.doi.org/10.3201/eid1710.110638
8. Valentin-Domelier AS, Girard M, Bertrand X, Violette J, François P, Donnio P-Y, et al.; Bloodstream Infection Study Group of the Réseau des Hygiénistes du Centre (RHC). Methicillin-susceptible ST398 *Staphylococcus aureus* responsible for bloodstream infections: an emerging human-adapted subclone? PLoS One. 2011;6:e28369. http://dx.doi.org/10.1371/journal.pone.0028369
9. Chroboczek T, Boisset S, Rasigade JP, Tristan A, Bes M, Meugnier H, et al. Clonal complex 398 methicillin susceptible *Staphylococcus aureus*: a frequent unspecialized human pathogen with specific phenotypic and genotypic characteristics. PLoS One. 2013;8:e68462. http://dx.doi.org/10.1371/journal.pone.0068462
10. Uhlemann AC, Hafer C, Miko BA, Sowash MG, Sullivan SB, Shu Q, et al. Emergence of sequence type 398 as a community- and healthcare-associated methicillin-susceptible *staphylococcus aureus* in northern Manhattan. Clin Infect Dis. 2013;57:700–3. http://dx.doi.org/10.1093/cid/cit375

Address for correspondence: Paul Jewell, St. Mary's Hospital, Imperial College Healthcare, NHS Trust, London, UK; email: pauljewell@nhs.net

Severe Disease Caused by Community-Associated MRSA ST398 Type V, Australia, 2017

Geoffrey W. Coombs, Stanley Pang, Denise A. Daley, Yung Thin Lee, Sam Abraham, Marcel Leroi

Author affiliations: PathWest Laboratory Medicine WA, Murdoch, Western Australia, Australia (G.W. Coombs); Murdoch University, Murdoch (G.W. Coombs, S. Pang, Y.T. Lee, S. Abraham); Australian Group on Antimicrobial Resistance, Murdoch (D.A. Daley); Austin Health, Heidelberg, Victoria, Australia (M. Leroi)

DOI: https://doi.org/10.3201/eid2501.181136

Using whole-genome sequencing, we identified a community-associated methicillin-resistant *Staphylococcus aureus* (CA-MRSA) sequence type (ST) 398 type V (5C2&5) isolate (typically found in China) in Australia in 2017. This CA-MRSA ST398 variant was highly virulent, similar to other related CA-MRSAs of ST398. This strain should be monitored to prevent more widespread dissemination.

The Australian Group on Antimicrobial Resistance (http://agargroup.org.au/) manages multiple national antimicrobial drug resistance surveillance programs, including the Australian *Staphylococcus* Sepsis Outcome Programme. This program involves 38 hospitals across Australia continuously providing antimicrobial MIC data and demographic data on episodes of *Staphylococcus aureus* sepsis. Specimens are referred to a central reference laboratory where whole-genome sequencing is performed for all methicillin-resistant *S. aureus* (MRSA) isolates.

In 2017, a MRSA sequence type (ST) 398 type V (5C2&5) isolate, typically referred to as livestock-associated MRSA (LA-MRSA), which has been isolated in many parts of the world including Australia (*1*,*2*), was cultured from a 56-year-old man from Singapore who was working as a chef in a suburb of Melbourne, Victoria, Australia. He sought hospital care for a 2-week history of a nonspecific illness and was found to have mitral valve endocarditis with embolic disease involving the spleen, brain, and lungs. Because his MRSA bacteremia failed to resolve after 10 days of vancomycin therapy, he required a mechanical mitral valve replacement. His bacteremia resolved 24 hours after valve replacement. Because of glycopeptide hypersensitivity and concerns of vancomycin heteroresistance, he was prescribed various nonglycopeptide antimicrobial drug therapies (e.g., clindamycin monotherapy, moxifloxacin monotherapy) for variable durations throughout the remainder of his treatment. While he was in the hospital, acute renal injury developed, requiring hemodialysis support. After 3 months' hospitalization, he was transferred to a hospital in Singapore. At the time of transfer, he was improving and undergoing rehabilitation. We were not able to establish if the patient had direct contact with livestock, but as a chef, he presumably had contact with raw meat.

We identified the patient's isolate (S23009-2017) as *S. aureus* by matrix-assisted laser desorption/ionization time-of-flight mass spectrometry using the Bruker MALDI Biotyper (https://www.bruker.com/) and confirmed this finding by DNA microarray using the *S. aureus* Genotyping Kit 2.0 (Alere Technologies, https://alere-technologies.com/). We performed susceptibility testing by using the VITEK 2 automated microbiology system (bioMérieux, https://www.biomerieux.com/) and performed whole-genome sequencing of the isolate using the Illumina NextSeq 550 Sequencing System (https://www.illumina.com/). We performed DNA extraction on an overnight subculture using the Invitrogen MagMAX DNA Multi-Sample Kit (ThermoFisher, https://www.thermofisher.com/). We prepared a library of the extracted DNA using the Illumina Nextera XT Library Preparation Kit and sequenced libraries having 150-bp paired-end chemistries. We identified single-nucleotide polymorphisms and performed core genome alignments using Snippy version 3.2 (https://github.com/tseemann/snippy). We constructed a phylogenetic tree using the resulting single-nucleotide polymorphisms in MEGA version 7.0 (https://www.megasoftware.net/) with the maximum parsimony algorithm. We identified antimicrobial resistance and virulence genes, multilocus sequence type, staphylococcal cassette chromosome *mec* (SCC*mec*) type, and *spa* type using available pipelines (https://cge.cbs.dtu.dk/services/) and confirmed the virulence and antimicrobial resistance gene profile by DNA microarray. We performed a phylogenetic comparison of S23009-2017 with 22 previously published MRSA ST398 whole-genome sequences and rooted the tree with an outgroup of single-locus Panton-Valentine leukocidin (PVL)–positive variants.

We identified S23009-2017 as a PVL-negative, t011-carrying, MRSA ST398 type V (5C2&5) isolate. *spa* type t011 and SCC*mec* element type V (5C2&5) are frequently identified in LA-MRSA ST398 isolates (*3*,*4*). However, unlike LA-MRSA ST398, which is typically phenotypically multidrug resistant and harbors multiple antimicrobial drug resistance genes, including *tetM* (*5*), S230090-2017 was only resistant to β-lactams (penicillin and oxacillin) and harbored only the *blaZ* and *mecA* antimicrobial drug resistance genes. Furthermore, S23009-2017 harbored the *sak*, *chp*, and *scn* human evasion genes, which are not typically found in LA-MRSA ST398 (*6*).

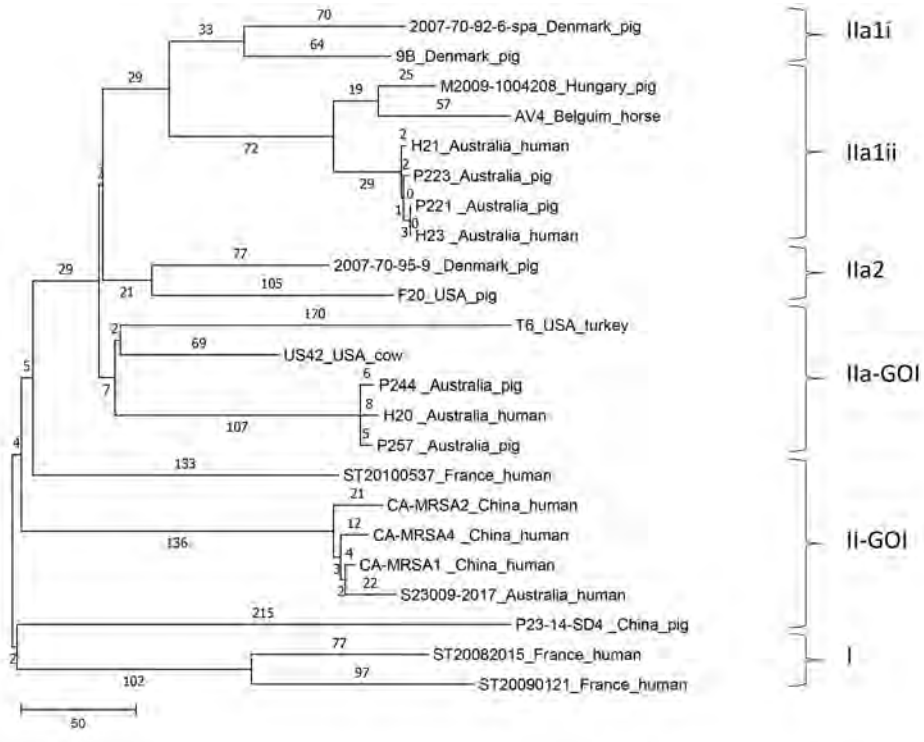

Figure. Phylogenetic tree of MRSA sequence type (ST) 398 isolate S23009-2017, recovered from a man in Australia in 2017, and related MRSA ST398 isolates from around the world (*2*,*6*,*7*). The tree was constructed by using single-nucleotide polymorphism differences and is rooted with MRSA ST398 isolates containing a single Panton-Valentine leukocidin locus. Isolates are grouped into clusters as described by Price et al. (*6*). Scale bar represents number of nucleotide substitutions per residue. CA-MRSA, community-associated MRSA; GOI, gene of interest; MRSA, methicillin-resistant *Staphylococcus aureus*.

Phylogenetic analysis showed S23009-2007 had a much closer relationship to the PVL-negative MRSA ST398 isolates from China reported by He et al. than to LA-MRSA ST398 isolates from Australia (Figure) (*7*). These isolates are grouped within the II-GOI (group of interest) clade from the Price et al. study of worldwide MRSA ST398 isolates (*6*).

He et al. reported several cases of severe and fatal infections with community-associated MRSA (CA-MRSA) ST398 and proposed that the strain arose from human-adapted predecessors and not from a livestock-adapted strain. Although all of the China isolates harbored a type V SCC*mec*, only 1 isolate harbored the type V (5C2&5) SCC*mec* element found in S23009-2017. Like S23009-2017, CA-MRSA ST398 isolates from China harbor *sak, chp*, and *scn* genes and lack the *tetM* resistance gene.

MRSA ST398 has not been previously reported to cause serious disease in Australia. Although LA-MRSA ST398 is frequently identified in pig herds in Australia, the isolate from this patient was not LA-MRSA but CA-MRSA and presumably originated in China. Because of immigration irregularities, we were not able to investigate whether the patient had visited China shortly before his illness or if his house companions were from China. Unlike LA-MRSA ST398, CA-MRSA ST398 has been shown to be highly virulent and has become the predominant CA-MRSA circulating in Shanghai, China. Thus, continued monitoring of this strain's epidemiology and preventing its widespread transmission are essential.

Acknowledgments

The authors thank the staff of the Australian Commission on Safety and Quality in Health Care (https://www.safetyandquality.gov.au/) and the participants of the Australian Group on Antimicrobial Resistance (http://agargroup.org.au/).

This study was partially funded by the Australian Commission on Safety and Quality in Health Care.

About the Author

Dr. Coombs is Chair of Public Health at Murdoch University, Murdoch, Australia, and Chair of the Australian Group on Antimicrobial Resistance. His research focuses on the antimicrobial drug resistance and molecular epidemiology of *S. aureus* and *Enterococcus faecium.*

References

1. Cuny C, Friedrich A, Kozytska S, Layer F, Nübel U, Ohlsen K, et al. Emergence of methicillin-resistant *Staphylococcus aureus* (MRSA) in different animal species. Int J Med Microbiol. 2010;300:109–17. http://dx.doi.org/10.1016/j.ijmm.2009.11.002
2. Sahibzada S, Abraham S, Coombs GW, Pang S, Hernández-Jover M, Jordan D, et al. Transmission of highly virulent community-associated MRSA ST93 and livestock-associated MRSA ST398 between humans and pigs in Australia. Sci Rep. 2017;7:5273. http://dx.doi.org/10.1038/s41598-017-04789-0
3. Stegger M, Lindsay JA, Sørum M, Gould KA, Skov R. Genetic diversity in CC398 methicillin-resistant *Staphylococcus aureus* isolates of different geographical origin. Clin Microbiol Infect. 2010;16:1017–9. http://dx.doi.org/10.1111/j.1469-0691.2009.03003.x

4. Monecke S, Slickers P, Gawlik D, Müller E, Reissig A, Ruppelt-Lorz A, et al. Variability of SCC*mec* elements in livestock-associated CC398 MRSA. Vet Microbiol. 2018;217:36–46. http://dx.doi.org/10.1016/j.vetmic.2018.02.024
5. Kadlec K, Fessler AT, Hauschild T, Schwarz S. Novel and uncommon antimicrobial resistance genes in livestock-associated methicillin-resistant *Staphylococcus aureus*. Clin Microbiol Infect. 2012;18:745–55. http://dx.doi.org/10.1111/j.1469-0691.2012.03842.x
6. Price LB, Stegger M, Hasman H, Aziz M, Larsen J, Andersen PS, et al. *Staphylococcus aureus* CC398: host adaptation and emergence of methicillin resistance in livestock. MBio. 2012;3:e00305-11. http://dx.doi.org/10.1128/mBio.00305-11
7. He L, Zheng HX, Wang Y, Le KY, Liu Q, Shang J, et al. Detection and analysis of methicillin-resistant human-adapted sequence type 398 allows insight into community-associated methicillin-resistant *Staphylococcus aureus* evolution. Genome Med. 2018;10:5. http://dx.doi.org/10.1186/s13073-018-0514-9

Address for correspondence: Geoffrey W. Coombs, Murdoch University, Antimicrobial Resistance and Infectious Diseases Laboratory, School of Veterinary and Life Sciences, Murdoch, WA, Australia; email: g.coombs@murdoch.edu.au

Candida auris Sternal Osteomyelitis in a Man from Kenya Visiting Australia, 2015

Christopher H. Heath,[1] John R. Dyer, Stanley Pang, Geoffrey W. Coombs, Dianne J. Gardam[1]

Author affiliations: Royal Perth Hospital, Perth, Western Australia, Australia (C.H. Heath); University of Western Australia, Crawley, Western Australia, Australia (C.H. Heath); Fiona Stanley Hospital, Murdoch, Western Australia, Australia (C.H. Heath, J.R. Dyer); PathWest Laboratory Medicine WA, Murdoch (C.H. Heath, S. Pang, G.W. Coombs, D.J. Gardam); Murdoch University, Murdoch (S. Pang, G.W. Coombs)

DOI: https://doi.org/10.3201/eid2501.181321

In Australia in 2015, *Candida auris* sternal osteomyelitis was diagnosed in a 65-year-old man with a history of intensive care treatment in Kenya in 2012 and without a history of cardiac surgery. The isolate was South Africa clade III. Clinicians should note that *C. auris* can cause low-grade disease years after colonization.

Candida auris, first reported in Japan in 2009 (*1*), is an emerging pathogen that has caused severe disease in hospitalized patients in many countries, including India, South Africa, Spain, the United Kingdom, the United States, and Venezuela (*2*–*4*). In July 2015, a 65-year-old man from Kenya visiting Australia for the first time sought treatment in Perth, Western Australia, Australia, for chronically discharging sternal sinus persisting for >1 year. His active medical problems included severe hypercapneic chronic obstructive pulmonary disease with pulmonary hypertension, ischemic heart disease, and chronic kidney impairment. In July 2012, he had unstable angina treated by coronary stenting that was complicated by cardiac arrest with cardiopulmonary resuscitation, which resulted in sternal injuries and a 3-month intensive care unit hospitalization in Nairobi, Kenya. At hospital admission, computed tomography scan of the chest showed a 3.3-cm subcutaneous collection and bony changes from chronic sternal osteomyelitis (Figure). Surgical debridement confirmed sternal osteomyelitis with parasternal abscesses. Posaconazole was given as pragmatic oral therapy, and trough serum levels of 2.0 mg/L at week 2 and 2.60 mg/L at week 4 were achieved. The patient died from progressive cardiorespiratory failure 3 months later.

Deep operative sternal bone samples yielded a yeast on Difco CHROMagar Candida medium (Becton Dickinson, https://www.bd.com/) that did not produce pseudohyphae or germ tubes. The isolate grew well at 40°C and 42°C but not 45°C. Matrix-assisted laser desorption/ionization time-of-flight mass spectrometry (MALDI version 3.1; Bruker Daltonics, https://www.bruker.com/) identified the pathogen as *Candida auris* (score >2.1).

Sequencing of the 18S rDNA internal transcribed region and 28S rDNA D1–D2 regions confirmed pathogen identification (Appendix Figure 1, https://wwwnc.cdc.gov/EID/article/25/1/18-1321-App1.pdf). We edited the DNA sequences, assembled consensus sequences using SeqScape (Applied Biosystems, https://www.thermofisher.com/us/en/home/brands/applied-biosystems.html), and performed sequence alignments with BLAST (https://blast.ncbi.nlm.nih.gov/Blast.cgi). The internal transcribed regions of our isolate matched 100% with *C. auris* reference strain KP131674.1. The D1–D2 regions of the isolate also matched 100% with those of multiple *C. auris* isolates (GenBank accession nos. JQ219331–2, KM000828, KM000830, KU321688). Susceptibility testing with the Sensititre YeastOne YO10 panel (Trek Diagnostic Systems, https://www.thermofisher.com/) showed fluconazole resistance (MIC >256 mg/L) and posaconazole susceptibility (MIC 0.06 mg/L) (Appendix Table).

[1]These authors contributed equally to this article.

We performed whole-genome sequencing (WGS) on the isolate (FSMC57608) using the NextSeq platform (Illumina, https://www.illumina.com/) and then assembled Illumina paired-end sequencing data using SPAdes, St. Petersburg genome assembler 3.1.1 (http://spades.bioinf.spbau.ru/release3.1.1/manual.html). We identified core genome single-nucleotide polymorphisms (SNPs) using Snippy version 4.0 (http://www.vicbioinformatics.com/software.snippy.shtml), using the *C. auris* B8441 genome for reference and previously described methods (*2*), and mapped ≈97.77% of the reads. A maximum-parsimony phylogenetic tree was constructed by using MEGA version 7.0 (https://www.megasoftware.net/) and 10 other *C. auris* genomes (*2*). Results showed that FSMC57608 (GenBank accession no. SRP156632) is a South Africa clade III isolate (Appendix Figure 2) with SNPs V125A and F126L and wild-type at amino acid positions 132 and 143 of Erg11 (gene associated with azole class antifungal drug resistance) (Appendix Figure 3).

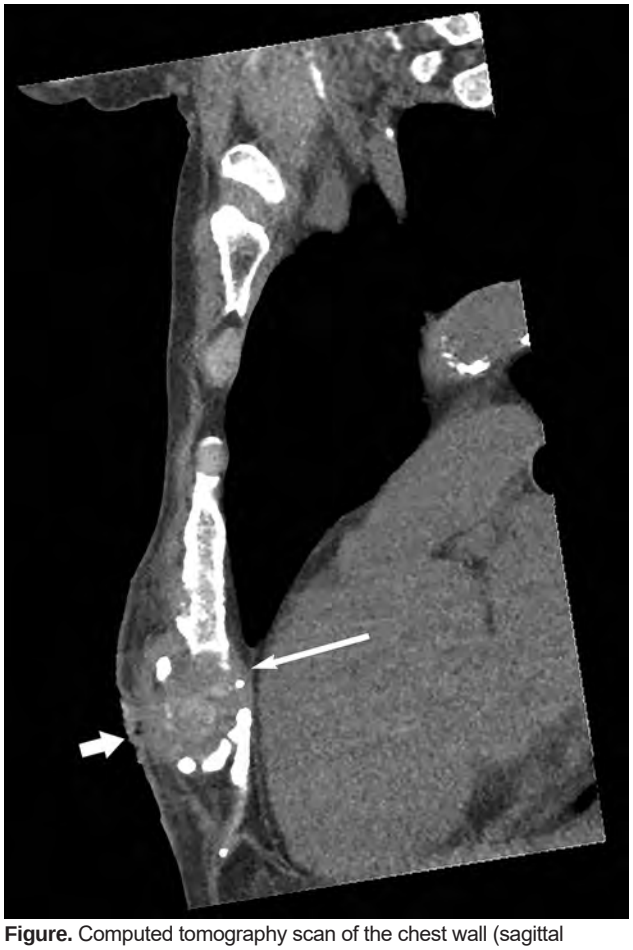

Figure. Computed tomography scan of the chest wall (sagittal section, bony windows) of man from Kenya with *Candida auris* sternal osteomyelitis, Australia, 2015. Image shows bony erosion and fragmentation of distal sternum (thin arrow), together with a 3.3-cm abscess and a sinus tract in the subcutaneous tissues (thick arrow).

Extensive nosocomial transmission of *C. auris* has been documented, and mortality rates of 40%–60% have been reported for patients with candidemia (*2*–*4*). *C. auris* can colonize human skin for months (*5*,*6*). Of 620 cases of *C. auris* infection linked to outbreaks in Europe during 2013–2017, a total of 466 (75.2%) patients became colonized (*3*). We postulate that our patient became colonized in 2012 in an intensive care unit in Kenya. This case also illustrates that clinical manifestations of *C. auris* infection can progress slowly for >12 months.

C. auris is multidrug resistant and, therefore, poses a risk for all patients, given the limited antifungal options available. Tentative *C. auris*–specific MIC breakpoints exist, pending further correlation between MICs and clinical outcomes (*2*). Proposed breakpoints are derived from expert opinion and/or those of closely related *Candida* species for antimicrobial drugs (e.g., amphotericin B) that do not have breakpoints. Despite breakpoint uncertainty and concerns about emergent multidrug resistance among *C. auris* isolates, we had prescribed oral posaconazole for our patient because of the in vitro MIC results and his strong preference for oral antifungal therapy.

WGS results show *C. auris* isolates fall into 4 distinct clades that appear to have emerged almost simultaneously in different geographic regions of the globe (*2*–*4*). Isolate FSMC57608 has SNPs V125A and F126L in Erg11, the latter SNP, F126L, having been described in previous investigations (J.F. Muñoz, unpub. data, https://doi.org/10.1101/299917) (*2*,*7*). This isolate was also wild type at amino acid positions 132 and 143 of Erg11, as seen in Africa isolates (J.F. Muñoz, unpub. data, https://doi.org/10.1101/299917), further supporting that the infection originated in Africa (*7*).

In summary, we describe a case of travel-linked *C. auris* infection manifesting as chronic sternal osteomyelitis, diagnosed in Australia in 2015. The patient had a history of intensive care treatment in Kenya, a country with documented *C. auris* transmission (*2*); he required treatment in Australia 3 years later and exhibited clinically significant disease associated with South Africa clade III *C. auris* infection.

Acknowledgments

The authors thank the patient's next of kin for providing permission to publish this case.

About the Author

Dr. Heath is an infectious diseases physician in the Department of Infectious Diseases at Fiona Stanley Hospital and Royal Perth Hospital in Perth, Western Australia, Australia, and a clinical microbiologist for *PathWest* Laboratory Medicine, FSH Network, Perth; he has research interests in laboratory

mycology and diagnostics and a special interest in infections in the immunocompromised host, particularly invasive fungal infections. Mrs. Gardam is the senior medical scientist in mycology for PathWest Laboratory Medicine; she has an active interest in diagnostics for pathogenic fungi and antifungal susceptibility testing, together with undergraduate and postgraduate education and teaching of medical mycology.

References

1. Satoh K, Makimura K, Hasumi Y, Nishiyama Y, Uchida K, Yamaguchi H. *Candida auris* sp. nov., a novel ascomycetous yeast isolated from the external ear canal of an inpatient in a Japanese hospital. Microbiol Immunol. 2009;53:41–4. http://dx.doi.org/10.1111/j.1348-0421.2008.00083.x
2. Lockhart SR, Etienne KA, Vallabhaneni S, Farooqi J, Chowdhary A, Govender NP, et al. Simultaneous emergence of multidrug resistant *Candida auris* on three continents confirmed by whole genome sequencing and epidemiological analyses. Clin Infect Dis. 2017;64:134–40. http://dx.doi.org/10.1093/cid/ciw691
3. Kohlenberg A, Struelens MJ, Monnet DL, Plachouras D; The *Candida auris* Survey Collaborative Group. *Candida auris*: epidemiological situation, laboratory capacity and preparedness in European Union and European Economic Area countries, 2013 to 2017. Euro Surveill. 2018;23. http://dx.doi.org/10.2807/1560-7917.ES.2018.23.13.18-00136
4. Chowdhary A, Sharma C, Meis JF. *Candida auris*: a rapidly emerging cause of hospital-acquired multidrug-resistant fungal infections globally. PLoS Pathog. 2017;13:e1006290. http://dx.doi.org/10.1371/journal.ppat.1006290
5. Centers for Disease Control and Prevention. Tracking *Candida auris*. 2018 Oct 3 [cited 2018 Jul 17]. https://www.cdc.gov/fungal/candida-auris/tracking-c-auris.html
6. Welsh RM, Bentz ML, Shams A, Houston H, Lyons A, Rose LJ, et al. Survival, persistence, and isolation of the emerging multidrug-resistant pathogenic yeast *Candida auris* on a plastic health care surface. J Clin Microbiol. 2017;55:2996–3005. http://dx.doi.org/10.1128/JCM.00921-17
7. Rhodes J, Abdolrasouli A, Farrer RA, Cuomo CA, Aanensen DM, Armstrong-James D, et al. Genomic epidemiology of the UK outbreak of the emerging human fungal pathogen *Candida auris*. Emerg Microbes Infect. 2018;7:43. http://dx.doi.org/10.1038/s41426-018-0045-x

Address for correspondence: Christopher H. Heath, Fiona Stanley Hospital, Department of Infectious Diseases, 102-118 Murdoch Dr, Murdoch, PO Box 404, Bull Creek, WA 6149, Australia; email: chris.heath@health.wa.gov.au

Biological Safety: Principles and Practices, 5th Edition

Dawn P. Wooley, Karen B. Byers; ASM Press, Washington, DC, USA, 2017; ISBN-10: 1555816207; ISBN-13: 978-1555816209; Pages: 741; Price: $150.00

The 5th edition of *Biological Safety: Principles and Practices* is still the leading comprehensive biosafety textbook available and is a page-turner as well. The book extensively covers the identification, assessment, and management of biological hazards, as well as special environments as they relate to biohazardous substances. It broadly deals with bacterial, viral, and fungal pathogens; biological toxins; and recombinant DNA used in academic research, medical, pharmaceutical, and veterinary laboratories. The book provides extensive background on the biohazards and details the risk to humans, animals, and, if applicable, to plants. For example, in the chapter "Viral Agents of Human Disease: Biosafety Concerns," Rozo, Lawler, and Parags present an overview of the viral life cycle, epidemiology, and diversity. They also summarize the clinical manifestation of viral disease and provide extensive examples of viral classes known for laboratory-associated infections, with information on postaccident management.

The 5th edition has added 8 new chapters covering topics that gained relevance in more recent years, such as a chapter on molecular agents describing genome editing, the use of recombinant T-cells for cancer therapy, and prions. Other new chapters deal with specialized biocontainment for research on virus-transmitting mosquitoes and research on aerosolized microorganisms. The 5th edition also expands on training programs, veterinary and greenhouse biosafety, field studies, and clinical laboratory safety.

Biological Safety: Principles and Practices stands out as a safety textbook because it is not purely focused on regulatory requirements, and it is enjoyable to read. All chapters are supplemented with useful tables summarizing essential information, and many contain descriptive diagrams. I appreciated the Laboratory Animal Allergy Questionnaire and the sample Biosafety Level 2 checklists, which can be very useful for faculty who begin to work in these areas. Furthermore, the chapters provide numerous references to relevant current publications and regulatory guidelines from the National Institutes of Health and Centers for Disease Control and Prevention. There is some overlap in chapters regarding details on bacterial virulence factors, viruses, and biosafety cabinets, which could be consolidated should a revision be considered.

The attention to detail and the assemblage of leading experts contributing to this book is clearly a labor of love by editors Dawn Wooley and Karen Byers. Both additionally authored chapters; for example, Dawn Wooley, who is well known for her work on risk assessment of viral vectors, contributed to chapters on molecular agents and on risk assessment of biologic hazards. Karen Byers lent her expertise to a chapter on laboratory-acquired infections, an area she has researched extensively. Because the material extends beyond academic research and includes clinical and veterinary laboratory practices, it is also appropriate for medical and veterinary personnel. Finally, the book can easily serve as a textbook for biosafety courses and even complement microbiology courses.

I found all topics of the book highly engaging and worth reading; the concisely written chapters can be read alone according to area of interest or serve as a reference for questions that might arise. The book is evidence based and illustrates data-driven best practices. It provides a modern view of biosafety practices; as such, it is a valuable resource not only for biosafety professionals but also for researchers working with biohazards.

Imke Schröder

Author affiliation: University of California at Los Angeles, Los Angeles, California, USA

Address for correspondence: Imke Schröder, UCLA–UC Center for Laboratory Safety, 607 Charles E. Young Dr E, 4881 Slichter Hall, Los Angeles, CA 90095-1569, USA; email: ischroeder@ehs.ucla.edu

Miracle Cure: The Creation of Antibiotics and the Birth of Modern Medicine

William Rosen; Viking, New York, NY, USA, 2017; ISBN-10: 0525428100; ISBN-13: 978-0525428107; Pages: 368; Price: $28.00

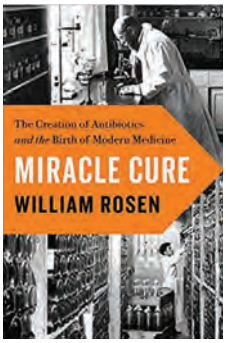

Miracle Cure: The Creation of Antibiotics and the Birth of Modern Medicine engagingly describes what is arguably the most significant development in the history of medicine: antibiotics. The book chronicles captivating accounts from the conception of the germ theory of disease and the scientific discovery of these life-saving medications to the interplay among the countless contributing idiosyncratic and imperfect individuals and organizations involved, including the pharmaceutical titans. With the contemporary emergence and spread of antibiotic resistance, the book's message is timely and poignant.

Miracle Cure is relevant for both the science enthusiast and the science novice. Although slightly tangential at times in its background narratives, it intertwines the creation of antibiotics as intricately tied to the evolution of modern medicine and paints both as not just a product of science but as a culmination of economic, political, and social influences. In so doing, it sheds a human light on the discovery and production of antibiotics.

Many medical professionals and nonmedical persons envision the discovery of antibiotics, especially penicillin, as a providential occurrence that revolutionized previously unenlightened medical practices characterized by bloodletting and poisoning. However, *Miracle Cure* paints them more accurately as products of the iterative process of scientific discovery in an attempt to improve public health and, in some instances, generate personal profit and fame. The lifesaving properties of antibiotics are a secondary theme to the real-life problems overcome, the challenging ethics decisions made, and the delicate scientific egos bruised along the way.

For readers seeking a book that provides insight into the current public health crisis of antibiotic resistance, *Miracle Cure* does not provide answers or potential solutions, nor was it intended to do so. However, it goes beyond the most apparent impacts antibiotics have had on human health to explore the less publicized effects of antibiotics on regulatory agencies, drug marketing, physician–pharmaceutical industry relationships, research study design, and the practice of medicine.

One of the book's most important arguments is that antibiotics have forced us to calibrate and recalibrate our idea of medication safety as we transitioned from unregulated mixtures of strychnine, mercury, and arsenic for which the adverse effects were inextricably tied to the morbidity and mortality of underlying disease to tightly regulated, carefully calibrated antibiotics for which safety and efficacy were the norm. *Miracle Cure* demonstrates that this shift, facilitated by a mix of altruism and greed, caused the "[p]rescription of antibiotic without a specific cause" to reach "disturbing proportions." The book is a fascinating and important read that translates to a deep understanding of the history of antibiotic development leading up to the current state and its problems.

Keith W. Hamilton

Author affiliation: The University of Pennsylvania, Philadelphia, Pennsylvania, USA

Address for correspondence: Keith W. Hamilton, Hospital of the University of Pennsylvania, Ste 110 Silverstein Bldg, 3400 Spruce St, Philadelphia, PA 19104, USA; email: keith.hamilton@uphs.upenn.edu

In Memoriam: Katrin Susanne Kohl (1964–2018)

Nina Marano, Stephen H. Waterman

Katrin Susanne Kohl, MD, PhD, MPH, who served over a decade as Deputy Director of the Division of Global Migration and Quarantine, National Center for Emerging and Zoonotic Infections, at the Centers for Disease Control and Prevention (CDC; Atlanta, Georgia, USA), died suddenly and unexpectedly at her home in Atlanta on May 20, 2018, at the age of 54. She was a beloved physician epidemiologist leader at CDC who made major contributions in international health and vaccine safety.

While at CDC's Immunization Safety Branch starting in 2000, Kohl brilliantly succeeded in launching and coordinating The Brighton Collaboration, an international effort of >800 participants in 80 countries to enhance vaccine safety. The collaboration was a new global initiative to improve the rigor of immunization safety science at a time of increasing public controversy and vaccine hesitancy. She worked tirelessly to promote the new collaboration among key policymakers in the global immunization community, resulting in publication of the first set of Brighton case definitions in the journal Vaccine.

Kohl was born in Duisburg, Germany, in 1964. Her Austrian father was a prominent architect there. She attended medical school in Graz, Austria, and completed her MD in 1991 and PhD in 1993 at the Free University of Berlin, Germany. In 1996, she earned her MPH from Tulane University School of Public Health and Tropical Medicine (New Orleans. LA, USA). She joined CDC in 1997 as an Epidemic Intelligence Service Officer assigned to the Louisiana Department of Health, where her work focused mainly on infectious disease epidemiology and sexually transmitted diseases. Tom Farley, her Epidemic Intelligence Service supervisor and later the New York City Commissioner of Health, remarked that the Louisiana staff fell in love with this German woman who made disease investigation a happy and exhilarating experience.

Katrin Susanne Kohl

At the Division of Global Migration and Quarantine, working with the division's director Martin Cetron, she participated in CDC quarantine and border health responses for Middle East respiratory syndrome, the 2009 (H1N1) influenza pandemic, the 2014–2015 Ebola epidemic in West Africa, and the 2016 Zika epidemic. She also played a key role in strengthening a new unit addressing United States–Mexico binational and border health. Kohl was the division's champion for helping to implement the World Health Organization's 2005 International Health Regulations, skillfully educating staff from US federal and state agencies, and liaising with World Health Organization member states and regional offices to help implement enhanced transparency and collaboration in international disease and outbreak reporting. Kohl also published in and reviewed articles for Emerging Infectious Diseases.

In addition to her scientific accomplishments, Kohl will be remembered for her passionate, caring, and ebullient personality, which made her such an effective ambassador, bringing together persons with diverse scientific viewpoints to reach technical and public health policy consensus. She will be greatly missed by her husband, Gene Spiegel; her son, Alexander, and daughter, Clara; her mother, Christel Kohl; her brother, Christian; and her many colleagues at CDC and around the world.

Author affiliation: Centers for Disease Control and Prevention, Atlanta, Georgia, USA (N. Marano); Centers for Disease Control and Prevention, San Juan, Puerto Rico, USA (S.H. Waterman)

DOI: https://doi.org/10.3201/eid2501.180961

Address for correspondence: Nina Marano, Centers for Disease Control and Prevention, 1600 Clifton Rd NE, Mailstop E03, Atlanta, GA 30329-4027, USA; email: nbm8@cdc.gov

Anna Dumitriu (1969). *Make Do and Mend* (detail)**, 2017**. Ampicillin antibiotic susceptibility discs and fabric, 12 in x 12 in/30.48 cm x 30.48 cm. First exhibited at LifeSpace Dundee, 2017. Made in collaboration with Nicola Fawcett (University of Oxford) and Sarah Goldberg (Technion). Digital image courtesy of Anna Dumitriu.

Repurpose and Reuse: Artistic Perspectives on Antimicrobial Resistance

Byron Breedlove

Antimicrobial resistance ranks among the most urgent global challenges of the 21st century. When penicillin became widely available in 1943, the specter of antimicrobial resistance was already stalking this seemingly miraculous drug. As new antimicrobial agents have been developed, they, too, have gradually lost effectiveness because of their misuse and overuse for human, animal, and agricultural health.

British artist Anna Dumitriu, who served as the 2018 president of the Science and the Arts Section of the British Science Association, has focused on the issue of antimicrobial resistance in her recent work. She states, "We are confronted by a very difficult situation now, where important antibiotic drugs we have relied on for many years have simply stopped working, because bacteria have evolved strategies to beat them. I'm fascinated how the drug discovery process works, how infectious diseases were treated in the past, and in what is happening now in scientific research to improve health."

Working with an array of traditional fine arts and craft materials and with bacteria, antibiotics, and DNA sequences, Dumitriu melds microbiology with fine art to create works within the genre of "bioart." Interestingly, Sir Alexander Fleming, discoverer of penicillin, created some of the earliest examples of this art form. He indulged his creative side by using laboratory instruments to "paint" ephemeral figures and landscapes, growing microbes with different natural pigmentations on agar-filled petri dishes and waiting for the images to develop.

Dumitriu is among the vanguard of a small cadre of interdisciplinary practitioners who wield their creative skills in studios and laboratories. Featured on this month's cover art is one component of her 2017 project *Make Do and Mend*, a section of quilt that comprises 16 irregular silk squares. The brown, blue, pink, and plum squares are flecked and dappled with splotches of contrasting colors, and assembled into a quilt with a combination of backstitch, running stitch, and satin stitch. As is the case with many quilts, the final product came from a cooperative effort—in this case, the artist and her scientific collaborator Nicola Fawcett.

Each silk square is stained with diluted fecal samples from individual patients in Oxford, UK, who had consented to their samples being used in artworks. Those samples were grown on silk cloth squares using chromogenic agar. The blue/pink patches that display different-sized colonies of bacteria indicate a diverse gut microbiome. All-blue or all-pink sections

Author affiliation: Centers for Disease Control and Prevention, Atlanta, Georgia, USA

DOI: https://doi.org/10.3201/eid2501.AC2501

The installation *Make Do and Mend* by Anna Dumitriu explores CRISPR gene editing and antibiotic resistance. It features an altered antique women's suit with CC41 mark, antique toy sewing machine, silk impregnated with CRISPR edited bacteria, altered vintage leaflets, ampicillin antibiotic susceptibility discs, fabric, wood and glass frames. First exhibited at LifeSpace Dundee, 2017. Made in collaboration with Sarah Goldberg and Roee Amit (Technion) with elements in collaboration with Nicola Fawcett (University of Oxford). Digital image courtesy of Anna Dumitriu.

suggest a gut microbiome that has reduced diversity from antibiotic use. Clustered near the center are three embroidered shapes with trailing flagella that represent *Escherichia coli* bacteria. Nine ampicillin susceptibility discs are stitched into the quilt. (For anyone interested in protocols, Fawcett states, "Dumitriu works with expert microbiologists to integrate compliance with health and safety standards into her work.")

In another aspect of this project, Dumitriu and Dr. Sarah Goldberg used CRISPR (short for clusters of regularly interspaced short palindromic repeats) to edit the genome of a strain of *E. coli* bacteria. They removed an ampicillin antibiotic resistance gene and replaced it with a fragment of DNA (converted into ASCII code and then to base 4) that encoded the World War II slogan "Make Do and Mend." That slogan came from the title of a pamphlet issued by the British Ministry of Information encouraging homemakers to repair and reuse clothing during wartime. The cover of that leaflet is also part of the exhibit.

Dumitriu conceived of this exhibit as a way to commemorate the 75th anniversary of the first use of penicillin in patients and to increase awareness about the rapid development of antibiotic-resistant strains of pathogens. Her *Make Do and Mend* project may help stimulate creative thinking about antimicrobial resistance and stewardship. Perhaps new serendipitous breakthroughs will allow us to repurpose and reuse some of our diminished antimicrobials in keeping with Fleming's famous quote, "One sometimes finds what one is not looking for."

Bibliography

1. British Library. Make do and mend, 1943 [cited 2018 Nov 16]. http://www.bl.uk/learning/timeline/item106365.html
2. Centers for Disease Control and Prevention. Antibiotic/antimicrobial resistance (AR/AMR) [cited 2018 Nov 14]. https://www.cdc.gov/drugresistance/index.html
3. Dumitriu A. FEAT (future emerging art and technology): make do and mend. Bioart and bacteria [cited 2018 Oct 26]. http://www.normalflora.co.uk/
4. Dunn R. Painting with penicillin: Alexander Fleming's germ art [cited 2018 Nov 19]. https://www.smithsonianmag.com/science-nature/painting-with-penicillin-alexander-flemings-germ-art-1761496/
5. Fawcett NJ, Dumitriu A. Bacteria on display–can we, and should we? Artistically exploring the ethics of public engagement with science in microbiology. FEMS Microbiol Lett. 2018;365 fny101. http://dx.doi.org/10.1093/femsle/fny101
6. Fernández CF. Art made with CRISPR aims to raise awareness of antibiotic resistance [cited 2018 Nov 14]. https://labiotech.eu/bioart/anna-dumitriu-crispr-antibiotic-resistance/
7. Medina MÁ. CRISPR gene editing meets the art world. The CRISPR Journal. 2018;1 [cited 2018 Nov 26]. https://doi.org/10.1089/crispr.2018.0035
8. Spencer M. A brief history of quilts [cited 2018 Nov 5]. https://blog.parachutehome.com/history-of-quilting/
9. Swain K. BioArt: materials and molecules. Lancet. 2018;391:e7. http://dx.doi.org/10.1016/S0140-6736(18)30562-2
10. Tacconelli E, Pezzani MD. Public health burden of antimicrobial resistance in Europe. Lancet Infect Dis. 2018; Nov 5:pii: S1473- 3099(18)30648-0.

Address for correspondence: Byron Breedlove, EID Journal, Centers for Disease Control and Prevention, 1600 Clifton Rd NE, Mailstop H16-2, Atlanta, GA 30329-4027, USA; email: wbb1@cdc.gov

EMERGING INFECTIOUS DISEASES®

Upcoming Issue

- International Biologic Reference Preparations for Epidemic Infectious Diseases
- Trends of Human Plague, Madagascar, 1998–2016
- Human Pasteurellosis, Health Risk for Elderly Persons Living with Companion Animals
- Ebola Virus Infection Associated with Transmission from Survivors
- Acute and Delayed Deaths after West Nile Virus Infection, Texas, USA, 2002–2012
- Macrophage Activation Marker sCD163 Associated with Fatal and Severe Ebola Virus Disease in Humans
- Epidemiologic and Ecologic Investigations of Monkeypox, Likouala Department, Republic of the Congo, 2017
- Zika Virus–Specific IgM Antibody Detection and Neutralizing Antibody Profiles 12–19 Months after Illness Onset
- Oasis Malaria, Northern Mauritania
- Killing Clothes Lice by Holding Infested Clothes Away from Hosts for 10 Days to Control Louseborne Relapsing Fever, Bahir Dah, Ethiopia
- Identification of *Leishmania* Species in Naturally Infected Sand Flies from Refugee Camps, Greece
- Seroprevalence of Heartland Virus Antibodies in Blood Donors, Northwestern Missouri, USA
- Incidence and Prevalence of West Nile Virus Infections, Continental United States, 1999–2016
- Rift Valley Fever Reemergence after 7 Years of Quiescence, South Africa, 2018
- *Cytauxzoon felis* Infection in Domestic Cats, Yunnan Province, China, 2016
- Tick-Borne Encephalitis Virus in Roe Deer, the Netherlands
- No Evidence of Zika Virus Exposure in Wild Long-Tailed Macaques, Peninsular Malaysia
- Clinical Characteristics of Ratborne Seoul Hantavirus Disease
- Severe Respiratory Illness Associated with Human Metapneumovirus in Nursing Home, New Mexico, USA
- *Schistosoma haematobium–S. mansoni* Hybrid Parasite Infecting Migrant
- West Nile Virus Infection in Travelers Returning to United Kingdom from South Africa

Complete list of articles in the February issue at http://www.cdc.gov/eid/upcoming.htm

Upcoming Infectious Disease Activities

March 4–7, 2019
Conference on Retroviruses and Opportunistic Infections
Seattle, WA, USA
http://www.croiconference.org/

April 13–16, 2019
European Congress of Clinical Microbiology and Infectious Diseases
29th Annual Congress
Amsterdam, Netherlands
http://www.eccmid.org/

April 16–18, 2019
International Conference on One Health Antimicrobial Resistance
Amsterdam, Netherlands
https://www.escmid.org/ICOHAR2019/

May 5–9, 2019
ASM Clinical Virology Symposium
Savannah, GA, USA
https://10times.com/clinical-virology-symposium

June 20–24, 2019
ASM Microbe 2019
San Francisco, CA, USA
https://www.asm.org/index.php/asm-microbe-2018

February 20–23, 2020
ISID
19th International Congress on Infectious Diseases
Kuala Lumpur, Malaysia
https://www.isid.org/

Announcements

Email announcements to EID Editor (eideditor@cdc.gov). Include the event's date, location, sponsoring organization, and a website. Some events may appear only on EID's website, depending on their dates.

Earning CME Credit

To obtain credit, you should first read the journal article. After reading the article, you should be able to answer the following, related, multiple-choice questions. To complete the questions (with a minimum 75% passing score) and earn continuing medical education (CME) credit, please go to http://www.medscape.org/journal/eid. Credit cannot be obtained for tests completed on paper, although you may use the worksheet below to keep a record of your answers.

You must be a registered user on http://www.medscape.org. If you are not registered on http://www.medscape.org, please click on the "Register" link on the right hand side of the website.

Only one answer is correct for each question. Once you successfully answer all post-test questions, you will be able to view and/or print your certificate. For questions regarding this activity, contact the accredited provider, CME@medscape.net. For technical assistance, contact CME@medscape.net. American Medical Association's Physician's Recognition Award (AMA PRA) credits are accepted in the US as evidence of participation in CME activities. For further information on this award, please go to https://www.ama-assn.org. The AMA has determined that physicians not licensed in the US who participate in this CME activity are eligible for AMA PRA Category 1 Credits™. Through agreements that the AMA has made with agencies in some countries, AMA PRA credit may be acceptable as evidence of participation in CME activities. If you are not licensed in the US, please complete the questions online, print the AMA PRA CME credit certificate, and present it to your national medical association for review.

Article Title

Enterovirus A71 Infection and Neurologic Disease, Madrid, Spain, 2016

CME Questions

1. You are seeing a 2-year-old girl with a 3-day history of fever and upper respiratory symptoms. She developed lethargy and ataxia today, and presents now to the emergency department. What should you consider regarding the epidemiology of potential enterovirus infection among children in the current study by Taravilla and colleagues?

A. Enterovirus was isolated from all 42 children in the study
B. Almost all patients were younger than 1 year of age
C. Most patients were girls
D. The peak incidence of illness occurred in July

2. Which one of the following symptoms or signs was present in the majority of children included in the current study?

A. Catarrhal symptoms
B. Fever
C. Diarrhea
D. Mucocutaneous findings

3. You decide to admit this patient to the hospital. Which one of the following findings was most associated with a worse prognosis in the current study?

A. Positive cerebrospinal fluid (CSF) testing for enterovirus
B. An elevated serum procalcitonin level
C. An elevated peripheral white blood cell count
D. A low CSF glucose level

4. The patient recovers after treatment with intravenous immunoglobulins. What was the most common sequela associated with enterovirus infection in the current study?

A. Facial paralysis
B. Cerebellar dysfunction
C. Limb paralysis
D. Intellectual disability

Earning CME Credit

To obtain credit, you should first read the journal article. After reading the article, you should be able to answer the following, related, multiple-choice questions. To complete the questions (with a minimum 75% passing score) and earn continuing medical education (CME) credit, please go to http://www.medscape.org/journal/eid. Credit cannot be obtained for tests completed on paper, although you may use the worksheet below to keep a record of your answers.

You must be a registered user on http://www.medscape.org. If you are not registered on http://www.medscape.org, please click on the "Register" link on the right hand side of the website.

Only one answer is correct for each question. Once you successfully answer all post-test questions, you will be able to view and/or print your certificate. For questions regarding this activity, contact the accredited provider, CME@medscape.net. For technical assistance, contact CME@medscape.net. American Medical Association's Physician's Recognition Award (AMA PRA) credits are accepted in the US as evidence of participation in CME activities. For further information on this award, please go to https://www.ama-assn.org. The AMA has determined that physicians not licensed in the US who participate in this CME activity are eligible for AMA PRA Category 1 Credits™. Through agreements that the AMA has made with agencies in some countries, AMA PRA credit may be acceptable as evidence of participation in CME activities. If you are not licensed in the US, please complete the questions online, print the AMA PRA CME credit certificate, and present it to your national medical association for review.

Article Title

Prescription of Antibacterial Drugs for HIV-Exposed, Uninfected Infants, Malawi, 2004–2010

CME Questions

1. You are advising a public health department in sub-Saharan Africa about antibiotic usage in HIV-exposed, uninfected (HEU) infants. On the basis of the analysis from the Breastfeeding, Antiretrovirals and Nutrition (BAN) Study by Ewing and colleagues, which one of the following statements about antibiotic usage in the first year of life among 2,152 HEU infants who were breast-fed through 28 weeks of age is correct?

A. About one third received an antibiotic prescription
B. Urinary infection was the most common indication for antibiotic use
C. Sulfonamides were the most commonly prescribed antibiotic class
D. HEU infants received a median of 2 antibiotic prescriptions during the 48 weeks of study follow-up

2. According to the analysis from the BAN Study by Ewing and colleagues, which one of the following factors was to be associated with a lower hazard of antibiotic prescription during the first year of life among 2,152 HEU infants who were breast-fed through 28 weeks of age?

A. Cotrimoxazole preventive therapy (CPT) exposure
B. Younger age
C. Male sex
D. Lack of antiretroviral exposure

3. On the basis of the analysis from the BAN Study by Dr. Ewing and colleagues, which one of the following statements about clinical implications of antibiotic usage in the first year of life among 2,152 HEU infants who were breast-fed through 28 weeks of age is correct?

A. Studies in Western Europe and Australia show higher rates of antibiotic prescriptions per person-year for infants in the first year of life than in the BAN Study
B. The antibacterial properties of CPT are its only documented benefit
C. Expanding lifelong antiretroviral therapy coverage and increasing availability of effective vaccines in Malawi and other areas of high HIV prevalence may reduce infectious morbidity and antibiotic use
D. Guidelines for HIV-infected pregnant women now recommend stopping breast-feeding by 12 months

EID SPOTLIGHT

These spotlights highlight the latest articles and information on emerging infectious disease topics in our global community.

Antimicrobial Resistance

Food Safety

Ebola

HIV/AIDS

Lyme Disease

Influenza

MERS

Pneumonia

Rabies

Tuberculosis

Ticks

Zika

EMERGING INFECTIOUS DISEASES®

http://wwwnc.cdc.gov/eid/page/spotlight-topics

CDC YELLOW BOOK 2018

HEALTH INFORMATION FOR INTERNATIONAL TRAVEL

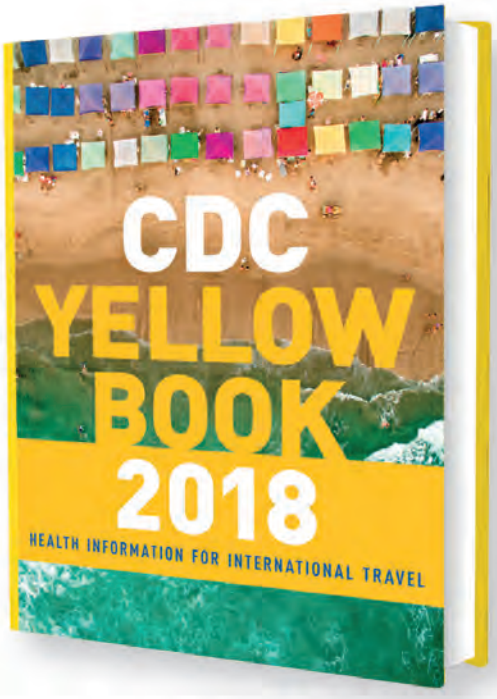

Available Now - New for 2018

The fully revised and updated *CDC Yellow Book 2018: Health Information for International Travel* codifies the U.S. government's most current health guidelines and information for clinicians advising international travelers, including pretravel vaccine recommendations, destination-specific health advice, and easy-to-reference maps, tables, and charts.

ISBN: 9780190628611 | $49.95 | May 2017 | Paperback | 704 pages

The 2018 Yellow Book includes important travel medicine updates:

- **The latest information about emerging infectious disease threats such as Zika, Ebola, and sarcocystosis**
- **New cholera vaccine recommendations**
- **Updated guidance on the use of antibiotics in the treatment of travelers' diarrhea**
- **Special considerations for unique types of travel such as wilderness expeditions, work-related travel, and study abroad**

IDSA members: log in via **www.idsociety.org** before purchasing this title to receive your **20% discount**

OXFORD
UNIVERSITY PRESS

Order your copy at:

www.oup.com/academic

Emerging Infectious Diseases is a peer-reviewed journal established expressly to promote the recognition of new and reemerging infectious diseases around the world and improve the understanding of factors involved in disease emergence, prevention, and elimination.

The journal is intended for professionals in infectious diseases and related sciences. We welcome contributions from infectious disease specialists in academia, industry, clinical practice, and public health, as well as from specialists in economics, social sciences, and other disciplines. Manuscripts in all categories should explain the contents in public health terms. For information on manuscript categories and suitability of proposed articles, see below and visit http://wwwnc.cdc.gov/eid/pages/author-resource-center.htm.

Summary of Authors' Instructions

Authors' Instructions. For a complete list of EID's manuscript guidelines, see the author resource page: http://wwwnc.cdc.gov/eid/page/author-resource-center.

Manuscript Submission. To submit a manuscript, access Manuscript Central from the Emerging Infectious Diseases web page (www.cdc.gov/eid). Include a cover letter indicating the proposed category of the article (e.g., Research, Dispatch), verifying the word and reference counts, and confirming that the final manuscript has been seen and approved by all authors. Complete provided Authors Checklist.

Manuscript Preparation. For word processing, use MS Word. Set the document to show continuous line numbers. List the following information in this order: title page, article summary line, keywords, abstract, text, acknowledgments, biographical sketch, references, tables, and figure legends. Appendix materials and figures should be in separate files.

Title Page. Give complete information about each author (i.e., full name, graduate degree(s), affiliation, and the name of the institution in which the work was done). Clearly identify the corresponding author and provide that author's mailing address (include phone number, fax number, and email address). Include separate word counts for abstract and text.

Keywords. Use terms as listed in the National Library of Medicine Medical Subject Headings index (www.ncbi.nlm.nih.gov/mesh).

Text. Double-space everything, including the title page, abstract, references, tables, and figure legends. Indent paragraphs; leave no extra space between paragraphs. After a period, leave only one space before beginning the next sentence. Use 12-point Times New Roman font and format with ragged right margins (left align). Italicize (rather than underline) scientific names when needed.

Biographical Sketch. Include a short biographical sketch of the first author—both authors if only two. Include affiliations and the author's primary research interests.

References. Follow Uniform Requirements (www.icmje.org/index.html). Do not use endnotes for references. Place reference numbers in parentheses, not superscripts. Number citations in order of appearance (including in text, figures, and tables). Cite personal communications, unpublished data, and manuscripts in preparation or submitted for publication in parentheses in text. Consult List of Journals Indexed in Index Medicus for accepted journal abbreviations; if a journal is not listed, spell out the journal title. List the first six authors followed by "et al." Do not cite references in the abstract.

Tables. Provide tables within the manuscript file, not as separate files. Use the MS Word table tool, no columns, tabs, spaces, or other programs. Footnote any use of boldface. Tables should be no wider than 17 cm. Condense or divide larger tables. Extensive tables may be made available online only.

Figures. Submit editable figures as separate files (e.g., Microsoft Excel, PowerPoint). Photographs should be submitted as high-resolution (600 dpi) .tif or .jpg files. Do not embed figures in the manuscript file. Use Arial 10 pt. or 12 pt. font for lettering so that figures, symbols, lettering, and numbering can remain legible when reduced to print size. Place figure keys within the figure. Figure legends should be placed at the end of the manuscript file.

Videos. Submit as AVI, MOV, MPG, MPEG, or WMV. Videos should not exceed 5 minutes and should include an audio description and complete captioning. If audio is not available, provide a description of the action in the video as a separate Word file. Published or copyrighted material (e.g., music) is discouraged and must be accompanied by written release. If video is part of a manuscript, files must be uploaded with manuscript submission. When uploading, choose "Video" file. Include a brief video legend in the manuscript file.

Types of Articles

Perspectives. Articles should not exceed 3,500 words and 50 references. Use of subheadings in the main body of the text is recommended. Photographs and illustrations are encouraged. Provide a short abstract (150 words), 1-sentence summary, and biographical sketch. Articles should provide insightful analysis and commentary about new and reemerging infectious diseases and related issues. Perspectives may address factors known to influence the emergence of diseases, including microbial adaptation and change, human demographics and behavior, technology and industry, economic development and land use, international travel and commerce, and the breakdown of public health measures.

Synopses. Articles should not exceed 3,500 words in the main body of the text or include more than 50 references. Use of subheadings in the main body of the text is recommended. Photographs and illustrations are encouraged. Provide a short abstract (not to exceed 150 words), a 1-line summary of the conclusions, and a brief biographical sketch of first author or of both authors if only 2 authors. This section comprises case series papers and concise reviews of infectious diseases or closely related topics. Preference is given to reviews of new and emerging diseases; however, timely updates of other diseases or topics are also welcome. If detailed methods are included, a separate section on experimental procedures should immediately follow the body of the text.

Research. Articles should not exceed 3,500 words and 50 references. Use of subheadings in the main body of the text is recommended. Photographs and illustrations are encouraged. Provide a short abstract (150 words), 1-sentence summary, and biographical sketch. Report laboratory and epidemiologic results within a public health perspective. Explain the value of the research in public health terms and place the findings in a larger perspective (i.e., "Here is what we found, and here is what the findings mean").

Policy and Historical Reviews. Articles should not exceed 3,500 words and 50 references. Use of subheadings in the main body of the text is recommended. Photographs and illustrations are encouraged. Provide a short abstract (150 words), 1-sentence summary, and biographical sketch. Articles in this section include public health policy or historical reports that are based on research and analysis of emerging disease issues.

Dispatches. Articles should be no more than 1,200 words and need not be divided into sections. If subheadings are used, they should be general, e.g., "The Study" and "Conclusions." Provide a brief abstract (50 words); references (not to exceed 15); figures or illustrations (not to exceed 2); tables (not to exceed 2); and biographical sketch. Dispatches are updates on infectious disease trends and research that include descriptions of new methods for detecting, characterizing, or subtyping new or reemerging pathogens. Developments in antimicrobial drugs, vaccines, or infectious disease prevention or elimination programs are appropriate. Case reports are also welcome.

Research Letters Reporting Cases, Outbreaks, or Original Research. EID publishes letters that report cases, outbreaks, or original research as Research Letters. Authors should provide a short abstract (50-word maximum), references (not to exceed 10), and a short biographical sketch. These letters should not exceed 800 words in the main body of the text and may include either 1 figure or 1 table. Do not divide Research Letters into sections.

Letters Commenting on Articles. Letters commenting on articles should contain a maximum of 300 words and 5 references; they are more likely to be published if submitted within 4 weeks of the original article's publication.

Commentaries. Thoughtful discussions (500–1,000 words) of current topics. Commentaries may contain references (not to exceed 15) but no abstract, figures, or tables. Include biographical sketch.

Another Dimension. Thoughtful essays, short stories, or poems on philosophical issues related to science, medical practice, and human health. Topics may include science and the human condition, the unanticipated side of epidemic investigations, or how people perceive and cope with infection and illness. This section is intended to evoke compassion for human suffering and to expand the science reader's literary scope. Manuscripts are selected for publication as much for their content (the experiences they describe) as for their literary merit. Include biographical sketch.

Books, Other Media. Reviews (250–500 words) of new books or other media on emerging disease issues are welcome. Title, author(s), publisher, number of pages, and other pertinent details should be included.

Conference Summaries. Summaries of emerging infectious disease conference activities (500–1,000 words) are published online only. They should be submitted no later than 6 months after the conference and focus on content rather than process. Provide illustrations, references, and links to full reports of conference activities.

Online Reports. Reports on consensus group meetings, workshops, and other activities in which suggestions for diagnostic, treatment, or reporting methods related to infectious disease topics are formulated may be published online only. These should not exceed 3,500 words and should be authored by the group. We do not publish official guidelines or policy recommendations.

Photo Quiz. The photo quiz (1,200 words) highlights a person who made notable contributions to public health and medicine. Provide a photo of the subject, a brief clue to the person's identity, and five possible answers, followed by an essay describing the person's life and his or her significance to public health, science, and infectious disease.

Etymologia. Etymologia (100 words, 5 references). We welcome thoroughly researched derivations of emerging disease terms. Historical and other context could be included.

Announcements. We welcome brief announcements of timely events of interest to our readers. Announcements may be posted online only, depending on the event date. Email to eideditor@cdc.gov.

In This Issue

Perspective

Synopses

Research

Dispatches

ISSN 1080-6040

DEPARTMENT OF HEALTH & HUMAN SERVICES
Public Health Service
Centers for Disease Control and Prevention (CDC)
Mailstop D61, Atlanta, GA 30329-4027

Official Business
Penalty for Private Use $300
Return Service Requested

MEDIA MAIL
POSTAGE & FEES PAID
PHS/CDC
Permit No. G 284